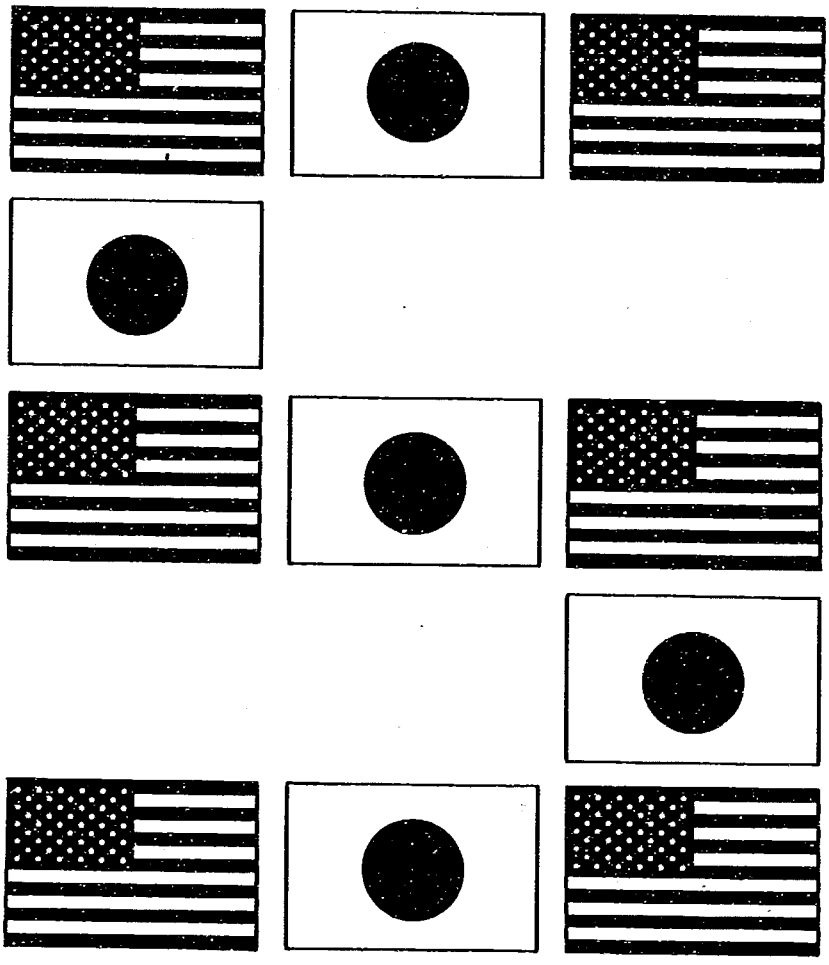
ISSN 0386-5878
Technical Memorandum
of PWRI No.3198

U.S.-JAPAN WORKSHOP ON EARTHQUAKE DISASTER PREVENTION FOR LIFELINE SYSTEMS



OCTOBER 26-27, 1992
PUBLIC WORKS RESEARCH INSTITUTE
TSUKUBA SCIENCE CITY, JAPAN

Copyright © (1993) by P.W.R.I.

All rights reserved. No part of this book may be reproduced by any means, nor transmitted, nor translated into a machine language without the written permission of the Director General of P.W.R.I.

この報告書は、土木研究所長の承認を得て刊行したものである。したがって、本報告書の全部又は一部の転載、複製は、土木研究所長の文書による承認を得ずしてこれを行ってはならない。

Technical Memorandum
of PWRI No.3198

PROCEEDING OF FIFTH U.S.–JAPAN WORKSHOP ON EARTHQUAKE DISASTER PREVENTION FOR LIFELINE SYSTEMS

OCTOBER 26 AND 27, 1992
PUBLIC WORKS RESERCH INSTITUTE
TSUKUBA SCIENCE CITY, JAPAN

by
Kazuhiko KAWASHIMA
Hideki SUGITA
and
Tomoru NAKAJIMA

Synopsis:

This proceedings document the results of the U.S.–Japan Workshop on Earthquake Disaster Prevention for Lifeline Systems which was held at the Public Works Research Institute, Tsukuba Science City, Japan, on October 26 and 27, 1992 under the auspices of the Panel on Wind and Seismic Effects, UJNR. The Workshop was organized by the Task Committee F "Disaster Prevention Methods for Lifeline Systems" (U.S. side chairman: R. D. Dikkers, NIST, Japan side chairman: Y. Iida, PWRI) of the Panel.

Key word: Earthquake Disaster Prevention, Lifeline Systems, Bridge, Pipeline, Gas, Telephone, Electricity, Water Supply, UJNR

FORWARD

The following proceedings document the results of the U.S.–Japan Workshop on Earthquake Disaster Prevention for Lifeline Systems which was held at the Public Works Research Institute, Tsukuba Science City, Japan, on October 26 and 27, 1992 under the auspices of the Panel on Wind and Seismic Effects, UJNR. The Workshop was organized by the Task Committee F "Disaster Prevention Methods for Lifeline Systems" (U.S. side chairman : R.D. Dikkers, Japan side chairman : Y. Iida) of the Panel. The Workshop was jointly coordinated by Mr. R.T. Eguchi of EQE Engineering and Design, and Dr. K. Kawashima, Head of Earthquake Engineering Division of the Public Works Research Institute.

The purposes of the Workshop were : (1) to bring together experts from both countries to discuss current research efforts in the area of lifeline seismic risk assessment and design, (2) to offer a forum for individuals to study specific measures being incorporated by agencies or companies to mitigate the effects of earthquakes on their systems, and (3) to identify future needs and opportunities between the two countries for cooperative research and exchange of data, information and research personnel. With this in mind, the Workshop program was developed so that it would help advance of the long-term objectives in lifeline earthquake engineering of both countries.

A broad range of special technical topics were presented at the Workshop. These included the following items.

1) Effect of liquefaction and large ground displacement
2) Network and system performance assessment
3) Observations and seismic monitoring
4) Seismic design and performance of lifeline systems, including telecommunication, electric power, water and natural gas systems
5) Seismic design and performance of highway bridges and tunnels
6) Socioeconomic impact of lifeline failures and disruptions

In total 34 papers were presented in the two days of plenary sessions; 19 papers from Japan and 15 papers from the U.S..

This proceedings includes (1) all technical papers that were presented during the Workshop in their order of presentation, (2) the resolutions that were unanimously approved by the participants during the closing session of the Workshop, and (3) Workshop program and list of participants.

In concluding the forward, we wish to express our profound gratitude and sincere appreciation to all participants in the Workshop for supporting the Workshop by active presentations and discussion. In particular, we would like to thank Dr. R. Chung, Mr. M.P. Singh, Mr. R. Eguchi and Prof. M. Shinozuka for organizing the U.S. members. And we would like to thank Dr. S.C. Liu his encouragement for holding the Workshop.

Greatful thanks are also extended to the Japan side members. Sincere appreciation goes to Prof. T. Katayama, Prof. E. Kuribayashi, Prof. H. Kameda, Prof. M. Hamada, Prof. T. Sato, Prof. S. Takada and the members involved in the Joint Research Program between PWRI and 8 private companies on the seismic design method for underground structures. Special appreciation also goes to Tokyo Metropolitan Government, Metropolitan Expressway Public Corporation, Trans-Tokyo Bay Highway Corporation, Tokyo Gas Corporation, Tokyo Electric Power Corporation, Central Research Institute of Electric Power Industry and NTT for the generous cooperation in the Workshop and during the study-tour. We also would like to thank the assisting staff members, Messrs. S. Unjoh, J. Hosikuma, H. Iida, H. Mukai, K. Nagaya and K. Tamura, and Miss. M. Ikeda at PWRI for the smooth progress of the schedule.

March 1993

Kazuhiko KAWASHIMA
Hideki SUGITA
Tomoru NAKAJIMA

Earthquake Engineering Division
Earthquake Disaster Prevention Department
Public Works Research Institute

TABLE OF CONTENTS

Papers

Session–2 Telecommunication 1

Earthquake and Lifeline Hazards Reduction Programs at National Science Foundation
(Mahendra P.Singh) 3

Aseismatic Countermeasures for Optical Fiber Cable in Liquefiable Ground
(Shinji MATAKI) 5

Post–Earthquake Performance of Telecommunications Networks
(Kenneth B.Boheim) 19

Seismic Considerations of Raised Floor Application for Telecommunication Network Facilities
(Alex K.Tang) 29

Session–3 Electricity, Water & Gas 41

Earthquake Engineering Researches for Electric Power Lifeline Systems
(Junichi TOHMA) 43

A Method of Evaluating Earthquake Resistance of Buried Pipelines——Recommened Practice of JGA and a Proposal for Its Improvement
(Nobuaki NISHIO) 55

Earthquake Hazard Reduction Program for a Water Lifeline Utility
(Ergun Bakall) 75

Seismic Design for Pipeline of Waterworks in Tokyo
(Ichiro YOKOTA) 93

Session–4 Effect of Liquefaction 111

Strees Analysis Method for Steel Pipelines Buried in a Liquefied Ground Layer
(Takashi IWATA) 113

Damage Assessment of Lifeline Facilities in Liquefied Area
(Masanori HAMADA) 127

Safety Estimation of Buried Pipes for Permanent Ground Deformation by Liquefaction
(Hideyo SUZUKI) 139

Experimental Study on Liquefaction Potential and the Uplift Deformation of Underground Structures
(Yoshio NINOMIYA) 161

Lateral Spread Effects on Reinforced Concrete Pile Foundations
(T.D.O'Rourke) 173

Session–5 Network Assessment 197

Seismic Reliability Analyses of Large Scale Lifeline Networks Using Fuzzy Set Theory
(Tadanobu SATO) 199

Network Performance of Highway Systems Under Earthquake Effects:
A Case Study of the 1989 Loma Prieta Earthquake
(Hioshi WAKABAYASHI and Hiroyuki KAMEDA) 215

GIS–Based Assessment of the Seismic Performance of a Water Delivery System
(Masanobu SHINOZUKA) 233

Session–6 Seismic Design 251

Earthquake Response Analysis Method for Shield Tunnels

(Yukio SHIBA) 253

A Seismic Design of a Large–In–Scale Shield Tunnel of Trans–Tokyo Bay Highway

(Kenji KURAISHI) 271

Design of Tama River and Kawasaki Fairway Tunnels in Expressway Bay–Shore Route

(Shinichi EGAWA) 285

Seismic Design Method of Underground Parking Garage Structures

(Kazuhiko KAWASHIMA) 301

Session–7 Bridge 319

Caltrans' Foundation Seismic Research Program

(Clifford J.Roblee) 321

Seismic Strengthening and Retrofitting of Highway Bridges in Japan

(Shigeki UNJOH) 357

Research Based Bridge Seismic Design and Retrofit Program Criteria, Standards and Status

(James E.Roberts) 379

Session–8 Hazard Mitigation 401

Pipeline Damage Mitigation Using TCLEE Pipeline Failure Databace

(Le Val Lund) 403

Study On Socio–Economic Effects of Lifeline Earthquake Disaster in Urbane Transportation Networks

(Leelawat Chartchai) 429

Lifeline Interaction and Post–Earthquake Functionality:
Case Study for Fire Following Earthquake

(Charles Scawthorn) 441

Proposed Plan for Developing and Adopting Seismic Guidelines and Standards for Lifelines

(Riley M.chung) 451

Session–9 Observation and Seismic Monitoring 465

Seismic Behavior of Beried Pipelines Through Field Observation

(Hideki SUGITA) 467

Seismic Monitering and System Control for Lifelines

(Shiro TAKADA) 481

Monitoring, Instrumentation and Innovative Devices for Lifeline Systems

(Donald Ballantyne) 503

Vulnerability of Fiber Optics Cables to Fault Rupture, A Proposed Field Experiment

(Felix S.Wong) 521

Session–10 Impact of Seismic Effects 533

Effective Measures for Reducing People's Anxiety in Undweground Spaces During Earthquakes

(Etsuro SAITO) 535

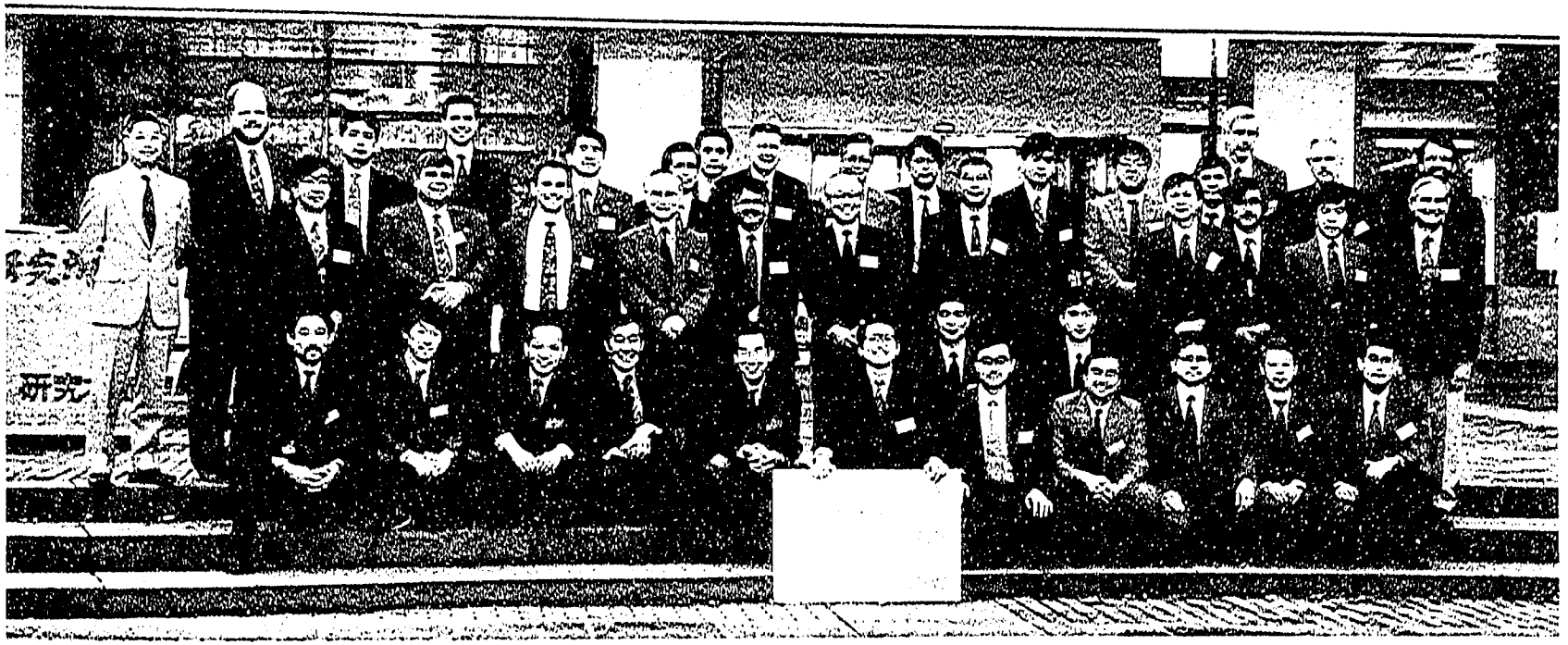
Indirect Losses Caused by Lifeline Damage or Disruption

(Ronald T.Eguchi) 549

Earthquake–Induced Congestion Impacts on Local Telephone Networks
. (L.J.Forys) 575

Resolution 595

Appendices 601
Workshop Program 603
Participants 618



Session-2

Telecommunication

U-1) Earthquake and Lifeline Hazards Reduction Programs at National Science Foundation
(Singh, M.P.)

J-1) Aseismic Countermeasures for Optical Fiber Cable in Liquefiable Ground
(Yagi, K., Mataki, S. and Sakurada, T.)

U-2) Post-Earthquake Performance of Telecommunications Networks
(Boheim, K.B. and Kelly, C.M.)

U-3) Seismic Considerations of Raised Floor Application for Telecommunication Network Facilities
(Tang, A.K.)

ABSTRACT

Earthquake and Lifeline Hazards Reduction Programs
at
National Science Foundation

Mahendra P. Singh
Program Director
Earthquake Hazard Mitigation Program
Directorate for Engineering
National Science Foundation

The National Science Foundation is one of the principal agencies involved in the National Earthquake Hazards Reduction Program. It has continuously supported research in earthquake engineering including research on lifelines and other civil infrastructure systems. This presentation will provide an overview of these research programs, and other related activities at the NSF.

Aseismic countermeasures for optical fiber cable in liquefiable ground

Koji Yagi 1), Shinji Mataki and Toshinori Sakurada
1) Senior Manager
NTT Telecommunications Field Systems R&D Center

ABSTRACT

This paper is concerned with the evaluation of aseismic performance of optical fiber cable joints and aseismic countermeasures for them. Ground deformation due to earthquake has caused manholes (MHs) to slide and raise, and cable joints within MHs have been damaged as tension moves cables or causes them to drop from their supports.Optical fiber cable joints would likely be damaged in an earthquake, because they are less able to resist tension than conventional metallic cable joints. As the communications network moves from metallic cable to optical fiber cable, optical fiber cable joints have become a new weak area in resisting earthquake. Aseismic countermeasures that prevent optical fiber cable joints from tension due to ground deformation are impotant subjects and needed.

INTRODUCTION

As part of its present strategy to diversify its range of telecommunications services, NTT is currently constructing a communications network that replaces conventional metallic cable with optical fiber cable, in order to benefit from its capacity to transmit greater volumes of data over long distances. However, previous earthquakes have caused damage to underground telecommunications facilities in liquified ground. Ground deformation has caused conduits to buckle, and joints to be damaged and severed. Collapsed highway banking resulted in shifting conduits and manholes. The cables that run within conduits have suffered damage to their sheath. Shifting between conduit sections has pulled the cable running through them into sharp changes of direction, leading to disrupted

communications. Cables and cable joints within manholes have also been damaged as tension moves cables or causes them to drop from their supports, but such incidents have not lead to any disruption in communications. The optical fiber network has not yet been exposed to an earthquake of a scale to damage underground facilities, but fears exist for the safety of the system.

As the communications network moves from metallic cables to optical fiber, the joints of optical fiber cables have become a new weak area in resisting earthquake. This paper reports on evaluations of the aseismic performance of optical fiber cable joints through assessment of the damage caused by past earthquakes and tests to reproduce the conditions of a similar disaster, and suggests measures to improve that performance.

CHARACTERISTICS OF CABLE JOINTS

Conventional metallic cables installed in underground facilities subjected to a major earthquake have been joined by a plumbing technique. As Fig. 1 shows, this method joins the cable's cores, covering the joints with a lead sleeve. Because the joint is attached intimately to the cable, the cable joint is able to withstand relatively high tension on the cable joint. In contrast, the characteristics of optical fiber cable cores mean that the cables are joined with a circular standard closure (SC), as shown in Photo.1. The SC's ability to withstand tension depends on the grip of the SC on the cable itself and the tension members inside the cable that connect to the SC. Experience has shown that this structure is less able to resist tension than the plumbing joint method.

PATTERNS OF SEISMIC DAMAGE TO UNDERGROUND FACILITIES

The extent of damage suffered by underground telecommunications facilities in an earthquake is greatly affected by the structure and quality of the surface soil above them. In the Niigata earthquake of 1964 and the Nihon Kai Chubu earthquake of 1983, soil liquefaction above underground facilities led to various types of damage, including sliding, raising, and inclination of manholes, and severance of conduit joints. Damage also

occurred within manholes, as cables were shifted or detached from their supports. (Photo.2) Figure 2 is a flow chart that analyses the effects of such damage on metallic cable.

As Table 1 shows, the damage sustained by cable within underground facilities can be classified into two types: that occurring in conduits, and that in manholes. The type of damage also differs according to whether the equipment houses metallic or optical fiber cable.

Damage to metallic cables in a conduit is generally in the form of cable severance due to damage or separation of the conduit, and leading to crossed circuits and other types of communications disruption. Optical fiber cable is judged to have less capacity to withstand bending and side stress, and its performance within a conduit during earthquake conditions are now being studied.

Metal cables within manholes have been known to suffer leakage of gas from the plumbing joint as a result of the cable or joint shifting, or separation from the cable supports. However, such incidents have not led to disruption of communications. Gas is inserted into the cable to prevent the ingress of water. When a tension large enough to shift the cable joint is exerted, the gas escapes through the space created between the cable and the lead sleeve.

The lesser resistance of SCs to tension means that optical fiber cables within a manhole are thought liable to increased transmission loss as the result of a tensile force great enough to cause shifting. However, the lack of examples of damage to optical fiber cable joints in a manhole in an actual earthquake mean that studies have been performed to assess cable shifting and severance of joints under such circumstances.

ANALYSIS OF CABLE SHIFTING AND JOINT SEVERANCE

In the Nihon Kai Chubu earthquake, soil liquefaction was especially severe in Noshiro city and along the route linking Noshiro and Oga. The damage to cables and cable joints in the form of shifting and separation from supports within manholes was analyzed (see Fig. 3).

Rate of damage caused by cable shifting within manholes

Within Noshiro, and along the Noshiro to Oga route, 78 manholes were positioned in ground where soil liquefaction occurred (see Fig.4). Of this total, 52 manholes suffered raising, cracking, intrusion of conduits into manholes, and other forms of damage. Twenty-eight of these manholes, or 36% of the total number sited in ground where soil liquefaction occurred, sustained cable shifting or separation of cable joints from their supports. Only one case was seen of a cable damaged when its conduit buckled due to ground deformation; this established that the effect on cable was greater within manholes than in conduits.

Amount of cable shifting within manholes

The amount of cable shifting within manholes was calculated through aerial surveys carried out before and after the earthquake (see Fig. 5). Data on the directional strains along the axis of conduits between manholes were first gathered from aerial measurements, and the relative displacement between manholes was calculated with reference to the distance between each manhole. When the relative displacement moved the manholes further apart, the length of the cable pulled out from each manhole was equal, and the amount of cable shifting within each manhole was classed as half the relative displacement between the manholes (see Fig. 6).

The survey showed that the relative displacement between manholes was a maximum 70 cm when pressed closer together, and a maximum 50 cm when pulled further apart. Since

70 cm shifting of manholes away from each other is also conceivable, maximum cable shifting within a single manhole is estimated at 35 cm (see Fig.7).

TESTING THE ASEISMIC PERFORMANCE OF OPTICAL FIBER CABLE

Outline of test

Further tests on cable shifting were performed to establish the extent of cable shifting within manholes calculated by the method described above, as well as the relative strengths of optical fiber SC joints and metallic cable plumbing joints. The tests involved placing cables and cable joints inside a manhole positioned on the surface, and measuring the cable shifting and optical fiber transmission loss when tension was applied to the cables (see Fig. 8).

Test results

Figure 9 shows the relation between degrees of cable shifting and the amount of tension applied to both optical fiber and metallic cables. Even a 35 cm shifting of metallic cables, causing gas leaks from the plumbing joints, did not disrupt communications through metallic cables. However, optical fiber cables suffered detachment of the SCs and other damage at a shift within the manhole of less than 35 cm, causing increased transmission loss and severance or disruption of communications.

These tests established that optical fiber cable SC joints are less resistant to earthquake than metallic cable plumbing joints. In an earthquake of a magnitude equal to some already witnessed, communication via optical fiber cables would likely be disrupted where it could be maintained with metallic cable.

ASEISMIC COUNTERMEASURES FOR OPTICAL FIBER CABLE

Requirements for Aseismic countermeasures

The tests to evaluate the aseismic performance of optical fiber cable established that the SC joints are the greatest problem in an earthquake. In the light of this, the following two requirements have been examined for countermeasures against earthquake damage.

1) Communications should not be disrupted, even if ground displacement in an earthquake causes cable shifting.

• Because the maximum amount of cable shifting inside a manhole resulting from soil liquefaction during an earthquake is about 35 cm, the cable joints in particular should be able to resist damage arising from this displacement.

2) Measures should be applied to existing cables as well as new installations.

Outline of the countermeasures

Rather than link the duct and cable joint within a manhole with the shortest possible length of cable, a certain length of extra cable was installed (see Fig. 10). However, this extra cable was shorter than the 35 cm maximum shift possible within a manhole. Therefore, consideration was given to creating a section of extra cable long enough that no tension is exerted on the SC joints even if a 35 cm cable shift occurs.

• Countermeasure for new cable installations (see Fig. 11)

Newly-installed cable is now fitted with a loop of extra cable inside manholes, so that no tension is exerted on the SC joints even if a maximum 35 cm cable shift occurs. In manholes without SC joints, a technique was examined by which the cable is attached to supports from which it can easily be detached when tension acts upon it, allowing the extra cable to be taken up smoothly. This is shown in Fig. 11. The cable loops have a diameter

of at least 30 cm, so that joints will not be affected even at a ground displacement between manholes of 70 cm.

• Countermeasure for existing cables (see Fig. 12)

Because it is difficult to insert loops in existing cable arrangements, the same supporter technique as for new installations is used in manholes without SC joints, but for manholes containing SC joints, cable holders are placed at duct entrances to prevent tension being applied to the SC joints.

CONFIRMING THE EFFECTIVENESS OF COUNTERMEASURES

Practical tests were carried out to confirm the ease of installation and the performance of the measures proposed for both existing cables and new installations. As shown in Fig. 13, tests were carried out to confirm the methods for both new and existing cables in and between two test-use manholes positioned on the surface. Tension was applied to the cables from the mid-point between the manholes, and the effect on cables within the manholes observed.

The tests established that a loop can be formed in newly-installed cable even if the optical fiber cable itself has a wide diameter. No engineering problems were encountered with existing cable either.

The following results were obtained in relation to the performance of the various measures:

1) Even in the event of a 100 cm cable shift from a manhole where a new cable loop was installed, there was no increase in transmission loss. With a shift of over 100 cm, the loop became smaller, and some cases of increased transmission loss were observed because the cable had exceeded its bending tolerance. Despite this, the measures were proved to comfortably satisfy requirements with a shift of over 35 cm.

2) The cable holders placed to prevent cable shifting in existing installations were able to prevent shifting of the SC joints. It was also confirmed that the cable in manholes without SC joints detached smoothly from the supports, and that the extra (15-27 cm) was taken up

smoothly within the conduit. It was also confirmed that no increase in transmission loss occurred when the cable was detached from the support.

These findings confirmed the effectiveness of the new measures. They suggest that 100 cm of extra cable could prevent damage to most SC joints in the event of an earthquake with the intensity of the Nihon Kai Chubu quake.

CONCLUSION

Tests to assess the aseismic performance of the SC joints of optical fiber cable established that the maximum shifting of cables within manholes during the Nihon Kai Chubu earthquake was 35 cm, and that this degree of shifting would damage the SC joints of current optical fiber cable. Appropriate measures to prevent this situation were examined, including positioning a loop of extra cable on either side of an SC joint within a manhole when installing new cables, and creating a mechanism in manholes without SC joints where cable could separate easily from its supports, allowing extra cable to be taken up smoothly. The effectiveness of these measures were confirmed through field testing.

FUTURE DIRECTIONS

Aseismic countermeasures that positions the extra cable within MHs also proved to be economical to install, and cost-effective in terms of damage prevention in the event of an earthquake. It is planned to introduce these measures to manholes sited in liquefiable soil to raise the aseismic performance of underground telecommunications facilities.
In the future, it is necessary to clarify the performance of optical fiber cable within a conduit during earthquake and develop the countermeasures for them.

REFFERENCES

1) " Investigation on Ground Deformation and Earthquake Damage of Underground Structures, " ADEP (JAPAN), Mar. 1990
2) " Report on Survey of Damage caused by the May 26, 1983 Nihonkai-chubu Earthquake, " OYO Corporation, Jan. 1984

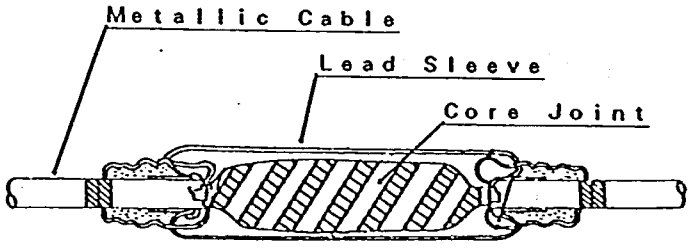


Fig. 1 Plumbing Joint

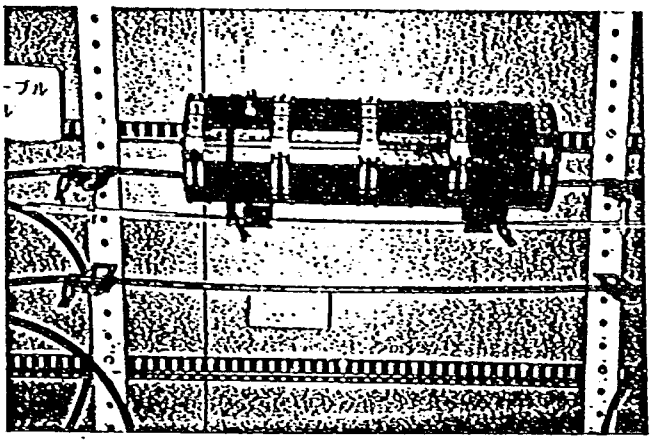


Photo. 1 Standard Closure

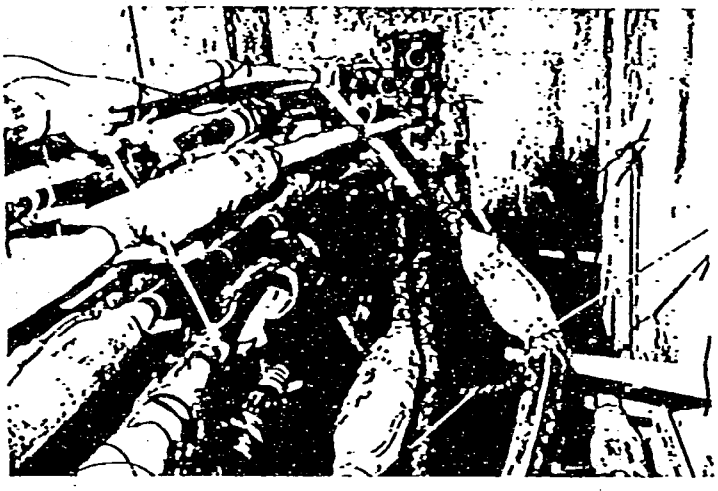
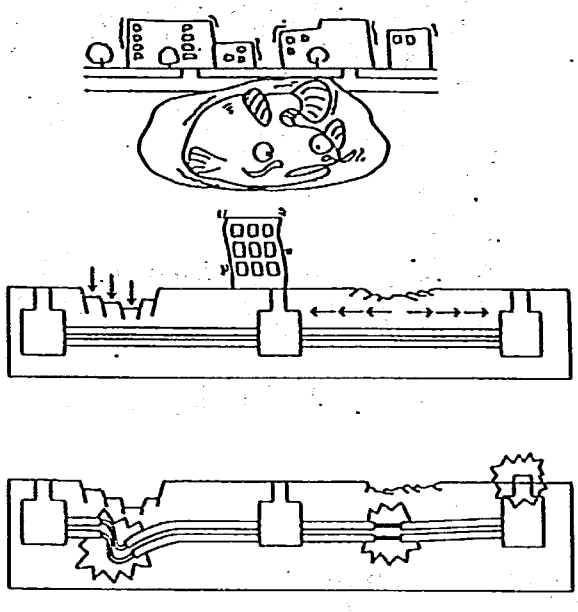


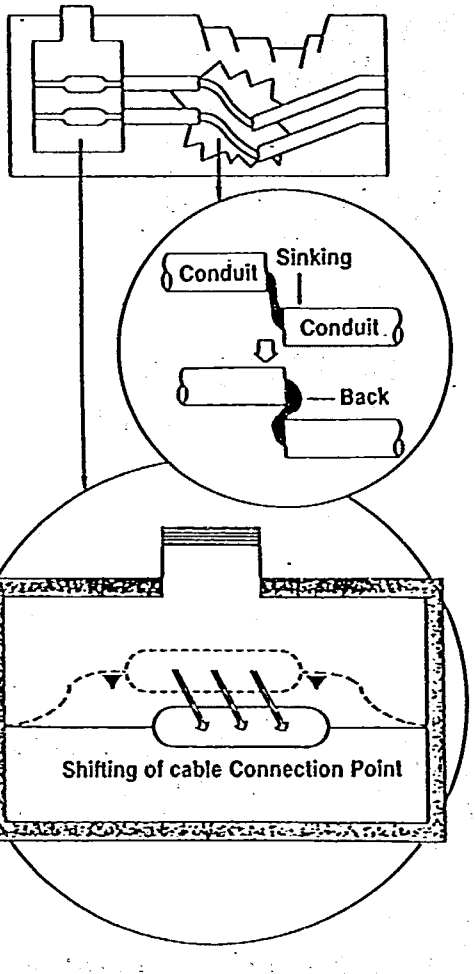
Photo. 2 Cable Joints Shifting and droping from their Supports

Table 1 Classification of Cable Damage Within Conduits and MHs

	Within Conduits	Within Manholes
Metallic Cable	Cables can be severed or become falsely interconnected, accoding to the type of damage or severance suffered by the conduit	Gas leaks as a result of movement or severanceof the cable
Optical Fiber Cable	Still investigating ; cables are prone to bending and lateral pressure	Damage is expected due to the weakness of cable connections

Patterns of Damage to Underground Facilities due to Ground Deformation





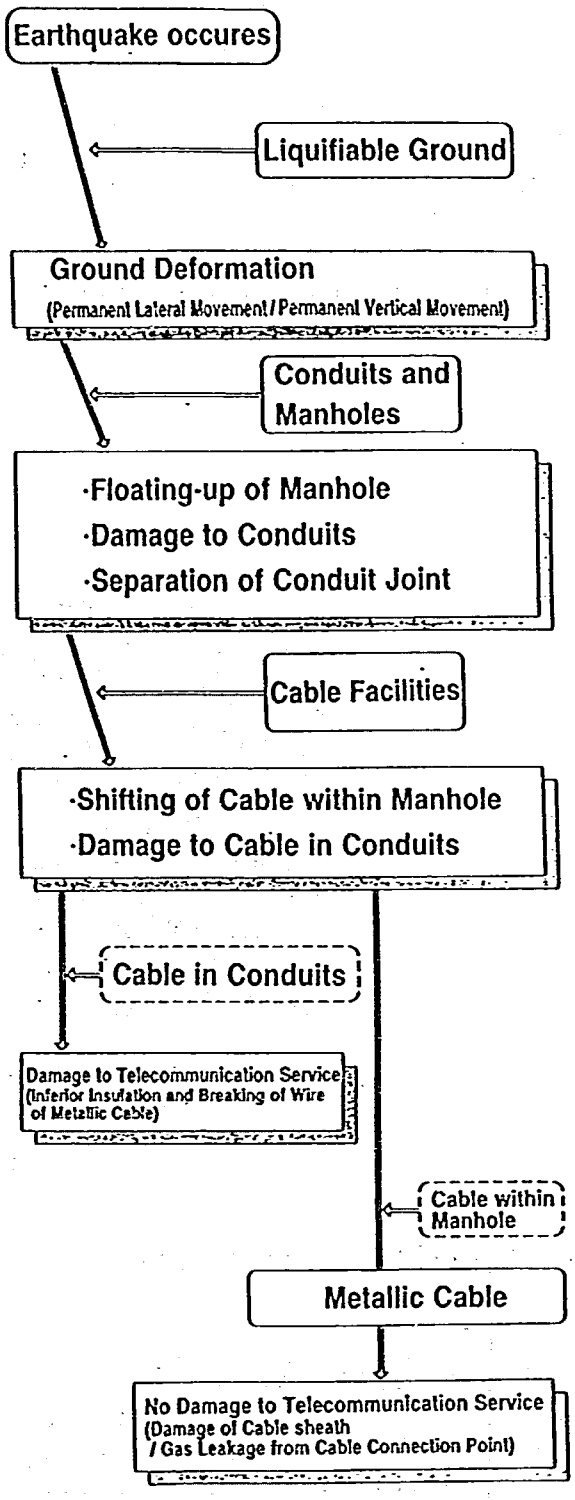


Fig. 2 Flow Chart that analyses the Damage of Metallic Cable

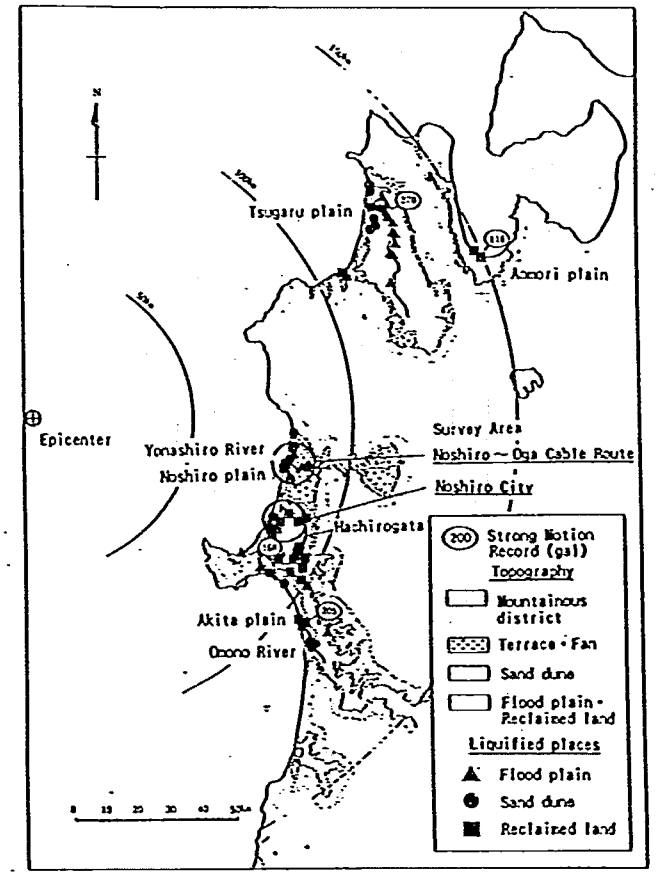


Fig. 3 Epicenter, Strong Motion Records and Liquefied Places

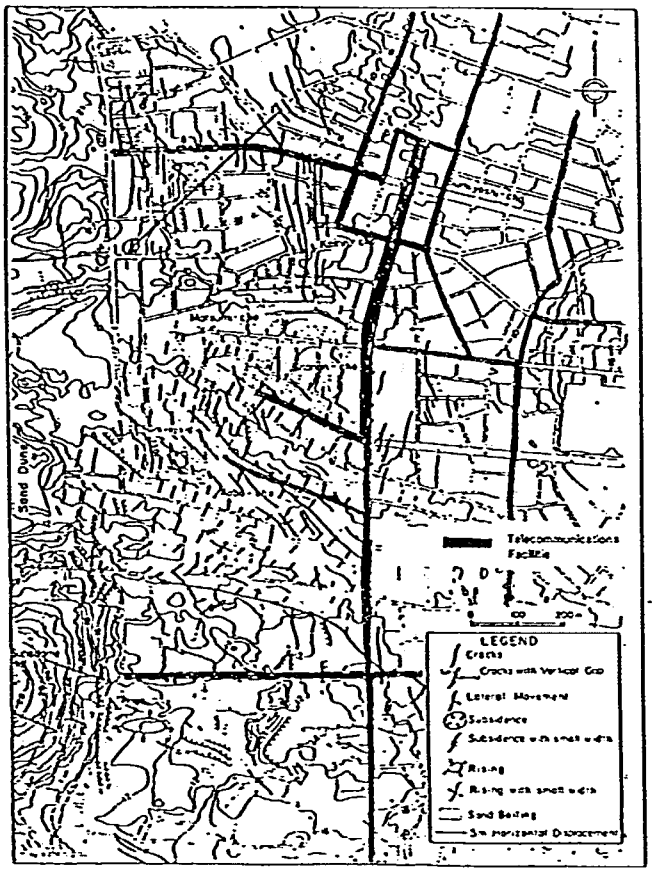


Fig. 5 Permanent Ground Displacements in Noshiro City

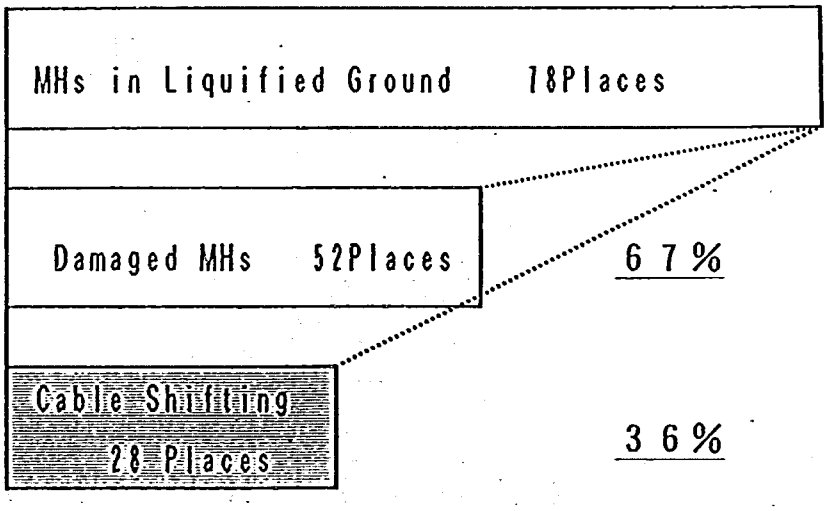


Fig. 4 Rate of Damage caused by Cable Shifting within MHs

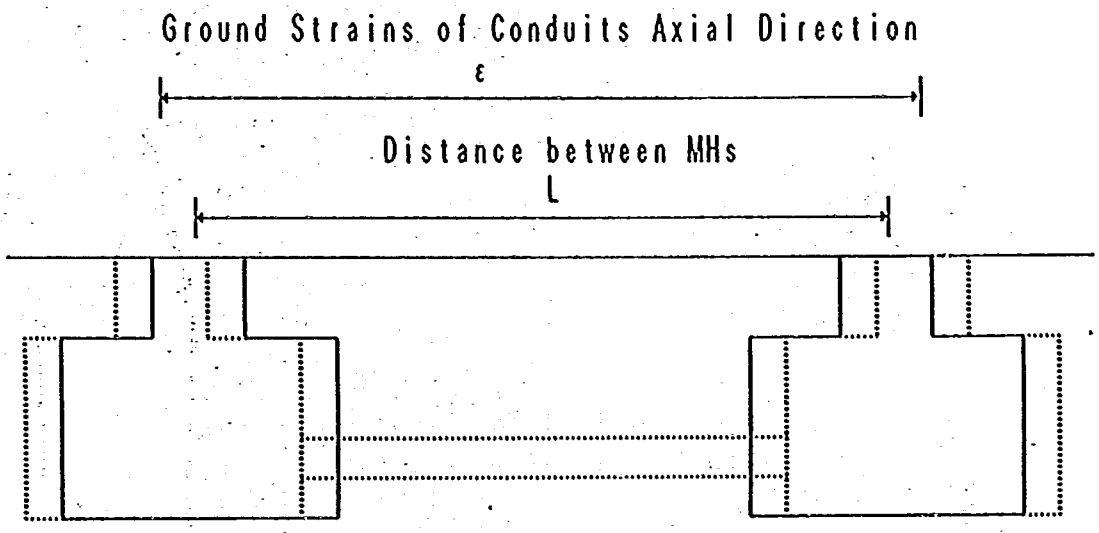


Fig. 6 Calculation Method of Amount of Cable Shifting within MH

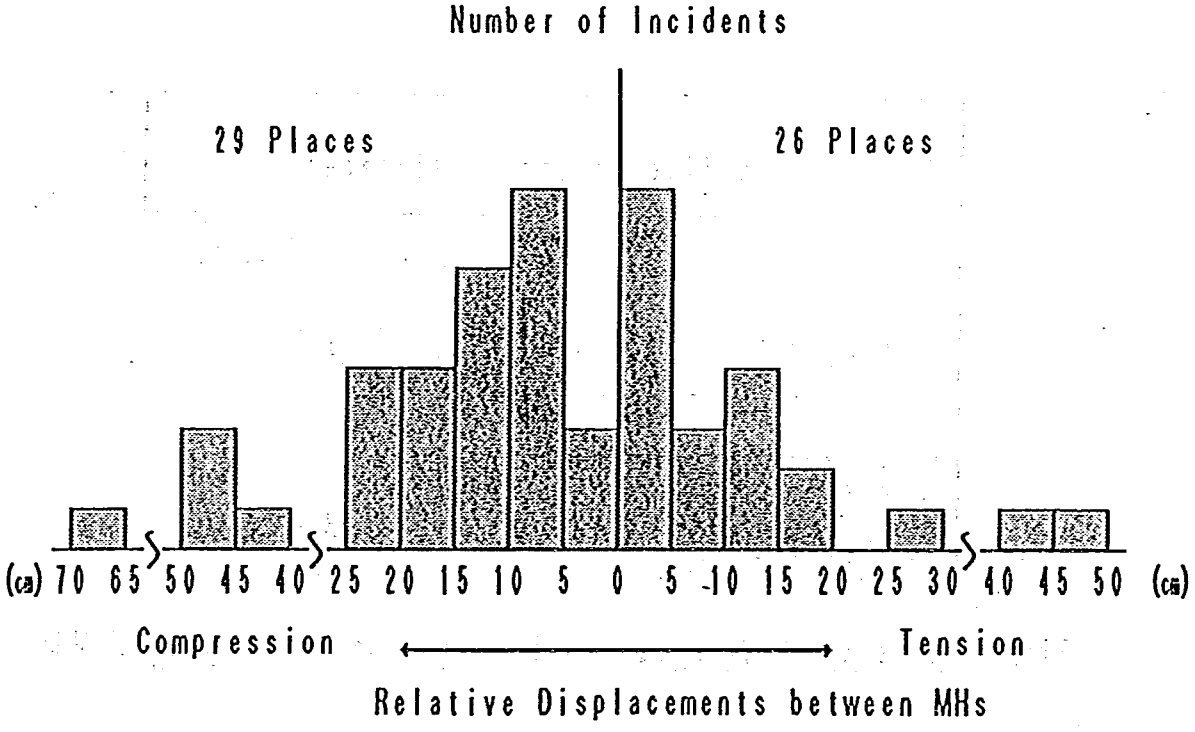


Fig. 7 Calculation Results of Amount of Cable Shifting within MH

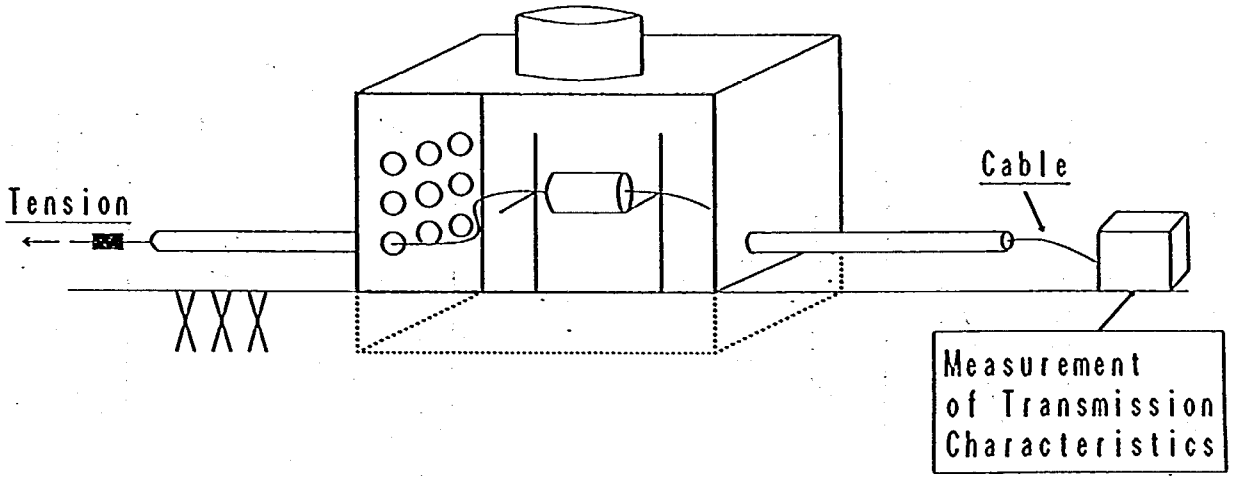


Fig. 8 Testing the Aseismic Performance of Optical Fiber Cable

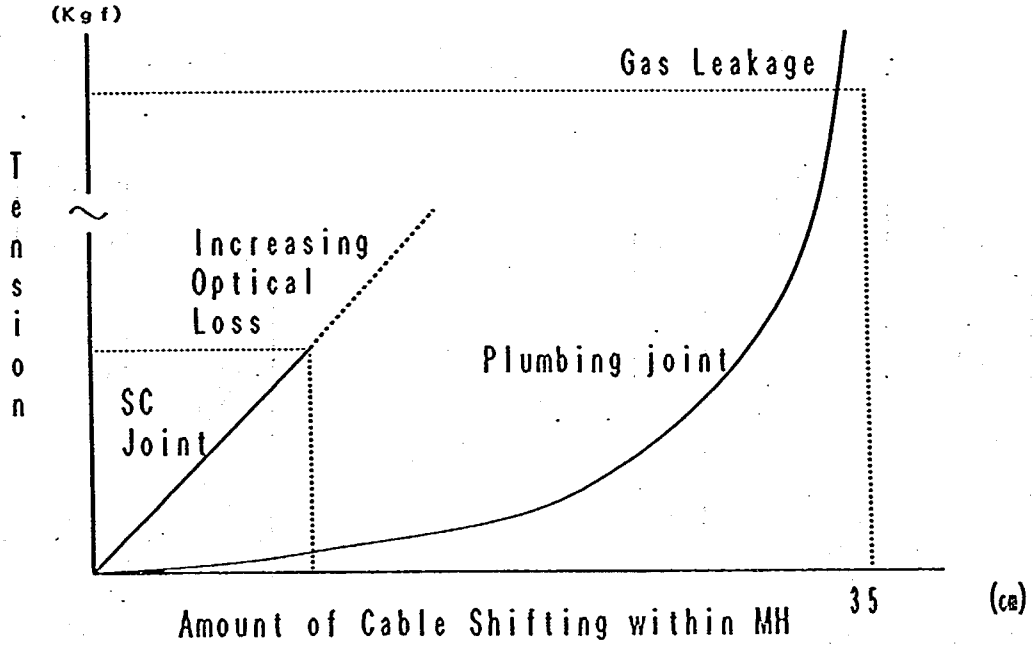


Fig. 9 Comparison between SC Joint and Plumbing joint

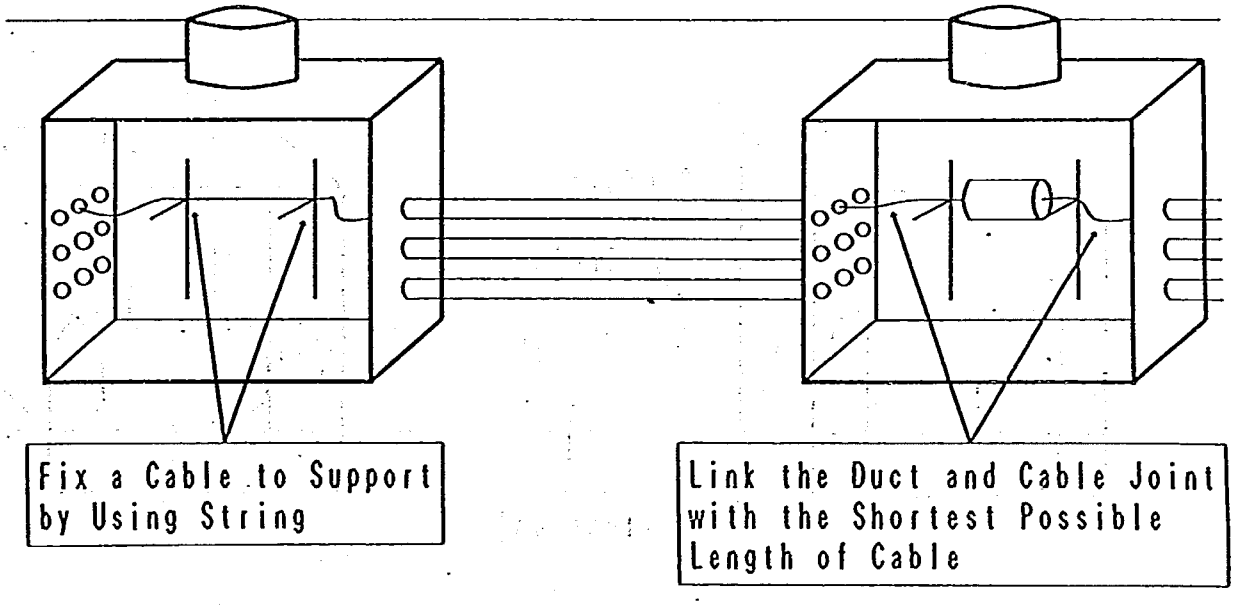


Fig. 10 Existing Cables within MHs

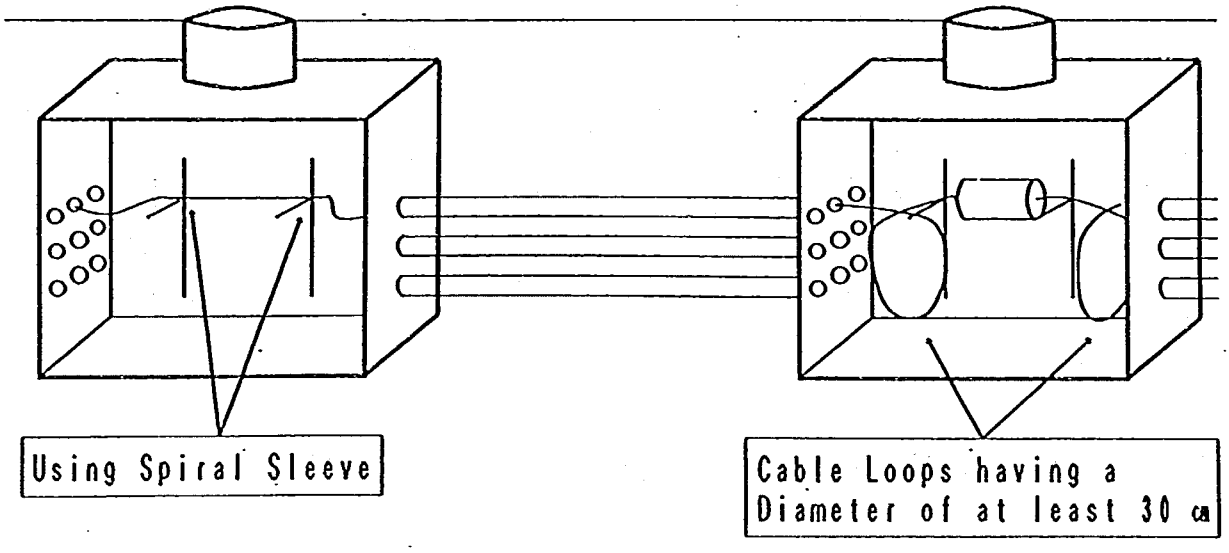


Fig. 11 Countermeasure for New Cable Installations

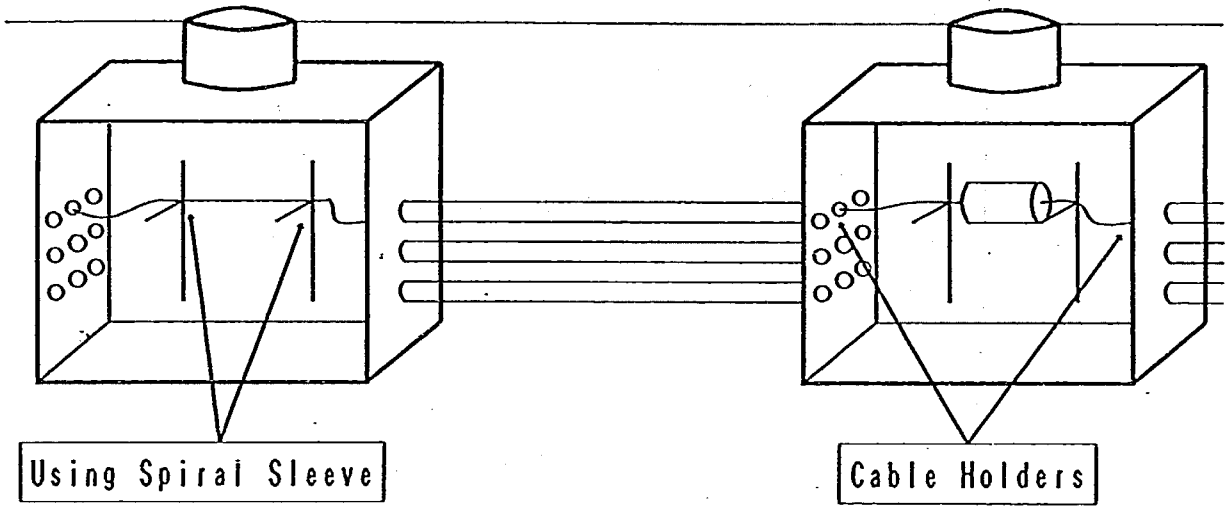


Fig. 12 Countermeasure for Existing Cables

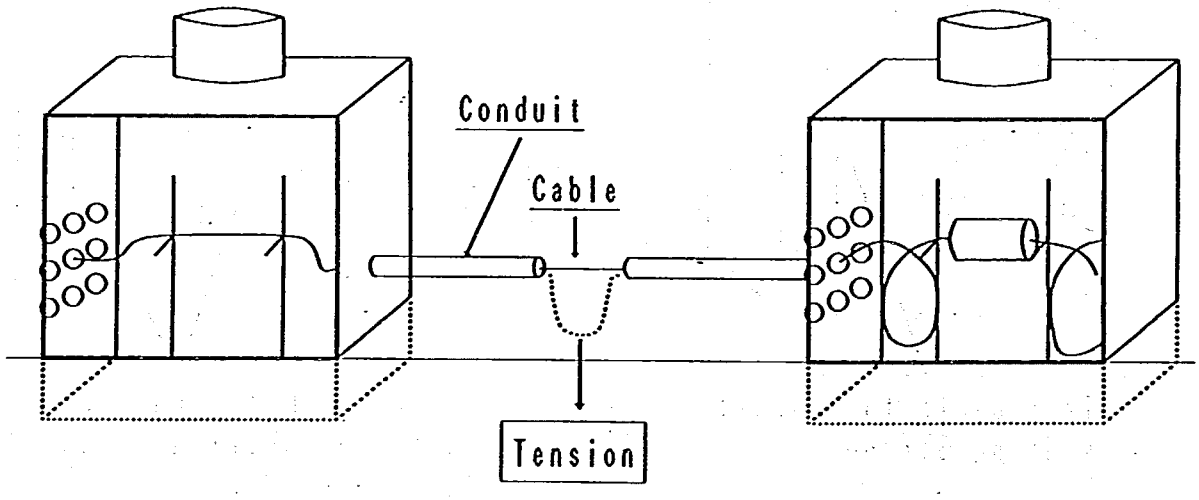


Fig. 13 Comfirming the Effectiveness of Countermeasures

POST-EARTHQUAKE PERFORMANCE OF TELECOMMUNICATIONS NETWORKS

Kenneth B. Boheim

Assistant Manager, Plans and Programs
National Communications System

Christopher M. Kelly

Senior Associate
Booz·Allen & Hamilton Inc.

ABSTRACT

United States Government policy directs the National Communications System (NCS) to ensure national security and emergency preparedness telecommunications for the entire spectrum of national emergencies. The Office of the Manager, NCS has developed a National Level National Security and Emergency Preparedness Telecommunications Program (NLP) to respond to this policy. The NLP is a set of programs that directly enhance the United States telecommunications infrastructure.

A key component in developing these programs is assessing the effects of damage and stress on the infrastructure. The NCS has assessed the effects of threats ranging from natural disasters to general war. Earthquakes are one of the natural disaster threats under study. The NCS, together with the National Science Foundation, is examining the impact of earthquakes on telecommunications. This paper describes the approach adopted by the NCS for assessing postearthquake performance of the United States telecommunications infrastructure and presents results of an initial study.

INTRODUCTION

For the past several years, the National Communications System (NCS) and its support contractors have been examining the postearthquake performance of telecommunication networks. These efforts have led to the development of an earthquake model for predicting damage to telecommunication facilities (reference 1). This paper discusses an application of the model to the assets of the United States public switched network (PSN) in the San Francisco Bay area.

The role of the National Communications System is to support the President of the United States in his roles as Head of State, Chief Executive, and Commander-in-Chief. The mission of the NCS is to assist the President in the exercise of his emergency telecommunication functions and coordinate the planning and provisioning of National Security and Emergency Preparedness (NS/EP) telecommunications for the Federal Government under all circumstances.

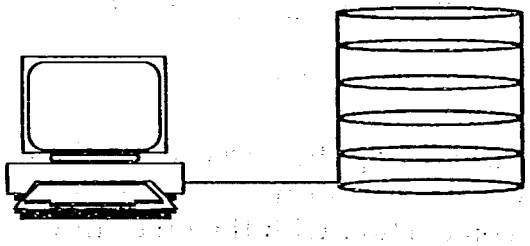
The NS/EP environment is defined by the critical needs that Federal agencies and departments fulfill under all conditions of emergency. These include, for example, the distribution of food and water, the restoration of electrical power and other energy sources, and the protection of the public. To support these functions, the agencies and departments require access to telecommunication services. As a result, the NCS focus is on provisioning communications to support the effective management of national resources by the Federal agencies and departments.

After careful study, the NCS has developed an architecture to meet NS/EP telecommunication requirements. A central theme of the architecture is leveraging the assets of the commercial carrier networks within the United States to support emergency needs. These networks are a critical resource because they represent billions of dollars per year of investment and are the core of operations for information transfer systems throughout the government. Government's reliance on these systems makes their use a necessity, and their ubiquity makes them an excellent and cost-effective foundation for building an NS/EP telecommunications capability.

The commercial carrier networks have specific characteristics that are well suited to support NS/EP needs. There are more than 25,000 switches in both the interexchange and local exchange carriers' networks. These switches provide service to almost every home and office in the nation. The hundreds of thousands of miles of fiber optics, digital microwave radio, and coaxial cable crossing the country offer significant redundancy. In addition, connections are available worldwide via satellite and undersea cable. This reach allows communications to the most remote locations.

The NCS has collected data on all of the major networks within the United States, see Figure 1. These networks include AT&T, MCI, Sprint, the Regional Bell Operating Companies, GTE, and the approximately 1,500 independent telephone companies. The NCS resource database contains a complete inventory of these assets and provides the basis for analyses of the commercial carrier networks' support for government emergency communications. Using these data, the NCS has determined that despite the richness of communications capability, the commercial carrier networks have intrinsic vulnerabilities unacceptable for NS/EP telecommunications. As a consequence, enhancements are required to ensure reliable NS/EP service. To that end, the NCS has built a National Level NS/EP Telecommunications Program (NLP) to enhance this basic infrastructure (reference 2).

THE NCS MAINTAINS AN EXTENSIVE DATA BASE ON THE TELECOMMUNICATIONS ASSETS WITHIN THE UNITED STATES



- INTEREXCHANGE CARRIERS (AT&T, MCI, US SPRINT, AND WILTEL)
- LOCAL EXCHANGE CARRIERS (RBOCS, GTE, AND OVER 1500 INDEPENDENTS)
- FAA/RCL NETWORK
- CELLULAR NETWORK CARRIERS

Figure 1

The NLP programs are designed to explicitly improve network connectivity and service to a damaged and congested network. The NLP through the Commercial Network Survivability (CNS) program includes enhancements to provide short-haul terrestrial connectivity around potentially damaged or isolated areas. Also, long-haul connectivity available in emergency conditions is included as part of the Commercial SATCOM Interconnectivity (CSI) program. Finally, the NLP through the Government Emergency Telecommunications Service (GETS) utilizes the network in nonstandard ways, introducing nonstandard routing and priority call treatment to deliver calls under stress conditions. The access to these services is available nationwide through a dedicated dialing plan and controlled by personal identification number codes.

NCS analyses of the commercial carrier networks have focused on the five distinct threat levels summarized in Figure 2. The examination of earthquake effects on NS/EP telecommunications focuses analyses on the threat from natural disasters.

THREAT FOCUS DURING TELECOMMUNICATIONS STRESS LEVELS

PEACETIME	CRISIS/ MOBILIZATION	LIMITED ATTACK	EXPANDED ATTACK	POST-ATTACK
• Equipment Outages and Service Failures • Natural Disasters • Hackers • Sabotage	• Terrorism • Insurrection • Low-Intensity Conflicts • Theater War • Conventional War	• Terrorists using weapons of mass destruction • Uncoordinated Attack using weapons of mass destruction - Accidental - Unauthorized	• Coordinated Attack using weapons of mass destruction	• Recovery • Reconstitution

Congestion is a problem to be addressed across all stress levels



Figure 2

Figure 3 is a composite picture showing the areas across the U.S. that are most affected by earthquakes, tornadoes, and hurricanes. These are the areas that the NCS intends to focus analyses on in conjunction with the other threats listed in Figure 2.

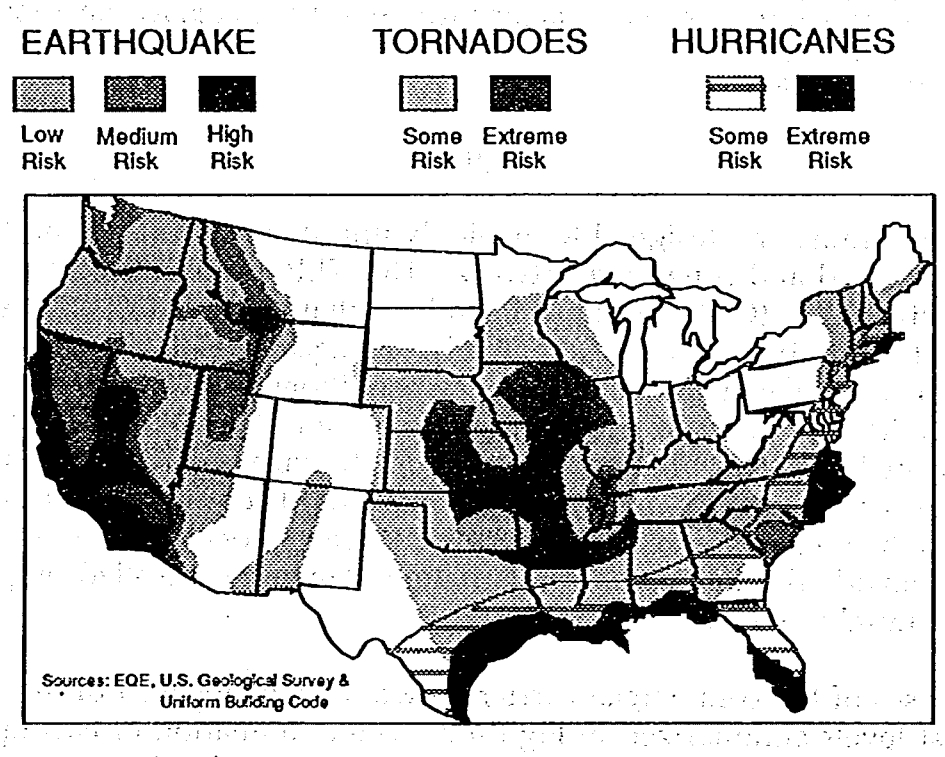


Figure 3

POSTEARTHQUAKE ASSESSMENT METHODOLOGY

In the aftermath of the Loma Prieta earthquake, the first priority for the earthquake analyses has been the San Francisco Bay Area. NCS long term goals are to improve and expand the initial modeling capability to include the effects from other natural disasters, model the performance of telecommunications, and develop mitigation strategies as needed.

In July 1991, the NCS and the National Science Foundation cosponsored a symposium to discuss and develop approaches to modeling earthquake effects and measures for predicting the resultant damage to the telecommunications infrastructure. The recommendations from the symposium are summarized here:

- Develop and acquire an earthquake model
- Validate model predictions against actual events, such as the Loma Prieta earthquake
- Define the user needs for communication during this type of time frame
- Collect data on the effects of earthquakes on telecommunications and industry's response to these types of disasters
- Establish exercise areas or pilot studies in one or more of the vulnerable areas for earthquake mitigation.

The NCS responded to the symposium recommendations and constructed a working model for estimating the structural damage to telecommunication assets due to earthquakes. In this manner, the predicted effects of the earthquake damage could be studied for the NS/EP community in this area using the network and NS/EP data maintained by the NCS.

The structure of the telecommunications damage assessment model is shown in Figure 4. As shown, there are two primary elements within the model, the telecommunications damage model and the PSN communications model. The telecommunications damage model characterizes and predicts damage to telecommunication assets. The damage model is composed of two specific models. The first estimates ground motion and the second assesses nodal fragilities. The PSN communications model assesses the postearthquake performance of NS/EP network services. The PSN communications model consists of algorithms and procedures developed over the past several years to estimate the performance of the PSN. A discussion of the PSN performance algorithms is not within the scope of this paper.

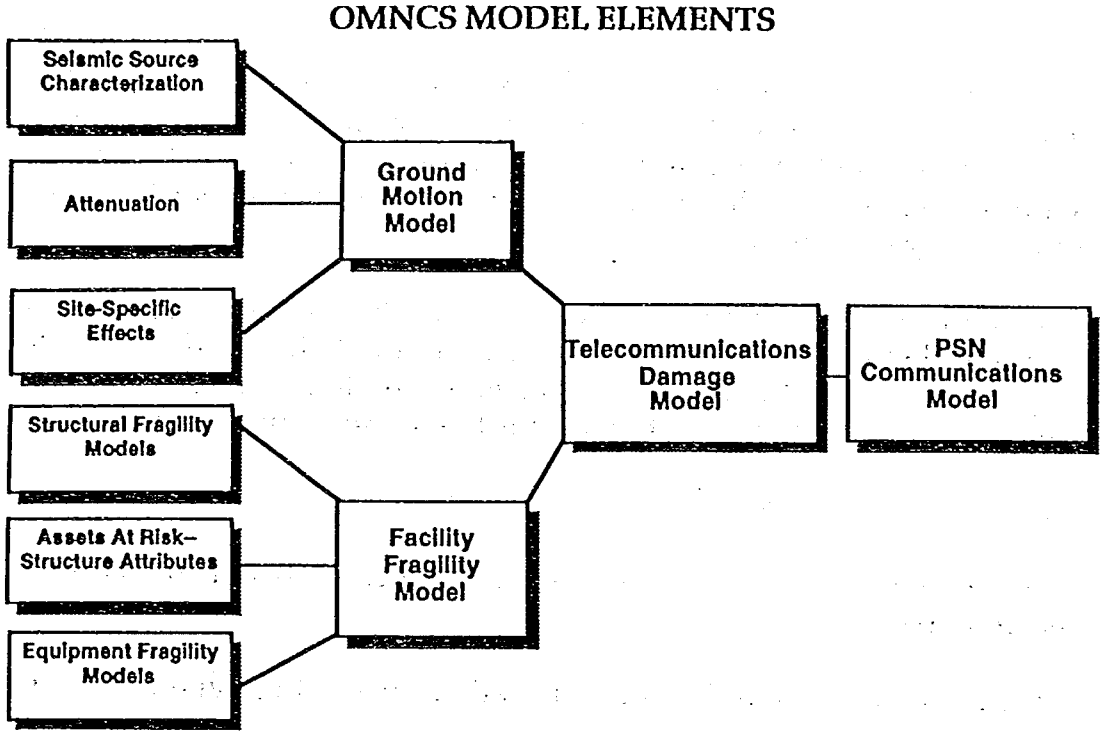


Figure 4

The ground motion model has three attributes: seismic source characterization, attenuation, and site-specific effects. Seismic source characterization calculates values for peak ground acceleration. The attenuation equations modify the calculated peak ground acceleration using the geological characteristics of the Bay area. Finally, site-specific effects associate soils from the area for each NS/EP and telecommunications structure under investigation (reference 1).

The facility fragility model has three principal components. First, structural fragility curves define the response of buildings to specific ground motions. For the NCS model, curves were developed for a number of building types found in and around the Bay area using data and practices developed under other efforts (reference 3). Structural attributes for each building under study are also assigned as part of the fragility model. The attributes include the particular construction of a building and are based on site survey data. The final component of the fragility model addresses equipment fragility. At this time, equipment fragilities have not been incorporated into the NCS model.

POSTEARTHQUAKE PERFORMANCE ASSESSMENT

An analysis using the model was performed for the Hayward fault to illustrate the impact a magnitude 7.5 earthquake may have on telecommunications. There were four key assumptions underlying the analysis:

- The maximum credible earthquake for the Hayward Fault is 7.5.
- The 30 percent damage level was assumed to produce loss of telecommunications functionality for a specific node.
- Interexchange and local exchange carrier network routing is based on data in the OMNCS resource database.
- NS/EP calls are provided priority treatment available through the National Level Program.

Figure 5 shows the area under study. The figure depicts the NS/EP assets and the more than 400 interexchange and local exchange carrier assets of AT&T, MCI, Sprint, GTE, and Pacific Telesis. The assets function as toll switches, multiplexers, and central offices. Links are not shown in the diagram but are included as part of the PSN communications model.

DISTRIBUTION OF ASSETS IN THE BAY AREA

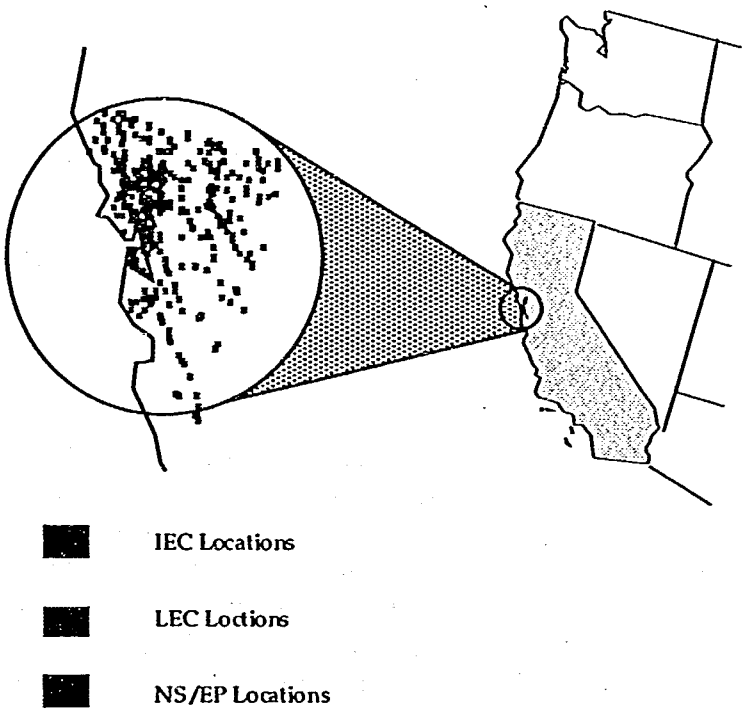


Figure 5

The results of the telecommunications damage model runs are shown in Figure 6. The distribution in the diagram illustrates the effects of peak ground acceleration to a building. The categories are based on definitions of costs to restore a building to

its predamage state. As depicted in the figure, most of the damage occurs in the light and moderate categories. The moderate and above regions equate to the 30 percent damage level assumed for the analysis. Buildings receiving this degree of damage were potentially nonfunctional.

RESULTS OF HAYWARD FAULT ANALYSIS

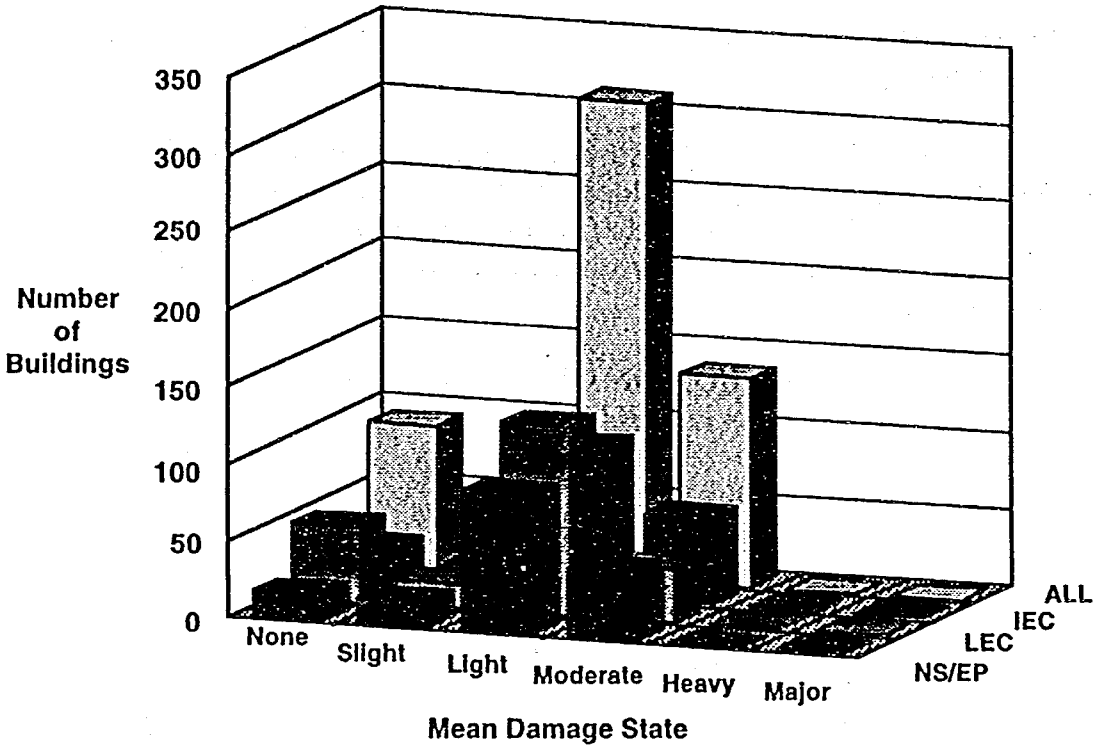


Figure 6

Calculations for performance are shown in Figure 7. As listed in the figure, the pre-event assets include 188 interexchange carrier assets, 223 local exchange carrier switches, and 167 NS/EP sites. The bar graph shows the number of assets with a predicted mean damage greater than or equal to 30 percent. The effect on NS/EP telecommunications caused a reduction in the availability of communications within California. NS/EP Telecommunications availability dropped to 83 percent ± 16 percent. Across the entire United States, NS/EP telecommunications availability ranged between 98 and 92 percent.

From the analysis, the following conclusions can be drawn. First, on a nationwide scale, the event had little or no effect on calls within other regions. The change was do mostly to connections to and from California. Service availability outside the area did not degrade. The network is robust and an outage in one part of the country typically will not affect other regions.

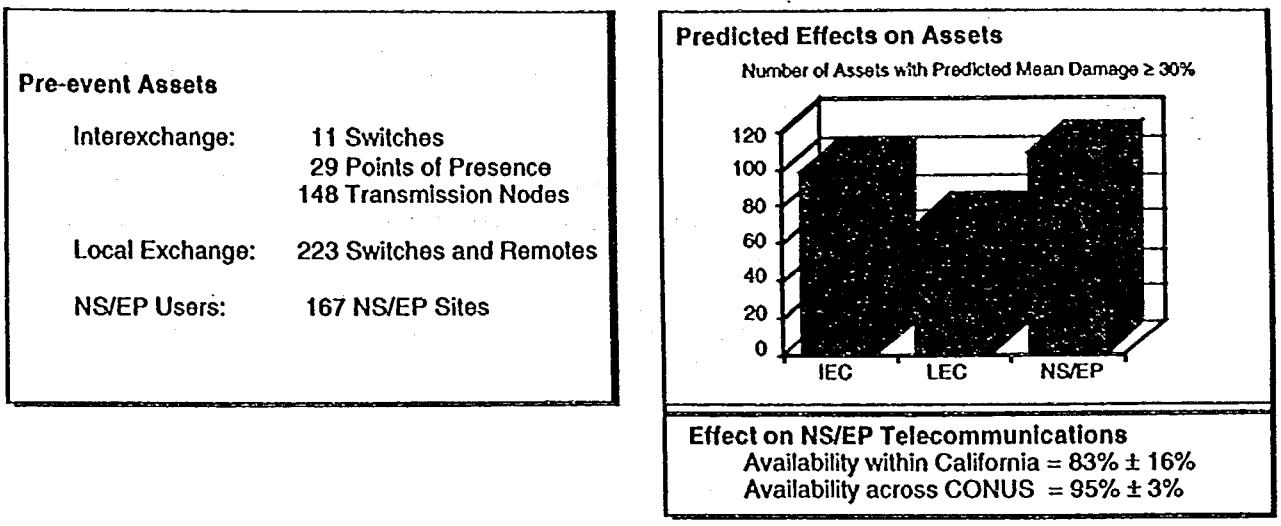


Figure 7

Regionally, network availability showed a wide variance. This variability was due to the effects of losing specific nodes during any given model iteration. The analysis indicates the need to identify the nodes or system designs that cause the greatest disruption and introduce enhancements to assure NS/EP service availability.

In addition, the analysis indicated that a number of areas require further definition or study. First, other analyses have shown that priority treatment is required to maintain high call completion rates following an outage; consequently, congestion effects must be included in future studies. Without priority treatment, NS/EP calls will not be afforded the necessary connections to establish communications. The NCS is developing models to examine the effects of congestion on NS/EP service following earthquakes. Efforts are underway to combine the telecommunications damage model with these PSN models.

The results for building damage and telecommunications are subjective and require additional study. The NCS is refining the assumption regarding telecommunications building damage and network functionality. As part of an ongoing effort to improve the model, the NCS is investigating methods for assessing the loss of telecommunications equipment functionality.

CONCLUSION

Since the development of the initial model, the NCS has undertaken new efforts to meet the goal of modeling natural disasters effects on telecommunications. Areas for future work include an examination of alternative models for predicting ground motion. The NCS and the National Science Foundation have defined work for the

National Center for Earthquake Engineering Research (NCEER) to survey the available models and complete a comparison of models as they would be applied to telecommunications infrastructure analysis.

The NCS continues to work with telecommunications carriers, gathering data on the effects of earthquakes on telecommunications structures. The purpose of this effort is to improve the statistical data used in analyses of ground motion effects on structures. Other plans include examining other regions of the U.S. that are earthquake risk areas such as the Los Angeles area of Southern California, the New Madrid fault area, and the regions in the Pacific northwest, southeast, and northeast United States.

ACKNOWLEDGMENTS

This work has been accomplished under contract to the Office of the Manager, National Communications Systems, DCA100-91-C-0015. Support has been provided by Booz·Allen and Hamilton, EQE Engineering and Design, a division of EQE International, and Dames and Moore. Contributors to the development of the earthquake components of the telecommunications damage model were Dr. Charles Scawthorn, Dr. Masoud Moghtaderi-Zadeh, and Dr. Kenneth Campbell of EQE Engineering and Design.

REFERENCES

1. National Communications System, "Earthquake Damage Assessment Report," August 6, 1992.

2. National Communications System, "National Level National Security Emergency Preparedness Telecommunications Program," May 28, 1992.

3. National Communications System, "Node Fragility Assessment Report," May 11, 1992.

Seismic Considerations of Raised Floor Application for Telecommunication Network Facilities

Alex K. Tang

Manager of Mechanical Engineering
and Regulatory Compliance
Northern Telecom Public Network Division

ABSTRACT

This paper describes the current trend in raised floor application in public network facilities (PNF) in high seismic regions. The raised floor environment for equipment installation is not new, e.g., data processing facilities, although its use in the PNF for switching and transmission equipment is. Existing overhead cable handling systems, commonly called ironworks, are one of the most vulnerable components of PNF to seismic hazards. When outdated equipment are replaced nowadays, it is often more cost effective to replace the ironworks as well with a raised floor system. The raised floor system is ideally suited for state-of-the-art telecommunication equipment as it improves seismic reliability and facilitates maintenance; cables can be routed under the floor and equipment can be rearranged without undue inconvenience. Benefits associated with the raised floor system are presented and discussed in this paper. Different design ideas for mitigating equipment damage in a raised floor environment are discussed and evaluated. Design guidelines and considerations are presented.

INTRODUCTION

Overhead cabling supported by massive ironworks in PNF is highly vulnerable to earthquake hazards. All post-earthquake investigations reported various forms of failure of the ironworks, and most failures are caused by using friction clamps to join sections of cable racks. Overloading of the cable racks beyond the load carrying capacity of the structural members is another major cause of failure Fig. 1 shows a typical failure in a PNF in California. The cable racks that have collapsed are supported temporarily by jiffy poles as indicated by the arrows in the figure. Some older facilities use cast-in cast-iron anchors to secure the ironworks. These anchors are brittle and damage to them is also observed. To date damage to ironworks has not affected service significantly, but there is no guarantee that future failure in a major earthquake may not affect network performance.

As equipment evolve with state-of-the-art switching and transmission technology in public network facilities (PNF), the facility environment also undergoes major changes. The usual scene of overhead cabling supported by massive ironworks is being replaced by panel lighting fixtures. This change is driven by the fact that the new equipment frames are much shorter, thus making overhead support awkward. The raised floor configuration as a means of equipment support is gaining popularity. It consists of a subfloor raised from the concrete slab, and the base of the equipment is level with the sub-floor. Cables can be routed under the sub-floor and a raised floor system provides an environment that can be controlled to yield superior conditions for equipment reliability and performance. Computer rooms have long use raised floors for easy cable handling, but the space under the raised floor is also used as an air plenum for cooling. PNF raised floors are not used as a plenum because a plenum enclosing cables becomes a fire hazard.

The raised floor presents a challenge to seismic protection of equipment. In the past years, several methods have been suggested by researchers and engineers to mitigate seismic damage in a raised floor environment. They are discussed in this paper. Other considerations associated with the use of raised floor in PNF also will be discussed to provide a comprehensive system overview. The factors considered are: (1) fire hazard, (2) cable routing, (3) cooling, (4) lighting, and (5) electronic packaging standards.

THEORETICAL ANALYSIS AND TESTS RESULTS

For seismic qualification of telecommunication equipment installed in North America, a floor response spectrum is available through NEBS (TR-EOP-000063) of Bell Communication Research (Bellcore, Ref. 3). One of the conditions for qualification is the equipment has to be mounted on concrete floor. For equipment mounted on raised floor, NEBS can be used as the starting point for the appropriate specification. Wong and Tso of McMaster University (Ref. 2) developed a straight line approximation of amplification curves for equipment mounted on raised floors based a simplified two degrees of freedom lumped mass model (see Fig. 2). Their work shows that equipment with natural frequency of 5-10 Hz and qualified to 100% NEBS on concrete floor, can be qualified for 50% NEBS on raised floor if the fundamental natural frequency of the raised floor is greater than 9 Hz. As the fundamental frequency of the raised floor increases, i.e., the floor becomes more stiff, the amplification approaches 100% NEBS as expected.

Results from tests performed by Wong and Tso on typical telecommunication equipment frames with simulated mass and several commercially available raised floors agree with the theoretical analysis in the first mode of vibration. For equipment and raised floor system with lower natural frequencies, the response of the system in the second mode of vibration requires further investigation.

Static load tests of commercially available raised floor reveal generally poor connection of the pedestal at the base plate that are anchored to the concrete floor. Adding gusset joints at the base plate as shown in Fig. 3 improves the load carrying capacity of the pedestal and increases its stiffness. The stringers that tie the pedestal tops together also contribute to the structural integrity of the raised floor, and the tiles seated on the stringers form a load carrying member. The load carrying capacity of the raised floor depends on the design of the stringer (a poorly designed cross-section failed prematurely in the test). The connection of the stringer and the pedestal head is also important. Poor connection details result in poor structural integrity. Tests show that clip-on connections perform poorly under load, while screw-on connections are much stronger. A basket-weave pattern is also very effective.

Raised floor systems with screwed on tiles have greater stiffness than systems with floor tiles that are not tied down and are free to be removed. Tiles in the latter configuration pop out quite frequently during vibration

tests, but tiles in the former configuration do not. Dislocated tiles cause some system failures in the vibration test. However, screwed on tiles hinder access to the sub-floor space.

METHODS USED TO PROTECT EQUIPMENT

The design criteria for seismic protection of network equipment are based on NEBS floor response spectra (Ref. 3) in most cases, but the ATC-3-06 specification (Ref. 5) is also used. Both criteria result in almost identical equivalent static forces (Fig. 4) and, hence, similar reinforcement designs for seismic protection. Three factors affect the method of reinforcement: the raised floor construction, the equipment frame structure, and the building facilities.

Most commercially available raised floors are not designed to resist seismic load imposed by equipment during an earthquake. Therefore, additional reinforcements are needed. There are two main approaches to provide the necessary reinforcements: Overhead bracing of the equipment and bracing of the raised floor. Overhead bracing is in general not preferred as this approach interferes with the elements that are an integral part of the raised floor environment as mentioned previously. Consequently, we will not discuss the overhead bracing approach in this paper.

Several methods are used to provide reinforcement at the raised floor level. The most commonly used methods are:

1. Bracing the pedestals to increased stiffness
2. Using a structural platform for the equipment, and
3. Bracing the equipment through the raised floor

Site specific conditions govern that of the above methods should be used. Very often, cost can be the major factor. The author has developed several designs in the past few years using all three methods, and examples in this paper are taken from in-service installations.

Base-isolation is another method for equipment protection, although it is not widely used in the PNF environment. OILES of Japan has designed a base-isolated computer floor system that reduces the vibration from earthquake motion, and this approach is ideal for vibration sensitive equipment. As this approach involves the entire floor, the allowable equipment weight, the equipment mounting methods and the allowable

displacement must be factored in the design. Consequently, base-isolation systems are not as cost-effective as rigid-mounting systems at present. As switching and transmission equipment for PNF become more compact, we expect base-isolated systems to become more popular.

Bracing The Raised Floor Pedestal (Fig. 5)

Figure 5 illustrates the pedestal bracing technique designed for a private network facility. The raised floor here is 900 mm high. Based on test results, effective bracing is confined to three modules with the equipment placed on the middle module. The primary objective of the design is to prevent the equipment from overturning and, hence, the shearing of cables. A bracket is installed to facilitate bracing as this particular raised floor is part of an existing facility for data processing equipment. Figure 6 shows the details of the bracket that is also used for other subsequent facilities. The bracket is clamped on the top and bottom of the pedestal where steel angles are bolted. The brackets provide mounting points for bracing in the transverse and longitudinal directions. They are located as near the top and bottom as possible to reduce moment load on the pedestal. This design increases the stiffness of the original raised floor by about 10 times; lateral load carrying capacity is increased and moment failure at the base plate of the pedestal is eliminated. Besides diagonal bracing, horizontal bracing is used to ensure structural integrity without relying on the stringers. No other modification to the raised floor is required.

The bracing members for this site are 50x50x7 mm steel angles, which are commonly used in PNF. The bracing method provides more space for cable routing. Other similar methods are presented in Ref. 1. The disadvantages of this method are reduced cable access and, for some facilities, the required anchoring may be overly extensive.

Structural Platform (Fig. 7)

Figure 7 shows a mounting system used by the author to protect equipment. A structural platform designed expressly for the equipment is anchored to concrete floor, and the equipment is mounted on the platform. The height of the platform is usually slightly less than that of the raised floor to allow for floor unevenness. The bolted connections allow the platform to be shipped in a smaller container for off-site installation. Welded connections are used for local installation for even better performance.

Structural platforms are easier to install than bracing, and this is especially true if they are installed at the same time as the raised floor. The platform design can be unique to a particular piece of equipment and features can be customized to fit special needs (e.g., cable entry and exit). Tests show that design detailing is critical to achieving the desired stiffness; local deformation reduces the stiffness of a structure that may appear extremely strong. Static load tests have identified the weak links to be the mounting points between the equipment and the platform, and the mounting points between the platform and the concrete floor. From personal experience, it is difficult to pinpoint the local weaknesses without static load tests. In one example, the calculated natural frequency is about 70 Hz but dynamic tests show only a 9 Hz first mode response. Again, good detailing at the connecting points between equipment, platform and concrete slab is essential to achieving design performance.

Bracing Equipment Through the Raised Floor (Fig. 8)

This method is usually used as an alternative to bracing the raised floor, when under floor obstructions rule out bracing the floor pedestals. It is an installation nightmare. The method requires anchoring the equipment through the raised floor to the concrete slab using threaded rods. The threaded rods are reinforced using a unistrut as shown in Fig. 8. The reinforcement helps prevent buckling caused by motion of the equipment during an earthquake. Diagonal bracings directly under the tile at the anchor points are terminated at the upper portion of the threaded rod while the other end is anchored to the concrete floor via a bracket (Fig. 8). This method effectively creates a structural platform using the floor tile as the platform, and allows some flexibility in anchoring the bracing members to the concrete floor. Bracing members can be designed to avoid interference with existing facilities under the floor.

BENEFITS OF RAISED FLOOR

Electronic switching and transmission systems are sensitive to temperature changes. An environment with a constant temperature can prolong the life of the equipment and improve their reliability. The raised floor environment fosters cost-effective temperature control as there are two layers of air insulation: the space above the drop ceiling and the space below the raised floor. Hence, the volume of air is smaller and more confined for effective temperature control.

Two methods are generally used for directing conditioned air to the equipment room: using air ducts from the ceiling, and using the raised floor as an air plenum. In terms of cost and fire/smoke control, air ducts from the ceiling is more effective. The few fires that occurred in PNF in North America in the past decade are caused by fires started from cables. Hence, the mix of cables and air plenum under the raised floor is highly undesirable as smoke will propagate very quickly with that combination. A gas fire suppression system can be used under the floor when air-conditioning is directed from the ceiling, and sprinkler under the raised floor can also be used as water does not damage cables. In the latter case, drainage under the floor should be provided.

Dust and other airborne contaminants can be controlled more easily when the free space is reduced. A cleaner environment is beneficial to densely packed electronics, and fosters reliability as several cases of equipment failure due to airborne contaminants have been reported. Lighting and noise control will also improve with reduced air space.

CONCLUSION

The raised floor systems presented in this paper are rigid-mounting systems. Of these the most viable system is the custom-designed structural platform. As there are no standards on equipment foot-print at present, custom platforms will be necessary until such time when a universal standard is in place and the platform can be standardized.

The structural platform should have a frequency at least five times that of the equipment frame to reduce or eliminate amplification. Engineering details of the mounting points are important; local deformation must be minimized to reduce unwanted amplification.

Future research and development should consider adding base-isolation systems on the raised floor for use with vibration sensitive equipment.

REFERENCES

1. Chang, I-Kwang, Experiments and Field Observations of Seismic Protection on Computer Facilities, US-Japan Workshop on Seismic Behavior of Buried Pipelines and Telecommunication Systems, Dec 4-6, 1984.

2. Wong, C.M. & Tso, W.K., Access Floor Response Spectra for Equipment Line-ups in Telecommunications Central Offices, Third U.S. Conference of Lifeline Earthquake Engineering, Aug 22-23, 1991.

3. Bell Communications Research, "Network Equipment Building System (NEBS) - General Equipment Requirements", Technical Reference TR-EOP-000063, Issue 4, Morristown, New Jersey, July 1991.

4. Tang, A. & Wong L., Seismic Performance of Telecommunications Systems and Earthquake Readiness of Telecommunications Facilities in North America, Pacific Conference on Earthquake Engineering, Auckland, New Zealand, Nov., 1991.

5. Applied Technology Council, Tentative Provisions for the Development of Seismic Regulations for Buildings, ATC-3-06, April, 1984 Second printing.

FIGURES

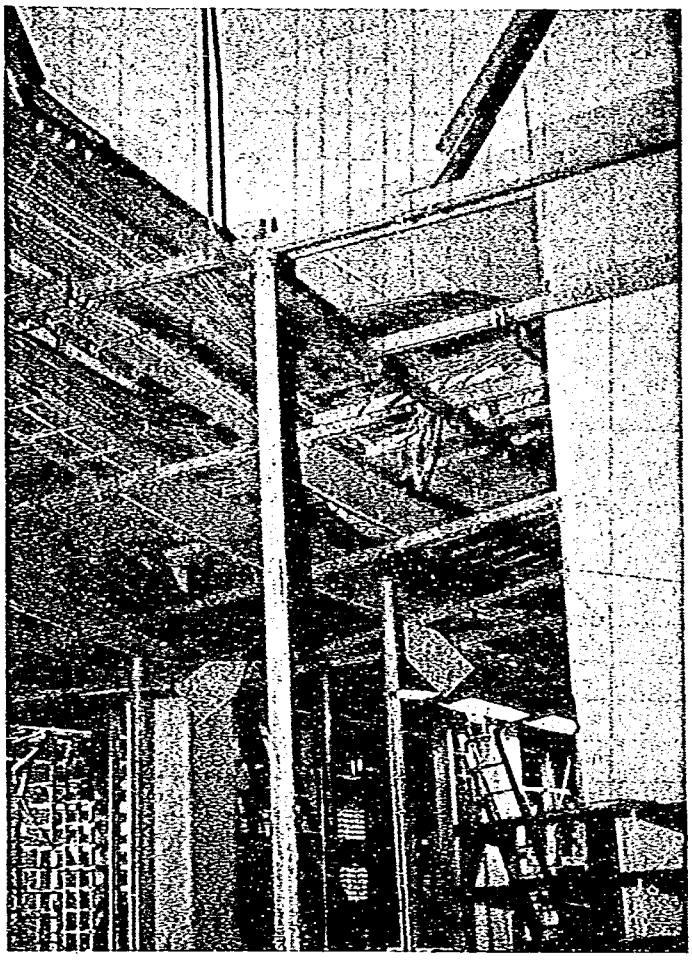


Fig. 1 Failed Ironwork in a Public Network Facility

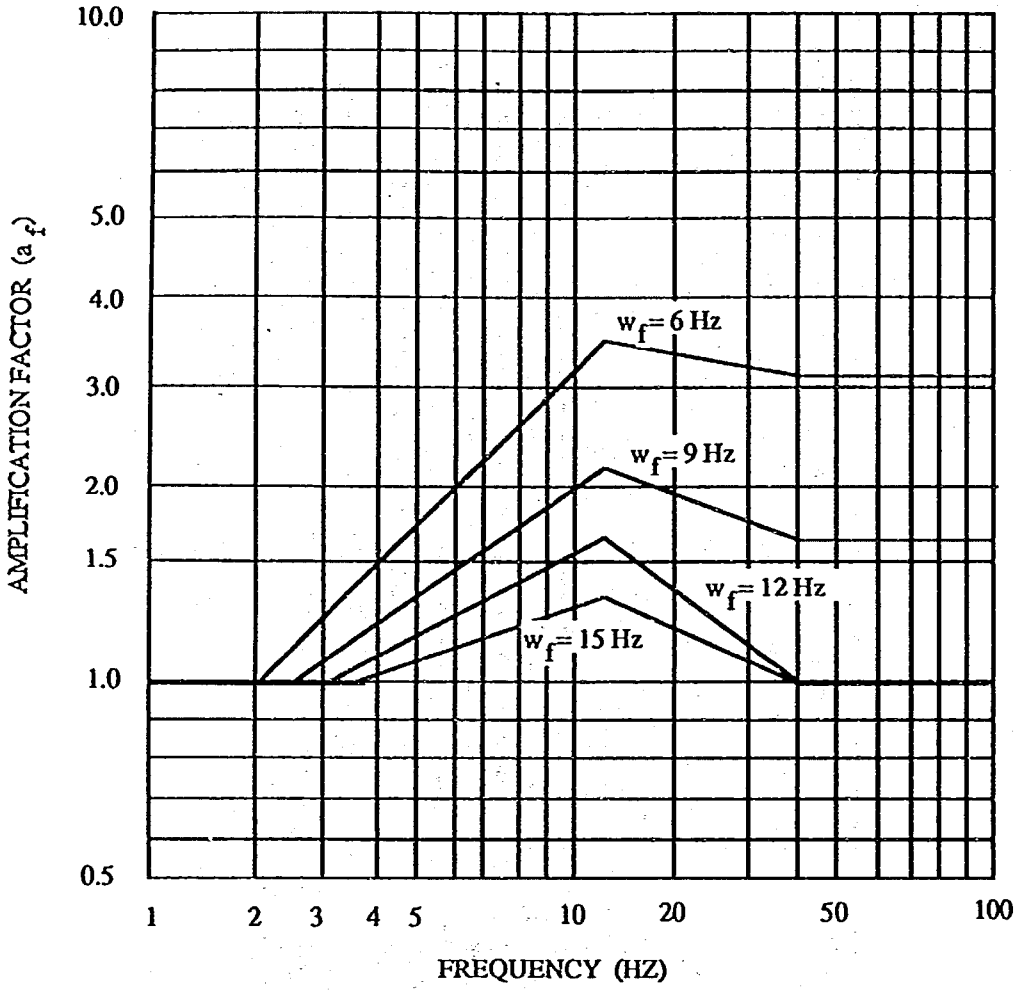


Fig. 2 Straight Line Approximation of Amplification Curves For Different Effective Raised Floor Frequencies
(Extracted from Reference 2)

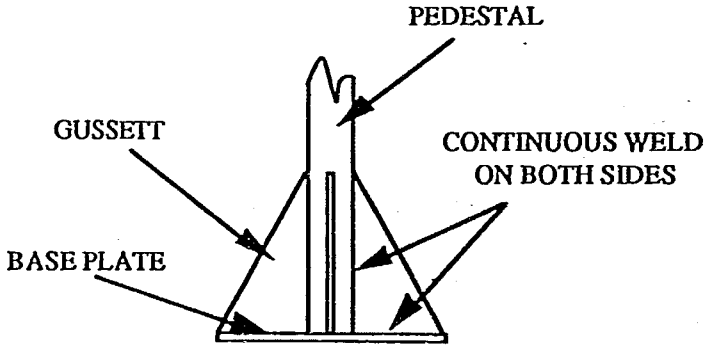


Fig. 3 Improvement to Raised Floor Pedestal

Specification / Force	ATC 3-06	NEBS
Base Shear	4.8W	3.75W
Base Moment	2.4WH	2.5WH

H = height of equipment

W = weight of equipment

Fig. 4 Equivalent Static Force for High Seismic Zones in North America. (Ref 5)

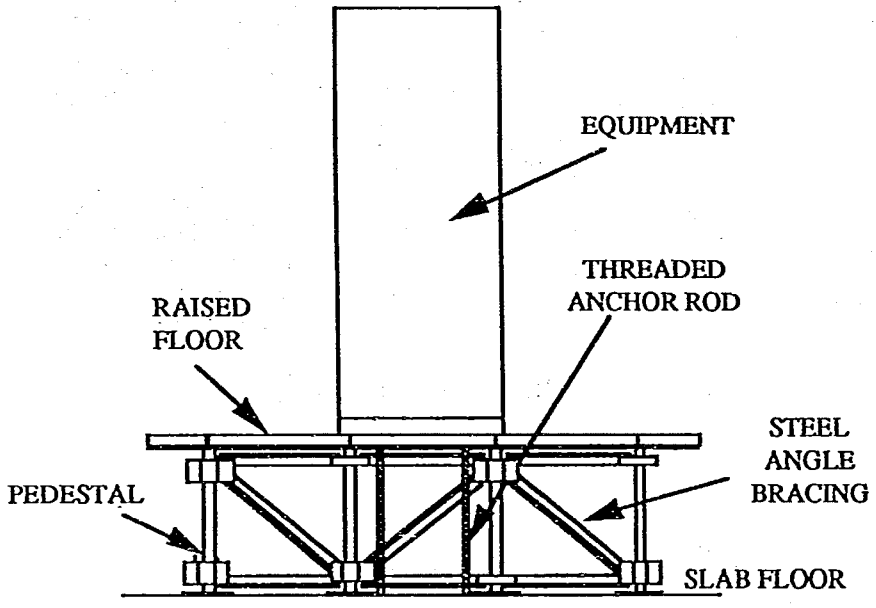


Fig. 5 Braced Raised Floor to Increase Stiffness

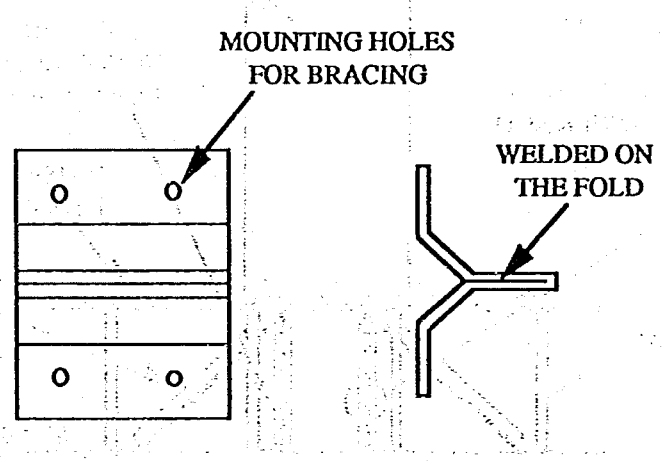


Fig. 6 Bracket for Bracing Raised Floor

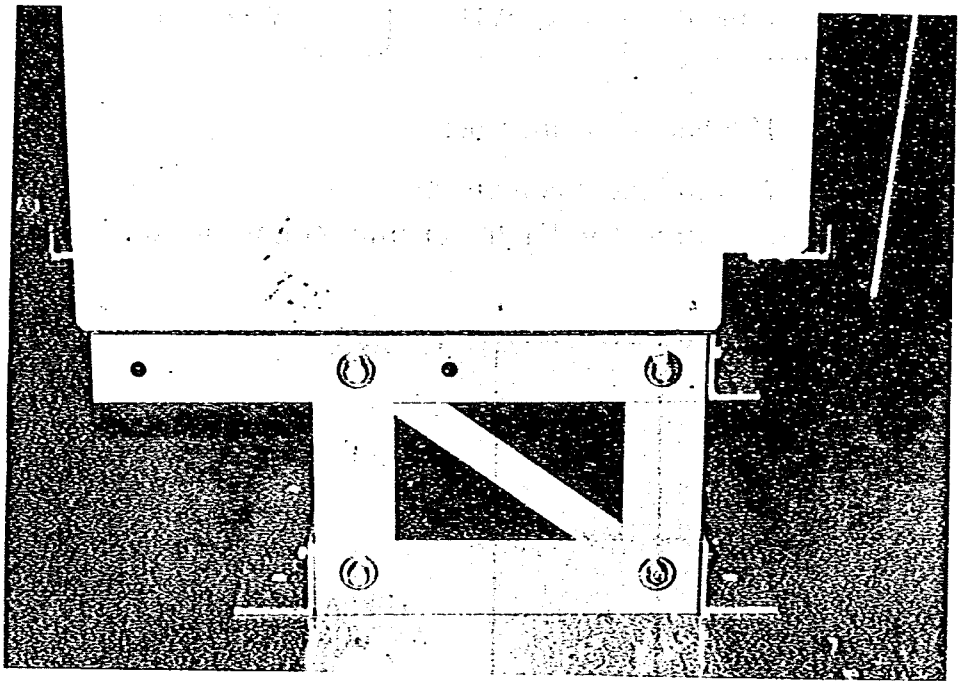


Fig. 7 Structural Platform for Equipment

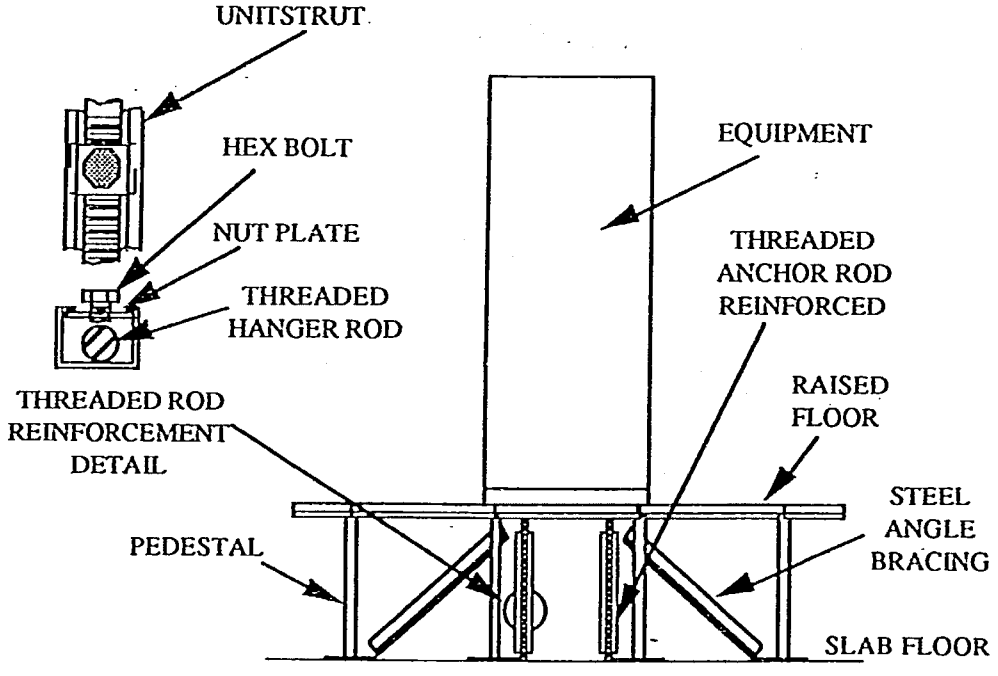


Fig. 8 Bracing Equipment through the Raised Floor

Session-3

Electricity, Water & Gas

J-2) Earthquake Engineering Researches for Electric Power Lifeline Systems
(Tohma, J., Iwatate, T., Yajima, H., Ohtomo, K. and Shumuta, Y.)

J-3) A Method of Evaluating Earthquake Resistance of Buried Pipelines –
Recommended Practice of JGA and a Proposal for Its Improvement
(Nishio, N.)

U-4) Earthquake Hazard Reduction Program for a Water Lifeline Utility
(Bakall, E., Decker, J. and Pyle, R.)

J-4) Seismic Design for Pipeline of Waterworks in Tokyo
(Yokota, I., Sato, S. and Chiba, T.)

Earthquake Engineering Researches for Electric Power Lifeline Systems

J. Tohma, T. Iwatate, H. Yajima,
K. Ohtomo and Y. Shumuta

In order to realize the efficient earthquake preparedness for the electric power delivery system, it is required to establish a facility plan that realistically minimize electric power failure in a region through preventing individual failures of the electric components and establishing relevant post-earthquake restoration method.

Central Research Institute of Electric Power Industry (CRIEPI) has been involved in research and development to provide a firm basis for requirements and practices for electric substation and transmission facilities. A project on the development of a methodology to evaluate the system reliability against earthquake hazards is being proceeded.

Introduction

The power delivery system is almost completed in the measures to be taken against single accidents and faults such as lightning and deterioration, and is least likely to cause large-scale supply failures. However, little evaluation has been made on the power serviceability of an entire system remaining available when power apparatuses are damaged simultaneously at many places as on a seismic occasion. Utility companies need a methodology to estimate the degrees of damage to individual apparatuses, to estimate the transmission capacity based on the results, and to establish the most effective preventive measures and a restoration procedure. These efforts will be able to contribute to a facilities plan with well balanced seismic margin.

The following paper outlines CRIEPI's current research activities related to this field.

Lessons learned from the recent earthquakes[1)2)]

Seismic effects and subsequent restoration process on the electric power facilities due to the 1989 Loma Prieta earthquake occurred in California, U.S.A., are investigated on the basis of the reconnaissance in San Francisco Bay area. From the investigation, although there were no or minor damages to the power stations and the overhead and underground transmission lines in the

Earthquake Engineerig Section
Central Research Institute of Electric Power Industry, Japan

area, a total of eleven (11) circuit breakers whose centers of gravity were designed at the upper part were severely damaged at some substations. This was an essential seismic effect and also a primary cause for the extensive power outages in the area. An estimated 1,400,000 customer services were affected by the power outages immediately after the earthquake, the services were restored within twenty four (24) hours with the aid of load transfer and prompt replacement for the damaged circuit breakers except some communities where the collapse of buildings and houses was concentrated. Consumed time back to normal service was almost the same as one experienced by the 1978 Off-Miyagi earthquake in Japan. Moreover, these power outages were found to have major effects on the daily activities of the transportation, city gas, water supply and sewerage systems and the industrial facilities in the area.

Seismic effects and subsequent restoration process on the electric power facilities due to the 1990 Philippines earthquake, which occurred in Luzon island, Republic of the Philippines, are also investigated in Luzon island. Extensive surface ruptures leading to extremely strong ground motion were triggered, since the earthquake was caused by a major rupture along the existing active fault ; Digdig fault. Thus, three rock filled dams and one earth dam located near epicenter were severely damaged with cracks and sliding on their embankments. The collapse of ceramic insulator parts and the oil leaks of substation equipment were major damages at some switchyards and substations in the heavily shaken area. Moreover, a number of poles were declined as the result of liquefaction in poor soil region such as Dagpan City. Immediately after the earthquake, power outages extended on the northern part of Luzon island. The power outages were restored within forty eight (48) hours in most of the affected area. Consumed time back to normal service for the rest of the affected area was more than one hundred (100) hours, because the replacement of the damaged equipment in some substations was considerably delayed by the interruption of the access roads mainly due to land slides. The loss of the traffic serviceability was found to have an essential effect on the restoration of the power outages in this case.

Earthquake observation and data base system[3)4)5)]

CRIEPI has been conducting earthquake observation for a total of fifty (50) observatories deployed on the rock outcrop and soil deposit as shown in Fig.1. The main purpose of the observation is to evaluate and improve the design earthquake ground motions currently applied to the electric facilities. A series of technical reports has been published on the strong earthquake records of the CRIEPI earthquake observation network. Event data of the earthquakes are listed with earthquake origin, outline of the observatory site condition, the maximum accelerations of all components. Data processing results are :

1) Corrected acceleration time histories
2) Integrated velocity and displacement time histories

3) Fourier and power spectra
4) Response spectra
5) Phase spectra

The digitized data can be delivered according to requests.

In order to perform a seismic risk analysis and a seismic zonation analysis, a data base concerning map of Japan, past earthquakes and active faults with some application programs is developed. Map data of Japan are closely sampled in geographical latitude and longitude for the lines of coasts, lakes and prefecture borders. Total number of sampling is about 43,000. Whole active faults in Japan are sampled and fault parameters are cataloged. Historical damage earthquakes in and around Japan based on Usami's lists, before 1884, and Utsu's lists since 1885 are cataloged. Whole earthquakes parameters in and around Japan since 1926 are cataloged. They are about 68,000 samples observed and analyzed by the Japan Meteorological Agency(JMA) network.

Plan view of earthquakes and/or active faults by districts, period and magnitude is plotted and listed on CRT and kanji-printer. Cross section view of earthquakes(JMA) by districts, period and magnitude is plotted and listed on CRT and kanji-printer. Seismic risk analyses based on some experimental formulas are computed and plotted. Their contents are mainly occurrence time table, distance vs. intensity of earthquake motion relation, return period of expected intensity and others as shown in Fig.2.

Earthquake safety evaluation of substation components[6)]

In order to clarify the seismic stability of the transformers during strong earthquakes and to verify the design values, earthquake observations have been carried out in some substations and seismic response analyses also have been performed by using the actual recorded earthquake motions. From 1979 to 1987, eighty nine (89) events (Maximum Magnitude is 6.6) were recorded. Maximum horizontal acceleration at the ground surface and the base of the transformers were 451 gal, and 381 gal, respectively.

The observed amplification between ground surface and the base from 178 earthquake horizontal acceleration is lower than those of design value, so the design value is understood to be conservative for strong earthquake motions.

The seismic response analyses of soil-structure systems with tank and bussing shown in Fig.3 were performed by using the actual recorded earthquake motions, the numerical results were well agreed with observed ones.

From above mentioned results, it is concluded that seismic design of the transformers is reasonable for strong earthquake motions.

Soil liquefaction / Large ground deformation[7)8)9)]

A probabilistic evaluation on spatial extent of liquefaction is reasonable when vulnerability assessment on underground transmission lines to be constructed in wide alluvial sites is concerned under insufficient soil profiles and data. In this respect, the practical method for constructing fragility curves for spatial extent of liquefaction on the basis of liquefaction potential index PL is developed. Monte Carlo simulation is combined with the simplified prediction method for liquefaction potential currently used among practical engineers for treating the uncertainty involved in SPT N values. Even more, in order to examine the correlation between PL value and the spatial extent of liquefaction, excess pore water pressure in sample soil columns, from which correspondent PL value can be also obtained, is evaluated with the aid of an one dimensional effective stress analysis. The ratio of computed excess pore water pressure to initial effective overburden pressure is then integrated along a soil column to derive the newly determined Q value. The existence of strong positive correlation is observed between PL and Q values. This validates that the fragility curves for liquefaction on the basis of PL value well represent the spatial extent of liquefaction.

Large ground movements triggered by liquefaction of sand layer is the most serious liquefaction hazards. It has well recognized that pile foundations and in-ground lifeline facilities were severely damaged by liquefaction-induced ground movements during the 1964 Niigata Earthquake, the 1971 San Francisco Earthquake and the 1983 Nihonkai-Chubu Earthquake and so on. For understanding such crucial damages in the area where is susceptible to liquefaction in the event of a future earthquake, a series of model shaking table tests was carried out as shown in Fig.4 to characterize the working load which is brought by liquefaction-induced ground movement. For the rigid body structure model, the lateral earth pressure on the model is found to be almost identical to the lateral pressure in liquid mud. This validates that the active earth pressure can be conventionally estimated with the aid of the coefficient of earth pressure equal to 1.0 and saturated unit weight for practical purpose. For the flexible structure model, the effective load necessary to cause critical deflection is uniformly distributed with respect to depth. The efforts to formulate this loading pattern correlating it with the flow velocity or other quantities are currently made.

System reliability evaluation of the transmission network[10)11)12)]

An algorithm to compute power failure was developed by modeling substations and transmission lines as a graphical network and a pilot computer program was prepared. In this analysis, various combinations of the damaged components are efficiently generated, then power failure is determined through the root searching method by bypassing the affected root. The method is

applied to an imaginary transmission network to illustrate the relationship between the power loss and its occurrence probability under a given earthquake condition. The graphical output may be used to identify the vulnerability within the system against earthquakes.

The main components of the developed PRA method consist of the following:

1) network modeling for a connectivity analysis of a power system which consists of generation, substation, and transmission facilities.

2) determination of the disconnected demanding substations and associated power loss in a network given the probability of failure at each node.

3) establishing a relationship between the power loss and its probability of occurrence.

A demonstrative example of a model substation/transmission network is shown in Fig.5. The model is an idealized primary network (over 154kV) for a metropolitan area. The functional failure of the substations was represented by the probability of failure of porcelain components. The probability of failure of underground transmission lines were represented by the number of manhole-pipe connections per unit length where seismic stress/strain exceed the limit state. A connectivity analysis of the network was then performed given the probability of failure for each node. In the analysis, the Monte Carlo simulation method and the shortest path search algorithm were used. Power failure at a demand node is defined as the condition for which the demand node is disconnected from all supply nodes. A number of 1,000 trials were carried out for each scenario earthquake. An amount of electric load loss is calculated at the each trial by summing the load of disconnected nodes at the event of an earthquake. Fig.5(b) exemplifies the relationship between the loss of electric load and excessive probability for the network shown in Fig.5(a). The loss of electric load is expressed in terms of the ratio of loss to the total demand just before the occurrence of power failure. It can be understood that the probability of occurrence gradually decreases according to the increase of amount of associated load loss. The occurrence of power failure over 10% is found to be nearly zero suggesting that the blackout of the total system is least likely to occur in this case. This curve is called the risk curve. Future parametric studies may enable us to observe the effect of seismic countermeasures for individual electric apparatus on the system reliability by generating various risk curves.

The quantitative evaluation of the power system reliability is desired in planning stage to supply the electricity of high quality with lower cost. Especially for the planning of the secondary network, which is done individually in each area, the evaluation of the reliability becomes important to adjust the reliability level of each area. The fundamental logic of analyzing the reliability for the secondary network was developed. The evaluation of minimum loss of load in case of a failure for the secondary network is one of the most difficult procedure which becomes a combination problem. The Branch Exchange Method and the Gradual Max Flow Method were developed by the CRIEPI's electric engineering specialists for this problem. The reliability index of loss of load and its frequency are calculated using probabilistic method for each load bus. The

application to the model system revealed effectiveness of the developed logic. The developed method will be also included in the seismic PRA.

Conclusion and future scope

Current research efforts on the earthquake engineering for electric power lifeline systems were presented. The PRA approach can be used to assess and predict the likelihood of power failure of an electric power supply system under an earthquake condition. This method is useful for the development of mitigations to reduce the impact of earthquakes on customer service and contribute to the efficient earthquake preparedness. Functional behavior of the power system such as power imbalance, abnormal voltage and unstable condition will be also considered to evaluate the system reliability more realistically. On the basis of these studies, CRIEPI will propose guidelines for earthquake hazard mitigation planning in the near future.

Reference CRIEPI reports (in Japanese)

1) Investigation of seismic effect and restoration on electric power facilities due to the 1989 Loma Prieta earthquake. U90027 (1990/7).

2) Investigation on seismic effect and restoration of electric power facilities due to the 1990 Philippines earthquake. U90072 (1991/4).

3) Development on data base concerning earthquakes and active faults with some application programs. U88025 (1988/11).

4) Development of earthquake data management system and data base concerning the earthquake motion records. U91047 (1992/1).

5) Strong motion earthquake records of CRIEPI earthquake observation network. U90058 (1991/2), U91038 (1992/10), U91039 (1992/10).

6) Seismic response characteristics of the ground and transformers in a substation based on earthquake observation. U90516 (1991/4).

7) Development of probabilistic evaluation for liquefaction potential during earthquake. U90055 (1991/3).

8) Development of earthquake resistant design taking lateral flow into consideration. (to be published).

9) Investigation on countermeasure against liquefaction for underground pipe. U91045 (1991/3).

10) Development of seismic reliability analysis method for electric power supply systems. U90061 (1991/3).

11) State-of-the-art report on restoration plan of electric power system against earthquake damage. U91063 (1992/4)

12) Reliability evaluation system for secondary networks. T91032 (1992/5).

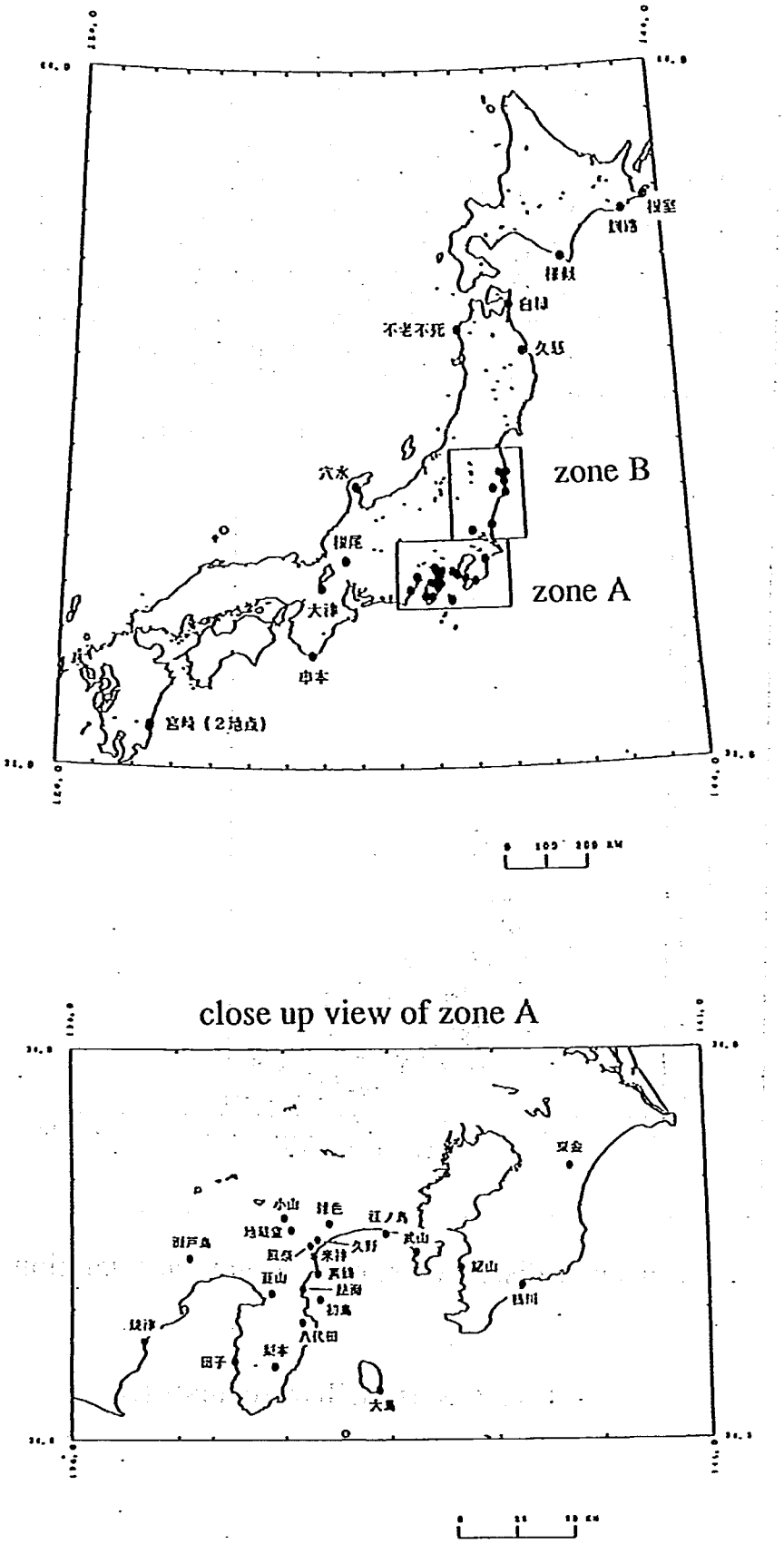
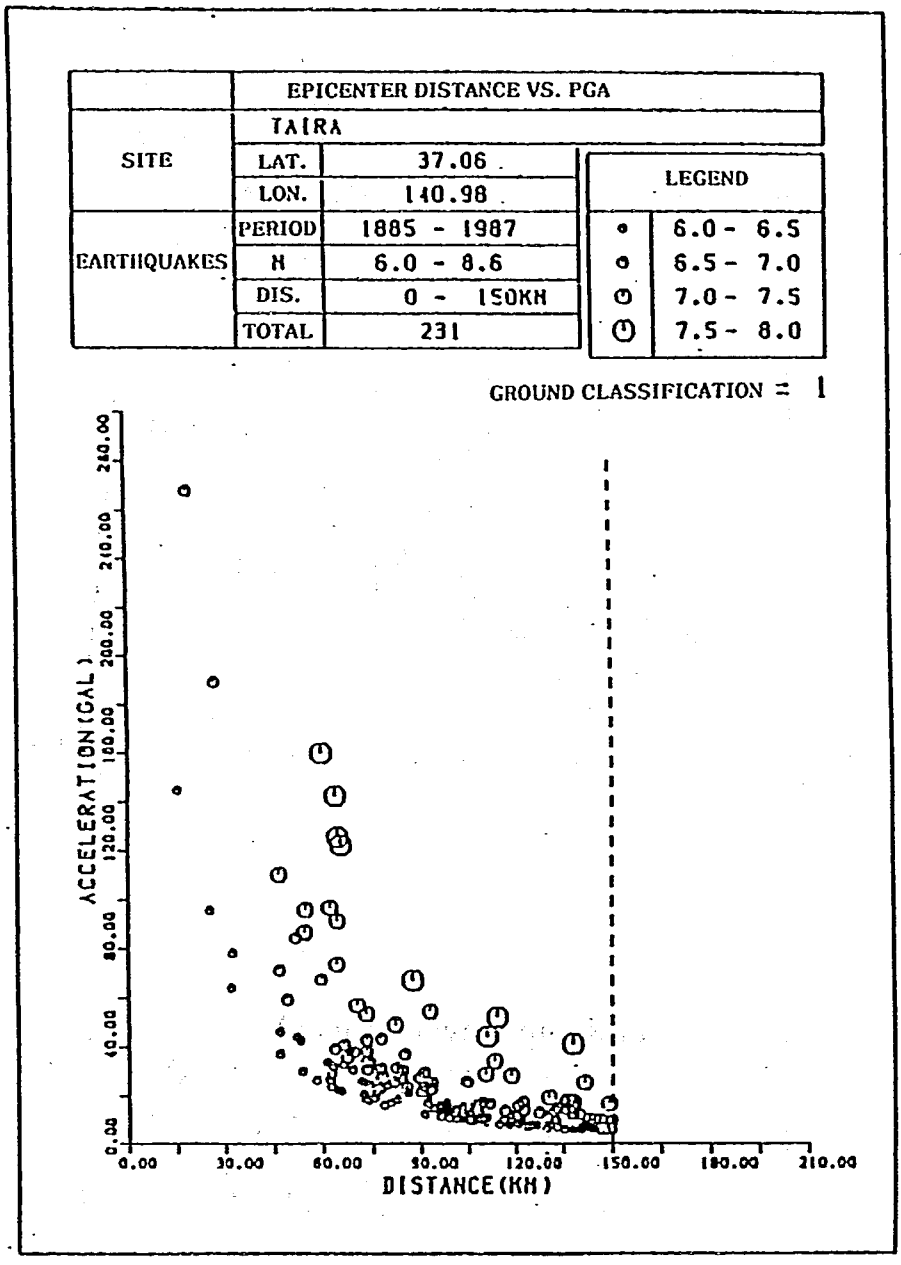
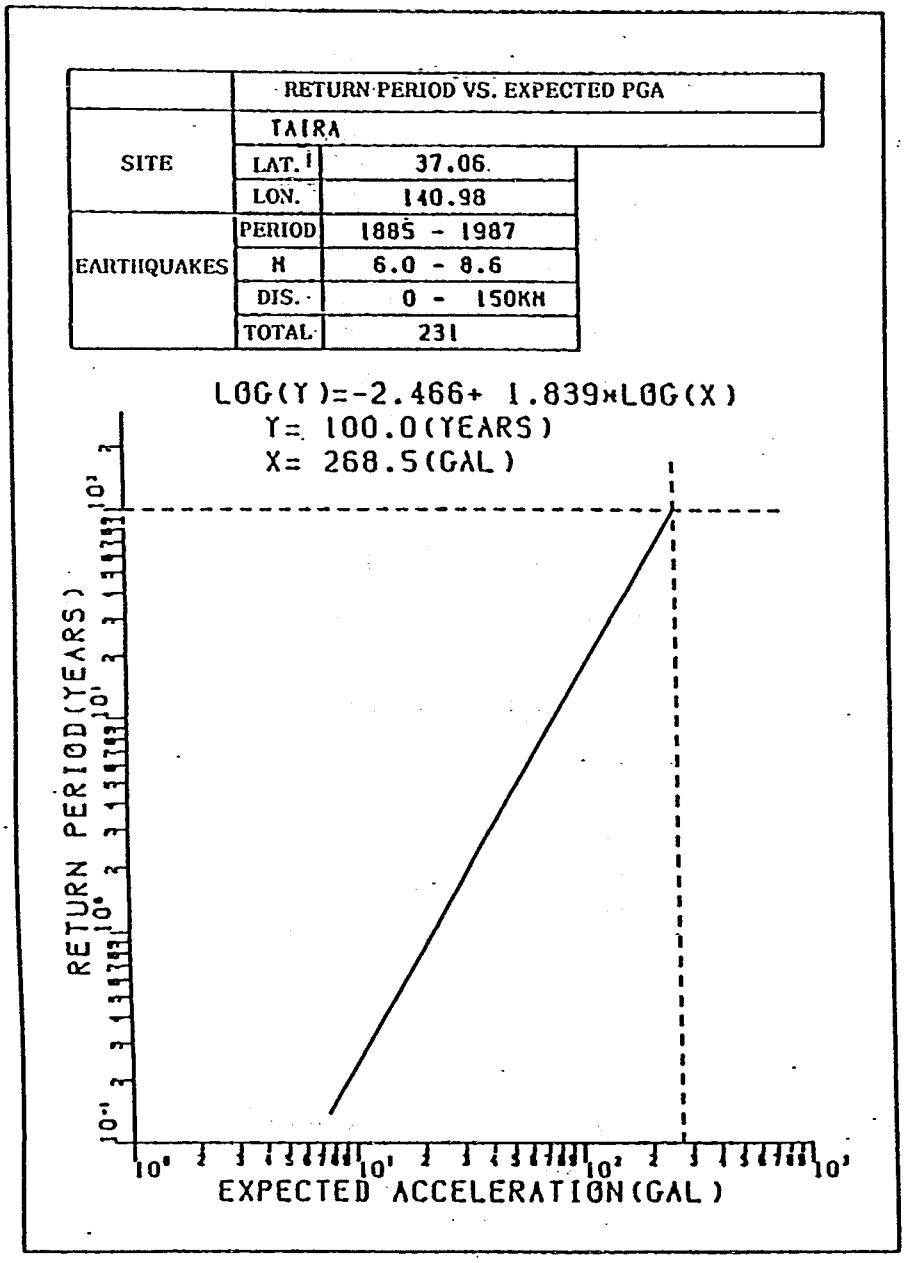


Fig.1 CRIEPI's earthquake observation network



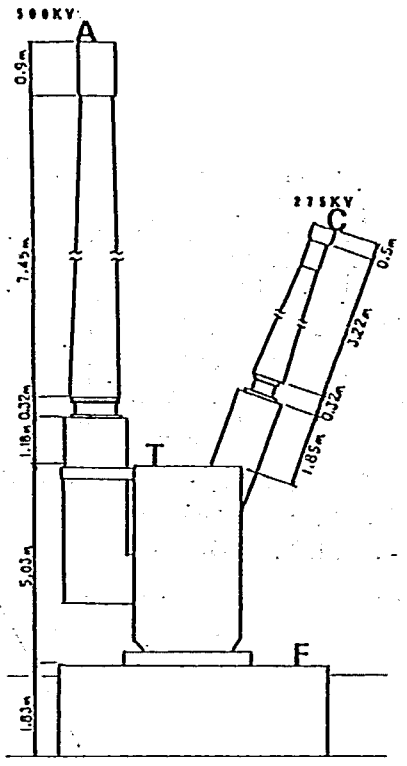
(a) Epicenter distance vs. peak ground acceleration(PGA)

Fig. 2 Seismic hazard analysis

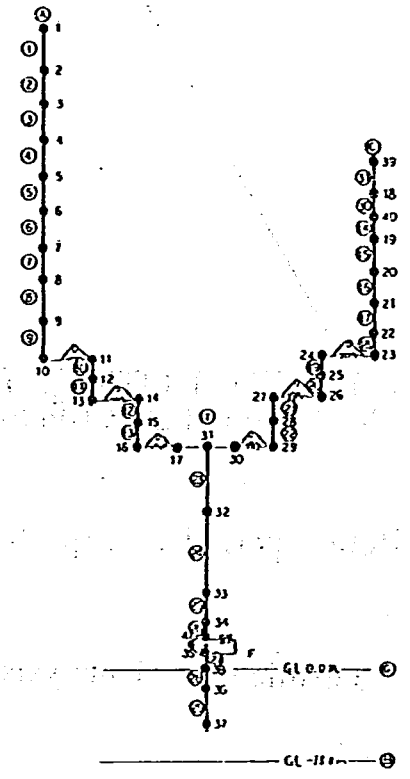


(b) Return period vs. expected PGA

Fig. 2 Seismic hazard analysis (continued)

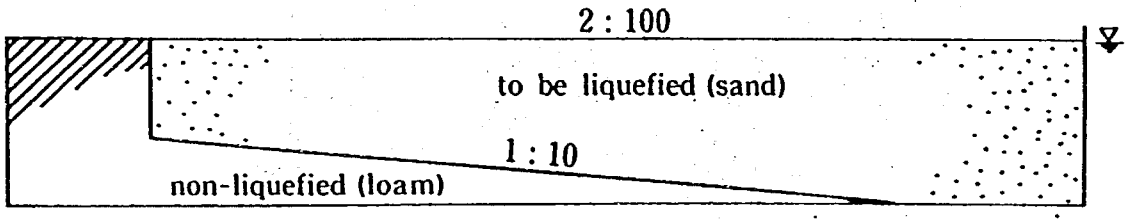


(a) 500kV transformer

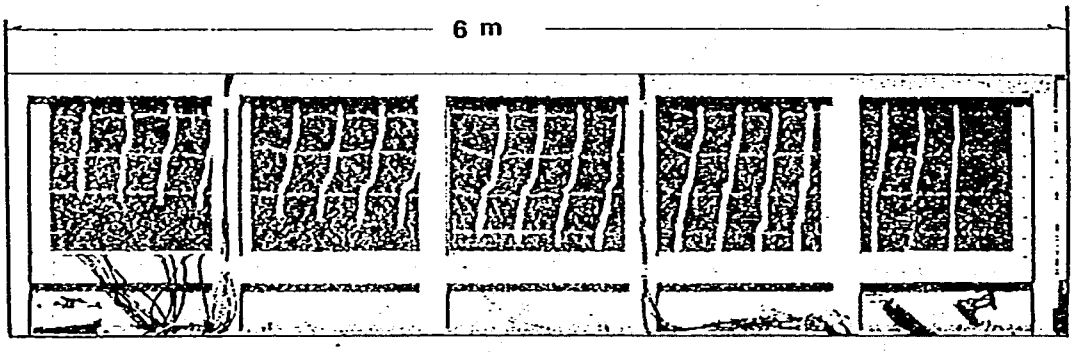


(b) Mathematical model

Fig.3 Earthquake response analysis of a substation component

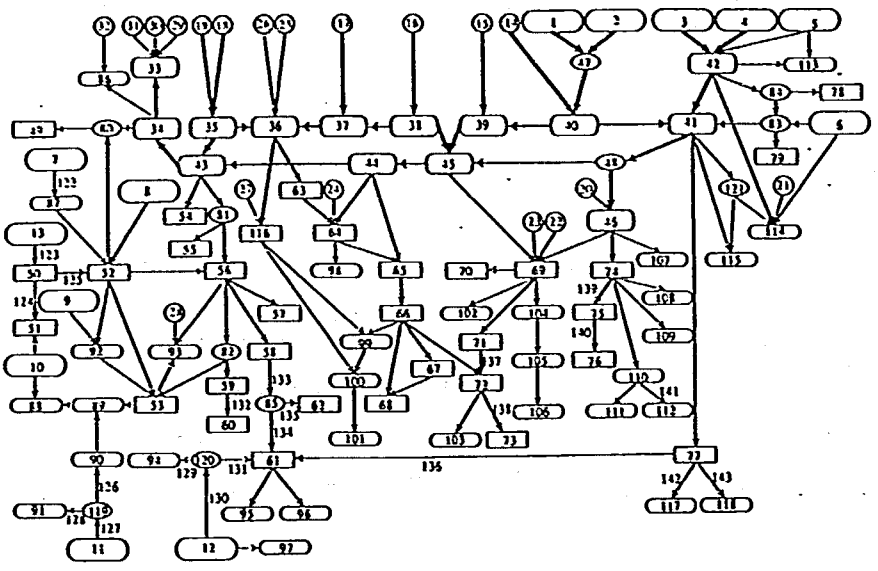


(a) Cross section of the model

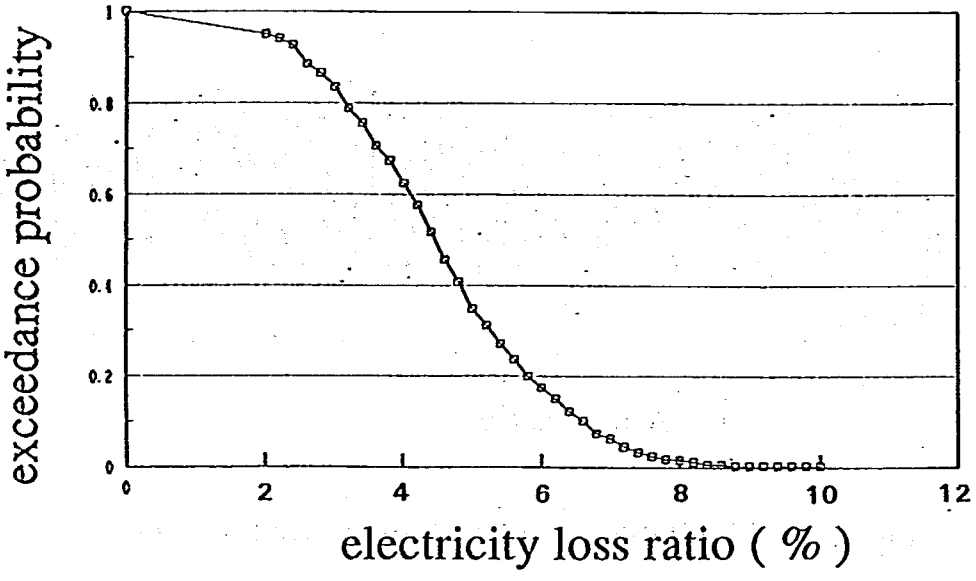


(b) After shaking

Fig.4 Shaking table test of a sloping ground model



(a) A primary power transmission network model



(b) A result of the connectivity analysis
by the Monte Carlo simulation

Fig.5 Seismic probabilistic reliability analysis
of the power flow network

A METHOD OF EVALUATING EARTHQUAKE RESISTANCE OF BURIED PIPELINES — RECOMMENDED PRACTICE OF JGA AND A PROPOSAL FOR ITS IMPROVEMENT

Nobuaki NISHIO
Fundamental Technology Research Laboratory
Tokyo Gas Company, Ltd.

SUMMARY

The Recommended Practice for Earthquake-Resistant Design of Medium- and Low-Pressure Gas Pipelines was drafted by the Japan Gas Association (JGA), in 1982, to give practical as well as effective means of earthquake-resistant design of gas distribution pipelines, on the basis of the knowledge and information obtained from damage to gas pipelines during the 1978 Miyagiken-oki Earthquake. This paper briefly describes the models and methods adopted in the Design Practice. Then, a proposal is made to improve the effectiveness of the Design Practice by introducing the new method of damage ratio prediction recently proposed by the present author. Several examples of earthquake-resistance evaluation are also presented.

INTRODUCTION

The 1978 Miyagiken-oki Earthquake caused heavy damage to low-pressure gas distribution pipelines in Sendai City and the surrounding areas. The damage to main pipelines was sustained mostly by thread-jointed steel pipelines (average nominal diameter was about 50 mm). Damage to mechanically-jointed cast-iron pipelines was much less significant than that to thread-jointed steel pipelines (average nominal diameter of cast-iron pipelines was about 150 mm). Arc-welded steel pipelines for medium-pressure transmission pipelines sustained no damage except for small leakages from flanges at an expansion joint and a valve. Service pipes connecting mains and customers also sustained serious damage; thread-jointed steel pipes (average nominal diameter was about 25 mm) were used for most of the service pipes.

Although a few major gas companies were already using newly-developed mechanical-joints for steel pipelines, thread-joints were almost the sole means of connecting steel pipelines in most gas companies in Japan, at that time.

In order to improve earthquake resistance of gas pipelines thus mitigating the probable damage during big earthquakes in the future, the Japan Gas Association (JGA) organized the Research Committee on Seismic Resistance of Gas Facilities, in 1979, under the auspices of the Ministry of International Trade and Industry, to study effective as well as practical method of evaluating the earthquake resistance of gas facilities. The Research Committee drafted three Recommened Design Practices in 1982. They are Design Practices for: (1) Water Sealed Gas Holders, (2) High Pressure Gas Pipelines, and (3) Medium- and Low-Pressure Gas Pipelines.

The method of evaluating seismic strain adopted in the Design Practice for high-pressure gas pipelines (Ref. 1) is basically similar to that adopted in the preceding technical standard for petroleum pipelines (Ref. 2) in that the method assumes a horizontally travelling wave as the cause of seismic strain in the ground and subsequent damage to the pipelines.

In contrast, the Design Practice for medium- and low-pressure gas pipelines (Ref. 3) is directly based on the knowledge and information obtained from the field investigation of seismic damage to buried pipelines, and the experiments on the "deformability" of pipelines and pipeline-ground interactions.

A simple method of evaluating the deformability of pipeline systems is used to make the Design

Practice effective and practical, and for the purpose of improving the earthquake resistance of miscellaneous types of pipelines which use miscellaneous kinds of joints and fittings.

This paper briefly describes the basic ideas of earthquake-resistance evaluation adopted in the Recommended Practice for Earthquake-Resistant Design of Medium- and Low-Pressure Gas Pipelines. Then, some improvements on the model and the method, used in the Design Practice, are proposed to further increase the effectiveness and the reliability of the Design Practice, on the basis of the new method of damage ratio prediction recently proposed by the present author (Refs. 4, 5).

OUTLINE OF THE RECOMMENDED PRACTICE FOR EARTHQUAKE-RESISTANT DESIGN OF MEDIUM- AND LOW-PRESSURE PIPELINES OF JGA

This Design Practice of JGA is aimed at giving sufficient deformability to pipelines to absorb the seismic displacements in the ground. As a result, the possible number of pipeline damage during a big earthquake is expected to decrease to a permissible degree.

The procedure of evaluation of earthquake resistance of a pipeline system can be roughly described as follows:

1. Design Ground Displacements

Required degree of deformability of a pipeline system should be greater than the Design Ground Displacements (we will call this degree of deformability the Deformability Index, hereinafter). The Design Ground Displacements are specified in accordance with: (1) the relative intensity of seismic activity of the area where the pipeline is laid, (2) the ground conditions of the site, and (3) the importance of the pipeline system. The values of the Design Ground Displacements are given by the following equations.

Horizontal displacements: $U = \alpha_1 \alpha_2 U_0$ (1)

Vertical displacements: $V = U/2$

where α_1 is seismic zone factor, α_2 is the factor determined in accordance with the combination of ground conditions and kind of pipeline, and U_0 is basic design ground displacement. Actually, the value of U_0=5 cm is designated.

The seismic zone factor α_1 represents the relative intensity of seismic activity in the area in consideration. The specified values of α_1 is as shown in Table 1, and the zoning of the land of Japan by the values of α_1 is as shown in Fig. 1.

The effect of ground conditions is expressed, in combination with the importance of the pipeline system, by the factor α_2 as shown in Table 2. The ground conditions are classified into three categories as shown in Table 3.

Category I in Table 3 represents stiff and stable ground, and is expected to sustain the least amount of damage to pipelines among three categories of grounds.

Category II represents uniformly layered soft as well as thick surface layer. This type of ground generally shows large response to incident earthquake, therefore, damage to pipelines is heavier than in the ground of Category I. However, the heaviest damage is considered to be sustained by the ground classified into Category III which represents soft and nonuniform ground.

The above idea of categorizing the ground conditions reflect the actual tendency of damage distribution observed during the 1978 Miyagiken-oki Earthquake (Refs. 6, 7). In addition, the important effect of nonuniformity in ground conditions on seismic strains in the ground (and in the pipelines also) has been verified through earthquake observations (Refs. 8, 9, 10), model experiments (Refs. 8, 11), and analyses of damage statistics (Refs. 12, 13).

In this Design Practice, the design ground displacement is defined as the relative displacement

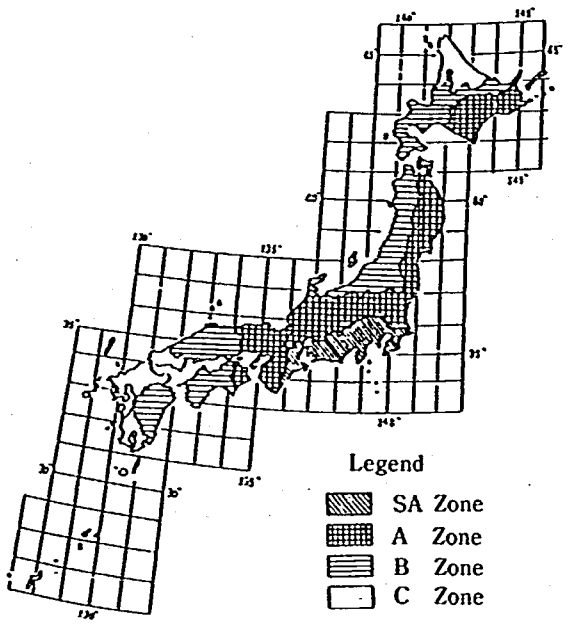


Fig. 1 The Zone Division of Japan by the Seismic Zone Factor

Table 1 Seismic Zone Factor (α_1)

Classification of Zones	SA	A	B	C
α_1	1.0	0.8	0.6	0.4

Table 2 Factor with Respect to the Combination of Ground Conditions and Importance of Pipeline System (α_2)

Classification of Pipeline based on Importance	Ground Conditions		
	I	II	III
Medium pressure A ($3 \leqq P < 10$ bar)	0.9	1.3	1.8
Medium pressure B ($1 \leqq P < 3$ bar)	0.7	1.0	1.4
Low pressure (main) ($P < 1$ bar)	0.5	0.7	1.0
Low pressure (service) ($P < 1$ bar)	0.7	1.0	1.0

Table 3 Classification of Ground Conditions

Category		Remarks
I		Stiff and stable ground Ground consisting of any one of, or the mixture of, the following three layers (1) Layer formed before Tertiary era (commonly called "rock") (2) Diluvium layer (3) Alluvium layer less than 10 m in thickness, or other soft soil layer less than 5 m in thickness
II		Horizontally-uniform soft ground Surface layer mainly consisting of alluvium more than 10 m in thickness, or soft soil layer more than 5 m in thickness
III	IIIa	Horizontally-nonuniform ground Area in which grounds I and II appear alternately, or mixed together
	IIIb	Discontinuous ground Locations where discontinuous displacement is anticipated with a high possibility; such as Category II ground adjacent to a rigid structure

between two ground blocks across which a pipeline is laid. This model of ground blocks is used to determine the Deformability Index of pipeline systems as will be described later.

The value of 5 cm for the basic design ground displacement U_0 is based on the facts that: (1) thread-jointed steel mains which has a Deformability Index of less than 3 cm sustained heavy damage during the 1978 Miyagiken-oki Earthquake, in the areas mainly consisting of very nonuniform grounds; (2) service pipes using thread-jointed steel pipes, the Deformability Index of which is also evaluated to be less than 3 cm, also sustained heavy damage; (3) while damage to mechanically-jointed cast-iron pipelines, the Deformability Index of which can be estimated at about 4–5 cm, was much less significant. Therefore, the basic design ground displacement of 5 cm was specified for the low pressure distribution mains in the ground classified as Category III, and it was decided that this value is varied in accordance with the kind (or importance) of pipeline and the ground conditions.

The vertical ground displacement V was simply decided to be one half of the horizontal ground displacement U. In fact, however, the occurrence of damage due to vertical ground displacement is limited to the locations where pipelines in subsiding grounds are connected to some rigid structures. The condition for such pipelines corresponds to Category IIIb of ground-conditions classification.

For the above reason, the discussions in this paper will mostly be concentrated to the horizontal ground displacements and subsequent axial deformations in the pipelines. Discussions will also be concentrated to main pipelines, the configuration of which is mostly straight.

2. Input ground displacement models

Four types of models of ground displacement is used to evaluate the deformability of pipeline systems (Fig. 2). Among them, the models in Figs. 2b and 2d are for the special (or rare) cases of pipelines fixed to rigid structures. Therefore, we will mainly pay attention to the model shown in Fig. 2a (the model in Fig. 2c is also less significant as suggested previously).

In this model, the strain in the ground is assumed to be concentrated to the boundry between two ground blocks. The axial soil restriction acting on the pipeline is assumed as a kind of frictional force which has a constant value over the length of pipeline in consideration. This makes it very simple to calculate the Deformability Index; and the calculated result will be somewhat conservative.

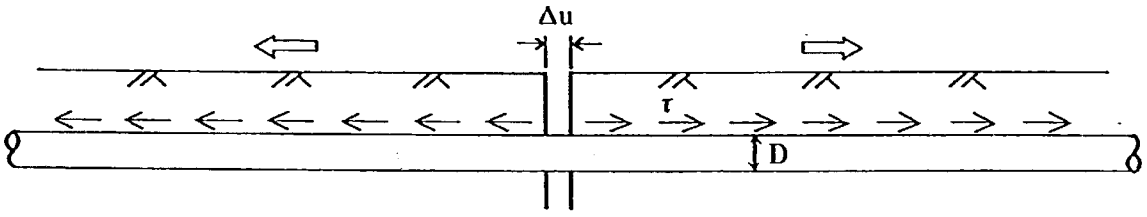
Actually, the stress-strain relationship with respect to shearing deformation of soils is approximately expressed by an elastic-perfectly plastic relationship; the elastic limit in terms of relative displacement between pipe-surface and the soil is estimated to be on the order of one tenth of a centimeter for common soils for backfill. Therefore, we can regard the soil as a perfectly plastic body when we take into account a great magnitude of ground displacement—as great as 5 cm for U_0.

As for the lateral soil restriction, elastic soil springs is assumed to resist the lateral displacement in the pipeline, because the relative displacements between pipeline and soil generally are small. However, the relative displacement, near the boundary between two ground blocks, becomes so great that slippage occurs between the pipe and the soil. As a result, calculation based on usual stiffness of the soil tends to give extremely conservative value of Deformability Index. Therefore, the value of coefficient of soil restriction is decreased to one third of that determined on the basis of the conventional subgrade reaction of the soil.

3. Calculation of Deformability Index δ

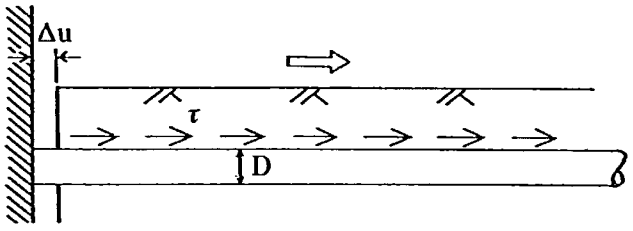
Although the symbol of Δu is used, in the Design Practice of JGA, for the Deformability Index for horizontal ground displacement, the symbol δ will be used in this paper, instead of Δu. Typical examples of calculating the Deformability Index in the horizontal direction are illustrated as follows.

In the case of a continuous pipeline (such as arc-welded steel pipelines and heat-fused polyethylene pipelines), the axial stress in the pipeline takes a linear distribution as illustrated in Fig.3. The strain distribution can be obtained from this stress distribution, by referring to the stress-strain relationship of the pipe material. Then the Deformability Index is obtained by integrating the strain between x=0 and x=L (where the stress takes the value of zero) for the given value of force F_0, or stress σ_0, at x=0 (or boundary between two blocks), and multiplying the obtained value by two, considering the elongation of the pipeline in the adjoining ground block. The allowable strains, ε_0, are prescribed by the Design Practice, and they are given values in the plastic range. This is because the period of recurrence of a disastrous earthquake, that can give such an extremely large ground

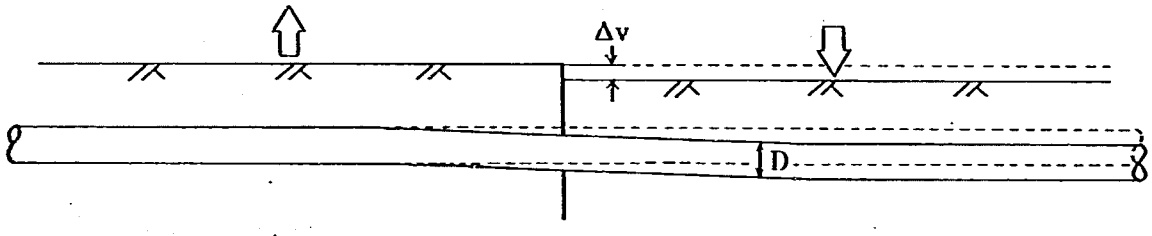


Δu : Allowable ground displacement = Deformability Index (Horizontal)
τ : Soil Restriction

a. Horizontal Relative Displacement between two Ground Blocks

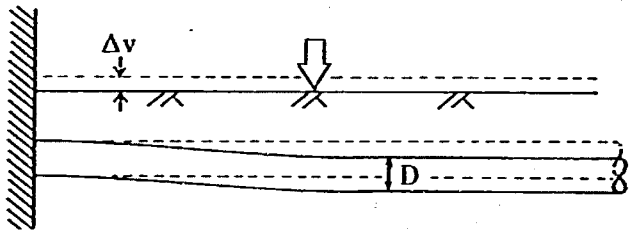


b. Horizontal Displacement in a Ground Block Adjacent to a Rigid Structure



Δv : Allowable ground displacement = Deformability Index (Vertical)

c. Vertical Relative Displacement between two Ground Blocks



d. Vertical Displacement in a Ground Block Adjacent to a Rigid Structure

Fig. 2 Ground-Displacement Models for Deformabilitty Evaluation for Buried Pipelines

displacements as 5 cm or more, is comparable to the lifetime of the pipelines.

The reduced elastic modulus, $\bar{E}$, is used together with the allowable strain ε_0 taking into account nonlinearity of stress-strain relationship beyond elastic limit.

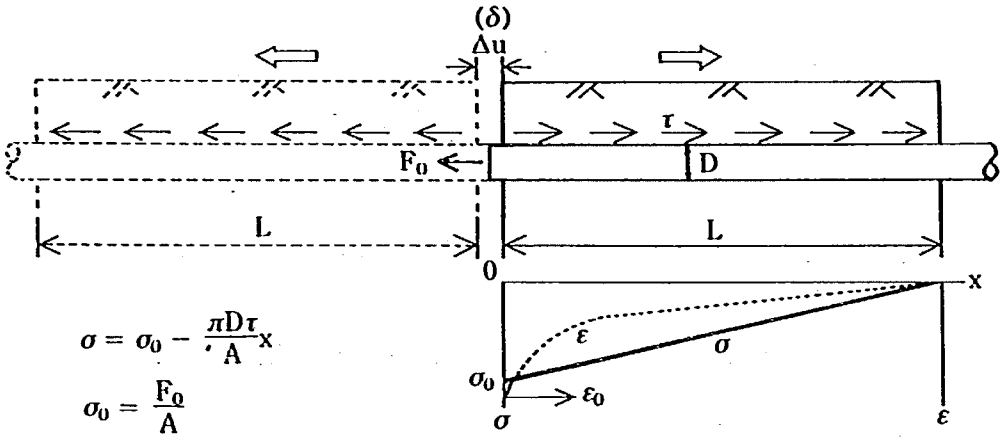
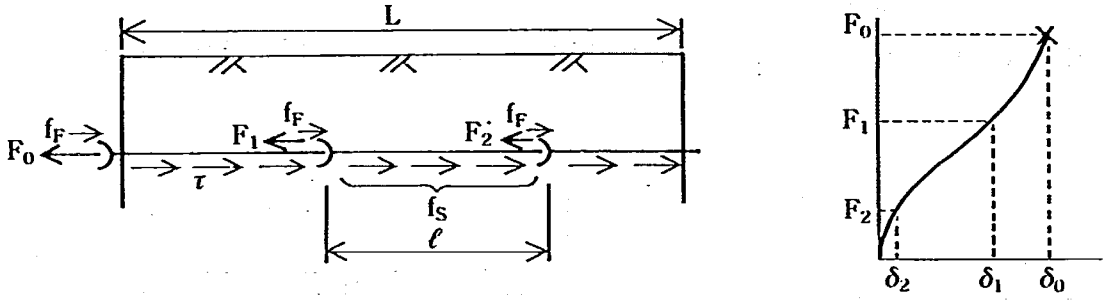


Fig. 3 Schematic Illustration of Equilibrium of Forces Acting on a Continuous Pipeline



a. Forces Acting on a Jointed Pipeline

b. Schematic Load-Displacement Diagram of Jointed Pipeline

$$F_1 = F_0 - (f_S + f_F) \approx F_0 - f'_F = F_0 - \pi D \tau' \ell$$
$$F_2 = F_0 - 2(f_S + f_F) \approx F_0 - 2f'_F = F_0 - 2\pi D \tau' \ell$$
$$F_3 = F_0 - 3(f_S + f_F) \approx F_0 - 3f_F' = F_0 - 3\pi D \tau' \ell$$
$$\vdots \quad \vdots \quad \vdots \quad \vdots \quad \vdots$$
$$F_n = F_0 - n(f_S + f_F) \approx F_0 - nf'_F = F_0 - n\pi D \tau' \ell$$
$$n \leqq F_0 / (f_S + f_F)$$
$$\delta = \delta_0 + 2(\delta_1 + \delta_2 + \cdots + \delta_n)$$

Fig. 4 Schematic Expression of Forces Acting on a Jointed Pipeline such as Cast-Iron Pipelines

The Deformability Indices of segmented pipelines which use joints and fittings is determined on the basis of the force-displacement characteristics combined with the equilibrium of forces with respect to the total pipeline system. In this case, the elongation of the pipe body is neglected because the pipe body is always far stronger than the joint (therefore, the strain produced in the pipe body is very small).

Fig. 4 shows an example of the equilibrium of forces for a segmented pipeline system. The symbol f_F in Fig. 4 denotes soil restriction against the joint due to the increased diameter of fitting or flange of the joint. The symbol f_S denotes the restrictive force due to the soil friction τ on one segment

of pipe. Recommended values for f_F and τ, which are based on experiments using actual pipes and soils, are provided in the Design Practice.

A method to simplify the calculation by representing the effect of two forces, f_F and f_S by an equivalent frictional force f'_S, based on the equivalent shear stress τ' is also provided in the Design Practice.

When the force acting on the joint at the center (boundary between two ground blocks) is reached the allowable value of the joint, the force, F_1, acting on the next joints, the force, F_2, acting on the joints next to the second joints, and similarly, the forces F_3, F_4, $\cdots$are determined by subtracting the forces f_F and f_S from the forces acting on the preceding joints. Then, the corresponding displacements in the joints, δ_0, δ_1, $\delta_2\cdots$, are determined referring to the force-displacement diagram, and the Deformability Index, δ, of the total pipeline system is obtained by summing up those displacements in the joints, as shown in Fig. 4.

For the pipelines constructed three-dimentionally by using bends and tees, which are mostly for service pipes, the Design Practice provides experimental data and results of FEM calculations for miscellaneous elements of 3-D pipelines.

It should be noted that the Deformability Indices, with respect to axial displacements, are calculated for tensile deformation in the pipelines because pipelines are substantially weaker for tension than for compression.

4. Evaluation of earthquake resistance

A pipeline system is recognized as earthquake-resistant with respect to horizontal displacement, if the Deformability Index, δ, obtained through the above-illustrated procedure is greater than the Design Ground Displacement, U. Similarly, a pipeline system is recognized as earthquake-resistant with respect to vertical displacement, if the Vertical Deformability Index, calculated by using the models of vertical ground displacement which are shown in Figs. 2c and 2d, is greater than the Design Vertical Ground Displacement, V.

EXAMPLES OF CALCULATING DEFORMABILITY INDEX, δ

In this chapter, examples of calculating Deformability Indices of several kinds of existing pipeline systems, by using the ground-block model shown in Figs. 3 and 4, and by referring to the data on soil restriction and strength of joints shown in the Recommended Practice of JGA. The earthquake-resistance of these pipelines will be evaluated in comparison with the Design Ground Displacements.

1. Thread-jointed steel pipelines 50 mm in diameter

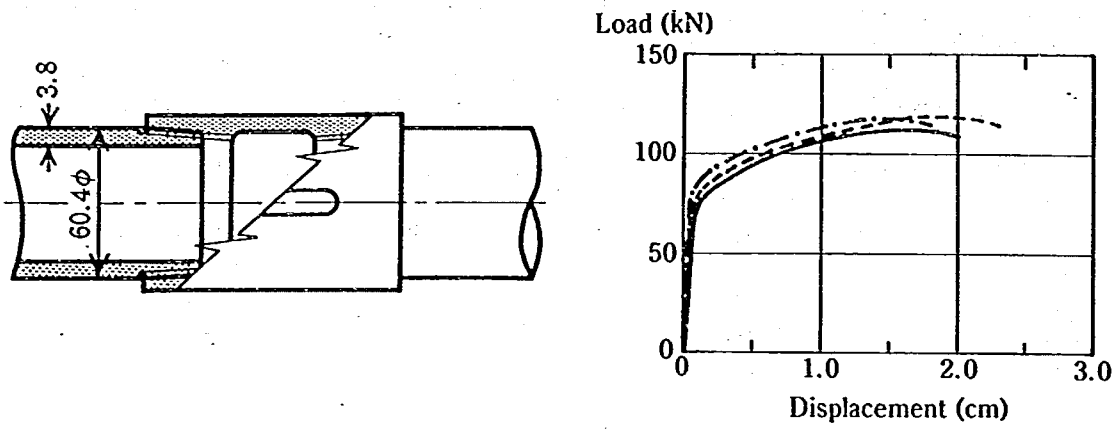
Fig. 5a shows the cross section of thread-jointed socket for steel pipelines commonly used in Japan until recently. The load-displacement diagrams for this type of joint 50 mm in diameter have been obtained as shown in Fig. 5b.

From these diagrams, we can assume that the strength of the joint, F_0, is approximately 115 kN (a little less than 12,000 kgf), and the corresponding displacement in the threaded part is about 2 mm.

The stress, σ_0, in the pipe corresponding to this value of F_0 is about 160 MPa($\sigma_0=F_0/A$). This stress is well below the yield strength of conventional mild steel (yield strength of such steel being σ_y=250–300 MPa, approximately), therefore, the strain in the pipe is simply given by dividing the stress by the conventional Young's modulus E, namely, $\varepsilon=\sigma/E$ where $E=2.06\times10^5$ MPa.

By expressing the equation of stress distribution, shown in Fig. 6, in terms of the strength of the joint, F_0, the equation of strain distribution is given as follows:

$$\varepsilon(x) = \frac{F_0 - \pi D \tau x}{AE} \qquad (2)$$



a. Cross Section of Thread-Joint (Socket, 50 mm)

b. Load-Displacement Diagram of 50 mm Thread-Joint (Axial Tension) (Ref. 3)

Fig. 5 Cross Section and Load-Displacement Diagram of 50 mm Thread Joint

The recommended value of soil restriction, taking into account the effects of increased diameter of socket and the existence of service branches at intervals of several meters, is given by the Design Practice as $\tau'=20$ kPa (0.2 kgf/cm^2). Then, by integrating the above equation between x=0 and x=L, and multiplying by two, the elastic elongation, δ_1, of the pipeline, 2L in length, is obtained as

$$\delta_1 = \frac{F_0^2}{\pi D \tau A E} \tag{3}$$

$$= 2.5 \text{ cm}$$

The elongation at the threaded part is $\delta_2=0.2$ cm as shown previously. Then the Deformability Index of this pipeline system is given as

$$\delta = \delta_1+\delta_2$$

$$= 2.7 \text{ cm}$$

In order for this pipeline system to be judged as earthquake-resistant, the product of the factors α_1 and α_2 must be smaller than 0.54. If we choose an area in zone A, $\alpha_1=0.8$ referring to Table 1. Therefore, the factor α_2 should take a value smaller than 0.675. This condition is satisfied only by a low-pressure pipeline in the ground of Category I. In other words, the thread-jointed pipeline is not regarded as earthquake-resistant, except for the case of low-pressure pipeline in stiff and stable grounds classified in Category I.

In the above calculation, the following equation for the value of L was used:

$$L = \frac{F_0}{\pi D \tau} \tag{4}$$

This value of L gives the minimum size of ground blocks which can cause damage to this pipeline system; and, in this case, L=30 m, approximately. This value can be related with the critical average strain in the ground which causes damage to this pipeline system.

This critical strain is given as follows:

$$\varepsilon_{cr} = \frac{\delta}{L} \tag{5}$$

$$= 900\times10^{-6}$$

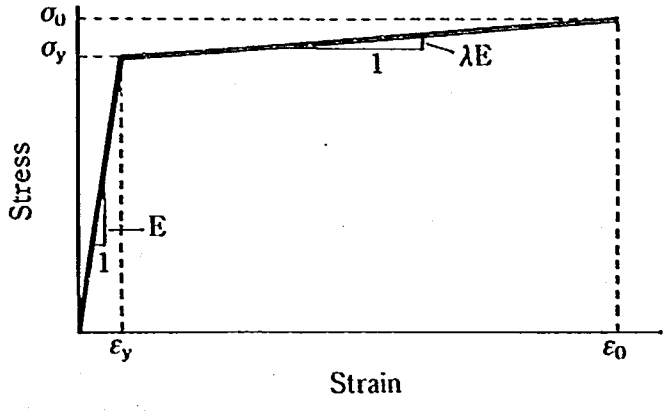


Fig. 6 Bi-linear Approximation of Stress-Strain Relationship for Steel

The above value approximately corresponds to the yield strain of grounds.

2. Continuous (arc-welded) steel pipeline 150 mm in diameter

The allowable strain for medium- and low-pressure steel pipeline is given by the Design Practice as ε_0=3% (of course, no harmful defect in the welded part is presumed). This value of ε_0 is far greater than the yield strain ε_y of about 0.12%. However, this value is small enough compared with the uniform-elongation limit of about 10–15% which gives the criterion of fracture under uniaxial tension.

Referring to the data of an experiment carried out using a pipe 150 mm in diameter (which is shown in Ref. 3), the stress-strain diagram can be approximately expressed with a bi-linear diagram as shown in Fig. 6 in which λE denotes the coefficient of strain hardening.

Based on this diagram, the elongation in the pipeline (or the Deformability Index), when the strain at x=0 reached the value of ε_0, is expressed as follows:

$$\delta = \frac{AE\{\varepsilon_y^2+\lambda(\varepsilon_0^2-\varepsilon_y^2)\}}{\pi D\tau} \tag{6}$$

The values for dimensions, coefficients and other quantities are given as follows:

E : Young's modulas = 2.06×10^5 MPa
λ : strain hardening ratio = 7×10^{-3}
ε_0 : allowable strain = 0.03
ε_y : yield strain = 0.0012
A : cross-sectional area of pipe = 25.2×10^{-4} m^2
D : outside diameter of pipe = 0.165 m

The recommended value of τ for polyethylene-coated steel pipelines without branches and other fittings is given, by the Design Practice, as

τ = 10 kPa (0.1 kgf/cm^2)

Substituting the above values in Eq. (6),

δ = 0.77 m

is obtained. This value is far greater than the required value of deformability. Thus the arc-welded continuous steel pipeline is sufficiently earthquake-resistant except for the cases of land slides and fault movements accompanied with extraordinarily great ground displacements.

For reference, the value of L is given, by substituting $F_0=A\sigma_0$ in Eq. (4), as

$L = 140$ m

The critical strain in the ground which is defined by Eq. (5) is calculated

$$\varepsilon_{cr}=5{,}500\times10^{-6}$$

This value is well in the plastic range of ground deformation. Moreover, it is necessary, for this steel pipeline to be damaged, that this level of great strain must be produced throughout the area as wide as L=140 m.

3. Steel Pipeline 50 mm in diameter using mechanical fittings

Fig. 7a shows the cross section of mechanical fitting currently used by Tokyo Gas Company and several other gas companies in Japan (for low-pressure mains only, in Tokyo Gas Company). Three broken lines in Fig. 7b show the force-displacement diagram obtained through pull-out tests of fittings (each diagram was obtained for one socket with another socket of the fitting fixed). The three diagrams show fairly great variation. However, we can assume a force-displacement diagram for earthquake-resistance evaluation as shown by the solid line in Fig. 7b. This model-diagram will give conservative result because; (1) the smallest value of the three actual diagrams is given for the maximum endurable force F_0, (2) the curve rising up from zero to the maximum force simulates the least-displacement curve of the three actual diagrams, (3) the ultimate displacement, δ_{01}, where leakage occurs, takes the smallest value of the three diagrams.

The recommended value of overall soil restriction, τ', for polyethylene coated pipeline (50 mm in nominal diameter), taking into account the increased diameter of fittings and the existence of service branches, is given by the Design Practice as

$\tau' = 20$ kPa (0.2 kgf/cm^2)

Using this value of soil restriction, and referring to Fig. 4, the forces acting on the fittings located at an interval of 5 m (ℓ=5 m) is given as follows:

$$F_0 = 45 \text{ kN}$$
$$F_1 = F_0-\pi D\tau'\ell = 26 \text{ kN}$$
$$F_2 = F_0-2\pi D\tau'\ell = 7 \text{ kN}$$

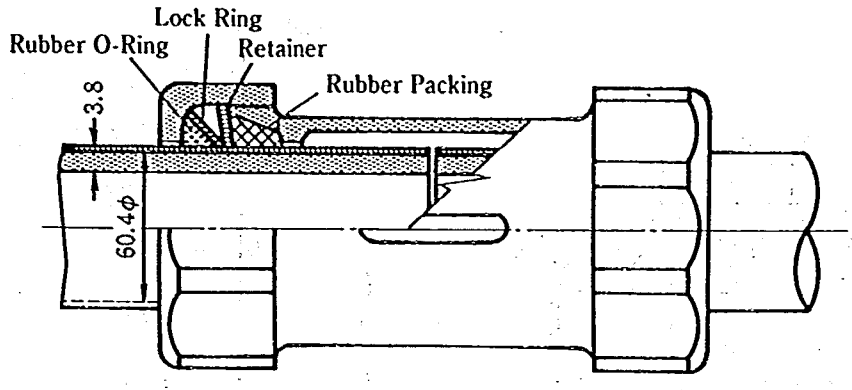
The displacements in the fittings corresponding to the above forces are given, from Fig. 7b, as

$$\delta_0 = \delta_{01}+\delta_{02} = 4.4+1.5 = 5.9 \text{ cm}$$
$$\delta_1 = 1.25\times2 = 2.5 \text{ cm}$$
$$\delta_2 = 0.3\times2 = 0.6 \text{ cm}$$

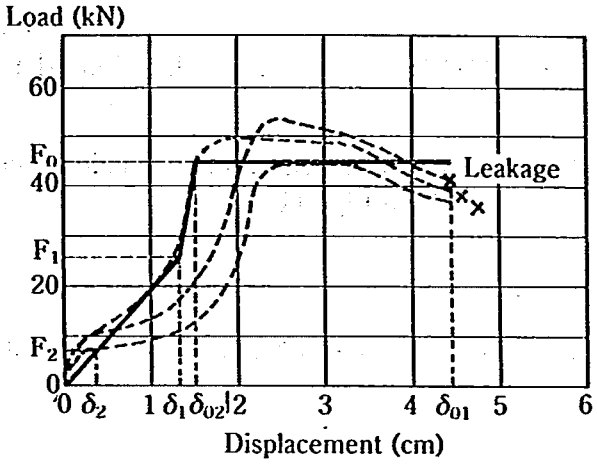
(note that one fitting has two sockets)
Therefore, the Deformability Index of this pipeline system is given as

$$\delta = \delta_0+2\delta_1+2\delta_2 = 12.1 \text{ cm}$$

This value of Deformability Index makes this pipeline system earthquake-resistant for all combinations of the conditions designated by Eq. (1) and Tables 1 and 2, although this pipeline system is actually



a. Cross Section of Mechanical Joint for Steel Pipe (Tokyo Gas LM-Type Socket, 50 mm)



b. Load-Displacement Diagram of 50 mm Mechanical Socket
- - - - - Experiments
——— Diagram for Calculation
(Ref. 3)

Fig. 7 Cross Section and Load-Displacement Diagram of Mechanical Joint for Steel Pipe (50 mm Socket)

used only for low-pressure distribution mains.

The value of L is given, by substituting τ' for τ in Eq.(4), as

$$L = 12 \text{ m},$$

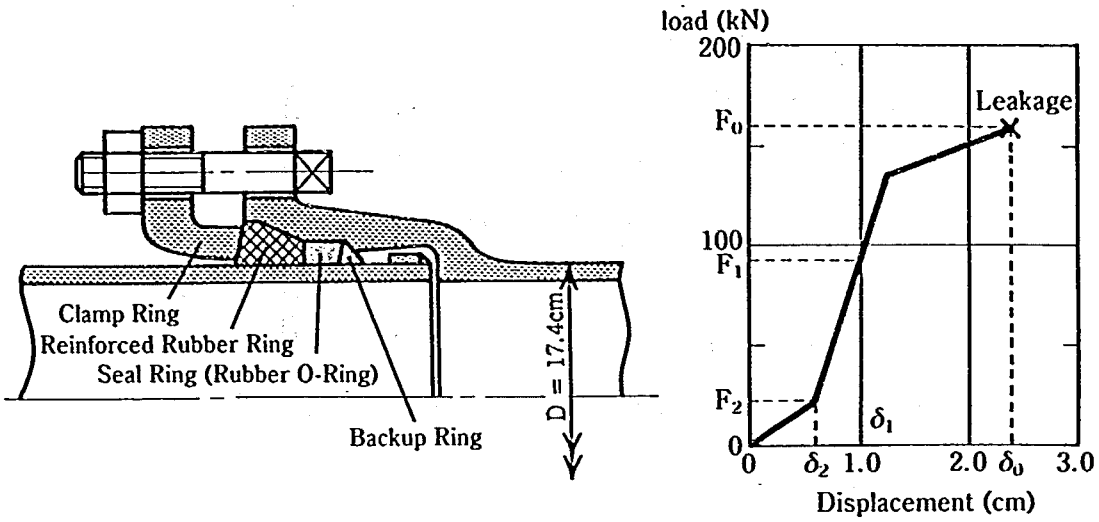
approximately. The corresponding critical average strain in the ground is then given, by Eq.(5), as

$$\varepsilon_{cr} = 10{,}000 \times 10^{-6} \text{ (or 1\%)}$$

4. Mechanically-jointed ductile cast-iron pipeline 150 mm in diameter

Fig. 8a shows the cross section of mechanical-joint of ductile cast-iron pipe, 150 mm in diameter, currently used by Tokyo Gas Company and several other gas companies in Japan (for low-pressure mains only, in Tokyo Gas Company). The force-displacement diagram of this joint is approximately expressed as shown in Fig. 8b.

The recommended value of overall soil restriction, considering the existence of wide flanges of joints is given approximately as



a. Cross Section of TM Joint

b. Load-Displacement Diagram for 150 mm TM Joint (Ref. 3)

Fig. 8 Cross Section and Load-Displacement Diagram of Tokyo-Gas Type Mechanical Joint (TM Joint) for Ductile Cast-Iron Pipe (150 mm)

τ' = 25 kPa (0.26 kgf/cm²)

Assuming the interval of joints as ℓ=5 m, the forces acting on the joints are given as follows:

F_0 = 160 kN
$F_1 = F_0 - \pi D \tau' \ell$
= 92 kN
$F_2 = F_0 - 2\pi D \tau' \ell$
= 23 kN

The displacements in the fittings corresponding to the above forces are given, from Fig. 8b, as

δ_0 = 2.4 cm
δ_1 =1.0 cm
δ_2 = 0.6 cm

Therefore, the Deformability Index of this pipeline system is given as

$\delta = \delta_0 + 2\delta_1 + 2\delta_2$
= 5.6 cm

From the above result, this pipeline system can be judged to be earthquake-resistant for all the conditions when used for low-pressure mains. As the medium-pressure mains, however, this pipeline is not earthquake-resistant depending on the sesmic zone and the ground conditions. Thus a pipeline system could be earthquake-resistant even though the deformability of each joint may not be greater than the specified ground displacement.

The value of L is given as

L = 12 m,

approximately, and the corresponding critical average strain in the ground is given as

$\varepsilon_{cr} = 4{,}700 \times 10^{-6}$

which is in the plastic range of ground deformation, as in the preceding examples.

PROBLEMS WITH THE RECOMMENDED DESIGN PRACTICE OF JGA

There are two problems to be considered in the Recommended Practice of Earthquake-Resistant Design of Medium- and Low-Pressure Pipelines. One problem is that soil liquefaction is not taken into account in the Design Practice, and the other arises from the fact that the Deformability Index alone is not sufficient to evaluate real earthquake resistance of pipeline systems.

The value of U_0=5 cm, associated with the ground block model for calculation of Deformability Index, is likely an excellent as well as quite appropriate criterion for assessing the earthquake resistance, if soil liquefaction is not taken into account. It is presumed that the earthquake resistance, taking into account soil liquefaction, is primarily the matter of the value of U_0. In other words, the earthquake resistance under the condition of soil liquefaction can be improved simply by increasing the Deformability Index, δ, unless extraordinary ground deformations, such as a lateral spreading due to the collapse of an embankment, are considered.

Then the remaining problem is what is the additional factor to be employed, in order to improve the method of earthquake-resistance evaluation.

The length L which represents the magnitude of effective range of ground block was calculated for different pipeline systems in the preceding chapter. The obtained values of L varied widely between 12 m for both mechanically-jointed steel pipeline and ductile cast-iron pipeline, and 140 m for continuous steel pipeline.

This length L gives the minimum size of ground blocks which can cause damage to straight pipelines, as previously mentioned. This fact implies that the length L gives the minimum distance between the possible locations of damage occurrence. Therefore, if the value of Deformability Index δ were the same, a pipeline system with a smaller value of L would have a possibility of sustaining greater number of damage, per unit length of pipeline, than a pipeline system with a greater value of L. Thus, the earthquake resistance, expressed in terms of possible damage ratio (number of damage per unit length of pipeline), should be evaluated on the basis of the values of both the Deformability Index, δ, and the minimum length of ground block L.

The present author has recently proposed a method of predicting seismic damage ratio for buried pipelines taking into account three fundamental factors affecting the damage ratio (Refs. 4, 5). They are: (1) the deformability characteristics of pipeline systems, (2) the nonuniformity in seismic ground displacement, and (3) the intensity of ground motion.

The deformability characteristics include both the Deformability Index δ and the "sample size factor" C which is given by the unit length of pipeline divided by the length of ground block, L. The both quantities, δ and L, are calculated by using exactly the same model of ground-blocks as is used in the Design Practice of JGA.

The nonuniformity in seismic ground displacement is defined as the standard deviation of ground displacement, σ_A. The surface soil layers are more or less nonuniform, in the horizontal direction, in geological structure. The seismic response characteristics of the layer, therefore, are also nonuniform, more or less. This nouniformity in seismic response (in terms of displacement) is expressed by the standard deviation σ_A, on the assumption that the displacement in the ground shows a probabilistic distribution having an average displacement $\bar{u}$ and a standard deviation σ_A.

The seismic displacement in a ground is basically proportional to the intensity of ground motion, in terms of acceleration, if the spectrum of ground motion is the same. Therefore, it can be assumed that both the average displacement and the standard deviation are proportional to the value of ground acceleration. Based on this fact, the subscript, A, of the standard deviation, σ_A, denotes that the value of standard deviation is defined for the intensity of acceleration of A, and the value of σ_A for the arbitrary intensity of acceleration A could be given by the following equation if the standard devia-

tion, σ_{A0}, for a particular value of acceleration, A_0, were known.

$$\sigma_A = \frac{A}{A_0}\sigma_{A0} \tag{7}$$

Thus the standard deviation σ_A is a quantity representing both the nonuniformity in the ground and the intensity of ground motion. This standard deviation of ground displacement is called, in the present paper, the "Nonuniformity Index" of ground.

Actually, the strain in the ground is expressed by the difference in displacements between adjoining ground blocks as demonstrated by the calculation of strains in the preceding chapter. This means that the average displacement $\bar{u}$ does not play any roll in determining the magnitude of strain in the ground, but the magnitude of strain is dependent only on the magnitude of standard deviation σ_A. (Consider that no strain is produced in a uniformly moving body, no matter how large its displacement may be.)

The strain, or differential ground-block displacements, thus related to the Nonuniformity Index, will not be given a one fixed value, but will show a distribution depending on the degree of nonuniformity of ground motion. Therefore, the earthquake resistance of a pipeline system should be evaluated on the basis of probability of damage, or the probability that the differential ground displacement between ground blocks exceeds the Deformability Index of the pipeline system.

A method of damage ratio prediction based on the above idea will be proposed in the following chapter.

EARTHQUAKE-RESISTANCE EVALUATION BASED ON DAMAGE-RATIO PREDICTION

A Method of Damage Ratio Prediction Using Ground-Block Model

The method of damage-ratio prediction proposed by the present author (Refs. 4, 5) uses the same ground-block model as that used in the Design Practice of JGA (Ref. 3). The Deformability Index δ and the minimum length of ground blocks L are calculated in the same procedure as illustrated in the preceding examples. (It should be noted that the symbol Δu is used in the Design Practice to express the Deformability Index. However, the same symbol Δu is used to represent the differential displacement between ground blocks, in this paper.)

On the other hand, the seismic displacement in each ground block is assumed to vary randomly according to a probabilistic distribution. In the proposed method, the displacement, u, is assumed to form a normal distribution with an average value of $\bar{u}$ and a standard deviation of σ_A. Then the probability density of the displacements is expressed as

$$p(u) = N(\bar{u},\ \sigma_A)$$

The relative displacement Δu between two ground blocks, which are sampled randomly, is also given by the form of probability density as

$$p(\Delta u) = N(0,\ \sqrt{2}\,\sigma_A)$$

in accordance with the theorem on the distribution of differences between two variables sampled from the same set.

The probability of occurrence of damage is then given, as the probability that the relative displacement of ground blocks Δu exceeds the Deformability Index δ, as

$$P(\Delta u > \delta) = \int_{\delta}^{\infty} p(\Delta u)\,d\Delta u \tag{8}$$

The damage ratio can then be determined by multiplying the above probability by a factor C which represents the size of sample set or the number of ground blocks constituting the sample set.

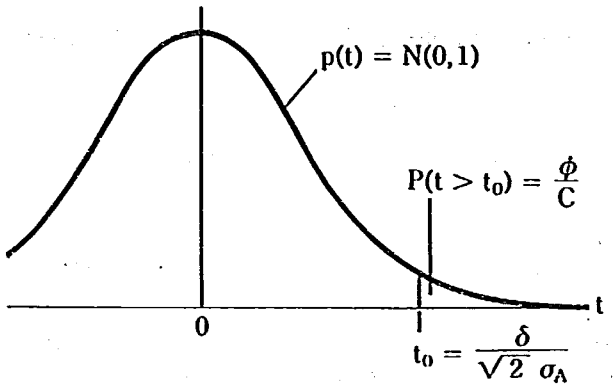


Fig. 9 Conceptual Expression of Probability of Damage in Relation with the Nonuniformity Index (σ_A) and the Deformability Characteristics of Pipeline (δ, C)

If we define the damage ratio in terms of a unit of "number of damaged parts per pipe-length of 1 km", then the factor C is given as

$$C = \frac{1{,}000\ (m)}{L\ (m)} \tag{9}$$

This factor is called the "sample size factor" in this paper.

Substituting $t=\Delta u/\sqrt{2}\,\sigma_A$ for the variable Δu in Eq.(8), the damage ratio ϕ is given in a normalized form as

$$\phi = CP(t > t_0)$$

$$= \frac{C}{\sqrt{2\pi}}\int_{t_0}^{\infty}\exp(-\frac{t^2}{2})dt \tag{10}$$

where

$$t_0 = \frac{\delta}{\sqrt{2}\,\sigma_A}$$

The value of ϕ/C can easily be obtained from the table of probability of exceedance for normal distribution. A schematic idea of damage probability is shown in Fig. 9.

Proposed Classification of Ground Conditions Based on Nonuniformity Index σ_{275}

The effectiveness of the above method of damage ratio prediction has been demonstrated, by the author, by applying this method to the damage statistics on gas distribution pipelines obtained during three earthquakes (1978 Miyagiken-oki Earthquake, 1983 Nihonkai-chubu Earthquake and 1989 Loma Prieta Earthquake). Based on the values of σ_A, obtained for different kinds of ground conditions through the analyses of the above damage statistics, classification of ground conditions based on the value of σ_{275} was proposed as shown in Table 4. The symbol σ_{275} denotes the Nonuniformity Index under the ground acceleration of A=275 cm/s^2 which represents the overall-maximum ground acceleration in Sendai City and the surrounding areas during the 1978 Miyagiken-oki Earthquake.

The classification of ground conditions in Table 4 is likely to correspond well to that in the Design Practice of JGA, although the latter is expressed in terms of required Deformability Index. In addition, this classification covers the condition of liquefiable ground. The applicability of the Nonuniformity Index to the liquefied ground has been demonstrated in the analysis of the above damage statistics which include the data obtained in the liquefied areas. It should be noted, however, the topography

Table 4 Classification of Ground Conditions Based on σ_{275} (A Proposal)

Degree of Nonuniformity	σ_{275} [cm]	Remarks (Corresponding Ground Conditions)	Examples from Existing Grounds and Estimated Values of σ_{275}
Very Uniform	< 0.5	Stiff diluvial deposit: Rock Mass	
Uniform	0.5 ~ 0.7	Moderately stiff diluvial deposit: Gravel Layer: Alluvium with a uniform thickness	Old downtown area of Sendai City (~ 0.6) Alluvial plain eastward of Sendai (~ 0.7)
Somewhat Nonuniform	0.7 ~ 1.0	Alluvium with somewhat nonuniform thickness: Alluvial fan: Ordinary residential land developed in a hilly area	Nagamachi-Kohriyama District of Sendai (0.8 ~ 0.9) Shiogama City (Total area) (~ 1.0)
Very Nonuniform	1.0 ~ 1.5	Alluvium with extremely nonuniform thickness such as a river basin and drowned valley: Areas containing liquefiable grounds to some extent: Land developed by cutting hills and filling valleys in vast scale	Oga City (Total area) (~ 1.2) Nanko-dai (housing area), Sendai (~ 1.5)
Extremely Nonuniform	1.5 <	Very soft alluvium with an extremely nonuniform thickness: Areas mostly consisting of liquefiable grounds	Port South District of Shiogama (~ 2.4) Concentrated-liquefaction area of Oga (~ 2.1) Noshiro City (Total area) (~ 2.2) Marina District, S.F. (~ 2.2)

of the areas studied was almost flat, and the lateral spreadings of ground were not very remarkable. Heavy lateral spreadings and landslides such as those observed in Niigata City during the 1964 Niigata Earthquake, which were mostly due to the collapse of river embankments, can be expressed in terms of the same Nonuniformity Index of enormous magnitude (such as around ten centimeters or more). However, we do not have accurate as well as sufficient amount of data to be analyzed, at the present.

Examples of Earthquake-Resistance Evaluation Based on the Proposed Method

(1) Critical damage ratio ϕ_{cr}

The above proposed model for damage ratio prediction shows that any type of pipeline systems will have some value of damage ratio larger than zero. Therefore, some critical value of damage ratio should be determined, referring to which a pipeline system will be judged whether earthquake-resistant or not. For low-pressure mains, a value of $\phi_{cr}=0.01$ (damage number/km) will be appropriate because this value, that is equivalent to one damaged part per 100 km of pipeline, is almost of the same level as that the gas industry deals with in its daily maintenance of pipeline networks. For example, Sendai City Bureau of Gas had low-pressure mains about 1,200 km in total length in the event of 1978 Miyagiken-oki Earthquake. Then, the probable number of damaged parts would have been smaller than twelve, if the expected damage ratio of those pipeline under an acceleration of A=275 cm/s^2 were smaller than 0.01. This number of damage is not very great compared with the number of leakage-repairing per day in daily maintenance. Actually, number of damaged parts due to this earthquake was 218 which was too great to be repaired in a short period by the staff of the City Gas Bureau alone.

(2) Deformability characteristics of pipeline systems used as examples

The pipeline systems to be used here as examples will be the four pipeline systems illustrated in the preceding chapter for examples of calculation of Deformability Index. The values of Deformability Index δ and sample size factor C for the four pipeline systems are as listed in Table 5.

(3) Predicted damage ratios under an acceleration of A=250 cm/s^2

Damage ratios for the above four pipeline systems are calculated by using Eq.(10) for the values of Nonuniformity Index σ_{275} shown in Table 4. The Nonuniformity Index σ_A for A=250 cm/s^2 is

Table 5 Deformability Characteristics (δ and C) for Four Types of Pipeline Systems

Type of pipeline	Nominal diameter (mm)	Deformability Index δ (cm)	Sample size factor C
① Thread-jointed steel pipeline	50	2.7	33
② Continuous (arc-welded) steel pipeline	150	77	7.1
③ Mechanically-jointed steel pipelilne (LM type)	50	12.1	83
④ Mechanically-jointed ductile cast-iron pipeline (TM type)	150	5.6	83

obtained by using Eq.(7). This value of ground acceleration, A=250 cm/s^2, is likely to be the greatest acceleration observed on (or estimated for) the liquefied ground. This may be due to the fact that liquefaction occurs under a relatively low acceleration such as 200 cm/s^2, and after the soil is liquefied, the surface ground is not excited further because the liquefied layer cannot transmit the earthquake wave. While the acceleration in non-liquefied ground is likely to be excited at much higher accelerations, such as 300 cm/s^2, and even as high as 400 cm/s^2 depending on the site conditions (however, very high acceleration is likely not necessarily be associated with great displacements).

Fig. 10 shows the calculated relationship between the damage ratio and the ground conditions (expressed in terms of Nonuniformity Index σ_{275}). The broken lines in Fig. 10 show the cases for the damage ratio under the acceleration of A=275 cm/s^2 which is the same as the ground acceleration estimated for Sendai City (for nonliquefied ground) during the 1978 Miyagiken-oki Earthquake.

(4) Evaluation of earthquake resistance of four pipeline systems

The pipeline system ① (thread-jointed pipeline) may be regarded as earthquake-resistant, referring to the critical damage ratio of ϕ_{cr}=0.01, in the "uniform" ground and under the acceleration of A=250 cm/s^2. However, the same pipeline system will not be earthquake-resistant, even in the uniform ground, if the acceleration is as intense as A=275 cm/s^2. In contrast, the earthquake resistance of pipeline system ③ (mechanically-jointed steel pipeline) is extremely improved compared to the thread-jointed system. This system will be sufficiently earthquake-resistant for almost all the ground conditions except for liquefiable ground conditions, and will be earthquake-resistant, even in the liquefiable conditions, unless substantial degree of lateral spreadings are expected (or if the Nonuniformity Index σ_{275} is smaller than about 3.0).

The pipeline system ④ (mechanically-jointed ductile cast-iron pipeline of Tokyo Gas Type) will be earthquake-resistant in most ordinary ground conditions excluding "extremely nonuniform" ground conditions. This system, however, will not be earthquake-resistant at all in the liquefiable ground conditions.

The arc-welded steel pipeline, 150 mm in diameter, (pipeline system ②) is expected to be sufficiently earthquake-resistant for almost all the ground conditions except for the case associated with substantial degree of lateral spreadings. The value of Deformability Index of continuous steel pipeline is proportional to the value of the ratio A/D, as shown in Eq.(6). Therefore, the larger the pipe diameter is, the greater the value of Deformability Index is. For example, a steel pipeline 600 mm in diameter will have the Deformability Index almost twice as great as that for 150 mm pipeline. At the same time, the size of the ground-block, L, will be almost nine times as great as that for 150 mm pipeline (therefore, the value of sample size factor, C, decreases to about one ninth). Thus the continuous steel pipeline, 600 mm in diameter, will show sufficient degree of earthquake resistance even

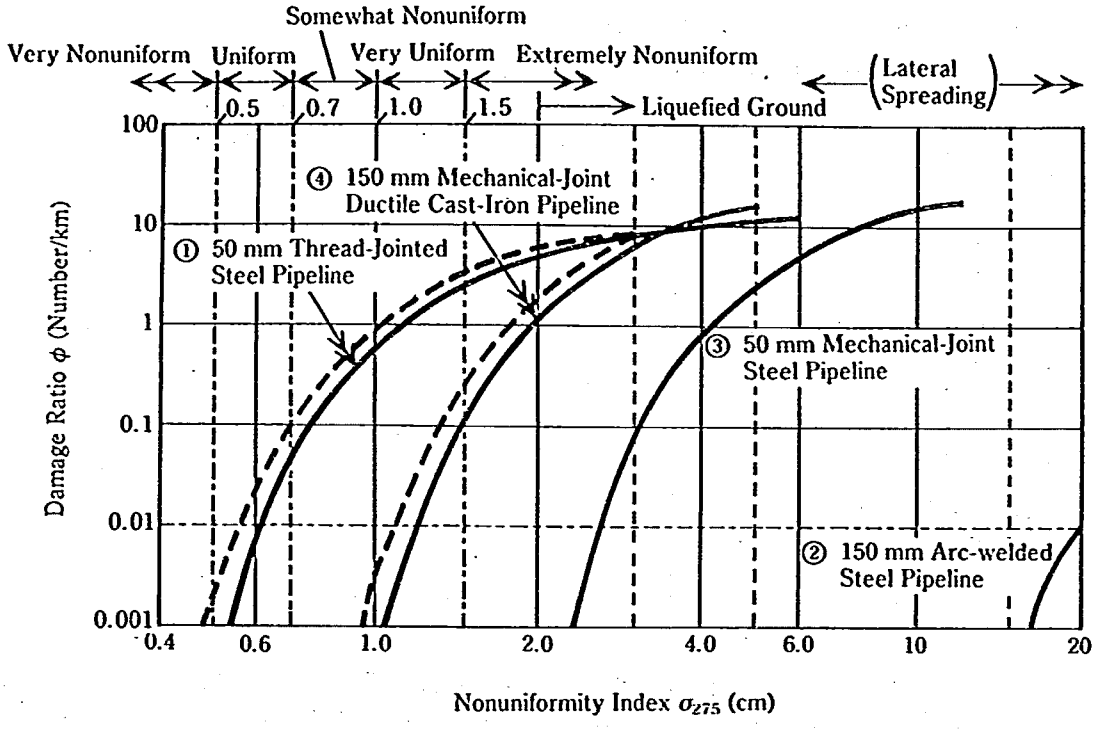


Fig. 10 Relationship Between the Damage Ratio and the Nonuniformity Index for Four Kinds of Pipeline Systems, under the Acceleration of A=250cm/s^2 (---- A=275cm/s^2)

for the ground conditions which give a value of σ_{275} as great as 50 cm or more (note that the value of probable damage ratio, ϕ, is the function of t_0, or the ratio δ/σ_A, and the value of C, as expressed by Eq.(10)). This fact suggests that 600 mm steel pipeline will be earthquake resistant even though an extremely large lateral spreading may be taken into account.

The medium-density polyethylene pipeline, 50 mm in diameter, is shown to have a value of Deformability Index of 400 cm, according to the Design Practice of JGA. This fact proves the polyethylene pipe to be one of the most earthquake-resistant materials for gas distribution.

CONCLUSION

The basic ideas of the Recommended Practice for Earthquake-Resistant Design of Medium- and Low-Pressure Gas Pipelines, drafted by JGA, were reviewed. It was demonstrated that the method of calculating earthquake resistance, by using the ground-block model, is simple and practical, and could be used to evaluate the deformability (in terms of the Deformability Index) of various types of (or, practically, any type of) pipeline systems if the stress-strain relationship of pipe materials or the load-displacement diagram of pipe-joints could be obtained.

The idea of Design Ground Displacement, which takes into account the nonuniformity in ground displacement, seems quite appropriate. The recommended values of horizontal ground displacement also seem to give appropriate criterion for evaluation of earthquake resistance, so far as extremely nonuniform ground conditions, including liquefiable grounds, are not taken into consideration.

However, the damage susceptibility of a pipeline system is not only related to the magnitude of Deformability Index but also related to the size of ground block which is also dependent upon the mechanistic characteristics of the pipeline system. The actual value of ground displacements, on the other hand, shows variation from place to place forming a certain type of distribution. Therefore, a method of improving the rationality of the Design Practice was proposed, which takes into account both the effect of the size of ground blocks and the variation of ground displacement mentioned above.

The examples of earthquake-resistance evaluation based on the proposed method demonstrated that the new method can evaluate the effect of ground-motion intensity on the damage susceptibility of pipeline systems. They also suggested that the new method can be applied for the earthquake-resistance evaluation taking into account the effect of soil liquefaction.

REFERENCES

1. Toki, K., Fukumori, Y., Sako, M. and Tsubakimoto, T., Recommended Practice for Earthquake-Resistant Design of High Pressure Gas Pipelines, Proc. of ASME PVP Conference, PVP-Vol.77, pp.349–356, 1983.
2. The Japanese Ministries of International Trade and Industry, Construction, and others, Technical Standard for Petroleum Pipelines, Ministrial Notification, 1973. (in Japanese)
3. Saito, K., Nishio, N. and Katayama, T., Recommended Practice for Earthquake-Resistant Design of Medium- and Low-Pressure Gas Pipelines, Proc. of ASME PVP Conference, PVP-Vol.77, pp.340–348, 1983.
4. Nishio, N., Damage Ratio Prediction for Buried Pipelines Based on Deformability of Pipelines and Nonuniformity of Grounds, Proc. of ASME PVP Conference, PVP-Vol.227, pp.13–22, 1992.
5. Nishio, N., Seismic Damage Ratio Prediciton for Buried Pipelines Considering Nonuniform Ground Displacement, Proc. of JSCE No.450/I-20, pp.63–74, 1992.
6. Japan Gas Association, Miyagiken-oki Jishin to Toshi-Gas (Miyagiken-oki Earthquake and Gas Facilities), 1979. (in Japanese)
7. Katayama, T. and Isoyama, R., Damage to Buried Distribution Pipelines During the Miyagiken-oki Earthquake, Proc. of ASME PVP Conference, PVP-Vol.43, pp.97–104, 1980.
8. Nishio, N., Ukaji, T. and Tsukamoto, K., Experimental Studies and Observation of Pipeline Behavior During Earthquakes, Proc. of ASME PVP Conference, PVP-Vol.43, pp.67–76, 1980.
9. Tsukamoto, K., Nishio, N., Satake, M. and Asano, T., Observation of Pipeline Behavior at Geologically Complex Site During Earthquakes, Proc. of 8WCEE, Vol.VII, pp.247–254, 1984.
10. Nishio, N., Hamura, A. and Sase, T., Earthquake Observation of a Buried Pipeline in a Non-uniform Subsurface Layer, Proc. of 9WCEE, Vol.VII, pp.23–28, 1988.
11. Nishio, N., Ukaji, T., Tsukamoto, K. and Ishita, O., Model Experiments on the Behavior of Buried Pipelines During Earthquakes, Proc. of ASME PVP Conference, PVP-Vol.77, pp.263–272, 1983.
12. Kubo, K., Katayama, T. and Sato, N., Quantitative Analysis of Seismic Damage to Buried Pipelines, Proc. of 4th Japan Earthquake Engg. Symposium, pp.655–662, 1975. (in Japanese)
13. Nishio, N., Studies on Seismic Behavior and Quantitative Prediction of Damage Ratio of Buried Pipelines, Thesis, 1989. (in Japanese)

EARTHQUAKE HAZARD REDUCTION PROGRAM FOR A WATER LIFELINE UTILITY

Ergun Bakall
Chief Engineer

Jan Decker
Administrative Analyst

Richard Pyle
Associate Civil Engineer
San Diego County Water Authority

ABSTRACT

The San Diego County Water Authority has long recognized that complete reliance on imported water to meet the water demands of its service area is imprudent given the possibility of seismic activity in the region and the potential for catastrophic failure of the aqueducts. Studies by the Authority have concluded that an emergency storage project is necessary to protect against the impacts of a sudden loss of imported water supply. In support of the emergency storage project, the Authority has initiated a seismic risk analysis to quantify the extent of damage and the time required to repair the pipelines. Also, the economic impacts caused by a lack of emergency storage, the consumers willingness to pay for a reliable water supply, and the costs for construction and operation of an emergency storage reservoir were also studied in order to appropriately size an emergency storage facility.

INTRODUCTION

The mission of the San Diego County Water Authority is to provide a safe and reliable supply of water to its member agencies who serve the San Diego region. Almost every year since the time the Authority was organized in June 1944, the Authority has imported a larger proportion of the total water used in San Diego County.

Prior to the time the Authority made the first imported water delivery in December 1947, the San Diego region was entirely dependent on local water resources. Three years later, the Authority provided more than half of the region's total water supply. The fact that in fiscal year 1990, the Authority delivered 647,500 acre-feet (800 million m^3) of imported water is indicative of how San Diego has come to rely on the Authority's imported water supply. This quantity comprised approximately 95 percent of the total water demand of the Authority's service area. The Authority is extremely vulnerable to interruptions of its imported water supply.

The Metropolitan Water District of Southern California (MWD) is the sole source of imported water to the Authority. The Authority takes delivery of water from MWD through five pipelines. Two parallel pipelines are known as the First San Diego Aqueduct. An additional three pipelines compose the Second San Diego Aqueduct. The Authority transmits the imported water to its member agencies through an aqueduct system made up of approximately 240 miles (384 km) of large diameter pipelines. The member agencies in turn distribute water to individual municipal, industrial, and agricultural customers.

MWD receives water from both the Colorado River and the State Water Project (Figure 1). Approximately 1.2 million acre-feet (1.5 billion m^3) of Colorado River water is carried annually from Lake Havasu on the river through the Colorado River Aqueduct to its terminus at Lake Mathews. Pumps along the Colorado River Aqueduct lift water a total of 1,350 feet (405 m) en route to Lake Mathews. The other water source, the State Water Project, delivers water through the 444-mile (710 km) long California Aqueduct to its terminus at Lake Perris.

MWD delivers both Colorado River water and State Water Project water to Lake Skinner, the main MWD storage facility for the Authority's aqueduct system. MWD operates a 340 million gallon (1,360,000 m^3) per day water filtration plant at the reservoir. The Authority receives both treated and untreated water from MWD. The First and Second Aqueducts have a total capacity of 1,275 cubic feet per second (cfs) (38 m^3/s), with 575 cfs (17 m^3/s) of treated capacity and 700 cfs (21 m^3/s) of untreated capacity available in the pipelines (Figure 2). The Authority's pipelines

range in size from 48-inches (1.2 m) to 108-inches (2.7 m) in diameter. The pipelines are predominately constructed of welded steel pipe and prestressed concrete cylinder pipe, with some precast concrete pipe.

The population of the Authority's service area has grown from 435,000 to over 2,350,000 since 1953. This was the last year a reservoir was constructed in the County exceeding 25,000 acre feet (AF) (30,825,000 m^3) was constructed. Much of the population growth since this time has occurred in the northern portion of the county, which has few storage facilities. Therefore, water to serve the majority of the daily needs of the north county's population must come directly from the Authority's aqueducts.

The Authority's aqueducts, the State Water Project, the Colorado River Aqueduct, and MWD's pipelines all cross major faults. The Authority has long recognized that complete reliance on the aqueduct system to meet the water demands of its service area is imprudent given the possibility of seismic activity in the region and the potential for catastrophic failure of the aqueducts. If the aqueducts are severed, water supplies to some areas of the county could be exhausted in a matter of days.

THE NEED FOR EMERGENCY STORAGE

The Authority does not own or operate any storage facilities. Although the Authority does have some contractual rights to store water in some of the region's reservoirs, all the reservoirs are owned by member agencies. As the agency responsible for providing all the supplemental water required for the county, the Authority has logically assumed the role for meeting emergency storage needs within the county. To meet the need for emergency storage, the Authority initiated the planning and design of a single surface storage site at Pamo Valley in the early 1980's. The Pamo Valley site has been considered for water supply purposes since the beginning of this century. The City of San Diego acquired the site in 1925 for water supply purposes.

By the late 1980's, the Authority realized that more extensive studies would be required to investigate all the potential emergency storage alternatives in order to successfully complete an emergency storage project. The Authority completed in July 1992 the Optimal Storage Study to identify the need for emergency storage and establish the preliminary planning criteria for the project.

The Optimal Storage Study report ranked 27 emergency surface and groundwater storage reservoir sites based upon environmental,

construction and operating costs. It more clearly identified the need for emergency storage. The study concluded that there is a definite need for emergency surface storage and the study recommended that five sites be carried into detailed engineering and environmental studies.

Of particular concern to the Authority is its ability to provide a safe and reliable service in the event of a significant interruption in service from MWD. As stated before, approximately 95 percent of the water used within the county is imported by the Authority. The balance comes from local production and surface supplies. The vulnerability of the delivery system to supply interruptions is evident from the number of faults the aqueduct system crosses. In order to quantify the risk, the Authority initiated a seismic risk & vulnerability assessment.

SEISMIC RISK AND VULNERABILITY ASSESSMENT

The Authority has initiated a seismic risk analysis to quantify the extent of damage from an earthquake and estimate the time required to repair the pipelines in order to assess the aqueduct systems's vulnerability. There are a five major geologic faults that present a significant seismic threat to the Authority's delivery and supply system. These earthquake zones are the San Andreas, San Jacinto, Elsinore, Rose Canyon and La Nacion faults.

The seismic risk analysis concluded that the geologic fault of major concern is the Elsinore fault. This fault threatens both aqueducts at their northern end where the region's water supply originates from MWD (Figure 3). Scientific research has shown that a credible earthquake event on the Elsinore fault, with a Richter magnitude greater than 7.0, could sever the County from imported supplies for up to two months.

The principal goal of the seismic risk analysis is to determine the risk of failure and the time to repair the aqueduct system. The study is divided into three areas of focus; pipeline failure due to ground motion, pipeline failure due to transient pressures caused by catastrophic pipe failure, and the estimated time and priority for repair.

Part I Quantification of Pipeline Vulnerability from Seismic Hazards

The first portion of the study quantified the number of failures along the Authority's aqueduct system due to potential seismic

events. For each of the five faults in this study, the magnitude for the maximum probable earthquake (MPE), defined as an event with a 475-year return period, and a maximum credible earthquake (MCE) was determined. Using the magnitude of the seismic events on each fault, the seismic hazard analysis then quantified the damage to the pipelines due to surface ground rupture and damage due to ground motion and liquefaction. The results of this portion of the study present the potential number of breaks per pipeline for each of the Authority's pipelines.

A large amount of information was needed to determine the number of failures due to seismic effects. The information included all the available data concerning the construction of the aqueducts and geotechnical information. The areas with a potential for soil liquefaction were identified and imposed on the pipeline routes. The pipe material, diameter, wall thickness and type of pipe joint were tabulated for each pipeline. With this information, the ground motion and liquefaction effects on the pipelines were quantified.

The analysis was performed by Eguchi and Honegger (1992). Pipe damage assessments from prior earthquake events were used to predict the performance of the Authority's pipelines during future events. Most of the data collected from prior events includes cast-iron pipe and pipe with diameters less than 24 inches (0.6 m). The data collected to date from prior events also does not differentiate between modes of pipe failure. Failure modes during seismic events may include failures related to corrosion, ground motion, subsidence, liquefaction, lateral spreading and fault rupture.

The Authority's pipelines are considerably larger and are constructed of different materials than failed pipelines studied after prior earthquake events. The aqueduct pipelines vary from 48 to 96 inches (1.2 to 2.7 m) in diameter. The pipelines are generally constructed of prestressed concrete cylinder pipe or welded steel pipe. Therefore, data on the performance of these large diameter pipelines was extrapolated from data on the performance of small diameter pipelines by comparison of the type of joint, joint strength, and differing material strengths.

Eguchi and Honegger (1992) assumed that the relative vulnerability of the pipelines is proportional to the joint strengths of the various pipeline materials. They found that joint strength generally increases with pipe diameter for each particular pipe material, except for steel pipe with a lap welded joint. For lap-welded steel pipe, the joint strength decreased with the increase in pipe diameter. The most interesting finding of their study was the large increase in vulnerability when comparing gasketed welded steel pipe with steel pipe with lap-

welded joints. The gasketed joints were found to be at least ten times more likely to fail than welded joints.

Using the relative joint strengths and pipe diameters, Eguchi and Honegger computed a set of vulnerability factors for the Authority's pipelines. The vulnerabilities are relative to 48-inch diameter precast concrete pipe without a steel cylinder, for which there are damage statistics from prior seismic events. The number of joint failures on the Authority's pipelines were calculated by using the relative vulnerability factors and damage statistics from prior seismic events.

The preliminary results of the seismic vulnerability study for the five faults are shown in Table 1. The table summarizes the number of repairs after each earthquake event for each of the pipelines. The length of each of the pipelines is also listed.

The results show that the Elsinore Fault is the predominate seismic threat to the Authority's aqueduct system. For a seismic event along the Elsinore fault, approximately 74 percent of the estimated repairs are due to liquefaction, 14 percent are due to fault rupture, and 12 percent are attributed to ground motion.

Part II Quantification of Pipeline Failure due to Transient Pressures Caused by Catastrophic Pipe Failure

The second portion of the study was a hydraulic analysis of the affects on the pipelines resulting from sudden pipeline rupture. A transient pressure analysis was conducted to determine the potential number and location of breaks for each of the pipelines as a result of transient pressure surges. The total number of failures is the sum of the failures due to the actual seismic event and the failures due to surge. The total number of failures is then used to prepare the estimates for the repair time.

The data for this portion of the analysis was derived mostly from the construction record drawings. The pipeline profiles and pipeline appurtenance information was tabulated. Two locations for catastrophic failure were assumed for each aqueduct, one at the San Luis Rey River and the second at the Elsinore Fault. These two locations are areas with a high potential for soil liquefaction.

The hydraulic analysis assumed that the pipeline failure would be a complete separation of the pipeline. This would allow water to flow out of the full diameter of the pipeline. All air/vacuum valves were assumed to be operating as designed.

The transient pressures are analyzed using Stoner & Associates, Inc.'s LIQT-PC computer program. The model divided the pipelines into reaches. The divisions occurred at high points, low points, changes in pipe diameter, and changes in pipe material. The model then determined the maximum and minimum pressures in each of the reaches. The total length of pipe that reaches vapor pressure was also calculated and is shown in Table 2.

The strength of each of the pipelines to resist the surge is being analyzed. By reviewing the transient pressures, the possibility of pipe collapse due to a vacuum or pipeline rupture due to a sudden increase in pressure will be quantified.

Negative pressure is of most significance to welded steel pipe while the positive pressure is most significant to prestressed concrete cylinder pipe. The steel pipe plate thickness is the least at the high points in the pipeline. The high points also correspond to the highest negative transient pressures. Therefore, the greatest potential for collapse is at these points. Conversely, concrete cylinder pipe material is capable of resisting pipe collapse. However, concrete cylinder pipe is susceptible to large increases in pressure. Typically, concrete cylinder pipe ruptures catastrophically due to a failure of the prestressing wires.

Part III Pipeline Failure Response Capability and Prioritization Study

The final portion of the study will analyze the number and locations of the failures to determine the required time and priority for repair. The repair times are continuing to be analyzed and refined by the Authority. The estimate of repair time will include:

- The accessibility of the repair site;
- Mobilization of repair forces;
- Procurement and/or fabrication of replacement pipe; and
- Removal of damaged pipe, construction and testing of the new pipeline segments and structures.

The repair time estimate will also take into consideration the effects of the earthquake on other infrastructure, such as highways, which may have an impact on emergency response and repair times. The Authority currently has agreements with construction contractors for mobilization during an emergency.

The Authority also stockpiles a small amount of pipeline repair sections for use in emergency repairs.

SERVICE CONTINUITY AND SYSTEM RELIABILITY STUDIES

Reliability Planning Study (Economic Study)

The economic impact of the lack of emergency storage, the costs for construction and operation of an emergency storage reservoir, and the consumers willingness to pay for a reliable water supply needed to be studied in order to provide a realistic level of service for an emergency storage facility. Prior assumptions for the sizing of facilities in the Optimum Storage Study and the Emergency Storage Project have used 75 percent of the normal level of service as the basis for sizing facilities. The fundamental economic issue with this planning assumption is the question of whether the public (the customer) is willing to make the financial investment to assure this level of reliability during emergencies, i.e., earthquakes. The Reliability Planning Study is an economic analysis designed to test the 75 percent level assumption as a true basis for planning.
The study consists of three areas of analysis; the residential consumers willingness to pay, the cost of emergency storage for various levels of service, and a determination of the maximum benefit to the consumer.

The first phase is an analysis of the amount the average customer is willing to pay for an emergency storage project. It estimates the value of the proportionate level of service during an emergency event. The research for this project consists primarily of random sample surveys of the public to determine the average monthly amount the customer is willing to pay to insure various levels of service during an emergency. The preliminary results are shown in Figure 4.

The second phase provides parallel data on the average monthly cost to the customer for the various reservoir alternatives of the emergency storage project. These are shown in the reservoir cost curve of Figure 5.

The final phase of this study overlays the results of both studies as shown in Figure 5. The net benefit is defined as the difference between the amount a customer is willing to pay for emergency storage and the estimated cost of emergency storage. The highest point on the net benefit curve is the maximum net benefit. This point corresponds to a 75 percent level of service.

This study is still in the analysis phase. Other issues that may impact this initial conclusion and may be relevant include economic impacts of a reliable water supply for industry and agriculture. However, the preliminary analysis supports the planning assumption of a 75 percent emergency level of service and verifies the conclusions of the Optimum Storage Supply and the need for the Emergency Storage Project.

Emergency Storage Project

Based on the conclusion of the risk analysis study that a significant threat for an interruption in service exists, and based upon the results of the Optimal Storage Study and the Reliability Planning Study (economic study), the Authority's Board of Directors on May 14, 1992 adopted a list of five surface storage sites to meet the need for emergency storage. These five sites (Figure 6) will move forward into preliminary engineering and final environmental review. Of the five sites, two are existing reservoirs that would be expanded, and three are surface reservoirs. The goal of the Emergency Storage Project is to provide sufficient emergency water storage for a significant interruption in service.

In order to meet the requirements of the environmental review process, the Authority is conducting an extensive analysis of the storage alternatives. This process began with the Optimal Storage Study and is continuing with the Emergency Storage Project. The Emergency Storage Project will complete all the environmental processing necessary at each of the five sites for construction of a reservoir. As a part of this process, preliminary engineering design will be completed at each of the surface reservoir locations.

In addition to a new reservoir alternative, the Authority is analyzing an alternative which optimizes the existing storage within the County for meeting emergency storage requirements. This alternative focuses on new pipeline and pumping facilities to take advantage of storage in the existing reservoirs to meet a portion of the emergency storage requirements. The existing aqueduct system transfers water from the north to the south by gravity flow. The most critical need for water would be in the northern part of the county since the majority of existing surface storage is in the south part of the county. To transfer water from the south to the north will require extensive modifications to the existing pipelines as well as the addition of new pipelines and pump stations.

CONCLUSION AND NEED FOR FURTHER STUDY

There is a need for the scientific community to continue to develop scientific data for assessing the impacts from seismic events on large diameter pipelines. The current method employs the extrapolation of data from small diameter pipeline failures to larger diameter pipelines. The extrapolation of the failure estimates using material strengths and joint design as described in this paper has given satisfactory results. However, methods of extrapolating data may be difficult to interpret to the layperson. Actual, validated scientific data concerning large diameter pipelines may be more readily acknowledged.

Reservoir projects will continue to be scrutinized by the public and environmental organizations due to their high cost and potentially large environmental impact. The more definite the underlying assumptions are for concluding that a need exists for reservoirs, the less likely there will be controversy from proposing any particular reservoir.

References:

James M. Montgomery Consulting Engineers (1992). "Storage Study Summary Report," Prepared for San Diego County Water Authority, San Diego, California.

Eguchi, R.T., Honegger, D.G. (1992). "Determination of Relative Vulnerabilities to Seismic Damage for San Diego County Water Authority Water Transmission Pipelines," Prepared for San Diego County Water Authority, San Diego, California

Ebasco Infrastructure (1992). "Project Status Report Pipeline Nos. 1,2,3,4, and 5 Hydraulic Study of Pipelines Rupture Scenarios," Prepared for San Diego County Water Authority, San Diego, California

Black & Veatch (1992). "Monthly Status Report Emergency Storage Project Risk Analysis," Prepared for San Diego County Water Authority, San Diego, California

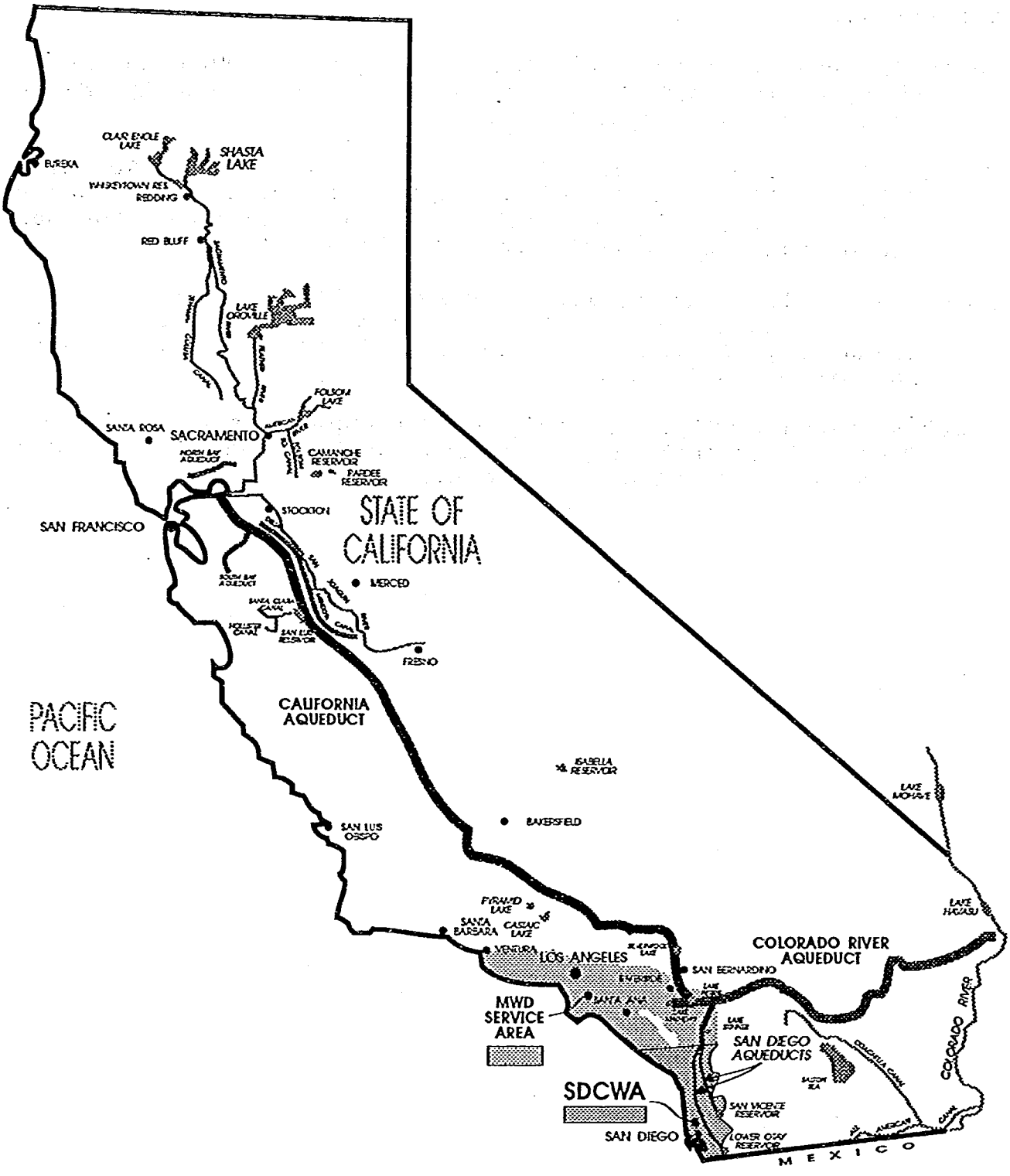


Figure 1

Major Water Conveyance Facilities to
Metropolitan Water District & San Diego County Water Authority

Figure 2

SAN DIEGO COUNTY WATER AUTHORITY
-With Member Agencies-

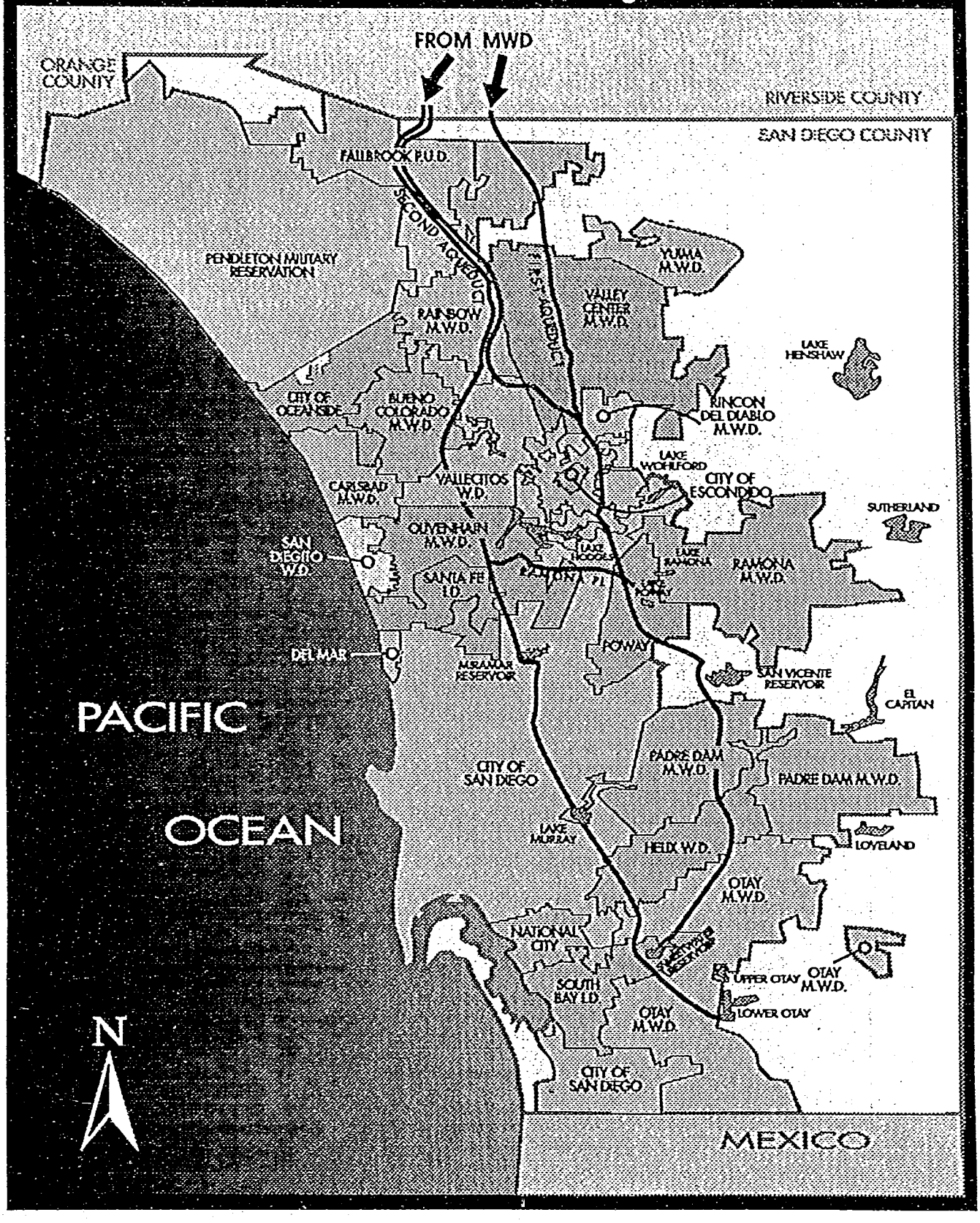
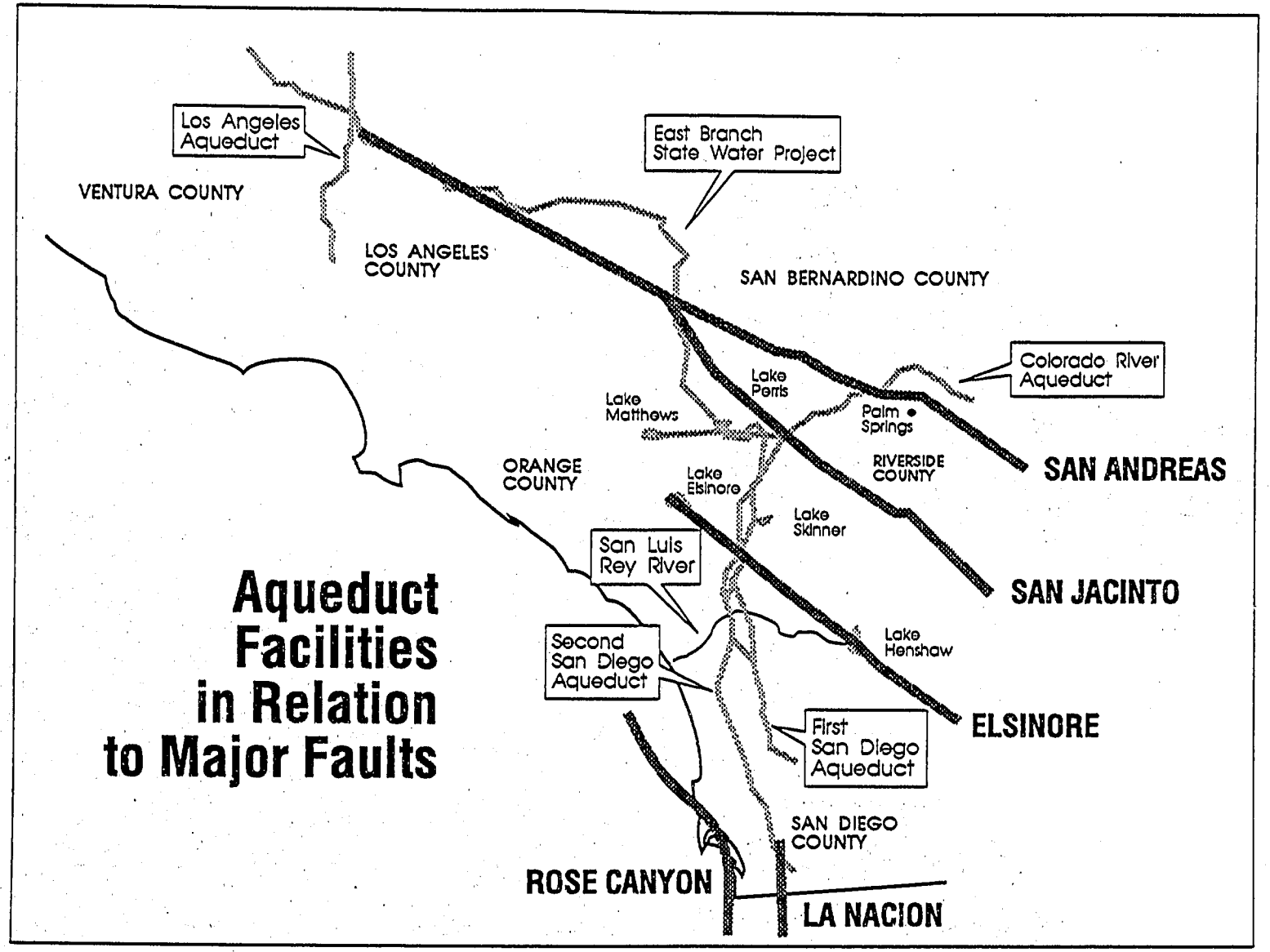


Figure 3


Los Angeles Aqueduct
East Branch State Water Project
VENTURA COUNTY
LOS ANGELES COUNTY
SAN BERNARDINO COUNTY
Colorado River Aqueduct
Lake Perris
Lake Matthews
Palm Springs
ORANGE COUNTY
RIVERSIDE COUNTY
SAN ANDREAS
Lake Elsinore
Lake Skinner
San Luis Rey River
SAN JACINTO
Lake Henshaw
Second San Diego Aqueduct
ELSINORE
First San Diego Aqueduct
SAN DIEGO COUNTY
ROSE CANYON
LA NACION
Aqueduct Facilities in Relation to Major Faults

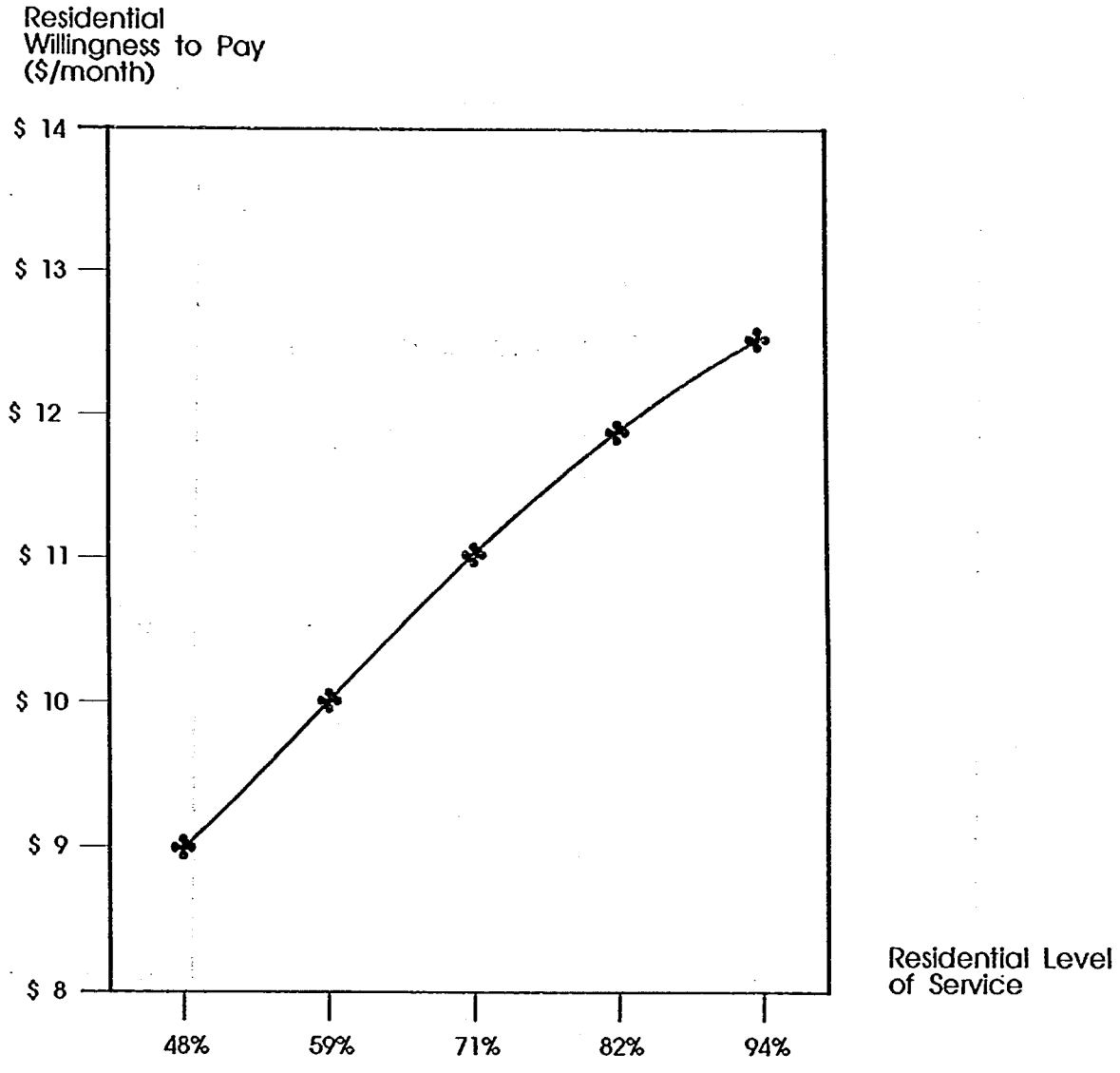


Figure 4
Residential Willingness-to-Pay Function

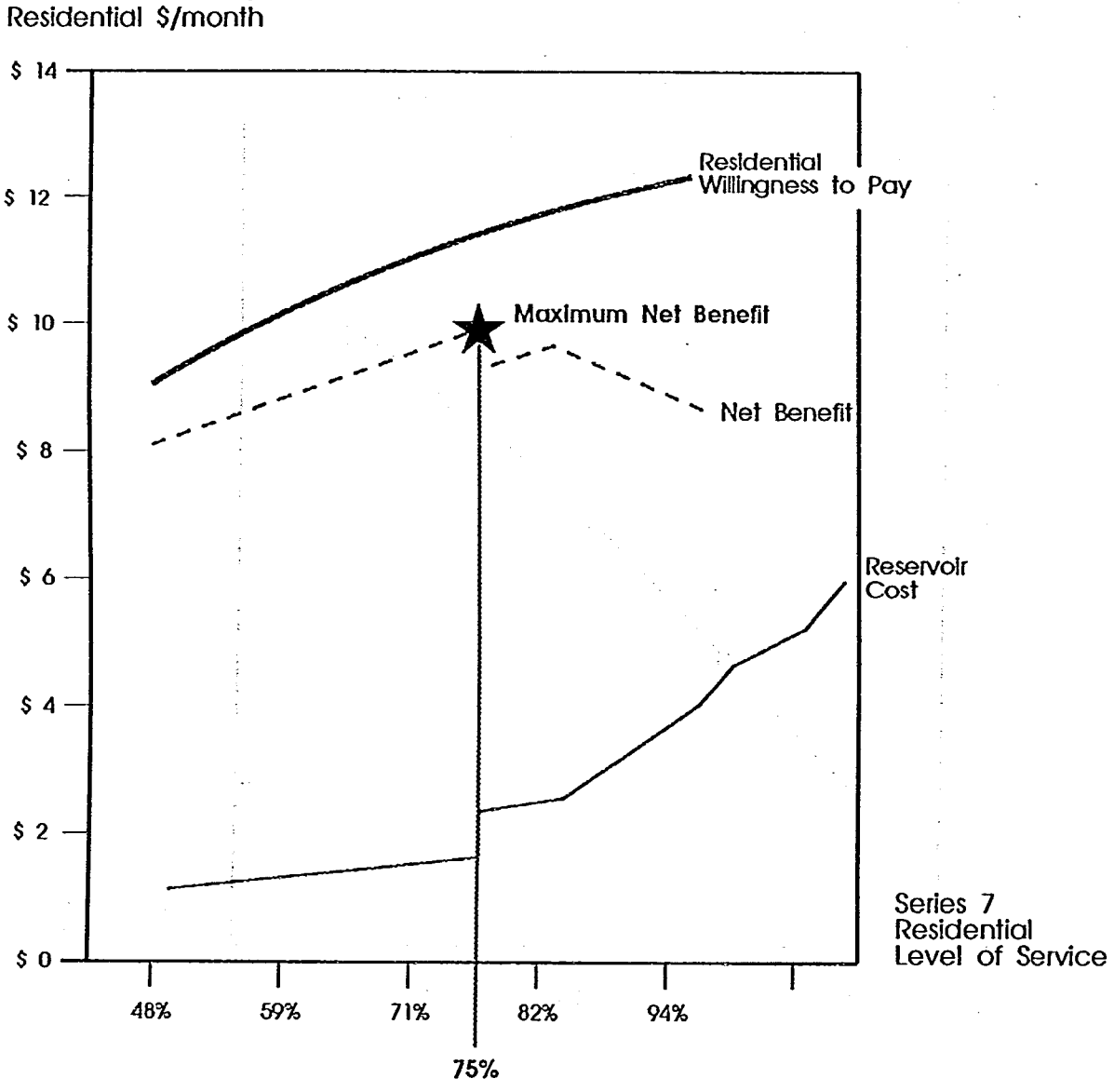
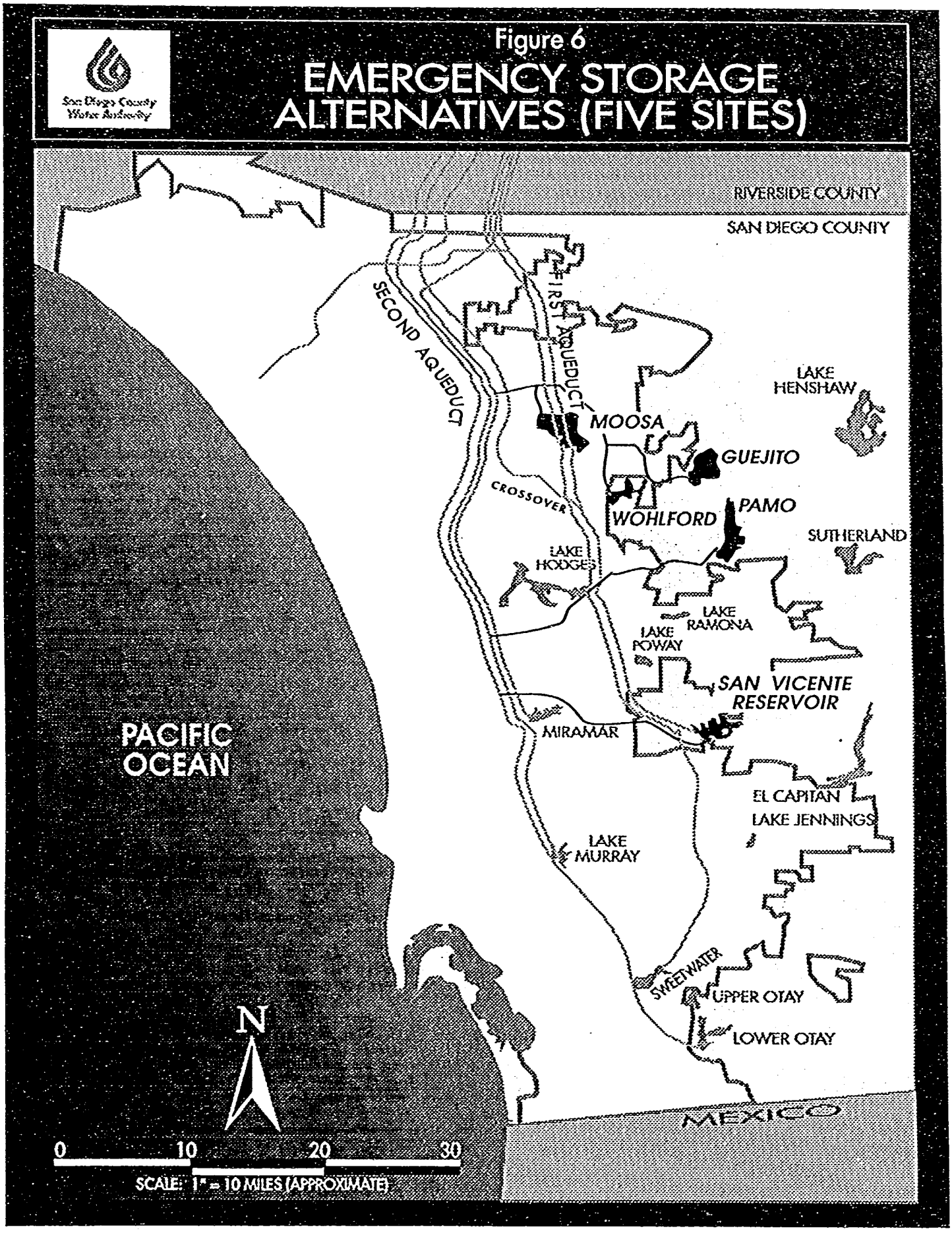


Figure 5
Residential Net Benefits: Series 7 Demands


Figure 6
EMERGENCY STORAGE ALTERNATIVES (FIVE SITES)
San Diego County Water Authority
RIVERSIDE COUNTY
SAN DIEGO COUNTY
SECOND AQUEDUCT
FIRST AQUEDUCT
MOOSA
LAKE HENSHAW
GUEJITO
CROSSOVER
WOHLFORD
PAMO
SUTHERLAND
LAKE HODGES
LAKE RAMONA
LAKE POWAY
SAN VICENTE RESERVOIR
MIRAMAR
PACIFIC OCEAN
EL CAPITAN
LAKE JENNINGS
LAKE MURRAY
SWEETWATER
UPPER OTAY
LOWER OTAY
MEXICO
N
0
10
20
30
SCALE: 1" = 10 MILES (APPROXIMATE)

Seismic Design for Pipeline of Waterworks in Tokyo

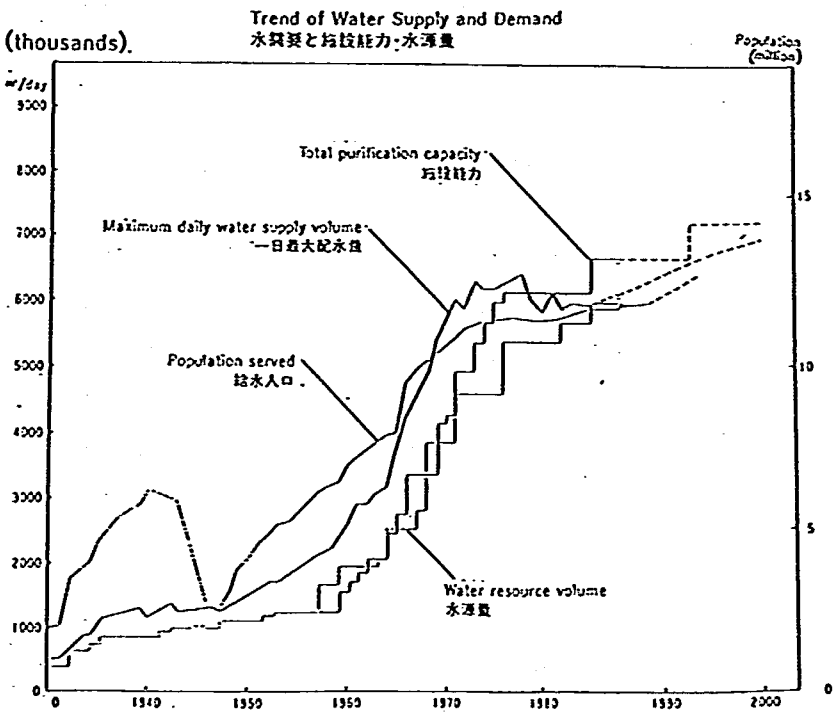
by Ichiro Yokota [1]
Syoji Sato [2]
Tadayoshi Chiba [3]

[1] Introduction of the Water supply System in Tokyo

The Bureau of Waterworks of the Tokyo Metropolitan Government is responsible for management and operation of water-supply to the area of 1,180 ㎢, almost the entire administrative area of Tokyo Metropolis, supplying potable water to about eleven million people.

The total volume of water supplied during fiscal year 1991 was 1,783 million ㎥, eauivalent to a daily average of 4.85 million ㎥, maximum daily supply was 5.96 million ㎥ which represented 542 ㎥ per capita.

The total length of water distribution main is 21,100㎞, the gross capacity of distribution reserviors is 1.26 million ㎥, and the goss installed daily water treatment capacity is 6,685 million ㎥.



The volume of water sources to which rights are currently held is 6.02 million ㎥ which correstponds approximately to the daily demand. However, this volume includes provisional water rihts which are subject

---

1) Chief, Second Designing Section, Construction Division, Waterworks Bureau of Tokyo Metropolitan Government, No.2Bldg. 13F, 2-8-1, Nishi-Shinjuku, Shinjuku-ku, Tokyo 163-01, Japan Tel:03-5320-6494 Fax:03-5388-1684
2) Deputy Chief
3) Assistant Chief

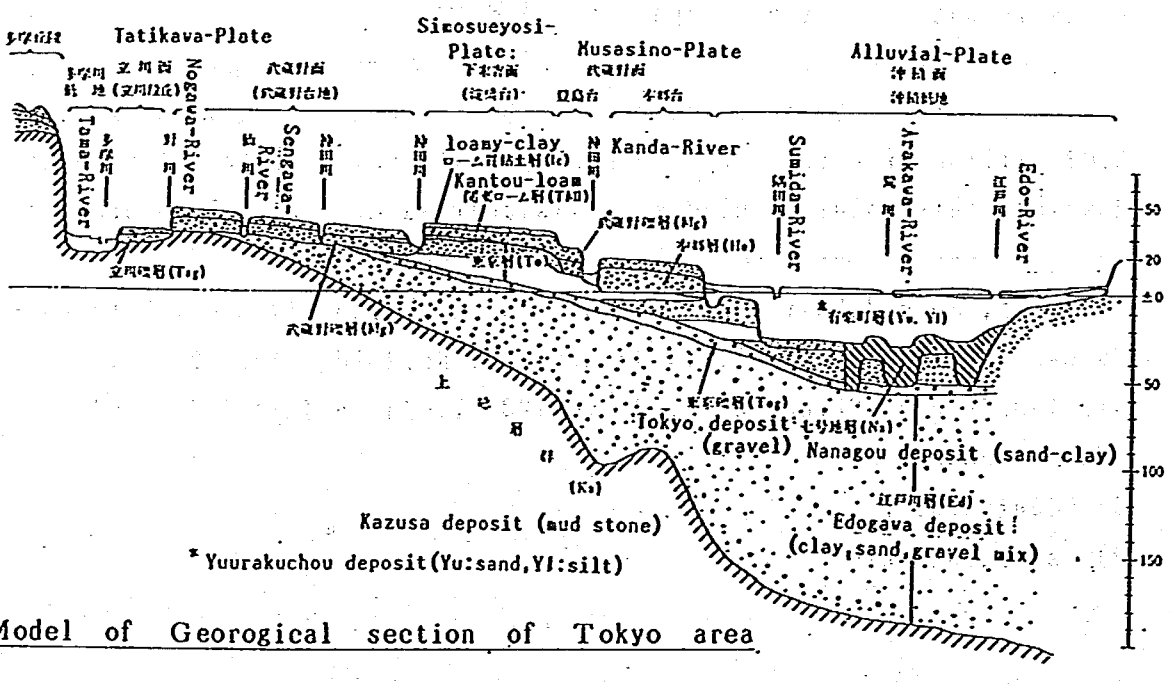
to restriction in the case of a water shortage. In summary, water resource rights are still extremely unstable.

Meanwhile, although overall water demand has remained more or less constant during the past few years by reason of a decrease in the leakage rate, pervasive use of water conserving devices and an increase in the number of buildings equipped with water recycling facilities, factors such as progressive urbanization of the Tama district, increasing numbers of high rise residential and commercial buildings and an increase in the number of buildings being constructed all point to gradual growth of water demand for the future.

Under the circumstances, it is the intent of the Bureau to actively encourage water conservation and recycling of water resources as a top priority, and to promote realization of the Water Conservation Conscious City concept.

[2] Georogical situation and seismic Design Criteria

The Kanto district including Tokyo Metropolis had to suffer from the serious damages of the Great Earthquake in 1923, and earthquakes of the similar magnitude had been recorded every 60 to 80 years in the past. Accordingly, seismic criteria of M = 8.0 and 50km distance to the epicenter which are equivalent to those of the Great Earthquake are adopted for the seismic design of waterworks in Tokyo.



Model of Georogical section of Tokyo area

Ground of Tokyo Metropolitan district is covered by a loamy surface soil plate (N ≒ 3) of 4 - 8m depth which sits on top of the alluvial deposit of soft viscous clay or sandy soil located 20m - 70m below the ground surface. Possibility of soil liquefaction is undeniable in a quarter of the geographically low lying section of Tokyo.

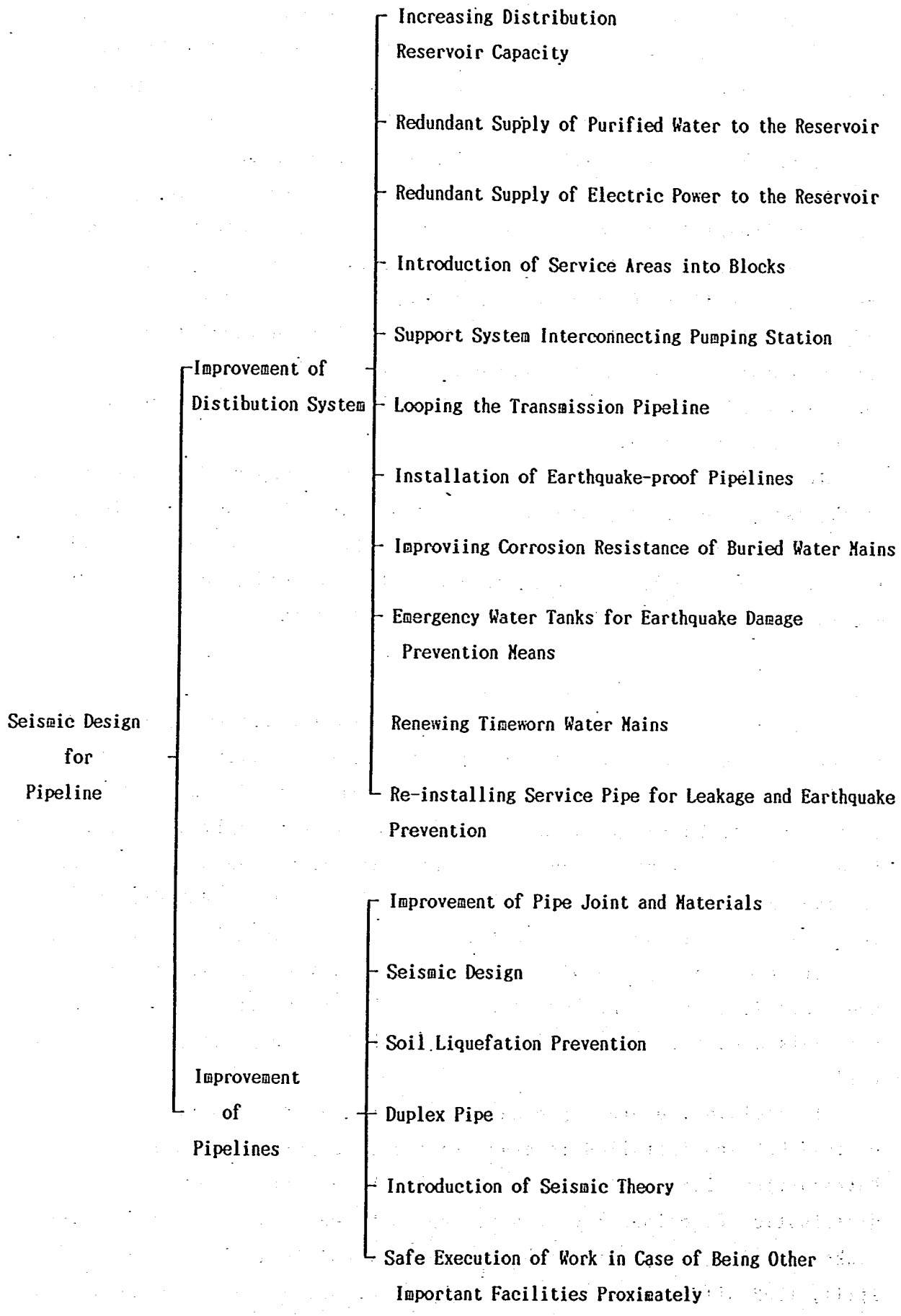
Damages to the pipelines inflicted upon by the Great Earthquake were most significant in the case of wooden housing which were found to have taken place more predominantly in the boundary between the hilly residential section of relatively solid ground in the west and geographically low lying section in the east than in the latter itself. This is considered due to the large relative displacement of ground because ground conditions vary significantly along the pipeline axis at the boundary of strata.

Similarly, damages inflicted upon the water supply pipelines by the earthquakes which took place recently in Niigata district or middle part of Japan Sea district were found predominantly in the breakaway of pipe joints,snapping or breakaway of pipe branches or bend pipes, snapping or breakaway at the connecting to structures and so on.

[3] Basic Policy of Seismic Design for Pipeline

The seismic design adopted is not only to upgrade the quality of the system as a whole but also to incorporate various measures aimed to localize failures in order to prevent dissemination of the faults to larger extent. Taking pipelines for example, water supply area is divided into small water supply blocks which are interconnected with each other, or pipelines are looped or laid in east-west or north-south directions so that the system is more resistant to faults or earthquakes. Likewise, most of water conveyance pipelines and important water distribution mains are designated to be earthquake resistant by virtue of the reinforced materials used for pipes and pipe joints while slip-proof pipe joints are used.

In addition, emergency clear water tanks as the measure to counter earthquakes are installed in order to ensure supply of potable water to Metropolitan citizens in preparation for the situation where water distribution functions had been disrupted by earthquakes. Clear water tanks of 1,500m³ capacity each were operational in 42 locations as of April, 1992 within Tokyo Metropolis, each of which can serve the area of 2km radius. Additional 18 clear water tanks are scheduled to be installed by the year 2000. When completed, those tanks together with


Seismic Design for Pipeline
Improvement of Distibution System
Increasing Distribution Reservoir Capacity
Redundant Supply of Purified Water to the Reservoir
Redundant Supply of Electric Power to the Reservoir
Introduction of Service Areas into Blocks
Support System Interconnecting Pumping Station
Looping the Transmission Pipeline
Installation of Earthquake-proof Pipelines
Improviing Corrosion Resistance of Buried Water Mains
Emergency Water Tanks for Earthquake Damage Prevention Means
Renewing Timeworn Water Mains
Re-installing Service Pipe for Leakage and Earthquake Prevention
Improvement of Pipelines
Improvement of Pipe Joint and Materials
Seismic Design
Soil Liquefation Prevention
Duplex Pipe
Introduction of Seismic Theory
Safe Execution of Work in Case of Being Other Important Facilities Proximately

water distribution tanks should be capable of serving the entire Tokyo Metropolis.

While water supply pipelines not only would have to be resistant to severe earthquakes and soft ground strata but also would be obliged to be laid under severer working conditions in conflict with city gas and sewagepipelines or underground railways beneath the public road, efforts are being made to establish seismic design applicable to pipelines.

As above reason, two approaches can be considered in order to achive earthquake-proof life line design.

One approach would be to upgrade earthquake-proof as a system, while the other would be to improve the earthquake-proof of individual components, constructed facilities and methods of construction.

[4] Seismic Design for Pipeline

[4-1]Improvement of distribution system

1) Increasing distribution reservoir capacity

The capacity of existing distribution reservoirs is equivalent to about eight hours' maximum daily water demand. In certain areas in the Tama district where support is not easy however, it is possible to secure distribution reservoir capacity equivalent to about 18 hours' water demand. In the future, it is intended to secure distribution reservoir capacity equivalent to at least ten hours' water demand.

2) Redundant supply of purified water to the reservoir

All water distribution facilities are capable of recieviing water from at least two water puritication plants, to prevent disruption in case of a failure affecting a purification plant or a conncting pipeline.

3) Redundant supply of electric power to the reservoir

All pumping stations are equipped with connections capable of receiving power from at least two supply systems.

4) Intrdction of service areas into blocks

The system has been changed to devide water supply service area into small block so that a fault in one will not affect the others. There is a pumping station for every block.

5) Support system interconnecting pumping stations

In anticipation of a pumping station failure or any similar problem,

the pipeline structure has been altered so that individual pumping stations shall henceforth be changed by operating valbes, and they can back each other up in case of failure.

6) "Looping" the transmission pipeline system: reinforcing the water suply network

Instead of viewing the water supply service areas of Tokyo Metropolis as a set of discrete points or lines, the entire system shall be reinforced by viewing the system as a continuous plane. To be more precise, the water supply pipeline system shall be made into a looped system that covers the entire service area. Work is now in progress to interconnect direction so that water can be conveyed toany point in the network.

7) Installation of earthquake-proof pipelins

Most distribution pipelines and important water mains are designated for earthquake-proof construction in which flexible anchoring joints are used.

8) Improving corrosion resistance of buried water mains

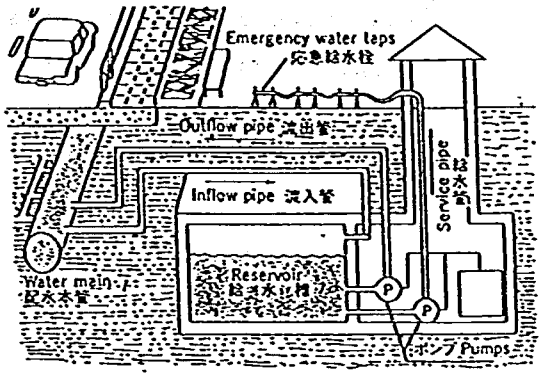
All buried pipelines installed since the year 1976 are covered by polyethylene-sleeves in order to prevent corrosion.

Buried pipelines are subject to attack by various agents of corrosion: iron bacteria, sulfate-reducing bacteria, acid soil, localized galvanic corrosion and electric corrosion due to stray current from electrified railways are all problems. Corrosion of the bolts used in joints is a particularly significant problem. Accordinly, buried pipelines are covered by polyethylene sleeves in addition to the coating applied to the pipes.

9) Emergency water tanks for earthquake damage prevention meanses

In order ti guarantee supply of potable water to Tokyo's citizens in the event of an earthquake, emergency water reservoir are being installed.Each reservoir stores 1,500 ㎥ of potable water at all times. 42 reservoirs, each expected to serve an area of 2 ㎞ radius, had been instaled in separate locations throughout Tokyo as of April,1992. An additional 18 earthquake-proof emergency reservoirs are expected to be installed by the year 2000 so that the entire metropolitan area can be covered.

Structure of Emergency Water Tank (EWT)
応急給水槽の構造



Water is piped into the tank from the distribution main via inflow pipes. A circulating pump returns the water to the main via the outflow pipe to circulate the entire contents of the tank.

10) Renewing timeworn water mains

The Tokyo water supply system will soon celebrate its centennial as a modern water supply system.

Those pipelines installed before World War II are of inferior quality and are quickly becoming superannauated. Most pre-war pipelines have already been renewed, while those installed within 10-20 years after the war are to be renewed progressively so that water leakage and earthquake-proof can be improved.

11) Reinstalling Service Pipe for Leakage and Earthquake prevntion

Lead pipes were used up until the year 1977 for service lines branching off to individual households. In order to reduce water leakage and improve earthquake-proof, those lead pipes have been replaced by flxible stainless steel pipes which are capable of withstanding land subsidence and earthquakes.

[4-2] Improvement of Pipelines

<Pipe joint and pipe materials>

Water conveyance and water distribution pipes are required to be water tight, high corrosion resistivity and durability.

Materials used and construction of pipe joint vary by the types of the pipe. The type to match the laying environment is selected in consideration of flexibility, expandability, toughness, slip resistivity and so on.

Water conveyance and distribution pipe materials actually used in the waterworks in Tokyo are cast-iron, high grade cast-iron, ductile cast-iron,steel, and stainless steel.

Also, pipe joints actually used are diverse in types and include socket type (hemp and lead), A type, K type, S II type; S type, U type, UF type, US type, PI type, flange pipe joint, and welded pipe joint.

During the period beginning in year 1892 through year 1960, the fixed type socket pipe joint water tightness of which was secured by the swelling of hemp packing which was held in position by molten lead was the only type available. This type is poor in flexibility and subject to pipe deformation and slippage of pipe joints.

Since year 1960, mechanical pipe joints and ductile cast-iron pipe were introduced, and then workability to lay pipe, and expandability and flexibility of pipeline have been improved. Through further improvements of pipe joints with expandability and slip-proof mechanism, highly earthquake resistant pipeline have been constructed.

External pipe joint is easy to work and better suited for medium and small diameter pipes.

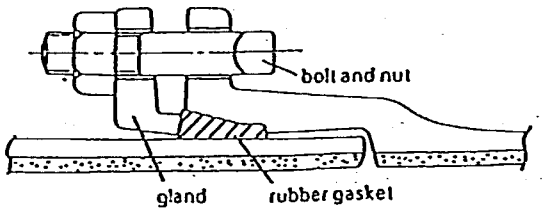
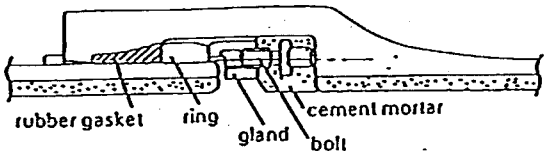
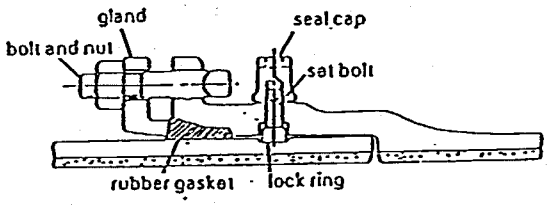
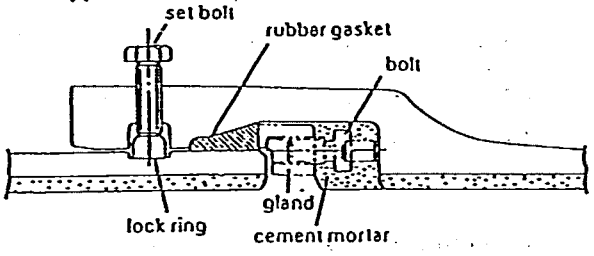
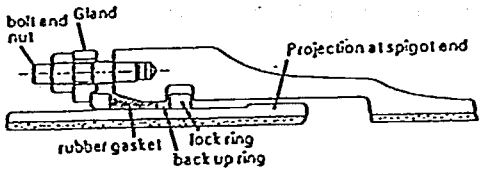
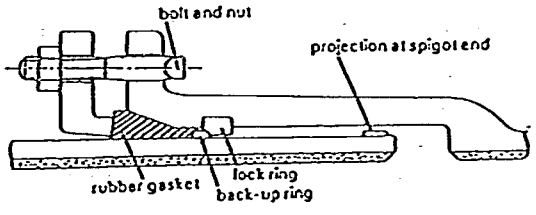
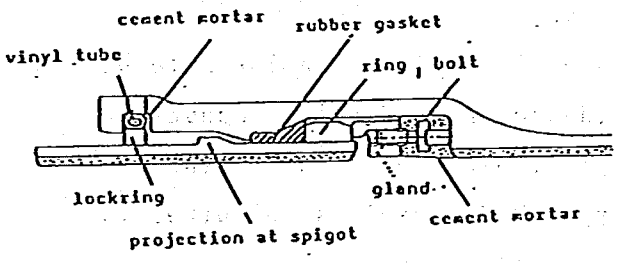
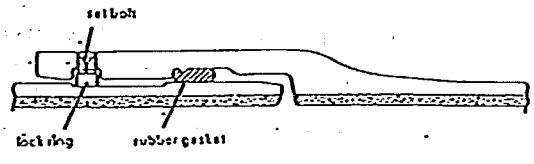
Internal pipe joint is rather complicated to work but is better suited for large diameter pipes because trench width can be smaller by virtue of the internal coupling. Advanced pipe joint designs and improved materials used have lead to the higher degree of safety of the earthquake resistant pipeline.

<Examples of the damage>

The total length of water distribution mains at the time of the Great Earthquake in year 1923 was 970km and the pipe used was ordinary cast-iron (brittle cast-iron of high carbon content having allowable tensile strength of 15kgf/mm² - 12.5kgf/mm²) to be coupled by the fixed type socket pipe joints.

Damages inflicted upon by the earthquake were significantly cracking

TYPICAL JOINT

STRUCTURE	STRUCTURE
FLEXIBLE JOINT	
K type 	U type 
RIGID JOINT	
KF type 	UF type 
CHAIN STRUCTURE JOINT	
S type 	SII type 
US type 	PII type 

of large diameter pipes longitudinal to the pipe axis and circumferential snapping of small diameter pipes. Damages due to the ground or topography are converged on the locations where solid strata changes being followed by the locations of soft ground, but not on the locations of diluvial ground. With respect to the structural form, damages were found often in deformed pipes (T-branch pipe, bend pipe) or near of aqueducts.

<Seismic Design>

Based on those experiences, seismic design for pipeline must incorporate measures to cope with (1) locations where ground strata shift and pipeline support structure varies, (2) change in the structure of pipeline (Bend pipe, T-branch pipe, reducer pipe, interface with pipeline support structure and so on), (3) soil liquefaction.

In the case of pipelines with couplings, pipe joints having expandability, flexibility and flexuosity (K type, U type, KF type, UF type and so on) are used for solid ground. In the locations of soft ground however, earthquake resistant pipe with chaine structure joints construction having slip-proof mechanism in addition to expandability and flexibility (S type, S II type, US type, P II type) are used.

Furthermore, collars or flexible pipes having sufficient expandability and flexibility are used continually in the locations where ground strata shift so that displacement can be absorbed or dispersed onto the pipeline.

In the locations where pipeline configuration varies, point of the shiftis locally protected by concrete and collars or flexible and expandable pipes are uses near the point of the shift so that displacement can be absorbed.

<Soil Liquefaction Prevention>

Soft sand strata containing fine grain sand of high percentage in its surface layer are extensively distributed in the geographically low lying section of Tokyo Metropolis where possibility of soil liquefaction is undeniable. A quarter of this section is expected to have possibility of soil liquefaction in the event of severe earthquake.

On the other hand, underground water level is not allowed to become lower in order to prevent ground subsidence. Accordingly, foundation improvement, pile foundation, duplex pipe, pipe joints of chained construction (S type, S II type, US type, P II type), steel pipes to construct a solid pipeline of high toughness are used.

P Ⅱ type pipe joint which is expandable and is provided with slip-proofmechanism and has such a construction capable of withstanding the frictionby preventing direct application of propulsive force to the pipe joint hadbeen developed for use in the medium and small diameter propulsion pipeline for a long distance.

<Duplex pipe>

Pipelines crossing important trunk road, railway, rivers are provided with centrifugal reinforced concrete outer pipes to be laid either by propulsion technique or open cut trench excavation technique in which water conveyance and distribution pipeline is laid in order to make the system into a duplex pipeline. In this case, seismic force and other external load is directly borne by external pipe and internal pipeline is provided with flexible and expandable pipe joints at the both end of external pipeline. Gap between external pipeline and internal pipeline is filled either by sand or by foamed mortar in order to provide cushion for the buoyancy or vibration of the internal pipeline.

In the case of large bore pipeline, water conveyance and distribution pipeline is drawn into a sealed tunnel in order to make the system duplex. In this case, sealed tunnel is either left unfilled in order to provide a passage for the inspection of water conveyance and distribution internal pipeline or filled with concrete.

<Introduction of Seusmic Theory>

During recent years, most of large bore pipelines are laid in shiled tunnels which are constructed at progressively increasing depths, more than 40m deep in certain locations.

In the case of medium and small bore pipeline, propulsion distance is more than 200m in certain locations.

Load conditions and impact of other factors are calculated by the finite element method at the time of design depending upon the significance of the route or unfavorable soil conditions or presence of significant proximate structures.

In addition, settlement gauges and clinometers are installed during the construction work in order to verify the design.

In the case of important trunk pipelines to be laid in the location where soil condition and other work environment are not favorable, seismic design theories including response displacement method, dynamic

response analysis and dynamic finite element method are applied in order to reflect the results in the earthquake resistance of pipelines.

<Safe Executiion of Work in Case of Being Other Important Facilities Proxmately>

Waterworks pipelines are generally buried underground similarly to the buried facilities of other public utilities (city gas, electric power, tele-communication, sewage and so on). As the result, waterworks pipelines are always proximate to other facilities, and in certain cases are obliged to be laid immediately above or under subways or immediately adjacent to bridge pier piles. It is therefore necessary to survey environmental conditions and soil conditions of the proposed pipeline route in advance to the work so that work method which takes earthquake resistance into consideration must be implemented. In the locations where ground conditions are not favorable, earthquake resistant slip -proof pipe joints and flexible and expandable pipe joints are used. Also, foundation works, foundation improvement works, and relief prevention works are implemented for the laying of small and medium bore pipelines with emphasis on trench excavation works.

For the laying of large bore pipelines by means of sealed tunnel technique, sealed technique by means of closed sealed equipment while impact of various factors is analyzed by means of finite element method and protection is implemented by means of peripheral foundation improvement for the works to pass under or the side of important structures (railway tracks, river works). Furthermore, in the case of waterworks pipelines being laid within the proximity of important structures, settlement gauges, clinometers and strain gauges will be installed directly onto adjacent structures as well as in proximate underground so that measurements can be compared to design values and simultaneously transmitted real-time through the telephone circuit to the central computer for centralized monitoring and control. By this arrangement, situation can be comprehended on real-time basis to be reflected upon safe execution of works and to serve future maintenance management.

[5] Example of the seismic design of sealed tunnel

(1) Outline

The sealed tunnel introduced herein is the one which crosses Arakawa River and Nakagawa River out of water conveyance trunk lines which start from Misato Water Purification Plant and arrive at Tokyo water front via Mizumoto Pumping Station and Kanamachi Purification Plant by crossing eastern part of Tokyo Metropolis from north to south.

Seismic design of the subject sealed tunnel was made by means of response analysis in order to calculate axial force to apply to the tunnel which was reflected on the design.

Design assumption of the subject sealed tunnel is scheduled to be verified by installing accelerometers and displacement gauges.

(2) Outline of calculation

a) Location

1-chome Seishincho, Edogawa-ku 3-chome Arasuna, Koutou-ku

b) Tunnel length

l = 922.4m

c) Outline of geological features

Geological formation within the vicinity of TP-30 through which the tunnel passes is lower Yurakucho deposit (Y1 deposit) which is an extremely soft silt deposit with average N value being 1 - 2. Tokyo deposit with N value being more than 50 lies underneath Yurakucho deposit in TP - 35 - 65m holding No.7 deposit in between.

d) Plan and vertical cross section

e) Scale of earthquake used in earth quake resistance calculation is equivalent to the scale of the Kanto Great Earthquake (M = 8, distance to epicenter (Delta) = 50km)

f) Calculation model

Calculation was made on the basis of following assumptions by means of multiple material points dynamic response analysis model including vertical shaft construction.

① Position of earthquake resistant layer of the ground is assumed to be in the Tokyo deposit having N value greater than 50.

② Deformation of bolts and face plates is taken into consideration in the event of tensile force applying to the tunnel.

③ Earthquake is assumed to be coped with by primary covering work only.

④ Vertical shaft junction is examined for the case of rigid junction and for the case of soft junction.

g) Process of calculation

Ground fluctuation as used in the verification of earthquake resistance is assumed to remain within allowable stress for the scale of underground multi-purpose duct design guideline (M = 7, distance to epicenter (Delta) = 50km) and within the extent the covering work body does not develop permanent deformation and within yield stress. However, in consideration of indeterminate factors involved in the evaluation of ground stratum and other elements, ground fluctuation was finally assumed to be within the allowable stress corresponding to the Kanto Great Earthquake. As the result of the calculation by dynamic analysis for the case of flexible segment being installed in the vicinity of vertical shaft for the former (scale of underground multi-purpose duct design guideline) (soft junction) and for the case of rigid junction between vertical shaft and the tunnel, it was confirmed that tensile force in axial direction is far smaller for soft junction than for rigid junction.

Accordingly, the subject sealed tunnel was to be constructed by soft junction where flexible covering work is installed in the vicinity of both vertical shafts while results of recalculation for the case of the latter (equivalent to the Kanto Great Earthquake) were adopted as design values.

(3) Reflection on the design

① Design of primary covering work (segment)

. Concrete covering work which is durable and economical was adopted for the construction of primary covering work.
. Vertical and horizontal earth load to apply to the primary covering work was assumed to be total earth covering load.
. Thickness of primary covering work was designed to be t = 300mm based on the concept of withstanding entire earth covering load.
. Construction of bolted joint of the covering work was ductile joint based on the examination of rigid joint which is theoretically durable.
. The joint was assumed to withstand tensile force in axial direction by itself. . Bolts which joint rings in longitudinal direction were

examined because construction of primary covering work is predominant in case tensile force applied to the covering work body. As the result, bolt size was determined to be M30 and made of material 10.9 (a = 4,500kgf/㎠).

② Design of secondary covering work

. Secondary covering work is to be constructed to protect and to reinforce primary covering work which is the main structure of sealed tunnel as well as the finish of vacant space in the tunnel.
. Construction of secondary covering work was designed to be such as to ensure safety when entire water pressure applies to the secondary covering work in the direction of longitudinal section of secondary covering work when water pressure applied to the sealed tunnel.
. Reinforcing steel bars having strength proportional to the ratio between the rigidity of primary covering work segment and secondary concrete covering work at the time of earthquake being equivalent to the strength of intering bolts to joint primary covering works were used.
. As the result, in order to upgrade degree of safety of the tunnel as a whole because the sealed tunnel is to be laid under the river bed, secondary covering work was provide by longitudinal and circumferential reinforcing steel bars. Thickness of secondary covering work was established to be 250mm in order to supplement objective of the secondary covering work and in consideration of the thickness sufficient to secure safety of the tunnel as a whole.

③ Design of water conveyance pipe

. Water conveyance pipe used was ductile pipe together with US type internal joint which is provided with slip-proof mechanism.
. Flexible segment was so configured to be capable of responding to maximum displacement.

④ Outline of earthquake monitoring instrumentation

Behavior of sealed tunnel and vertical shaft is monitored by installing an instrumentation system in order to comprehend in what manner analytical values obtained in advance by [study of earthquake resistance of sealed tunnel during earthquake] behave.

(a) Accelerometers are installed in the tunnel and in vertical shaft

while displacement gauges are installed in primary covering and secondary covering works.

(b) Monitoring is automatic for earthquakes of the intensity greater than 3.

(c) Results of monitoring shall be processed to be compared with preliminary analysis and to be verified by confirming performance of the construction of covering works in cross sectional plane of the tunnel obtained by engineering study and to monitor displacement of flexible segment.

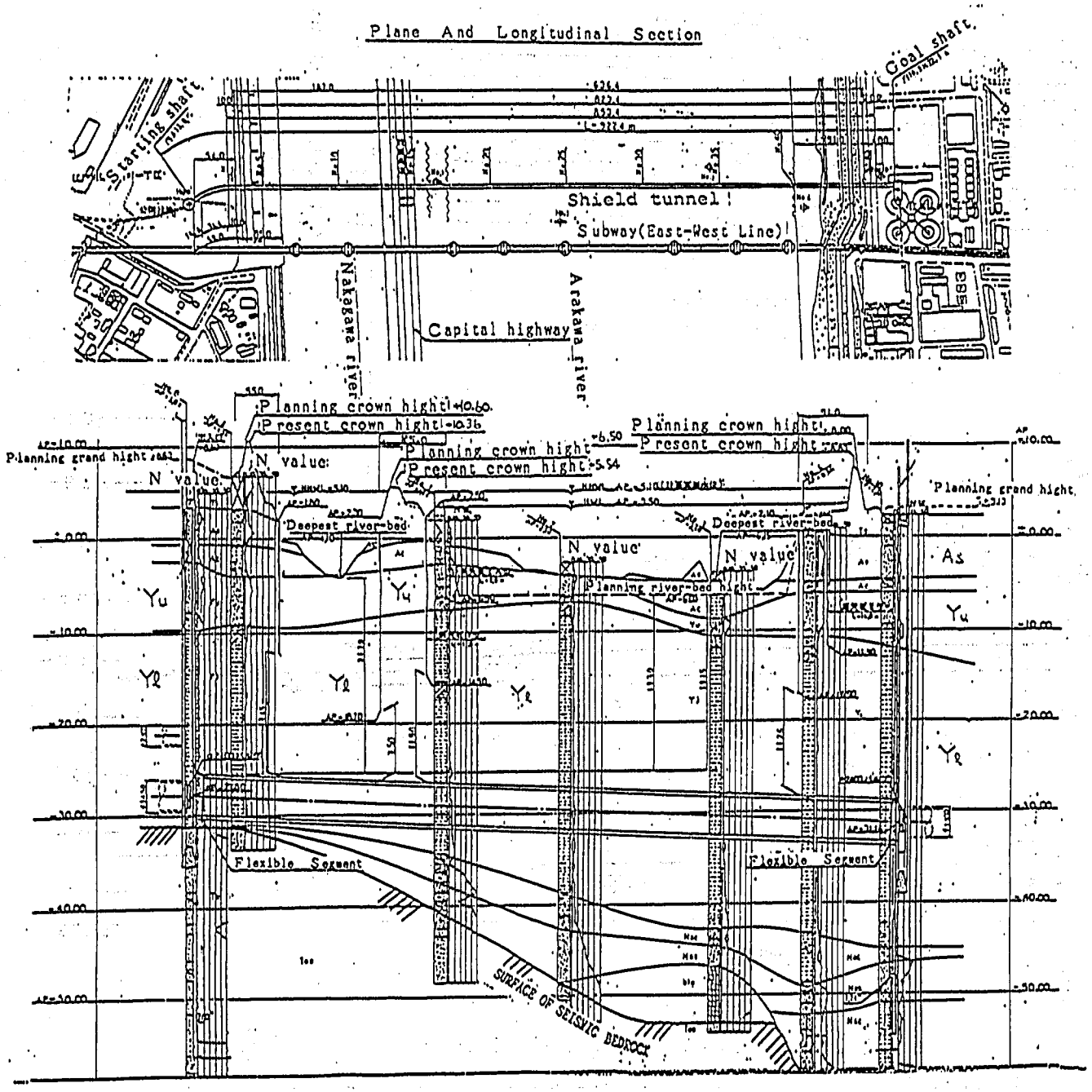
[6] Closing

Due to restrictions applying to the pumping of underground waater, enacted toalleviate land subsidence, there are practically no alternatives other than tap water for drinking water. Nevertheles, the increasing numbers of hospitls and office computer facilities which operate 24 hours a day, together with trends in the behavioral pattern of metropolitan citizens in the amusement quater, indicate an accelerating transition into arond-the-clock urban activity that necessitates a continual supply of water, even in the event of accident or earthquake.

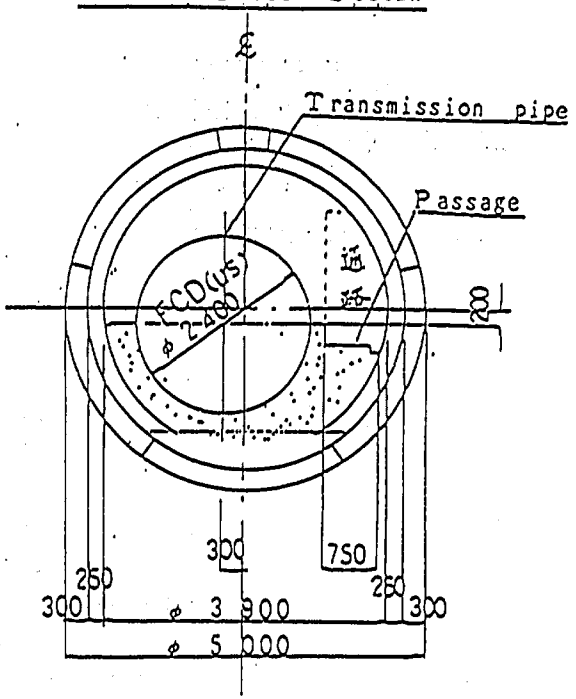
In consideration of the recent modification of the building code under which wooden houses are allowed now to be built to three stories instead of just two, the need has arisen to prepare for future high pressure water mains that can directly supply more buildings without a need for receiving tanks.

In order to cope with these various requiremens, the Bureau aim to improve both the quantity and quality of water supplied, to maintain appropriate water presssure, to prevent inadvertent incidents hindering water supply, and to guarantee stable water supply without disruption even by accidents and earthquakes.

Plane And Longitudinal Section



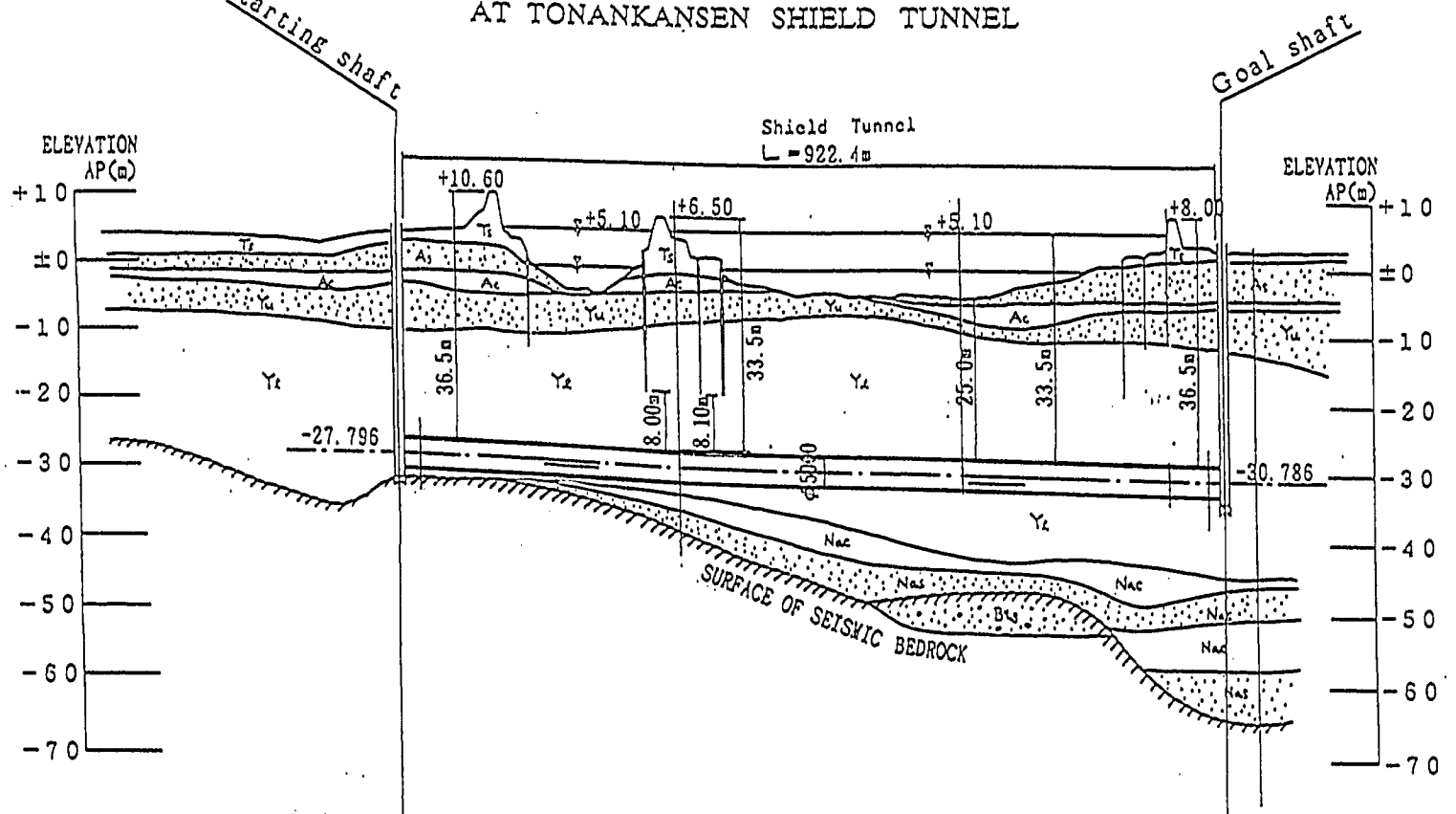
Tunnel Cross Sectin



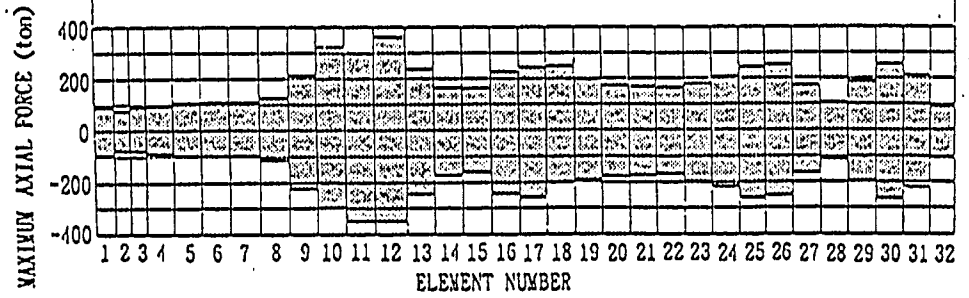
GEOLOGICAL FEATURE

Ts : TOP SOIL
Ac : ALLUVIAL CLAY LAYER
As : ALLUVIAL SAND LAYER
Yu : ALLUVIAL YURAKU-CHO CLAY LAYER (UPPER)
Yl : ALLUVIAL YURAKU-CHO CLAY LAYER (LOWER)
Mac: DILUVIAL MARITA CLAY LAYER
Mas: DILUVIAL MARITA SAND LAYER
Dtg: BURIED TERRACE GRAVEL

OBSERVATIONAL LOCATIONS OF EARTHQUAKE BEHAVIOR AT TONANKANSEN SHIELD TUNNEL



Result of Numerical Analyses of The Grate Kanto Earthquake in Case of Tunnel With Flexible Joint



GEOLOGICAL FEATURE

Ts : TOP SOIL
Ac : ALLUVIAL CLAY LAYER
As : ALLUVIAL SAND LAYER
Yu : ALLUVIAL YURAKU-CHO CLAY LAYER (UPPER)
Yl : ALLUVIAL YURAKU-CHO CLAY LAYER (LOWER)
Nac: DILUVIAL NARITA CLAY LAYER
Nas: DILUVIAL NARITA SAND LAYER
Btg: BURIED TERRACE GRAVEL

Session–4

Effect of Liquefaction

J–5) Stress Analysis Method for Steel Pipelines Buried in a Liquefied Ground Layer
(Iwata, T. and Ohtani, Y.)

J–6) Damage Assessment of Lifeline Facilities in Liquefied Area
(Hamada, M.)

J–7) Safety Estimation of Buried Pipes for Permanent Ground Deformation by Liquefaction
(Suzuki, H., Masuda, T., Sato, M. and Hamada, M.)

J–8) Experimental Study on Liquefaction Potential and the Uplift Deformation of Underground Structures
(Tokida, K., Ninomiya, Y. and Azuma, T.)

U–5) Lateral Spread Effects on Reinforced Concrete Pile Foundations
(Meyersohn, W.D., O'Rourke, T.D. and Miura, F.)

Stress Analysis Method for Steel Pipelines Buried in a Liquefied Ground Layer

Coauthors: Takashi Iwata, Senior Manager, Transmission Section, Tokyo Gas Co.; and
Yasuyuki Ohtani, Senior Engineer, Supercomputing Div. 3,
Fuji Research Institute

ABSTRACT

Extensive studies have been done on a phenomenon where the liquefied ground in which gas pipelines are buried, undergoes permanent displacement (incident to seismic impact), and the pipelines are damaged by ground displacement.

Using a large shaking table, we studied the permanent displacement caused by seismic impact on an inclined, liquefied soil layer. Precise measurements were taken of the changes in pore pressure during a process ranging from excited liquefication (caused by vibrating the ground layer), to initiation of permanent displacement (after halting the vibration), and eventually to recession of the displacement. Changes in the ground binding force and velocity of ground movement have also been measured. We expect that these studies are a significant breakthrough in the precise analyses of the effect that permanent displacement has on buried steel pipelines.

Because we expect that many researchers will announce the results of their research in this field, and because we want to precisely evaluate the effect of permanent displacement of liquefied ground on buried steel pipes as quantitatively as possible, we have developed a new nonlinear underground pipeline stress analysis system.

This system can precisely reproduce how the ground binding force,which is related to a change in pore pressure, can affect buried steel pipelines. In this process, liquefied ground, whose pore pressure peaks after the recession of ground vibrations, undergoes permanent displacement as its pore pressure decreases until the pressure vanishes and the displacement is terminated.

Specifically, given relevant data on changes in the ground binding force and the velocity of ground movement over time (in a process leading to final, permanent displacement), the system can simulate, even up to a nonlinear region, the specific magnitude of strain on buried pipelines after a period of time.

Given precise data on changes in the ground binding force and the velocity of ground movement which results from fluctuations in pore pressure (incident to the occurrence of permanent displacement), the system could precisely evaluate how a flexibly buried weld-jointed steel pipeline can withstand the impact of permanent displacement of liquefied ground induced by an earthquake. This is considered to be a serious issue facing public gas utilities.

INTRODUCTION

Damage to buried steel pipes in liquefied soil principally comes from dynamic displacement of liquefied ground (induced by an earthquake), and/or from permanent displacement of liquefied ground due to an inclination of the underlying ground layer, which remains unliquefied.

Our current studies focus on the permanent displacement caused by soil liquefaction, which is now one of the most popular themes of research. Specifically, we worked on a system that was capable of analyzing the impact of displacement on buried, weld-jointed steel piping. This system incorporates logic which is capable of precisely simulating a phenomenon where the ground binding force recovers following dissipation of pore pressure, and concurrently the ground displacement slows down. This occurs in a process where the permanent displacement of liquefied ground goes on after the cessation of seismic vibration. Therefore, this system should be available to effectively analyze the impact a permanent displacement of liquefied ground has on buried pipes.

ANALYSIS of BURIED PIPELINES in A LIQUEFIED GROUND LAYER

1. Analytical system

We have developed a technique for analyzing how the strain on a buried pipeline is affected by permanent displacement. The technique analyzes interim changes to the ground binding force and the velocity of ground movement during a process starting from the moment pore pressure starts, through diminishing pressure (after complete ground liquefication and recession of seismic vibration), to the moment the pressure vanishes.

1.1 System overview

This system is designed to analyze the behavior of buried pipes in a liquefied ground layer using the model of a three dimensional beam supported elastically.

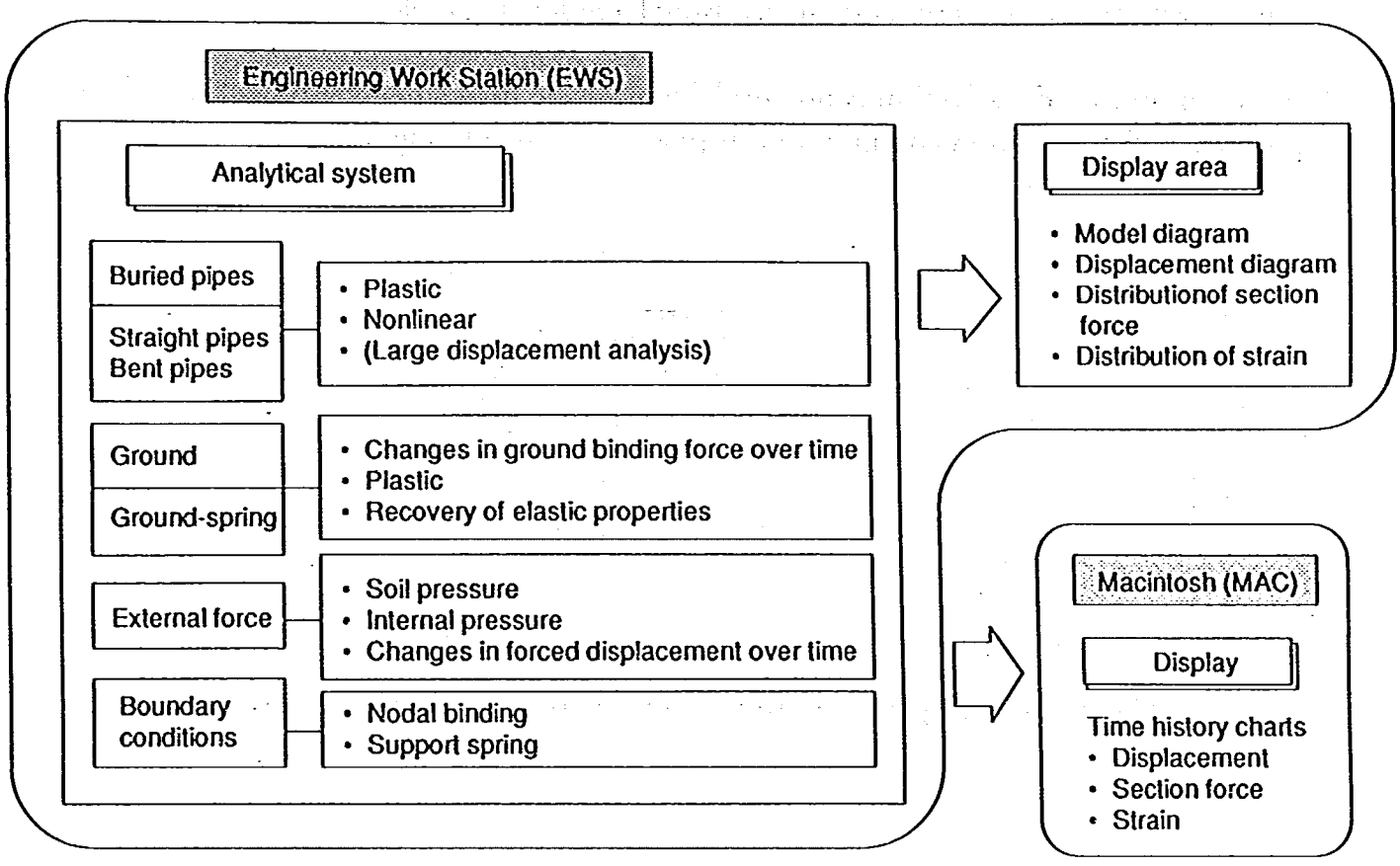


Fig. 1 System overview

1.2 Standard displacement input procedures

In the authors' view, changes overtime in the ground binding force and the velocity of ground movement following pore pressure changes have been generally identified from a qualitative point of view, but there has been no actual field measurement of these changes. At the moment, we are in an experimental stage, using large shaking tables.

Since optimum model selection is not available now, we used a general model capable of reproducing characteristics common to this phase, as shown in Fig. 2.

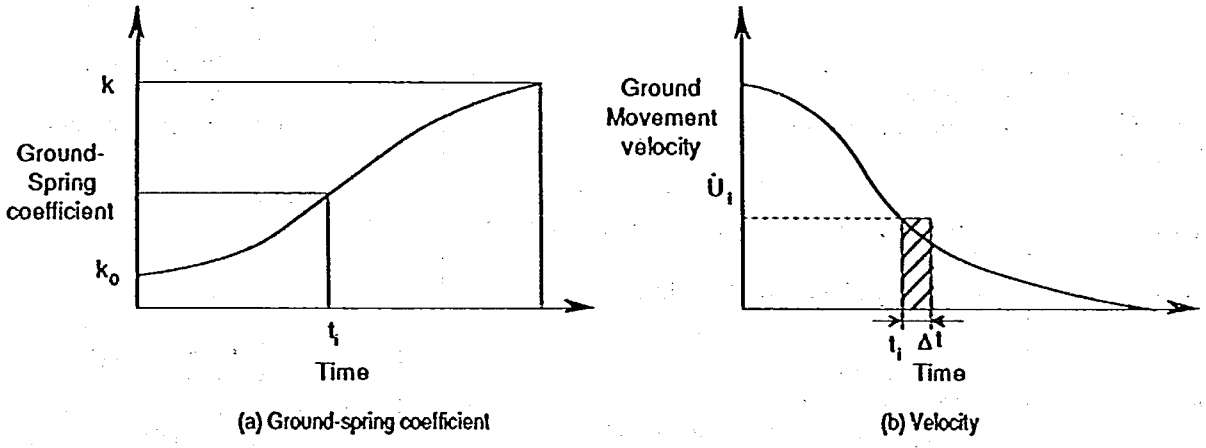


Fig. 2 Ground-spring reaction and velocity of ground movement

The system deals with these time-dependent changes as follows.

- The system can allow for arbitrary time-dependent changes to the ground binding force and the velocity of ground movement.

- Ground-spring coefficients and increments in permanent displacement between Δt_i at the time t_i through t_{i+1} are determined as follows:

$$k=k_i=k(t_i)$$

$$\Delta U=\Delta U_i=\dot{U}(t_i)\Delta t_i$$

The time step Δt_i can be set arbitrarily.

- Finite element analysis is made by incremental formula on ground-spring coefficients and permanent displacement.

- The slip limit of the ground-binding force is determined by the relevant k-value at t_i in the interval of Δt_i as follows:

$$\sigma_i^{cr} = k_i u^{cr} \text{ [kgf/cm}^2\text{]}$$

The analytical system also allows for an increase in the slip limit proportional to increase in the k-value.

Assuming that k-value changes as shown in Fig. 3(a), the system computes a relation between ground-binding forces and permanent displacement as shown in Fig. 3(b).

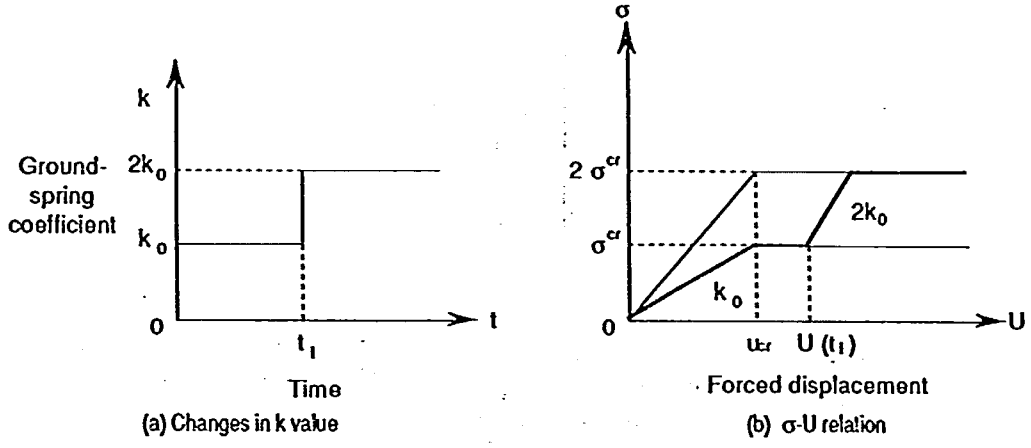


Fig. 3 Conditions for recovery of soil elasticity behavior

2. Analysis of permanent displacement effect

Considering changes to the ground-binding force and ground movement velocity with time, we analyzed a simply structured set of pipelines and ground, and examined the characteristics of this analytical system.

2.1 Analytical model

We analyzed the two different configurations of model pipelines illustrated in Figs. 4 (a) and (b). Assuming (a) that the Type A model has a bending of 90 degrees, and the Type B a bending of 135 degrees, and (b) that the ground has been liquefied around the bend in the range of 25 meters, we assume that two sets of 50-cm-long horizontal permanent ground displacement occurred along the pipeline opposite in directions. Ground spring varies during liquefaction and gradually increases as pore pressure dissipates.

Table 1 shows the physical properties of the buried pipeline.

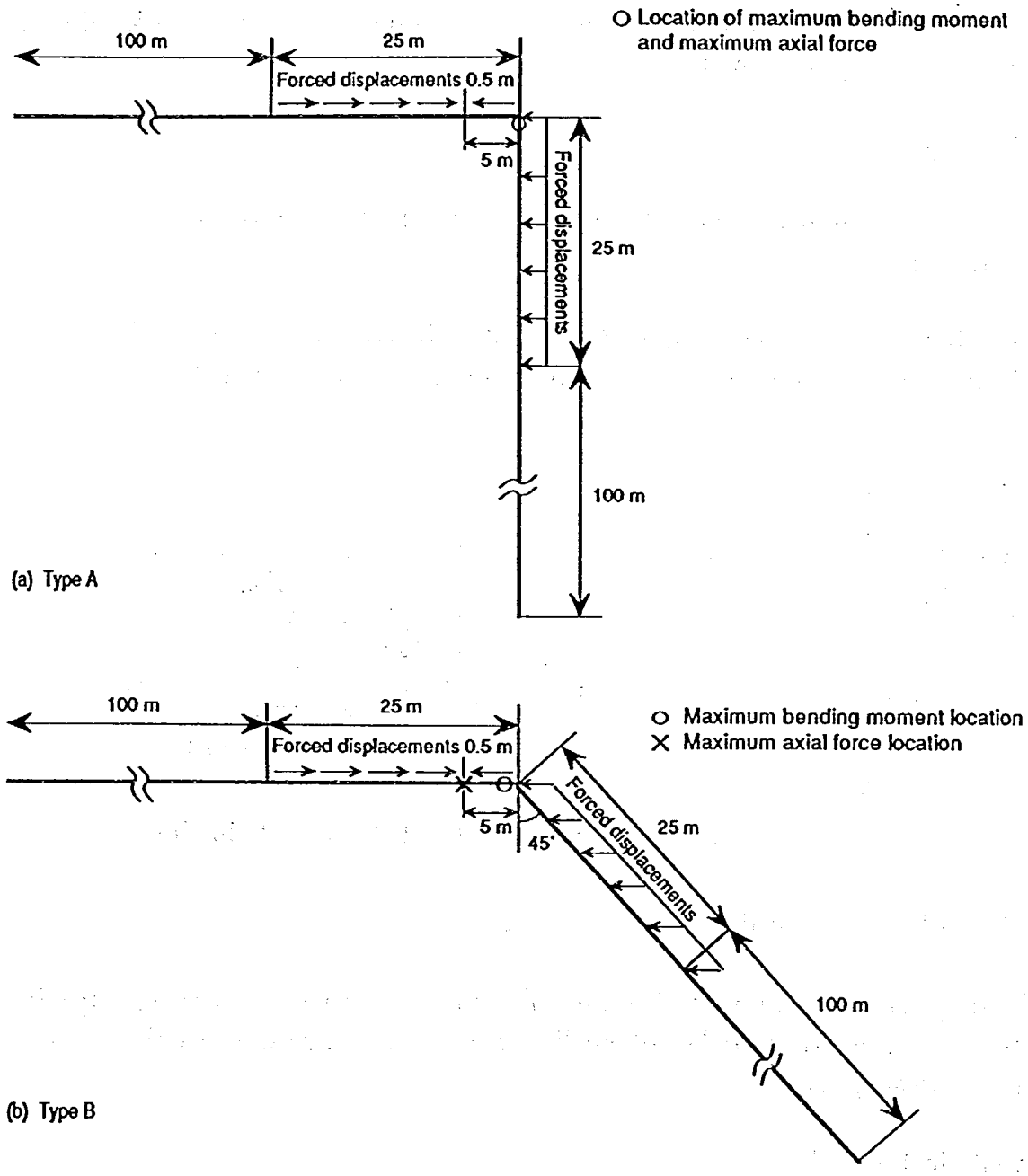


Fig. 4 Buried model pipeline model

Table 1 Physicul Properties of Buried Pipeline

Code name	O.D. (cm)	Thickness (cm)	Young's module (kg/cm^2)	Yield stress (kg/cm^2)
200 A	21.63	0.58	2.1×10^6	2079

Considering that ground spring acts in directions longitudinal and perpendicular to a pipe axis, we used the spring coefficient and critical binding force specified in the Recommended Practice for Earthquake Resistant Design of Gas Pipelines.

We assumed that the ground-spring coefficients in a liquefied phase had been reduced to one-tenth of the normal coefficient (Fig. 5).

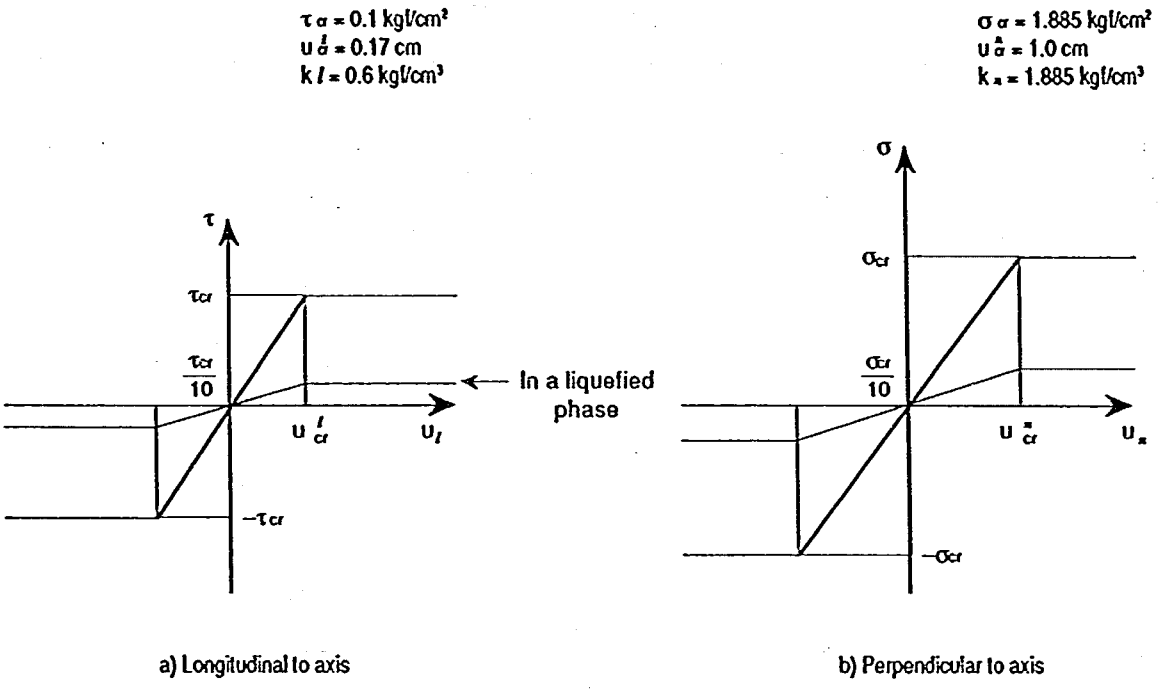


Fig. 5 Ground-spring coefficient

2. 2 Sensitivity analysis

We provide a number of models for time-dependent changes to ground-binding force and ground-movement velocity. We also conducted analyses of two cases where a ground-spring coefficient assumed a normal value of k_o and where it assumed one-tenth of the normal value because of ground liquefaction.

Table 2 lists the individual cases of analysis to be compiled in this report.

Table 2 Analysis Case Studies

Cases	Buried pipe model	Ground-spring and velocity
A1	Type A 90° bend	$k=k_o$, $\dot{U}$=constant
A2	"	$k=k_o/10$, $\dot{U}$=constant
A3	"	Fig. 6 (a)
A4	"	Fig. 6 (b)
A5	"	Fig. 6 (c)
A6	"	Fig. 6 (d)
B1	Type B 135° bend	$k=k_o$, $\dot{U}$=constant
B2	"	$k=k_o/10$, $\dot{U}$=constant
B3	"	Fig. 6 (a)
B4	"	Fig. 6 (b)
B5	"	Fig. 6 (c)
B6	"	Fig. 6 (d)

It is assumed that ground movement rapidly decelerates to some extent on recovery of ground binding force. In Case A3 (Case B3), changes occur quite linearly with time. For more reasonable variations with time, Cases A4 through A6 (Cases B4 through B6) are considered.

Figure 6 shows a model of changes to ground-spring coefficient and ground-movement velocity with time.

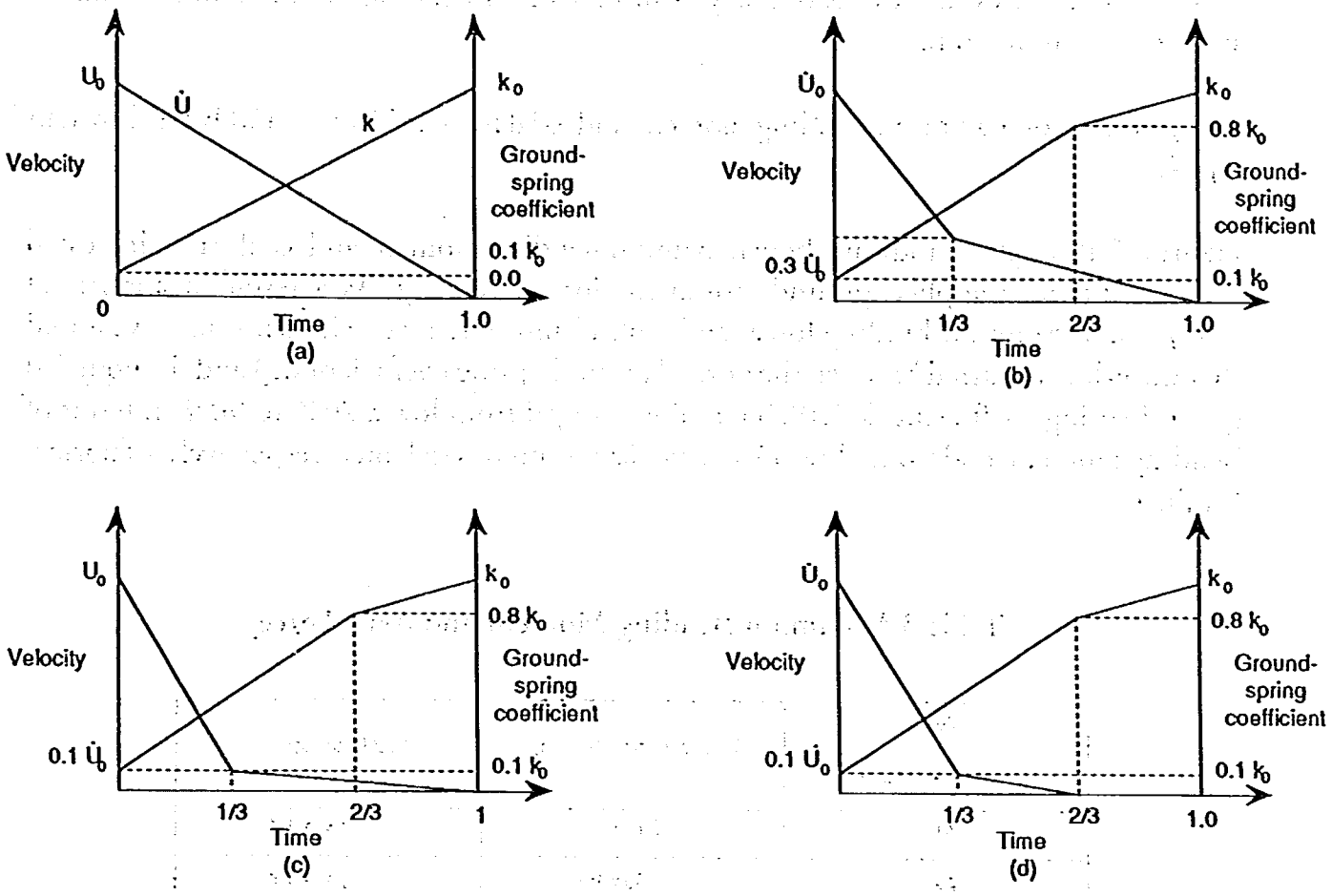


Fig. 6 Time-dependence models of ground-spring coefficients and ground-movement velocity

2.3 Results of analyses

Table 3 summarizes the results of analyses in maximum bending moment and maximum axial force of tested pipes.

The positions of maximum bending moment and axial force in Types A and B are shown in Fig. 4.

Figures 7 through 10 indicate how maximum bending moment and axial strain increased against externally applied ground-movement forced velocity. As a result of analysis of changes in the ground-binding forces and ground-movement velocity with time, we found that the values occurred between the normal ground-spring coefficient (k_o) and the liquefied ground-spring coefficient ($k_o/10$). The values ranged from low a 70% to 90% in terms of bending moment, and from a low 60% to 90% in terms of axial force, respectively, of normal k values.

Table 3 Maximum Bending Moment and Axial Force

Item Case name	Bending moment (kgf.cm)	Axial force (kg)
A1	2.71×10^5	2.65×10^4
A2	0.90×10^5	0.47×10^4
A3	2.45×10^5	2.40×10^4
A4	2.35×10^5	2.34×10^4
A5	2.09×10^5	2.15×10^4
A6	1.84×10^5	1.64×10^4
B1	1.94×10^5	4.04×10^4
B2	0.71×10^5	0.76×10^4
B3	1.75×10^5	3.61×10^4
B4	1.68×10^5	3.51×10^4
B5	1.51×10^5	3.22×10^4
B6	1.35×10^5	2.53×10^4

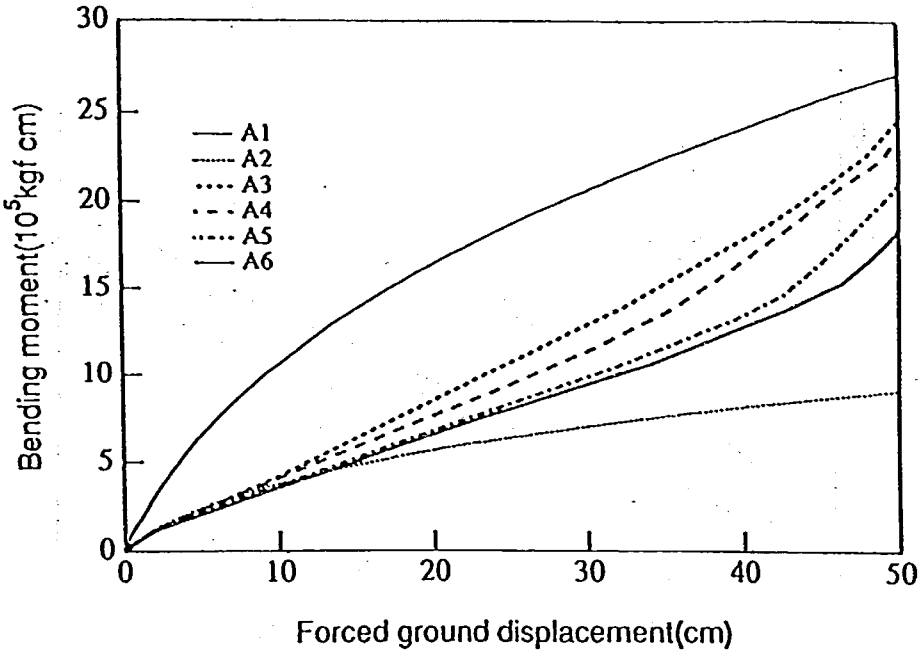


Fig. 7 Type A: bending moment versus forced ground displacement

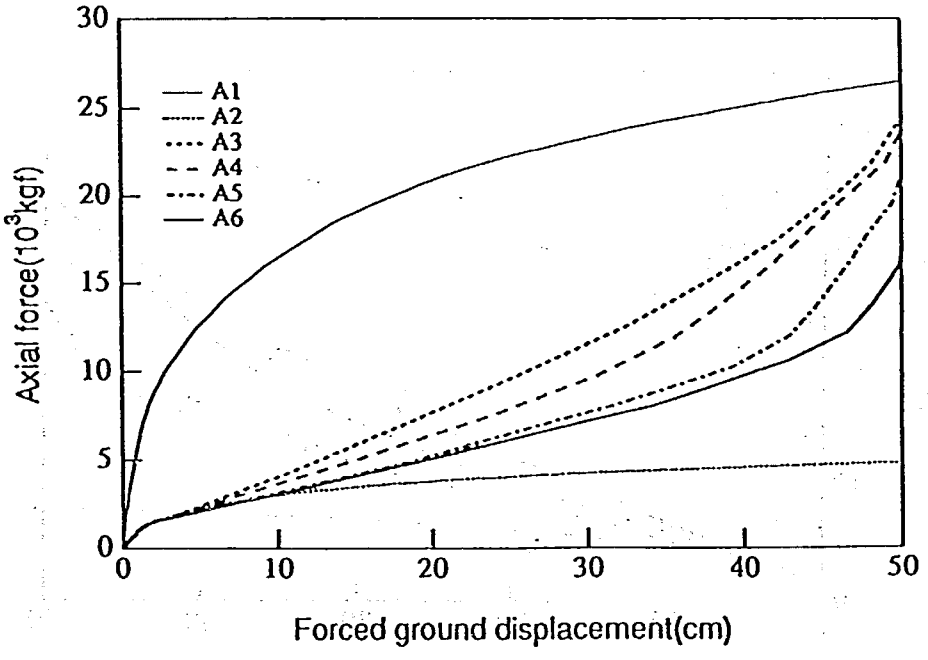


Fig. 8 Type A: axial force versus forced ground displacement

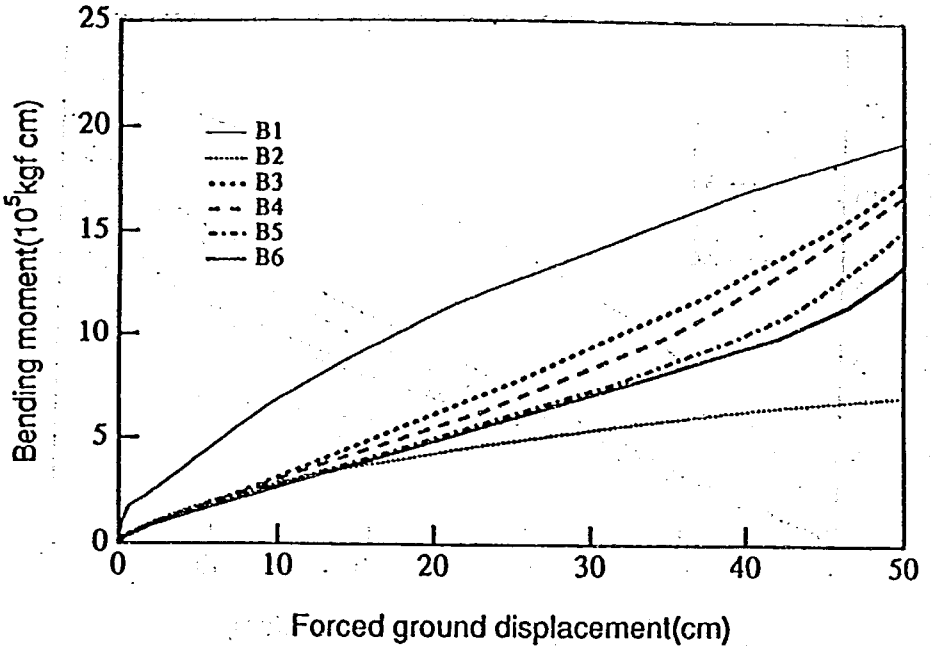


Fig. 9 Type B: bending moment versus forced ground displacement

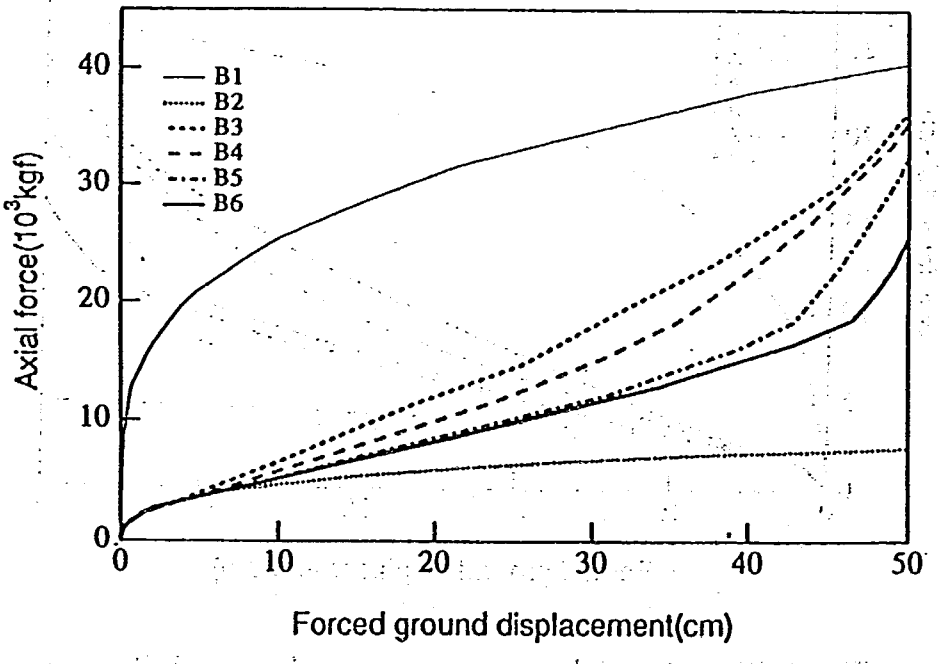


Fig. 10 Type B: axial force versus forced ground displacement

DISCUSSION

We conducted studies of changes to liquefied ground-spring coefficients and ground-movement velocity with time. In the initial stage where forced displacement ranged from 10 to 20 cm, there was no appreciable difference between time varying case and liquefied ground ($k=k_o/10$) in terms of effect on buried pipes. In the final stage, however, where forced displacement ranged from 40 to 50 cm, the effect on buried pipes sharply increased. In conventional analyses, pipe-to-ground slip displacement is constant. Accordingly once pipes and ground begin to slip against each other, forced displacement no longer can affect buried pipes regardless of the pipes' forced displacement.

This system, however, is designed according to the concept that the slip limits can increase in tandem with an increase in the ground-reaction factor. The critical ground-retaining force is thereby enhanced (Fig. 3).

For this reason, buried pipes are subjected to substantial external force when the k-value has increased in the final stage.

In this study, we conducted studies of the simplest case of linear changes with time as shown in Fig. 6 (a). We also studied cases of permanent displacement to piping occurring in earlier stages of the pore pressure dissipation process as shown in Figs. 6 (c) and (d). Between these, however, we found no substantial difference in the effect of permanent displacement because of time variations.

CONCLUSION

In the past, we often analysed the effect of permanent ground displacement on buried steel pipelines with regard to cases where the ground binding forces remain undiminished, or where the ground binding force decreases to one-tenth the normal value as a result of ground liquefaction. We found, however, that the effect of displacement allowing for time-dependent changes to pore pressure, interposes itself in the above cases. This also occurred in the present study.

These analyses provide relatively stable results, being minimally affected by differences in time according to the parameters used.

We hope that in the future, this analytical system will be used as an effective tool for precisely determining the effect of liquefied ground permanent displacement on buried weld-jointed steel pipelines. The system will be adopted after we come up with the results of extensive studies and experiments on permanent ground displacement using large shaking tables, as has been practiced by many research institutes.

DAMAGE ASSESSMENT OF LIFELINE FACILITIES IN LIQUEFIED AREA

Masanori Hamada

Professor of Civil Engineering
School of Marine Science and Technology
Tokai University, Shimizu, Japan

ABSTRACT

This paper first outlines the general procedure for damage assessment of lifeline facilities, including the estimation of loss of function. In particular, the method of the assessment of damage rate of buried pipes in liquefiable ground is introduced. Secondly, the present paper describes the current status of researches about liquefaction-induced large ground displacements and their effects on lifeline facilities, and propose future research subjects to be urgently solved for a reliable assessment of earthquake damage of lifeline facilities.

INTRODUCTION

Large-scale development projects are now proceeding along the waterfront in many major Japanese cities, including Tokyo and Osaka. These waterfront projects are often conducted on soft ground reclaimed from a sea or a river.

In the 1989 Loma Prieta earthquake, lifeline facilities were seriously damaged as a result of liquefaction of reclaimed land in the San Francisco Bay area. Furthermore, the 1990 Luzon, Philippines earthquake caused extensive liquefaction in Dagupan City and its surrounding area, resulting in serious of lifeline systems. These two earthquakes taught us the importance of earthquake resistant design of structures on and in reclaimed ground. Accordingly, local governments such as Tokyo Metropolitan Government and the companies providing lifeline services, such as electricity and gas, are now conducting a series of analyses for the assessment of damage resulting from a strong future earthquake. Pre-earthquake measures to reinforce facilities and post-earthquake recovery strategies are also being investigated based on the results of the damage assessment. In these studies, the effects on lifeline facilities of liquefaction-induced ground displacements are also being examined. This paper describes the current status of damage assessment of lifeline facilities, in particular, in liquefied area, and the reseach subjects to be urgently solved for a reliable assessment of earthquake damage of lifelines.

GENERAL PROCEDURE OF DAMAGE ASSESSMENT OF LIFELINE FACILITIES AND SYSTEM FUNCTION

The assessment of the damage of lifeline facilities, the loss of the function, and the recovery process has been conducted according to the flow chart shown in Figure 1. Lifeline facilities are generally distributed over a wide area, so earthquake activity is surveyed for the whole area. For the cities on the Pacific coast, such as Tokyo and Osaka, an undersea earthquake of the magnitude 8 class and an inland one of magnitude 7 class with the hypocenter right under the cities, are considered. If the earthquake is assumed to occur under the ocean, the effects of tsunami must be taken into consideration because some lifeline facilities such as thermal power stations are located on the coast.

The earthquake motion on the bedrock throughout the area on which lifeline facilities are distributed is estimated by using attenuation formulae. A correct estimation of the earthquake motion in the neighborhood of earthquake faults will be one of the important subjects, since a number of facilities are located in the fault zone in the case of an inland earthquake and the high damage probability of those facilities has a great influence on the overall functioning of the system.

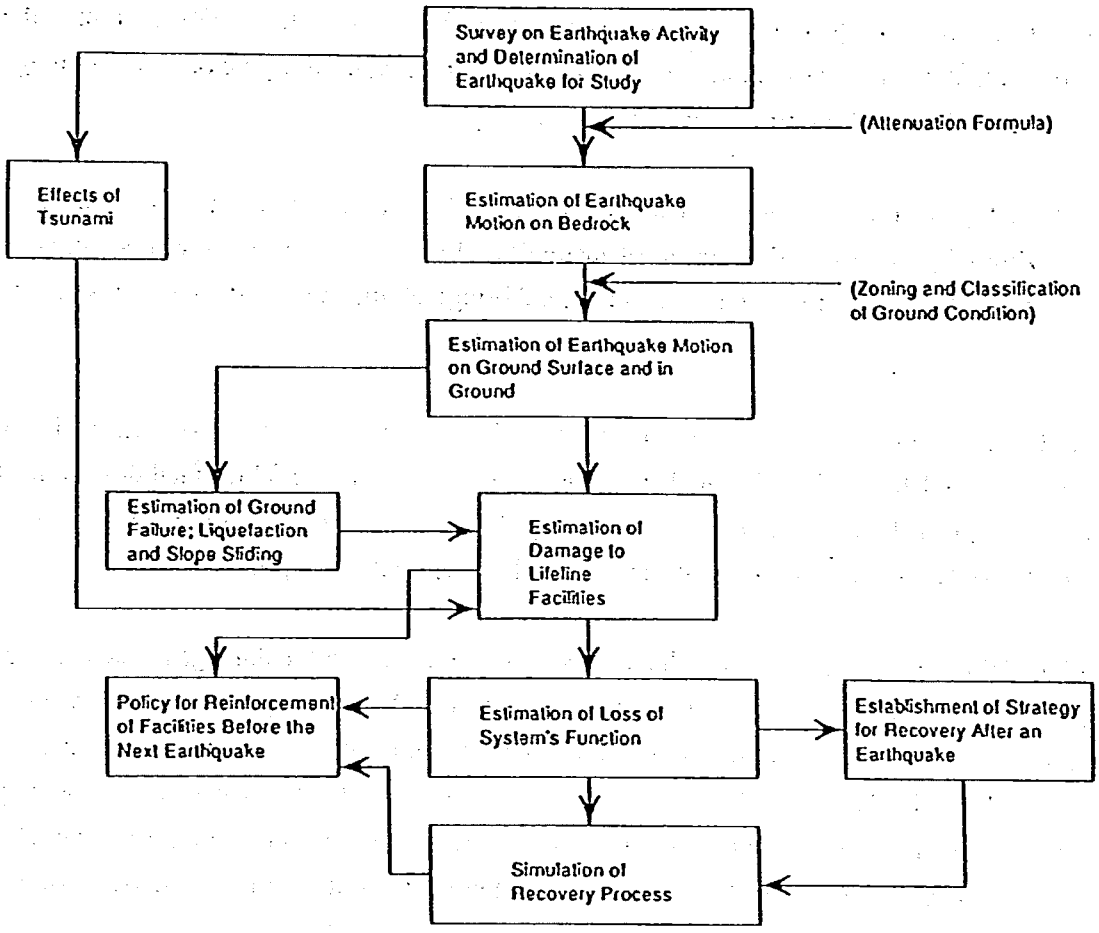


Figure 1. General Flow Chart of Damage Estimation of Lifeline Systems

The next step is to estimate the earthquake motion on the ground surface as well as in the ground by dynamic response analysis, the input for which is the earthquake motion on the bedrock. Besides acceleration, velocity, and displacement, it is required to determine the relative displacement and the strain in order to estimate the damage to buried lifeline facilities. Since lifeline facilities are distributed over a wide area, the area of interest is generally divided into meshes with a size of 1 kilometer to 500 meters, and the earthquake motion for each mesh, where the ground condition is assumed to be uniform, is calculated.

Based on the calculated earthquake motion on the surface and in the ground, the potential of liquefaction and slope sliding is examined. Since many areas of Japanese large coastal cities are constructed on reclaimed land, the exact estimation of liquefaction potential is one of the key subjects for damage assessment of lifeline facilities. The damage to lifeline facilities is assessed on the basis of the calculated earthquake motion, by taking into account the effects of ground failure such as liquefaction.

The damage rate to facilities is generally represented as a probabilistic quantity. For example, the damage rate of buried pipes is given as the number of failures per unit length of a pipe or as the damage probability at junctions with other structures such as manholes.

As for the effects of liquefaction, we must consider the effect of the permanent ground displacements, subsidence and heaving of ground and floating up of manholes. In places where lifeline pipes cross a river, the effects of the subsidence of the embankment behind bridge abutments must also be taken into consideration.

The two methods can be used to obtain the damage rate of buried pipes. The first method is by empirical formulae obtained by statistically analyzing the damage caused to lifeline facilities in past earthquakes. The second method is to numerically compare the stress, the strain and the deformation which are calculated based on predicted earthquake motion with the ultimate strength of the facilities.

The functionality of lifeline system after an earthquake is evaluated based on the damage assessment of the facilities. A number of numerical methods of network analysis has been proposed. However, networks of lifelines consist of an enormous number of elements and such an analysis covering all elements is extremely difficult. Thus, to achieve the objectives, some simplifications are always made by taking into account the characteristics of the network. An electricity supply substation, for example, consists of many transformers, circuit breakers, and other components, but is substituted by a simple system with fewer elements upon the judgement of experts.

The post-earthquake recovery strategy right after an earthquake is studied on the basis of assessed damage to facilities and the function. The recovery process is simulated in accordance with several probable recovery strategies, and based on the simulation the best strategy is chosen by referring to expert's opinions. The pre-earthquake policy for the reinforcement of the facilities is also determined based on the damage assessment and on the result of the simulation of recovery process.

LIQUEFACTION-CAUSED DAMAGE TO BURIED PIPES

Figure 2 shows the locations of damage to buried gas pipes, and the area of liquefaction in Noshiro City during the 1983 Nihonkai-Chubu earthquake (Noshiro City Government, 1983). It is clear that most of the locations of damage was caused in the liquefied area. Table 1 shows the number of the breakages of the gas pipes and the water pipes in the city, the damage rate, which is a mean number of breakages per 1.0 km, and the ratio of the damage rate in the liquefied area to that in non-liquefied area. The damage rate in the liquefied area is considerably high, mostly ten times that in the non-liquefied area.

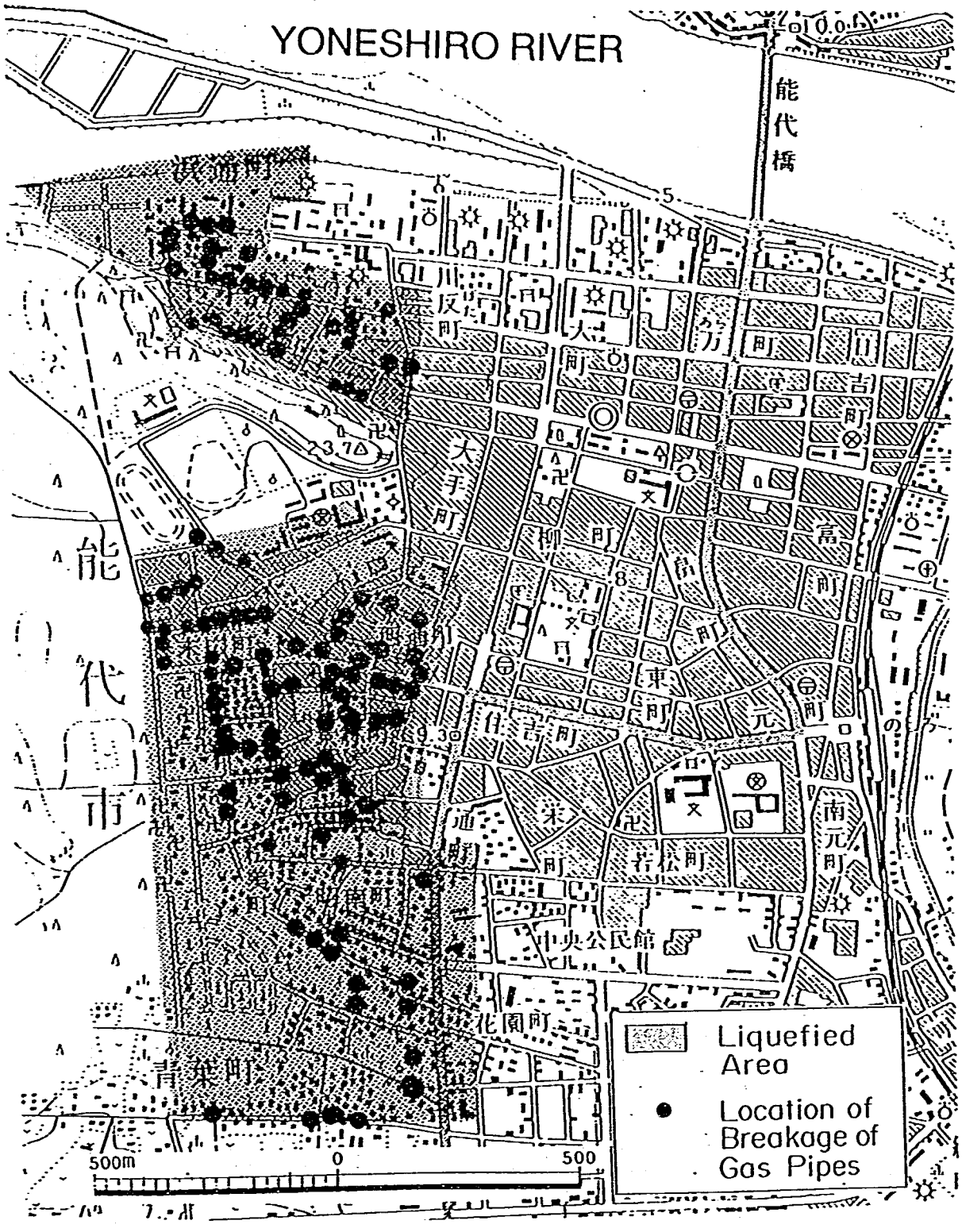


Figure 2. Locations of Damage of Buried Gas Pipes and Liquefied Area in Noshiro City during 1983 Nihonkai-Chubu Earthquake

Table 1 Damage Rate of Gas and Water Pipes in Noshiro City

	Liquefied Area	Non-Liquefied Area	Ratio of Damage Rate
Total Length of Pipe (km)	29.25	49.72	17.23/1.93
Number of Breakages	504	96	= 8.93
Damage Rate (1/km)	17.23	1.93	

During the 1989 Loma Prieta earthquake, buried pipes of lifeline systems were severely damaged in a reclaimed land in San Francisco Bay area. Figure 3 shows the locations of repairs of water pipes (MWSS: Municipal Water Supply System) at Marina district in San Francisco (O'Rourke et al. 1992). The dotted and solid lines are the waterfronts in 1857 and 1906, respectively. The area in the north of the dotted line had been reclaimed from the sea. It was reported that the district suffered severe and extensive liquefaction. The result of Figure 3 also shows that most of the damage to buried pipes occurred in the liquefied area. Figures 2 and 3 suggests that the liquefaction is the most critical factor for the assessment of damage to buried pipes.

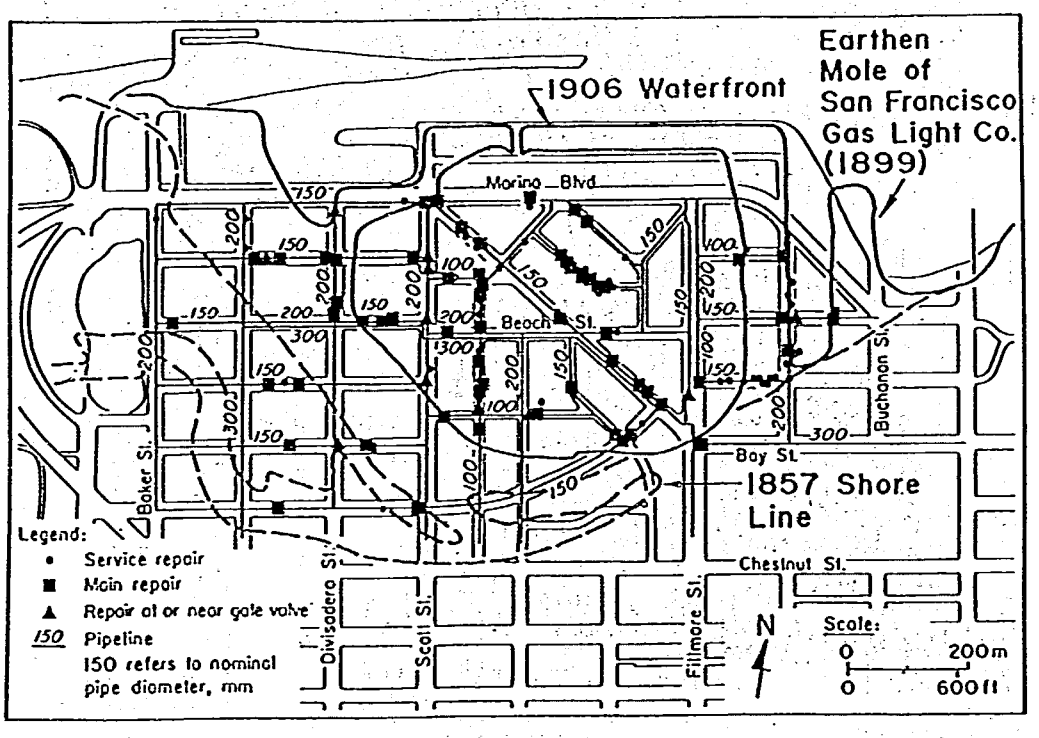


Figure 3. Locations of Repairs of Pipres at Marina District
(1989 Loma Prieta Earthquake, O'Rourke 1992)

ESTIMATION OF DAMAGE RATE OF BURIED PIPES IN LIQUEFIED AREA

The first method to estimate the damage rate of buried pipes, is based on an empirical formulae obtained from statistical analyses of the damage caused to lifeline facilities in past earthquakes. The following empirical formula is proposed for the buried pipes;

$$R_f = C_G \cdot C_L \cdot C_P \cdot C_O \cdot R_S$$

R_f: Damage rate of buried pipes
R_S: Standard damage rate
C_G: Coefficient for ground condition
C_L: Coefficient for liquefaction
C_P: Coefficient for pipe's material
C_O: Coefficient for pipe's diameter

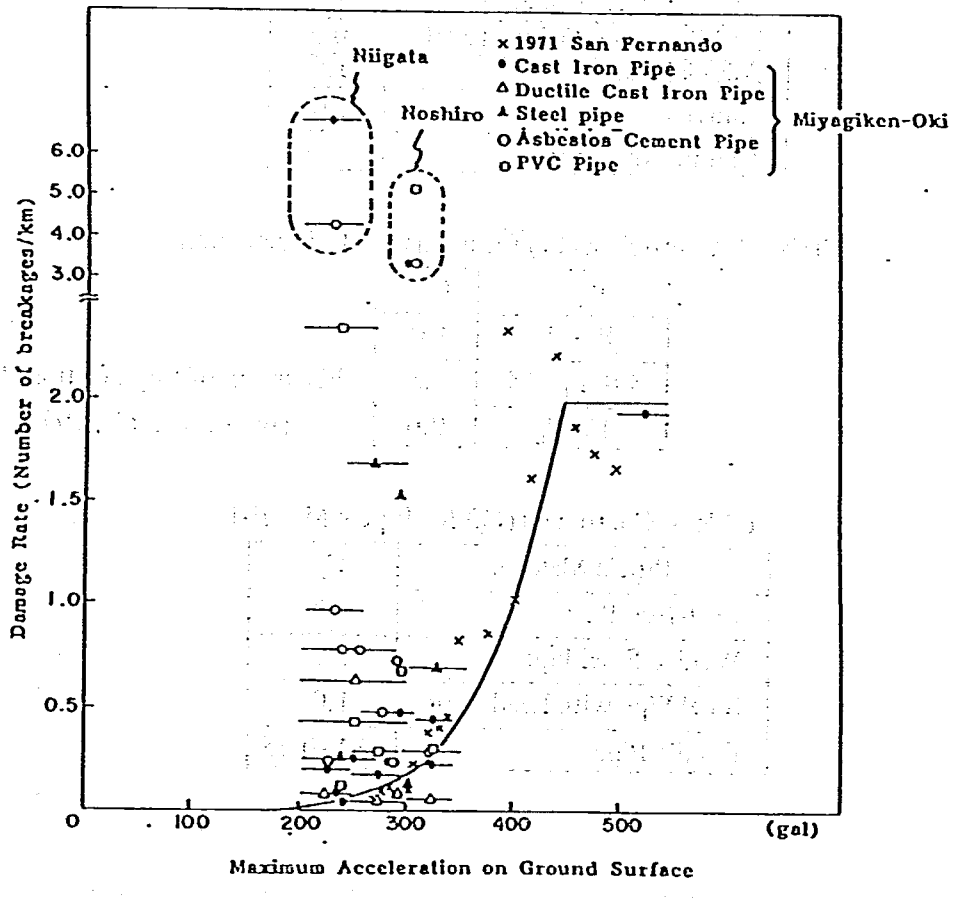


Figure 4. Water Pipe Damage Rate in 1971 San Fremando and 1978 Miyagiken-Oki Earthquakes (Isoyama, 1980)

Figure 4 shows a damage rate of buried pipes (mean number of the failure points per 1 km) obtained from 1971 San Fernando and 1978 Miyagiken-Oki earthquakes. From these data the standard damage rate R_S can be determined with respect to the maximum acceleration at the ground surface. However, it is necessary to make a correction to the standard damage rate according to the ground condition C_G, the intensity of the liquefaction C_L, and the material of the pipe C_P and the diameter of the pipe C_D. The coefficients C_G and C_L are determined by analyzing the damage caused by past earthquakes, while the coefficients C_P and C_D are estimated by comparing the strength of the pipe under the study with those of the damaged pipes, during past earthquakes, most of which had a relatively small diameter and low strength.

One example of the values of the coefficients, which were used for the damage assessment of buried water pipes is shown Tables 2~5.

Table 2 Coefficient (C_G) for Ground Condition

Ground Condition	C_G
Bed Rock and Dilluvial Soil	0.5
Alluvial Clay	1.0
Alluvial Sand	1.0
Peat in Low Land	2.0

Table 3 Coefficient (C_L) for Intensity of Liquefaction

P_L	C_L
$P_L < 5$	1.0
$5 \leq P_L < 15$	4.5
$15 < P_L$	9.0

PL: Index of Liquefaction Potential (Iwasaki, et al., 1978)

Table 4 Coefficient (C_P) for Pipe's Material

Pipe's Material	C_P
Cast-Iron Pipe	1.0
Welded Steel Pipe	0.1
Steel Pipe with Lead Joint	1.0
Ductile Pipe	0.1~0.25

Table 5 Coefficient (C_0) for Pipes Diameter

Pipe's Diameter (mm)	C_0
$\phi \leq 125$	1.3
$150 \leq \phi < 350$	0.7
$400 \leq \phi < 1000$	0.5
$1000 < \phi$	0.2

It should be noted that the coefficient for the intensity of liquefaction, which was determined based on the damage in liquefied area in Nishiro City during the 1983 Nihonkai-Chubu earthquake, is remarkably high and is the most influential parameter for the assessment of the damage rate.

The second method for the assessment of the damage rate of facilities is based on the comparison of the stress, the strain and the deformation, which are calculated on the basis of earthquake motion, with the ultimate strength of the facilities. Figure 5 shows the procedure of calculation of damage rate of buried pipes. Besides the relative ground displacement and the ground strain resulting from propagating earthquake waves, the permanent ground displacements due to liquefaction are taken into consideration in the calculation of the stress and the strain of buried pipes.

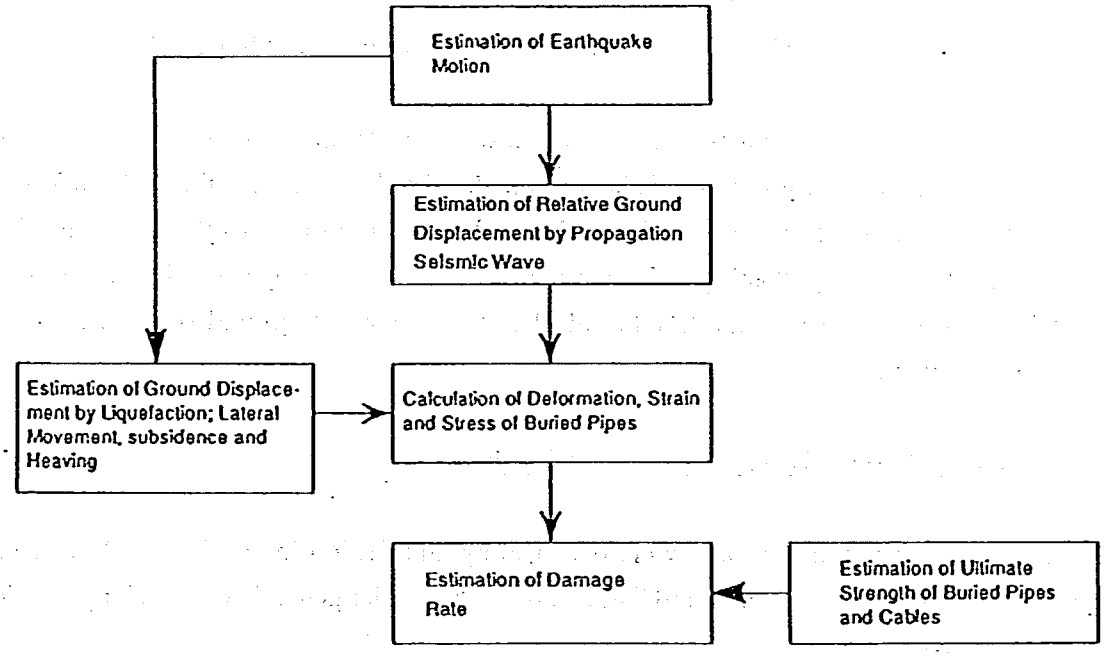


Figure 5. Flow Chart for Estimating Damage Rate for Buried Pipes

CURRENT STATUS OF RESEARCHES ON EFFECT OF LIQUEFACTION ON BURIED LIFELINE FACILITIES

Liquefaction-Induced Permanent Ground Displacement

The author and his co-workers reported that liquefied ground was displaced as much as several meters in the horizontal direction, depending on topographical and geological conditions at the time of the 1983 Nihonkai-Chubu earthquake (Hamada, et al., 1986). Since then case studies of liquefaction-induced ground displacements caused by ten earthquakes in Japan, the U.S. and Philippines have been compiled by the Japan-U.S. joint research team (Hamada and O'Rourke 1992). Furthermore, the mechanism of the occurrence of liquefaction-induced ground displacements has been investigated by shaking table test and by numerical methods. However, no mechanism which gains a consensus of researchers has been found so far. Some empirical formulae have been proposed: One example of those formulae is as follows;

$$D = 0.75 \sqrt{H} \sqrt[3]{\theta} \qquad (1)$$

D: Liquefaction-induced ground displacement (m)
H: Thickness of liquefied soil layer
θ: Larger value of gradient of ground surface or that of liquefied soil layer (%)

The assessment of the effects of liquefaction-induced displacements on lifeline facilities, especially on buried pipes, requires accurate estimation of the magnitude, the direction and the distribution of the displacements. To make this information available, the mechanism of ground displacements needs to be fully clarified. Model tests using shaking tables are now being carried out by several research institutes in Japan, while work on numerical models to calculate the permanent ground displacement is also proceeding simultaneously.

Effects of Permanent Ground Displacement on Lifeline Facilities

Many buried pipes and foundation piles were damaged by liquefaction-induced ground displacement during the 1964 Niigata and 1983 Nihonkai-Chubu earthquakes. The general effects of liquefaction on lifeline facilities are as follows;

1) Settlement and inclination of structures due to reduction of the ground's bearing capacity.
2) Uplifting of embedded structures such as manholes due to buoyancy in the liquefied soil.
3) Damage due to Liquefaction-induced ground displacements.

Effects 1) and 2) are already taken into consideration in the earthquake-resistant design of facilities, but effects of liquefaction-induced ground dispalcements are at present not considered. When large permanent ground displacements with a magnitude of several meters are considered in the earthquake-resistant design of buried pipes, two problems arise; One is whether "the seismic response displacement method," which has conventionally been used for the design of underground structures, is applicable or not. And if it is applicable,then the problem is how to evaluate the coefficient of the subgrade reaction of partially liquefied ground.

The other one is the evaluation of the ultimate strength of facilities. It is extremely difficult to design facilities by the conventional allowable stress method, when the ground displacement reaches several meters. The information about the ultimate strength of lifeline facilities such as buried pipes is insufficient at present

The former problem has been studied through experiments on pile foundation models in liquefied soil, and it was reported that the force acting on the pile during lateral movement of liquefied soil was proportional to the velocity of the ground movements and was caused by the flow of the liquefied ground. The second problem is now being studied by laboratory tests on piles and pipes.

CONCLUSIONS

In this paper, the current status of damage assessment of lifeline facilities, particularly in liquefied ground, are described and the subjects, which should be solved in near future, are described. As stated in the introduction, large-scale waterfront projects have already progressed at major cities in Japan. To create an earthquake-proof urban society, the study of reliable damage assessment of lifeline facilities should be proceeded more strongly.

RERERENCES

Noshiro City Government, The 1983 (May 26) Nihonkai-chubu Earthquake; A Document of the Hazard Experienced in Noshiro City, 1984 (in Japanese).

O'Rourke, T.D. and Pease, J.W., Large Ground Deformations and Their Effects on Lifeline Facilities: 1989 Loma Prieta Earthquake, Case Studies of Liquefaction and Lifeline Performance During Past Earthquakes, Volume 2, United States Case Studies, Technical Report NCEER-92-0002, National Center for Earthquake Engineering Research, Feb., 1992.

Iwasaki, T., Tatsuoka, , Tokida, K. and Yasuda, S., A Practical Method for Assessing Soil Liquefaction Potential Based on Case Studies at Various Sites in Japan, Proceedings of the Fifth Japan Earthquake Engineering Symposium, 1978 (in Japanese).

Hamada, M., Yasuda, S., Isoyama, R., and Emoto, K., Study on Liquefaction Induced Permanent Ground Displacements, A Technical Report, Association for the Development of Earthquake Prediction, Nov., 1986.

Hamada, M., and O'Rourke, T.D., Case Studies of Liquefaction and Lifeline Performance During Past Earthquakes, Volume 1, Japanese Case Studies, Technical Report NCEER-92-0002, National Center for Earthquake Engineering Research, Feb., 1992.

Isoyama, R., Seismic Performance Evaluation of Urban Utility System, Doctor Thesis of University of Tokyo, Dec., 1980.

Safety Estimation of Buried Pipes for Permanent Ground Deformation by Liquefaction

by Hideyo Suzuki[1], Tamio Masuda[1], Masayuki Sato[2] and Masanori Hamada[3]

1) Tokyo Electric Power Company
2) Tokyo Electric Power Services Company
3) Tokai University

ABSTRACT

This paper describes a methodology to assess the safety of buried pipes for electric power transmission against Permanent Ground Deformation. In this paper, the Pipe-Protected Type of transmission cable is considered; and the deformation components of the ground movement is assumed to be horizontal; i.e., neither vertically settlement nor floating are considered.

At first, the various types of the underground transmission lines are introduced. Among the various types of the transmission lines, the Pipe-Protected Type of the cables (POF) is selected for the investigation.

The outline of the past study on Permanent Ground Deformation is summarized, and the assumptions for assessing the safety of the Pipe-Protected Type transmission lines are described. The calculation procedure of the failure probability is proposed, in which both the beam structure of the steel pipes and reaction spring of surrounding ground are used to calculate the strain in the pipe using the response displacement method. In this procedure, the estimation of the thickness of the liquefied layer, maximum values of the Permanent Deformation and their pattern are simplified. Using these deformations, the "critical acceleration" for a Pipe-Protected Type of the buried pipes are obtained. Using the critical acceleration, failure probability is obtained, being considering the assumed probability distribution of acceleration, which is derived from the observed acceleration in Kanto Area.

An example of the numerical results is given and discussed; in which a structural system consisted of a pipe and a manhole is presumed for one type of the ground condition. Consequently, a practical methodology can be proposed to compare the probability of different conditions of types of pipes and ground conditions.

INTRODUCTION

The strong earthquakes in the past showed several features of failure of buried pipes[1], from which we have learned important lessons such that the welded steel pipes have relatively high durability to earthquake loads, compared with the ductile pipes. From these valuable lessons, we have already established a Design Code for Buried Pipes for transmission of electric power[2]. Meanwhile, the research efforts on the Permanent Ground Deformations (PGD) during liquefaction have been made by many researchers in Japan and the US so far. In the practical design of the buried pipes for power transmission lines, the consideration of PGD is just at onset, and most of the buried pipes, which have been already buried in the soft sand ground in the past, have not been investigated their durability for PGD.

In the vast area of Tokyo and its surrounding urban area, the total length of the underground transmission line, including a low voltage of 6.6 kV through an ultra high voltage of 275 kV, is counted more than seven thousands kilometers. Some of the power cables of the underground transmission lines are installed in tunnels or conduits, and the others are installed within protecting pipes. In the pipe-protected cables, a precise estimation of failure is needed to assess the safety of transmitting capacity of the power following strong earthquakes.

The underground transmission lines are divided into mainly two types as shown in Figure 1; one is a Pipe/Trough-Protected Type, and the other is a Tunnel Type. The Pipe/Trough-Protected Type includes the followings; (A) Steel Pipe-Protected Type, (B) Trough-Protected Type, (C) Concrete Pipe-Protected Type, and (D) Jacked Hume-Pipe-Protected Type, respectively. Representative structural drawings of the underground transmission system are shown in Figure 1, together with the Tunnel Type. In this paper, some results of the safety assessment for the Steel Pipe-Protected Type are described, as this type of transmission line is mostly used. The major aspects of the Steel Pipe-Protected Type are:

- Most of the pipes are installed in shallow part of the grounds, usually, 2 to 5 meters from the surfaces.
- The pipes are welded or screw-tighten, and attached to manholes.
- The intervals of the manholes are usually 200 to 300 meters.

The Tokyo Electric Power Company is now undertaking a project in regard to the safety assessment of the transmission networks against the various class earthquakes. A methodology to evaluate the failure probability of buried pipes has been proposed for this investigation, based upon the experience of the past strong earthquakes, and upon results of experiments on the

strength and stress-strain behavior of the pipes and cables. As stated above, the total length of the pipes is too long for assessment, so that a simplified method is adopted for both the structural strength and the estimation of ground deformations as inputs.

In this paper, we present a method to assess the safety of buried pipes for electric power transmission cables against earthquakes. The buried pipes of Pipe-Protected Type*)1 are discussed by assuming the loading due to a horizontal displacement of ground during liquefaction.

ASSESSMENT OF MAGNITUDE AND DISTRIBUTION OF "PGD"

Magnitude of Permanent Ground Deformation (PGD)

It has been observed by aerial surveys that the grounds have displaced with a magnitude of several meters due to soil liquefaction in Niigata City during the 1964 Niigata earthquake as well as in Noshiro City during the 1983 Nihonkai-Chubu earthquake. These permanent ground deformations caused extensive damage to inground structures such as foundation piles and buried pipelines. Therefore, the influential factors for the occurrence of the ground deformations and their mechanisms have been studied. However, any consensus is not yet achieved among the researchers.

Hamada et al.[3] conducted regression analyses by using data from the 1964 Niigata, the 1971 San Fernand and the 1983 Nihonkai-Chubu earthquakes and proposed the following empirical formula:

$$D = 0.75 \sqrt[2]{H} \sqrt[3]{\Theta} \qquad (1)$$

D : Magnitude of permanent ground deformation in horizontal direction (m)
H : Thickness of liquefied layer (m)
Θ : The greater gradient of ground surface or lower boundary of liquefied layer (%)

The proposed correlation given by Equation (1) only provides an approximate fit to the field data. The measured ground deformations are actually scattered between values half and twice the values given by the above formula. In particular, the empirical formula shows a

*)1 Within the pipe of Pipe-Protected Type, so named "Pipe-type Oil Filled Cables (POF)" are installed.

comparatively low correlation between the ground deformation (D) and the greater gradient of the ground surface or lower boundary of liquefied layer(Θ), since D is proportional to the cubic root of the gradient.

If the sloping ground is deformed due to the gravity under the condition of a great reduction of its shear modulus, resulting from the liquefaction, the ground deformation should be proportional to the gradient of the ground surface. A high correlation could be expected with the gradient. However, the proposed empirical formula, which was obtained from regression analyses, seems to be in contradiction to the above assumption.

Furthermore, it is practically difficult to determine the gradient of the lower boundary of the liquefied layer, since the gradient is usually less than few percents. Therefore regression analyses were re-conducted using the data from the area where the gradient of the ground surface is comparatively low, below 1 % in Niigata and Noshiro Cities to develop more simplified empirical formula for easier application. The formula is focussing on the effects of the thickness of the liquefiable layer for the prediction of the magnitude and the distribution of the liquefaction-induced ground deformation on the alluvial flat plane such as Tokyo area in the present study.

The regression analyses clarified that a comparatively good correlation could be found between the magnitude of the ground deformation and the thickness of the liquefiable layer. But the degree of the effect of the thickness on the ground deformation largely varies, depending upon the areas under the study as shown in Figure 2. The effect of the thickness is smaller in the vicinity of the Niigata Railroad Station, compared with Ebigase-Shitayama District in Niigata City, and Noshiro City. The vicinity of the Niigata Railroad Station was already urbanized at the time of the earthquake, and many in-ground structures such as basements and foundation piles of the buildings had a great influence to reduce the magnitude of the ground deformations. Consequently, the following two formulae were proposed for this study:

$$D = 0.34\,H \qquad (2)$$

$$D = 1.2\,H \qquad (3)$$

where, D : the ground deformation in the horizontal direction (m)
H : the estimated thickness of the liquefied layer (m).

Formula (2) is applied to the urbanized area, and Formula (3) to non-urbanized area.

Pattern of Horizontal Ground Deformation

The pattern of the ground deformation essentially depends on the topographical and geological conditions of the sites. Figure 3(a) and (b) show the distribution of the length of the compressive and the tensile zones from the data of Niigata and Noshiro Cities. The length ranges 150 to 450 meters with a mean value of 320 meters in the compressive zone as well as 100 to 450 meters with a mean value of 240 meters in the tensile zone. The pattern of the deformations, shown in Figure 4, was used for the present study.

The width of the ground deformation zone ranges 100 to 400 meters with a mean value of 240 meters, and the pattern, shown in Figure 4, was used for the study. This pattern is used for the analyses of the lateral deformation of the buried pipes. A sinusoidal curve was applied for the analysis of lateral deformation of the pipe, in order to prevent large stress concentration at the nodal point of the triangle shaped pattern.

CALCULATION OF FAILURE PROBABILITY

Outline of The Procedure

The main flow chart of the calculation of the failure probability is shown in Figure 5. As seen in this figure, major steps of the procedure are:

a) To estimate thickness of liquefied layer according to the strength of Peak Ground Acceleration (PGA) at the surface
b) To establish a relationship between the PGA and the thickness of liquefied layer
c) To model a ground-pipe structural system, using continuous beam and ground springs, in which the triangular and sinusoidal patterns of ground deformation are assumed for axial and lateral direction on the basis of the past investigations
d) To determine a maximum deformation of the triangular/sinusoidal patterns, when the strains of the pipe exceed the ultimate strain
e) To establish a relationship of the axial length of manholes vs. the maximum deformation of the triangular and sinusoidal patterns with respect to the spring constants of the surrounding ground
f) To determine Critical Acceleration using the relationships of (b) and (e) for assessing the critical durability of the buried pipe
g) To calculate failure probability of the pipe, using the probabilistic distribution of acceleration derived from the attenuation curves observed by Tepco

Procedure of Estimation of Failure Probability

Failure probability of each failure mode

Both compressive and tensile failures associated with axial deformation in the pipe, and bending failure in the perpendicular direction are considered as the failure modes of the pipes due to Permanent Ground Deformations. In this study, the failure probabilities due to each mode are calculated based on the principles described below.

Generally, the principal factors influencing the failure of structures during an earthquake are the characteristics and intensity of the earthquake motion, and the deformation and strength characteristics of the ground and structure. There will be a statistical variation in the values of all of these quantities. Clearly it is required to base any assessment of structural failure probability on all of these causal factors with consideration of the relevant variations. To carry out such an investigation, a study of the cross-correlations between all factors with a variation is first needed. However, in this study, the variation of maximum acceleration in the earthquake motion is considered to be the controlling factor on failure, and other factors are assumed to act deterministically.

A *'performance function'* of **Z** is given below for assessing whether a particular form of failure will occur or not.

$$Z = A_r - A_s \qquad (4)$$

$$Z \geq 0 : \textit{Non-failure}$$

$$Z < 0 : \textit{Failure}$$

Where, A_r : critical acceleration for each point; i.e., maximum ground surface acceleration at which no failure occurs

A_s : peak ground surface acceleration.

The total failure probability, P_f, is then given by:

$$P_f = P(Z<0) = P(A_r<A_s) \qquad (5).$$

The critical acceleration will posses a statistical variation as a result of many factors. In this study, however, since all quantities apart from the peak ground acceleration are considered deterministically, the critical acceleration becomes a deterministic quantity. The failure probability for a particular failure mode may be determined as shown in Figure 5.

To calculate the failure probability of buried pipes due to permanent deformations as a result of ground liquefaction, it is first necessary to calculate the critical acceleration. In this study the critical acceleration was evaluated as described below using the response displacement method.

The interactive effects of PGD on buried pipes are presently being investigated in various research institutions, and are gradually becoming clear. However, there is still no accepted method for practical evaluation. It is therefore a subject for subsequent debate as to whether the behavior of buried pipes under permanent ground deformations may be adequately analyzed by using the response displacement method. In this study, it was assumed that the ground had reached the liquefied state, and the analysis was made with reduced values of ground stiffness and strength to evaluate the critical acceleration for a buried pipe due to permanent deformations of the liquefied ground.

In the response displacement method, the buried pipes and manholes were modeled as a beam with ground spring having a bi-linear behavior. As shown in Figure 5, the critical value of maximum deformation (D_{max}) at which the strain of the pipe exceed ultimate strain, was determined varying the axial length of the manholes and the spring stiffness of the ground. In this way, a table was produced showing the relationship between the D_{max} causing failure of the pipe and physical conditions of the buried pipe. As a separate study, the depth of liquefaction (H) and maximum values of permanent deformations ($D_{max} = 0.34$ H) were obtained from ground conditions, by varying the value of the ground surface acceleration (α_{max}). A relationship between α_{max} and D_{max} was thus obtained. By comparing these results it is possible to evaluate the critical acceleration for the buried pipe, as shown in Figure 5.

Using this method, if the very laborious non-linear analysis of the pipe-ground system can be made with various parameters using the response displacement method just once, then regardless of the ground conditions in which the pipe is located, it is possible to evaluate the critical acceleration just by establishing the relationship between the ground acceleration and the depth of liquefaction. As a result, the investigation can be applied over a wide range, and even when a large number of design conditions need to be studied, the method is relatively easy.

Total probability of failure

The above-mentioned probability is only for one particular form of failure. For example, the failure probability calculated from the critical acceleration in an axial compression analysis refers to a conditional probability of failure at the point of interest under permanent deformation in the axial direction, provided that the point lies within a compression zone. It is therefore necessary to make a calculation of the probability of occurrence of each of the postulated failure modes.

To determine this total probability, let us first separate the occurrence of deformation under liquefaction by direction relative to the pipe. In reality, the deformation will occur at some angle to the axis of the pipe. However, here the situation will be simplified by taking the deformation to occur either at 0 or 90 degree(s) to the pipe, with a probability of occurrence of 0.5. In addition, amongst the cases in which deformation occurs in the pipe axis direction there will be cases such that the pipe lies either within a compression or a tension zone, and this probability was taken as the ratio of the deformation pattern length in compression zones (L_c=240 meters) or length in tension zones (L_t=320 meters) to the sum of these two lengths (L_c+L_t=560 meters). According to this approach the probabilities that the pipe will lie in a deformation pattern in a compressive zone (R_c), or in a tension zone (R_t), or the pipe is subject to deformation in the direction perpendicular to the pipe axis, are as follows.

$$R_c = 0.5 \frac{L_c}{L_c + L_t} \quad (= 0.286) \qquad (6a)$$

$$R_t = 0.5 \frac{L_t}{L_c + L_t} \quad (= 0.214) \qquad (6b)$$

$$R_m = 0.5 \qquad (6c)$$

The total failure probability can then be obtained by multiplying these values of R_c, R_t, R_m by the failure probabilities in each of the failure modes, and then summing up the resulting probabilities, as below.

$$P_f = R_c P_{fc} + R_t P_{ft} + R_m P_{fm} \qquad (7)$$

where, P_f : Total failure probability,
P_{fc} : Failure probability of compression
P_{ft} : Failure probability of tension
P_{fm} : Failure probability of bending moment

Numerical Model of Buried Pipe

Physical properties of the pipe are shown in Figure 6(a) and (b). The limiting tensile strain for the pipe was taken as 8% with a consideration of fatigue failure. Compressive failure strain was the buckling strain for the pipe determined from Equation (8). A bi-linear load-strain relationship was employed. Equation (8) is the same as that in the code for aseismic design of high-pressure gas pipes[4] for the allowable buckling strain in straight pipes with the safety factor

being unity.

$$\varepsilon_{ab} = 44 \cdot t / D_m \qquad (8)$$

Where, ε_{ab} : pipe buckling strain (%)
t : pipe thickness (cm)
D_m : average pipe diameter (cm)

The bi-linear load-strain relationship was formed using a straight line between the origin and the yield point as the primary gradient, followed by a secondary gradient after yield taking a value of the primary gradient multiplied by a coefficient of 7×10^{-3}. This coefficient is determined from the code for aseismic design of high-pressure gas pipes[4].

For the bending properties of the POF pipe, a bi-linear moment-strain relationship was used on the basis of the properties of the pipe material. Bending failure was assumed to occur when the compressive strain at the ends of the pipe reached the buckling strain.

Among the ground springs of the model, those acting in the pipe axis direction were assumed to have a bi-linear stiffness as shown in Figure 7(a), based on the code for aseismic design of high-pressure gas pipes[4]. The ground stiffness ($k_a = 0.6$ kgf/cm^3) and critical shear stress ($t_{cr} = 0.1$ kgf/cm^2) are approximately the average values obtained from load tests on gas pipes. Springs supporting the pipe perpendicularly in the horizontal direction have a linear relation as shown in Figure 7(b).

The above-mentioned ground stiffness and critical shear stress were modified by the coefficients shown in Table 1 depending on the FL value and the depth of the pipe. Table 1 is taken Japan Highway Bridge Code[5].

Since the stiffness of the manholes is much greater than that of the pipe, stress concentrations occur at the connection between pipe and manhole. In this study, it is assumed that failure only occurs at the connections. The typical distance of neighboring two manholes is 200 to 300 meters. For this reason, the design point of one pipe-manhole junction would not be influenced by other manholes, and the analysis was made using one manhole with a connected pipe only. The analysis model for the permanent deformations in the pipe axis direction is shown in Figure 8(a). The analysis model for deformations perpendicular to the pipe is shown in Figure 8(b).

For the analysis of the pipe in the perpendicular direction, a deformation pattern was used where the point of maximum curvature of the distribution coincided with the manhole junction, as shown in Figure 8(b).

Critical Ground Deformations

The critical ground deformations for the pipe in the axial direction are shown in Figure 9, with respect to the manhole length. Similar results from the analysis of the pipe in the perpendicular direction are shown in Figure 10. For the pipe under axial tensile load, no failure occurs, because the limiting tensile strain of 8% is large enough.

From Figures 9 and 10, for the same critical deformation, failure is more likely to occur in cases in which the ground deformation occurs in the direction of axial compression in the pipe than in cases in which the deformation is in the perpendicular direction.

AN EXAMPLE OF NUMERICAL RESULTS AND CONSIDERATION

The assumed pipe, manhole, and ground conditions are shown in Figure 11. As seen in the figure, the POF pipe is assumed to be installed at 3.8 meters below the ground level, attached to manholes with 25 meters in axial length. The thickness of liquefaction was assessed in accordance with the method given in the "*Japan Highway Bridge Code*[5]", with liquefaction taken to occur in sand layers. The probability distribution of maximum ground surface acceleration was taken as a log normal distribution as shown in Figure 12. The mean value (α_{max}) was varied at 100 and 200 Gals, and the failure probability was determined. The standard deviation was assumed as $\sigma = 0.269$, which is calculated by using the attenuation of maximum acceleration in Kanto District observed by Tepco.

The results of the failure probability are shown in Table 2. In this table, there was no failure due to permanent deformation in the direction perpendicular to the pipe axis. As a result, because there is neither probability of tensile failure nor bending failure, the value of the total failure probability was considerably reduced.

CONCLUSION

The methodology to assess the safety of buried pipes for electric power transmission against Permanent Ground Deformation have been proposed. And an example of the calculation in one case was presented. Although the calculated values of the failure probability are regarded not to have meanings, from the results of the calculation, the proposed procedure may be a practical method to assess the safety assessment of many buried pipes of different pipes in different ground conditions.

References

(1) Editors; M. Hamada and T.D. O'Rourke; Case Studies of Liquefaction and Lifeline Performance During Past Earthquakes, Technical Report NCEER-92-0001

(2) Tokyo Electric Power Company; Seismic Design Guideline for Underground Power Cable Structures (Draft), 1987 (in Japanese)

(3) M.Hamada et al.: Study on Liquefaction-induced Permanent Ground Displacement, Association for the Development of Earthquake Prediction, November 1986, Tokyo

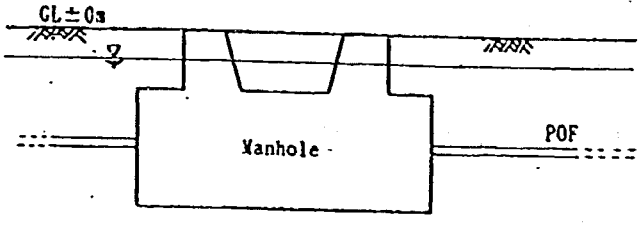
(4) Japan Gas Association; Recommended Practice for Gas Pipeline Aseismic Design, 1982 (in Japanese)

(5) Japan Road Association; Japan High Way Bridge Code, 1990 (in Japanese)

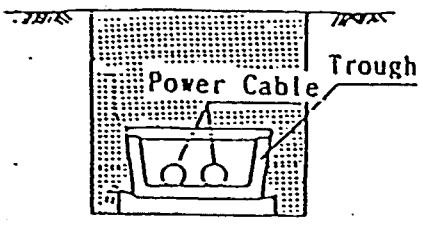
Table 1 Reduction Factor for Soil Spring during Liquefaction

Depth	$F_L \leqq 0.6$	$0.6 < F_L \leqq 0.8$	$0.8 < F_L$
$0 \leqq Z < 10$	1/3	1/3	2/3
$10 \leqq Z < 20$	1/3	2/3	2/3

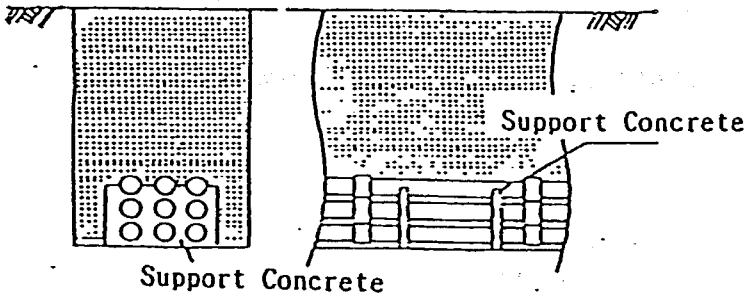
I. Pipe/Trough Protected-Type



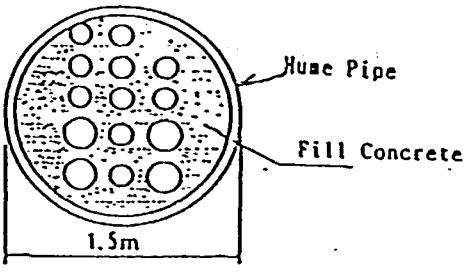
(A) Steel Pipe Protected-Type



(B) Trough Type

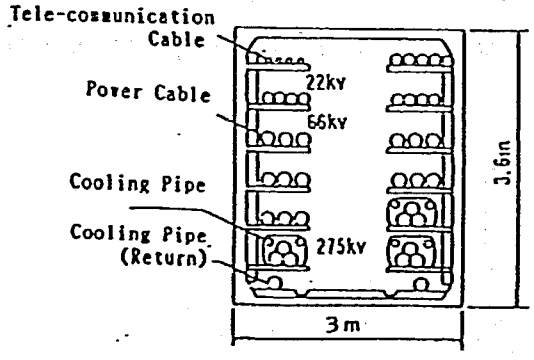


(C) Concrete Pipe-Protected Type

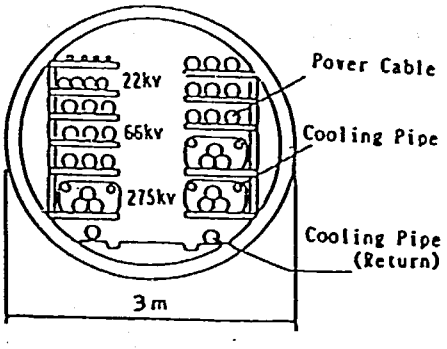


(D) Jacked Hume-Pipe-Protected Type,

II. Tunnel Installed Type



(A) Box Culvert Tunnel Type



(B) Shield Tunnel Type

Figure 1 Representative Types of Underground Transmission Lines

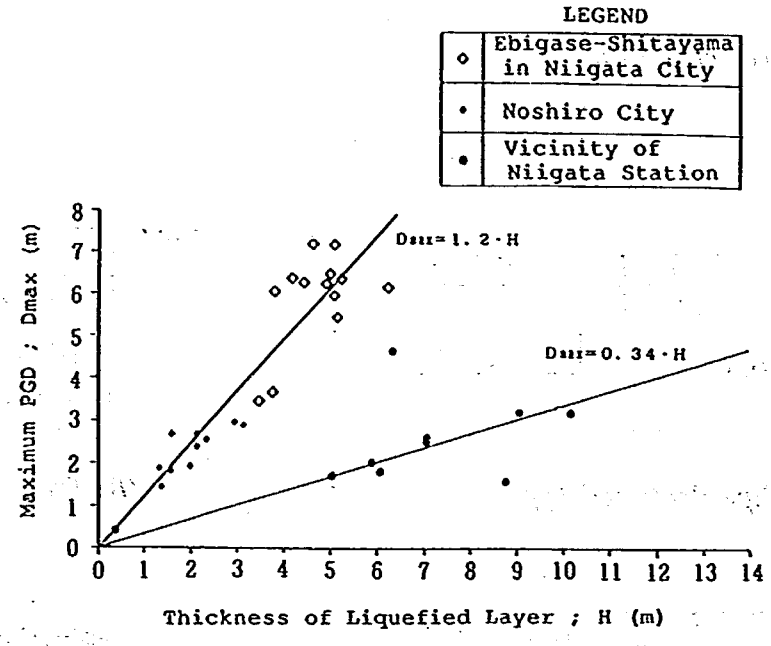


Figure 2 Relationship between Thickens of Liquefied Layer and Maximum Deformation

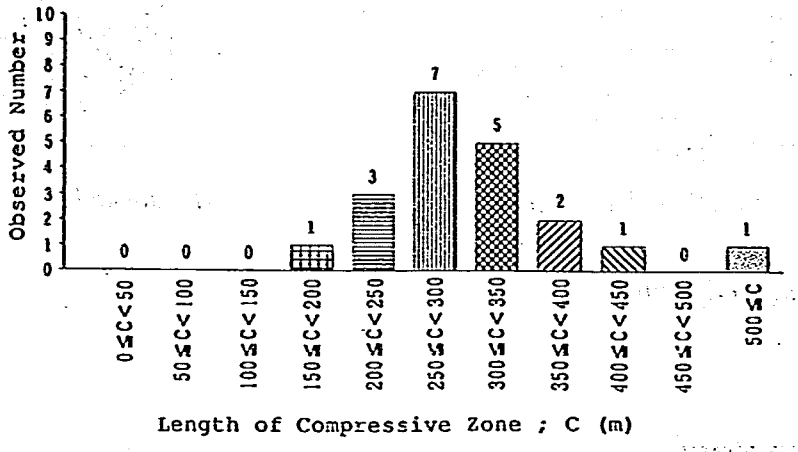


Figure 3(a) Diagram of Frequency versus Slope Length in Compression Strain Zone

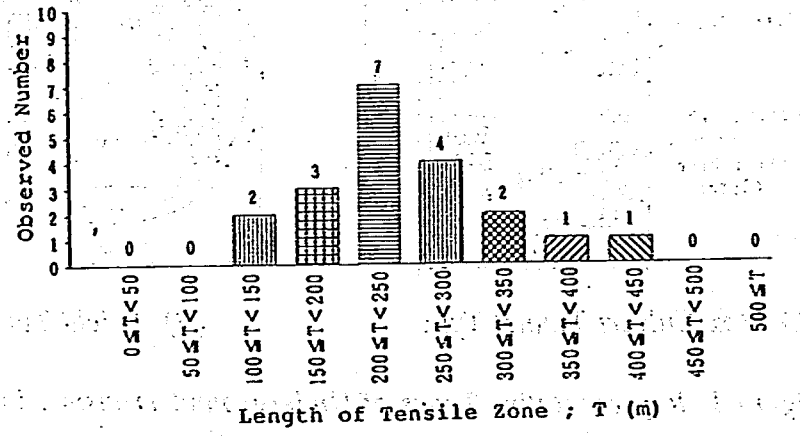


Figure 3(b) Diagram of Frequency versus Slope Length in Tensile Strain Zone

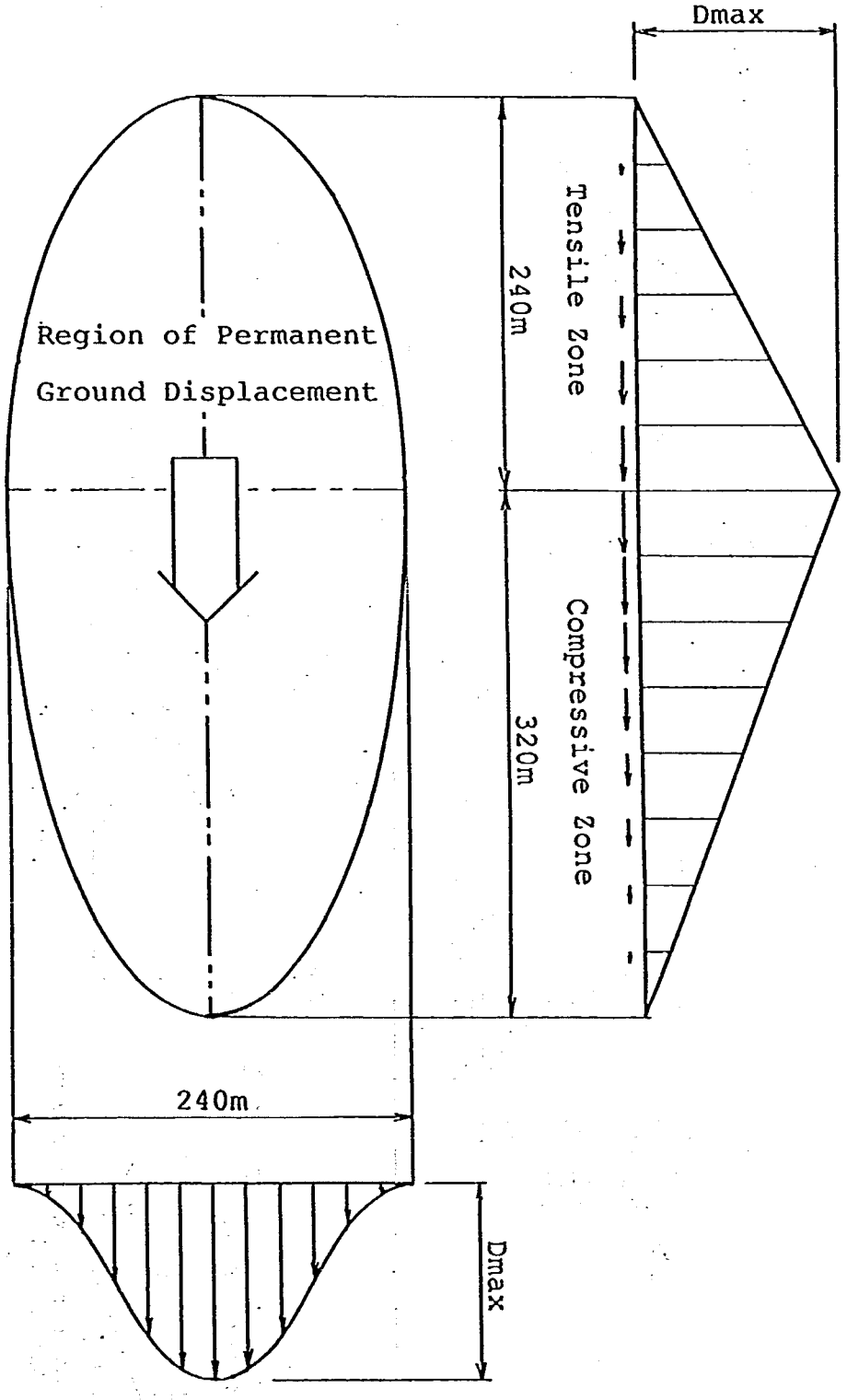


Figure 4 Idealized Pattern of Permanent Ground Deformation Used for the Study

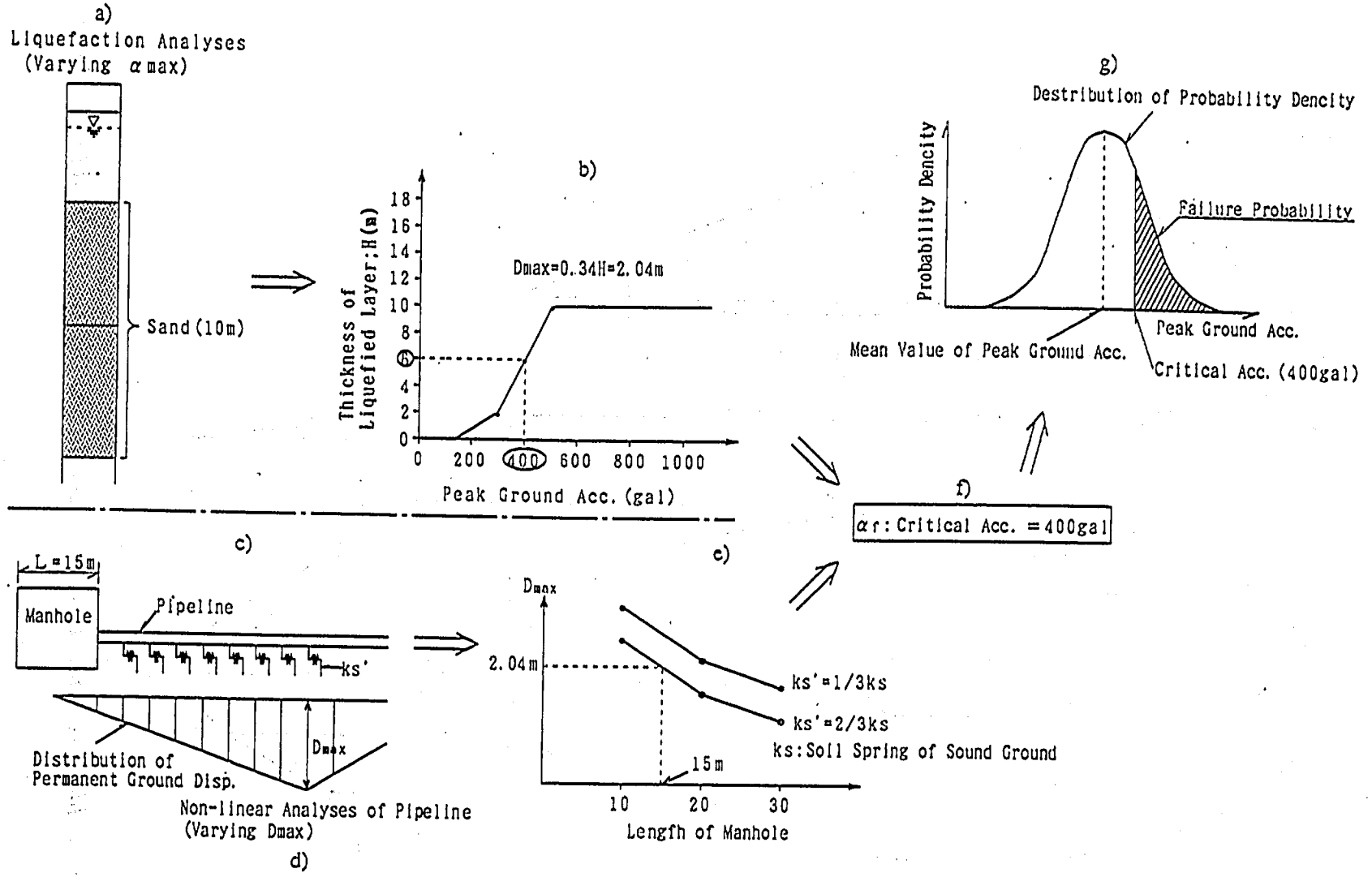
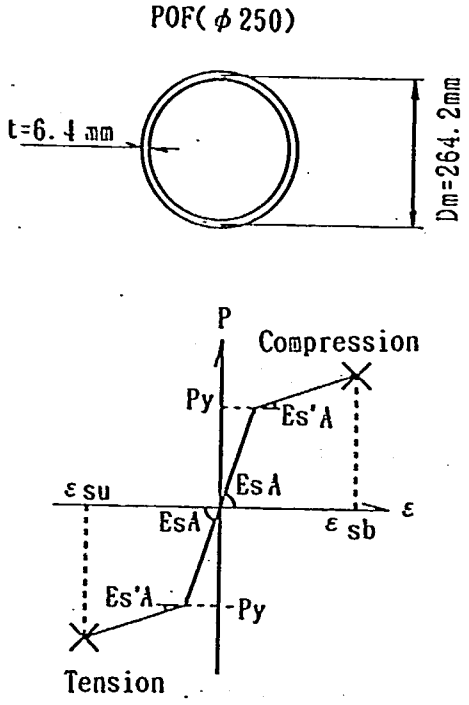


Figure 5 Flow Chart of Procedure for Estimation of Failure Probability



A : Section area of pipe

Es : Young modulus of steel
Es=2.1×10⁶(kgf/cm²)

Es' : Second modulus of steel
Es'=Es×10⁻²

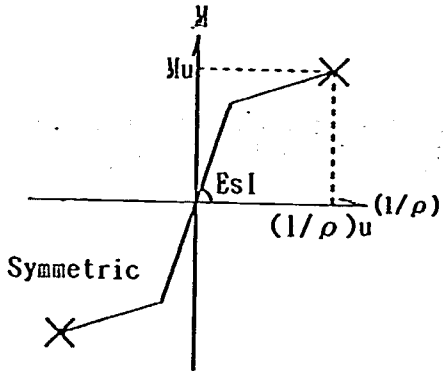
Py : Yield load of pipe
Py=A·σsy

σsy: Yield stress of steel
σsy=2900(kgf/cm²)

εsu: Critical tensile strain of steel
εsu=8(%)

εsb: Critical compressive strain of steel
εsb=44·t/Dm(%)

Figure 6(a) Physical Property of Pipe-protected Type Pipe (POF)
(In the Case of Axial Force Load)



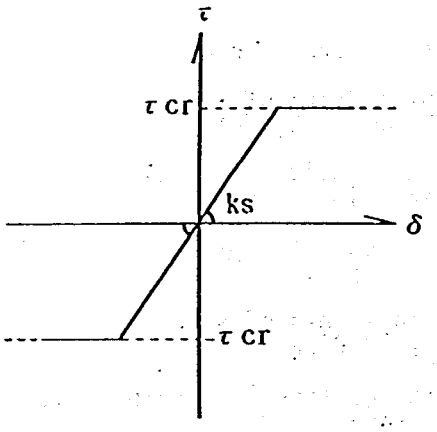
Es : Young modulus of steel
Es=2.1×10⁶(kgf/cm²)

I : Inertia moment of section area

Mu : Failure moment of pipe

(1/ρ)u: Failure bending strain of pipe

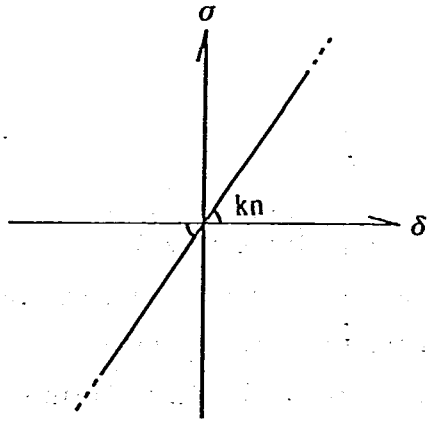
Figure 6(b) Physical Property of Pipe-protected Type Pipe (POF)
(In the case of Bending Load)



ks : Soil spring constant per unit area
in longitudinal direction
ks=0.6(kg/cm²)

τ cr: Critical shear stress
τ cr=0.1(kg/cm²)

Figure 7(a) Spring Characteristics of the Surrounding Ground
(In the Case of Axial Force Load)



kn : Soil spring constant per unit area
in orthogonal direction
kn=3×ks

Figure 7(a) Spring Characteristics of the Surrounding Ground
(In the Case of Bending Load)

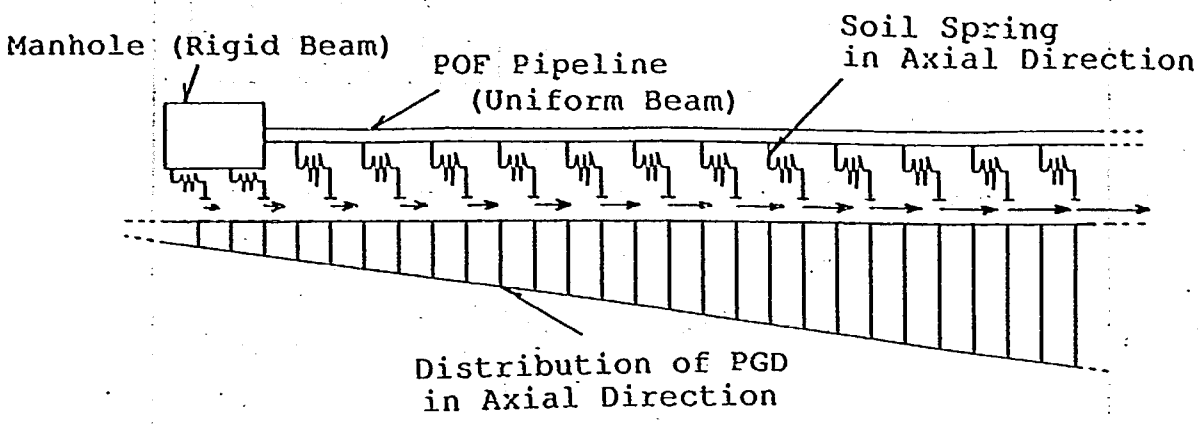


Figure 8(a) Analysis Model for Axial Direction of the Pipe

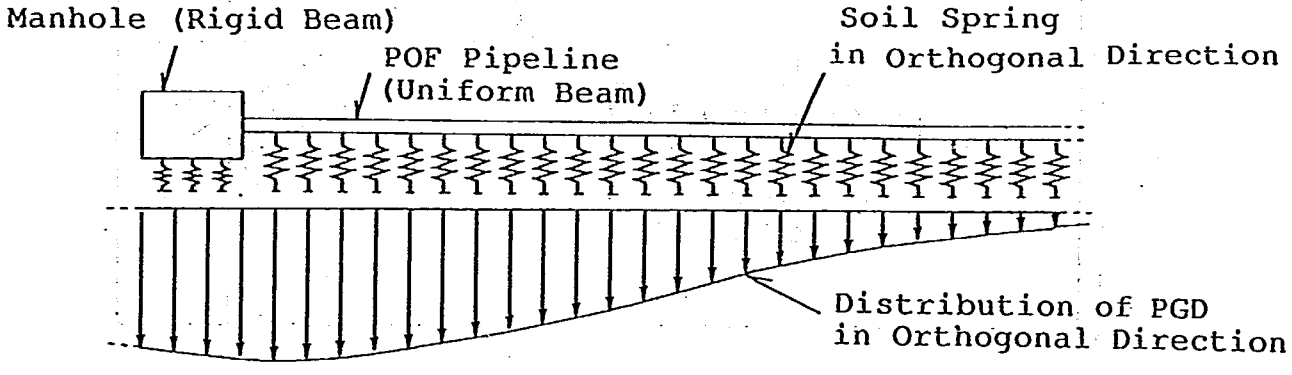


Figure 8(b) Analysis Model for Lateral Direction of the Pipe

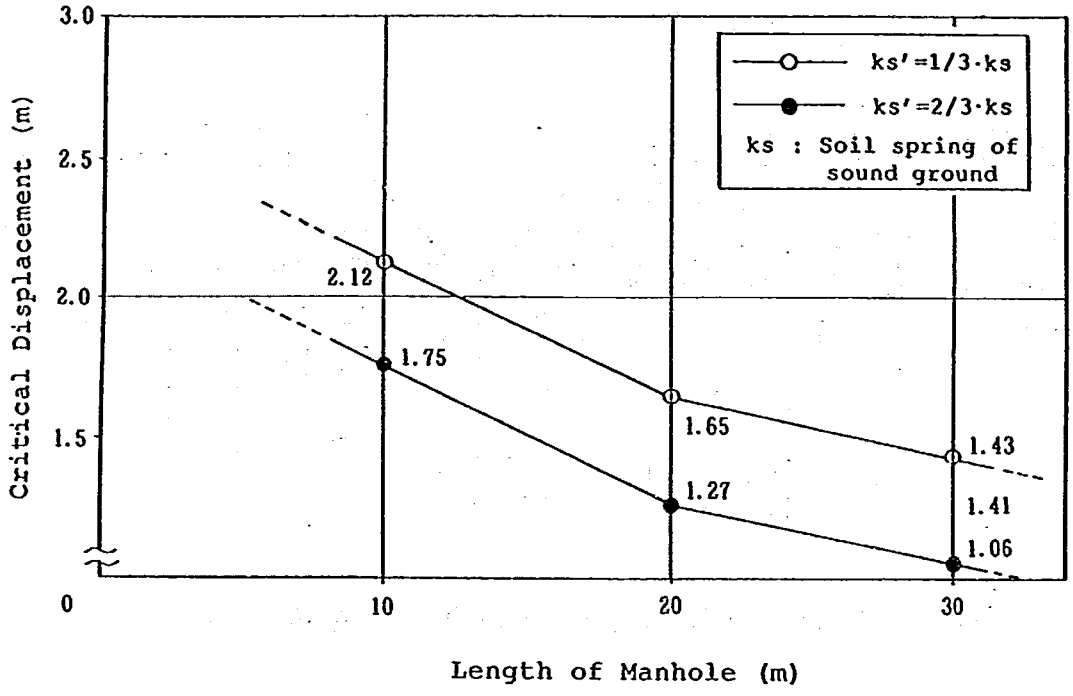


Figure 9 Relationship between Interval of Manholes and Critical Deformation (Axial Direction Force Load, Compressive Failure)

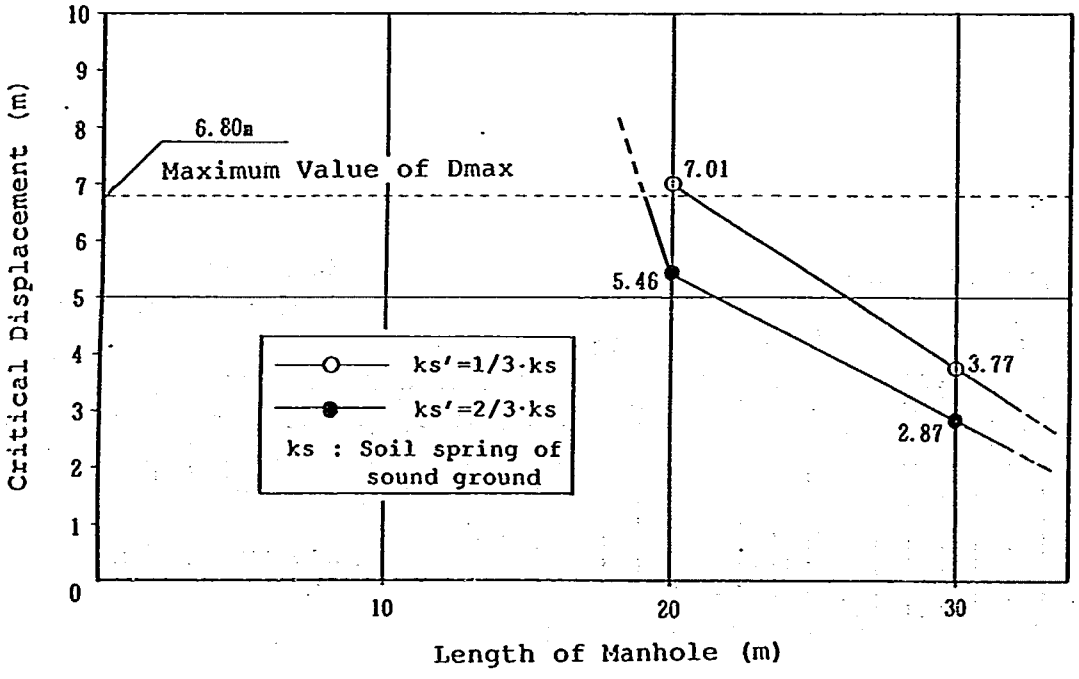
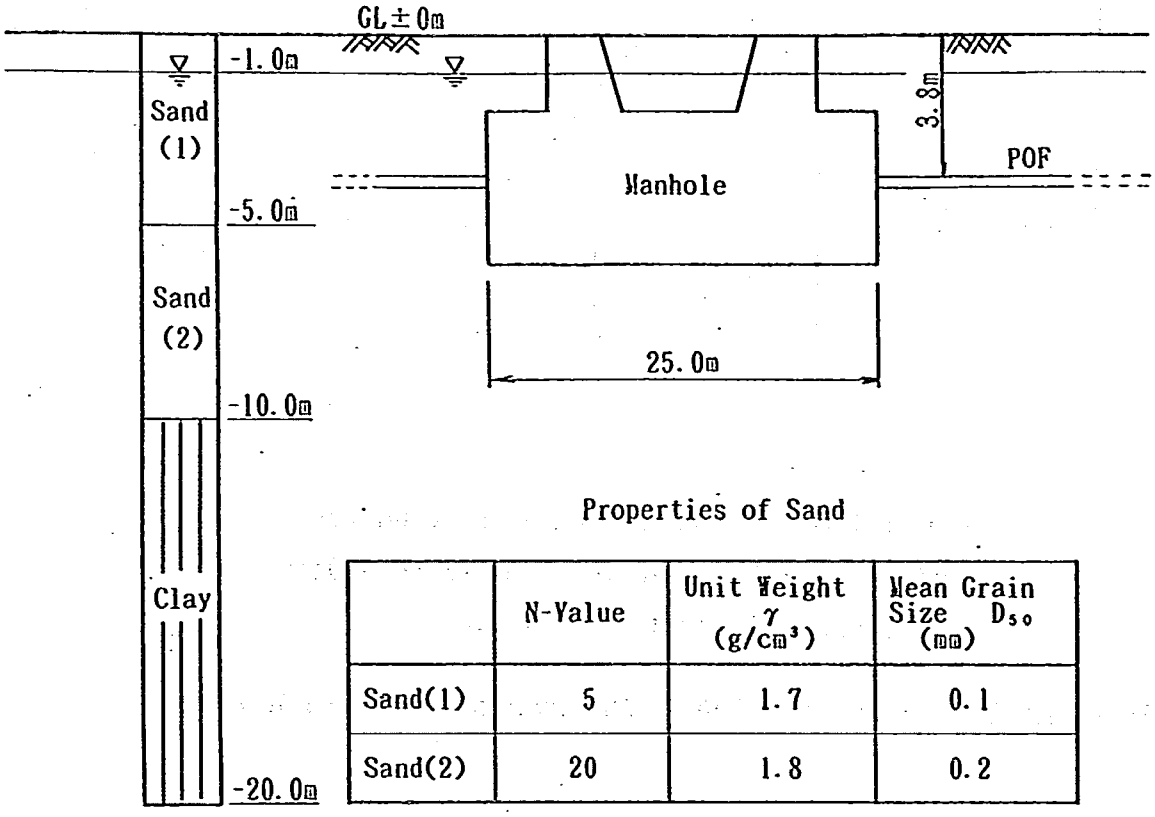


Figure 10 Relationship between Interval of Manholes and Critical Deformation (Lateral Direction Force Load, Bending Failure)

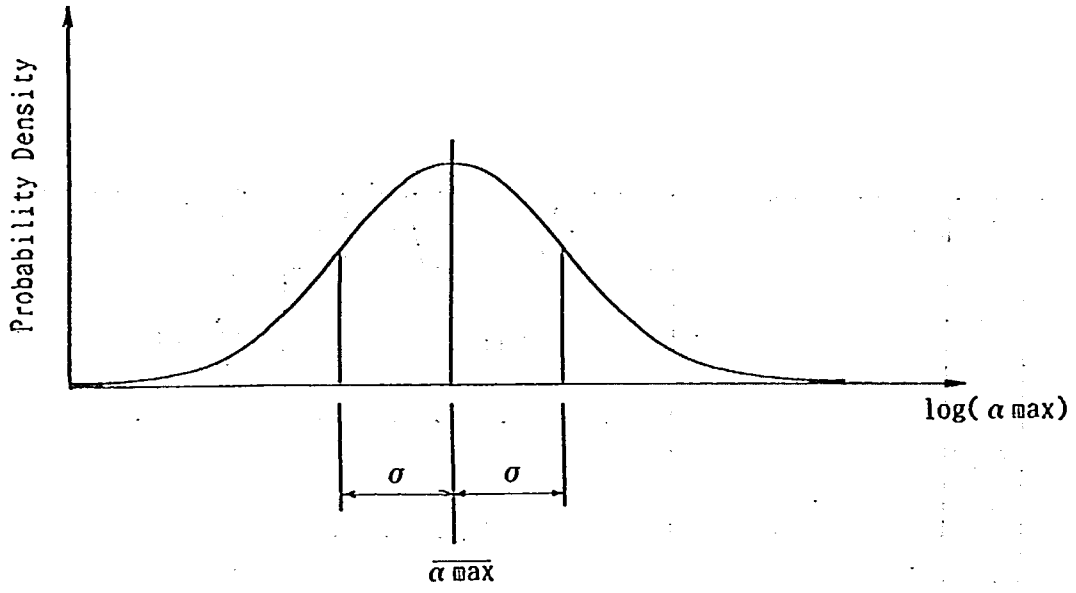
Soil Profile



Properties of Sand

	N-Value	Unit Weight γ (g/cm³)	Mean Grain Size D_{50} (mm)
Sand(1)	5	1.7	0.1
Sand(2)	20	1.8	0.2

Figure 11 Model POF Attached to a Manhole and Ground Conditions for the Calculation of Failure Probability



α max : Maximum ground acceleration at surface.

$\overline{\alpha \text{ max}}$: Mean Value of α max (α max=100gal, 200gal

σ : Standard deviation (σ =0.269)

Figure 12 Distribution of Probability Density of the Maximum Acceleration

Table 2 Results of the Estimation of Failure Probability

Mean Value of PGA $\overline{\alpha_{max}}$ *(Gal)*	*Failure Mode of Pipe*	*Critical PGA* α_{cr} *(Gal)*	*Failure Probability for Each Failure Mode* P_{fc} P_{ft} P_{fm}	*Total Failure Probability* P_f
100 (53.8 to 185.8*)	compression:fc	220	0.101	0.029
	tension:ft	non-failure	0	
	moment:fm	non-failure	0	
200 (107.7 to 371.6*)	compression:fc	220	0.440	0.126
	tension:ft	non-failure	0	
	moment:fm	non-failure	0	

*) *Notice : "(-- to --)" denotes log variation of* $-\sigma$ *to* $+\sigma$

EXPERIMENTAL STUDY ON LIQUEFACTION POTENTIAL AND THE UPLIFT DEFORMATION OF UNDERGROUND STRUCTURES

Ken-ichi Tokida[1], Yoshio Ninomiya[2] and Takuo Azuma[3]

ABSTRACT

As for the earthquake resistant design of underground structures, the important point is the method to evaluate excess pore water pressure which causes uplift force acting on an underground structure. In this paper, uplift deformation of underground structures with a rectangular section such as a common utility duct due to soil liquefaction during earthquake is considered. And the relation between the uplift deformation of underground structures and excess pore water pressure in the ground surrounding the underground structure is observed using two dimensional ground models and underground structure models whose conditions are varied in the shaking table test . Furthermore, the factors relating to the uplift deformation of underground structures due to soil liquefaction are discussed.

INTRODUCTION

Waterfront area at urban district in Japan is recently being developed. At this area, there are a lot of underground structures buried in liquefiable sand layer. It is especially important to consider reasonable earthquake resistant design and economical countermeasures against uplift of underground structures such lifeline systems as sewage pipes and common utility ducts.

From this point of view, this paper is intended as an experimental investigation of the relation between occurrence of excess pore water pressure in liquefied layer and uplift of an

---

[1]Head, Ground Vibration Division, Public Works Research Institute, Ministry of Construction
1 Asahi, Tsukuba-shi, Ibaraki-ken 305 Japan
[2]Senior Research Engineer, ditto
[3]Assistant Research Engineer, ditto

underground structure, using a shaking table. The ground models and the underground structure models of these tests is varied in the following conditions; the thickness of liquefiable layer below the structure model, the width of the structure and the barrier wall which is considered to work as one of countermeasures against uplift of the structure.

METHOD OF EXPERIMENT

The condition of test models and measurements are shown in Figure 1 and Table 1. The ground models are constructed in a square container placed on a shaking table. This container is 600 mm wide, 1,800 mm long and 1,100 mm high. The front and back plates of it are acrylic resin. The ground model consists of a liquefiable sand layer and a non-liquefiable sand layer. The total thickness of the two layers and the thickness of a liquefiable layer above the underground structure model are set to be constant in each test, and the thickness of liquefiable sand layer below every structure model is respectively varied in three or two cases.

The material of the ground model is a clean sand called as Toyoura Sand. These characteristics of the material is shown in Table 2. The liquefiable sand layer is constructed by the underwater drop method. The non-liquefiable sand layer is firstly compacted enough not to liquefy during exciting. These characteristics of liquefiable sand in each test is shown in Table 3.

The underground structure model is buried in the liquefiable sand layer in each test. In this study, four types of underground structure models whose condition are shown in Table 4, are used. These are made of aluminum and hollow models with a rectangular section. Sponge is stuck on the front and back surfaces of the structure model to reduce a friction force between the container and the structure model.

In each test, constant sinusoidal acceleration with a frequency of 3HZ was employed for 20 seconds(60 cycles). Several levels of maximum acceleration(80-230 gal) are applied stepwise to the shaking tables as an input motion. The input maximum acceleration are shown in Table 5.

As shown in Figure 1, pore water pressure meters , accelerometers and bench mark points are installed in or on the ground models to measure the time history of excess pore water pressure, acceleration and displacement of ground surface. Furthermore, at the surface of the underground structure models, pore water pressure meters, accelerometers, slide wire displacement meters, earth pressure meters and a friction meter are installed to measure the time history of excess pore

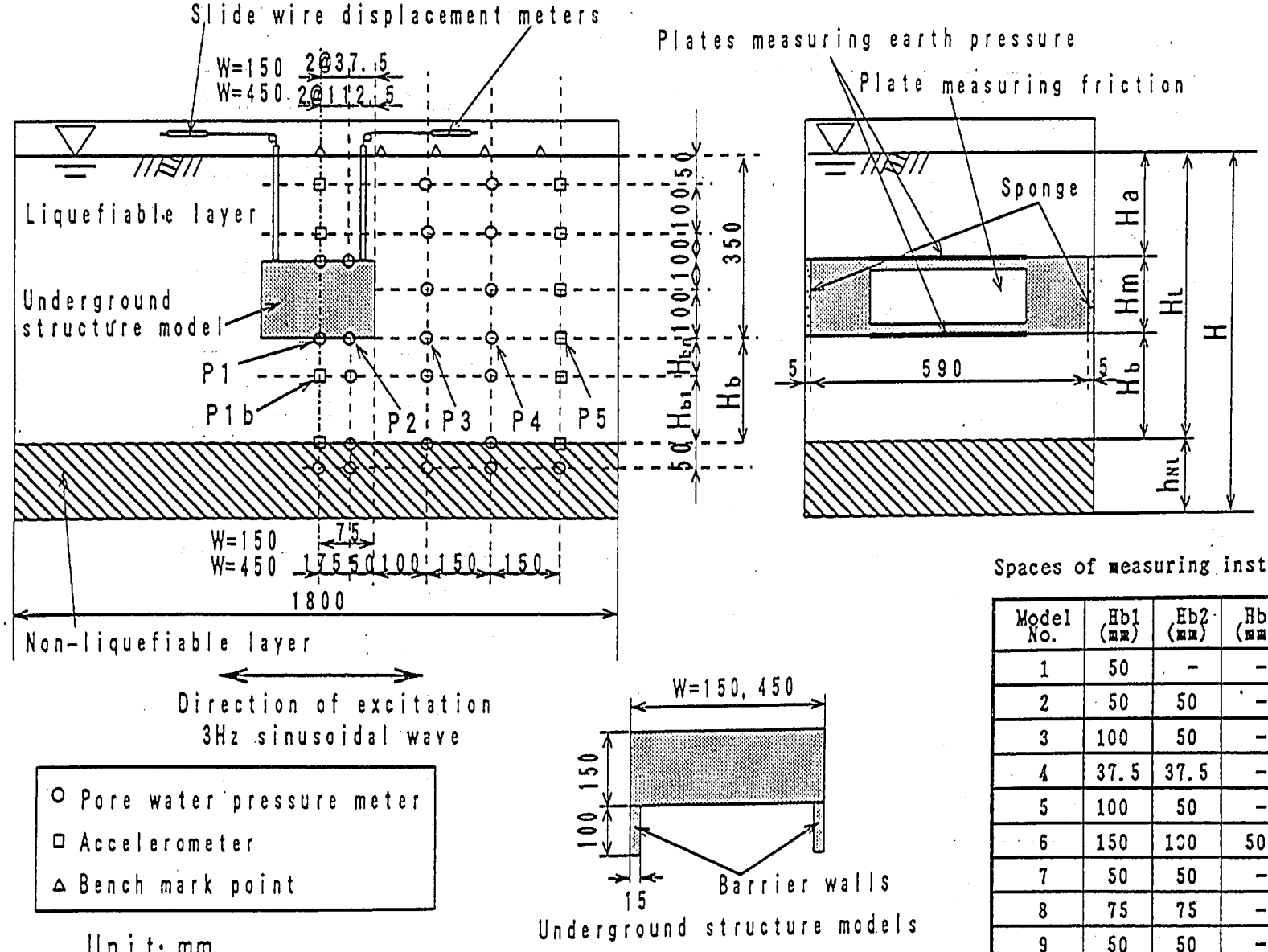


Figure 1 Test models and measurements

Spaces of measuring instruments

Model No.	Hb1 (mm)	Hb2 (mm)	Hb3 (mm)	Hb (mm)
1	50	-	-	50
2	50	50	-	100
3	100	50	-	150
4	37.5	37.5	-	75
5	100	50	-	150
6	150	100	50	300
7	50	50	-	100
8	75	75	-	200
9	50	50	-	100
10	75	75	50	200

water pressures, an acceleration, uplift displacements, earth pressures, a friction between sand and the structure model.

Table 1 Conditions of ground models

Model No.	Layer thickness (mm)						Width	Remarks
	Ha	Hm	Hb	HL	hNL	H	W	
1	200	150	50	400	550	950	150	-
2	200	150	100	450	500	950	150	-
3	200	150	150	500	450	950	150	-
4	200	150	75	425	525	950	450	-
5	200	150	150	500	450	950	450	-
6	200	150	300	650	300	950	450	-
7	200	150	100	450	500	950	150	BW
8	200	150	200	550	400	950	150	BW
9	200	150	100	450	500	950	450	BW
10	200	150	200	550	400	950	450	BW

BW:With barrier walls

Table 2 Characteristics of sand used for the experiments (Toyoura sand)

Specific gravity of soil particle Gs	2.648
Maximum void ratio emax	0.940
Minimum void ratio emin	0.621
Coefficient of uniformity Uc	1.6
Maximum size(mm)	0.85

Table 3 Characteristics of ground models

Model No.	Dry density ρ_t(tf/m^3)	Saturated density ρ_{sat}(tf/m^3)	Relative density Dr(%)
1	1.426	1.887	26.0
2	1.441	1.897	32.0
3	1.434	1.892	29.2
4	1.469	1.914	43.0
5	1.444	1.899	33.2
6	1.443	1.898	32.8
7	1.434	1.892	29.2
8	1.433	1.892	28.8
9	1.469	1.914	43.0
10	1.442	1.897	32.4

Table 4 Conditions of underground structure models

Model No.	Width (mm)	Length (mm)	Height (mm)	Specific gravity	Remarks
1	150	590	150	0.94	-
2	450	590	150	0.85	-
3	150	590	150	1.03	BW
4	450	590	150	0.89	BW

BW:With barrier walls whose length is 100mm.
Note:Specific gravity of model 3,4 is one of the structure models with barrier walls.
Model 1,2 and 3,4 are the same model respectively except for barrier walls.

Table 5 Conditions of input motion

Model No.	Maximum acceleration of input motion (gal)	Frequency and duration
1	80	
	110*	
	170	
2	80	
	110*	
	140	
3	80	
	110*	
4	80	
	110	
	170*	3Hz
	230	
5	80	20 sec
	110*	
6	140*	
7	80	
	140*	
	200	
8	80	
	140*	
9	80	
	140*	
	200	
10	80	
	140*	

*:The uplift of a structure model was observed first.

RESULTS OF EXPERIMENT

As for uplift of underground structures due to soil liquefaction, it is important to investigate the rise of excess pore water pressure on the bottom plate of the structure. In this study, the uplift deformation of underground structures and the rise of excess pore water pressure were investigated experimentally in the different models: the thickness of the liquefiable layer below the structure models(Hb), the width of the structure models(W) and the existence of barrier walls.

The following figures show that the values of excess pore water pressures are maximum values and the values of vertical displacements are mean values calculated in the time step of 0.33 seconds. And the results in this paper show ones as for the input conditions when the uplift of the structure models began first (see Table 5).

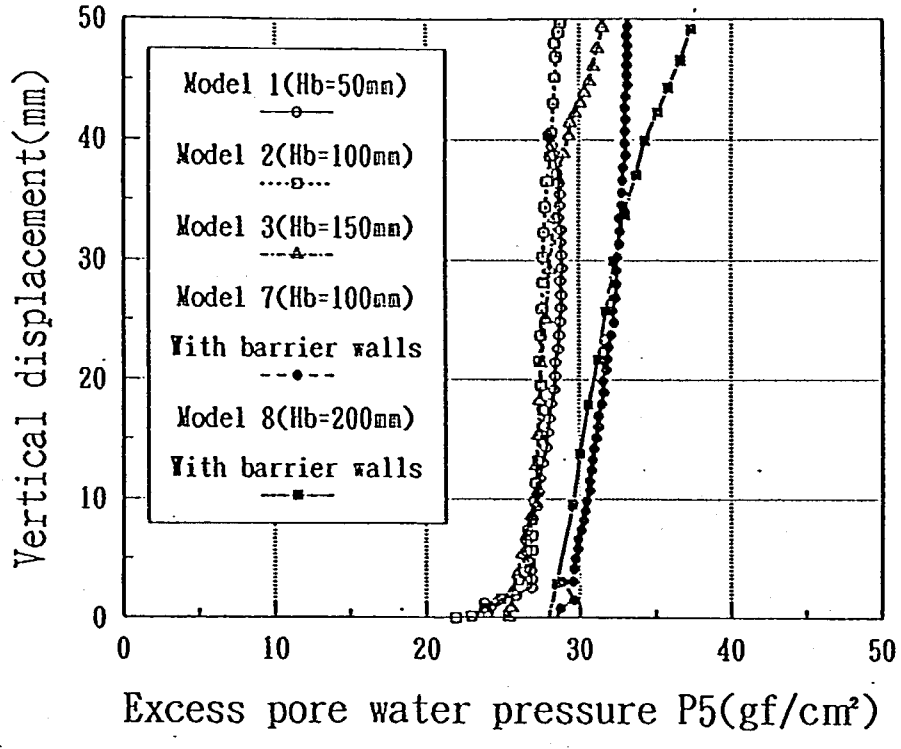
Figure 2 (a) and (b) show the relation between the vertical displacements of the structure models and the excess pore water pressures in surrounding ground at the same depth as the bottom plate of the structure model(P5 in Figure 2). It can be noticed from these figures that the excess pore water pressure at P5 at the beginning of uplift do not depend on the thickness of the liquefiable layer below the structure model, but the characteristics of the structure models. Furthermore, since the excess pore water pressures at the beginning of uplift of Structure Model 2 (specific gravity 0.94) are smaller than Model 3(1.03, see Table 4), the excess pore water pressures at the beginning of uplift of the structure models with barrier walls are larger than those without barrier walls.

Figure 3 shows the time histories of the vertical displacements of the Structure Model 1. This figure indicates that the structure model begin to uplift more early and the uplift velocity, in other words, the gradient of the line shown in Figure 3 becomes large according to the increase of Hb.

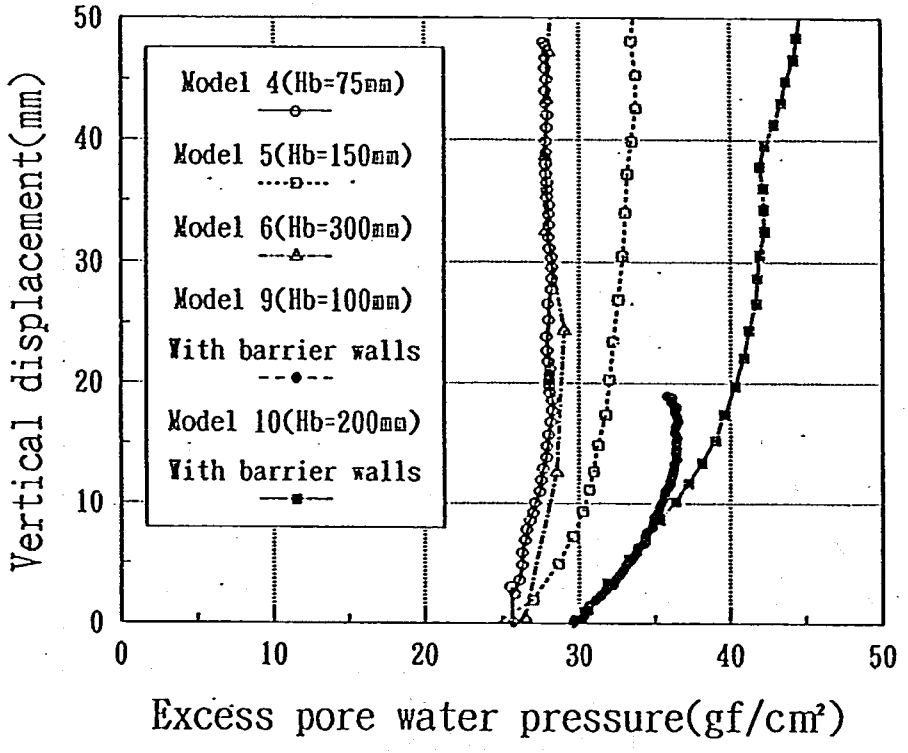
Figure 4 shows the time histories of the vertical displacements of the Structure Model 3 and 4 with barrier walls. This figure indicates that the uplift velocity of Structure Model 3 (W=150 mm) is larger than Structure Model 4 (W=450 mm). Thus, it can be indicated that the uplift velocity of the structure model becomes small according to the increase of W. The effect of Hb can be also indicated in this figure as indicated in Figure 3.

Figure 5 (a) and (b) show the time histories of the vertical displacements of the structure models. It is clear that the uplift velocities of Ground Model 7 and Ground Model 9 (structure models with barrier walls) are smaller than Ground Model 2 and Ground Model 4 (structure models without barrier walls), respectively. Therefore, it can be noticed that barrier walls work effectively to reduce the uplift velocity of the underground structure models.

Figure 6 shows the time histories of the excess pore water pressures in the ground surrounding the structure model (P5) and at the point under the center of the bottom plates (P1b in Figure 1). This figure indicated that the rise of excess pore water pressures at P5 and P1b become large according to the increase of Hb.



(a) Models 1, 2, 3, 7 and 8 (W=150mm)



(b) Models 4, 5, 6, 9 and 10 (W=450mm)

Figure 2 Relations between vertical displacements and excess pore water pressures

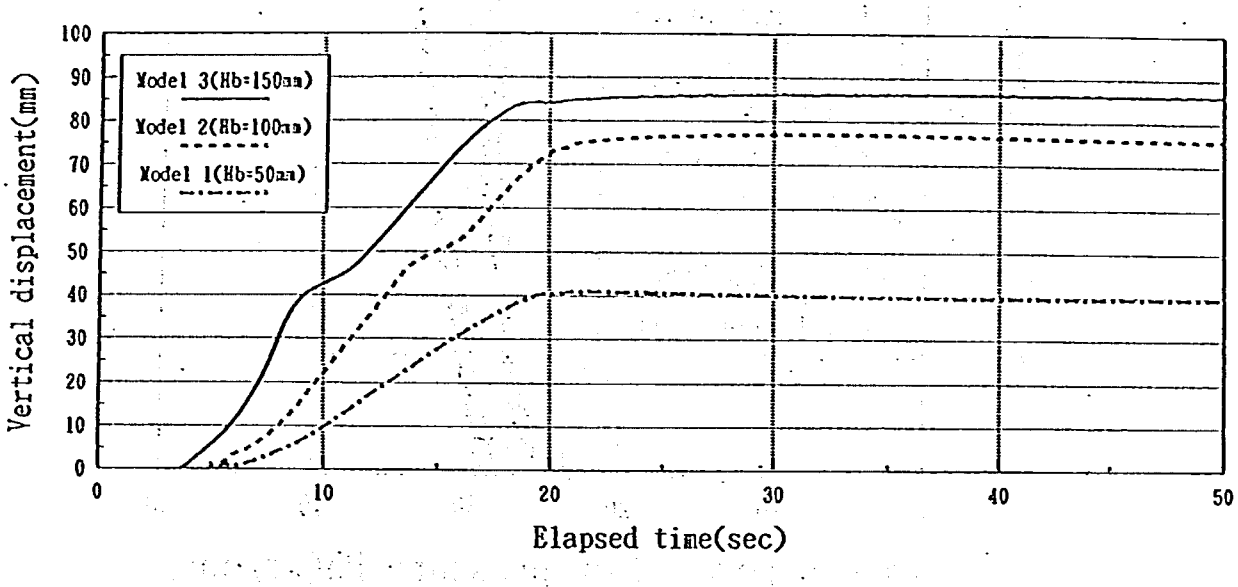


Figure 3 Time histories of vertical displacements
Models 1, 2 and 3 (W=150mm)

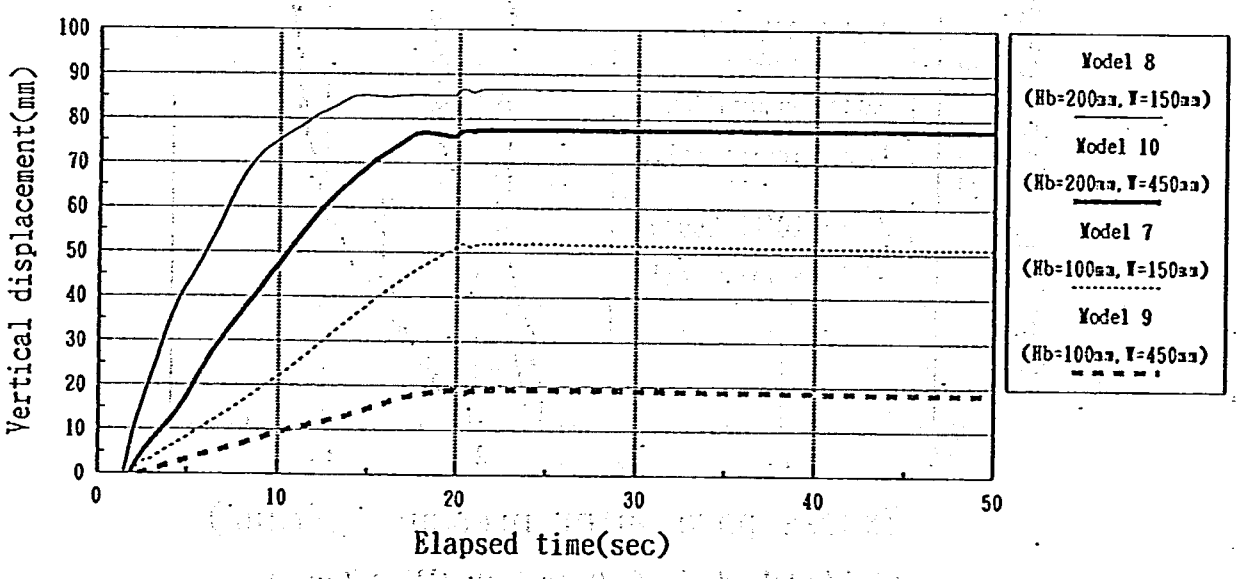
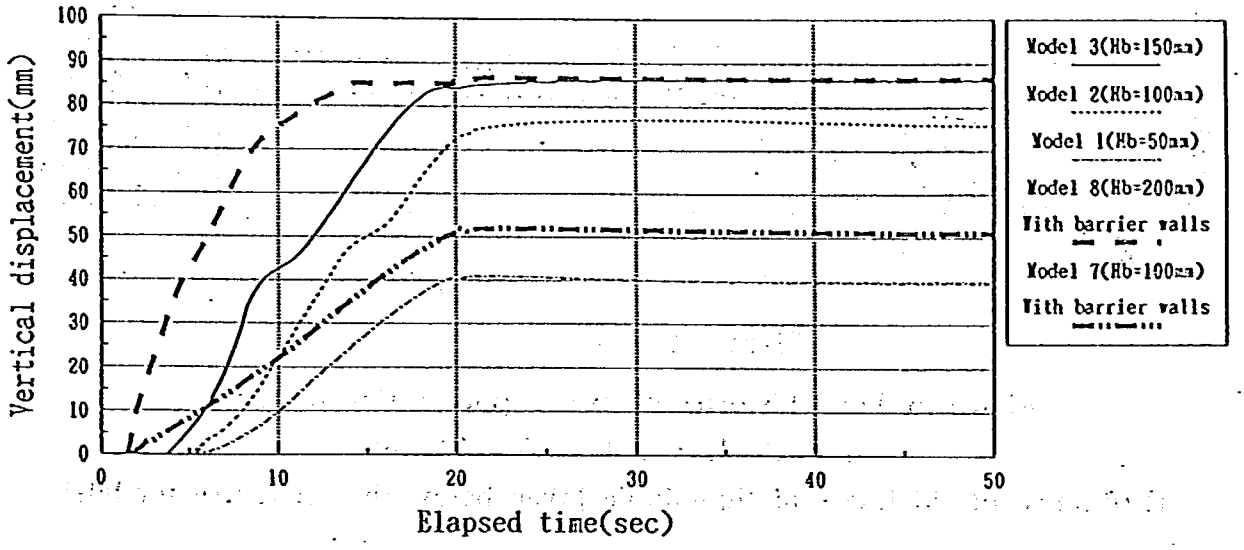
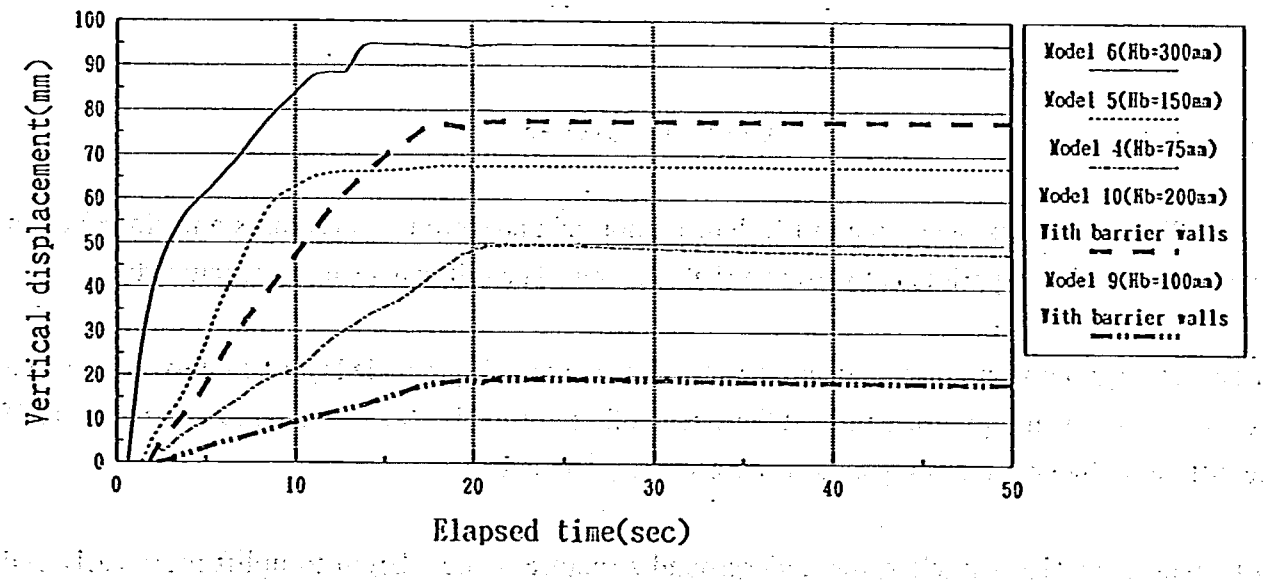


Figure 4 Time histories of vertical displacements
Models 7, 8, 9 and 10: with barrier walls



(a) Models 1, 2, 3, 7 and 8 (W=150mm)



(b) Models 4, 5, 6, 9 and 10 (W=450mm)

Figure 5 Time histories of vertical displacements (Comparison of with and without barrier walls)

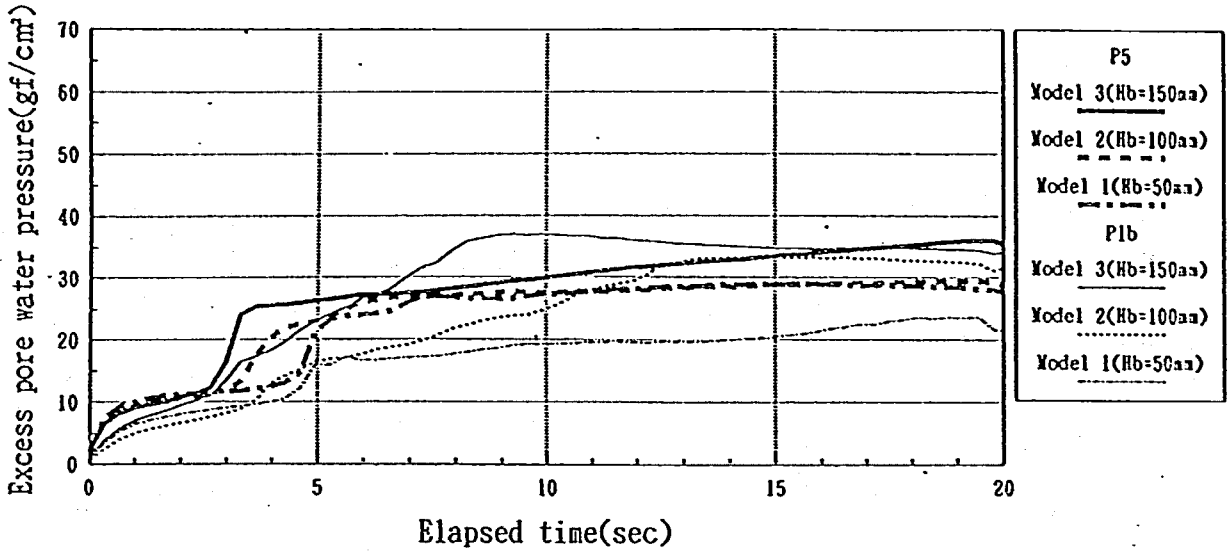


Figure 6 Time histories of excess pore water pressures
Models 1, 2 and 3 (W=150mm)
(Influence of thickness of liquefiable layer below the structure models)

CONCLUSIONS

The relation between the uplift deformation of underground structures and liquefaction potential is studied experimentally using a shaking table. The following can be concluded:

1) The underground structure models set at the same depth in liquefiable layer begin to uplift, when the excess pore water pressure ratio at the surrounding ground is almost the same value in spite of the different thicknesses of layers below the structure model

2) However, as Hb is thicker, the underground structure models begin to uplift more early and uplift faster. Because the excess pore water pressure below the structure model increase early and fast according to the increase of the thickness of liquefiable layer below the structure model. And

another reason why the structure model uplift faster is that the soil and water flow from the surrounding ground to the below of the structure model may become easy.

3) As the width of the structure models is smaller, the structure models uplift faster, because the soil and water flow from the surrounding ground to the below of the structure model may become easy.

4) It is important to pay attention to the thickness of liquefiable layer below underground structures and the width of ones, when we discuss the countermeasures of underground structures.

5) The barrier walls installed on the underground structure models are effective to reduce the uplift velocity of the structure models.

FUTURE DIRECTIONS

Future subjects on the uplift deformation of underground structures caused by liquefaction can be considered as the following;

1) Investigation of other factors such as overburden load on the top plate of the underground structure and friction acting on the side plates of that relating to uplift deformation of underground structures.

2) Influence of shape of the cross section: rectangular and circle, upon the uplift deformation of underground structures.

3)Establishment of method to estimate the safety factor considering the uplift deformation characteristics of underground structures.

4) Establishment of reasonable countermeasures such as barrier walls to prevent or decrease the uplift deformation of underground structures.

ACKNOWLEDGEMENT

The authors wish to express his sincere gratitude to Mr.Hideo Matsumoto, Deputy Head of Planning Division of PWRI for his helpful comments to conduct experiment.

REFERENCES

1.Japan Road Association: "Design Guidelines for Common Utility Duct', March, 1986(in Japanese)

2.Tokida K. Ninomiya Y.: Experimental Study on the Uplift Deformation of Underground Structures Induced by Soil Liquefaction, Fourth Japan-U.S. Workshop on Earthquake Resistant Design of Lifeline Facilities and Countermeasures Against Soil Liquefaction, May 1992

LATERAL SPREAD EFFECTS ON REINFORCED CONCRETE PILE FOUNDATIONS

W.D. Meyersohn[1], T.D. O'Rourke[2], and F. Miura[3]

ABSTRACT

The paper presents the results of analytical studies focused on the response of reinforced concrete piles to lateral spreads caused by soil liquefaction. A numerical procedure was applied for this study, which represents the refinement and expansion of an existing computer program, B-STRUCT, developed as part of a cooperative U.S.-Japan research project. The procedure models the pile by means of beam elements and rotational springs. The surrounding soil is modeled by means of transverse and longitudinal bilinear spring-slider elements. The beam elements account for both geometric nonlinearities and buckling states. The program accounts for nonlinear material performance by means of rotational springs, which utilize a trilinear moment-rotation law to represent the cracking and ultimate flexural states of reinforced concrete piles. The moment-rotation relationship reflects the composite action of the concrete and reinforcing steel, as well as the levels of thrust and moment in the pile.

Analytical results of the program are shown to be in good agreement with the observed performance of piles during previous Japanese earthquakes. The results of a parameter study are presented in which the maximum lateral displacements affecting deep foundations are related to the subsurface conditions, displacement magnitude, pile diameter, and the thickness and stiffness of the liquefied soil. Recommendations for planning and design are made on the basis of the analytical findings. The engineering recommendations and computer model are applicable to deep foundations for bridges, waterfront structures, and buildings.

1,2 - Graduate Research Assistant and Professor, respectively, School of Civil and Environmental Engineering, Cornell University, Ithaca, NY

3 - Professor, Computer Science and Systems Engineering, Yagamuchi University, Ube, Japan

INTRODUCTION

Case studies of liquefaction-induced ground deformation and damage to pile foundations during the 1964 Niigata earthquake (Hamada, et al., 1986) have emphasized the critical effects lateral spreads can have on deep foundations. As a consequence, there has been considerable analytical effort in modeling the response of pile foundations to lateral spreads (e.g., Kawishima, et al., 1988; Miura, et al., 1991; Yoshida and Hamada, 1991; Miura and O'Rourke, 1991). Relatively sophisticated models have been developed that predict the deformation pattern and failure mechanisms observed in the field.

This paper describes a computer model to evaluate pile response to large ground deformation. The analytical results of the model are shown to compare favorably with observed patterns of pile deformation. The failure modes of piles subjected to liquefaction-induced movements are discussed, with emphasis on failure by either buckling or excessive flexure. The results of parametric studies are summarized to provide dimensionless plots for identifying axial loading conditions that may result in buckling, and for predicting the maximum lateral soil displacement associated with excessive bending of the pile. An engineering approach is proposed in which a safe level of axial pile load is chosen to prevent buckling, and the maximum lateral soil movement at flexural failure is estimated.

ANALYTICAL MODEL

The computer program, B-STRUCT, a code based on the finite element method, has been developed over a number of years as a research tool to solve soil-structure interaction problems. In its original conception, B-STRUCT was developed in FORTRAN at Cornell University (Trautmann, 1981) to evaluate buried pipeline response to permanent ground displacement patterns induced by trench construction. Later, the code was upgraded by Ahmed (1990) to account for simultaneous axial and transverse soil-interaction and different force-displacement relationships for transverse upward and downward relative movements between the pipe and soil. However, the program was, at this stage, restricted to the limitations of small deflection theory.

Miura and O'Rourke (1991) expanded the range of applicability of the program by including rotational joints with a trilinear moment-curvature relationship. This adjustment allowed for material nonlinearities of the pile in terms of moment and the relative rotation between consecutive beam elements. In the present stages of development, B-STRUCT takes into account both geometric nonlinearities and material nonlinearities of pile and soil. Each beam element is formulated as a nonlinear elastic member, with material nonlinearities concentrated at nodal points. An Updated Lagrangian formulation is used to account for geometric nonlinearities in the simulation of large deformation. A solution algorithm, based on the modified Newton-Raphson method with a mixed-step iteration technique, is used for convergence. Beam elements are formulated with the capability of detecting buckling states.

Figure 1a shows the soil-pile system with various geometric parameters used in the present study. The water table designates the top of the liquefiable stratum of thickness, H_L, above which is the nonliquefiable soil cover, l_L. The pile is embedded a distance, l_b, into a firm, nonliquefiable soil. Soil displacement is specified as an input parameter and applied in a series of load increments until the final magnitude of maximum soil displacement at the ground surface, d_h, is achieved. Any distribution of soil displacement can be specified, with a trapezoidal distribution illustrated in the figure. Axial load, shear, and moment can be specified at the top of pile.

As shown in Figure 1b, the program models the pile foundation by a series of beam elements, while the surrounding soil is modeled by means of transverse and longitudinal bilinear spring-slider elements. Although the diagram shows only springs offering lateral resistance, the program accounts for the effects of skin friction and adhesion as well. The two-dimensional beam elements account for geometric stiffening of the pile. In addition, the effect of axial thrust on the bending capacity of the pile is incorporated in the model.

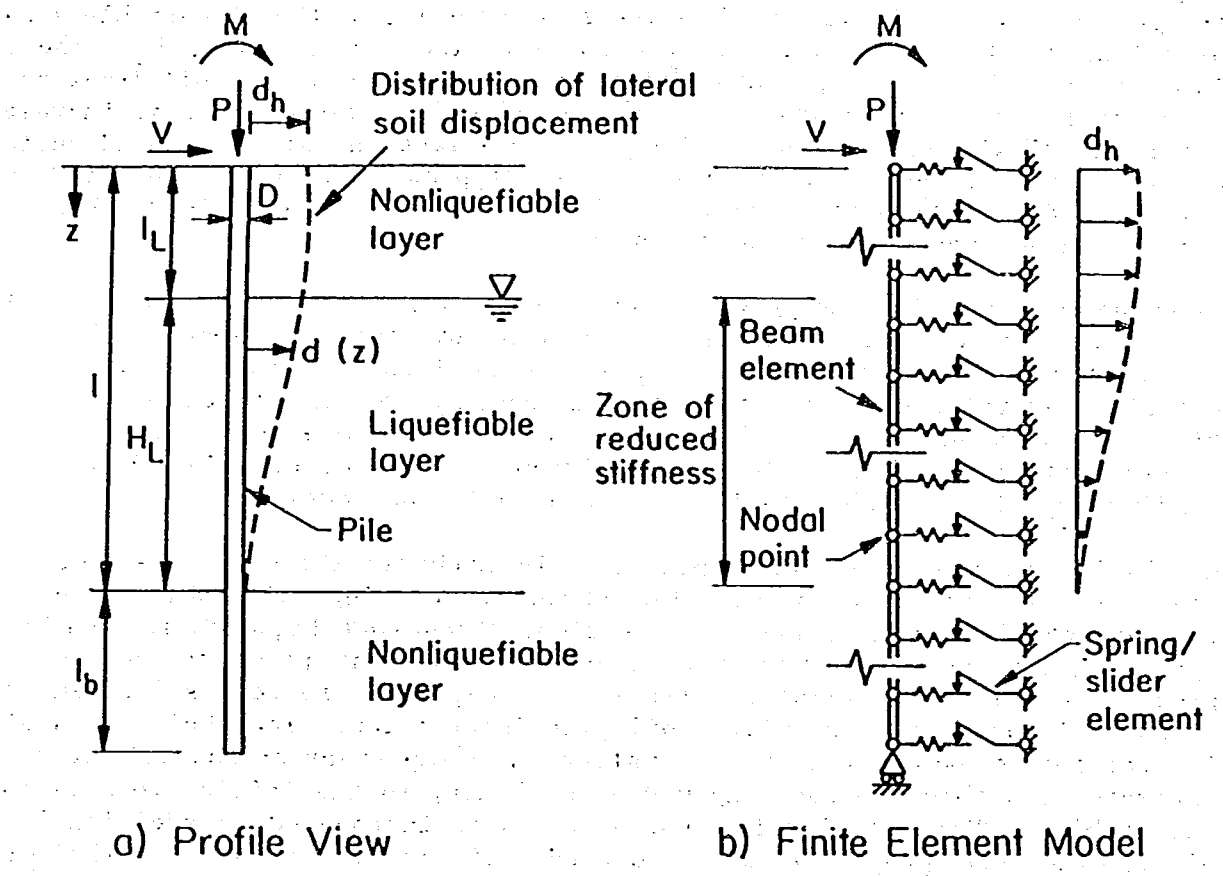
A relatively simple model is adopted in this study for the horizontal force-displacement relation between the pile and the surrounding soil, which is based on the concept of horizontal subgrade reaction. Given that liquefaction and lateral spreading involve a stiffness reduction mechanism that is poorly understood at present, a relatively simple, bilinear elasto-plastic force-displacement relationship is adopted to simulate soil-pile interaction. The choice of a simple interaction mechanism permits the evaluation of important trends and influential parameters, without introducing undue complexity in the initial formulation of the problem. More complex formulations can be introduced as additional tests of liquefied soil properties are conducted, and a better delineation of the problem is achieved through parametric studies.

The soil yielding force is determined from lateral bearing capacity factors proposed by Hansen (1961). The soil spring stiffness was determined from the coefficient of horizontal subgrade reaction, k_h, proposed by Terzaghi (1955), which is given by the expression:

$$k_h = n_h \frac{z}{D} \tag{1}$$

in which n_h is the constant of horizontal subgrade reaction, z is the depth, and D is the pile diameter. The yielding spring displacement was determined by dividing the yielding force by the spring stiffness. Stiffness reduction due to liquefaction is accomplished by dividing k_h by a reduction factor larger than 1. The spacing of the spring-slider elements was chosen to conform with the maximum spacing required for beam on elastic foundation analysis (i.e., Boresi, et al., 1978).

Nonlinear flexural behavior of the pile material is accounted for by means of rotational springs, which utilize a trilinear moment-rotation law. The rotational springs, which connect individual beam elements, are used to represent cracking and ultimate flexural states of reinforced concrete piles. Figure 1c



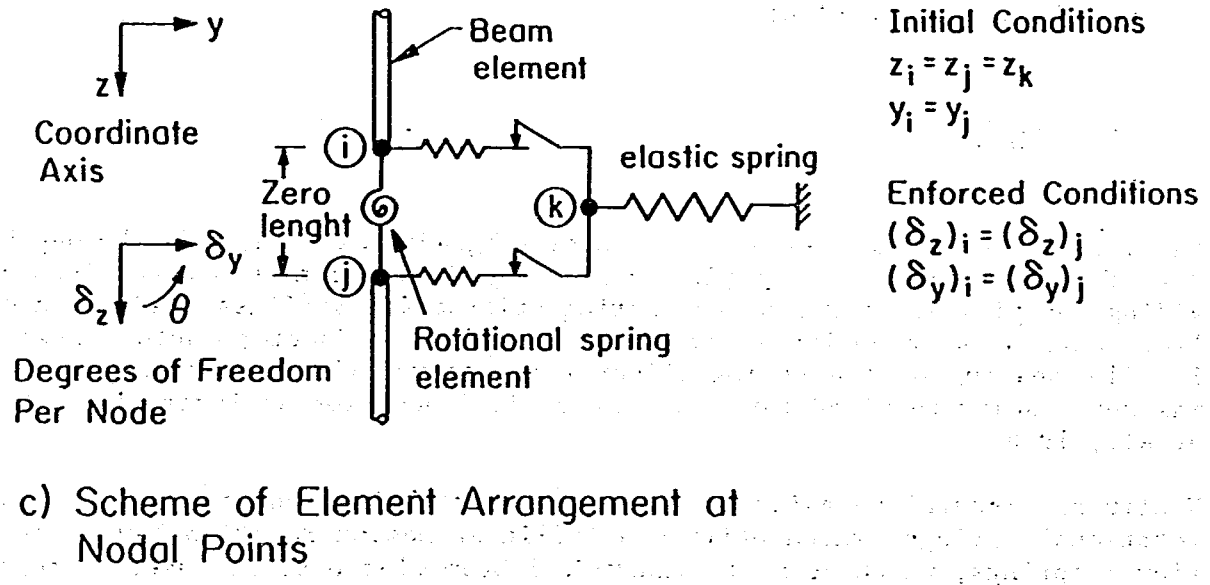


FIGURE 1. Analytical Model for the Soil-Pile System

illustrates a typical beam element-rotational spring connection. A zero-length rotational spring is placed between adjacent beam elements. A condition is enforced in which both axial and transverse displacements of nodes i and j are the same. As a result of the double-node scheme, two soil springs are required in parallel at both nodes. The stiffness of each soil spring is, in this case, one-half of what it would be if only one spring were used.

Both soil springs are connected in series to a very stiff elastic spring. Soil displacements are specified indirectly by a force applied at node k. The magnitude of this force is determined such that the resulting displacement at node k is exactly the specified soil displacement. Although this arrangement of elements produces a larger structure, it substantially improves numerical convergence.

Since the material nonlinearity of the model is concentrated at the rotational springs, the lateral deflection of the pile is the combined result of elastic bending of the beam elements and nonlinear rotation of the connecting rotational springs. Therefore, the relation between moment and curvature of the pile has to be converted into a relation between moment and rotation of the rotational spring elements. As explained in Appendix A, the angle of rotation of the rotational spring is related to a step-wise moment-rotation relation of the pile by means of the expression:

$$\theta = \frac{2}{n+1}\frac{1}{L}\left[d - \frac{ML^2}{2EI}\right] \tag{2}$$

in which L is the total length of the pile, n is the number of rotational springs present in the model, M is the bending moment, E is the Young's modulus of the pile material, and I is the moment of inertia of the pile cross-section. The term d is a transverse pile deflection given by the equation:

$$d = \frac{1}{\psi} - \sqrt{\frac{1}{\psi^2} - L^2} \tag{3}$$

where ψ is the curvature associated with the moment M. Equation 2 indicates that the spring rotation depends on geometric and elastic properties of the pile, as well as on its moment-curvature relation.

COMPARISON OF FIELD OBSERVATIONS AND ANALYTICAL RESULTS

During the 1964 Niigata earthquake, many foundation piles of bridges and buildings were damaged by liquefaction-induced permanent ground displacement (e.g., Hamada, et al., 1986; Kawashima, et al., 1988). The extent of pile damage, however, was not realized until 1985, when excavations were made at a number of buildings to investigate reinforced concrete pile damage. As indicated in recent work by Hamada (1992), most of the piles were damaged beyond repair as a result

of the earthquake. Surprisingly, the buildings had remained serviceable, even with extensive pile damage.

Two cases were selected for this study to assess the ability of B-STRUCT to predict damage states in pile foundations. The NHK and the Niigata Family Court House (NFCH) pile foundations were chosen for analysis because information regarding pile properties, subsurface conditions, and extent of ground displacement were available. Figure 2 presents a map of the City of Niigata, highlighting the location of the two sites. The NHK building is located on the right bank of the Shinano River, while the NFCH is on the left bank. The distance between both structures is about 2 km. The subsurface conditions at the two sites consist of fluvial and beach deposits of sands and silty sands.

The NHK Building

The NHK building was a four-story reinforced concrete building supported on 35-cm-diameter reinforced concrete piles. Excavations performed 20 years after the earthquake revealed extensive pile damage (Hamada, 1992; Kawamura, et al., 1985). Figure 3a shows a schematic diagram of a typical broken pile, in conjunction with the results of Standard Penetration Tests (SPTs) performed at the site. Severe concrete rupture was observed at 2.5 to 3.5 m from the pile top, and at about 2 to 3 m from the bottom.

Based on the surface ground deformation, pile damage characteristics, and boring records given by Hamada, et al., (1986), it was possible to develop a simplified model for the site, which is presented in Figure 3b. The soil properties used to determine the coefficients of subgrade reaction and ultimate lateral resistances were those of a loose-to-medium sand for the upper 8.5 m, having an angle of internal friction of 32° and a unit weight of 16.7 kN/m^3. The lower 2.5 m was taken as a dense sand with a friction angle of 40° and a unit weight of 17.6 kN/m^3. The analysis, with these input conditions, was similar to that reported by Stewart, et al. (1988) using a previous version of B-STRUCT.

The assumed soil displacement pattern increases linearly from the bottom of the liquefied layer to the top. Within the upper nonliquefiable layer, the soil displacement is constant. The maximum specified soil displacement at the ground surface was set at 1.0 m.

There is laboratory and field evidence that displacement is linearly distributed in soil subjected to lateral spreading. Shake table tests conducted by Yasuda, et al., (1991) indicate that soil displacement of liquefied sands increases linearly in the vertical direction from zero at the bottom of the liquefied layer to a maximum value at the surface. In addition, no relative displacement at the boundary between liquefied and nonliquefied layers was observed. Inclinometer measurements reported by Mejia (1992) after the 1989 Loma Prieta earthquake at a site where liquefaction and lateral spreads occurred show an approximately linear pattern of horizontal movement, thus corroborating the laboratory test observations.

Cracking and ultimate moments and curvatures of the pile were determined from the cross-section of the pile and the estimated axial load acting on the pile

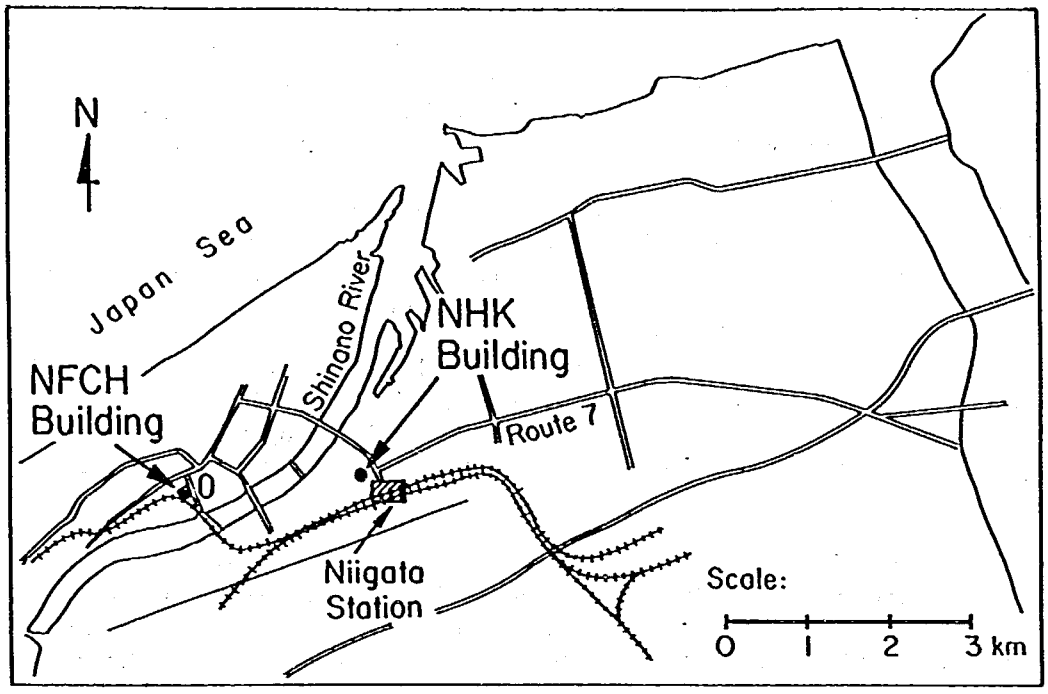


FIGURE 2. Map of Niigata Showing Locations of Buildings and Pile Foundations Used for Analysis

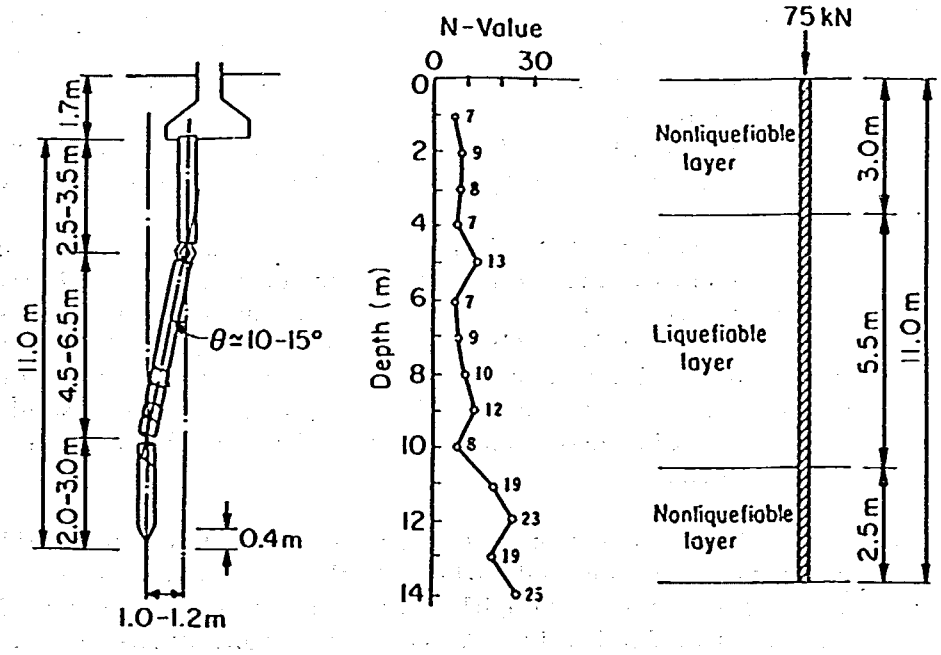


FIGURE 3. Schematic of Typical Damaged Pile at NHK Building

(75 kN). From these values, the moment-rotation characteristics of the rotational springs were calculated using Equations 2 and 3. These values are presented in Table 1. The maximum lateral resistance and the stiffness of the liquefied soil were reduced by a factor of 50. Bending moments were taken as zero at the top and bottom of the pile. Field observations indicate that the pile cap connection behaved as a hinge under the effects of large soil movement.

The results of the simulation are presented in Figure 4. It shows the bending moment distribution along the pile, as well as the deformed shape of the pile at several stages of soil displacement. The analysis predicts the formation of the dual plastic hinge-pattern of the pile. The first plastic hinge is formed at the lower interface, and occurs when the maximum soil displacement reaches a value of about 0.45 m. The upper plastic hinge develops at a maximum soil displacement of 0.62 m. Since the second plastic hinge is formed shortly after the first one, there was not much opportunity for bending moment redistribution, and the pile continued to deform as a rigid body, following closely the soil deformation.

The model successfully predicts the deformed shape of the pile and the locations of the plastic hinges. Furthermore, the model indicates that rigid body displacement would have occurred for maximum soil movement greater than about 0.62 m. The observed pile deformations are consistent with this mechanism of movement.

The NFCH Building

The Niigata Family Court House (NFCH) was a three-story reinforced concrete building founded on concrete piles. As a result of lateral spreading during the 1964 Niigata earthquake, the building displaced horizontally between 0.90 and 1.10 m, according to photogrametic studies performed by Yoshida and Hamada (1991). The building did not collapse, and was placed in service shortly after the earthquake. It was not until demolishing operations during construction of new buildings that the state of the original pile foundation was uncovered.

Two 35-cm-diameter piles, referred to here as Piles 1 and 2, were carefully excavated and examined. Each of them supported a small footing. Figure 5 shows a scale diagram of the damage state of each pile, along with the measured SPT values. The N values are mostly less than 10 for depths up to 8 m, but sharply increase at greater depths. The water table is located at a depth of 1.70 m, however, that value was measured 25 years after the earthquake (Hamada, 1992). It can be assumed that the soil below the water table and above a depth of 8.0 m liquefied during the earthquake.

As shown in Figure 5, Pile-1 did not reach the lower interface, while Pile-2 penetrated into the lower nonliquefied soil. Both piles were damaged at about 2 m from the ground surface, which roughly coincides with the upper interface between liquefied and nonliquefied soil. At this location, Pile-1 showed bending cracks, while Pile-2 showed a severe shear dislocation of about 0.18 m. In addition, severe bending cracks at depths between 6.5 to 8.5 m were observed in Pile-2. The general shape of Pile-2 is similar to that of the NHK piles. It shows a double plastic hinge formation with reverse curvature.

TABLE 1. Rotational Spring Constants of Selected Piles

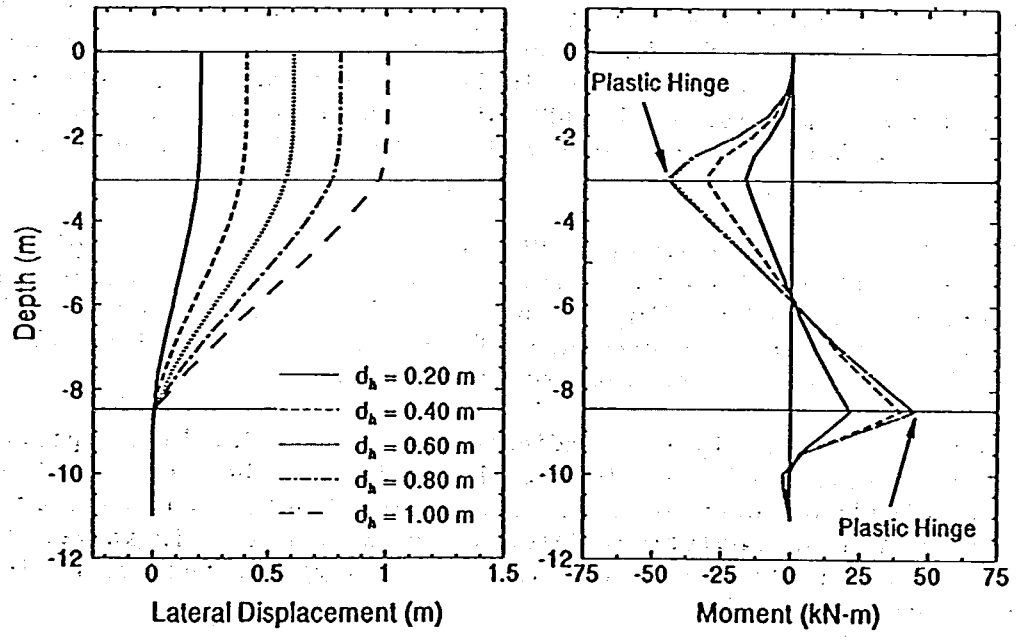
a) Cracking State

Case	D (m)	L (m)	P_a (kN)	n	M_c (kN-m)	ψ_c (m^{-1})	θ_c (rad)
NHK	0.35	11	75	21	2.51	$1.27\ 10^{-4}$	$1.03\ 10^{-5}$
NFCH-1	0.35	7	29	13	2.65	$1.38\ 10^{-4}$	$1.27\ 10^{-5}$
NFCH-2	0.35	9	290	17	15.12	$7.93\ 10^{-4}$	$7.48\ 10^{-5}$

b) Ultimate State

Case	D (m)	L (m)	P_a (kN)	n	M_u (kN-m)	ψ_u (m^{-1})	θ_u (rad)
NHK	0.35	11	75	21	45.03	$5.07\ 10^{-2}$	$2.67\ 10^{-2}$
NFCH-1	0.35	7	29	13	60.76	$4.60\ 10^{-2}$	$2.23\ 10^{-2}$
NFCH-2	0.35	9	290	17	87.05	$3.40\ 10^{-2}$	$1.56\ 10^{-2}$

Symbols:
D = Pile diameter
L = Pile length
n = No. of rot. springs
P_a = Axial load
M_c = Cracking moment
ψ_c = Cracking curvature
θ_c = Cracking rotation
M_u = Ultimate moment
ψ_u = Ultimate curvature
θ_u = Ultimate rotation



a) Pile Displacement b) Bending Moment

FIGURE 4. Analytical Results for the NHK Pile Foundation

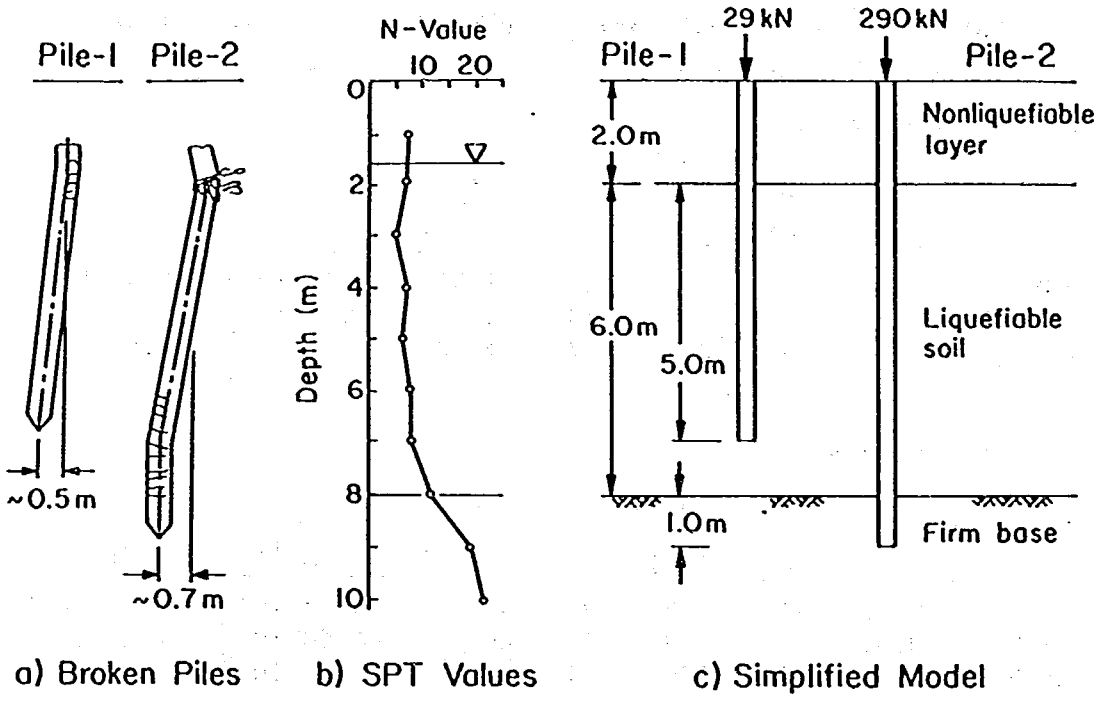
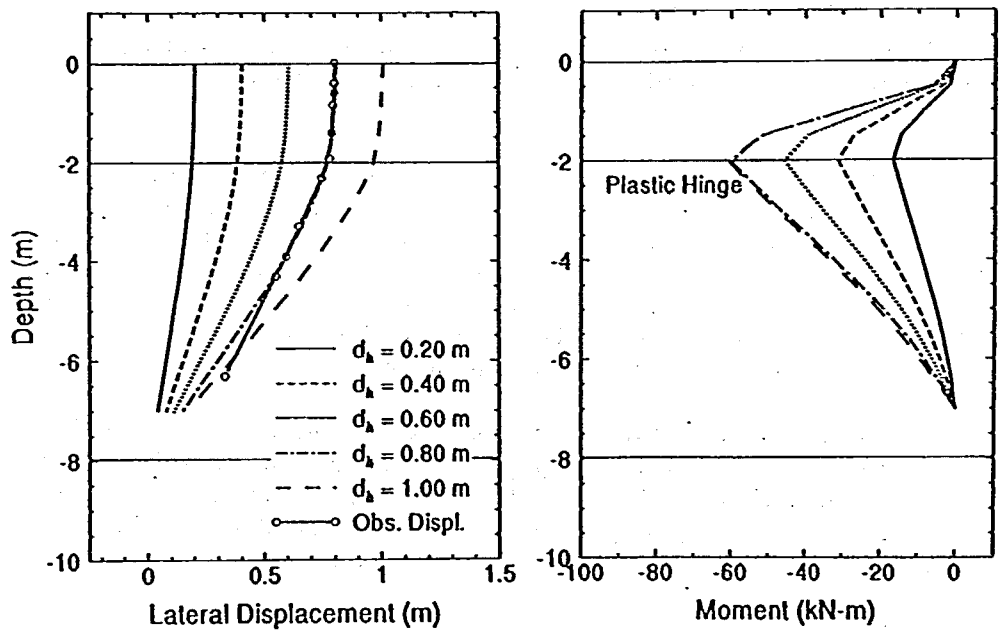


FIGURE 5. Observed Pile Deformation and Soil Conditions at NFCH Building

Table 1 lists the calculated cracking and ultimate moments and curvatures of the cross-sections of both piles. The load in Pile-2 was taken as 290 kN, as given by Yoshida and Hamada (1991). The load in Pile-1 was taken as one-tenth of this value, to reflect the reduced bearing capacity due to soil liquefaction. It should be recognized that further reduction in axial load will not affect the analytical results. Because of the similarity of N-values at both sites, the same geotechnical properties at the NHK building were assumed for the NFCH building. The maximum lateral resistance and stiffness of the liquefied soil were reduced by a factor of 50.

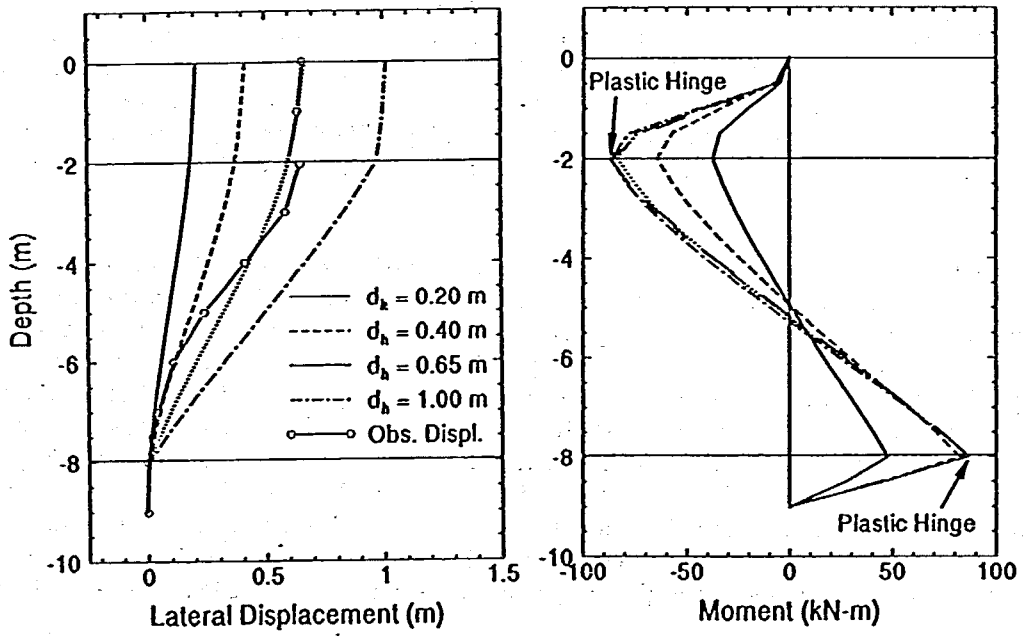
The simplified soil profile given in Figure 5 was used to compute pile response to the assumed soil displacement. The results, presented in Figures 6 and 7, show pile deflections and bending moments at different stages of soil displacement. Superimposed are measurements of transverse deflections obtained by Yoshida and Hamada (1991) from the excavated piles.

The numerical results in Figure 6 indicate that Pile-1 develops a plastic hinge at the upper interface of the liquefiable soil when the maximum displacement reaches a magnitude of about 0.75 m. The observed deflected shape of the pile agrees closely with the analytical deformation pattern at this stage. The bending moment diagram in Figure 6 indicates that no moment redistribution occurs after hinge formation.



a) Pile Displacement b) Bending Moment

FIGURE 6. Analytical Results for Pile-1, NFCH Building



a) Pile Displacement b) Bending Moment

FIGURE 7. Analytical Results for Pile-2, NFCH Building

The analytical results in Figure 7 show that the formation of a plastic hinge in Pile-2 occurs first at the lower interface, when the soil displacement is about 0.42 m, while it develops later at the upper interface, at a soil displacement of about 0.65 m. Like the NHK building, almost no variation in bending moment occurs after the second plastic hinge appears and the pile starts to displace as a rigid body.

A direct comparison between observed and analytical pile displacements is complicated by the shear offset observed in the field. If it is assumed that upper plastic hinge formation weakened the pile, thereby contributing to shear offset at this location, the analytical results for 0.65-m-displacement appear to be consistent with the observed deformation. In this case, hinge formation would have been followed by shear offset, leading to the observed relative movement between the head and underlying body of the pile.

The analytical results show deformed shapes consistent with pile deformations observed in the field. The results imply that the actual displacement of upper intact soil was approximately 0.65 to 0.75 m, which is low relative to the horizontal movement of the building reported by Yoshida and Hamada (1991), but still well within the bounds of measurement error (Hamada, 1992).

PILE FAILURE MODES

Two distinct failure modes can be recognized in piles subjected to lateral spreads resulting from soil liquefaction. In the first one, the lateral deflection of the pile may result in the pile reaching its bending capacity, thus developing a plastic hinge. On the other hand, the combined action of lack of sufficient lateral support, due to the reduced stiffness of the liquefied soil, and the lateral movement that is imposed on the pile, may result in an unstable condition. Whether a pile develops excessive bending or undergoes buckling depends primarily on the stiffness of the liquefied soil, the length of pile exposed to the liquefied soil, the axial load carried by the pile, and the pile stiffness.

Figure 8 illustrates the possible failure mechanisms. The depth of water table in the diagrams simply indicates the possible extent of an upper nonliquefied layer. Whether the bending capacity of the pile is first reached in the vicinity of the lower or the upper interface depends on the amount of lateral restraint offered by the nonliquefied soil. In general, hinge formation will tend to occur at the lower interface, since the higher confining effective stress at a greater depth results in larger lateral resistance than at a shallower depth (Figure 8b). However, it also is possible for the pile to develop a plastic hinge near the upper interface if the foundation system to which the pile is attached provides sufficient lateral movement restraint, if the liquefied soil is relatively deep, or if the pile is not long enough to penetrate the lower firm base (Figure 8c).

Buckling may occur before the development of a plastic hinge, since the critical buckling load of the pile decreases as the pile displaces from its original straight position. It is convenient to regard the lateral displacement of the pile top as an imperfection. The larger the imperfection, the smaller the

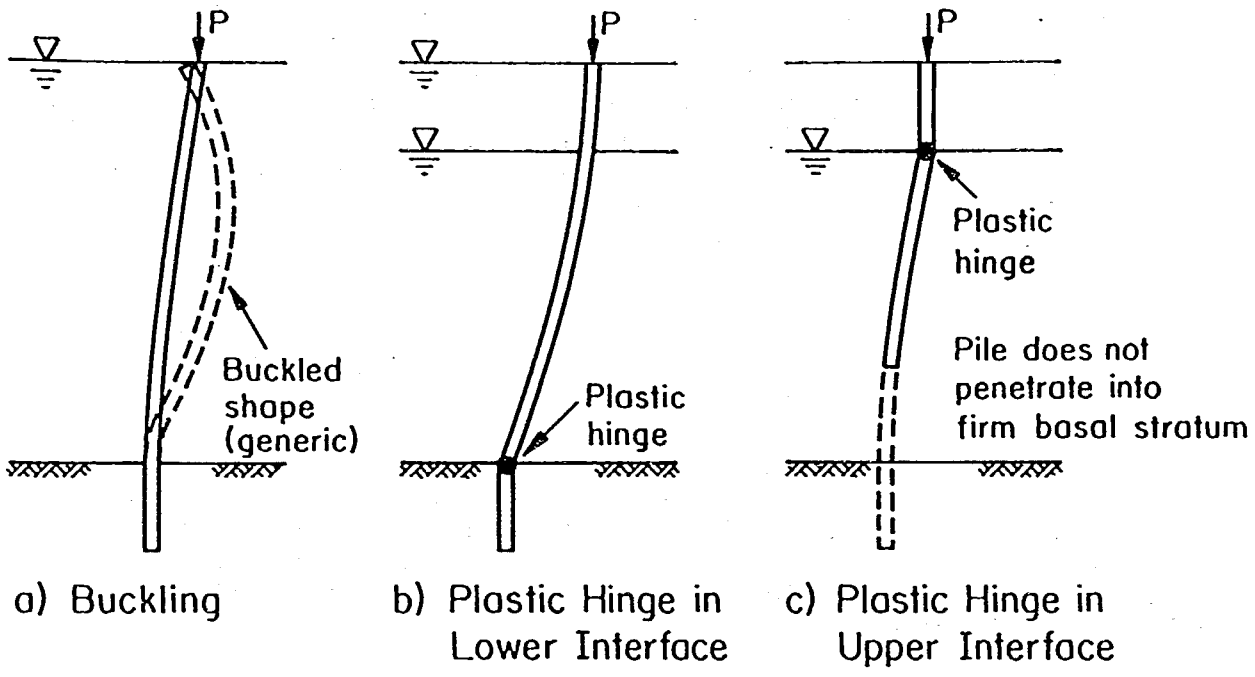


FIGURE 8. Pile Failure Modes

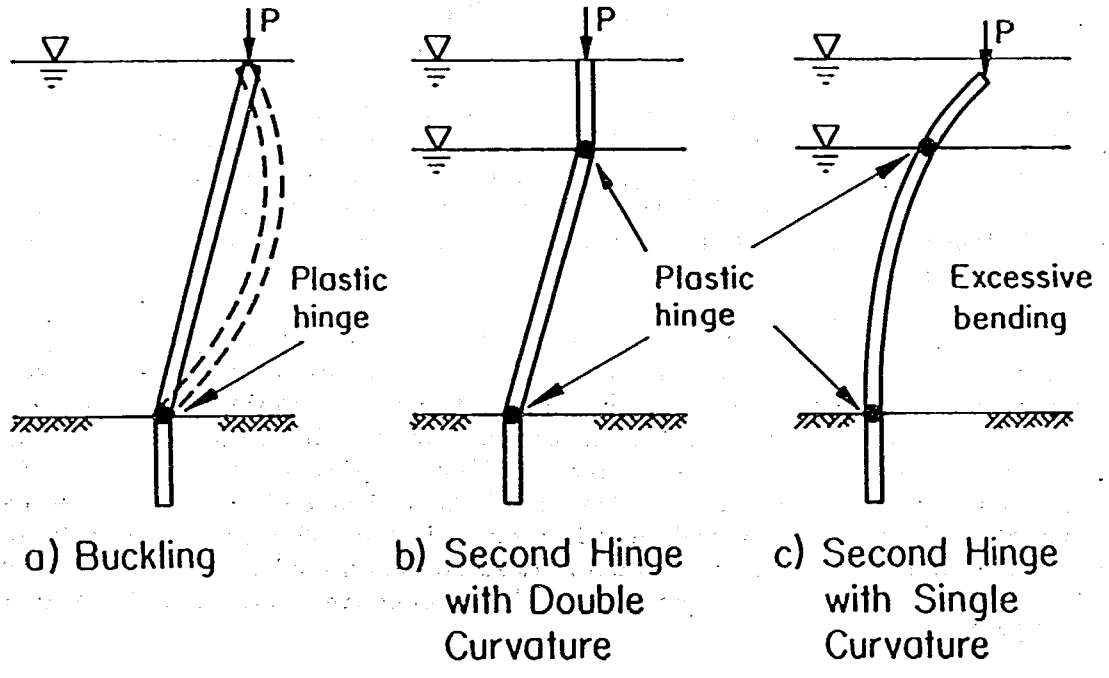


FIGURE 9. Post-Hinge Behavior of Piles

critical load. Depending on the axial load being carried by the pile, this critical displacement could be smaller than the displacement required to cause bending failure. Buckling occurs, for the most part, in situations where there is not sufficient lateral support to counteract the movement of the pile. Such is the case when the water table is at, or near to, the ground surface.

Even after bending failure, the pile may be able to deform without actual collapse (as was evinced by the case histories presented in the previous section). Post-hinge formation behavior is illustrated in Figure 9. The pile could either buckle, or develop a second plastic hinge. Assuming that the first hinge forms at the lower interface, two situations may arise. If the pile is flexible, or if the upper nonliquefiable layer extends sufficiently deep, the pile will bend following a double curvature, trying to comply with the soil displacement pattern. A plastic hinge will tend to form at the upper interface, as shown in Figure 9b. The resulting configuration may be stable, and the pile might be able to continue displacing as a rigid body without significant changes in the stress field.

On the other hand, if the pile is relatively rigid, it will tend to flex, forming a single curvature. After the first hinge develops, further pile displacement will result in moment redistribution over other portions of the pile. The bending moment will increase rapidly over a significant length of pile until deterioration of the pile under high moment occurs (Figure 9c), leading to structural collapse of the pile.

If the pile is sufficiently rigid and strong, it may resist the soil forces imposed by lateral spreading. Under these conditions, a relatively stiff pile will flex until the soil has mobilized its full resistance against the pile. Additional soil movement occurs as a flow relative to the pile.

PARAMETRIC STUDY

The above discussion illustrates various forms of failure that a pile subjected to lateral spreads may undergo. It is vital, therefore, to be able to predict whether a pile will fail in bending, or whether it will buckle as a result of the induced deflection. In addition, it is important to assess the amount of lateral soil displacement that a given concrete pile can absorb before it develops a failure mechanism.

To this end, a parametric study was performed using the computer program B-STRUCT. The basic geometrical configuration is that of Figure 1a. Two pile lengths were used, 11 and 15 m. The extent of the upper nonliquefied layer, H_L, was varied from 0 to 3 m, and the length of the lower embedment, l_b, was assumed to be constant and equal to 2.5 m. Three different pile diameters, 35, 45, and 60 cm, were used in the analysis. The axial load imposed on each pile ranged from 5% to 50% of the calculated bearing capacity of the pile. Cracking and bending moments and curvatures were determined for each combination of pile diameter and axial load, in accordance with the procedure described by Miura and O'Rourke (1991).

The degree of lateral stiffness reduction due to liquefaction is not known, or very difficult to evaluate. Therefore, to explore the stiffness reduction effect on lateral displacement capacity of piles, the stiffness of the liquefied soil was set equal to the stiffness of the nonliquefied soil divided by a reduction factor, R_f. Four values were assigned to R_f: 50, 10, 5, and 1. It was assumed that stiffness reduction takes place uniformly through the liquefied layer.

Typical analytical results are given in Figure 10, which shows soil displacement versus axial load for different values of R_f. The soil displacement in the vertical axis is that at which the pile either buckles or develops a plastic hinge. The abrupt change in slope in three of the four curves indicates a transition load, P_t. The transition load denotes the load at which the pile buckles simultaneously as it develops a plastic hinge. Thus, at axial loads smaller than P_t, the pile will always fail by excessive bending, while at higher loads the pile will buckle. Note that, as the axial load increases above P_t, the soil displacement, d_h, decreases significantly.

The ability to predict the potential for buckling is of significant practical importance. If a pile develops a plastic hinge, it generally can accommodate more lateral soil displacement than if it were to buckle. If it undergoes buckling, a catastrophic pile failure may follow. To provide guidance for this problem, transition loads were identified from the computer results and are plotted in Figure 11. The horizontal axis, $\beta_c H_L$, is a characteristic length that depends on the flexural rigidity of the pile, as well as the stiffness of the soil. The parameter β_c is the characteristic of the system, and is defined as:

$$\beta_c = \sqrt[4]{\frac{n_h D}{(EI)_c}} \tag{4}$$

in which n_h is the constant of horizontal subgrade reaction (see Equation 1). It should be recognized that, for liquefied soil, the constant of horizontal subgrade reaction will be obtained by dividing the value for intact soil by the reduction factor (i.e., n_h/R_f). The value of $(EI)_c$ is the value of EI after concrete cracking takes place. $(EI)_c$ is given by the expression:

$$(EI)_c = \frac{M_u - M_c}{\psi_u - \psi_c} \tag{5}$$

in which M represents the bending moment, and ψ the is curvature. The subindices c and u designate cracking and ultimate states, respectively. The grounds for defining β_c as a function of the cracked pile stiffness result from the fact that, when the pile buckles, a large portion of the pile is in a post-cracking state.

Most buckling occurred in the absence of the upper nonliquefied layer (or when the water table is at the ground surface). Figure 11 indicates that the transition load increases as the characteristic length increases. The observed

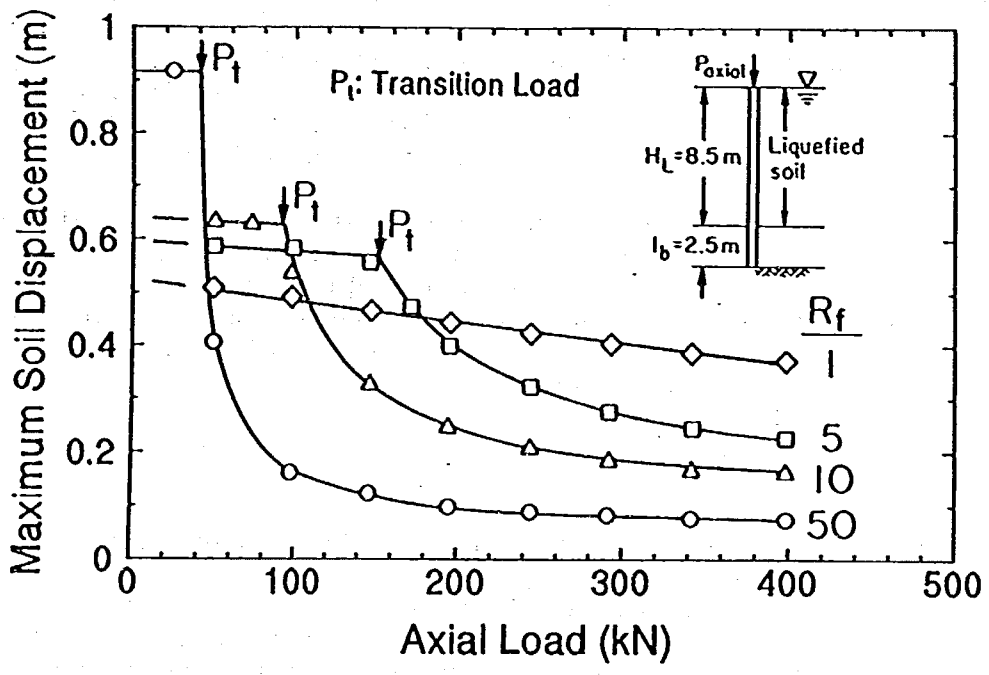


FIGURE 10. Maximum Soil Displacement versus Axial Pile Load for a 35-cm-Diameter Pile, H_L = 8.5 m, ℓ_b = 2.5 m

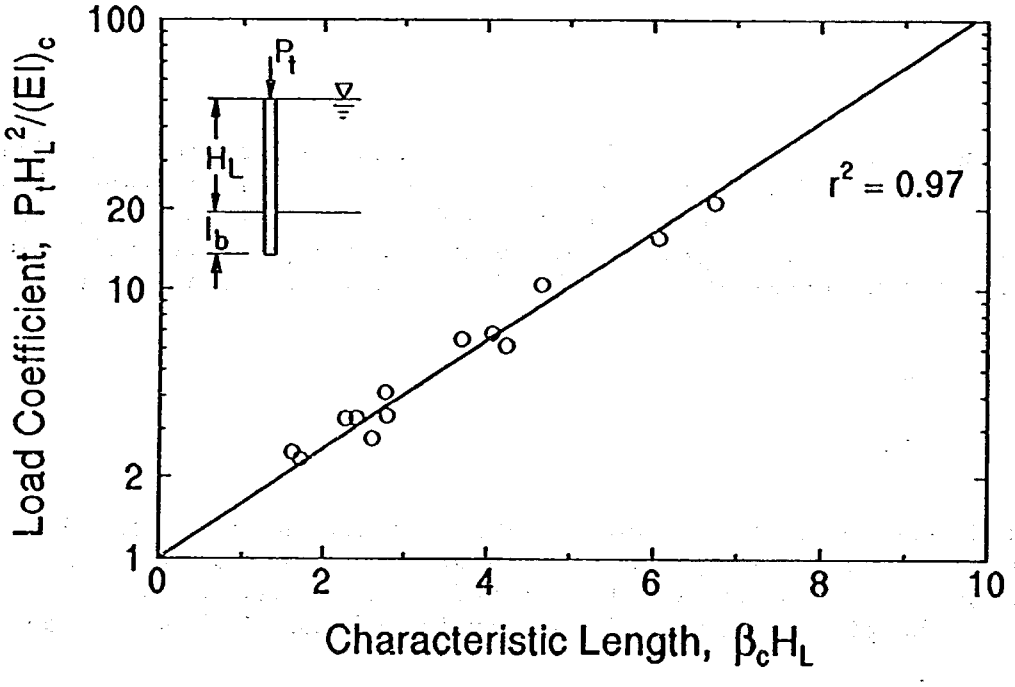


FIGURE 11. Dimensionless Load Coefficient as a Function of Characteristic Length to Evaluate Transition Load

scatter arises mainly as a result of the nonlinearities of the system. However, a power regression fitted to the data shows a coefficient, r^2, of 0.97. Thus, by knowing the characteristic of the system and the thickness of the liquefied layer, H_L, it is possible to assess the magnitude of the transition load.

Once a load less than the transition load has been determined such that the pile will not buckle, the next logical step is to assess the amount of soil displacement required to cause bending failure. Soil displacements at bending failure were determined, and are plotted in Figure 12. The horizontal axis is the normalized length, $\beta_c H_L$, while the vertical axis is given as a function of the dimensionless expression $d_h D/H_L^2$. (For a practical meaning of this quantity, see Appendix B.)

The curve in Figure 12 was developed for axial loads less than the transition load, P_t, and generally equal to about one-fourth to one-third the ultimate bearing capacity of the pile. The curve represents a reasonable practical range of working loads that contribute to moments in the pile, and hence, to flexural failure under horizontal soil displacement. In some cases of axial load, the analyses showed flow failure of the soil around the pile with no bending failure apparent. These cases are not represented in the figure.

Figure 12 indicates a decrease in the soil displacement, d_h, as the characteristic length increases. A very flexible pile will have a larger characteristic length than a relatively stiff pile. Since the flexible pile will try to conform to the soil displacement, large curvatures will develop near the interfaces between liquefied and intact soil. The pile will, therefore, experience bending failure at a relatively low value of soil deformation. A stiff pile will provide a greater resistance to soil displacement, allowing for larger movement.

The scatter observed in Figure 12 is, basically, the effect of the nonlinear behavior of the pile, which cannot be accounted for completely by the terms used to define both axes. Nevertheless, a power regression fitted to the analytical data shows a r^2 of 0.86.

Given that Figure 12 presents a generic curve that permits correlation of dimensionless displacement as a function of the characteristic length, it is possible to show the influence of soil liquefaction by adjusting the curve for reduced stiffnesses caused by liquefaction. In this case, the curve in Figure 12 is taken as representing the stiffness of intact soil. Curves representing reduced stiffnesses can be generated by displacing the reference curve for intact soil a distance $(R_f)^{1/4}\ \beta_c H_L$ to the right.

In Figure 13, three additional curves are shown for R_f = 5, 10, and 50. The estimation of dimensionless displacement varies by 1.4 to 2.1 as the R_f, or stiffness reduction, varies by an order of magnitude from 5 to 50. Such comparisons show how sensitive predicted movements are to the estimated degree of liquefaction, and help to point out the analytical consequences of our uncertainty in accounting for stiffness reduction because of liquefaction. The differences in dimensionless displacement with respect to variations in stiffness reduction are moderate, and a convenient range in estimated movements can be defined between R_f of 5 and 50.

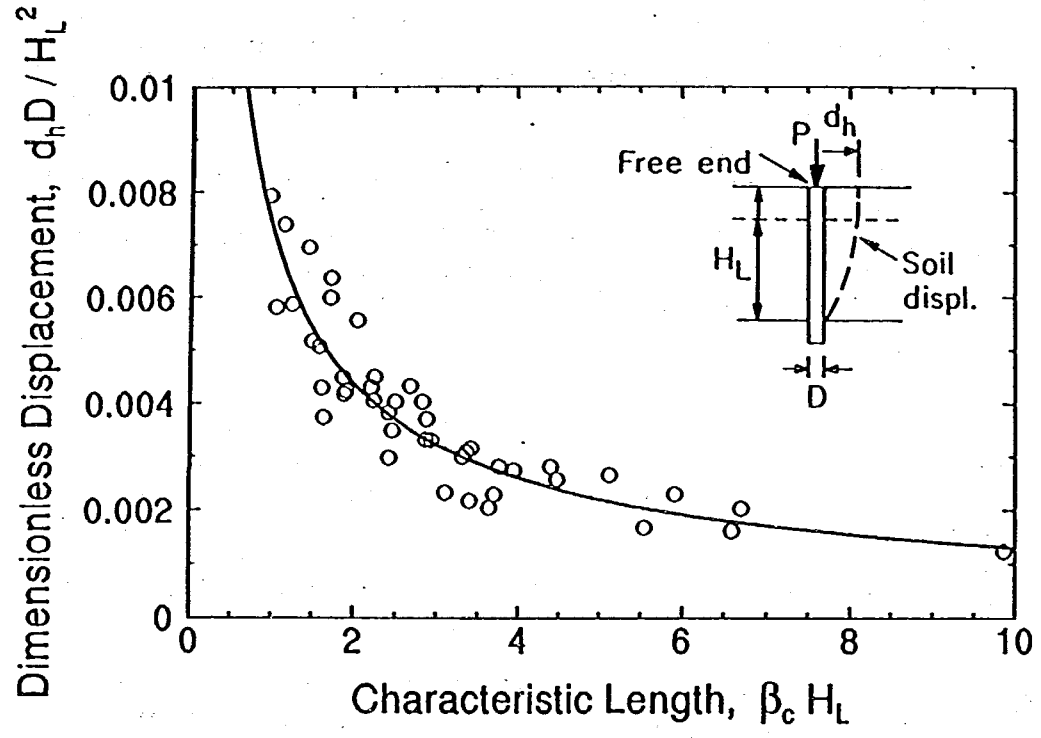


FIGURE 12. Dimensionless Displacement versus Characteristic Length to Evaluate Maximum Lateral Spread Movement at Pile Bending Failure

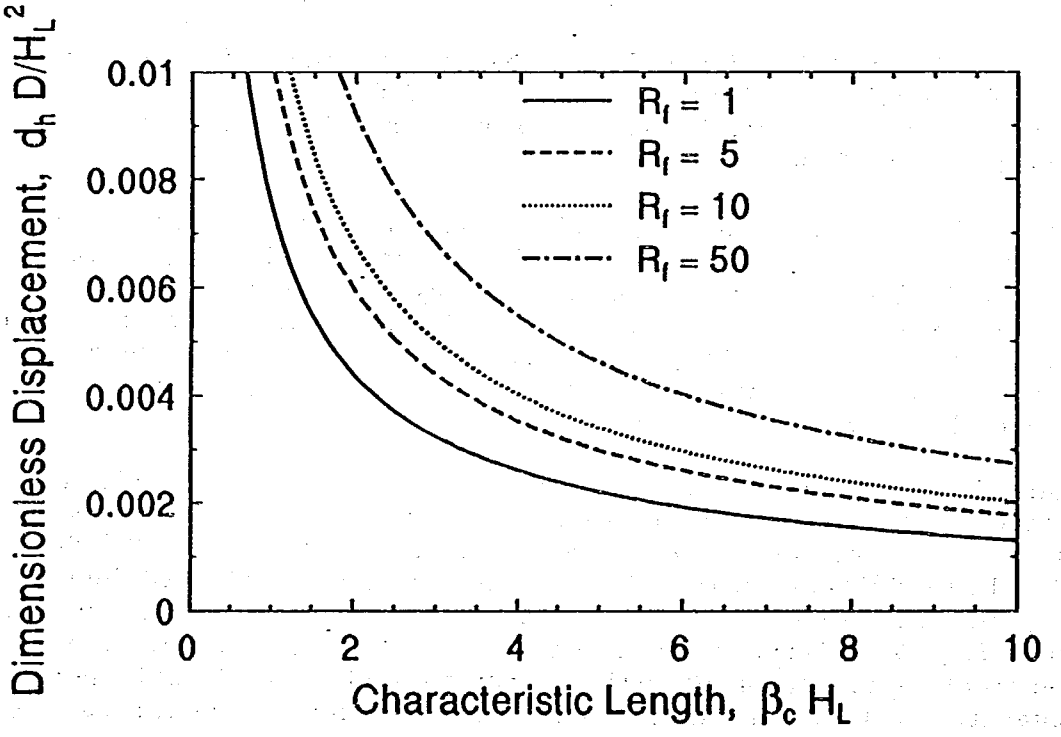


FIGURE 13. Curves Illustrating Effect of Reduced Soil Stiffness Caused by Liquefaction on the Estimation of Dimensionless Displacement

The practical application of the dimensionless curves in Figures 11 and 12 can be illustrated with an example. Consider a bridge abutment founded on 45-cm-diameter reinforced concrete piles, similar to those described by Miura and O'Rourke (1991). The piles penetrate a 6-m-thick stratum of potentially liquefiable sand into an end-bearing stratum of dense gravel. The axial load acting on each pile is 300 kN. The $(EI)_c$ for the pile is about 19.6 MN-m^2, as determined following the procedures of Miura and O'Rourke (1991). Assuming a reduction factor of 50 for the potentially liquefiable stratum, the characteristic length is about 0.95. Accordingly, the load factor in Figure 11 is about 1.56. The transition load, then, is 850 kN. Since the transition load is larger than the applied load, the pile will not buckle. The maximum soil displacement the pile can tolerate before forming a plastic hinge can be determined from Figure 12. From the calculated characteristic length of 0.95, the dimensionless displacement is about 0.0077. Thus, the maximum soil displacement is 0.62 m.

CONCLUSIONS

A computer model, B-STRUCT, has been described which evaluates pile response to large permanent ground displacement. The model is shown to give analytical results which compare favorably with observed pile deformations caused by lateral spreads. Parametric studies are used to develop two sets of dimensionless curves, which provide for 1) the determination of acceptable levels of axial load that do not result in pile buckling, and 2) the maximum lateral soil movement at which excessive pile flexure occurs, given that axial load is below the buckling limit. An engineering approach for estimating acceptable axial loads and maximum soil movement from lateral spreading is explained, based on the use of the dimensionless curves. The general trends given by the curves can be used for a first-order evaluation of liquefaction effects, and the computer model, B-STRUCT, can be used for site-specific analysis. The engineering approach and computer analysis are applicable to deep foundations for bridges, waterfront structures, and buildings.

ACKNOWLEDGEMENTS

Support for this paper and its associated research was provided by the National Center for Earthquake Engineering Research, Buffalo, NY under Project No. 912341. The assistance of Michael Palmer, who performed many computer analyses, is appreciated. The authors thank Ali Avcisoy, who drafted the figures, and Kristin J. Stewart, who prepared the manuscript.

LIST OF REFERENCES

Ahmed, I., "Pipeline Response to Excavation-Induced Ground Movements," Ph.D. Dissertation, School of Civil and Environmental Engineering, Cornell University, Ithaca, NY, 1990.

Boresi, A.P., O.M. Sidebottom, and J.O. Smith, Advanced Mechanics of Materials, 3rd Ed., John Wiley and Sons, Inc., New York, 1978.

Hamada, M., "Large Ground Deformations and Their Effects on Lifelines: 1964 Niigata Earthquake," Case Studies of Liquefaction and Lifeline Performance During Past Earthquakes, Vol.1, Japanese Case Studies, Technical Report NCEER-92-00001, NCEER, Buffalo, NY, Feb. 1992.

Hamada, M., S. Yasuda, R. Isoyama, and K. Emoto, "Study on Liquefaction-Induced Permanent Ground Displacements," Association for the Development of Earthquake Prediction, Tokyo, Japan, Nov. 1986.

Hansen, J.B., "The Ultimate Resistance of Rigid Piles Against Transversal Forces," Bulletin 12, Danish Geotechnical Institute, Copenhagen, 1961, pp. 1-9.

Kawamura, S., T. Nishizawa, and T. Wada, "Damage to Piles Due to Liquefaction Found by Excavation Twenty Years after Earthquake," Nikkei Architecture, Tokyo, Japan, 1985, pp. 130-134 (in Japanese).

Kawashima, K., K. Shimizu, S. Mori, M. Takagi, N. Suzuki, and S. Nakamura, "Analytical Studies on Damage to Bridges and Foundation Piles Caused by Liquefaction-Induced Permanent Ground Displacement," Proceedings, 1st Japan-U.S. Workshop on Liquefaction, Large Ground Deformations, and Their Effects on Lifeline Facilities, Tokyo, Japan, Nov. 1988, pp. 99-117.

Mejia, L., "Liquefaction at Moss Landing," Contribution to the NEHRP Report to Congress on the Loma Prieta, California, Earthquake of October 17, 1989, Woodward-Clyde Consultants, April, 1992.

Miura, F. and T.D. O'Rourke, "Nonlinear Analyses of Piles Subjected to Liquefaction-Induced Large Ground Deformation," 3rd Japan-U.S. Workshop on Earthquake-Resistant Design of Lifeline Facilities and Countermeasures for Soil Liquefaction, Technical Report NCEER 91-0001, NCEER, Buffalo, NY, Feb. 1991, pp. 497-512.

Miura, F., H.E. Stewart, and T.D. O'Rourke, "The Effects of Liquefaction-Induced Lateral Spreading on Pile Foundations," Soil Dynamics and Earthquake Engineering, Vol. 10, No. 5, July, 1991, pp. 271-279.

Stewart, H.E., F. Miura, and T.D. O'Rourke, "Pile Damage Due to Large Ground Displacement," Proceedings, 1st Japan-U.S. Workshop on Liquefaction, Large Ground Deformations, and Their Effect on Lifeline Facilities, Tokyo, Japan, Nov. 1988, pp. 173-182.

Terzaghi, K., "Evaluations of Coefficients of Subgrade Reaction," Géotechnique, Vol. 5, No. 4, Dec. 1955, pp. 297-326.

Trautmann, C.H., B-PIPE, Computer Program, School of Civil and Environmental Engineering, Cornell University, Ithaca, NY, 1981.

Yasuda, S., H. Nagase, H. Kiku, and Y. Uchida, "A Simplified Procedure for the Analysis of Permanent Ground Displacement," 3rd Japan-U.S. Workshop on Earthquake-Resistant Design of Lifeline Facilities and Countermeasures for Soil Liquefaction, Technical Report NCEER 91-0001, NCEER, Buffalo, NY, Feb. 1991, pp. 225-236.

Yoshida, N. and M. Hamada, "Damage to Foundation Piles and Deformation Pattern of Ground Due to Liquefaction-Induced Permanent Ground Deformations," 3rd Japan-U.S. Workshop on Earthquake-Resistant Design of Lifeline Facilities and Countermeasures for Soil Liquefaction, Technical Report NCEER 91-0001, NCEER, Buffalo, NY, Feb. 1991, pp. 147-161.

APPENDIX A: Moment-Rotation Relation

This Appendix presents the derivation of Equation 2. The program, B-STRUCT, models a pile as a series of beam elements connected by trilinear rotational springs. As a consequence of this element arrangement, bending deformation of the pile will be the result of elastic flexure of the beam elements, plus rotation of the rotational springs.

Figure A.1 presents the moment-curvature relationship of the pile and its trilinear simplification in dashed lines. The objective is to determine the properties of the rotational springs such that the simplified (dashed) line is followed by the model. Two conditions have to be satisfied: 1) the curvature of the model and the pile, for a given bending moment, have to be equal, and 2) the corresponding lateral displacements also must be the same.

Consider a pile of length, L, subjected to a constant moment, M, which causes the free end of the member to displace laterally a distance, d (Figure A.2). The resulting curvature will be constant along the pile, irrespective of whether the pile is still elastic, or has surpassed its elastic limit. The total distance, d, can be resolved into an elastic component, d_e, and a plastic component, d_p. The relation between the displacement, d, and the curvature, ψ, is given by Equation 3 in the text.

Figure A.3 shows the combined elastic and non-elastic moment-curvature of the pile. The horizontal axis could be either curvature or deflection, given their one-to-one relation. The steep straight line of slope EI represents the elastic contribution of the beam elements, while the hatched area represents the non-elastic contribution of the rotational springs.

Figure A.4 illustrates the deflection of the structure if it were modeled by elastic beam elements and one, two, or n rotational springs. The plastic deflection at the free end of the structure modeled by n rotational springs is given by:

$$d_p = \frac{n + 1}{2} \theta \, L \qquad (A.1)$$

and the elastic displacement, d_e, (assuming it is small compared to d_p) is:

$$d_e = \frac{ML^2}{2EI} \qquad (A.2)$$

Combining Equations A.1 and A.2, and solving for the angle θ, one obtains Equation 2 in the text.

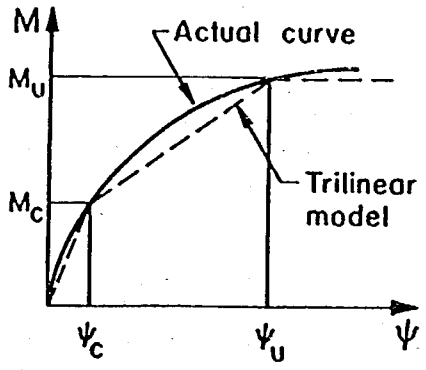


FIGURE A.1. Typical Moment-Curvature Relationship of Reinforced Concrete Pile

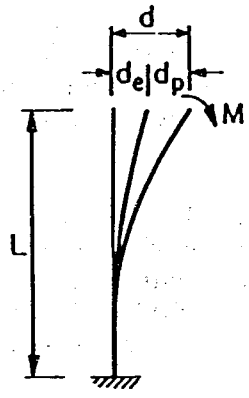


FIGURE A.2. Pile Deflection from the Application of External Bending Moment

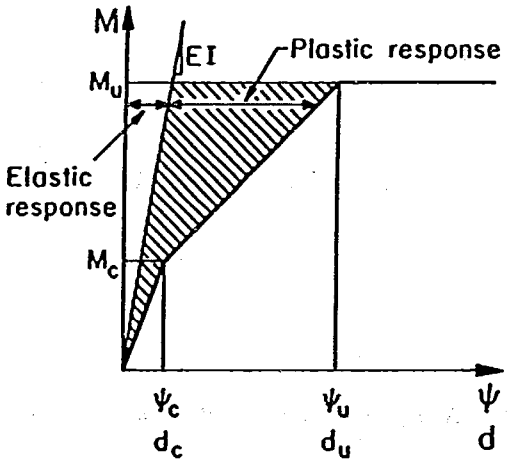


FIGURE A.3. Elastic and Plastic Moment-Curvature and Moment-Displacement Relationship

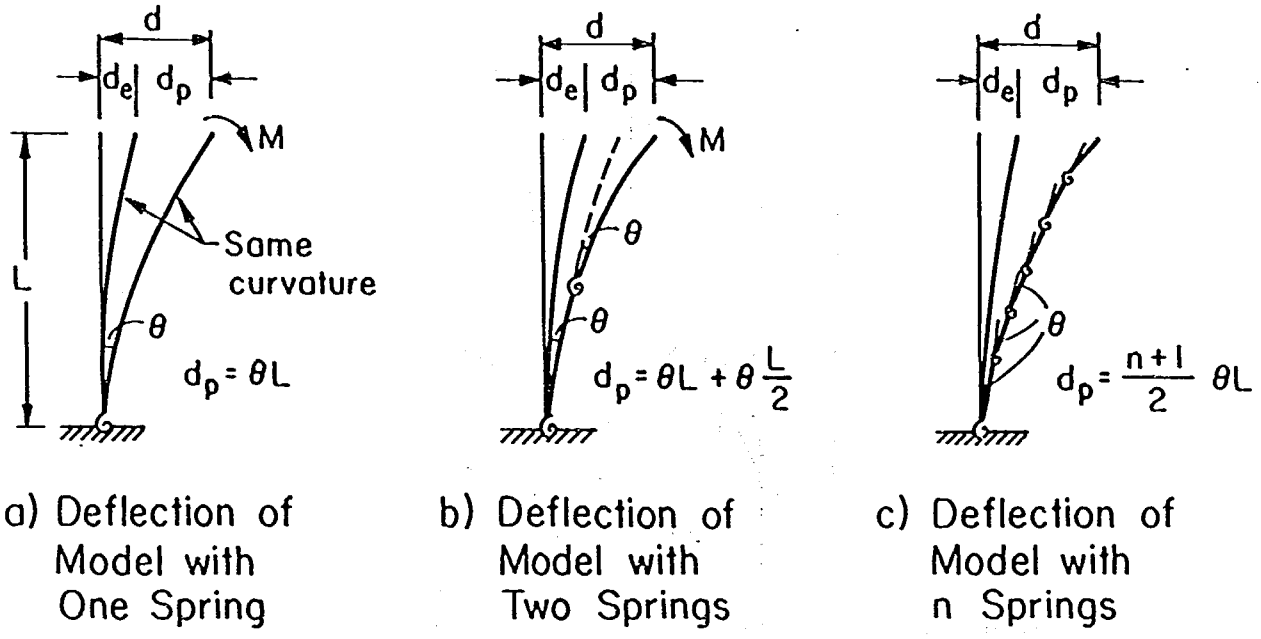


FIGURE A.4. Elastic and Plastic Pile Deflection with 1, 2, and n Rotational Springs

APPENDIX B: Geometric Interpretation of Dimensionless Displacement

Consider a pile which, as a result of soil displacement, deforms as in Figure B.1. For simplicity, it is assumed that the pile deforms into two circular arcs, each of radius R. The total pile offset, d_h, is small, compared to the distance, H_L. The ratio between the rise, ED, and the half-chord, BD, is approximately equal to the ratio between BD and the radius R, that is:

$$\frac{\overline{ED}}{\overline{BD}} \approx \frac{\overline{BD}}{R} \tag{B.1}$$

However,

$$\overline{BD} \approx \frac{H_L}{4} \tag{B.2}$$

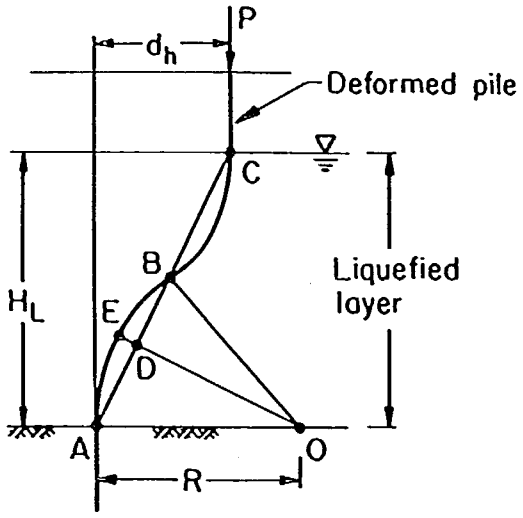


FIGURE B.1. Simplified Geometry of Pile Deflection

therefore,

$$\frac{1}{R} = \psi = \frac{16\ \overline{ED}}{H_L^2} \tag{B.3}$$

where ψ is the curvature. The distance ED can be approximated as a fraction of the pile offset, d_h. Therefore:

$$\psi = \frac{16\ \alpha\ d_h}{H_L^2} \tag{B.4}$$

in which α is a positive constant smaller than 1. The strain, ϵ, is simply the curvature multiplied by the radius of the pile, or D/2. Therefore:

$$\epsilon = \frac{D\psi}{2} = A\ \frac{D\ d_h}{H_L^2} \tag{B.5}$$

where A is a constant equal to 8α. The factor multiplying the constant A in Equation B.5 is proportional to the strain in the pile, and is the same dimensionless displacement used in the vertical axis of Figures 12 and 13 in the text.

Session–5

Network Assessment

J–9) Seismic Reliability Analyses of Large Scale Lifeline Networks Using Fuzzy Set Theory
(Sato, T., Toki, K. and Fujita, Y.)

J–10) Network Performance of Highway Systems Under Earthquake Effects: A Case Study of the 1989 Loma Prieta Earthquake
(Wakabayashi, H. and Kameda, H.)

U–6) GIS–Based Assessment of the Seismic Performance of a Water Delivery System
(Shinozuka, M., Hwang, H.H.M. and Tanaka, S.)

SEISMIC RELIABILITY ANALYSES OF LARGE SCALE LIFELINE NETWORKS USING FUZZY SET THEORY

By Tadanobu SATO, Knzo TOKI and Yusuke FUJITA

ABSTRACT

To evaluate uncertainty of failure probability of network components requires a large and long-term statistical survey. We, therefore, attempt to use the fuzzy sets theory to assess the seismic reliability of large scale lifeline networks and taking into account uncertainty of failure probability of the components. We developed an algorithm which has only polynomial complexity to enumerate paths in the network. Using this algorithm we have calculated the fuzzy membership function of seismic reliability of a given network. The uncertainty of the attenuation law, response velocity value per unit seismic coefficent and natural period of ground are defined by using normal convex fuzzy membership functions. A check of applicability of our new method is made by hypothetical seismic reliability analysis of a gas supply network composed of 387 nodes and 391 links.

INTRODUCTION

Because damage to a single location in a utility network often affects a major portion of the entire system, the reliability of lifeline networks during earthquake is a major concern for the prevention of urban hazards. When we are to assess the seismic reliability of lifeline systems, the following items must be considered: seismic activity and the attenuation of seismic waves; microzonation that takes into account to the local geological nature of each area; structure response and system analyses with proper modeling of components; and lifeline serviceability requirements. Seismic reliability analysis should include an efficient method for computing the reliability of the lifeline as a network interconnected nods and links. Because enumeration of network states in a seismic environment usually has exponential complexity, seismic reliability analyses of large scale networks have not been feasible as the number of components increases. To overcome this deficiency we proposed already an efficient procedure for assessing the seismic reliability of lifeline networks (Ref.1). For a fixed earthquake on an active fault zone, we proved that the network took at most $2n^2-2n+2$ states, n being the number of components. In the algorithm, we used the concept of the critical distance to the earthquake fault (Ref.2). A network is assumed to consist of links and nodes, and a node and link to fail if the seismic response exceeds a particular level at any point in each component. The intensity of the seismic response, Y, at a particular point in the network components is given through an attenuation law in terms of the earthquake magnitude, M, the shortest distance to the rupture zone,r, and the parameters $C_k(k = 1, 2, \cdots)$ which express the source mechanisms and the effect of local geological parameters around the point. If the network component can sustain the magnitude of response expressed by Y^*, the shortest safe distance (the critical distance) between the component and the fault rupture is inversely solved from the attenuation law

$$r^* = f(M, C_k, Y^*) \tag{1}$$

The sphere of the radius with this distance centered at the element point defines the critical boundary for the component because it divides three dimensional spare into the component of working and non-working states. The shape of the critical boundary for

a node is a sphere. For a link it is a combination of a row of spheres and idealized by a circular cone with spheres at both end provided that there is linearity of the failure distances along the link.

The purpose of this paper is to relax this binary condition of component's failure probability. The seismic reliability of a network may have uncertainty if we take into account uncertainties of several factors. Especially the effect of uncertainty of attenuation law must be examined carefully.

SEISMIC DURABILITY OF PIPE ELEMENTS

Network components are assumed to fail when the strain induced in the pipe exceeds a threshold level. The Japanese specification for the earthquake resistant design of gas pipes (Ref.3) defines the formula with which to calculate pipe strain as

$$\varepsilon = \beta \cdot \delta, \quad \delta = (1-\alpha) \cdot U \tag{2}$$

in which β is the coefficient for transferring relative displacement between the pipe and ground into the pipe strain, α the transmission coefficient, U the ground displacement given by

$$U = \frac{2}{\pi^2} \cdot T \cdot S_V \cdot K \cdot cos(\frac{\pi z}{2H}) \tag{3}$$

in which T is the natural period of the ground, S_V the response velocity value per unit seismic coefficient, K the design seismic coefficient and z the depth of the pipe. By substituting Eq.(3) into Eq.(2) the strain induced in a pipe is expressed as follows:

$$\varepsilon = \beta \cdot (1-\alpha)\frac{2}{\pi^2} \cdot T \cdot S_V \cdot K \cdot cos(\frac{\pi z}{2H}) \tag{4}$$

To calculate ε the value of K must be expressed by an attenuation law in terms of the earthquake magnitude, M, and the shortest distance to the rupture zone, r. Because the attenuation laws proposed so far are functions of the magnitude and epicentral distance, we have used the following relation for K (Ref.4)

$$K \cdot g = 227 \cdot 10^{0.308M}(r+30)^{-1.201} \tag{5}$$

in which g is the acceleration of gravity. By substituting Eq.(5) into Eq.(4), the strain induced in a pipe is expressed as a function of the earthquake magnitude, M, and the distance between the component and the fault, r. If the allowable strain on the pipe ε^* is given the critical distance for the pipe, r^*, can be calculated using Eqs.(4) and (5).

SEISMIC ENVIRONMENT

The gross parameters of the seismic source, which are required to reliability analysis of lifeline network, are the fault length and width, the seismic moment and the magnitude of the earthquake. The seismic moment, M_o, is the fundamental parameter used to measure the magnitude of an earthquake caused by a fault slip, but the surface magnitude,m_s, is used in engineering. We have the relation between m_s and M_o given by Geller (Ref.5). The fault area, S, also is related to M_o ;

$$S = 1.88 \cdot 10^{-15} M_o^{2/3} \tag{6}$$

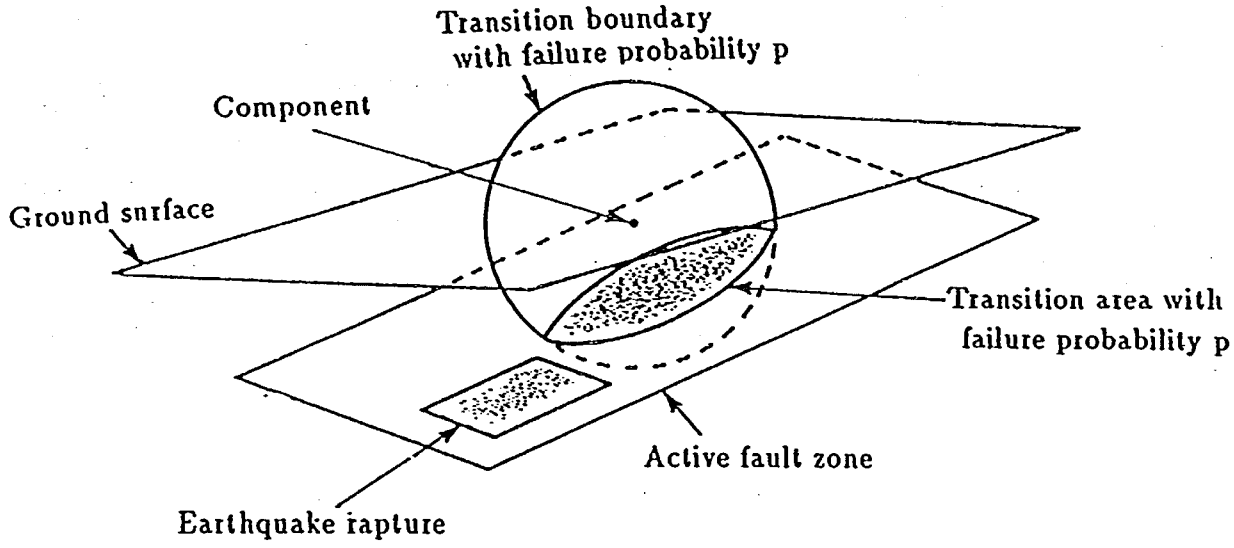


Fig.1 Transition boundary, collocation of an earthquake rapture in the active fault zone and transition boundary of a component

The network component will fail, if the critical boundary with the critical distance r intersects the earthquake rupture area. Taking into account the probabilistic nature of an earthquake occurring, we have defined an active fault zone. The collocation of earthquake rupture on this active fault zone is determined from a probabilistic concept. We assume rectangular areas (the length of fault to be twice of the width) for the active fault zone and for a rupture caused by an earthquake as shown in Fig.1. The collocation of both rectangles is arranged with the axes of symmetry parallel. We define the transition area as the intersection between the critical boundary of a component of the network and the active fault zone as shown in Fig.1. For a node it is a circle; for a link it is the cross section between the active fault plane and a circular cone with a sphere at both end. To formulate network reliability, we must assume that this transition area may intersect an earthquake rupture with magnitude m. Therefore, it is convenient to look at the positions of rupture from the center of the earthquake. We defined a coordinate transformation (Ref.1) by which the position of earthquake rupture can be represented by the center of the rupture. An example of the collocation of this newly defined transition area for a simple network composed of four nodes and links is shown Fig.2. A influence region is defined as an intersection of several transition areas. The network condition changes from one region to the other. For example the influence region 9 expresses the network condition that links of 1,2 and 4 fail simultaneously.

NETWORK RELIABILITY COMPUTATION

In order to illustrate the reliability computation a multi-terminal reliability measure is used that is defined as the probability that the given source nodes can be connected to all specified terminal nodes in the network. Let $I_i(x, y/M)$ be an reliability index of influence region i defined by the probability to satisfy the function of a network after a magnitude M earthquake with a rupture centered at (x, y). How to calculate the reliability index of region 5 in Fig.2 (I_5) is explained in Table 1. The connectivity from node 1 to node 4 is chosen as the reliability measure. There are four cases based on components failure condition. $I_5(x, y/M)$ becomes 0.75 by adding all probabilities of network functioning.

For simplicity we consider only one active fault zone in the following analysis. The transition areas divide the active fault zone into some m influence regions $A_i (i = 1, 2, \cdots, m)$ Each A_i, region corresponds to some state of the network and $I(x, y/M)$ is constant within A_i so that the reliability of the network, G, conditioned on magnitude M is

$$R(G/M) = \sum_{i=1}^{m} \{I_i(A_i/M) \cdot A_i\} / \sum_{i=1}^{m} A_i \qquad (7)$$

in which we assume uniform distribution of earthquake occurrence on the active fault zone.

Point matching method : The most time consuming part of the developed program is the calculation of area of influence region A_i. After detail check of program statements we found that the order of enumeration for a network with n elements was $O(n^6)$ due to the existence of nested DO ROOPS to calculate A_i although our algorithm guarantees the order of $O(n^2)$ (Ref.1). To overcome this deficiency we have developed an algorithm named "point matching method". The idea of the method is simple. Evaluation points are uniformly distributed on the active fault zone and the area of region A_i is assined to be proportional to the number of evaluation points included in the region A_i. The value of reliability index defined by $I(x, y/M)$ is assumed to each evaluation point. If the number

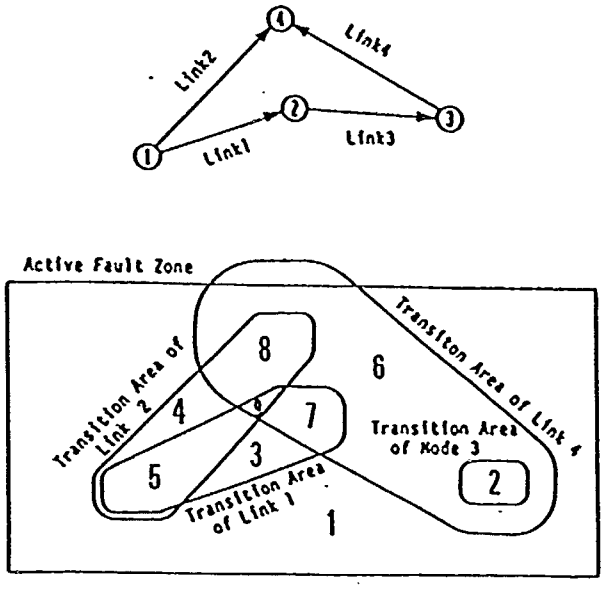


Fig.2 The collocation of the transition area for a simple network

Table 1 Calculation of Reliability index

	Link 1	Link 4	Reliabilty measure	Probability
1	F	F	NS	
2	F	F	NS	
3	NF	F	S	$(1-0.25)\times 0.5 = 0.375$
4	NF	NF	S	$(1-0.25)\times(1-0.5) = 0.375$
				Reliability index $I_5 = 0.750$

F: Failure S: Satisfy

NF: Non failure NS: Not satisfy

of evaluation points in the region A_i is N_i then Eq(7) is rewritten as follows :

$$R(G/M) = \sum_{i=1}^{m} \{I_i(N_i/M) \cdot N_i\} / \sum_{i=1}^{M} N_i \tag{8}$$

Application of minimal cutset : In Table 1 we counted out all possible case for calculating reliability index. But this is not feasible as the number of collectively exhaustive regions increases. For an illustrative purpose a network shown in Fig.3 is considered. The reliability measure is connectivity from nodes S_1, S_2, and S_3 to nodes D_2 and D_3. The transition areas of nodes A, B, C and D are intersected with active fault zone and only single failure probability for each transition area is assigned as given in Table 2. If we calculate the reliability index of shaded influence region by taking into account all possible cases we have to count out 16 (2^4) cases because this region is included inside of four transition areas composed of nodes A, B, C and D. The computation time to calculate the reliability index expands exponentially as the number of related transition areas of an influence region increases. To avoid this difficulty we use minimal cutset which is the subset of network components. If only one component in this subset survives the connectivity of the network is satisfied. In the example given in Table 3 the minimal cutset is the combination of nodes C and D because both nodes must survive to satisfy the reliability measure. The reliability index of this influence region, therefore, can be calculated by counting out all cases satisfying reliability measure for nodes A and B and multiplying survival probability of nodes C and D as shown in Table 4.

THE FUZZY DEFINITION OF CRITICAL DISTANCE

An interval of confidence using lower and upper bounds is one way of reducing the uncertainty. As shown in Fig.4, to define an uncertain number we use α level (grade) fuzzy number in which α gives the level of presumption and ($[a_1^\alpha, a_2^\alpha]$) is the pair of lower and upper bounds for uncertain number a at α level. A curve defining the fuzzy number is called as a fuzzy membership function. In the following analyses we treat two types of fuzzy membership functions. One is used for expressing the uncertainty of survival probability of component as shown in Fig.5. Four fuzzy membership functions are shown for four survival probabilities (0.5, 0.7,0.9 and 1.0) of a component. The other is used for expressing the uncertainty of critical distance originated in the uncertainties of attenuation law of acceleration, response velocity value per unit seismic coefficient and natural period of ground. For example the fuzzy membership function of critical distance at node 385 in the network shown in Fig.8 is given in Fig.6. Left-hand side of figure is fuzzy membership functions of the concerned values and right-hand side is those of critical distance transferred mathematically from the left-hand fuzzy membership function using the relationship between critical distance and the concerned values given by Eq.(1).

A MODEL OF GAS NETWORK AND AN ACTIVE FAULT ZONE

We considered a gas supply network (Fig.7) composed of 387 nodes and 391 links. The network shown in Fig.7 is an idealization of the southern portion of the middle pressure A line (gas pressure; $10 > p > 3kg/cm^2$). Four source nodes, A, B, C, and D are connected to the high pressure line through regulator stations, and 147 terminal nodes are connected to source nodes of the middle pressure line ($1 < p < 3kg/cm^2$) through district regulators. To evaluate the reliability of this network we have chosen a simple connectivity measure,

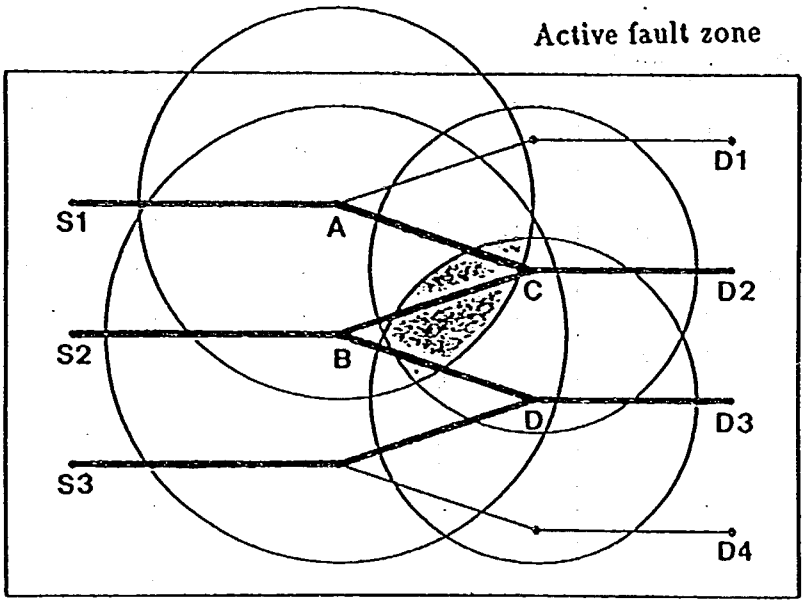


Fig.3 A network to apply the minimal cutset

Table 2 failure probability and non failure probability of transition area

P_f: Failure probability
P_l: Non failure probability

Node	P_f	P_l
Node A	0.3	0.7
Node B	0.4	0.6
Node C	0.9	0.1
Node D	0.8	0.2

Table 3 Calculating reliability index without using minimal cutset

	Node A	Node B	Node C	Node D	Reliability measure	Probability
1	o	o	o	o	o	0.7×0.6×0.1×0.2=0.0084
2	o	o	o	×	×	
3	o	o	×	o	×	
4	o	o	×	×	×	
5	o	×	o	o	o	0.7×0.4×0.1×0.2=0.0056
6	o	×	o	×	×	
7	o	×	×	o	×	
8	o	×	×	×	×	
9	×	o	o	o	o	0.3×0.6×0.1×0.2=0.0036
10	×	o	o	×	×	
11	×	o	×	o	×	
12	×	o	×	×	×	
13	×	×	o	o	×	
14	×	×	o	×	×	
15	×	×	×	o	×	
16	×	×	×	×	×	
						Reliability index 0.0176

Table 4 Calculation of Probability using minimal cutset

	Node A	Node B	Reliability measure	Probability
1	o	o	o	0.7×0.6=0.42
2	o	×	o	0.7×0.4=0.28
3	×	o	o	0.3×0.6=0.18
4	×	×	×	
				0.88
				Reliability index 0.1×0.2×0.88=0.0176

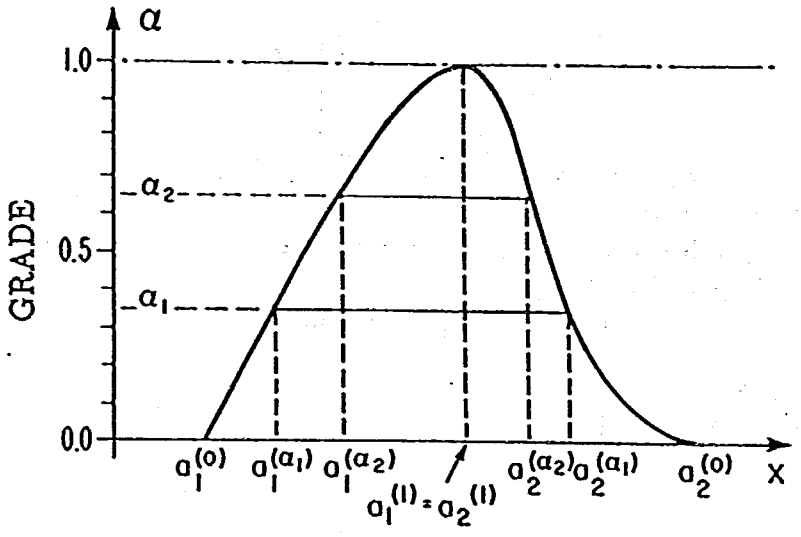


Fig.4 Definition of fuzzy numbers

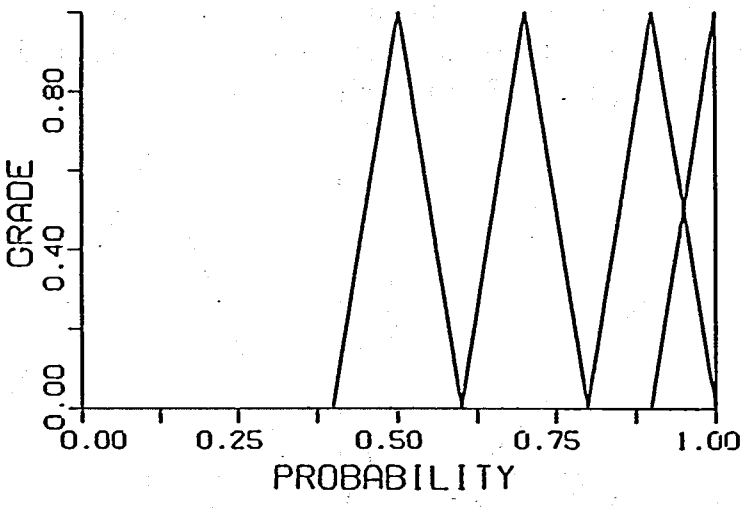
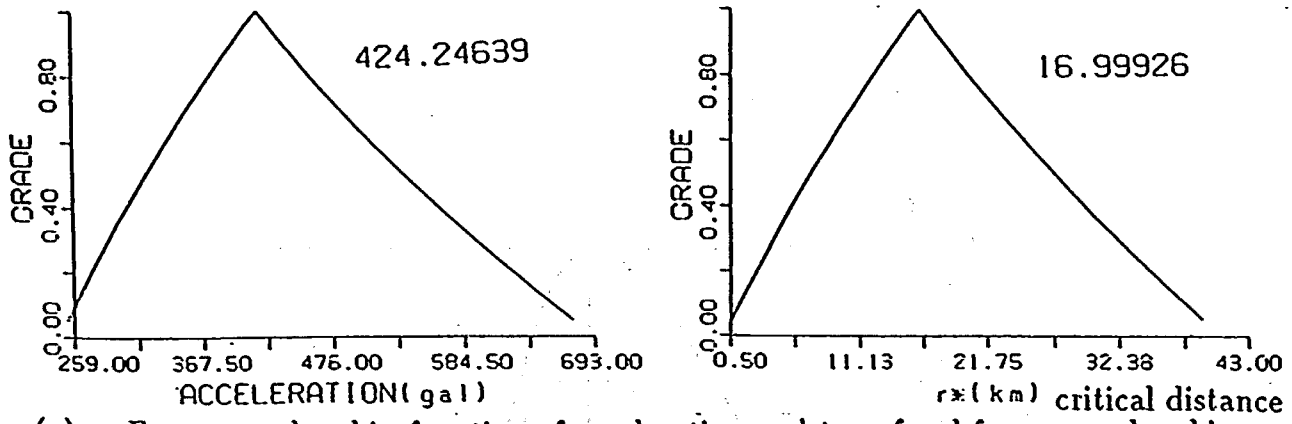
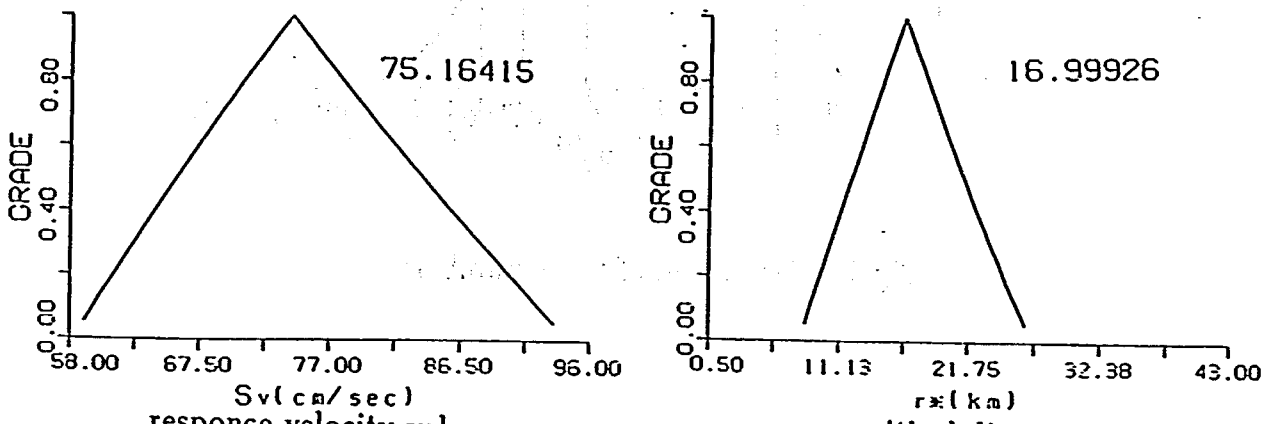


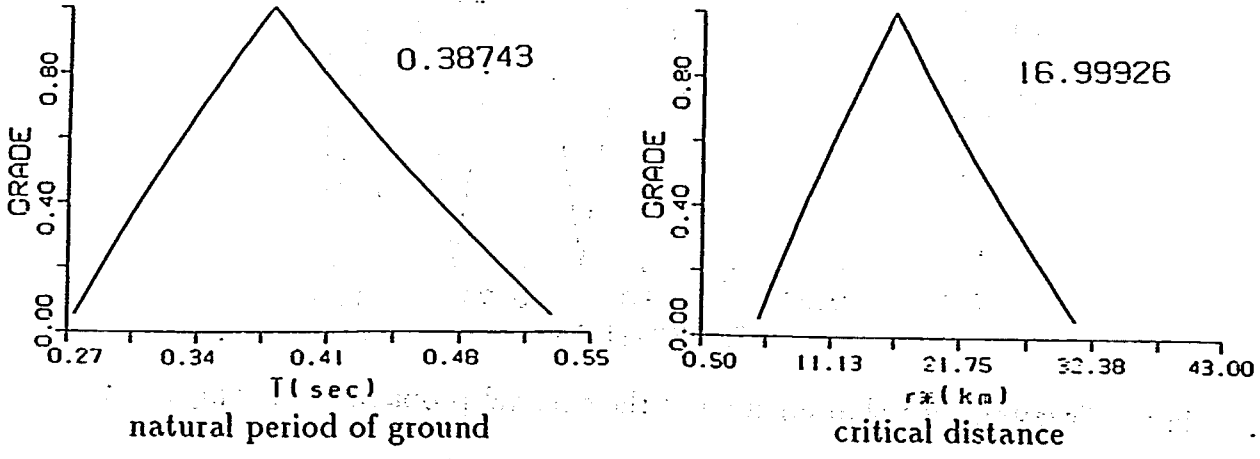
Fig.5 Fuzzy membership function of the survival probability of component



(a) Fuzzy membership function of acceleration and transfered fuzzy membership function of critical distance
(node 385 ; magnitude 7.4)



(b) Fuzzy membership function of responce velocity value per unit seismic coefficient and trancefered fuzzy membership function of critical distance
(node 385 ; magnitude 7.4)



(c) Fuzzy membership function for natural period of ground and transfered fuzzy membership function of critical distance
(node 385 ; magnitude 7.4)

Fig.6 Fuzzy membership function

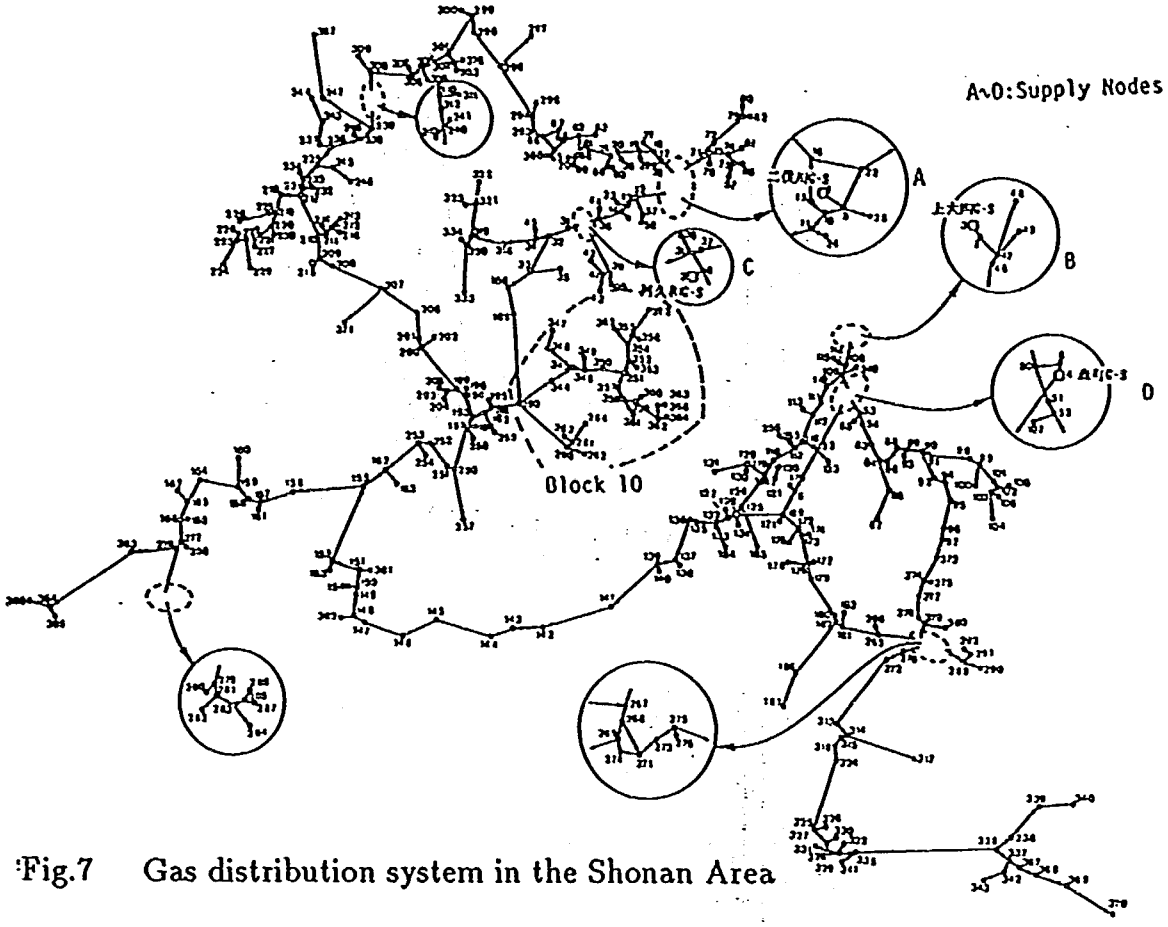


Fig.7 Gas distribution system in the Shonan Area

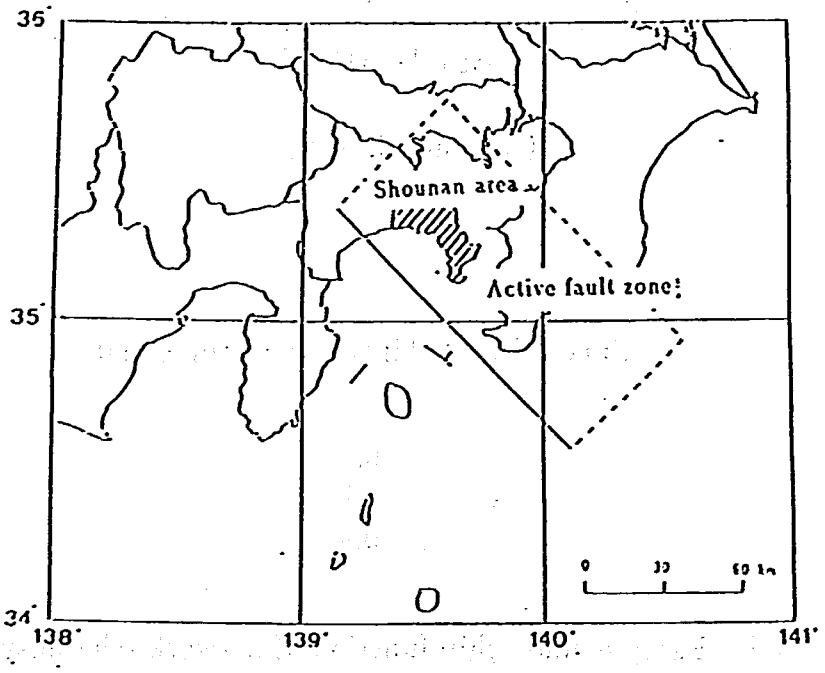
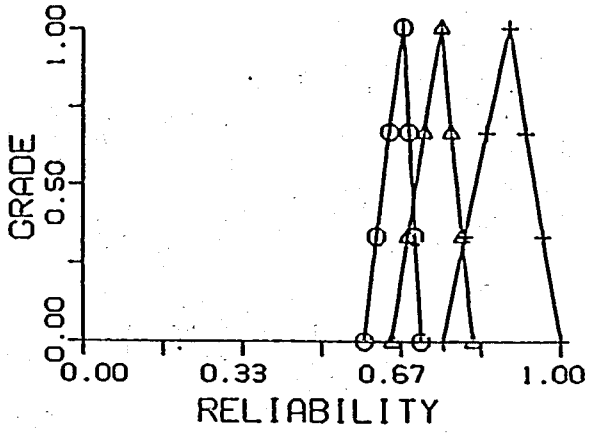
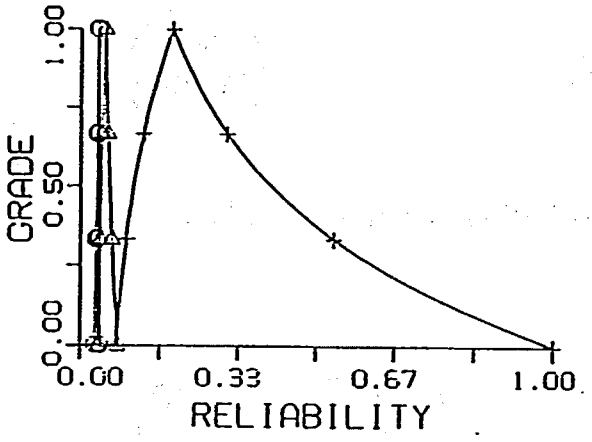


Fig.8 Relation between seismic reliability and earthquake magunitude



(magnitude 7.4)

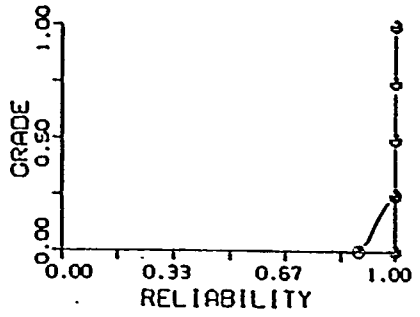


(magnitude 7.8)

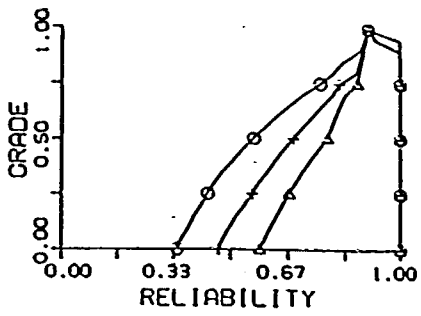
Survival probability of all component

⊙	:	0.5
△	:	0.7
+	:	0.9

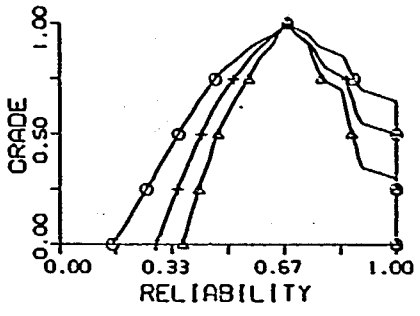
Fig.9 Fuzzy membership function of network reliability for earthquakes with magnitude 7.4 and 7.8



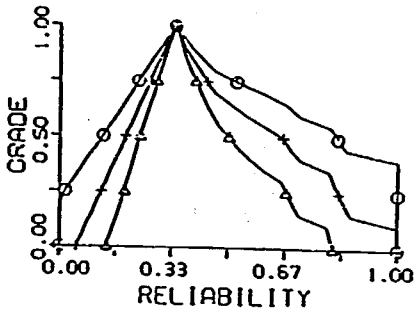
(magnitude 6.6)



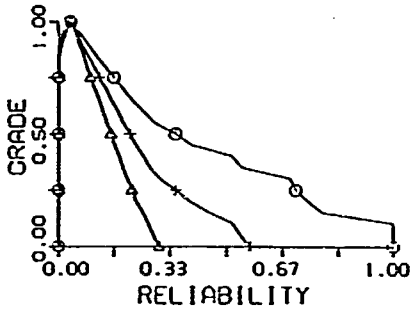
(magnitude 7.2)



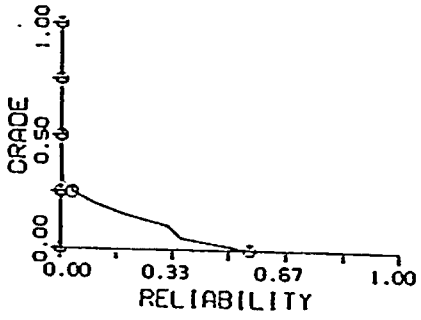
(magnitude 7.4)



(magnitude 7.6)



(magnitude 7.8)



(magnitude 8.0)

⊙ acceleration
△ responce velocity value per unit seismic coefficient
\+ natural period of ground

Fig.10 Fuzzy membership function of network reliability for earthquakes with magnitude 6.6,7.2,7.4,7.6,7.8 and 8.0 taking into account uncertainties of attenuation law , responce velocity value per unit seismic coefficient and natural period of ground.

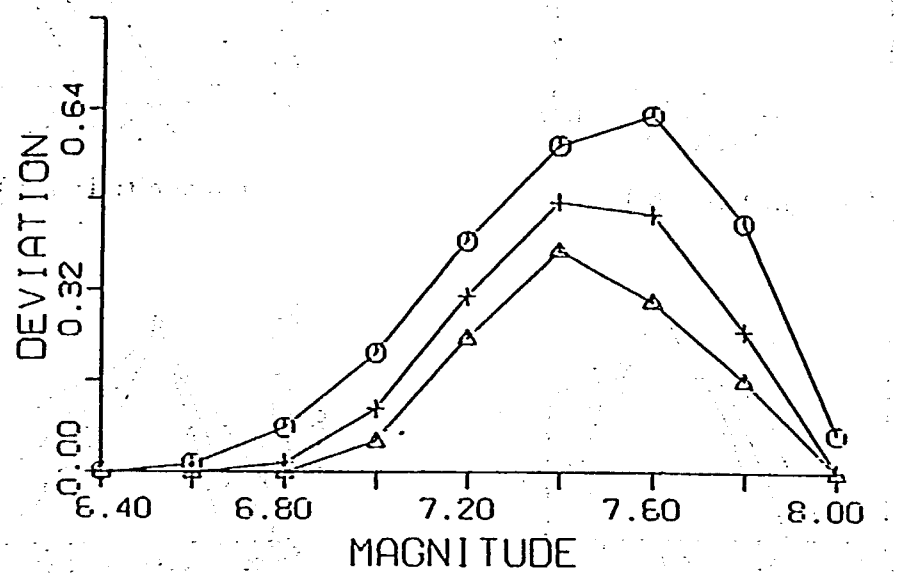


Fig.11 Deviation of fuzzy membership function of network reliability

the probability that gas can reach all the termini. An active fault zone is considered (Fig.8). This zone includes the fault fault area of the 1923 Kwanto Earthquake. The shear wave velocity and thickness of the ground at each node are determined by using the geological data base constructed from the results of standard penetration tests conducted at 1618 points in the area concerned. The depth of the buried pipe elements is assumed to be $1.2m$.

APPLICATION

A work station, NEWS-3860, with 25 MIPS processing speed is mainly used for calculating seismic reliability of the gas network shown in Fig.7. The seismic reliability of the network is calculated for random earthquakes with magnitude 7.4 and 7.8 on the active fault zone. To use the fuzzy membership function given in Fig.5 we assume that survival probability of all components have same value within the critical boundaries. The calculated seismic reliability and its membership function is given in Fig.9. When the uncertainty of survival probability of component is not take into account, the network reliability is given by an ordinary number with a value at grade (α) being equale to 1.0. For example the seismic reliability of the network is 0.88 when the survival probability of all components for earthquake magnitude 7.4 is an ordinary number of 0.9. The component survival probability is, however, defined as an fuzzy number with membership function as shown in Fig.5. The seismic reliability of network is, therefore, expressed by a fuzzy number with distributing nature. As can be seen the width between the upper and lower bounds for certain α level becomes large if the survival probability is increased. This tendency is amplified as the earthquake magnitude is increased

To apply the fuzzy membership functions given in Fig.6 for calculation of seismic reliability of the network we define pair sets of critical distances based on the lower and upper bounds for an α level. Using both sets of critical distances we can calculate lower and upper bounds of seismic reliability of the network for a given α level. Changing α level we can compose the fuzzy membership function of the seismic reliability of the network. The calculated results for random earthquakes with magnitude 6.6, 7.2, 7.4, 7.6 7.8 and 8.0 on the active fault zone are shown in Fig.10. When the critical distances are ordinal numbers the seismic reliability of the network is also ordinal number which is equal to the fuzzy membership function with the grade at 1.0. For example seismic reliability of the network is 0.67 when the all critical distances of components are ordinal numbers for random earthquakes with magnitude 7.4. To take into account uncertainties of attenuation law, response velocity and natural period of ground we define the fuzzy numbers shown in Fig.6. Because the fuzzy membership function of critical distance obtained from the fuzzy value of attenuation law of acceleration spans wide range of critical distance, the fuzzy membership function of reliability also spans wide range of reliability. To compare the range of distribution of the fuzzy membership function the area of fuzzy membership function is calculated and shown in Fig.11 as a function of earthquake magnitude. From this figure we can conclude that the uncertainty of the seismic reliability becomes large when the uncertainty of attenuation law is considered.

CONCLUSION

Using the concept of fuzzy uncertainty uncertainties of several factors for assessing seismic reliability of large scale lifeline system have been implemented in the algorithm with which to analyze the seismic reliability. It uses a new approximate calculation scheme

called point matching method and minimal cutset theory. Calculation of the seismic reliability of an example network shows that newly developed program package can be used with large networks. The result reveals that the effect of uncertainty of attenuation law is the largest on the seismic reliability analyses of networks.

REFERENCES

(1) Sato, T., "Seismic reliability analysis of lifeline networks taking into account fault extent and local ground conditions", Natural Disaster Science, Vol.6, No.2, 51-72, (1984).
(2) Moghtaderizadeh, M., Wood, R.K., Der-Kiureghian, A., Barlow, R.E. and Sato, T., "Seismic reliability of flow and communication networks", Lifeline Earthquake Engineering, The Current State of Knowledge, ASCE, 81-96 (1981).
(3) Japan Gas Association, "Specification for earthquake resistant design of gas pipelines", March(1982)(in Japanese).
(4) Kawashima, K., Aizawa, K. and Takashina, K., "Attenuation of peak ground acceleration,velocity and displacement based on multiple regression analysis of Japanese strong motion records", Earthquake Engineering and Structural Dynamics, Vol.14, pp.199-215 (1986).
(5) Geller, R.J., "Scaling relation for earthquake source parameters and magnitude", Bull.Seism.Soc.America, Vol.66, No.5, pp.1501-1523 (1976).

NETWORK PERFORMANCE OF HIGHWAY SYSTEMS UNDER EARTHQUAKE EFFECTS: A CASE STUDY OF THE 1989 LOMA PRIETA EARTHQUAKE

Hiroshi WAKABAYASHI
Associate Professor
of Civil Engineering
Osaka Prefectural College
of Technology
Neyagawa – Japan

Hiroyuki KAMEDA
Professor
Urban Earthquake Hazard Research Center
Disaster Prevention Research Institute
Kyoto University
Uji – Japan

ABSTRACT

The effects of the Loma Prieta Earthquake of October 17, 1989 on the highway network system are presented. First, the importance of highway network reliability as a lifeline system is discussed. Next, the impact of the Loma Prieta Earthquake on Japanese lifeline researchers is discussed with emphasis on investigations of the one-month closure of the Bay Bridge and its effects on the Bay Area transportation system. On this basis, a highway network reliability analysis is performed to explain the actual consequences of the Loma Prieta Earthquake. The OD matrix is estimated from the observed link flows under normal conditions as a basis for the analysis. Functional effects of highway network capacity and average travel time are identified for the periods before and after the earthquake considering the modal shift between the highway and BART and the effects of the temporary HOV lanes. Finally, a new efficient reliability analysis method developed by Wakabayashi and Iida is applied to the Loma Prieta case, by which the terminal reliability is evaluated for the pre- and post-earthquake periods.

INTRODUCTION

Reliable highway networks provide sure and stable traffic service by offering drivers alternative routes even when a part of the network is damaged. They should also enable smooth restoration activities during disaster operations. As basic studies for realizing such a goal, it is important to develop methodologies for evaluating highway network performance under the disaster emergency. A special feature of the reliability analysis of highway network systems, unlike other types of lifeline systems, is that it should take into account route choice behaviour of drivers. During a disaster emergency, detour traffic due to the damage of network components can cause congestion in another part of the network. Consideration of multi-commodity is another important factor in traffic flows. Single-commodity flows like electric power can reach any destinations as long as supply and demand node pairs are connected. In contrast, every driver on the highway has his own destination. Therefore, the identification of Origin-Destination flow is required in highway network analysis. The traffic flows on a network is a consequence of "User Equilibrium" which works under the individual optimum principle. Thus, it is difficult to control the network flows towards the "System Optimum".

The closure of the San Francisco Oakland Bay Bridge due to the 1989 Loma Prieta Earthquake brought heavy functional damage to the San Francisco Bay Area highway network. For successful highway construction and efficient disaster traffic management, the assessment of the consequences of the disaster is essential. However, no opportunity for disaster analysis from the viewpoint of traffic engineering has been provided due to the lack of basic data. In this regard, the case of the closure of Bay Bridge provided the first chance to conduct this type of investigation.

This paper presents the analysis of functional effects of highway network based on San Francisco Bay area traffic data. Functional effects of highway network capacity, average travel time and terminal reliability are estimated for pre- and post-earthquake periods. The output also includes an evaluation of the modal shift between highway and BART(Bay Area Rapid Transit) and the effects of the temporary HOV(High-Occupancy-Vehicle) lanes.

THE IMPORTANCE OF SEISMIC RELIABILITY OF THE HIGHWAY NETWORK AS A LIFELINE SYSTEM

The highway network reliability under seismic hazard is an important issue in modern urban regions, particularly in those large metropolitan areas both in the U.S.A. and Japan. Their highway networks constitute major transportation lifeline systems. The essential requirements for the highway systems under seismic environment is "Just in Time" transport. This concept is important for emergency operations immediately after the earthquake. As the entire region recovers, its significance shifts towards the time value under normal economic activities. It is, therefore, important to incorporate just-in-time evaluation in the highway network reliability assessment in every stage of post-earthquake period. The state-of-practice of earthquake countermeasures for urban highway systems has been stressed on structural design and retrofit. However, operations under earthquake emergency is an equally important issue. This aspect of the problem still needs great research and development efforts coming from the following reasons:

1) There is more traffic demand than highway stock.

2) No major urban highway systems have experienced large earthquakes. For this reason, there is lack of study cases and basic data for the development of disaster management planning for highway systems.

3) Appropriate methodological systems for highway network reliability assessment have not been established.

No opportunity for disaster analysis from the viewpoint of traffic has so far been provided. Thus, there are too large uncertainties for road planners to understand and assess the disaster effects in the event of major earthquake. In addition, with the lack of a sufficient methodological system, systematic and rational countermeasures are difficult to design. At the same time, the reality of the importance for disaster prevention promotion is lacking.

THE MOTIVATION IN JAPAN TO ANALYZE THE EFFECTS OF THE LOMA PRIETA EARTHQUAKE ON THE TRANSPORTATION SYSTEM

For the establishment of effective countermeasures after a disaster, the identification of the effects of disaster on a quantitative basis is essential. Traffic data for the periods before and after the 1989 Loma Prieta Earthquake were collected from the Bay Area freeway network. Using these data, analysis of functional effects of the earthquake and the evaluation of traffic management could be carried out. The effects of the Loma Prieta Earthquake in the San Francisco Bay Area, which are similar to the potential earthquake effects in Japan, have the following characteristics:

a) The population of the Bay Area is 6 million, which is close to the population of the Chukyo (Nagoya) Area at approximately 7 million. Amplification of the earthquake motion and liquefaction of the soft ground in the San Francisco Bay Area produced widespread damage in the lifeline networks. Soft ground is common to big cities in coastal areas in Japan, such as the Tokyo Metropolitan area with a population of 27 million and the Keihanshin Area (Kyoto-Osaka-Kobe) with 15 million.

b) San Francisco Bay Area has much more highway network stock than any Japanese large cities. At the same time, however, a considerably large demand for trip production in the Bay Area exists at the peak periods. Thus, serious traffic congestion occurs in the San Francisco Bay Area, which will be discussed in the chapter on network capacity. The Japanese highway network has similar traffic congestion problems.

c) Although the Loma Prieta Earthquake brought severe damage, it was fortunately restricted

to localized cases with very poor soil conditions and very poor structural conditions. Consequently, the capability for the socio-economic activities in the Bay Area recovered quickly. These activities naturally generate great traffic demands. Suffering from partial damage of the network, including the Bay Bridge, the remainder of the network had to support the traffic. This situation could appear in Japan.

Therefore, the characteristics of Loma Prieta Earthquake have been of big concern among Japanese engineers in earthquakes and related fields.

In this study, highway network performance is evaluated as follows:

(1) The method for explaining traffic conditions in the network is developed. Next, on the basis of the traffic indicators obtained, the system of evaluating the network performance is developed.

(2) Applying this system to the Loma Prieta Earthquake, the validity of the system is tested. And the effects of the actual traffic managements are quantified.

There was no Origin-Destination(OD) Table available for the Bay Area, which is indispensable for this kind of traffic analysis. Thus, the OD table is estimated from the observed link flow data using the maximum likelihood theory. After the estimation of the OD table before and after the earthquake, the network is loaded with OD flow using the traffic assignment method. Then the set of traffic indicators is obtained. On the basis of this data set, highway network capacity, average travel time and terminal reliability are identified before and after the earthquake. At the same time, the share effects between highway and BART are evaluated, as well as the effect of the temporary HOV lanes.

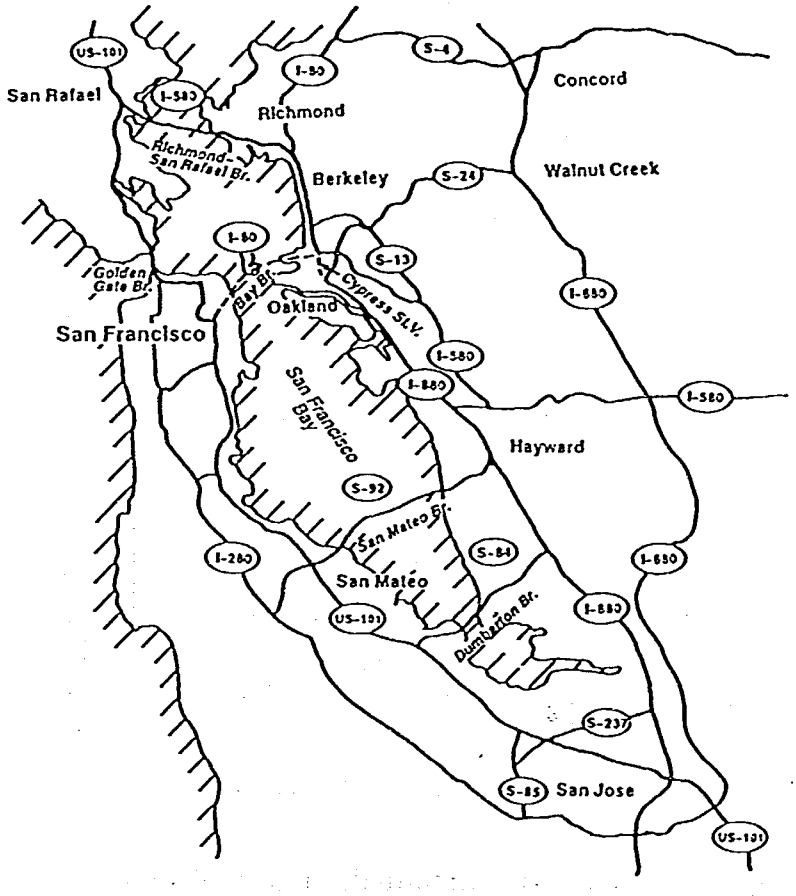


Figure 1. Highway Network of San Francisco Bay Area: Dotted lines depict closed sections.

OUTLINE OF THE FUNCTIONAL DAMAGE OF THE HIGHWAY TRAFFIC

The Loma Prieta Earthquake occurred at 5:04:15 p.m. on 17 October, 1989 on Pacific daylight time. The magnitude was 7.1.

The Bay Bridge is the main route and the shortest route for vehicles between San Francisco and Oakland (Fig.1). Due to the collapse of the deck at pier E9, the Bay Bridge became unavailable for a one-month period. The closure of the bay Bridge had tremendous effects on the transportation system of the entire Bay Area. During the period of the closure from 17 October to 17 November, the only major short route was BART (Bay Area Rapid Transit), and the number of passengers increased significantly. At the same time, a great amount of detoured traffic took alternative routes using other bridges. The traffic volume on these bridges increased heavily as illustrated in Fig.2. CALTRANS, then, established HOV (High-Occupancy-Vehicle) lanes and auxiliary/through lanes adding to the existing lanes to reduce traffic congestion as much as possible.

Although the heavy detour traffic was dissolved after the reopening of the Bay Bridge one month later, serious effects continued on other parts of the highway network. In the San Francisco City Area, since many distributors of US-101 and I-280 have been closed, heavy congestion

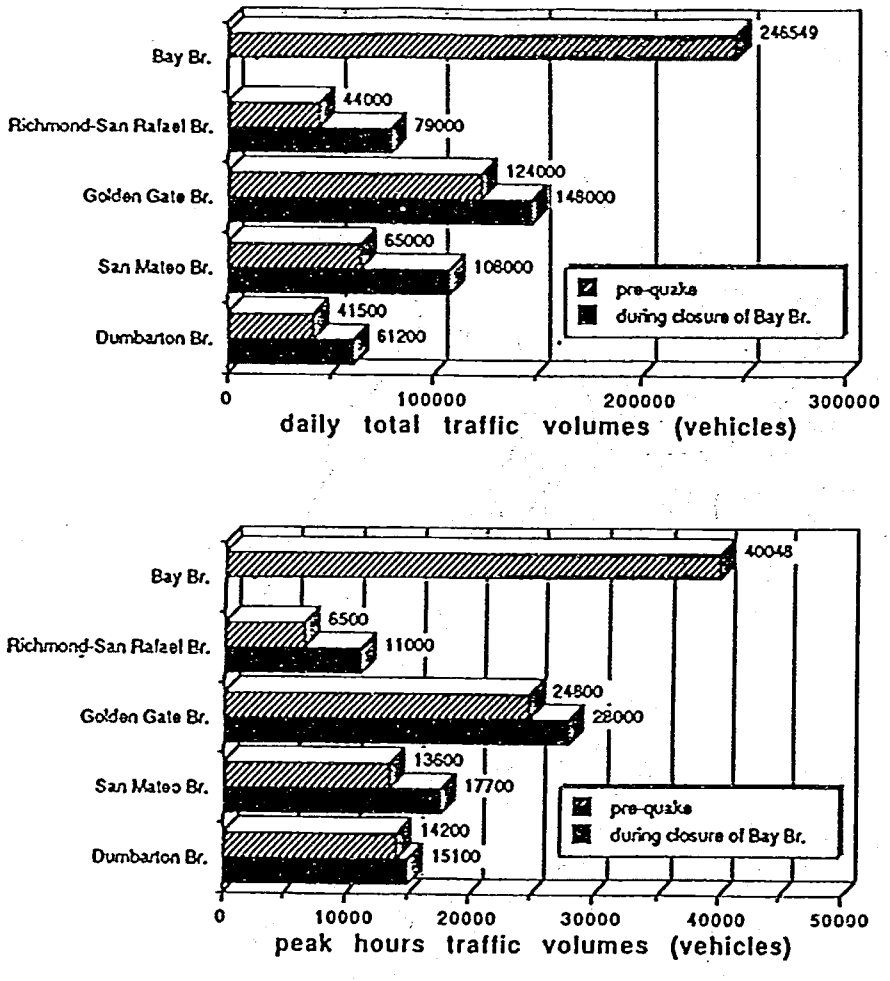


Figure 2. Pre- and Post-Earthquake Traffic Volumes on Five Bridges across the San Francisco Bay: (provided by Mr. Nojima of Urban Earthquake Hazard Research Center; Data source: CALTRANS)

occurs especially for the commuting period. In Oakland, the Cypress Street Viaduct of I-880 collapsed killing many. The failure of the loop road of the freeway in Oakland has affected the through traffic.

ESTIMATION OF OD MATRIX

For the highway network traffic analysis, Origin-Destination(OD) flow data is essential. However, there is no OD matrix surveyed before and after the earthquake available for the San Francisco Bay Area. The OD flow should be estimated then from other observed traffic data. The only data collected before and after the earthquake is the traffic volume at several highway side sites.

Many methods for estimating OD flow from observed link flow data have been proposed so far. These methods are basically divided into two categories. One is the case that the OD matrix previously surveyed exists, and the other is the case that no OD matrix was previously surveyed. For the latter case, the method by J.Holm et al.(1976) and the method by H. Inoue(1983) are known. Inoue's method requires the data set of the ratio of route choice. In the present study, there is neither a OD matrix previously surveyed nor available route choice data.

The method proposed by J.Holm et al. requires only the observed link flow data and the number of inhabitants of each zone besides the specifications of the network. The methodological structure combines the gravity type model and the maximum likelihood method. Using the method by Holm et al., the OD matrix before the earthquake is estimated.

In the method of Holm et al., the gravity model is

$$T_{ij} = p\, E_i\, E_j\, d_{ij}^{q}\,, \tag{1}$$

where T_{ij} is the number of car trips from zone i to zone j;
E_i is the number of inhabitants in zone i;
d_{ij} is the travel time from i to j;
p is a constant (trip generation factor); and
q is a negative constant (trip length exponent).

The link volume, estimated in the model, can be expressed with the aid of the gravity model as a sum of the traffic flow between all zones:

$$\begin{aligned} v_a &= \sum_{i,j} T_{ij}\, h_{aij} \\ &= p \sum_{i,j} E_i\, E_j\, d_{ij}^{q}\, h_{aij}\,, \end{aligned} \tag{2}$$

where v_a is the traffic volume on link a, i.e. link flow; and
h_{aij} is the portion of the traffic T_{ij} which uses link a.

Link flows are given using Smock's algorithm where the traffic capacity and the level of service on each highway link are taken into account;

$$v_a^{(n)} = (1 - 1/n)\, v_a^{(n-1)} + 1/n\, u_a\,, \tag{3}$$

where $v_a^{(n)}$ is the traffic volume on link a after the n'th iteration;
u_a is an auxiliary variable and equal to v_a, and is the traffic volume assigned along the minimum time path to link a after the n'th iteration.

The observed traffic flows v_a^* are assumed to be mutually independent, normal-distributed stochastic variables, with the means $v_a^{(n)}$ and with variances which vary with $v_a^{(n)}$ as follows:

$$v_a^* = v_a^{(n)} + \varepsilon_a,\quad \varepsilon_a \in N(0, (v_a^{(n)})^{\omega}\, \sigma^2)\,, \tag{4}$$

where ω is a real constant, and

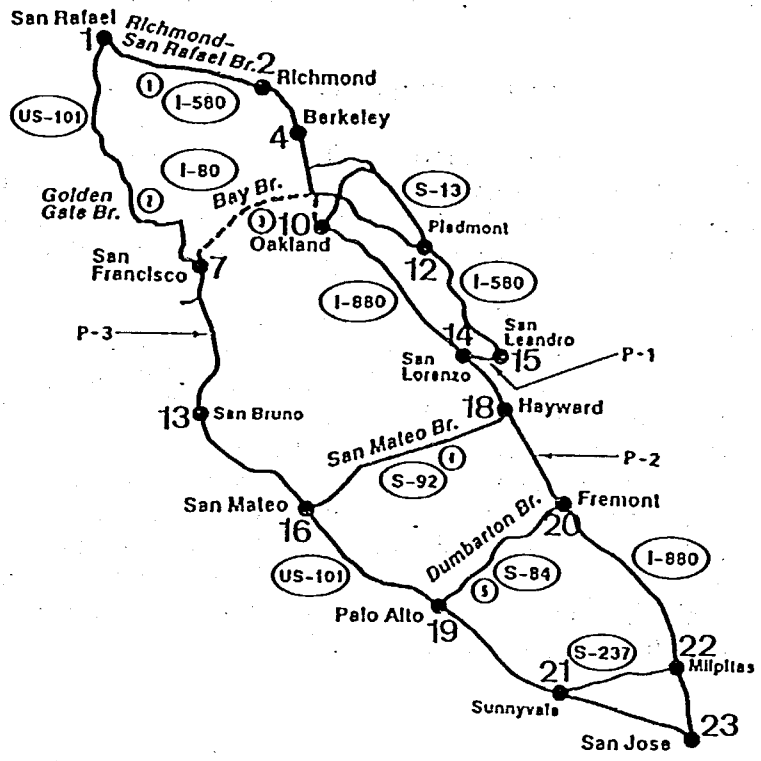


Figure 3. Study Area Highway Network of San Francisco Bay Area
Dotted lines depict closed sections; and ① to ⑤,
and P–1 to P–3 are traffic observation sites.

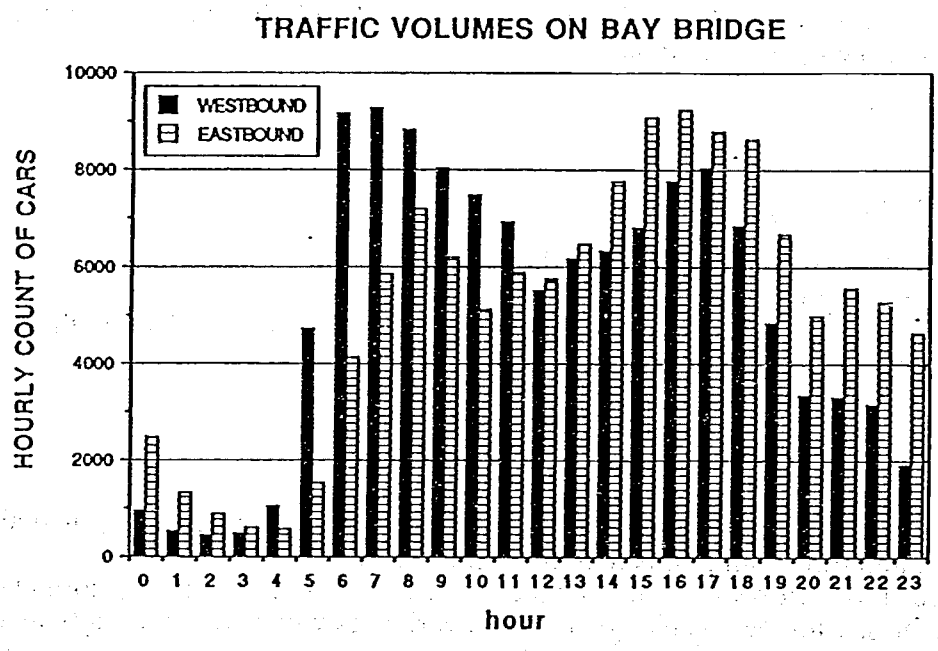


Figure 4. Traffic Volumes on Bay Bridge (Autumn, 1988):
(provided by Mr. Nojima of Urban Earthquake
Hazard Research Center; Data source: CALTRANS)

σ^2 is independent of a.

The value of ω indicates the weighting of the differences between observed and estimated traffic flows on the individual link if these differences are to be minimized.

The parameter p and σ^2 are estimated by means of the maximum likelihood method. The joint probability function is computed and its logarithm calculated. The function can be maximized by differentiation.

Figure 3 represents the Bay Area freeway network focused particularly on the absence of the Bay Bridge. The set of the observed link flows before the earthquake collected by CALTRANS and reported by Kameda et al.(1991) is used. The time of observation was autumn, 1988 except a few data. For observed sites from ① to ⑤ in Fig.3, traffic volume was measured for 24 hours. For observed sites from P–1, P–2 and P–3, traffic volumes for only 5 hours at the morning peak period from 4 a.m. to 10 a.m. were collected. To estimate the OD matrix, traffic volume per 24 hours is desired. Traffic volumes per day at these sites are estimated from the proportion of the 5 hours traffic to 24 hours traffic at the 24 hours period observation site (Fig.4).

Next, the specifications of the network for traffic assignment are described. The distances between every two nodes of Fig.3 are given using the road map of the American Automobile Association (AAA). The numbers of lanes for links are given from VCR pictures that one of the authors had taken actually driving on the Bay Area freeway network. The travel time function is the B.P.R.(Bureau of Public Roads) function,

$$t_a = t_{a0} \{ 1 + \alpha (v_a / C_a)^{\beta} \}, \tag{5}$$

where t is the travel time at flow v_a on link a;
t_{a0} is the travel time at zero flow on link a;
v_a is the flow on link a;
C_a is the capacity of link a; and
α and β are parameters.

The BPR engineers suggested values of 0.15 and 4 for α and β (Branston, 1976). Here, C_a is used as the practical capacity per day, and this is calculated from the hourly capacity and the *K–factor*. According to the HCM 1985, the *K–factor* varies from 7% to 11.5% (Transportation Research Board, 1985). In spite of the sensitivity analysis for the OD matrix varying the *K–factor*, the OD matrix obtained scarcely changed because of the roughly structured network. The travel time at zero flow, t_0, is given at 60 miles per hour since the speed limitation on the freeway is 55 to 60 m.p.h. and the actual steady state flow is such a state.

Next, as the land use characteristics, the number of inhabitants in every zone is calculated using the interpolation between 1985 and 1990 census populations or the latest estimates (Rand Mc.Nally & Company Offices, 1986 and 1990). The longitudinal changes in populations between 1985 and 1990 are small.

On the basis of these data, every OD flow between zone pairs i, j is estimated. The set of values of p and q resulting in the lowest weighted difference between observed and estimated traffic is chosen as the correct solution using the variance of Holm et al. (1976). In addition, the value of ω in Eq.(4) is important:

$\omega = 0$ indicates that the standard deviation of the traffic is independent of its magnitude. With $\omega = 1$, mean and variance are in proportion. $\omega = 2$ indicates that the standard deviation of traffic is proportional to the magnitude of the traffic; i.e., that the relative deviation σ_a / v_a is constant. In this study, $\omega = 2$ is adopted from the results of Iida and Takayama (1981). Using the maximum likelihood method, the values of $p = 9.9 * 10^{-4}$ and $q = -0.28$ are obtained. The total number of car trips is approximately 2,050,000 excluding the intrazonal car trips.

For testing the validity of the OD matrix obtained, the estimated and observed link flows are shown in Fig.5. The estimates are obtained using the Smock's method and the Incremental Assignment method. According to the study by Holm et al.(1976), the 95 % confidential interval, of course, depending on the traffic volume, is ±5,200 vehicles per a day when estimated traffic is 10,000 vehicles per a day. In our study, many link flows are well–estimated. However, some link flows are not. This is because in the network representation shown in Fig.5, the traffic flows

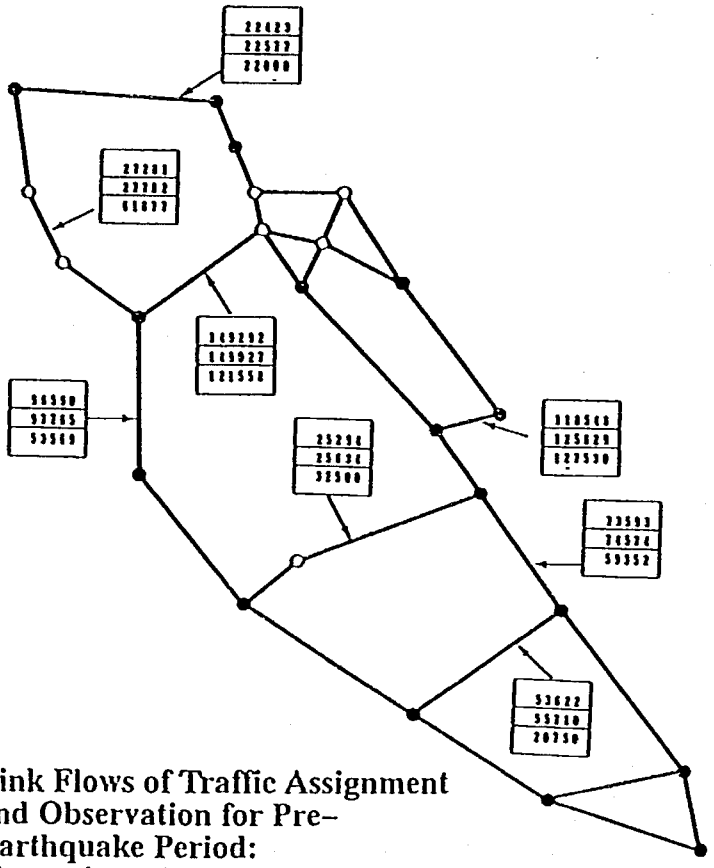


Figure 5. Link Flows of Traffic Assignment and Observation for Pre-Earthquake Period:
Figures in each box indicate
(1) link flow by incremental assignment;
(2) link flow by Smock's method; and
(3) observed link flow (vehicles/day/1 direction), respectively.

to/from the outside of the study area are replaced with the traffic flows to/from the boundary nodes, since the network cannot be extended due to the limited observation sites for traffic flows. From the model structure of estimating OD flows using the gravity model, the error between the observed and estimated flow becomes large, especially when the inhabitants in the zone for the boundary node is small. However, the major purpose of this study is the evaluation of the effects of the Bay Bridge closure, and the traffic flow there is well-estimated. Thus the analysis hereafter is based on this OD matrix.

HIGHWAY NETWORK EVALUATION BEFORE AND AFTER THE LOMA PRIETA EARTHQUAKE

Four cases are considered as follows:
(1) The network before the earthquake is loaded with the OD matrix before the earthquake.
(2) The network after the earthquake is loaded with the OD matrix before the earthquake.
(3) The network after the earthquake is loaded with the OD matrix after the earthquake. The OD matrix after the earthquake is the matrix after the modal shift from the choice of using a vehicle to using BART.
(4) The network after the earthquake with temporary HOV (High-Occupancy-Vehicle) lanes etc. is loaded with the OD matrix after the earthquake.

Case study (1) is to explain the traffic condition before the earthquake. Case study (2) is to

evaluate the traffic condition if the traffic demand before the earthquake continues with no change onto the surviving network, i.e., the network without the Bay Bridge and Cypress Street Viaduct. Case study (3) is based on the data that about 112,000 persons switched their modal choice from using a car to using BART during the Bay Bridge closure. On the basis of this fact and using the number of average persons per vehicle, the OD matrix after the earthquake is estimated. The OD matrix after the earthquake cannot be estimated exactly and directly from the observed link flows after the earthquake, because the observed traffic is congested and it does not reflect the real traffic demand; consequently the OD matrix is underestimated. In case study (3), the actual traffic condition after the earthquake can be evaluated. The important point is that this case study evaluates the alleviation of some congestion by the use of BART. In case study (4), rigorous analysis for the contribution of HOV lanes etc. cannot be carried out since the OD matrix for High-Occupancy-Vehicles cannot be estimated. Thus, the analysis here is limited to the average effect of temporary lanes from the viewpoint of the reduction of congestion.

GLOBAL EVALUATION OF THE NETWORK WITH NETWORK CAPACITY

Network capacity is defined as the maximum number of car trips that the network can deal with without over-saturated traffic when OD flow is increased using the given assignment principle under a fixed OD pattern. In other words, given the set of link capacities of the network, network capacity is the maximum number of vehicles in which every OD traffic can travel without encountering of heavy congestion. In this chapter, the network capacities are calculated for the four cases, using the route search method that is used in the course of the traffic assignment. This method is as follows:

Step 1: Obtain the unit OD matrix, $\{ x_{ij} \}$,

$$\text{where } x_{ij} = T_{ij} / \sum_{i,j} T_{ij}, \tag{6}$$

and T_{ij} is the number of car trips from zone i to zone j.

Let ΔX be the incremental number of total trips, and consider the incremental OD matrix $\{ \Delta X x_{ij} \}$. Let $m = 1$.

Step 2: Execute the incremental assignment for the incremental OD matrix $\{ \Delta X x_{ij} \}$ of m'th iteration. Update the travel times for all links. Set the travel times as infinity for the links where the assigned link flow exceeds the link capacity.

Step 3: The shortest travel time path is found for every OD pair.

Step 4: When there are paths with finite travel times for all OD pairs, go to Step 5. If there is a path with infinite travel time, go to Step 6. The occurrence of the path with infinite travel time means that the network becomes disconnected, namely, that the cut set in the graph theory occurs.

Step 5: Let $m = m + 1$, and go to Step 2.

Step 6: Stop computing. The network capacity is obtained as $m\Delta X$.

This procedure quantifies the effect of the Bay Bridge closure and the contribution of BART and HOV lanes from the viewpoint of macroscopic properties. The results are shown in Table 1. Case 1 shows that the network capacity before the earthquake is approximately 1,440,000 trips. It is less than the total demand of car trips, 2,050,000 (except the intrazonal car trips) that is the basis of this analysis. The degree of congestion, that is defined as the ratio of the demand to the capacity, is used for the measure of congestion levels in Japan. From this criteria, this means that serious congestion had already occurred before the earthquake, especially during the daily peak periods.

In case 2, the network capacity drastically decreases from 1,440,000 to 620,000. The ability of the network to deal with the traffic demand without heavy delay is less than half that of before the earthquake. The impact of the Bay Bridge closure was quite serious from the viewpoint of network capacity. Figure 6 shows the network capacity state and it illustrates that the cut set occurs around Richmond. The occurrence of the cut set is caused by the detour of traffic to/from Berkeley adding to the usual traffic to/from Richmond.

Table 1. EVALUATION OF NETWORK CAPACITY

Case Studies	Network Capacity $\times 10^3$ trips
(1) Pre-Earthquake Network and Pre-Earthquake OD Matrix	1,440
(2) Post-Earthquake Network and Pre-Earthquake OD Matrix	620
(3) Post-Earthquake Network and Post-Earthquake OD Matrix (Consideration of Modal Shift)	790
(4) Post-Earthquake Network with Temporary Lanes and Post-Earthquake OD Matrix	790

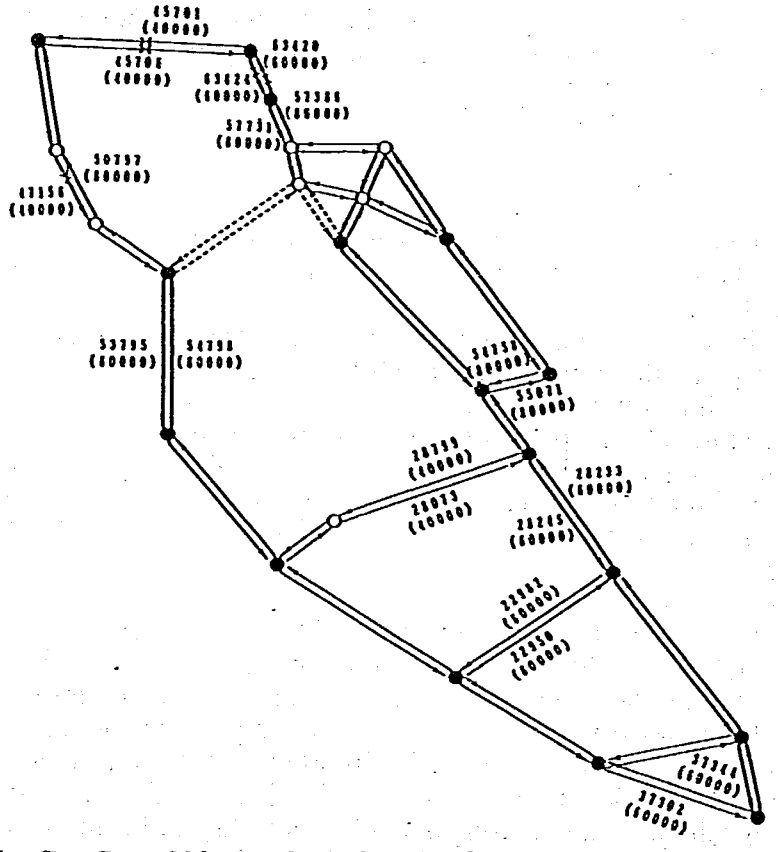


Figure 6. Cut Set of Network under the State of Network Capacity For Case Study 2: Network Capacity is 615,163 and figures indicate link flows under the state of network capacity and figures in brackets are link capacities.

In case 3, the network capacity is 790,000 trips, recovering 180,000 trips from case 2. This increase is the contribution of BART which absorbed trips from the highway delaying the occurrence of the cut set.

In case 4, no gain in network capacity is obtained from that in case 3. This is because the temporary lanes, such as HOV lanes and auxiliary/through lanes, are placed at the partial section of a bridge and at the approach to a bridge between the sections without temporary lanes. If the temporary lanes added to the links are included in the cut set, the network capacity had increased. However, the highway sections with large traffic demand are usually operated to their limits of highway width. The introduction of HOV lanes and auxiliary/through lanes has its own limitation, therefore, from the viewpoint of the network capacity. The effect of temporary lanes from another point of view is recognized; however, the multiple evaluation is, therefore, also important.

EVALUATION OF OD TRAVEL TIMES

In contrast to the network capacity of the global evaluation, evaluation of the network performance for each OD pair is also important. Here, we focus on the travel times between all Origin and Destination nodes before and after the earthquake. The travel times are the mean travel times that are computed in the procedure of the traffic assignment. Considering space, travel times for only three OD pairs are reported;

a) Travel time between San Francisco and Oakland;
b) Travel time between San Francisco and Berkeley; and
c) Travel time between San Francisco and San Jose.

Hourly traffic demand is discussed. The network specifications are the same as those used in the OD estimation, except for the hourly based characteristics:

The traffic capacities are given two cases: 1,600 and 2,000 passenger car units per lane per hour, which reflect the level of service for D and E respectively, shown in the Highway Capacity Manual 1985. The hour factors that are used for converting daily traffic to hourly traffic, are given in three cases: 0.10 and 0.08 for peak commuting period.and 0.06 for the daytime activity period excluding the peak period. The analysis will be carried out for these 6 combinations of levels of service and hour factors.

The results are shown in Table 2. For example, in the first and second columns in case 1(a), the mean travel time between San Francisco and Oakland is 17 to 27 minutes before the earthquake. After the earthquake, the shortest travel route being via the San Mateo Bridge, the mean travel time becomes 100 to 165 minutes in case 3(a). Table 2 also shows the upper figures in (1) representing travel times on the Bay Bridge route and lower figures indicating travel times for the same route in the post-earthquake period for comparison. Despite the difficulty of computing travel time in a jam condition, these results well-explain the actual travel time reported. For example, the travel time on the San Mateo Bridge reported by the Japanese reconnaissance team on November 1989 was about 90 minutes for the eastern direction at P.M. peak period (Kameda Ed., 1990). The computed travel time is about 60 minutes. The error between the observed and computed travel time is caused by the fluctuation of day-to-day traffic dynamics and by the use of the over-saturated section of travel time function. Another experience reported was that a person left home to go to work three hours earlier than usual.

The results shown in Table 2 were the mean travel times calculated at a steady state traffic flow without fluctuation, and without merging and weaving conflicts. For the actual travel time estimation in an over-saturated traffic flow, travel time in Table 2 should, therefore, be recognized at least as the necessary travel time.

Table 2. EVALUATION OF OD TRAVEL TIMES (Min.)

Hour Factor Capacity(v.p.h.)	0.10 2,000	0.10 1,600	0.08 2,000	0.08 1,600	0.06 2,000	0.06 1,600
(1) Pre–Earthquake Network and Pre–Earthquake OD Matrix						
(a) San Francisco – Oakland*	17.80 56.76	27.10 66.37	13.61 52.79	17.80 56.76	11.72 50.87	12.97 52.15
(b) San Francisco – Berkeley*	19.30 37.34	28.31 43.34	15.00 34.76	19.30 37.34	12.95 33.56	14.32 34.37
(c) San Francisco – San Jose*	62.23 62.23	81.58 81.58	53.25 53.25	62.23 62.23	48.98 48.98	51.83 51.83
(2) Post–Earthquake Network and Pre–Earthquake OD Matrix						
(a) San Francisco – Oakland	140.18	247.10	89.42	138.04	59.41	82.10
(b) San Francisco – Berkeley	135.70	259.02	83.52	135.70	55.78	72.40
(c) San Francisco – San Jose	101.84	184.49	66.89	101.84	52.16	62.30
(3) Post–Earthquake Network and Post–Earthquake OD Matrix (Consideration of Modal Shift)						
(a) San Francisco – Oakland	100.52	165.28	67.46	100.52	53.61	61.74
(b) San Francisco – Berkeley	86.13	162.23	62.12	86.13	46.83	58.84
(c) San Francisco – San Jose	81.60	129.96	59.44	81.60	50.26	56.01
(4) Post–Earthquake Network with Temporary Lanes and Post–Earthquake OD Matrix						
(a) San Francisco – Oakland	90.04	143.54	63.03	90.04	52.28	58.74
(b) San Francisco – Berkeley	74.91	122.58	55.04	74.91	44.08	52.16
(c) San Francisco – San Jose	77.27	125.88	57.95	77.27	49.74	54.96

* Upper figures indicate the travel times on Bay Bridge route.
Lower figures indicate the travel times on the same route in the post–earthquake period.

RELIABILITY ANALYSIS OF THE BAY AREA HIGHWAY NETWORK

Finally, the reliability of the Bay Area highway network is identified for pre- and post-earthquake periods. In this paper, highway network reliability is treated as terminal reliability, defined as the probability that two given nodes are connected for certain traffic service levels for given periods. This reliability is an indicator of alternativity and redundancy.

For example, let the service level be a simple physical connection between two nodes under unusual conditions. A highway network at this reliability level provides traffic service by offering vehicles alternative routes even when some part of the network is damaged. This indicator therefore can be used to assess network invulnerability during disasters. However, because this indicator illustrates only simple connectivity, traffic conditions and travel distances are not considered. If the traffic conditions do not matter, at least minimum transport service will be available for the transportation of relief goods.

Next, let the traffic service level be smooth without heavy delay. A highway network at this reliability level provides sure and unfluctuating traffic by offering drivers alternative routes even when a given route is down. This reliability indicator therefore shows the stability of the highway network performance. At the same time, it explains the network conditions under which detour traffic, due to damage of some part of the network, affects the congestion of another part of the network. In other words, it represents the network service level which follows network failure caused by a disaster. This indicator can be used for traffic management during restoration after a disaster to ensure smooth restorative activities.

Fortunately, in the Loma Prieta Earthquake, serious damage to the facilities could be avoided. Consequently, the capability for the socio-economic activities in the Bay Area to recover was quick, and this comes out as the traffic demand. Thus, the surviving network had to support traffic until the recovery of the entire network. Therefore, the indicator of reliability is important to ensure a high standard of service.

The highway network reliability analysis should include the phenomenon in its procedure that the change in path flows affects the change in terminal reliability. It should also consider the aforementioned characteristics of traffic flows. In this study, the highway network reliability analysis methods developed by Iida and Wakabayashi (1989) and by Wakabayashi and Iida (1991a, 1991b) are applied. This reliability analysis method consists of the estimation of link reliability and reliability analysis for terminal reliability.

Estimation of Link Reliability

First, the method for estimating the link reliability is briefly shown (Wakabayashi and Iida, 1991a). Link reliability is determined by the following assumptions:

(1) The link reliability on link a, r_a, is the result of variations in link flow, v_a. Link reliability is defined as the probability that the demand flow on the link does not exceed the capacity of the link for a given time period.

(2) Demand flow range obeys a normal distribution. The mean of the demand flow is $\bar{v}_a$.

(3) Variances in the normal distribution, σ_a^2, are functions of the demand flow and link capacity on link a, C_a. Coefficients of variation (COV), $\sigma_a / \bar{v}_a$, are given using the following function:

$$\mathrm{COV} = \sigma_a / \bar{v}_a = \alpha \exp \{ -\beta (\bar{v}_a / C_a + \delta)\} + \gamma , \qquad (7)$$

where α, β, γ and δ are parameters, and α and β are different from those used in Eq.(5).

In (1), the capacity is determined corresponding to the desired service levels. Here, the same capacities are given as used in the previous chapter; 1,600 and 2,000 passenger car units per lane per hour, which reflect the level of service D and E. When link flow variation is identified as a probability density function, link reliability can be determined from demand flow and link capacity. This method has an advantage that the set of link reliability can be determined from the re-

sults of traffic assignment with only one time computation. Thus, this method is capable of reliability assessment and of comparison of alternatives of transportation planning under restriction of sufficient data collection.

The Intersection Method: An Efficient Terminal Reliability Analysis Method

Reliability analysis for a network system, such as a telecommunication network system, should involve, in general, all the minimal path sets and cut sets regardless of their length or cost, since the connectivity between two given nodes is more important than the time or distance between the nodes. In the reliability analysis of a highway network system, however, routes expected to be used by drivers should be taken into major consideration.

Therefore it is necessary to choose the significant path sets and cut sets which contribute greatly to the determination of the reliability value in the highway network reliability analysis. To attain this, a partial network actually used by vehicles should be excerpted from the highway network. Through this excerpt technique, the number of path sets and cut sets can be reduced.

In this paper, we introduce a new approximation method using partial minimal path sets and cut sets (Iida and Wakabayashi, 1989 and Wakabayashi and Iida, 1991b). Two reliability functions are introduced as

$$R_p = 1 - \prod_{s=1}^{p'} \left(1 - \prod_{a \in P_s} r_a \right), \tag{8}$$

and

$$R_k = \prod_{s=1}^{k'} \left\{ 1 - \prod_{a \in K_s} (1 - r_a) \right\}, \tag{9}$$

where r_a is link reliability, and

$$r_a = \mathrm{E}[X_a]. \tag{10}$$

X_a is a binary indicator variable for link a, as follows:

$$X_a = \begin{cases} 1, \text{ if link } a \text{ provides the given traffic service level,} \\ 0, \text{ otherwise.} \end{cases} \tag{11}$$

A set of link reliability is determined using the aforementioned method. "Functioning" or "failure" of links is assumed to be independent of each other, where "failure" is caused by natural disaster, traffic accidents, maintenance of link, and traffic congestion; and where every link is sufficiently long so as not to affect another link. P_s represents s–th minimal path set and K_s denotes s–th minimal cut set, and the subscripts p of R_p and k of R_k stand for "path" and "cut". And, p' and k' are the number of partial minimal path sets and cut sets respectively and,

$$p' \leq p \ , \ k' \leq k \, , \tag{12}$$

where p and k are the total number of minimal path sets and minimal cut sets respectively.

The value of R_p is characterized as follows: R_p is the increasing function of the number of path sets. When the number of the minimal path sets p' is small, Eq.(8) provides the lower bound value of reliability. When all the minimal path sets are employed in Eq.(8), the value R_p yields

the upper bound value of reliability. This upper bound is known as Esary and Proschan's upper bound (Barlow and Proschan, 1965), and is

$$U = 1 - \prod_{s=1}^{P} \left(1 - \prod_{a \in P_s} r_a\right). \tag{13}$$

Hence, the value R_P increases monotonically with an increase in the number of path sets from the lower bound of reliability to Esary and Proschan's upper bound of reliability.

Similarly, the value of R_k decreases monotonically with the increase in the number of cut sets from the upper bound of reliability to the lower bound of reliability. This lower bound of reliability is known as Esary and Proschan's lower bound and is

$$L = \prod_{s=1}^{k} \left\{1 - \prod_{a \in K_s} (1 - r_a)\right\}, \tag{14}$$

and

$$L \leq R \leq U. \tag{15}$$

Therefore, the two functions will cross at a certain point between Esary and Proschan's upper and lower bounds. The value at the intersection is proposed as an approximation for the reliability value.

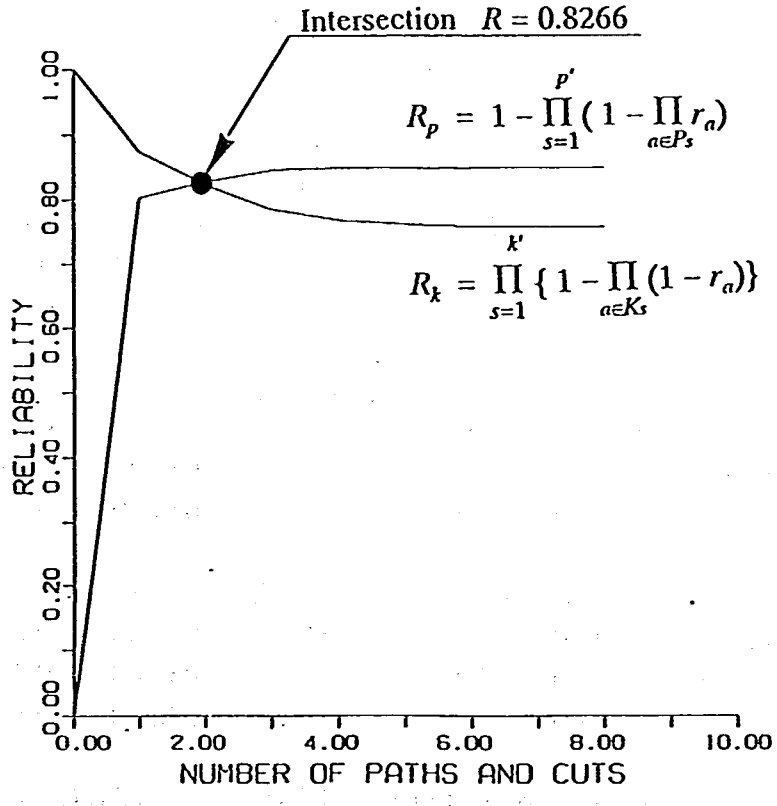


Figure 7. Illustration of the Intersection Method: Terminal reliability between San Francisco and Oakland for Case Study (1), Hour Factor 0.06, Service Level D

The intersection method provides sound approximations. The necessity for computational work is extremely limited due to the incorporation of non-Boolean absorption (Iida and Wakabayashi ,1989) and the use of partial minimal path sets and cut sets. The CPU-TIME is 1/200 to 1/20,000 times more efficient than the exact method and the Monte Carlo method (Wakabayashi and Iida ,1991a and 1991b). Since it is simplistic and easily calculable, the intersection method can be applied to a large scale highway network.

In addition, the partial path sets and cut sets employed in the reliability analysis procedure correspond to the existing traffic routes and screen lines. Thus, we can use the reliability analysis results in connection with actual highway planning and traffic management.

The way in which the partial minimal path sets and cut sets are determined is described in Wakabayashi and Iida (1991b).

The procedure of the intersection method is demonstrated in Fig.7.

The Reliability Analysis of the Bay Area Highway Network

The results are shown in Table 3. The four columns of the left hand side reflect the peak period terminal reliability. It is presumed that heavy congestion had occurred during pre-earthquake peak periods and the terminal reliability at this period is estimated as very small. Thus, the terminal reliability in every case for the post-earthquake period is also extremely small.

The two columns of the right hand side represent the daytime period excluding the peak peri-

Table 3. EVALUATION OF TERMINAL RELIABILITY

Hour Factor	0.10	0.10	0.08	0.08	0.06	0.06
Capacity(v.p.h.)	2,000	1,600	2,000	1,600	2,000	1,600
(1) Pre-Earthquake Network and Pre-Earthquake OD Matrix						
(a) San Francisco – Oakland	0.0038	0.0000	0.5918	0.0038	1.0000	0.8266
(b) San Francisco – Berkeley	0.0000	0.0000	0.1244	0.0000	0.9971	0.5221
(c) San Francisco – San Jose	0.0000	0.0000	0.0284	0.0000	0.9264	0.1159
(2) Post-Earthquake Network and Pre-Earthquake OD Matrix						
(a) San Francisco – Oakland	0.0000	0.0000	0.0000	0.0000	0.0438	0.0000
(b) San Francisco – Berkeley	0.0000	0.0000	0.0000	0.0000	0.0192	0.0000
(c) San Francisco – San Jose	0.0000	0.0000	0.0000	0.0000	0.0952	0.0000
(3) Post-Earthquake Network and Post-Earthquake OD Matrix (Consideration of Modal Shift)						
(a) San Francisco – Oakland	0.0000	0.0000	0.0000	0.0000	0.6586	0.0009
(b) San Francisco – Berkeley	0.0000	0.0000	0.0000	0.0000	0.4017	0.0000
(c) San Francisco – San Jose	0.0000	0.0000	0.0000	0.0000	0.6494	0.0012
(4) Post-Earthquake Network with Temporary Lanes and Post-Earthquake OD Matrix						
(a) San Francisco – Oakland	0.0000	0.0000	0.0001	0.0000	0.9234	0.0080
(b) San Francisco – Berkeley	0.0000	0.0000	0.0000	0.0000	0.3932	0.0000
(c) San Francisco – San Jose	0.0000	0.0000	0.0001	0.0000	0.8740	0.0050

ods. The connectivity with given service levels is relatively high for pre-earthquake period. In case study (2) in which the traffic demand before the earthquake is generated without change in the surviving network, the terminal reliability considerably decreases. In case study (3) which considers the modal shift between highway and BART, the terminal reliability improves more than in case (2). The contribution of BART that bore the traffic between San Francisco and the opposite bank is evaluated. In case study (4), despite the treatment of HOV lanes as just temporary additional lanes for all vehicles, terminal reliability increases. This fact demonstrates that the terminal reliability can be raised by the addition of temporary lanes. It is one of the strongest ways to improve reliability but is impossible under such congested traffic. In Japan, HOV lanes are unfamiliar, but exclusive lanes for buses and taxis are familiar. These exclusive lanes also contribute to the smooth travel of ambulances and fire engines to their destinations in order to administer quick medical care and to prevent the escalation of a disaster.

CONCLUSION

For successful highway construction and efficient disaster traffic management, the identification of the consequences of a disaster is essential. This paper presented the impact of the 1989 Loma Prieta Earthquake with emphasis on investigations of the one-month closure of the Bay Bridge and its effects on the Bay Area transportation system. The importance of the highway network reliability as a lifeline system and the impact of the Loma Prieta Earthquake on Japanese lifeline researchers were discussed. After these discussions, the methodologies for evaluating highway network performance under the disaster emergency were presented. It was pointed out that the consideration of the characteristics of traffic is important in the course of the highway network performance analysis. Functional effects of highway network capacity, average travel time and terminal reliability are estimated for pre- and post-earthquake periods, including the evaluation of modal shift between the highway and BART and the effects of the temporary HOV lanes. These analyses quantified the contribution of BART and temporary lanes that could mitigate the functional damage of the network, compared to the case in which there were no alternative transportation systems and no management of highway systems for the post-earthquake period.

San Francisco Bay Area has a larger highway stock than any large Japanese city. In even such a highway network system, detour traffic due to the damage of network components, the collapse of the Bay Bridge, caused heavy congestion in other parts of the network.

In contrast, Japanese highway systems are operated under critical condition with heavy traffic demand. In addition, there are few alternative reasonable routes when a given route is down. With the mass transit systems already being operated under congestion with a heavy passenger demand, there is little room to accept the modal shift from the highways. Therefore, it is a urgent theme to establish invulnerable highway network systems and management systems for a disaster emergency period.

ACKNOWLEDGEMENTS

This work has been performed as a cooperative research, integrating the investigation of the effects of the 1989 Loma Prieta Earthquake conducted by Kameda et al.(1991) and the highway reliability analysis methods developed by Wakabayashi and Iida (1991a, 1991b).

We are grateful to Professor Yasunori Iida of Kyoto University for his enthusiastic support and encouragement. Mr. Souta Dei, an undergraduate student of the Urban Earthquake Hazard Research Center, helped us in the calculation. Mr. Nobuoto Nojima of the Urban Earthquake Hazard Research Center was pleased to provide us with some figures that will also be used in his doctoral dissertation.

REFERENCES

Barlow,R.E. and Proschan,F. (1965). Mathematical Theory of Reliability. John Wiley & Sons, Inc., New York. 1965.

Branston,D. (1976). Link Capacity Functions: A Review. Transpn. Res. Vol.10, pp.223–236, Pergamon Press, 1976.

Holm,J., Jensen,T., Nielsen,S.K., Christensen A., Johnsen,B. and Ronby,G. (1976). Calibrating Traffic Models on Traffic Census Results Only. Traffic Engineering and Control, Vol.17, No.4,pp.137–140,1976.

Iida,Y. and Takayama,J. (1981). Statistical Analysis of the Characteristics of Traffic Fluctuation on Expressway. Expressways and Automobiles, Vol.24, No.12, pp.22–32, 1981.

Iida,Y. and Wakabayashi,H. (1989). An Approximation Method of Terminal Reliability of Road Network Using Partial Minimal Path and Cut Sets. Transport Policy, Management and Technology Towards 2001 (Selected Proceedings of The Fifth World Conference on Transport Research), Vol.4,pp.367–380, Western Periodicals, Co., 1989.

Inoue,H. (1983). Statistical Estimation of Traffic Demand using Traffic Census Results. Proceedings of Japan Society of Civil Engineering, pp.85–94, 1983.

Kameda,K., Asaoka,K., Ogawa,N. and Nojima,N. (1991). Effects of the 1989 Loma Prieta Earthquake on the San Francisco Bay Area Transportation System. Investigation of the effects of the Loma Prieta Earthquake, Vol.3, Part 4, Urban Earthquake Hazard Research Center UEHR Report No.E7, Disaster Prevention Research Institute, Kyoto University, 1991.

Kameda,H. Editor, Japanese Group for the Study of Natural Disaster Science (1990). Loma Prieta Earthquake of October 17, 1989 Reconnaissance Report. Natural Disaster Research Report Supported by the Japanese Ministry of Education, Science and Culture (Grant No.01102044), 1990.

Rand Mc.Nally & Company Offices (1986). 1980 Census Populations or Latest Available Estimates, Rand Mc.Nally 1986, Road Atlas. p.120, Rand Mc.Nally & Company Offices, 1986.

Rand Mc.Nally & Company Offices (1990). 1980 Census Populations or Latest Available Estimates, Rand Mc.Nally 1990, Road Atlas. p.120, Rand Mc.Nally & Company Offices, 1990.

Transportation Research Board (1985). Highway Capacity Manual 1985. Special Report 209, Transportation Research Board, 1985.

Wakabayashi,H. and Iida,Y. (1991a). Evaluation of Reliability of Road Network for Better Performance, Advanced Management and Future Network Design. Applications of Advanced Technologies in TRANSPORTATION ENGINEERING, Proceedings of the Second International Conference, pp.121–125, American Society of Civil Engineers, 1991.

Wakabayashi,H. and Iida,Y. (1991b). An Efficient Evaluation Method for Road Network Reliability in Disaster. International Symposium on Natural Disaster Reduction and Civil Engineering, Japan Society of Civil Engineers, pp.397–405, 1991.

GIS-BASED ASSESSMENT OF THE SEISMIC PERFORMANCE OF A WATER DELIVERY SYSTEM

Masanobu Shinozuka

Sollenberger Professor of Civil Engineering
Department of Civil Engineering and Operations Research
Princeton University, Princeton, NJ 08544

Howard H. M. Hwang

Professor of Civil Engineering
Center for Earthquake Research and Information
Memphis State University, Memphis, TN 38152

Satoshi Tanaka

Visiting Scholar
Department of Civil Engineering and Operations Research
Princeton University, Princeton, NJ 08544

ABSTRACT

This paper presents the recent improvement of a GIS-based computer program, LIFELINE-W, for evaluating the seismic performance of a water delivery system. First, damage to water supply source such as pumping stations has been included in the analysis. Second, the occurrence of a pipe break is considered as a function of peak ground acceleration, pipe material, pipe diameter, and soil condition. By using Memphis water delivery system as an example, the system performance in the event of an earthquake is evaluated using the improved LIFELINE-W program.

INTRODUCTION

The water delivery system in a large city is usually very complex and covers a large area. The water delivery system may suffer from pipe breaks, joint leakages, and mulfunctions of pumping stations in the event of an earthquake. These damages could result in a considerable reduction of both flow rate and water pressure and thus lead to a significant loss of fire-fighting capability and supply of potable water. Sato and Shinozuka (1991) developed an interactive and graphic computer program, LIFELINE-W, for evaluating the seismic performance of a water delivery system. This program includes ARC/INFO, a Geographic Information System (GIS) software package (ESRI 1991). Thus, LIFELINE-W has various functions such as digitizing a water delivery network, interactive editing of features and attributes, performing seismic risk analysis, and displaying results in graphic form. Furthermore, these functions can be integrated using macro language and menu interface of the ARC/INFO software package so that the LIFELINE-W computer code can be used easily and effectively.

The LIFELINE-W program has been used to evaluate the seismic performance of the Memphis water delivery system subject to a 7.5 moment magnitude earthquake, which is assumed to occur at Marked Tree, Arkansas (Shinozuka et al. 1992). The adequacy of post-earthquake water supply and the possible impacts on the residents and industries in the Memphis area have been assessed. In that study, however, the supply nodes such as pumping stations were assumed not to be damaged by ground motions. The pumping stations of the Memphis water delivery system, however, may be quite vulnerable to ground shaking, because these facilities were not designed to resist earthquakes. In addition, the pipes in the entire system were assumed as cast iron pipes, even though ductile pipes were used since 1975. The occurrence of pipe breaks was considered as a function of the MMI intensity and pipe diameter; the variation of soil condition in the study area was not taken into account.

In this paper, we presents the recent improvement of the LIFELINE-W computer program. First, damage to water supply source such as pumping stations has been included in the analysis. Second, the occurrence of a pipe break is considered as a function of peak ground acceleration, pipe material, pipe diameter, and soil condition. The performance of Memphis water delivery system in the event of an earthquake is evaluated again by using the improved LIFELINE-W program.

CONNECTIVITY AND FLOW ANALYSIS

For the connectivity and flow analysis of a water network, the LIFELINE-W computer code uses the analysis algorithm proposed by Takakuwa (1978) with modifications to include booster pumps and treatment of negative pressure. For the pipe attached to a booster pump, the water lift by the booster pump is added to the water head at the downstream nodes. The leakage at the nodes is also taken into consideration. In addition, a supply node such as a pumping station is modelled by using a supply station, a demand node, and a supply link as shown in Figure 1. In the event of an earthquake, the supply station remains intact with a fixed water head, while the probability of failure of the pumping station is taken care of by the failure of the supply link. The LIFELINE-W computer program can be used to evaluate a water delivery system under an intact condition or a seismically damaged condition.

MEMPHIS WATER DELIVERY SYSTEM

The Memphis water delivery system is operated by Memphis Light, Gas and Water Division (MLGW). The system supplies water in both the City of Memphis and Shelby County, Tennessee, except for a few incorporated municipalities inside the county. The water is taken from underground aquifer by deep wells and delivered to the public after treatment. The Memphis water delivery system consists of a large low-pressure system and several high-pressure systems on the outskirts of the city. The system is comprised of about 1300 links and 960 nodes. The total length of the buried pipes is about 1370 km and the pipe diameter ranges from 15 cm to 122 cm. The unlined and cement-lined cast iron pipes were used for those installed before 1975, while the ductile iron pipes were used afterwards. As of 1990, there are eight pumping stations in the low-pressure system and one small pumping station in the high-pressure system. In addition to these pumping stations, six elevated tanks are used in the high-pressure systems and nine booster pumps connect the low-pressure and high-pressure systems.

Data pertinent to the entire Memphis water delivery system have been collected, digitized, and implemented into a GIS database. The GIS coverage of the water network is shown in Figure 2. A flow analysis of the Memphis water network under an intact condition is carried out. The water heads at the nodes in the suburban area tend to be smaller than those inside Memphis, although the output flow rate can meet the demand at most of these nodes.

SUBSURFACE CONDITIONS

Memphis is located in the Mississippi embayment, which consists of unconsolidated sedimentary deposits. Ng et al. (1989) collected about 8500 existing boring logs in the Memphis area. These data were compiled and analyzed to establish representative boring logs for the cells resulting from applying a grid system to the entire study area. On the basis of these representative boring logs, the subsurface conditions in the study area are revealed. By using the classification of soil profiles specified in the Uniform Building Code, Hwang (1991) developed a generalized map showing the soil-profile classifications in the Memphis area (Figure 3). In this study, the soil conditions S_2 and S_3 shown in Figure 3 are considered as average soil condition, while S_4 is considered as poor soil condition.

SEISMIC GROUND SHAKING

Memphis is close to the southwestern segment of the New Madrid seismic zone (NMSZ). Thus, significant seismic hazards exist in the Memphis area. Hwang et al. (1990) evaluated ground shaking in the Memphis area caused by a 7.5 moment magnitude earthquake assumed to occur at Marked Tree, Arkansas. The values of peak ground acceleration at 424 sites were determined by nonlinear site response analyses. These values were then interpolated for the entire study area as shown in Figure 4 (Shinozuka et al. 1992). Because of the location of the scenario earthquake, ground shaking is more severe in the northwestern part of the county.

FRAGILITY ANALYSIS OF SHEAHAN PUMPING STATION

The Sheahan pumping building is a one-story steel frame building built in 1931 without seismic resistant design. By using the ABAQUS computer program (1989), seismic response of the building is determined from the response spectrum analysis with the site-specific response spectrum developed by Hwang and Lee (1990). On the other hand, structural capacities is determined by using the criteria set forth in the AISC LRFD Manual (1986). Uncertainties in both structural response and structural capacity are quantified and 10,000 simulations are carried out to construct the fragility curve for the Sheahan pumping building (Figure 5). Detail of the derivation of the fragility curve is shown in Hwang et al. (1992). Other pumping stations in the Memphis water delivery system are similar to Sheahan pumping station; thus, the fragility curve of Sheahan pumping station is also used for other pumping stations.

ESTIMATION OF PIPE BREAKS

The existing pipes in the Memphis water delivery system are made of either cast iron or ductile iron. For the cast iron pipe, the pipe break rate Y estimated by Katayama et al. (1975) is used in this study.

$$\text{Log}(Y) = 6.424\ \text{Log}(PGA) + 4.822 \quad \text{For poor soil conditions}$$
$$\text{Log}(Y) = 6.005\ \text{Log}(PGA) + 3.434 \quad \text{For average soil conditions}$$
$$\text{Log}(Y) = 5.322\ \text{Log}(PGA) + 1.602 \quad \text{For good soil conditions}$$

where Y is the number of pipe breaks per km and Y is limited to 16 breaks/km. PGA is the horizontal peak ground acceleration in g. For ductile iron pipe, the pipe break rate is estimated by following the procedure suggested in Monograph No. 2 issued by the ASCE Technical Council on Lifeline Earthquake Engineering (Craig 1991).

$$\text{Log}(Y) = 6.424\ \text{Log}(PGA) + 3.999 \quad \text{For poor soil conditions}$$
$$\text{Log}(Y) = 6.005\ \text{Log}(PGA) + 2.611 \quad \text{For average soil conditions}$$
$$\text{Log}(Y) = 5.322\ \text{Log}(PGA) + 0.779 \quad \text{For good soil conditions}$$

Figures 6 and 7 show the pipe break rate for the cast iron pipe and ductile iron pipe, respectively. The pipe break rate described above is for the pipe diameter D of 25 cm and is independent of the pipe diameter. However, the pipe performance in actual earthquakes indicated that large diameter pipes have less chance to be broken. In this study, the C_d factor suggested by Okumura and Shinozuka (1991) is used to include the effect of pipe diameters on the pipe break rate. The C_d factor is taken as 1.0 for $D < 25$ cm; 0.5 for $25 < D < 50$ cm; 0.2 for $50 < D < 100$ cm; and 0 for $100 < D$ cm. It is noted that the pipe break rate established in this study is preliminary. Further research is needed to refine the model.

By assuming that the occurrence of a pipe break follows the Poisson process, the failure probability of the i-th pipe P_i can be determined as

$$P_i = 1 - \exp(-r_i * L_i) \qquad (1)$$

where L_i and r_i are the pipe length in km and pipe break rate per km of the i-th pipe, respectively. The pipe break rate of the i-th pipe under the scenario earthquake is automatically assigned by laying the GIS coverages of PGA and soil-profile over the coverage of water network, in which pipe diameter and pipe material are established as link attribute data.

SEISMIC PERFORMANCE

Damage to the water network caused by ground shaking is simulated by using the Monte Carlo method. A random number uniformly distributed between 0 and 1 is generated for each pipe. If the random number is smaller than P_i, the pipe is considered to have been broken and thus it is removed from the network. Flow analysis of the damaged network is then performed to determine the flow parameters such as the water head and output flow rate at each node. On the basis of 20 simulation results, the average output flow rate at each node can be determined (Figure 8). Furthermore, the simulation results are laid over the census tract coverage to estimate the ratio of the output under damaged condition to the demand in each census tract (Figure 9). A moderate decline in water output occurs in the northern part of the county. The results reflect the stronger ground shaking as well as the poor connectivity of the network in this part of the county. Other areas in Memphis and Shelby County maintain the predicted water output at the level more than 70% of the demand except a few areas inside the city where the water output flow is quite low. This is especially true in the downtown area near the Mississippi River. The impact of water supply on the residents and industries in the study area will be carefully examined in the future.

CONCLUSIONS

This paper presents the recent improvement of the GIS-based LIFELINE-W computer program for evaluating the seismic performance of a water delivery system. This study demonstrates that the interactive and graphic computer program, LIFELINE-W is a very powerful tool for performing seismic risk analysis of a lifeline network. Spatial information such as the topography, census tracts, soil conditions, and ground motion intensity can be easily utilized in the analysis. In addition, the display of results in graphic form makes it easier for the user to examine analytical results and to make decisions effectively.

In this study, the pipe break rate is estimated on the basis of the available results in the literature and further research is required to refine the model. Furthermore, the ground shaking is the only seismic hazard considered in the analysis. Other seismic hazards such as soil liquefaction may also have great potential to damage the network. Such a study will be undertaken in the future.

ACKNOWLEDGMENTS

This work is supported by the National Center for Earthquake Engineering Research under contract numbers NCEER 913311, 913312 and 913313 (NSF grant number BCS-9025010). Any opinions, findings, and conclusions expressed in the paper are those of the authors and do not necessarily reflect the views of NCEER or NSF of the United States.

The authors appreciate the generous assistance provided by the Memphis Light, Gas and Water Division (MLGW), City of Memphis. In particular, the assistance given by Mr. Tommy Whitlow of MLGW is greatly appreciated.

REFERENCES

Craig, E. T. (1991), Seismic Loss Estimates For a Hypothetical Water System, Monograph No. 2, Technical Council on Lifeline Earthquake Engineering, American Society of Civil Engineers, New York.

Environmental Systems Research Institute (1991), ARC/INFO Users Guide, Redlands, CA.

Hibbit, Karlsson and Sorensen Inc. (1989), "ABAQUS Users Manual," Providence, RI.

Hwang, H., and Lee, C.S. (1990), "Site-Specific Response Spectra for Memphis Sheahan Pumping Station," Technical Report NCEER-90-0007, National Center for Earthquake Engineering Research, SUNY, Buffalo, NY.

Hwang, H., Lee, C.S., and Ng, K.W. (1990), "Soil Effects on Earthquake Ground Motions in the Memphis Area," Technical Report NCEER-90-0029, National Center for Earthquake Engineering Research, State University of New York at Buffalo, Buffalo, NY.

Hwang, H (1991), "Seismic Hazards for Memphis Water Delivery Systems," Proceeding of the Third U. S. Conference on Lifeline Earthquake Engineering, Los Angeles, CA, pp. 510-519.

Hwang, H., Ch'ng, A.L., and Hsu, H.M. (1992), "Seismic Fragility Analysis of Memphis Sheahan Pumping Building," Technical Report, Center for Earthquake Research and Information, Memphis State University, Memphis, TN.

Katayama, T., Kubo, K., and Sato, N. (1975), "Earthquake Damage to Water and Gas Distribution System," Proceedings of U. S. National Conference on Earthquake Engineering, pp. 396-405.

"Manual of Steel Construction--Load and Resistance Factor Design," (1986), American Institute of Steel Construction, Inc., Chicago.

Ng, K.W., Chang, T.S., and Hwang, H. (1990), "Subsurface Conditions of Memphis and Shelby County," Technical Report NCEER-89-0021, National Center for Earthquake Engineering Research, State University of New York at Buffalo, Buffalo, NY.

Okumura, T., and Shinozuka, M. (1991), "Serviceability Analysis of Memphis Water Delivery Systems," Proceedings of the Third U.S. Conference on Lifeline Earthquake Engineering, Los Angeles, CA, pp. 530-541.

Sato, R., and Shinozuka, M. (1991) "GIS-Based Interactive and Graphic Computer System to Evaluate Seismic Risks on Water Delivery Networks," Proceedings of the Third U.S. Conference on Lifeline Earthquake Engineering, Los Angeles, CA, pp. 651-660.

Shinozuka, M., Hwang, H., and Murata, M (1992), "Impact on Water Supply of a Seismically Damaged Water Delivery System," in Lifeline Earthquake Engineering in the Central and Eastern U.S., ed. Ballantyne, D. B., Monograph No. 5, Technical Council on Lifeline Earthquake Engineering, American Society of Civil Engineers, New York, pp. 43-57.

Takakuwa, T. (1978), "Analysis and Design of Water Distribution Network (Haisui Kan-mou no Kaiseki to Sekkei)," Morikita Shuppan, (in Japanese).

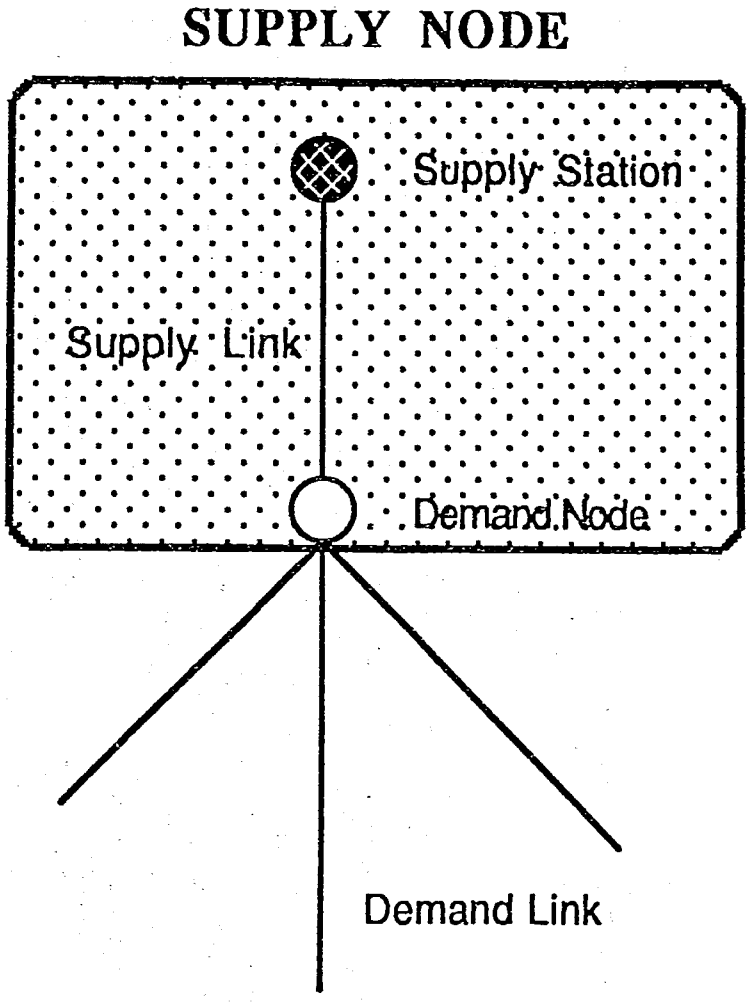


Figure 1. Modeling of a Supply Node

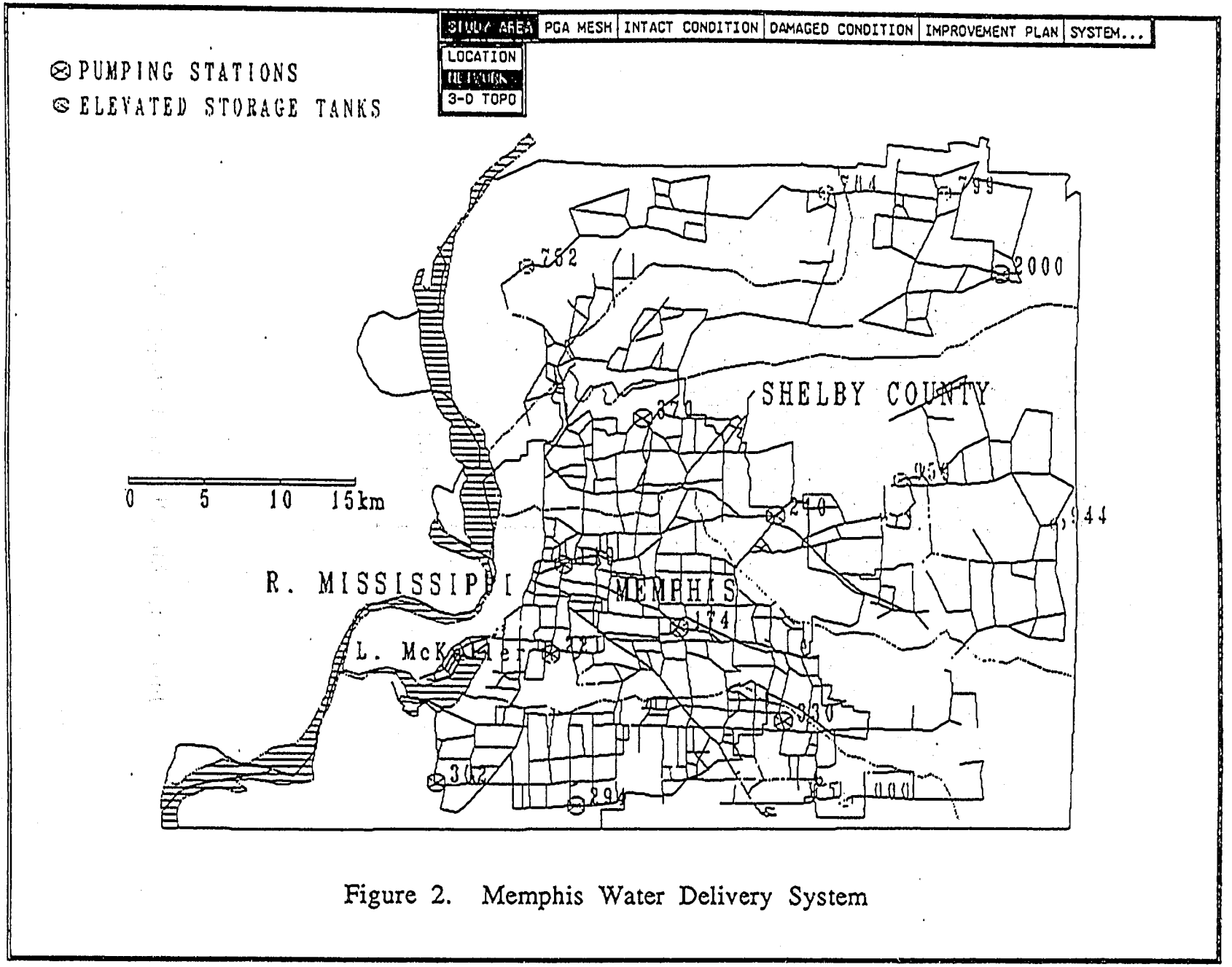


Figure 2. Memphis Water Delivery System

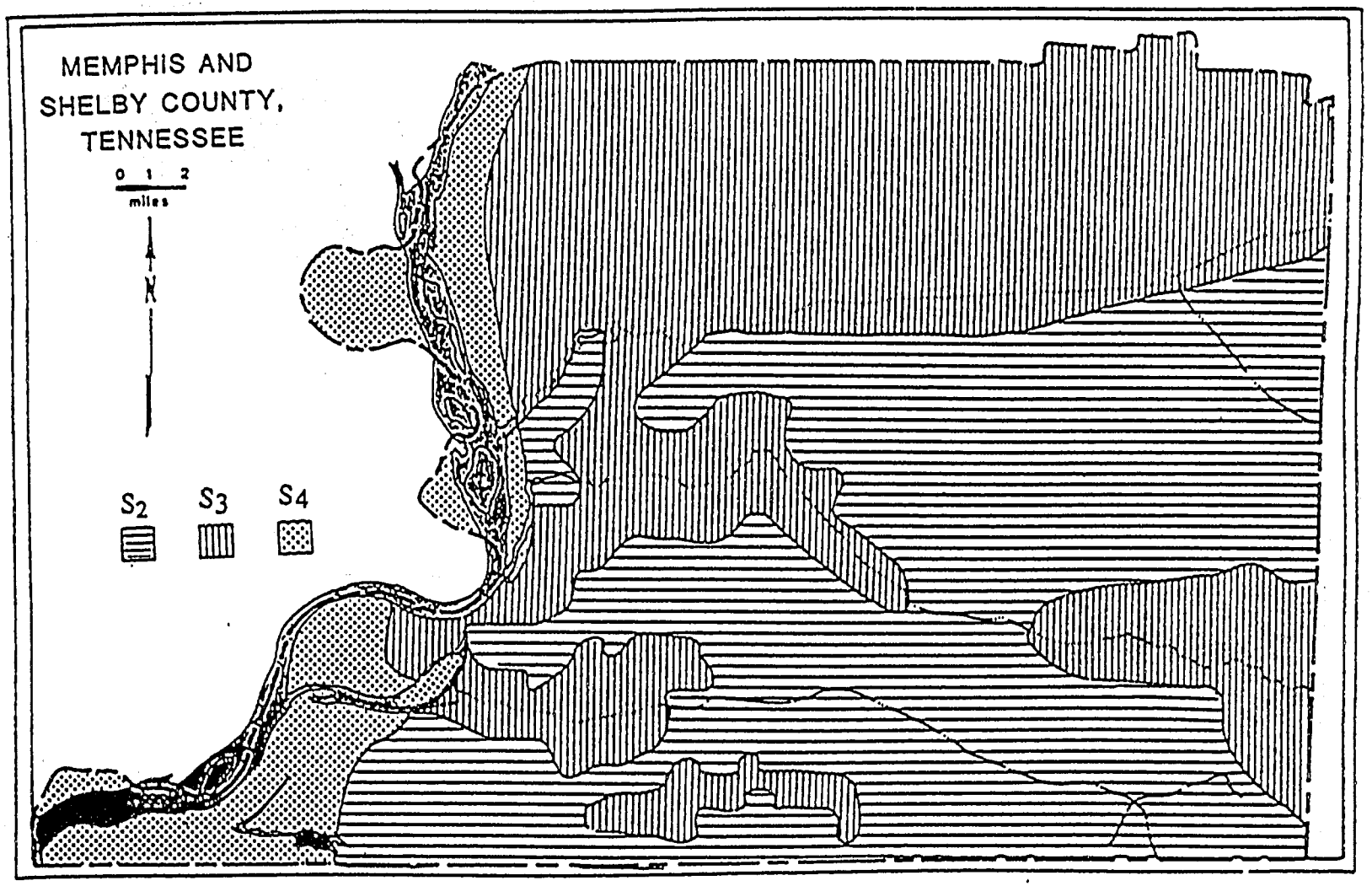


Figure 3. GIS Coverage of Soil-Profile Classification in Shelby County

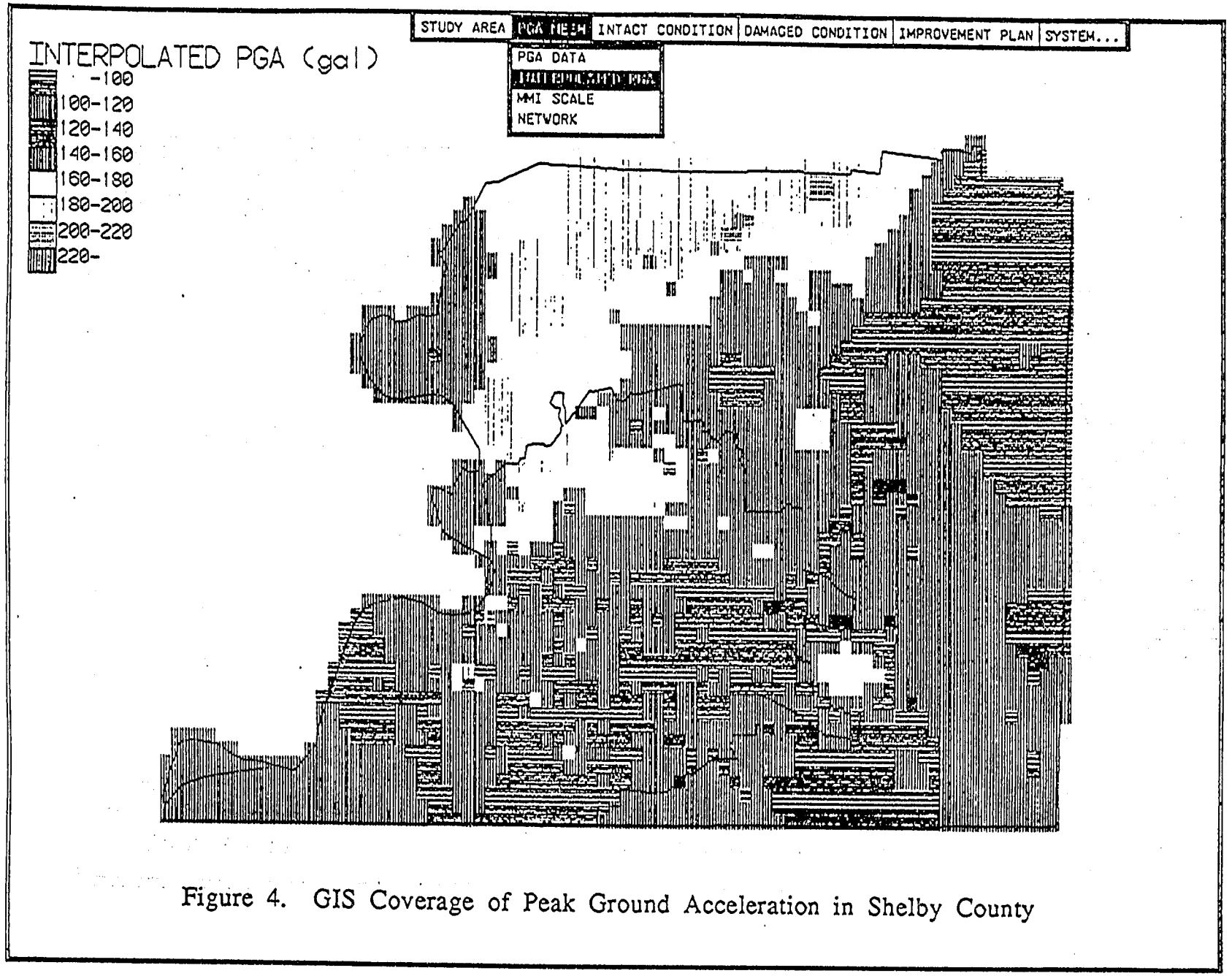


Figure 4. GIS Coverage of Peak Ground Acceleration in Shelby County

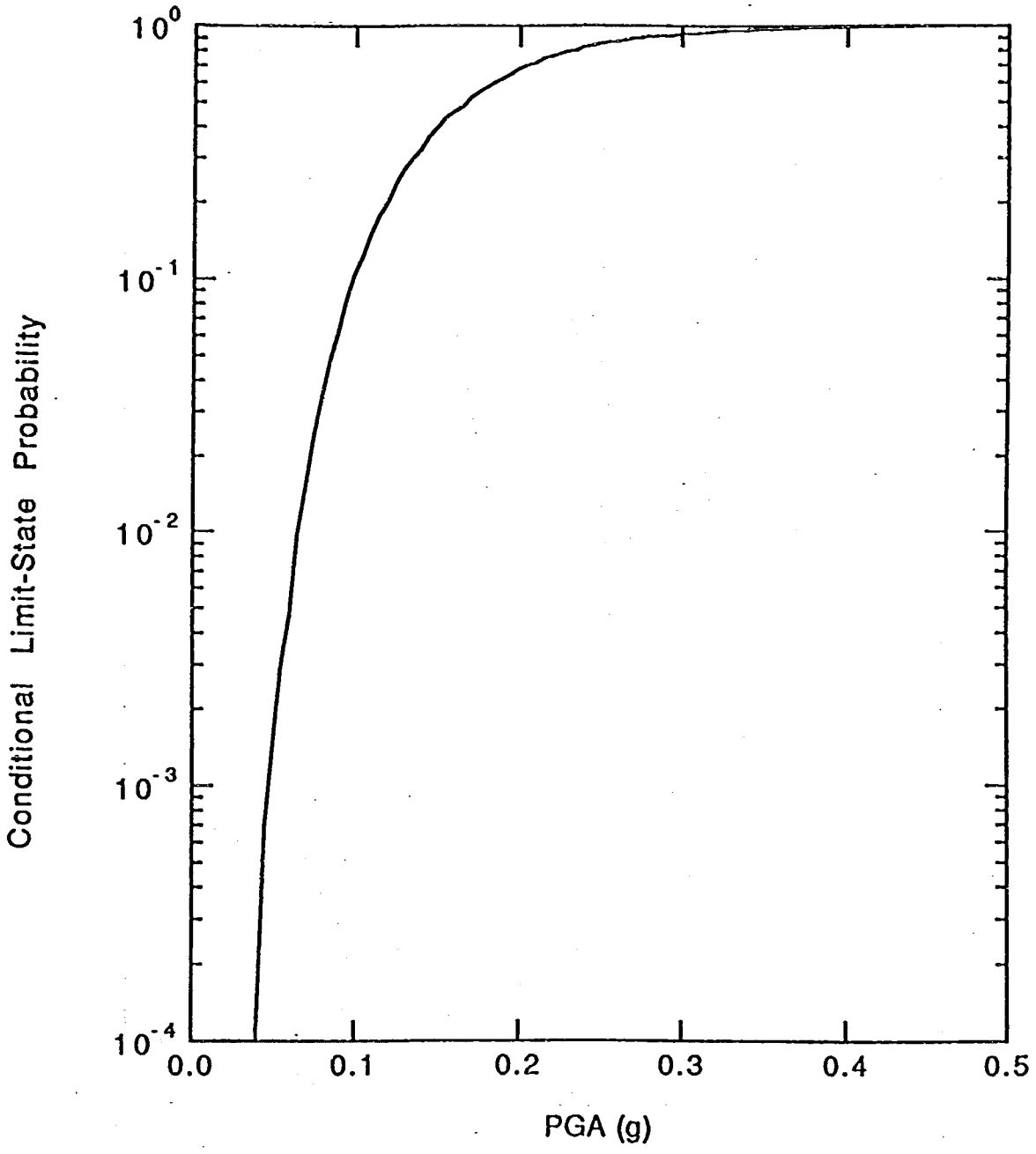


Figure 5. Fragility Curve of Sheahan Pumping Station

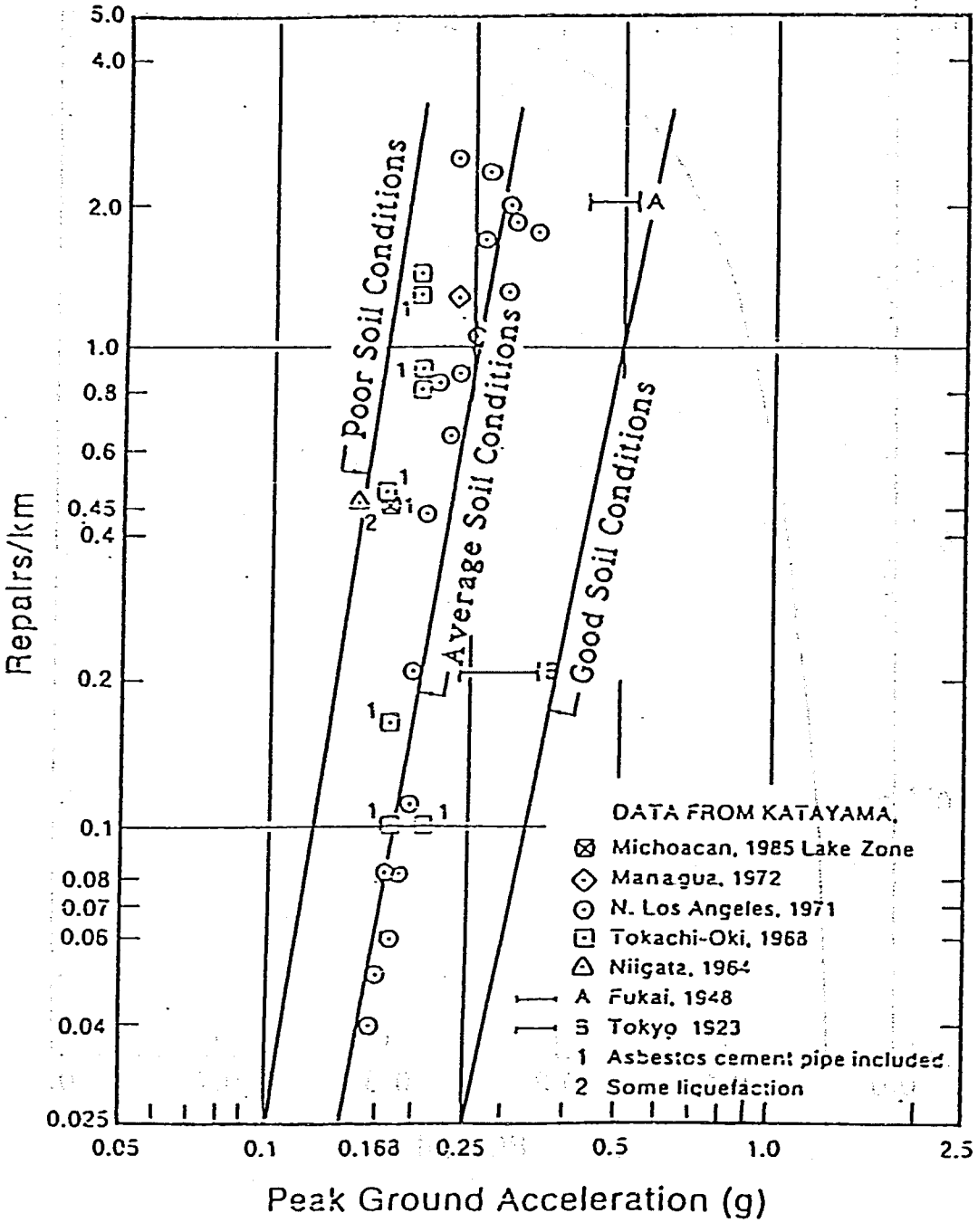
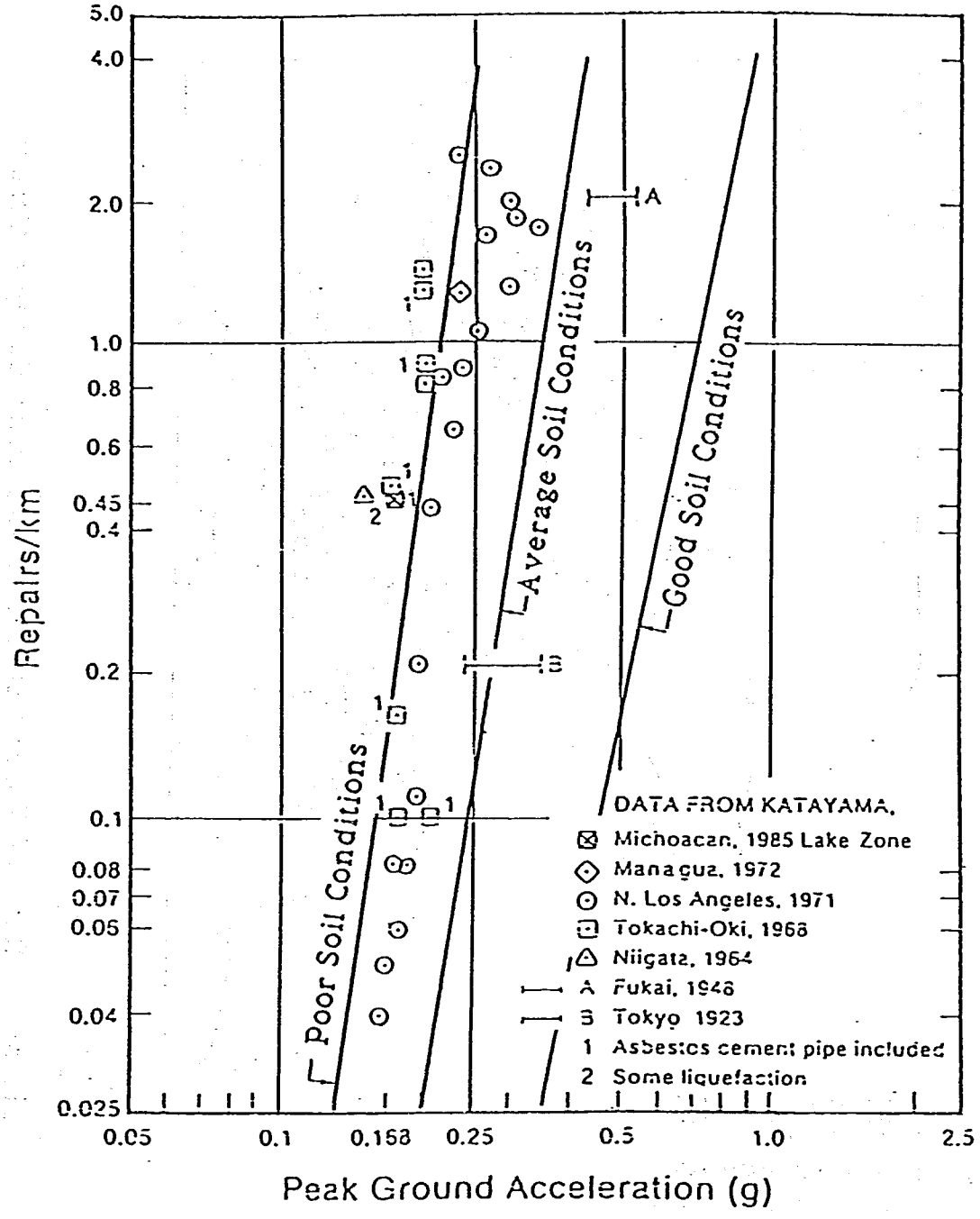


Figure 6. Pipe Break Rate for Cast Iron Pipe (after Katayama et al. 1975)



. Figure 7. Pipe Break Rate for Ductile Iron Pipe

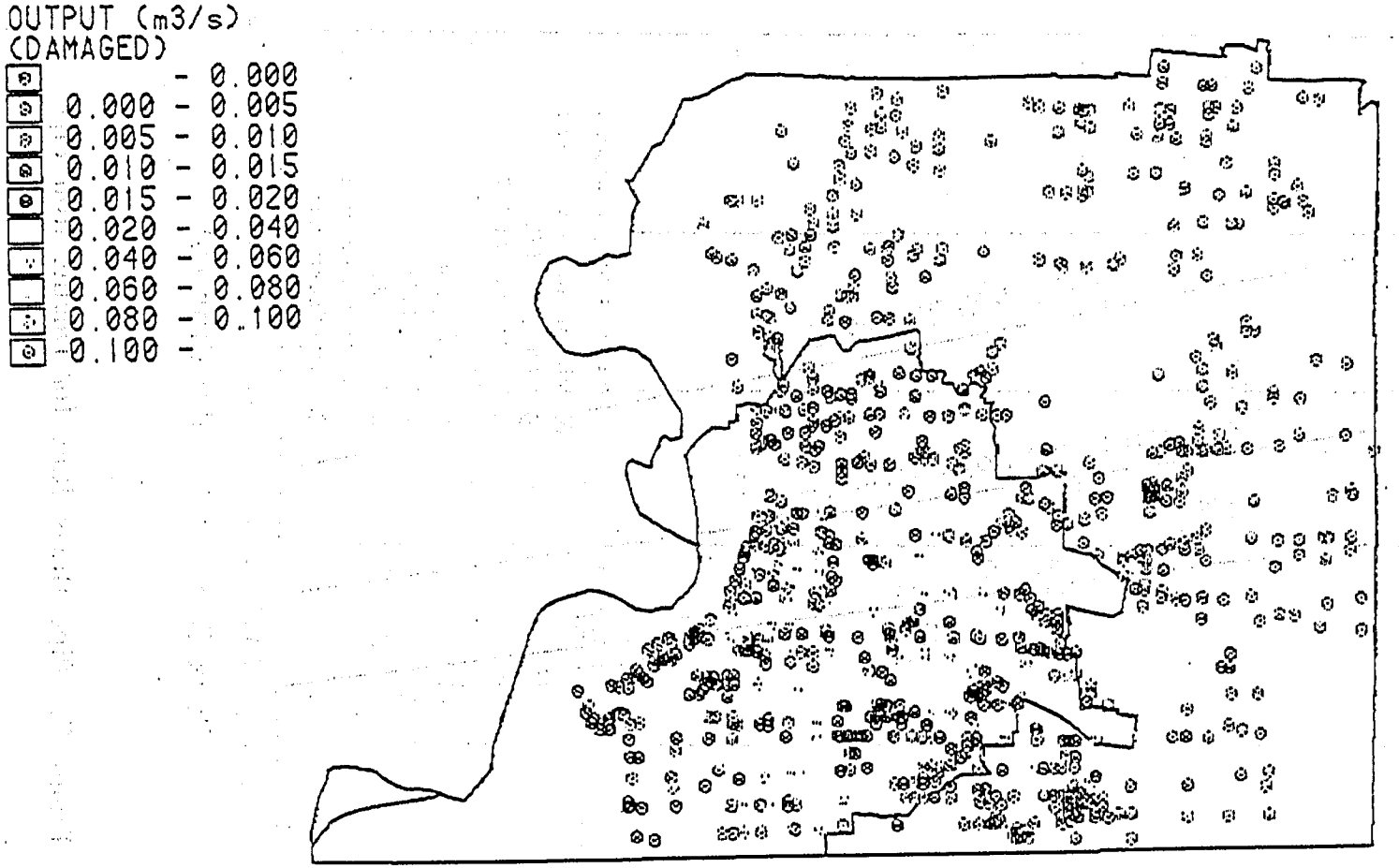


Figure 8. Ratio of Water Output at Nodes under Damaged Condition

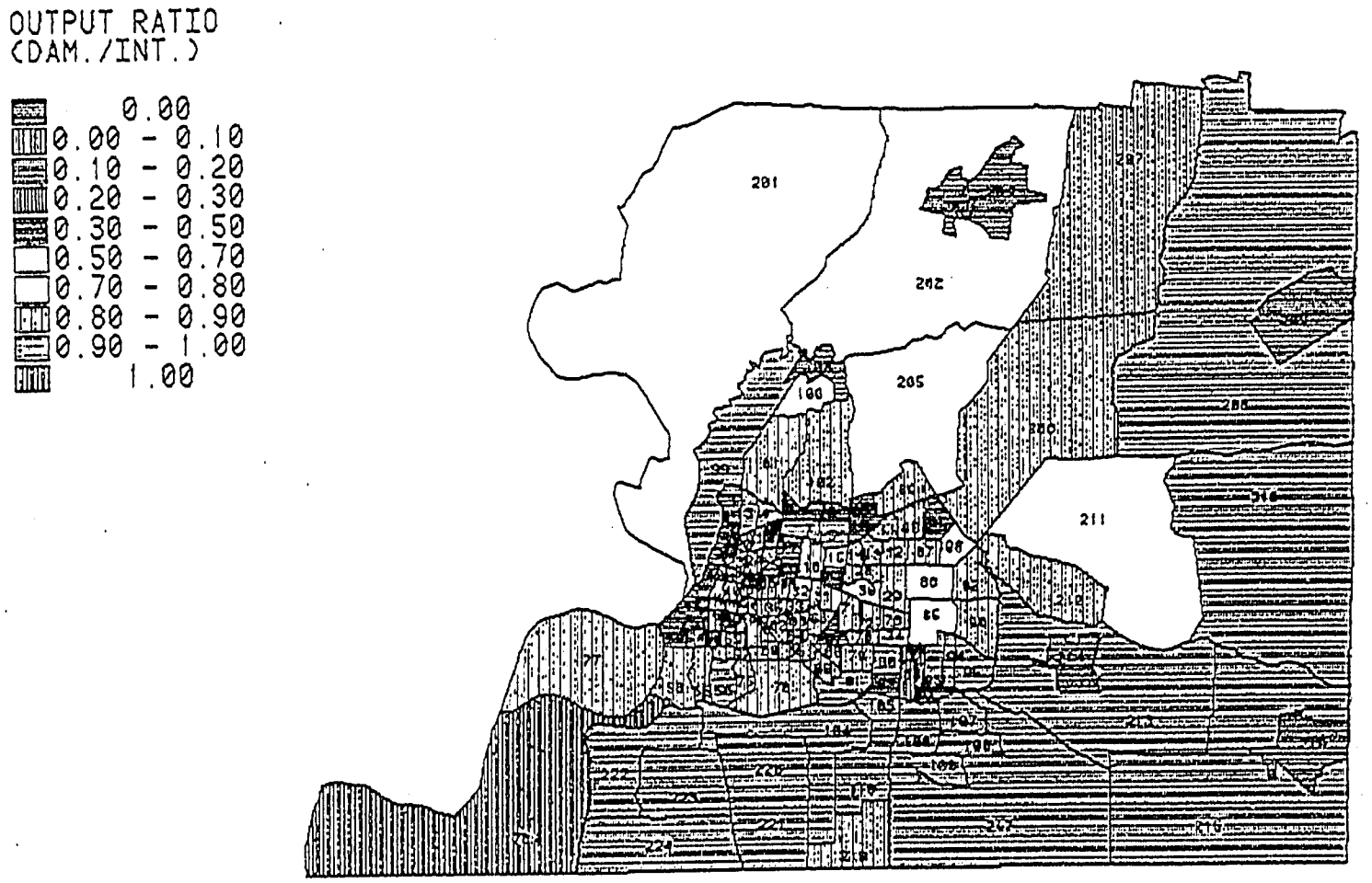


Figure 9. Ratio of Water Output in Census Tracts under Damaged Condition

Session-6

Seismic Design

J-11) Earthquake Response Analysis Method for Shield Tunnels
(Shiba, Y.)

J-12) A Seismic Design of a Large-in-Scale Shield Tunnel of Trans-Tokyo Bay Highway
(Uchida, K., Shioi, Y., Kudo, I. and Kuraishi,K.)

J-13) Design of Tama River and Kawasaki Fairway Tunnels in Expressway Bay-Shore Route
(Kubota, N., Egawa, S. and Tachibana, Y.)

J-14) Seismic Design Method of Underground Parking Garage Structures
(Kawashima, K., Sugita, H. and Nakajima, T.)

EARTHQUAKE RESPONSE ANALYSIS METHOD FOR SHIELD TUNNELS

Yukio Shiba

Research Engineer
Earthquake and Wind Engineering Group,
Technology Research Center, Taisei Corporation

ABSTRACT

Shield tunnels are the most popular and vital structures for lifeline facilities in Japan. This paper describes the method for earthquake response analysis of the shield tunnels. Firstly, it describes analysis method in the longitudinal direction. It presents the techniques for modeling of the tunnel, whose lining is longitudinally segmented into short rings, and performs seismic stress analysis under a sinusoidal ground displacement. Secondly, the paper describes analysis method in the cross-sectional direction. It presents an analytical model for cylindrical tunnel buried in simple ground. Then it gives approximate formulae for seismic stresses induced by the dynamic ground displacement. These formulae can be directly used in the seismic design.

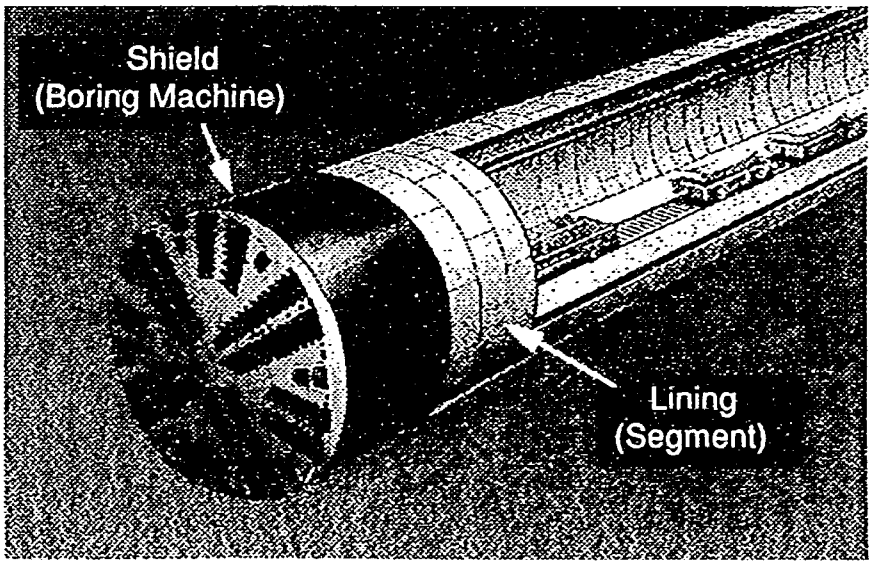


Fig. 1 Shield Tunneling Method

INTRODUCTION

In Japan, in recent years, a number of tunnels for urban lifeline facilities which include sewer trunk lines, power/communication pipelines, subways, trans-bay highway, etc., have been constructed by Shield Tunneling Method, as illustrated in **Fig.1**. The lining of the tunnel is usually cylindrical and is fabricated with lining members called "segments." Since the shield tunnels are vital structures supporting various urban functions and are usually constructed in soft ground, they are required to be safe against earthquakes both in the longitudinal and cross-sectional directions.

Typical structure of the tunnel lining is shown in **Fig.2**. The cylindrical lining is divided into segment-rings in the longitudinal direction, and a segment-ring is divided into segments as smaller pieces in the circumferential direction. This lining structure is the very peculiarity that distinguishes the shield tunnel from other types of tunnel and pipes, and makes it difficult to develop a practical seismic design procedure.

This paper describes the method for earthquake response analysis of the shield tunnels based on the research results obtained by the author and other colleagues.

ANALYSIS METHOD IN THE LONGITUDINAL DIRECTION

Loading Test on Tunnel Lining

In order to develop an analytical model of the shield tunnel, as well as to understand the finer points of its seismic design, it is necessary to investigate the deformation characteristics and failure mode of the tunnel lining. For this purpose, loading tests are performed on the lining.

As an example, **Photo 1** shows a loading test performed by PWRI. The model lining used for the test was a 4-ring model with 16 pieces of segments made of reinforced concrete. The outer diameter, thickness, and length of each ring are 1.8 m, 0.125 m, and 0.9 m, respectively. The model lining was subjected to alternate compressive/tensile load in the longitudinal direction.

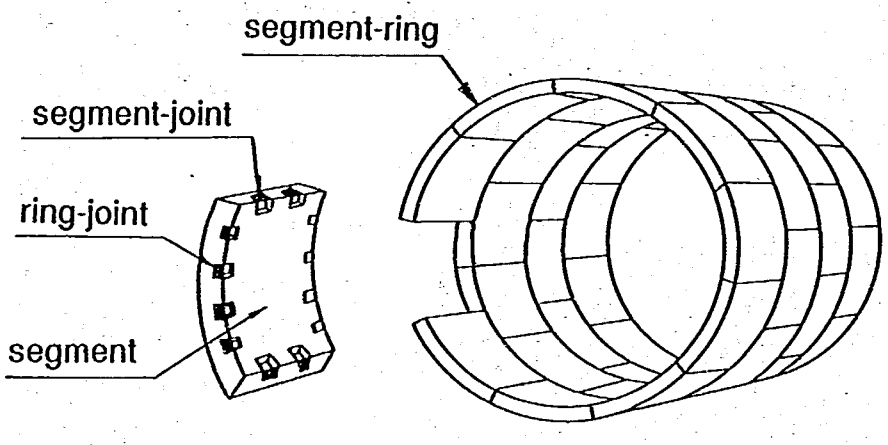


Fig. 2 Structure of Shield Tunnel Lining

The test results are summarized as follows:

1) The tensile stiffness of the model was very small in comparison with the compressive stiffness: the deformation of the model when subjected to tensile load was much larger compared with the deformation when subjected to the compressive load of the same magnitude.

2) Most of the tensile deformation of the model occurred at ring-joints, and segment-rings themselves were hardly deformed.

3) The final break of the model occurred at a certain joint section of segment-rings, where all ring-joints broke with their anchor bars having been cut as shown in **Photo 2.**

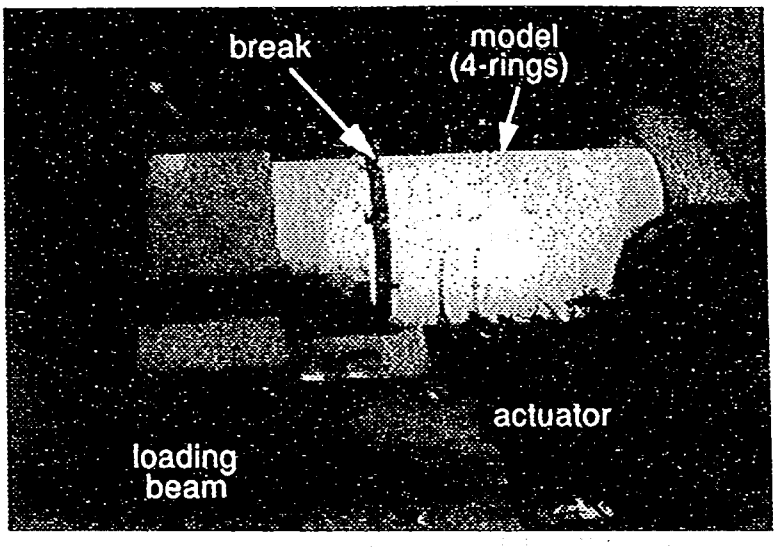


Photo 1 Loading Test on Model Tunnel

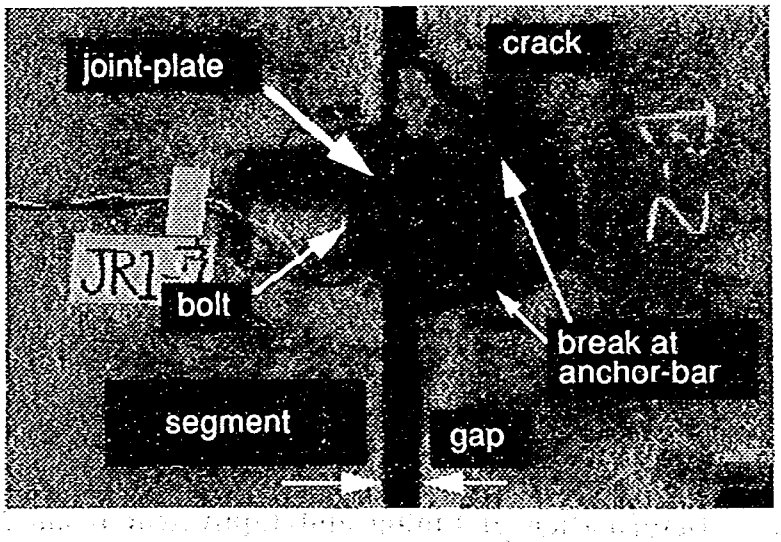


Photo 2 Breaking in a Ring-joint of the Model Tunnel

Modeling Technique

Since a shield tunnel consists of a succession of segment-rings, it suggests an analytical model consisting of a succession of beam and spring elements, which elements respectively model segment-rings and ring-joints. However, when we adopt the model for the analysis of a tunnel with the length of hundreds/thousands meters, we have to use at least hundreds/thousands of analytical elements to model the whole tunnel. So, it is necessary for practical design procedure to devise a more simple analytical model.

Fig.3 shows the "Equivalent Beam Model" which was developed as a simple model for the shield tunnel. In this model, the lining of a shield tunnel is modeled by a uniform beam, based on the idea that while the lining is divided into segment-rings, its behavior of deformation is macroscopically considered as that of a uniform beam, because the length of segment-ring is usually much smaller than its diameter.

Equivalent Stiffness of Tunnel Lining

When a uniform beam is substituted for the tunnel lining, the stiffness of the beam should be adequately determined taking into account the following characteristics of the lining deformation (see **Fig.3**):

1) Under compressive axial force, the lining is deformed due to the compression of segment-rings only; ring-joins are hardly compressed.
2) Under tensile axial force, the lining is deformed due to the tension of both segment-rings and ring-joints.
3) Under bending moment, the lining is bent due to the coupling of the tension of both segment-rings and ring-joints on the tensile stress side of the moment and the compression of segment-rings only on the compressive stress side.

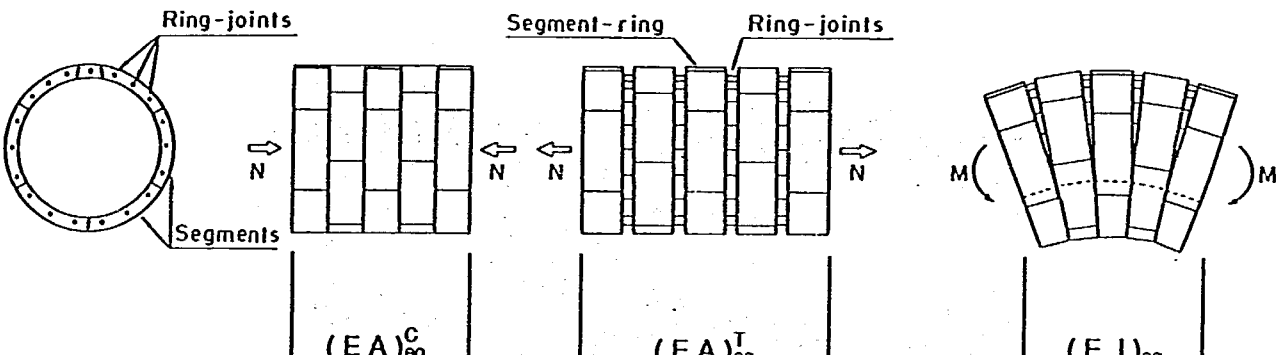


Fig. 3 Deformation of Lining and Equivalent Beam Model

"Equivalent stiffness", meaning the axial and bending stiffnesses assigned to the beam model which models the tunnel lining, is evaluated as discussed below.

Fig.4 shows the method of evaluating equivalent axial stiffness. A ring portion of length unity in which a joint is included is considered. This procedure is thought sufficient to represent the whole of tunnel.

When the tunnel is subjected to the compressive force N_C, the deformation δ_C of the portion is given by

$$\delta_C = \frac{N_C}{E_S A_S} l_S \tag{1}$$

where E_S = Young's modulus of the segment-ring;
A_S = cross-sectional area of the segment-ring;
l_S = length of the segment-ring.

On the other hand, when the equivalent beam with the axial stiffness $(EA)^C_{eq}$ is subjected to the same compressive force, the deformation δ_{eq} of the portion with length l_S is given by

$$\delta_{eq} = \frac{N_C}{(EA)^C_{eq}} l_S \tag{2}$$

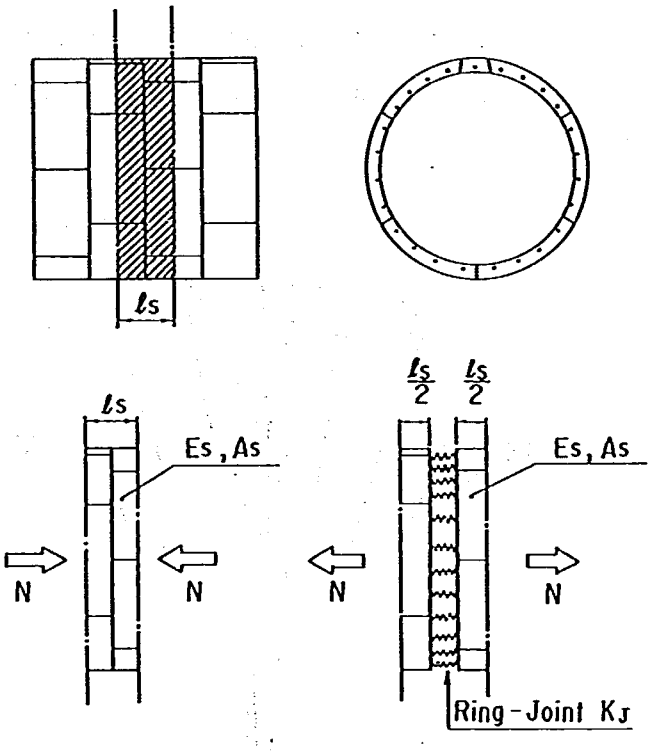


Fig. 4 Evaluation of Equivalent Axial Stiffness

Equating Eq.(2) to Eq.(1), the equivalent compressive stiffness of the lining $(EA)^{C}_{eq}$ is determined as

$$(EA)^{C}_{eq} = E_S A_S \tag{3}$$

Using the same procedure, the equivalent tensile stiffness of the lining $(EA)^{T}_{eq}$ can be determined. That is, when the portion in lining is subjected to the tensile force N_T, the tensile deformation δ_T is the sum of the deformations of a segment-ring and a joint, given by

$$\delta_T = \frac{N_T}{E_S A_S} l_S + \frac{N_T}{K_J} \tag{4}$$

where K_J = the tensile stiffness of joint section which can be evaluated by summing up the spring constants of all ring-joints on the section.

With the deformation of the equivalent beam expressed as in Eq.(2), the equivalent tensile stiffness of the lining, $(EA)^{T}_{eq}$, results in the following equation.

$$(EA)^{T}_{eq} = \frac{E_S A_S}{1 + \dfrac{E_S A_S}{l_S K_J}} \tag{5}$$

The method of evaluating the equivalent bending stiffness is shown in **Fig.5**. The stress-deformation condition of the portion with length l_S is considered here also. When the lining is subjected to bending moment M, the intersectional angle θ is formed between the two planes each of which passes through the center of the segment-ring. The parameter θ/l_S corresponds to the "curvature" in the beam theory.

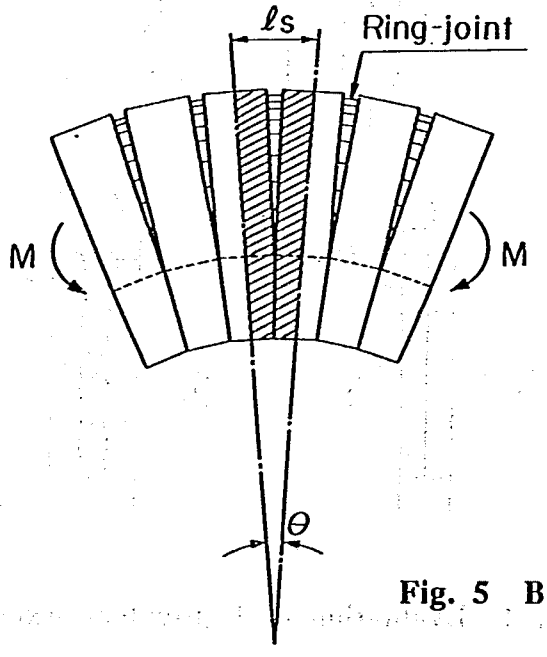


Fig. 5 Bending Deformation of Lining

The relationship between M and θ can be obtained by introducing the following assumptions.

1) At a joint section, the segment-ring only is deformed on the compression side, while both the segment-ring and the ring-joint are deformed on the tensile side.
2) The segment-ring and the ring-joint are deformed in proportion to the distance from the neutral axis.
3) The position of the neutral axis and the condition of stress in the segment-ring do not vary along the tunnel axis, because a segment-ring is short in comparison to its diameter.
4) The ring-joints discretely arranged on a bolt-circle are idealized as incompressive line-spring continuously distributed on the centroid circle of the segment-ring.

Fig.6 shows the stress-strain condition in the lining derived from the above assumptions. Thus, considering equilibrium condition and strain compatibility, the curvature θ/l_S of the lining is derived as the following equation.

$$\frac{\theta}{l_S} = \frac{\cos\phi + (\pi/2 + \phi)\sin\phi}{\cos^3\phi} \frac{M}{E_S I_S} \tag{6}$$

where I_S = moment of inertia of the cross section of the lining; $\phi = \sin^{-1}(x/R)$ = position angle of the neutral axis, which is the solution of the following equation:

$$\phi + \cot\phi = \pi\left(\frac{1}{2} + \frac{l_S K_J}{E_S A_S}\right) \tag{7}$$

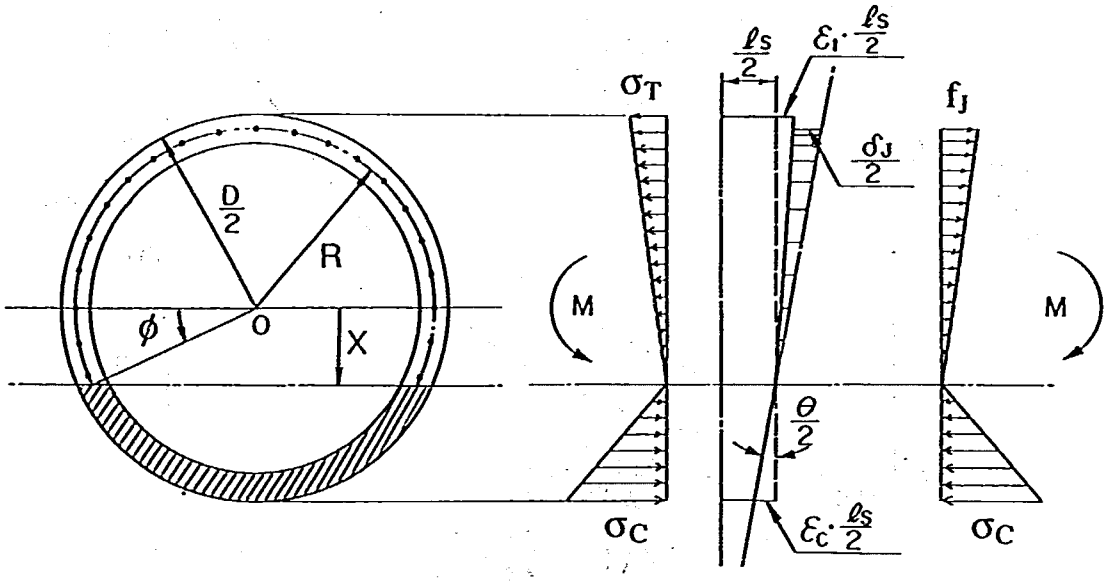


Fig. 6 Stress-Strain Condition in the Lining Subjected to Bending

Since the curvature of the equivalent beam with bending stiffness $(EI)_{eq}$ and subjected to bending moment M may be written as

$$\frac{\theta_{eq}}{l_S} = \frac{M}{(E\,I)_{eq}} \tag{8}$$

equating Eq.(8) to Eq.(6), the equivalent bending stiffness $(EI)_{eq}$ results in the following equation:

$$(E\,I)_{eq} = \frac{\cos^3\phi}{\cos\phi + (\pi/2 + \phi)\sin\phi} E_S\, I_S \tag{9}$$

Fig.7 shows the equivalent bending stiffness and the neutral axis position in relation to the tensile stiffness of the ring-joint, which are calculated by Eqs. (7) and (9).

In the above process, the stresses in the lining are also derived: i.e., the compressive stress, σ_C , and the tensile stress, σ_T , in segment-ring, and the tensile force, f_J , in the ring-joint outermost from the neutral axis are given by the following equations:

$$\sigma_C = \frac{M}{I_S} \frac{\cos\phi + (\pi/2 + \phi)\sin\phi}{\cos^3\phi} \left(\frac{D}{2} - x\right) \tag{10a}$$

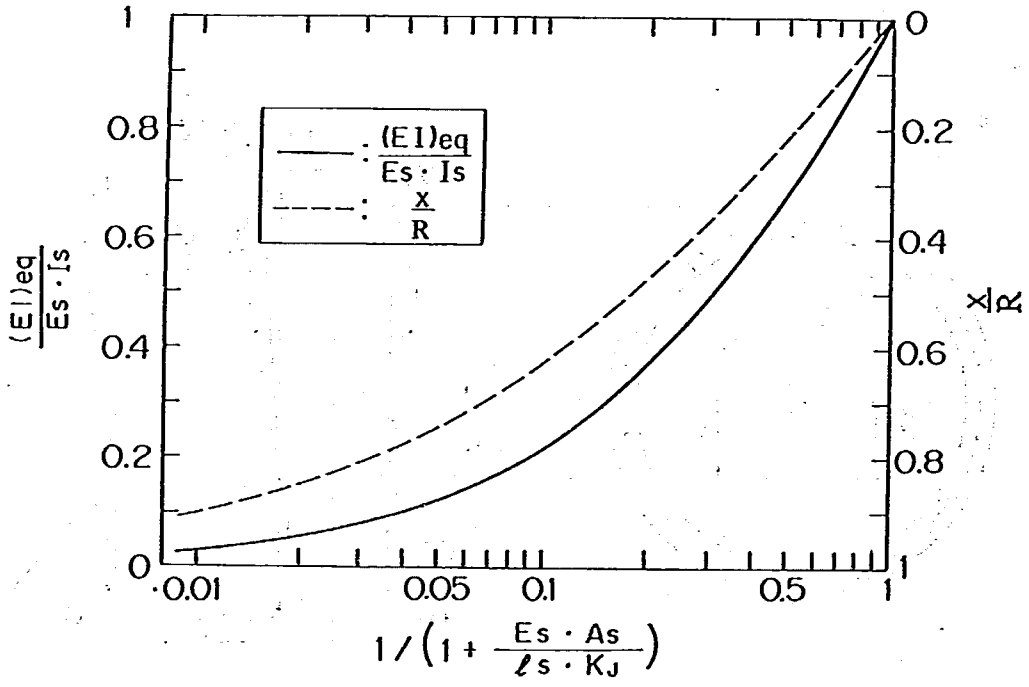


Fig. 7 Equivalent Bending Stiffness and Neutral Axis Position

$$\sigma_T = \frac{M}{I_S} \frac{\cos\phi - (\pi/2 - \phi)\sin\phi}{\cos^3\phi} \left(\frac{D}{2} + x\right) \tag{10b}$$

$$f_J = \frac{M l_S}{E_S I_S} \frac{\pi \sin\phi}{\cos^3\phi} (R + x)\, k_J \tag{10c}$$

where D = outer diameter of segment-ring; R = radius of centroid circle of segment-ring; x = position of neutral axis ($x = R\sin\phi$); and k_J = the tensile stiffness of a ring-joint.

Evaluation of Seismic Stresses due to Sinusoidal Ground Displacement

In this section, a practical calculation method of seismic stresses in a shield tunnel is presented.

Fig.8 shows a model for the analysis. The tunnel is assumed to be infinitely long and is subjected to sinusoidal ground displacement which expediently expresses the ground motion along the tunnel axis during an earthquake. The seismic stresses induced in the tunnel are analyzed using "Seismic Deformation Method" : in the method a tunnel-ground system is modeled as a beam on elastic support, and the support is statically deformed so as to correspond to the ground displacement. The beam as an analytical model for the tunnel is characterized by the equivalent stiffness evaluated in the previous section. The ground displacement as seismic force to the tunnel is regarded as the sinusoidal wave with amplitude U and wave length L.

At first, the evaluation method of bending moment induced in the tunnel is described. In this case, direction of the ground displacement is assumed to be perpendicular to the tunnel axis as shown in **Fig.8**. Displacement of the tunnel axis due to the ground displacement is governed by the following differential equation.

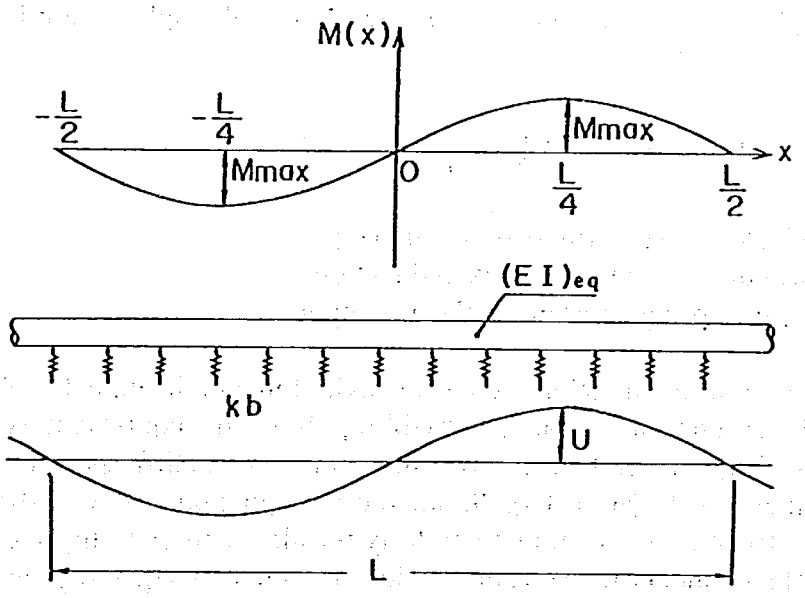


Fig. 8 Analytical Model for Evaluation of Bending Moment

$$(E\,I)_{eq}\frac{d^4 v}{d x^4} + k_b v = k_b U \sin\left(2\pi\frac{x}{L}\right) \tag{11}$$

where $(E\,I)_{eq}$ = equivalent bending stiffness of the tunnel ;
v = tunnel displacement in the direction perpendicular to its axis ;
k_b = normal spring constant of elastic support ;
x = distance along the tunnel axis.

Tunnel displacement v is obtained by solving the differential equation (11), which can be easily solved under the assumption of the beam's being infinitely long. Derived from the tunnel displacement, the maximum bending moment induced in the tunnel thus results in the following.

$$M_{max} = \alpha_M \frac{4\pi^2 U}{L^2}(E\,I)_{eq} \tag{12}$$

where

$$\alpha_M = \frac{1}{1 + (2\pi/\lambda_M L)^4} \qquad \lambda_M = \sqrt[4]{\frac{k_b}{(E\,I)_{eq}}} \tag{13}$$

Substituting M_{max} of Eq.(12) for M in Eq.(10), maximum stresses in the tunnel lining can be evaluated.

Next, the method for evaluating the axial force induced in the tunnel is described. Note that if ground displacement is either perpendicular or parallel to the tunnel axis, no axial force is induced in the tunnel. Therefore, the direction of ground displacement is assumed to be inclined to the tunnel axis; the amplitude and the wave length of ground displacement then apparently vary with the inclination: for example, if the inclination is 45 degree, the apparent amplitude and wave length are $U'=U/\sqrt{2}$ and $L'=\sqrt{2}L$, respectively.

Thus, the displacement of the tunnel axis due to ground displacement is expressed by the following differential equation:

$$(EA)_{eq}\frac{d^2 u}{d x^2} - k_a u = -k_a U' \sin\left(2\pi\frac{x}{L'}\right) \tag{14}$$

where $(EA)_{eq}$ = equivalent axial stiffness of the tunnel ;
u = tunnel displacement in the axial direction ;
k_a = shearing spring constant of elastic support.

The displacement of the tunnel as well as the axial force in the tunnel is obtained by solving Eq.(14) which includes a nonlinear parameter $(EA)_{eq}$. Since the equivalent axial stiffness of the shield tunnel has nonlinearity in the sense that the compressive stiffness and the tensile stiffness differ from each other, as shown in **Fig.9**, one must assign compressive stiffness to the section where compressive force is induced, and similarly tensile stiffness to the section where tensile force is induced. The boundary between the sections is a unknown quantity, and is determined by solving the following equation:

$$\frac{2\pi}{\lambda_T L'}\alpha_T \tanh(\lambda_T \eta) + \frac{2\pi}{\lambda_C L'}\alpha_C \tanh\left\{\lambda_C\left(\frac{L'}{2}-\eta\right)\right\} = (\alpha_T - \alpha_C)\tan\left(2\pi\frac{\eta}{L'}\right) \tag{15}$$

where η = position of the boundary ;

$$\alpha_T = \frac{1}{1 + (2\pi/\lambda_T L')^2} \qquad \alpha_C = \frac{1}{1 + (2\pi/\lambda_C L')^2}$$

$$\lambda_T = \sqrt{\frac{k_a}{(EA)^T_{eq}}} \qquad \lambda_C = \sqrt{\frac{k_a}{(EA)^C_{eq}}} \tag{16}$$

The solution of η is in the range of 0 to L'/4, while η = L'/4 in case of the ordinary tunnel with linear axial stiffness.

The displacement and the axial force of the tunnel are then solved for each of the two sections, and the maximum axial forces induced in the tunnel result in the followings.

$$\left.\begin{matrix} N_{Tmax} \\ N_{Cmax} \end{matrix}\right\} = \alpha_C \frac{2\pi U'}{L'}(EA)^C_{eq}\left\{\begin{matrix} \beta_T \\ \beta_C \end{matrix}\right. \tag{17}$$

where N_{Tmax} = maximum tensile force ; N_{Cmax} = maximum compressive force ;

$$\beta_T = \frac{(EA)^T_{eq}}{(EA)^C_{eq}}\frac{\alpha_T}{\alpha_C}\left\{1 - \frac{\cos(2\pi\eta/L')}{\cosh(\lambda_T \eta)}\right\} \tag{18a}$$

$$\beta_C = 1 + \frac{\cos(2\pi\eta/L')}{\cosh\left\{\lambda_C(L'/2 - \eta)\right\}} \tag{18b}$$

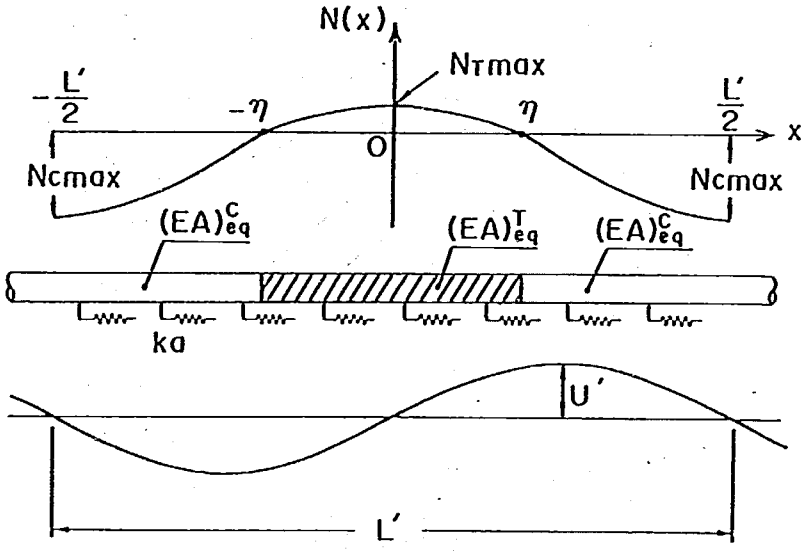


Fig. 9 Analytical Model for Evaluation of Axial Force

If the lining of the shield tunnel were a jointless tube, not divided into segment-rings, then the axial stiffness of the tube, EsAs, would be equal to equivalent compressive stiffness $(EA)^C_{eq}$, and the maximum axial force could be written by the following equation:

$$N_{Tmax} = N_{Cmax} = \alpha_C \frac{2\pi U'}{L'} (EA)^C_{eq} \qquad (19)$$

The coefficients β_T and β_C in Eq.(17), therefore, express the influence of the existence of ring-joint on axial forces responses. **Fig.10** shows β_T and β_C versus the dimensionless parameter $\lambda_C L'$, based on Eqs.(15), (16), and (18).

Dynamic Response Analysis Method

In the case when structural or geological condition of surrounding ground along the tunnel is complicated, and when the ground displacement can not be expressed by a simple sinusoidal wave, another analysis method is needed which takes the ground condition into consideration.

Fig.11 shows the analytical model available for such case. The model is based on the one which has generally been used for the analyses of submerged tunnels, pipelines, etc., and consists of two principal parts; one is the dynamic analysis model of surrounding ground, and the other is the equivalent beam model for shield tunnel. The two parts are connected by spring elements which express soil-structure interaction (correspond to elastic support in the above simple analysis method). It is peculiar to the analysis of shield tunnel that time-domain nonlinear analysis is required for the response analysis in the direction of tunnel axis because of the nonlinearity in axial stiffness of the equivalent beam.

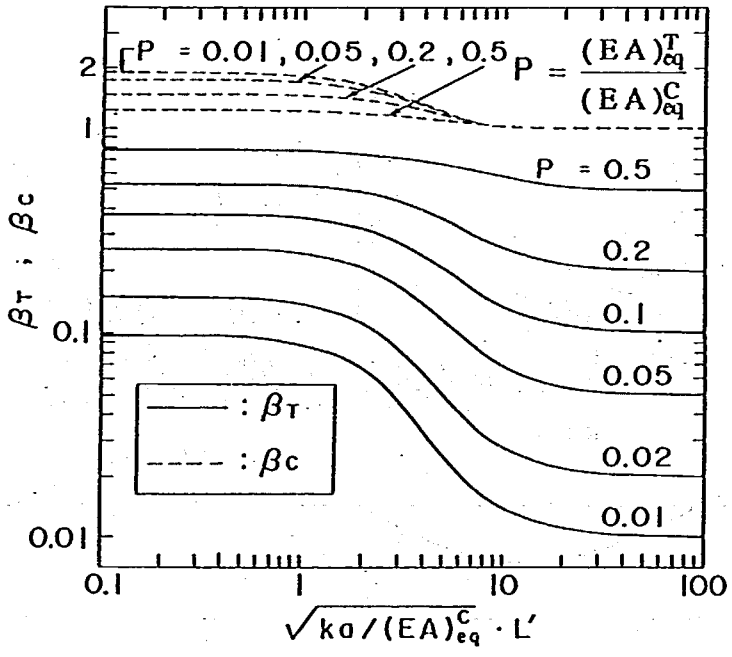


Fig.10 Coefficients β_T and β_C

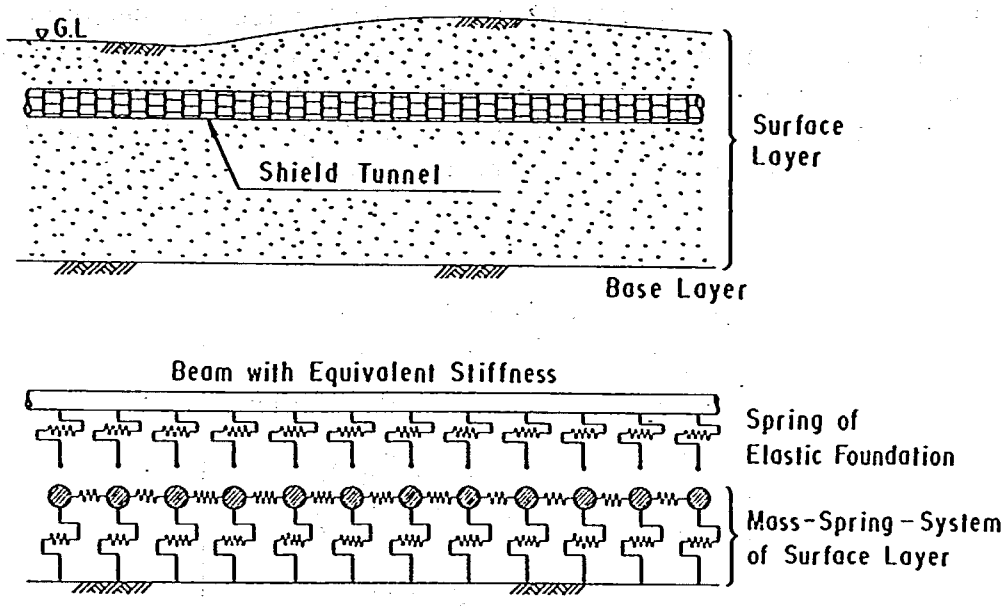


Fig.11 Dynamic Response Analysis Model of Tunnel-ground System

ANALYSIS METHOD IN THE CROSS-SECTIONAL DIRECTION

Object of Analysis

The earthquake response analysis method for the cross section of a cylindrical shield tunnel is presented in this chapter. The object here is shown in **Fig.12**. The surrounding ground consists of two layers; a homogeneous soft surface layer with thickness H_g and a rigid base layer. The shield tunnel is buried with its center being at depth H.

The ground condition is assumed to be rather simple, so that the simple analysis method presented in the following section can be applied. In the case of complicated ground condition, more complex analysis method such as a 2-D Finite Element Method should be employed.

Analytical Model

Fig.13 shows the analytical model of the tunnel-ground system. While divided into some segments in the circumferential direction, the tunnel lining is modeled as an uniform ring with unit length along the tunnel axis, taking the influence of the division and segment-joints into consideration in the same manner as is generally performed in static analyses. The interaction spring, which expresses interaction effect between the tunnel and the surrounding ground, is distributed in the normal and tangential directions of the ring continuously. The interaction spring used in this model is not of the Winkler type but of the coupled type, which mutually acts on the normal and tangential directions, and the spring constant of which varies according to the deformation mode of the tunnel.

The ring-on-elastic-support model is subjected to two seismic forces; ground displacement

and ground stress. As shown in **Fig.13**, these seismic forces are determined from the earthquake-induced displacement and shearing stress at the position of tunnel-ground interface in free-field ground where no tunnel exists. According to the technique of "Substructure Method", the ground displacement acts on the ring through the interaction spring, and the ground stress acts directly on the ring, the both being decomposed into normal and tangential components.

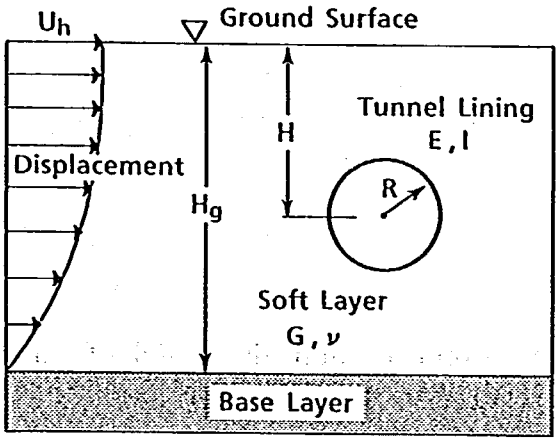


Fig.12 Cross Section Subjected to Lateral Ground Displacement

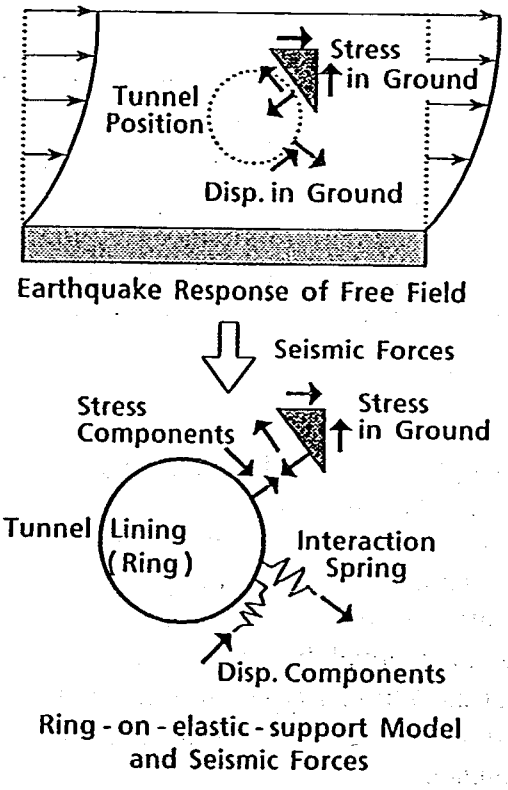


Fig.13 Analytical Model of Cross Section of Shield Tunnel

Seismic Stresses Induced in Tunnel Lining

If the following assumptions are introduced into the analytical model, then the seismic stresses induced in the tunnel lining can be described in the form of mathematical formulae.

1) The surface layer oscillates in fundamental vibration mode.
2) The influence of inertia force of the lining is negligibly small.
3) The nonlinear characteristics of soil is not taken into consideration.
4) The depth of tunnel crown is larger than the diameter of the tunnel, and the tunnel invert is not close to the rigid base layer.

With the above assumptions, solving the differential equation that describes the stress-strain relationship of a ring leads to writing the seismic stresses induced in the tunnel lining in the form of Fourier series which includes the first kind of Bessel function. Although the seismic stresses calculated by this solution are comparable to those by 2-D Finite Element Method, a more simple expression is desirable for the structure design practice. So by making approximation with regard to the exact solution, approximate formulae to calculate the seismic stresses are derived, as in the following simple form:

$$M = -\frac{3 E_S I_B}{R} \gamma C \sin 2\theta \tag{20a}$$

$$Q = -\frac{6 E_S I_B}{R^2} \gamma C \cos 2\theta \tag{20b}$$

$$N = -\frac{6 E_S I_B}{R^2} \left(1 + \frac{G R^3}{6 E_S I_B} \right) \gamma C \sin 2\theta \tag{20c}$$

where

$$C = \frac{4 (1 - \nu) G R^3}{(3 - 2\nu) G R^3 + 6 (3 - 4\nu) E_S I_B} \tag{21a}$$

$$\gamma = \frac{\pi U_h}{2 H_g} \sin \left(\frac{\pi H}{2 H_g} \right) \tag{21b}$$

M, Q, N = respectively, bending moment, shearing force, and normal force induced in the tunnel lining when the ground surface moves toward the right, as shown in **Fig.12**; positive directions of the stresses are shown in **Fig.14**;

θ = angle clockwise from crown of the tunnel;
E_S = Young's modulus of the segment-ring;
I_B = moment of inertia of the curved beam;
R = radius of centroid circle of the segment-ring;
G = shear modulus of the surface layer;
ν = Poisson's ratio of the surface layer;
H_g = thickness of the surface layer;
H = depth of the tunnel center;
U_h = amplitude of the ground displacement at the surface.

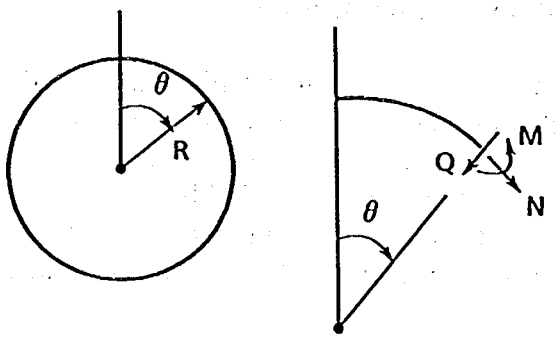


Fig.14 Coordinate System of Ring

The γ given by Eq.(21b) represents the magnitude of shearing strain induced at the tunnel center depth in the free-field ground which oscillates in the fundamental vibration mode. The seismic stresses, consequently, are induced in proportion to the shearing strain in the surrounding ground.

Since Eq.(20) to (21) are derived as approximate formulae for the exact solution, the seismic stresses calculated by the formulae, as a matter of course, include some error. According to the detailed comparison between the formulae and the exact ones, the approximate formulae tend to underestimate the seismic stresses by at the most 20% of the exact solutions. Therefore, it is recommended that the seismic stresses calculated by the above equation should be multiplied by 1.2 to 1.3 so as to be on the safe side in the seismic design.

CONCLUSIONS

Earthquake response analysis method for shield tunnels was described in this paper. The method is summarized as follows.

1) As for the response analysis in the longitudinal direction, tunnel-ground system is modeled by an equivalent-beam on elastic support. The equivalent beam is a uniform beam for which the longitudinal stiffness is determined to be equivalent to that of the tunnel lining. The seismic stresses induced in the tunnel are analyzed by statically deforming the elastic support so as to correspond to ground displacement along the tunnel axis, and are formulated for the case that the mode shape of the ground displacement is sinusoidal.

2) As for the response analysis in the cross-sectional direction, tunnel-ground system is modeled by a ring on elastic support. Seismic forces which the model is subjected to are ground displacement and ground stress. For the case that a surface layer oscillates in the fundamental vibration mode, approximate formulae as well as exact ones to calculate the seismic stresses induced in the tunnel are formulated.

The methods described here are scheduled to be adopted into the guideline for seismic design of shield tunnels. The methods are required to be confirmed through sufficient number of earthquake experience in many real shield tunnels.

ACKNOWLEDGEMENT

A part of this paper is the result of the studies carried out as "Cooperative Research in Development of Seismic Design of Underground Structures." The author expresses his sincere appreciation to the cooperative research members.

The author thanks Dr. Kazuhiko Kawashima of Public Works Research Institute for allowing to use the photographs of loading test on shield tunnel performed by PWRI.

REFERENCES

1) Shiba, Y., Kawashima, K., Obinata, N., and Kano, T., "An Evaluation Method of Longitudinal Stiffness of Shield Tunnel Linings for Application to Seismic Response Analyses", Proceedings of JSCE, Vol. 398, pp. 319-327, 1988, (in Japanese).

2) Shiba, Y., Kawashima, K., Obinata, N., and Kano, T., "Evaluation Procedure for Seismic Stress Developed in Shield Tunnels Based on Seismic Deformation Method", Proceedings of JSCE, Vol. 404, pp. 385-394, 1989, (in Japanese).

3) Shiba, Y., and Okamoto, S., "A Proposal of Practical Earthquake Response Analysis Method of Cylindrical Tunnels in Soft Ground", Proceedings of the 4th U.S.-Japan Workshop On Earthquake Disaster Prevention For Lifeline Systems, Los Angeles, August 19-21, 1991.

A SEISMIC DESIGN OF A LARGE-IN-SCALE SHIELD TUNNEL OF TRANS-TOKYO BAY HIGHWAY

Keinosuke Uchida[1], Yukitake Shioi[2], Izumi Kudo[3], Kenji Kuraishi[4]

1) Director, Trans-Tokyo Bay Highway Corporation
2) General Manager, Design and Engeneering Dept., ditto
3) Manager, Design and Engeneering Dept., ditto
4) Design and Engeneering Dept., ditto

ABSTRACT

As the first phase of an ambitious plan to connect Kawasaki and Chiba directly crossing the Tokyo Bay over a 15km distance, the Trans-Tokyo Bay Highway project was approved by the Government to proceed with a participation of private sector. The Trans-Tokyo Bay Highway Corporation was established on Octover 1, 1986, and is responsible for the financing, design and construction. The paper introduces the design and engineering of the large bore tunnel lining system of the two-10km long slurry shield tunnels.

INTRODUCTION

The Trans-Tokyo Bay Highway will be a toll road extending about 15km to cross the center of Tokyo Bay and linking Kawasaki in Kanagawa with Kisarazu in Chiba. The plans call firstly for approximately 10km of highway in tunnels under Kawasaki waters where surface traffic is heavy, and the remaining 5km over the Kisarazu waters which have relatively sparse surface traffic and shallow depth to be a bridge structure.

The Trans-Tokyo Bay Highway Corporation was established on Oct. 1, 1986 as a private sector body to undertake the financing, engineering and construction. Construction has been in progress since May 27, 1989.

It is planned that the undersea tunnel will be constructed using a slurry shield tunneling method. However in the engineering and design, the following peculiar conditions need to be adequately considered and taken into account:

a) The external diameter of the primary lining is approximately 14m, much larger than any experienced so far.

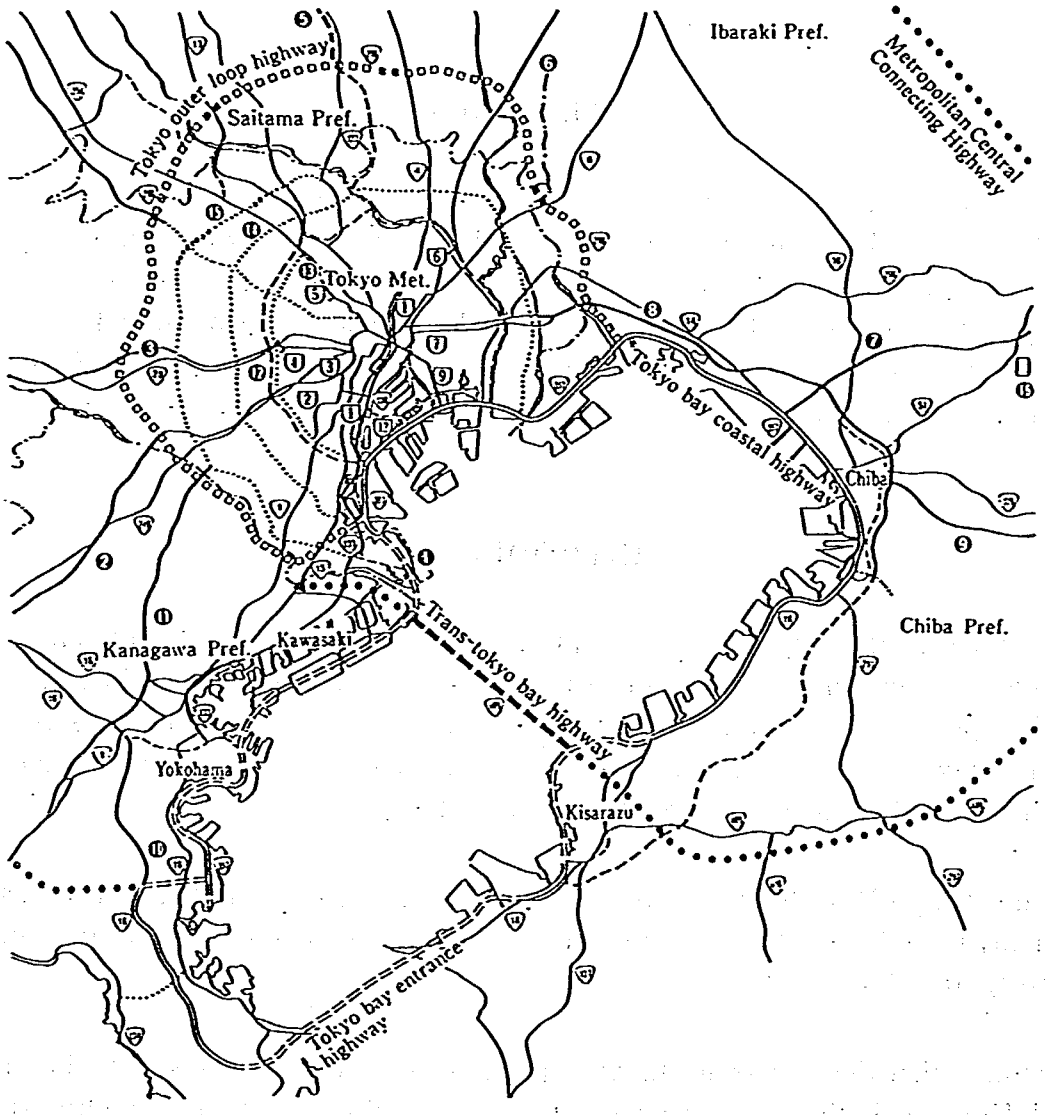
b) It is to be built in extremely soft ground under the sea.

c) It will be subjected to extremely high water pressure.

d) There is a high probability of the tunnel being affected by earthquakes.

Consequently, there were many areas where conventional design procedures were not appropriate. In view of this, extensive technical studies through various tests and numerical analysis were carried out, and the results were reflected in the detailed design.

This paper outlines those tests related to the aseismic design of the tunnel and describes how the results from those tests have been utilized to improve the detailed design.



Legend :

- Tokyo bay coastal highway
- Tokyo outer loop highway
- Metropolitan central connecting highway
- Metropolitan expressway
- Expressway & Toll roads
- National highways
- Principal local roads

❶Tokyo international airport (Haneda)
❷Tomei expressway
❸Chuo expressway
❹Kan-etsu expressway
❺Tohoku expressway
❻Joban expressway
❼Higashi kanto expressway
❽Keiyo highway

❾Chiba-togane highway
❿Yokohama-yokosuka highway
⓫Third-keihin highway
⓬Central loop route
⓭Loop No.6
⓮Loop No.7
⓯Loop No.8
⓰New tokyo international airport (Narita)

Fig. 1 Metropolitan Highway Network

PROJECT OUTLINE

a) Road Name : Trans-Tokyo Bay Highway

b) Route Name : National Highway No.409

c) Work Area : Ukishima, Kawasaki, Kanagawa-Nakashima, Kisarazu, Chiba

d) Length : 15.1km

e) Carriageway : Dual 2-lane (triple 2-lane in the future)

f) Design speed : 80 kph

g) Design Load : TL-20t and TT-43t

h) Road structure : Tunnels, bridge and man-made islands

i) Project Cost : Approx. ¥1,150 billion

j) Work Schedule : About 10 years starting from fiscal 1986

k) Traffic forecast : 33,000 veh/day in the opening year (64,000 veh/day 20 years later)

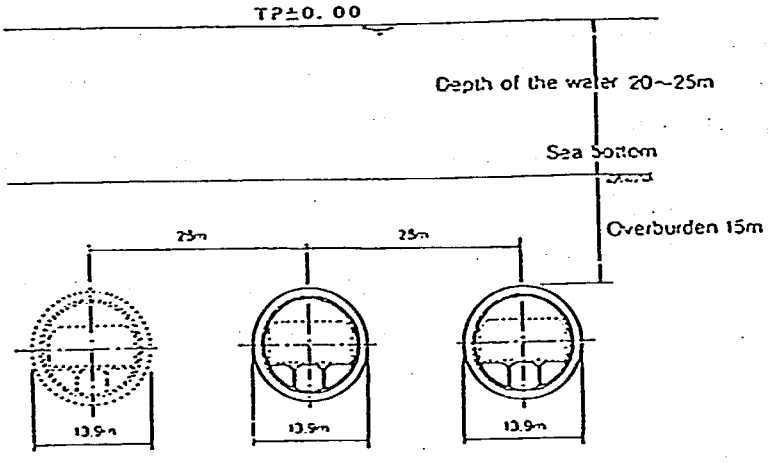


Fig. 2 Tunnel conceptual plan

NATURAL AND SOCIAL CONDITIONS

TOPOGRAPHICAL AND GEOTECHNICAL ASPECTS (See Fig.3)

The seabed along the planned road route forms a very gentle ship-bottom-like shape with a maximum water depth of about 30m in the midsection. From Ukishima on the Kawasaki side to the bay center, there exist very soft alluvial clayey soils of 20-30m thickness. On the Kisarazu side relatively compact sandy soils are thickly deposited.

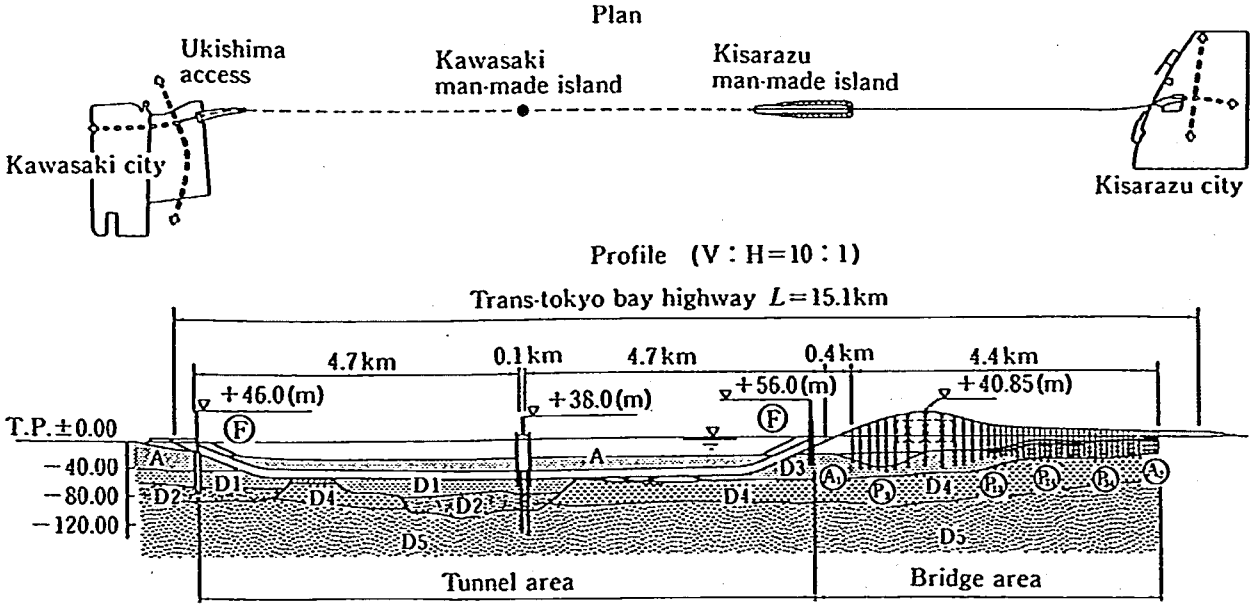


Fig. 3 Highway Plan and Profile

The soil properties at the tunnel face are as follows. On the Kawasaki side the upper half of the tunnel runs through alluvial deposits and the lower half diluvial deposits. On the Kisarazu side, the entire tunnel runs through diluvial deposits. The alluvial soils were deposited about 10,000 years ago and have a high plasticity index of 60-100, and a low unconfined compressive strength of 0.2-0.4kgf/cm^2. The diluvial deposits consist of alternating layers of relatively compact sandy soils and clayey soils. The slope sections on both the Ukishima and Kisarazu sides are man-made embankment fill with unconfined compressive strength of 6-30kgf/cm^2. From the design viewpoint, the geological foundation is considered to be diluvial soils lying beneath the road continuously with a depth of TP-80 to -90m and SPT of over 70.

EARTHQUAKES

Seismic activities are continuously experienced in the Tokyo Bay area. In the period from 818 to 1867 it is thought that 32 major earthquakes occurred. From 1868 to date, 23 earthquakes causing major damage have been experienced. Some were very large, typified by the Great Kanto Earthquake in 1923.

LINING STRUCTURE (See Fig.4)

The tunnel is lined by a 65cm thick primary lining of 11 equally divided precast RC segments and a 35cm thick secondary lining of in situ RC. The primary lining is so designed that it can withstand all loads. On the other hand, the function of the secondary lining is weight supplement to create resistance against buoyancy, and protection of the primary lining from fire.

Because the large bore tunnel is constructed in the very soft soils, the primary lining carries large earth and water pressure, and seismic forces. Consequently, in order to achieve highest degree of stability possible as a ring structure, highest rigidity and strength were required at the segment joints of the primary lining.

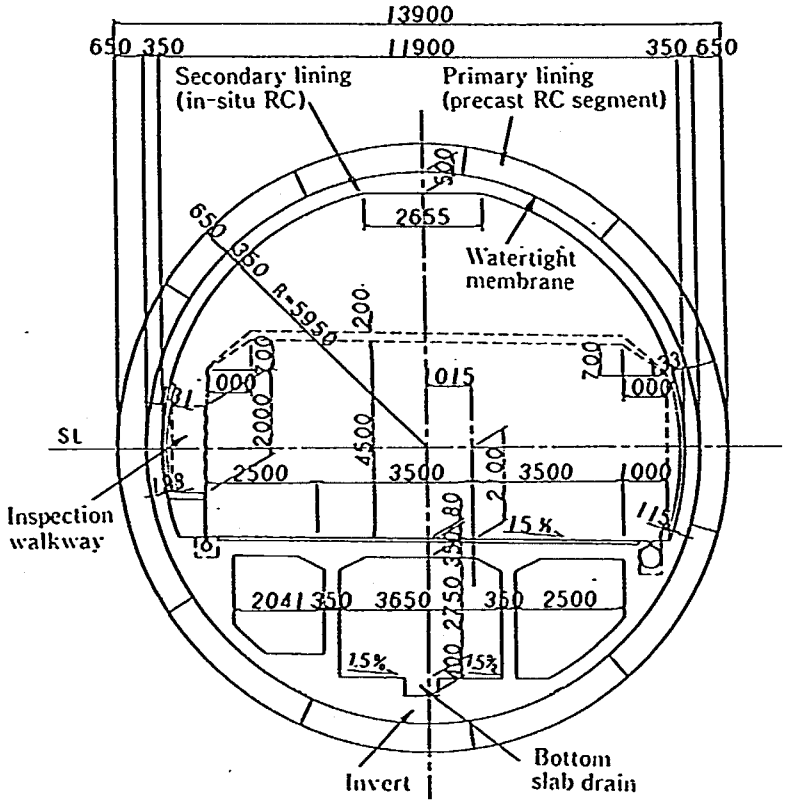


Fig. 4 Tunnel Configuration

ASEISMIC DESIGN

BASIC CONCEPT IN ASEISMIC DESIGN

Considering the active seismic activities of the area in question, two types of large-scale earthquake were employed as input seismic motions; L1 which represents an earthquake of magnitude having a relatively high probability of occurring during the life of the structure based on the seismic activity records in the Tokyo Bay area, and L2 which is the largest possible seismic motion to occur in the Kanto Region. The design concept is that, under L1 seismic motion, the structure shall be free from any damage, with each and every structural member under allowable stress or within elastic strain, and that, under L2 seismic motion, it shall be free from any functional damage as a highway and be repairable, with each and

every structural member under ultimate strength. The tunnel aseismic design was carried out in such a way that the response displacement (static) method was used to check the aseismic safety of the general portion of the tunnel, and then a dynamic analysis was applied to verify the tunnel behavior during the earthquake motion.

INPUT SEISMIC MOTION USED FOR SEISMIC RESPONSE ANALYSIS

As mentioned above, the input seismic motions are determined at the two levels, L1 and L2. The acceleration response spectra of L1 and L2 are shown in Fig. 5. They are given as acceleration response spectra representing the characteristics of each seismic motion on the design bedrock of the highway with a damping coefficient of 5%.

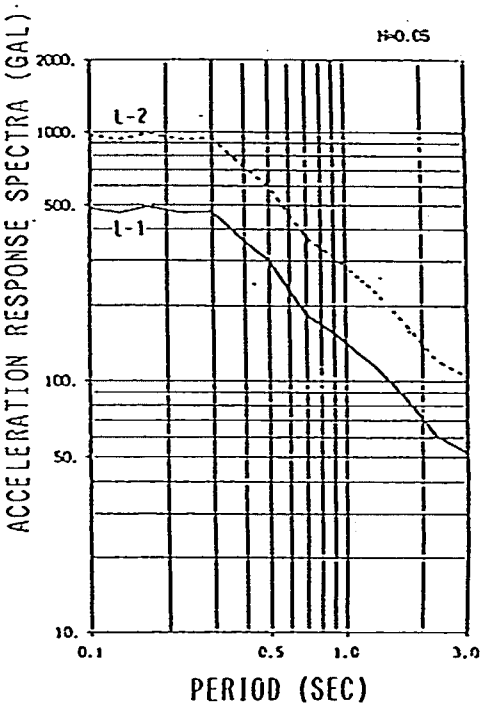


Fig. 5 Response spectra

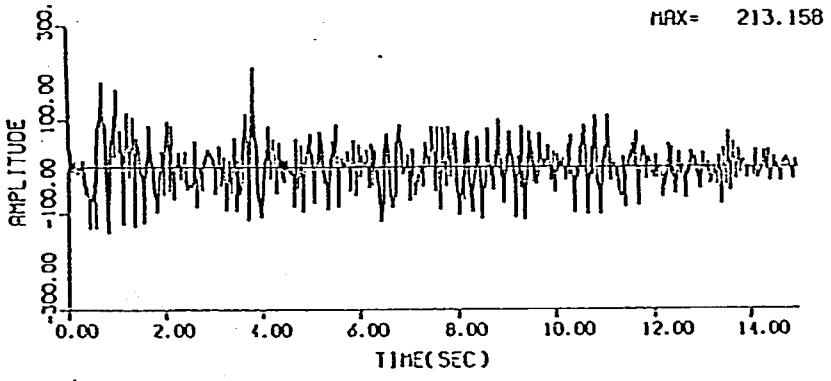


Fig. 6 L－1 Seismic motions

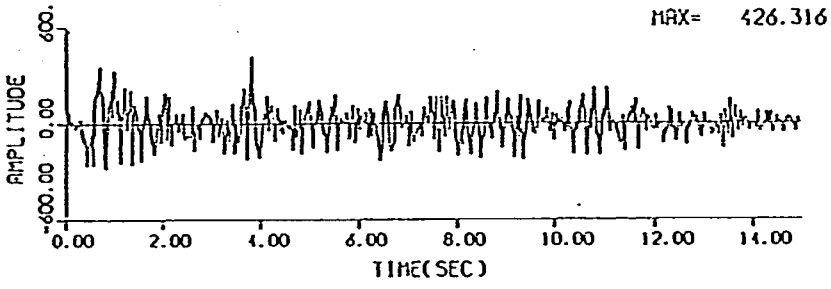


Fig. 7 L－2 Seismic motions

The acceleration wave form of L1 is shown in Fig. 6. This is a pseudo-acceleration wave form, obtained by adjusting the wave form recorded on the bedrock near Kaihoku Bridge at an epicentral distance of 100 km during the Miyagiken-Oki earthquake of 1978 (magnitude 7.4), so that it would agree with the acceleration response spectrum of L1 in the natural period range of 0.1 to 3 seconds.

The acceleration wave form of L2 is shown in Fig. 7. This is a pseudo-acceleration wave form obtained from the wave form recorded on the gravel bed at Hachinohe port, at an epicentral distance of 175 km (record at Hachinohe port), during the Tokachi-Oki earthquake of 1968 (magnitude 7.9) by first converting it into the seismic motion at the design bedrock (assumed to be 10 m below the surface) and then making adjustments so that it would agree with the acceleration response spectrum of L2 in the natural period range of 1 to 3 seconds.

ENGINEERING ISSUES IN ASEISMIC DESIGN

As far as the primary lining of shield tunnel is concerned, due to the existence of precast segment joints, a flexible structure is realized able to follow the displacements of the surrounding ground during earthquake. Consequently, this is a structure with excellent aseismic properties. However, the in-situ secondary lining increases longitudinal rigidity of the tunnel, resulting in mobilization of a large cross-sectional force by seismic deformation. Thus, the more resistance the tunnel is given against the mobilized seismic forces, such as by increasing axial reinforcing bars, the higher are the seismic forces which are mobilized, resulting in a contradiction. That is, the main issue in the tunnel aseismic design was to establish an optimum longitudinal rigidity evaluation for the secondary lining.

ASEISMIC PERFORMANCE TEST

The preliminary aseismic tests on the lining system were carried out as shown in Fig.8 to obtain an understanding of aseismic performance in terms of differences in the segment joint structure, differences for presence/absence of a secondary lining, and differences from the amount of reinforcing steel bars used in the secondary lining. The tests also verified the excellent aseismic performance of the long-bolt joint structure employed in the tunnel primary lining. In the longitudinal aseismic design for the tunnel structure, the following concept was employed:

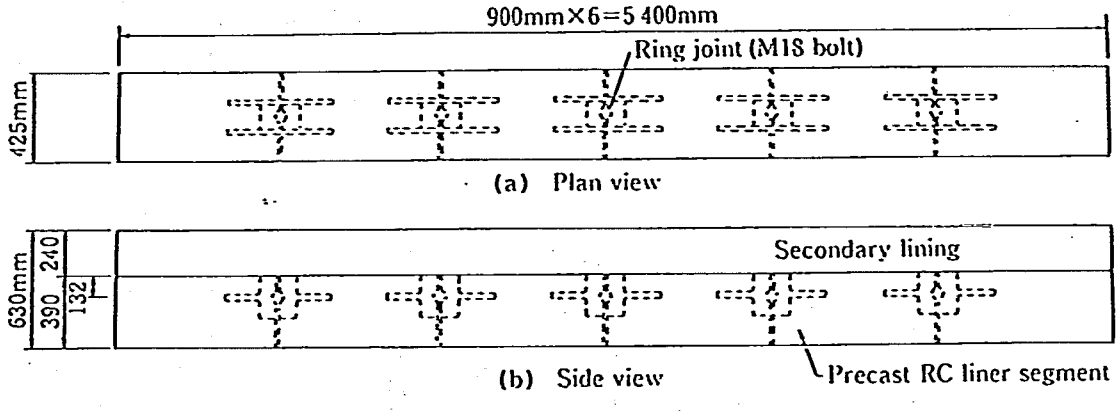


Fig. 8 Test Model to Evaluate Lining Longitudinal Rigidity

a) DESIGN OF JOINT IN THE SEGMENTAL RING

The segmental ring joints of the primary lining are subject to the severest loading condition without the secondary lining under seismic motion of the tunnel. Therefore, the ring joints were so designed to withstand this condition, i.e. the cross-sectional forces were calculated with the rigidity of only the primary lining, and the bolt stress and the ring joint opening was evaluated.

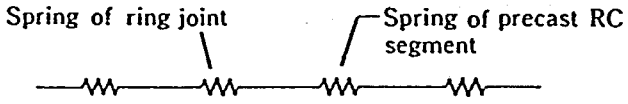


Fig. 9 Ring Joint Structural Analysis Model

b) DESIGN OF SEGMENT IN LONGITUDINAL DIRECTION

The longitudinal reinforcing steel bars of the precast RC segment are so designed to have an ultimate yield strength in excess of that of the ring joint bolts:

$$As \times \sigma sa \geq AB \times \sigma by \quad (1)$$

As : Longitudinal sectional area of steel bars in precast RC segment
σsa : Allowable stress of reinforcing steel bars in precast RC segment
AB : Cross-sectional area of ring joint bolts
σby : Yield stress of bolts

c) DESIGN OF SECONDARY LINING

The aseismic performance tests showed that cracking in the secondary lining occurs first in a certain spontaneous ring joint position. If the cross-sectional area of the longitudinal re-bar is not sufficient to transmit the mobilized axial force in the lining, the re-bar yields, and the opening at the joint position continues to increase resulting in destruction of the ring joint. However, if the area is sufficient, the re-bar does not yield but transmits the force, resulting in many dispersed cracks over many other locations in the secondary lining, which prevents any axial deformation from being concentrated at a specific ring joint.

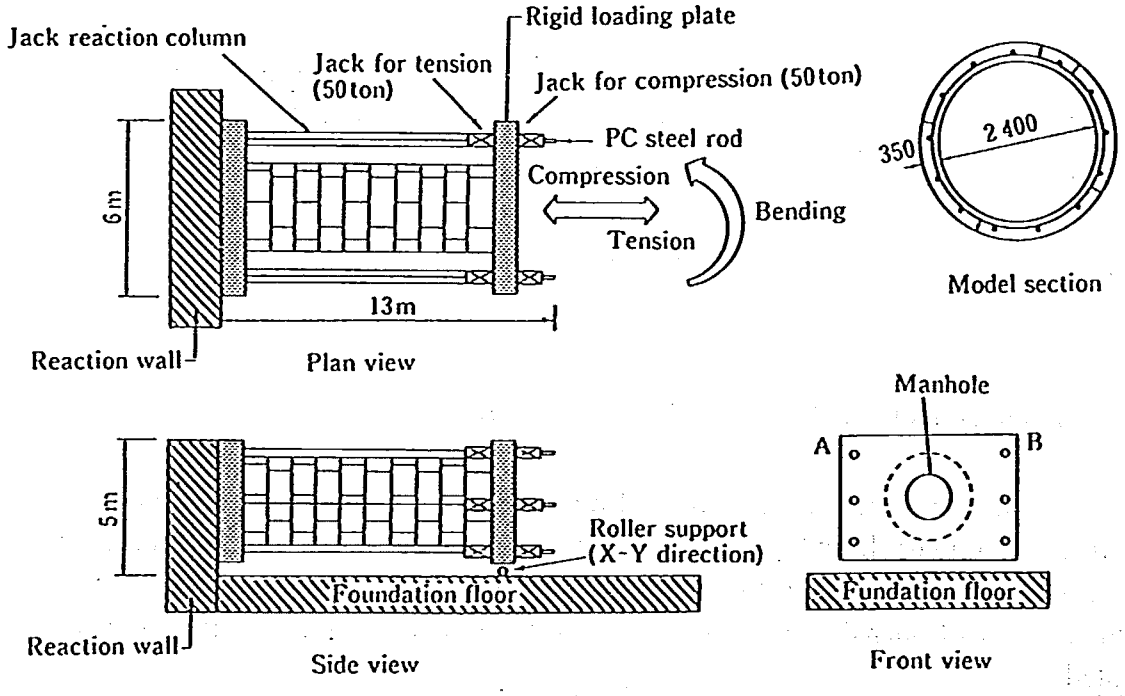


Fig. 10 Test Model to Evaluate Isolation Effect of Membrane on Lining Longitudinal Rigidity

Consequently the necessary cross-sectional area of the reinforcing bars of the secondary lining is given by the following formula. This allows transmission of sufficient force dispersing cracks in the secondary lining, and the bars should be arranged continuously in the axial direction.

$$A2s \cdot \sigma sy \geq 1.2A2L \cdot \sigma ct \qquad (2)$$

A2s : Cross-sectional area of reinforcing bars in secondary lining
σsy : Yield stress of reinforcing bars in secondary lining
A2L : Longitudinal cross-sectional area of secondary lining concrete
σct : Tensile strength of concrete

ASEISMIC EFFECT OF WATERTIGHT MEMBRANE

To effect watertightness of the tunnel, it is planned to install a waterproof membrane between the primary and secondary linings of the tunnel. The membrane was thought to have an isolation effect of reducing transmission of shear force between the linings. Therefore, it was necessary to verify the effects on the longitudinal rigidity of the tunnel, and an experimental evaluation of the rigidity isolation effect by the membrane between linings was carried out using a scale model as shown in Fig. 10. A numerical analysis model was created to first explain the test results, and then to simulate the seismic behavior of the tunnel as shown in Fig. 11. The simulation revealed that 95% of the primary lining deformation was transmitted to the secondary lining even with the existence of the membrane (EVA membrane of 1mm thickness with unwoven textile of 3mm thickness) between the linings, and contradicted the expected isolation effect. It was concluded that the membrane was not thick enough to absorb the shear resistance between the linings due to differences in level arising from assembly error of the lining segment.

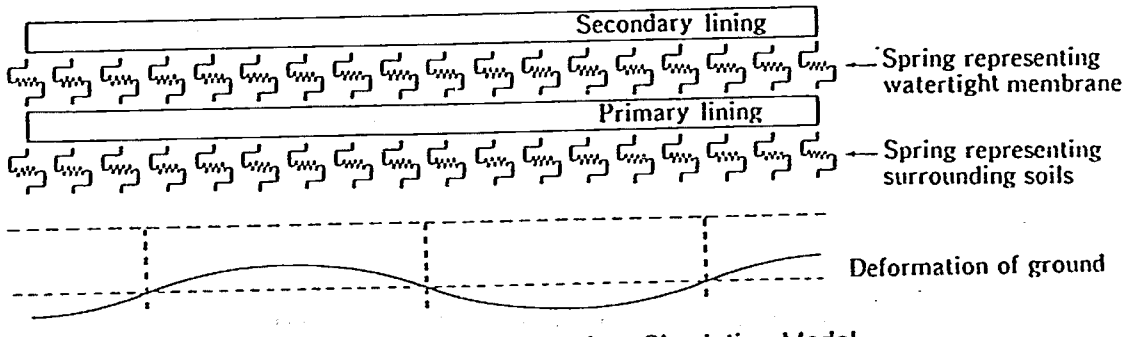


Fig. 11 Dynamic Behaviour Simulation Model

DESIGN OF SPECIAL SECTIONS

a) SPECIAL SECTIONS

The Trans-Tokyo Bay Highway Tunnel has parts connecting with other structures and areas subject to drastic changes in soil conditions. It is expected that behavior of these parts will be different from those of general portions during earthquakes. Since large strains concentrate on the segmental ring joints in these areas, the segmental ring joint structures usually used in the general portions do not satisfy the requirements. Therefore, reinforcing methods were examined for the following sections which show behavior different from those of the general sections of the tunnel.

① Connecting sections of a vertical shaft and a shield tunnel.

② Boundary sections of underground meeting points of a shield machine and a RC segment.

③ Sections of ground subject to drastic changes, such as a transition area for soil improvement methods in the Ukishima slope section (SCP to DMM) and soil improvement termination areas (DMM to existing ground).

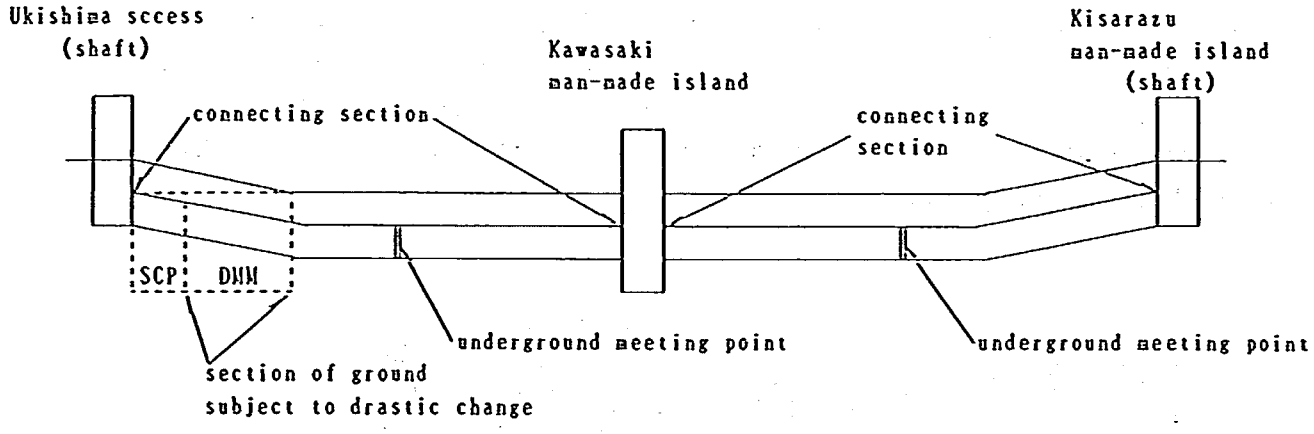


Fig. 12 Special Section

b) SHAFT ACCESS

Since shield tunnels are less rigid than surrounding ground and have apparent weight similar to that of the ground, deformation which is almost equal to soil displacement occurs. On the other hand, shafts are supported by underground diaphragm walls and piles, and affected by inertial forces due to being projected above the ground. Therefore shield tunnels and shafts, which show different behavior, may cause large cross-sectional forces at their connecting sections.

The following proposed structures were prepared in order to absorb the difference of displacement between shafts and tunnels in these sections.

① RC segments + elastic washers
② Ductile segments
③ Ductile segments + elastic washers
④ Flexible segments

Comparison and study of these proposed structures above in terms of safety, economical efficiency and workability concluded that the proposal using flexible segments was most appropriate.

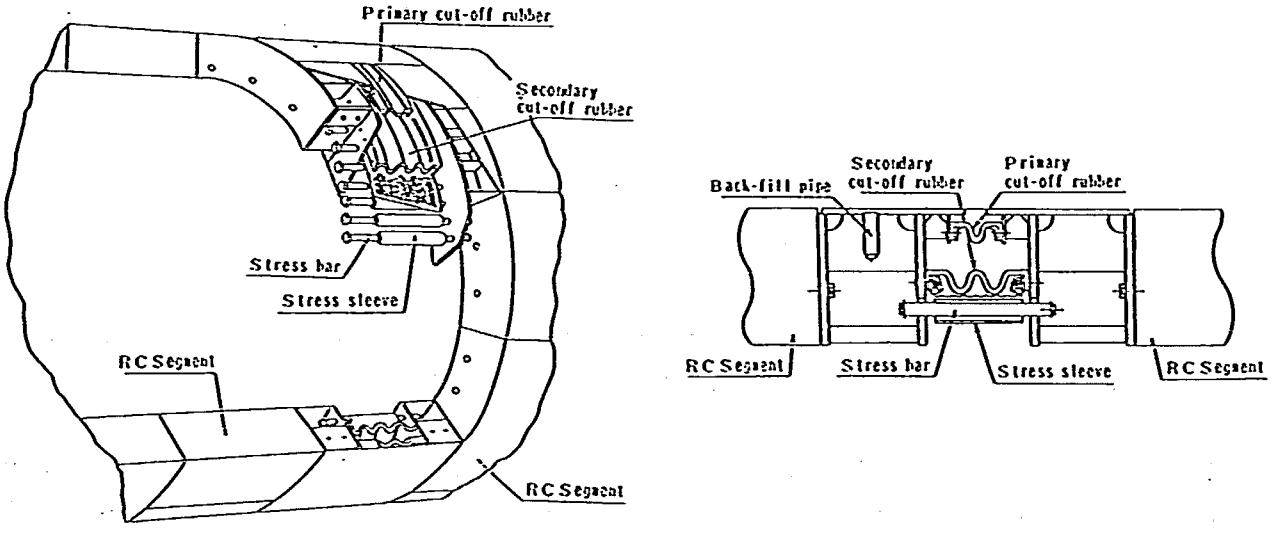


Fig. 13 Concept of Flexible segment

In order to avoid hindrance to the movement of flexible segments, this proposal eliminates the secondary lining at the flexible segments, provides discontinuity of floor slabs with rubber joints, and adopts a simple girder bridge form.

c) UNDERGROUND MEETING POINTS

In constructing the Trans-Tokyo Bay Highway, excavation will be started from each shaft and tunnels will meet each other below the sea bed.

At the underground meeting points, the lining will be constructed using the steel shell of a shield machine, which gives these areas considerably greater longitudinal rigidity compared with the RC segments. Therefore, as ground strains caused by earthquakes are absorbed in smaller quantities around the machine, the strains are concentrated on adjacent RC segment sections.

Since these sections cannot absorb all of these strains with usual ring joints alone, elastic washers will be placed in ten segment rings around the meeting points in order to absorb the strains.

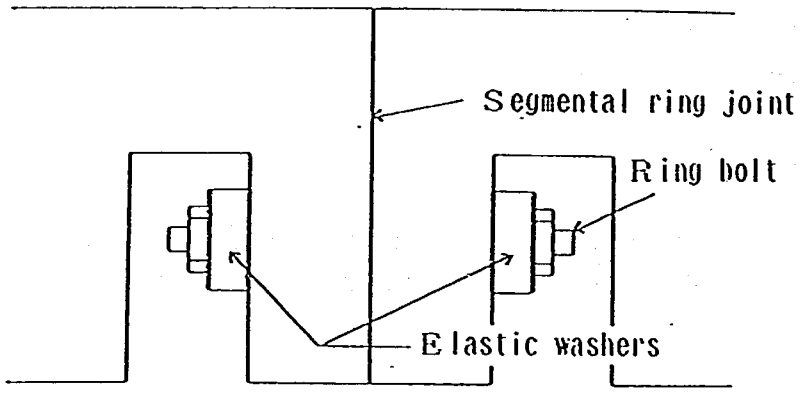


Fig. 14 Elastic washer

d) SECTIONS OF GROUND SUBJECT TO DRASTIC CHANGES

Where the soil conditions change drastically, different ground behavior occurs around the areas' boundaries during an earthquake, which results in large strains.

The present tunnels bring about relatively gradual changes in soil conditions of the existing ground and, except for the following two areas have no sections where large strains are produced. In these two areas, soil conditions change drastically and large strains are likely to occur.

① Transition area for soil improvement methods in the Ukishima slope section (SCP to DMM)

② Soil improvement termination area in the Ukishima slope section (DMM to alluvial clay of the existing ground).

Elastic washers will be placed in forty segment rings around these areas in order to absorb these strains.

AFTERWORD

Ordering procedures have already been finished for tunneling work and joint ventures are now preparing for the start of excavation.

In the process of detailed design for the tunnel structure, there were many engineering issues to be studied such as reasonable design of tunnel in very soft soils under both static and dynamic loading condition, design of watertight tunnel, design to prevent rust and corrosion, and the construction planning of safe, reliable and economical. Therefore various study groups were formed of experts and specialists to solve these technical issues, and the results and findings were successfully input to the tunnel design.

The Trans-Tokyo Bay Highway will be a main road in the metropolitan highway network to help promote a balanced growth of the region. It is also expected to allow a rearrangement of the transport functions in the metropolitan area. Twenty years after the preliminary feasibility study, the project has finally started under a newly organized system taking advantage of the vital capacity of private firms. In the project implementation, adequate considerations will be given to the natural and living environment, navigational safety in the area, and construction safety.

Design of Tama River and Kawasaki Fairway Tunnels in Expressway Bay-Shore Route

By N. Kubota[1], S. Egawa[2] and Y. Tachibana[3]

1) Manager, Design Section, Bay-Shore Route Construction Bureau, Metropolitan Expressway Public Corporation
2) Assistant Manager, Design Section, Bay-Shore Route Construction Bureau, Metropolitan Expressway Public Corporation
3) Chief Engineer, Oriental Consultants Co., Ltd.

INTRODUCTION

To support future development of the metropolitan area making up Tokyo and its outlying area for the 21st century, it is indispensable to complete an even more highly organized traffic network, to say nothing of relieving/eliminating of traffic congestion in central Tokyo.

For this purpose, road construction that becomes its nucleus is, now in being carried out, and what is planned as a part of the same is the Tokyo Bay Ring Road. The Tokyo Bay Ring Road is a general term for (1) [The Tokyo Bay-Shore Road] with a total length of 160 km, running along the shore of Tokyo Bay from Yokosuka to Futtsu via Yokohama, Kawasaki, Tokyo, Funabashi, Chiba and Kisarazu, (2) [Bay-Mouth Traverseway] of about 10 km on the sea, linking Miura and Boso peninsula, (3) [Trans Tokyo Bay Highway] with a length of about 15 km, linking Kawasaki and Kisarazu, and (4) [The Second Tokyo Bay-Shore Road] with a length of about 50 km, linking Haneda, Ichikawa, Chiba and Goi.

[The Tokyo Bay-Shore Road] is, in principle, a road with a total width of 50 ~ 100 m with 10 ~ 14 lanes in total. An fully-access-controlled highway out of a total length of 64 km from Namiki, Kanazawa-ku. Yokohama to Kohya, Ichikawa is being constructed by the Metropolitan Expressway Public Corporation as an express-way Bay-Shore Route. At present, 26 km between Tokai, Ota-ku and Kohya, Ichikawa and 2.8 km between Honmoku and Daikoku pier are in practical use.

The Tama River Tunnel and Kawasaki Fairway Tunnel being constructed by the Metropolitan Expressway Public Corporation now are one part of the Expressway Bay-Shore Route which makes up the Tokyo Bay Ring Road, located at the mouth of

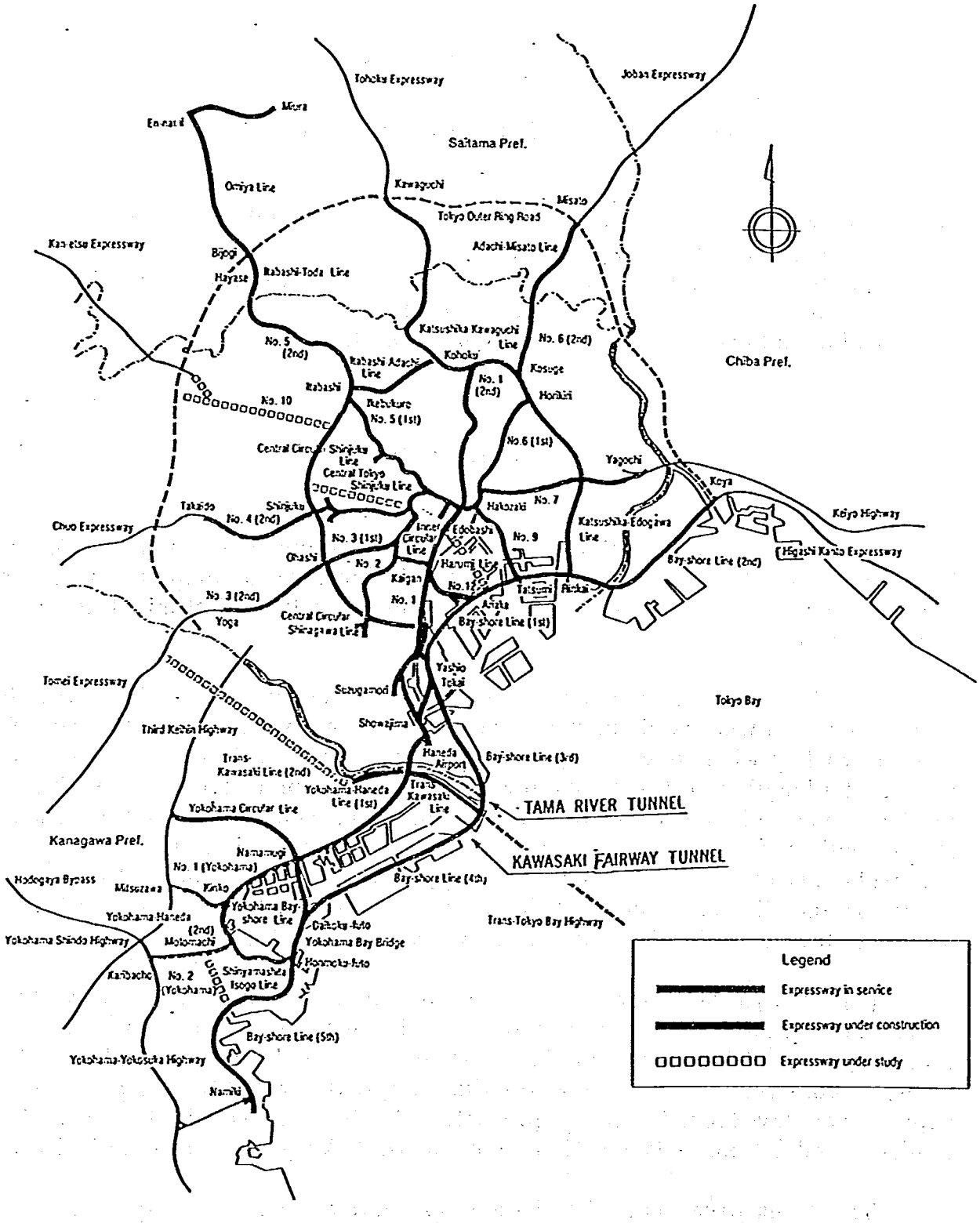


Fig.-1 The Metropolitan Expressway Network

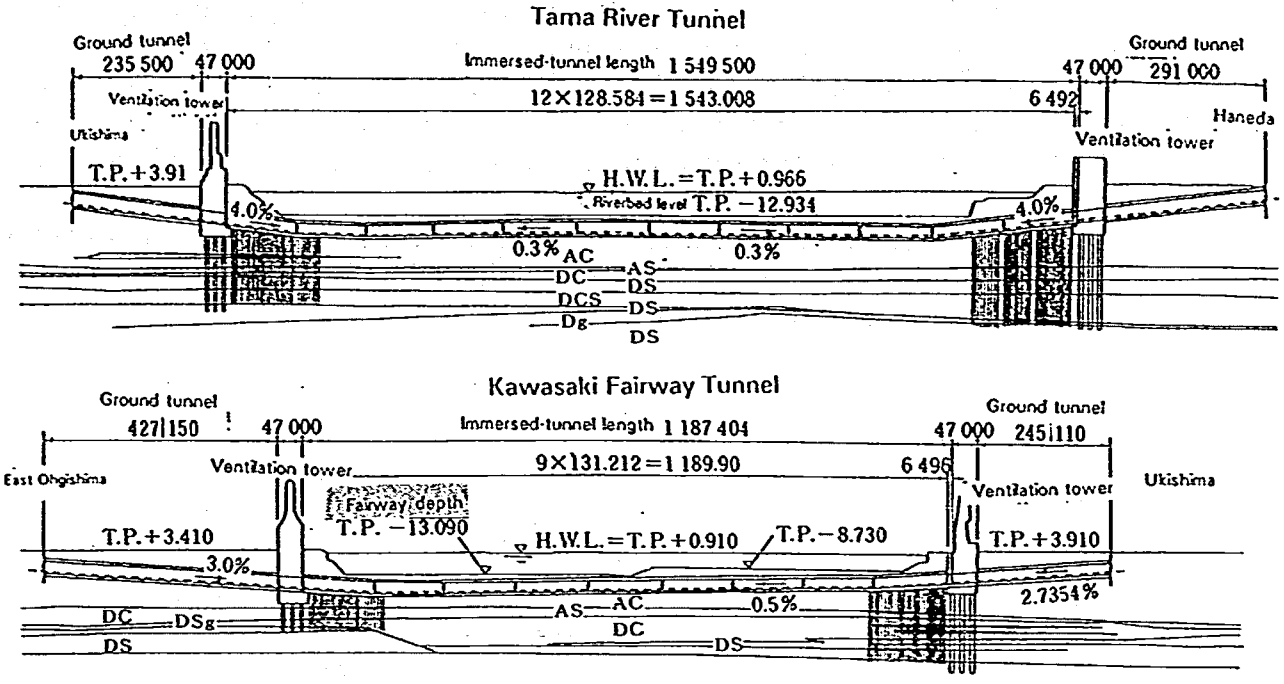


Fig.-2 Longitudinal Profile
Tama River And Kawasaki Fairway Tunnel

the Tama River and Kawasaki Fairway, respectively. These tunnels are the fully-access-controlled highways with 3 lanes in each direction, linking the reclaimed land of Haneda Airport and the Ukishima reclaimed land with East Ogishima. Since this district is closed to the Haneda Airport, it was decided to adopt a tunnel system to avoid aerial navigation area restriction and radio wave interference and adopt an immersed tunneling method for the sea bottom part due to the results a comparative study that was carried out. The Tama River Tunnel is made up of an immersed tunnel with a length of 1,549.5 m, ventilating towers and ground tunnel at both ends of the tunnel. The total length is 2,170 m.

However, the Kawasaki Fairway Tunnel is made up of an immersed tunnel with a length of 1,187.4 m, ventilating towers and ground tunnel at both ends. The total length is 1,953 m. This paper reports on outline of the structure and seismic design of the immersed tunnel at sea bottom.

OUTLINE OF STRUCTURE

The Tama River Tunnel is made up of 12 elements about 130 m in length, 10 m in height and 39.9 m in width with a reinforced concrete construction and a 4.5 m long steel shell block that is called the final joint, having cross sections shown in Fig. 3. On the other hand, the Kawasaki Fairway Tunnel consists of 9 elements of the same size as that of the Tama River Tunnel, except for a width of 39.7 m. For the joints between the elements, flexible joints that enable a substantial reduction in sectional force to be generated in the tunnels due to an earthquake are put to use. A conceptual diagram of the tunnel element is shown in Fig. 4. It is a 4-room reinforced concrete construction with roadway space, an escape pathway and facilities for gas and electricity. To ensure water-tightness, it is covered with 8 mm thick waterproof steel plates (the bottom and both sides) and a waterproof rubber

sheet and 15 cm thick protective concrete (top). Longitudinal tightening cables are arranged along the axis and pre-stress of some 10 kgf/cm^2 is introduced to prevent cracks. Its end-faces are covered with terminal steel shells for the purposes of ensuring fabrication accuracy and reinforcement, and the terminal steel shells have rubber gaskets and vertical shear keys necessary to connect the tunnel elements.

In addition, the element end faces are covered with steel bulk-heads to act as temporary water stopping walls so that it can be floated and towed. Primarily, the necessary numbers per element are shown in Table 1.

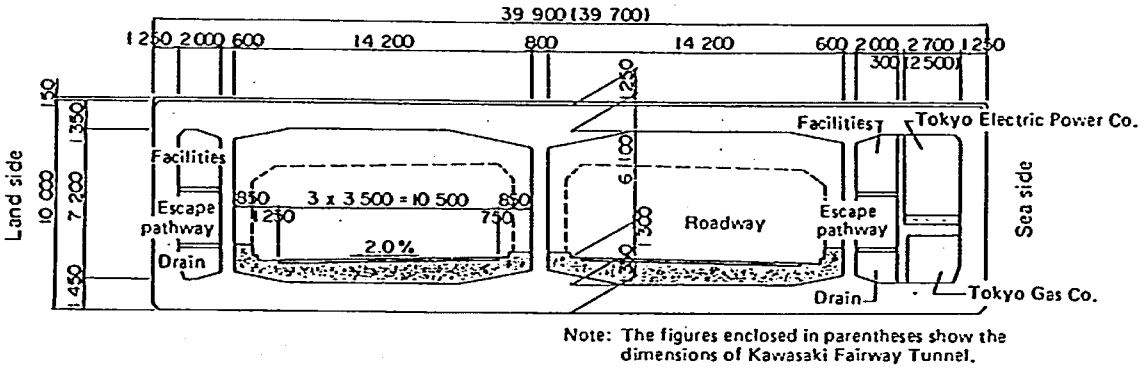


Fig.-3 Cross Section of Submerged Tunnel

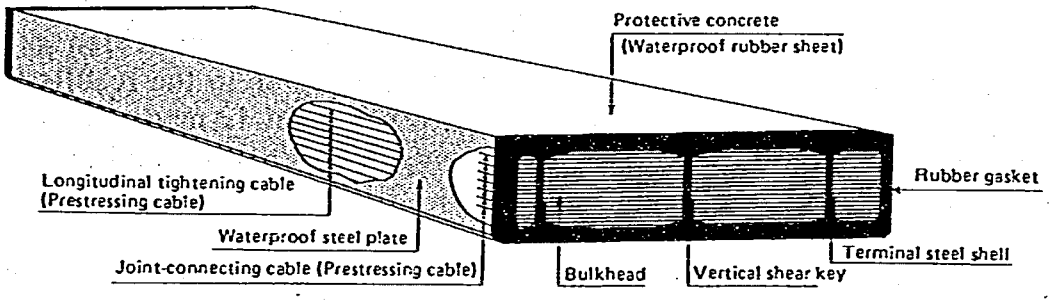
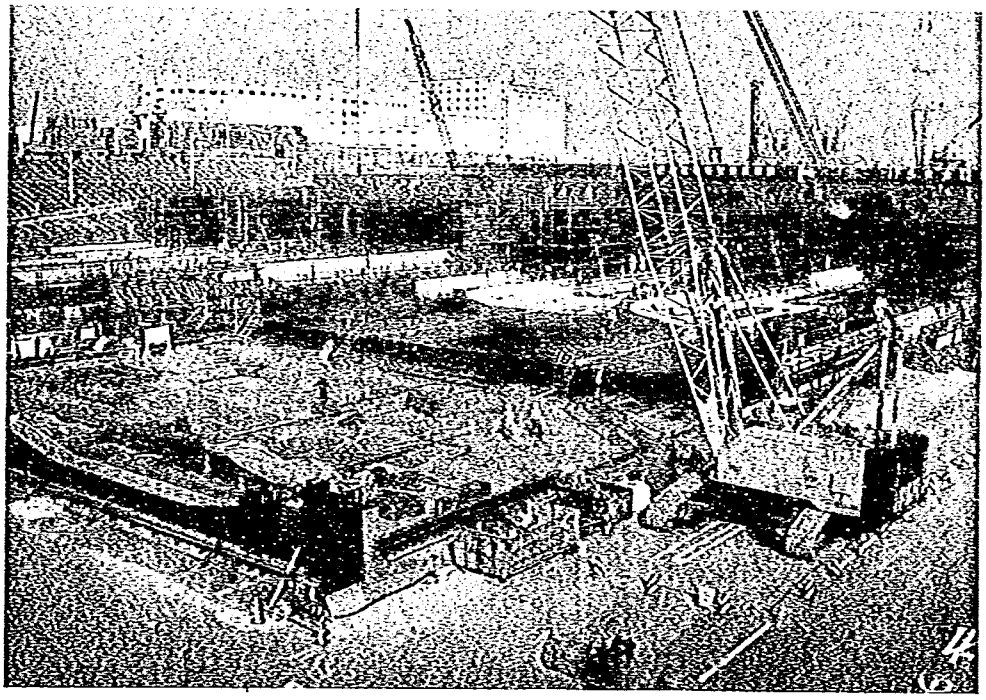


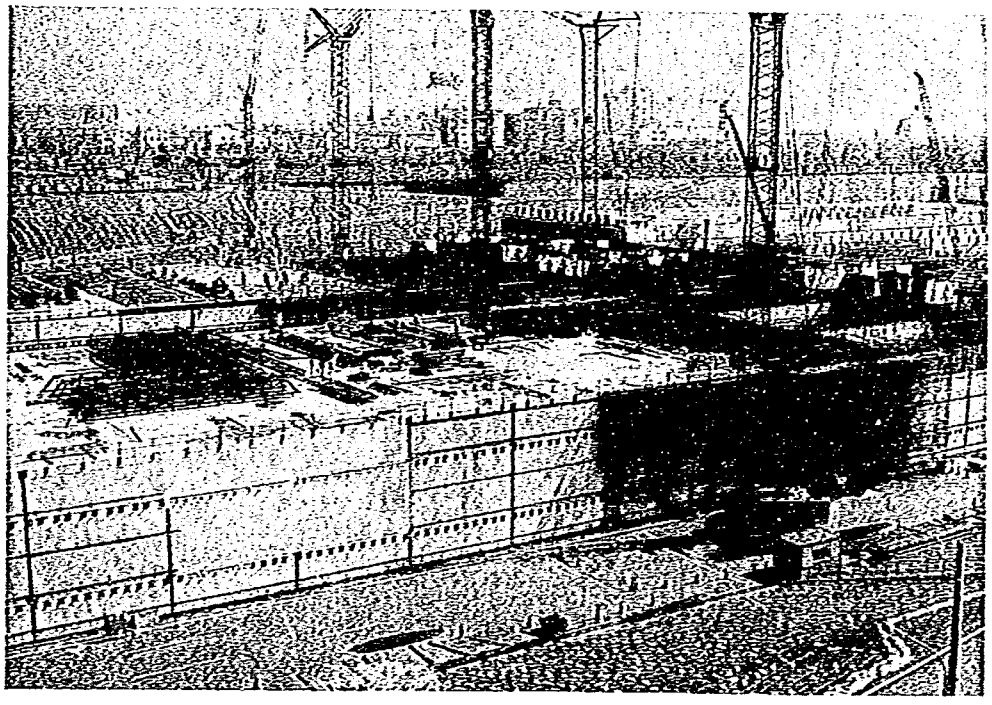
Fig.-4 Conceptual Diagram of Tunnel Element

Table-1 Quantity of Tunnel Element Construction Materials

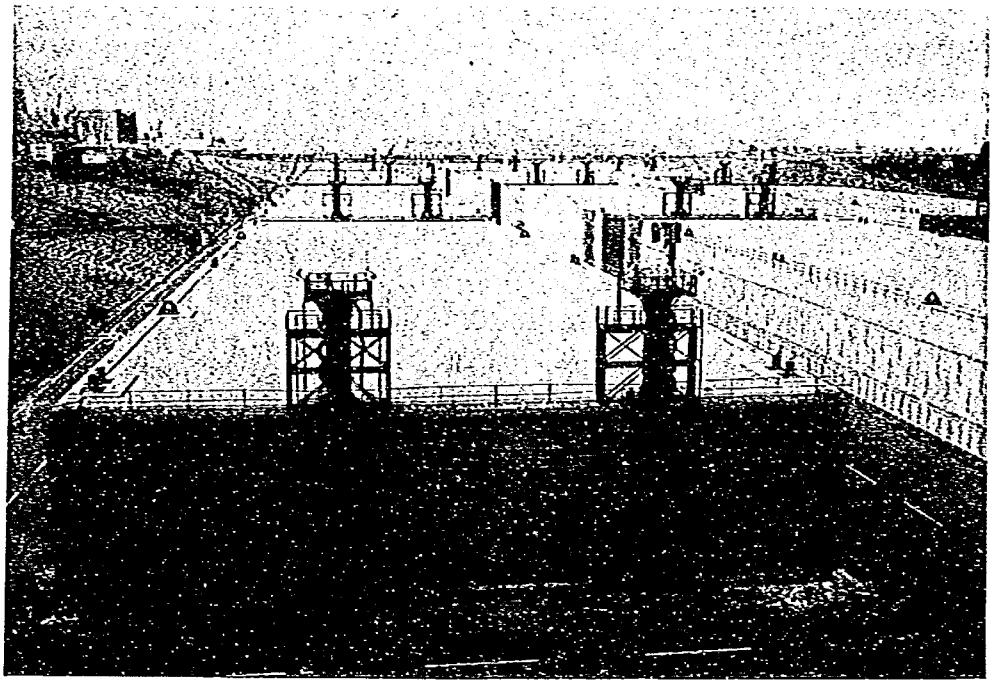
Items	Specifications	Quantity
Concrete	σ_{ck28}=350kg/cm^2 (BB352B)	19,000 m^3
Reinforcing Bar	SD345 D51~D16	5,370 t
Waterproof Steel Plate	SS400 t=8mm	500 t
Waterproof Rubber Sheet	Butyl Rubber t=2.5mm	5,000 m^2
Longitudial Tighteninng Cable	SWPR 7B 12-φ12.7	112 Cables
Joint-Connecting Cable	SWPR 7B 19-φ11.1	200 Cables
Terminal Steel Shell	SS400	300 t
Bulkhead	SS400	170 t



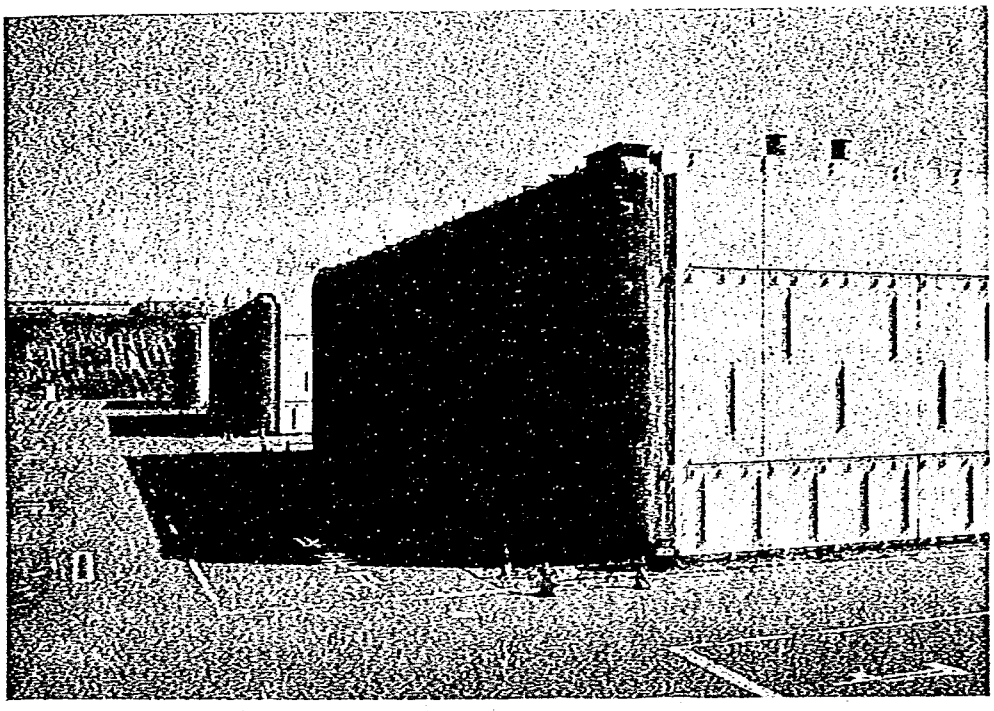
Picture-1 Fabricating Works of Lower Slab



Picture-2 Fabricating Works of Upper Slab



Picture-3 Tunnel Elements



Picture-4 Terminal Steel Bulkhead and Rubber gasket

DESIGN OF IMMERSED TUNNEL

Design of the element cross section

Cross section profile of immersed tunnel is determined in that freeboard amount during towing (about 10 cm) and floating safety after immersed installation (safety rate 1.1 or higher) is ensured. Also, the amount of reinforcing bars are determined by that intensity of member stress caused by combination of loads shown in Table 2 are confirmed to be within the allowable stress. Design at the time of earthquake will be described later. However, as far as the cross sections are concerned, these are determined by sectional force caused by combination of dead load, side earth pressure, hydraulic pressure and non-uniform settlement.

Design of the element axial direction

The model used for studying in the element axial direction is made of a beam on elastic foundation of ground spring and as the stationary load, dead weight, earth pressure, hydraulic pressure and top covering load are applied. Sectional forces in axial direction are scarcely generated under stationary load except the sea wall restored areas, and amount of reinforcing bars is calculated by sectional force cause by the effect of [earthquake + temperature]. Design at the time of earthquake will be described later.

Table-2 Combination of Loads Increment in Allowable Stress (for completed structure)

	Combination of Loads	Increment
A	Dead load*1 + Lateral earth pressure + Hydrostatic pressure (at H.W.L.)*2 + Load due to differential Settlement	0%
B	—〃— + —〃— + —〃— (at L.W.L.) + —〃—	0%
C	—〃— + —〃— + —〃— (at H.H.W.L.) + —〃—	30%
D	A + Load due to Temperature difference*3	15%
E	A + Seismic load	50%
F	A + Seismic load + Load due to Temperature difference	65%
G	A + Accidental load	50%

Note) *1 Dead load = Self Weight of Element + Weight of Protective Concrete + Weight of Road-bed + Weight of cover

*2 Increment in the allowable stress shall be same for the case where differential settlement is not taken into cosideration.

*3 · Temperature difference

(1) Top slab, Bottom slab and External walls at 0℃, while Internal walls at 10℃

(2) External surface of Top slab, Bottom slab and External walls at 0℃ while the Internal surface of the same at 10℃.

(3) External surface of Top slab, Bottom slab and External walls at 10℃ while the Internal surface of the same at 0℃.

Design of joint

The immersed tunnel elements are connected by joints. In general, there are flexible joints of which the rigidity is smaller than the element and rigid joint that has almost the same rigidity as the element. For this immersed tunnel, we adopted a flexible joint. In case flexible joints are used, we can largely reduce the sectional force caused by non-uniform settlement due to solid consolidation, the effects of temperature change and earthquakes. Therefore, economical tunnel element can be designed.

However, since deformability to absorb relative displacement between the elements and water-proof ability to maintain the function of a tunnel are required simultaneously for the flexible joint, it must be of a structure having these ability in combination.

Structure of the flexible joint is shown in Fig. 5. The components to make up this structure are as follows:

1) Rubber gasket: Member to stop water leakage at the joints and, at the same time, act as compressive and tensile springs in an axial direction. (Fig. 6)

2) Joint connecting cable: Member to form composite spring together with a rubber gasket and to restrict displacement that the joints tend to open in the tunnel axial direction.

3) Horizontal and vertical shear keys: Using members to prevent dislocation between elements in horizontal and vertical directions and to act as springs by means of inserting shock absorbing rubbers into the engaged points.

4) Secondary water stopping rubber: Water-proof member to enhance safety of the joint against water leakage.

5) Terminal steel shell: Member to reinforce the parts where rubber gaskets are fitted and ensure flatness of the end faces. This is a part of the element.

The flexible joint reduces the sectional force in the tunnel axial direction, but an accurate evaluation of joint rigidity is important in regarding. Before designing this tunnel, a mockup sample of the rubber gasket and joint connecting cable was made and to confirm the behavior of joint compression, a tension test and bending test was carried out.

As a result, we acknowledged that (1) deformation characteristics of the joint can be found by superpositioning of deformation curve of the rubber gasket and the joint connection cable, (2) dynamic spring constant is 1.05 times greater than static spring constant, and (3) effect of frequency on the dynamic characteristics is negligible. Deformation curves of the joints used for design are shown in Fig. 7.

Since loading and unloading act repeatedly during an earthquake, the relation between loading and deformation of the rubber gasket moves over both loading and unloading curves in the shape of the loop. Therefore, the smallest and largest point on the loop are present on the unloading curve and a secant gradient of these two points becomes the dynamic spring constant.

In consequence of the design, it was found that the amount of deformation at the joints ranged from 2.8 to 5.3 cm though they vary depending on points of the joints. The allowable amounts of deformation of the joints are determined by either one of the values resulting from subtracting the minimum compression amount that prevents water leakage (nose height of the rubber gasket) and amount of deformation due to rubber creeping from the initial amount of compression due to the hydraulic pressure of the rubber gasket (5 ~ 6 cm) or tensile strength of joint connecting cable (5.7 cm).

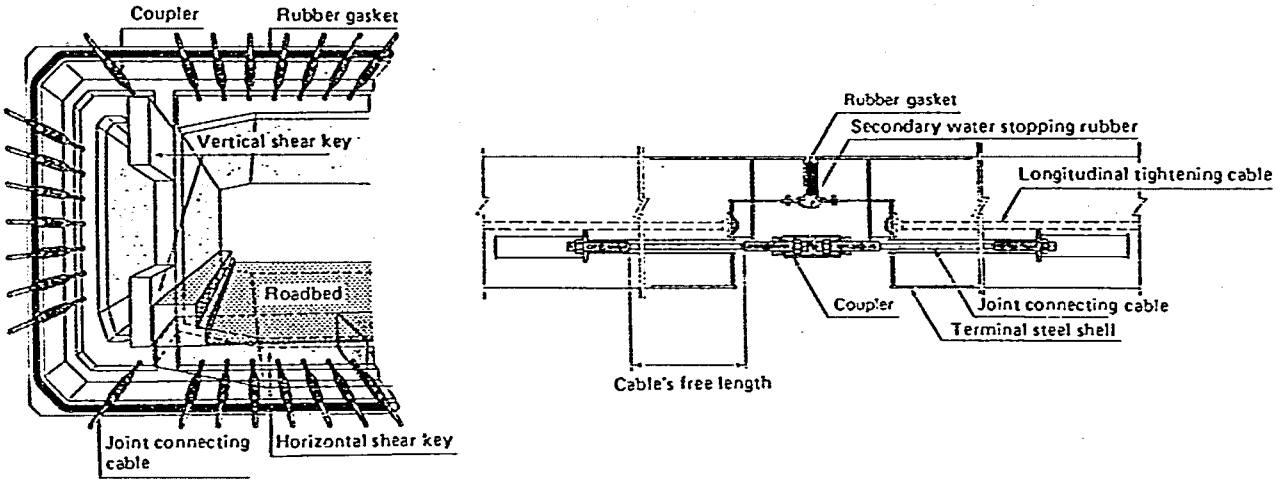


Fig.-5 Mechanism of Flexible Joint

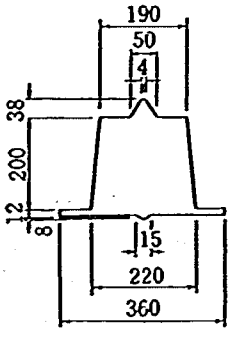


Fig.-6 Cross Section of Rubber Gasket

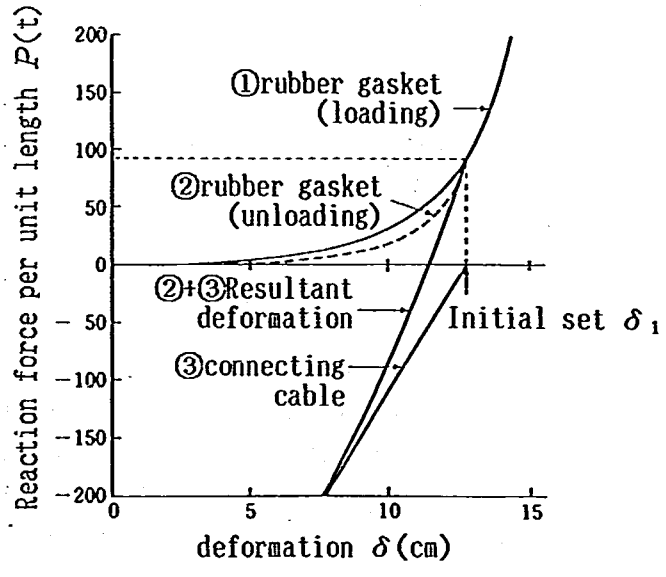


Fig.-7 Deformation curves of the joint (axial direction)

SEISMIC DESIGN

Basic policy

The seismic design of this tunnel is intended to be carried out by the allowable stress method by means of setting up an earthquake corresponding to the L-1 level, designing by an seismic deformation method, and checking by an earthquake response analysis with overall system models.

Set-up of input earthquake motion

The bedrock for the seismic design of this tunnel is assumed to be a diluvium sand layer with 50 or more of N-value, existing in the vicinity of TP-70 m. However, the shear wave velocity (V_S) of this layer is 300 ~ 400 m/s and the tertiary that is equivalent to the first kind ground is even deeper, and it is assumed to exist at a depth of TP-150 m. For this reason, we first set up earthquake intensity on the first kind ground, and performed an earthquake response analysis of the ground applying the superposed reflection theory, and then, set up input earthquake motion for the designing purpose on the bedrock for seismic design.

For the earthquake intensity for the seismic designs, we used the L-1 level intensity, based on the results of the study conducted by the Public Works Research Institute of the Ministry of Construction. Concretely speaking, we were looking for the acceleration response spectrum of the earthquake with a magnitude of M7 and an epicentral distance of 50 km and the earthquake with a return period of 75 years from seismic activities around the construction site, and decided the design spectrum to envelop this spectrum. This is shown in Fig. 8.

Next, we created an earthquake waveform having this spectrum intensity by means of adjusting the acceleration amplitude of the waveform that was observed near the Kaihoku Bridge at the time of Off Miyagi Prefecture Earthquake in 1978 having a frequency characteristic close to L-1 spectrum, with the frequency domain.

Next, we set up input earthquake motion on the bedrock for seismic design by means of inputting the previously obtained L-1 earthquake waveform into the layer equivalent to the first kind ground on this point, and carried out a response analysis of the ground based on the superposed reflection theory, and then, found the response waveform of the bedrock for the seismic design.

Seismic design of cross section

We sought the sectional force caused by an earthquake in the tunnel cross section by means of giving the response displacement of the ground (about 7 ~ 9 cm on top of the element) based on L-1 level spectrum to an FEM model with a surface layer ground. As a result, every stress was found within the allowable stress. The model for study and bending moment distribution are shown in Figs. 9 and 10, respectively.

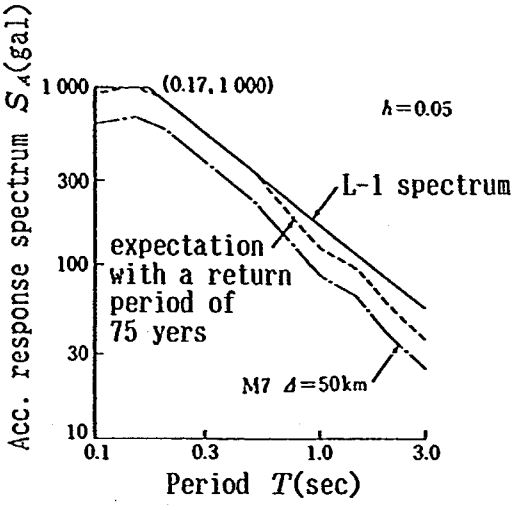


Fig.-8 L-1 spectrum

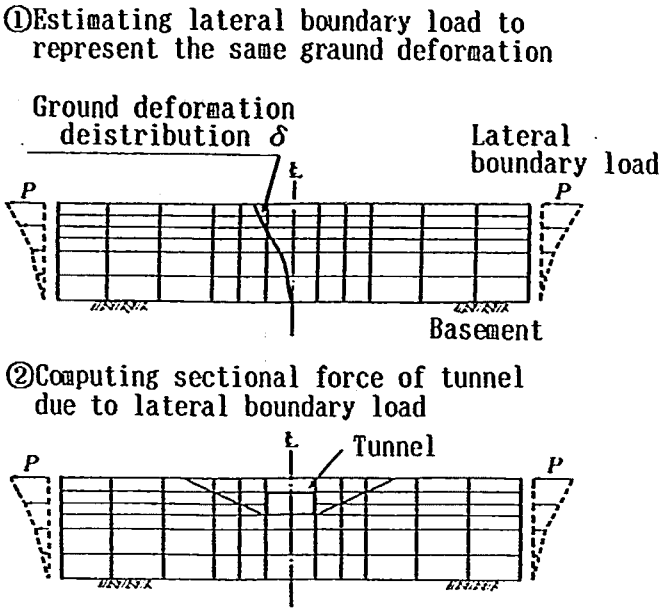


Fig.-9 Anelysis of Tunnel Cross Section by Seismic Deformation Method

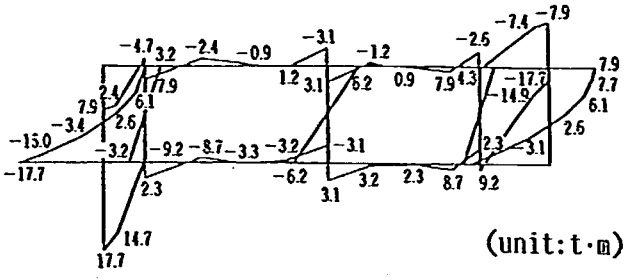


Fig.-10 Bending Moment in Cross Section (Kawasaki Fairway Tunnel)

Design of longitudinal direction

(a) Evaluation of the ground spring constant

Following two methods are applied to an algorithm of the ground spring constant to be used for analysis of the axial direction of a tunnel. These methods are (1) a method to calculate the ground spring using modulus of elasticity as shown in the guideline (plan) for the underground multi-purpose duct design (Japan Road Association, 1986) and (2) a method to calculate the ground spring on the basis of relation between load and displacement using the FEM model of the ground including the tunnel. Generally, the spring constant calculated from the FEM model is greater. When applying this spring, sectional force is calculated to be larger, resulting in an evaluation on the safer side. In this analysis, we calculated the ground spring by the both methods. Both methods of calculating the spring are shown below:

(1) Calculation of the ground spring by the FEM model

We have created an FEM model of the cross section of a tunnel and the ground with an unit length of the axial direction of the tunnel, and obtained a ground spring using the tunnel displacement at the time load is applied to the tunnel:

$$K = P \times \delta$$

where K : Spring constant between the tunnel and ground per unit length of the tunnel (t/m/m)
P : Load to be applied to the tunnel on the FEM model (t/m)
δ : Displacement of the tunnel (m)

We used a three-dimensional model in the calculation of the spring in the axial direction of the tunnel, and we used a two-dimensional model (plane strain) in the calculation of the spring in the right angle direction of the tunnel.

(2) Calculation of the ground spring by the underground multi-purpose duct design guideline

The ground spring is calculated with the following equations:

$$K_X = G_S' \qquad K_Y = G_S' \qquad K_Z = E_S'$$

where K_X : Spring constant in the axial direction of the tunnel (t/m/m)
K_Y : Spring constant in the right angle horizontal direction of the tunnel (t/m/m)
K_Z : Spring constant in the right angle vertical direction of the tunnel (t/m/m)
G_S': Equivalent shear deformation factor (t/m^2) estimated from the characteristic value of the surface ground layer
E_S': Equivalent deformation factor (t/m^2)

(b) Analysis by the seismic deformation method

In the seismic deformation method, we found deformation and sectional force of the tunnel by means of: (1) modelling the tunnel as the beam on elastic foundation by the ground spring, (2) assuming ground deformation along the tunnel to be a sine waveform and (3) giving the ground displacement to the tunnel via the ground spring as the forced displacement. In this case, we assumed the load to the tunnel not to exceed the bearing strength of the ground as shown in Fig. 11. As for bearing strength of the ground, we made it the frictional resistance between the tunnel element and peripheral ground for the tunnel axial direction, and we made it the passive earth pressure strength at the time of an earthquake for the horizontal direction and ultimate bearing capacity for a vertical direction.

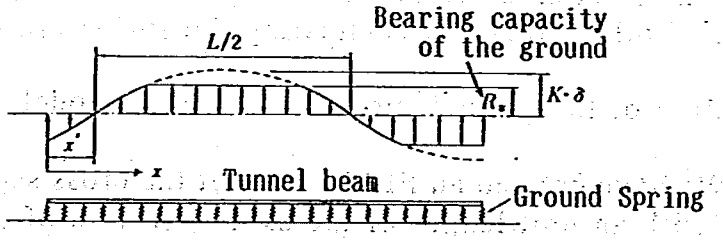


Fig.-11 Seismic Deformation Method to the Longitudinal Direction

Displacement amplitude of the ground that was assumed to be a sine wave is estimated by the following equation:

$$U_h = m \cdot \beta \cdot S_D$$

where U_h : Displacement amplitude of the ground at the tunnel level (m)
m : Mode amplitude ratio to the ground surface at the tunnel depth
β : Participation factor of shearing oscillation primary mode of the surface ground layer
S_D : Response displacement (m). This is found from displacement response spectrum in Fig. 12. Figure 12 is a result of finding the displacement response spectrum of the input earthquake motion shown in Fig. 8 and assuming the damping constant of the ground to be h=10%.

We found the natural period of the surface ground layer T, m and β by means of modelling the ground as a multilayer ground. Wavelength of the ground deformation is estimated by the following equations according to the underground multipurpose duct design guideline (Japan road Association).

$$L = \frac{2L_1 \cdot L_2}{L_1 + L_2}$$

$$L_1 = V_{DS} \cdot T = 4H$$
$$L_2 = V_{BS} \cdot T$$

where L : Wavelength of the ground deformation (m)
V_{DS}: Equivalent shearing elastic wave velocity of the surface ground layer (m/s)
V_{BS}: Shearing elastic wave velocity of the bedrock (m/s)
T : Natural period of the surface ground layer (sec)
H : Thickness of the surface ground layer(m)

The ground spring, the ground response displacement and wavelength of the ground deformation in the Tama River and the Kawasaki Fairway Tunnels are shown in Table 3. Results of analysis are shown in Fig. 13.

Earthquake response analysis

A dynamic analytic model made up of the tunnel and ventilating tower as shown in Fig. 14. The ground is divided into a number of segments along the axial direction of the tunnel and each segment is replaced by one mass-one spring system. In the analysis, we assumed a segment width that divides one tunnel element into quarters. It was 32 meters. We found the deformation amount, sectional force and joint relative displacement of the tunnel by; (1) assuming that dynamic characteristic of the ground is not affected by the tunnel's. (2) finding the response displacement of the ground disregarding existence of the tunnel, and (3) giving it as the ground displacement.

A comparison of the maximum response value by earthquake response analysis and allowable values is shown in Table 4. For input earthquake motion, we also checked the large-scale earthquakes of the Kanto Earthquake class (L-2 earthquake being proposed by the Public Works Research Institute of the Ministry of Construction) in addition to L-1 earthquakes. Distribution of sectional force is shown in Fig. 13.

Table-3 Ground Spring, Displacement of ground, Wavelength of Ground Deformation

		Kawasaki Fairway Tunnel	Tama River Tunnel
Ground Spring	Axial (tf/m/m)	5 330~ 10 500	4 000~ 9 000
	Transversial Horizontal (tf/m/m)	26 800~ 47 700	19 700~25 900
	Transversial Vertical (tf/m/m)	57 500~259 000	45 300~85 500
Displacement of the Ground (cm)		3.8~7.8	7.2~10.7
Wavelength of the Ground Deformation (m)		190~390	350~500

Note:Displacement responce is at Tunnel Level

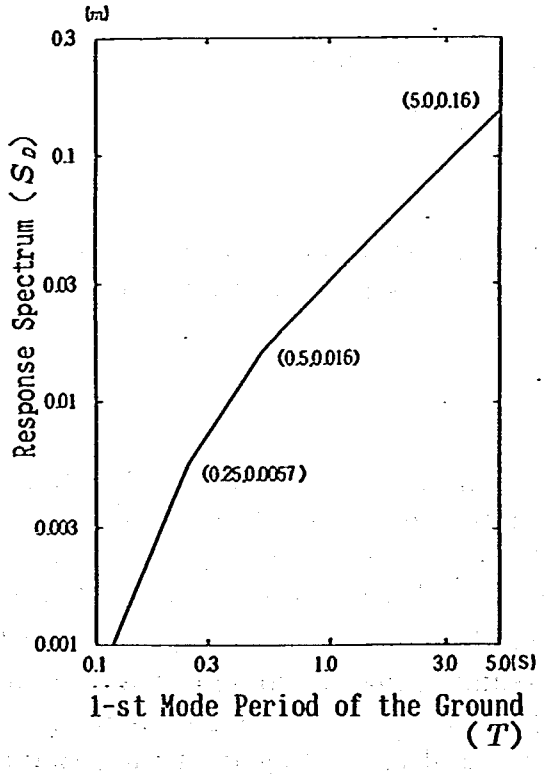


Fig.-12 Displacement Response Spectrum

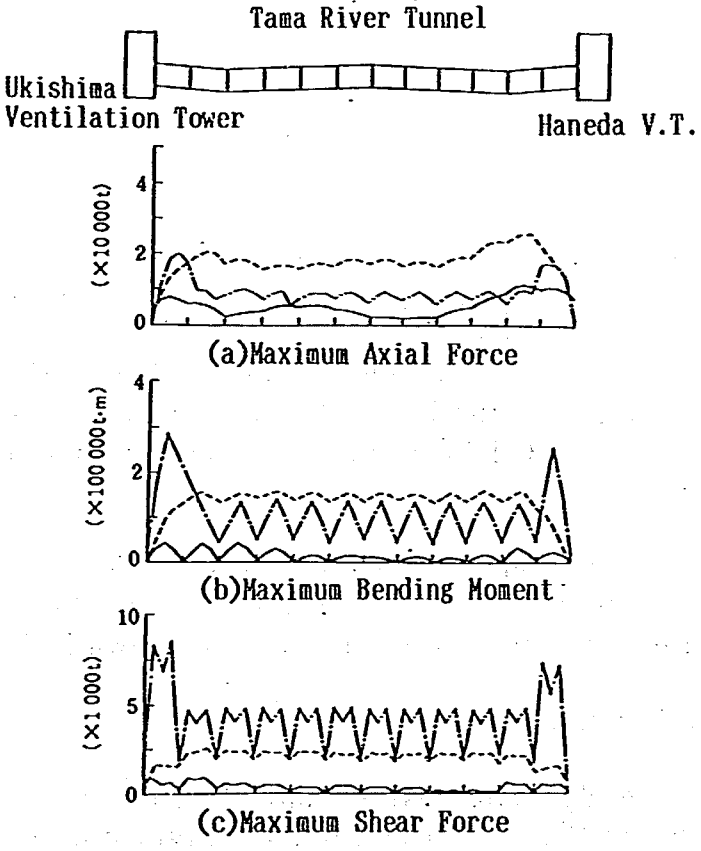


Fig.-13 Results of Seismic Response Analysis

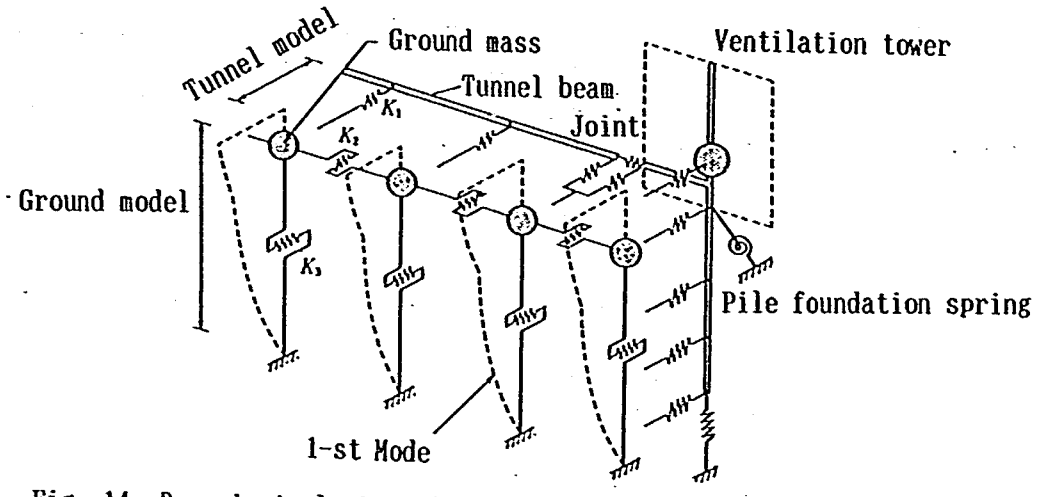


Fig.-14 Dynamic Analysis Model for Integrated Tunnel System

Table-4 Comparison of the Resuls by Dynamic Analysis with the Allowable Values

		Kawasaki Fairway		Tama River	
		L-1	L-2	L-1	L-2
Tunnel Element	Axial Tensile Force (tf)	11 000 (47 000)	32 200 (56 600)	11 400 (49 300)	33 800 (62 400)
	Bending Moment (tf·m)	326 000 (584 000)	651 000 (1 120 000)	40 200 (607 000)	110 000 (818 000)
	Shear Force (tf)	6 560 (40 100)	14 500 (47 300)	1 050 (40 400)	3 290 (47 500)
Tunnel Joint	Elongation (cm)	1.5 (5.9)	4.8 (8)	1.8 (5.7)	4.8 (8)
	Expansion due to Rotation (cm)	0.3 (5.9)	0.4 (8)	0.2 (5.7)	0.8 (8)
	Shear Dislocation (cm)	1.8	5.8	1.1	1.3

Note:Values parenthesized indicate allowable values.

(1) For L-1 earthquake

For L-1 earthquakes we made a comparison of the generation values and allowable values corresponding to allowable stress (yield stress for joint connecting cable).
In result, we found that both of generation sectional force and joint relative displacement are below allowable values and it seemed that sufficient earthquake resistance is being maintained.

(2) For L-2 earthquake

For L-2 earthquake, we made a comparison of generation value and allowable value at the ultimate limit state. In result, we found that both of generation of sectional force and joint relative displacement are below the allowable values, and it seemed that a sufficient amount of earthquake resistance is being maintained.

We think that the result of this study should be an example of a verification against large-scale earthquakes assumed on the basis only of knowledge we acquired in the past, even if we consider the fact that the amount of accumulated data of large-scale earthquake is not enough.

CONCLUSION

The immersed tunnel construction works of the Tama River Tunnel and the Kawasaki Fairway Tunnel began with preparation of the dry dock in March 1986, the first period construction of the element fabrication in September 1987 and then the second period construction in July 1990, and now fabrication of 21 elements are almost completed.

REFERENCES

1) Ministry of Construction: Method of Determination of Input Earthquake Motion for Dynamic Analysis, Technical Memorandum of Public Works Research Institute, No. 2120, 1984. 3
2) Metropolitan Expressway Technical Center: Report of Design and Construction Method of Immersed Tunnel, 1987-1989
3) Tezuka, S. and Tomizawa, S.: Crack Control Method for Construction of Immersed Tunnel Element, Concrete Journal, Vol 27, No. 5, PP. 38-49, Japan Concrete Institute, 1989. 5
4) Kubota, N., Egawa, S., Matsuoka, A. and Shimizu, T.: Design and construction of Tama River and Kawasaki Fairway Immersed Tunnels on The Tokyo Bay-Shore Road, CONCRETE JOURNAL, Vol. 30, No. 5, PP. 29-43, Japan Concrete Institute, 1992. 5

SEISMIC DESIGN METHOD OF UNDERGROUND PARKING GARAGE STRUCTURES

by Kazuhiko KAWASHIMA[1], Hideki SUGITA[2] and Tomoru NAKAJIMA[3]

ABSTRACT

Presented in this paper is the outline of seismic design method of reinforced concrete underground structures for parking garage based on the Guide Specifications of Design and Construction of Parking Garage issued by the Ministry of Construction in 1992. Background of seismic design by means of the Seismic Deformation Method is described.

INTRODUCTION

Resolving traffic congestion in urban area is a significant importance. Providing enough space for parking is one of the key solutions for decreasing the traffic congestion and traffic accident. For this purpose, the Ministry of Construction revised the Road Law in 1991 so that the bodies who construct the road, such as the Ministry of Construction and Regional Governments, can construct parking garages as the "Supplementary Structures of Road". It is anticipated that many garages would be constructed underground of roads in urban areas because of various limitation of space available and restriction of land use on ground.

For facilitating the construction of parking space and garage, the Guide Specifications of Design and Construction of Parking Garage was notified by the Ministry of Construction in March 1992. Main body of the notification as well as the supplementary explanation was published by the Japan Road Association in

---

1 Head, Earthquake Engineering Division, Public Works Research Institute, Ministry of Construction, Tsukuba Science City, Japan
2 Research Engineer, ditto
3 Research Engineer, ditto

November 1992[1]. The Guide Specifications cover planning, design and construction of parking space and garage. In the chapter of Planning, the overall procedure of planning, basic considerations for type selection, lay-out, size and height of parking lots are described. In the chapter of Design, description is given to design and construction of reinforced concrete underground structures for parking garage, because they are the major type adopted in urban area and they require specific design and construction considerations. When other type of structures such as prestressed concrete structures are used, appropriate modifications are required to adopt the Guide Specifications. General design procedure of main body of the structures including seismic design and design of facilities such as electricity, lightning and ventilation are described. Construction procedure with emphasis on the fact that the construction of underground parking garage structures is made in highly populated city areas are described in the chapter of Construction.

Table of contents of the Guide Specifications is as :

Chapter 1 General
Purpose
Scope
Chapter 2 Planning
1 Survey
2 Basic Planning
Chapter 3 Design
1 General
1.1 Scope
1.2 Definition of terms
2 Design of Main Body of Parking Garage Structures
2.1 Loads
2.2 Materials
2.3 Allowable stress
2.4 Soil properties for design
2.5 General provisions for design of strctural members
2.6 Design of strctural members
2.7 Strctural details
2.8 Design of foundation
2.9 Special consideration for wall and floor
3 Seismic Design
3.1 Basic principle for seismic design
3.2 Loads and load combination

3.3 Evaluation of soil liquefaction
3.4 Seismic design
3.5 Evaluation for uplift due to liquefaction and countermeasaure
3.6 Evaluation of safety by dynamic response analysis
4 Design of Temporary Works for Construction
Chapter 4. Constrction
1 General
2 Planning of Construction
3 Notes for Construction

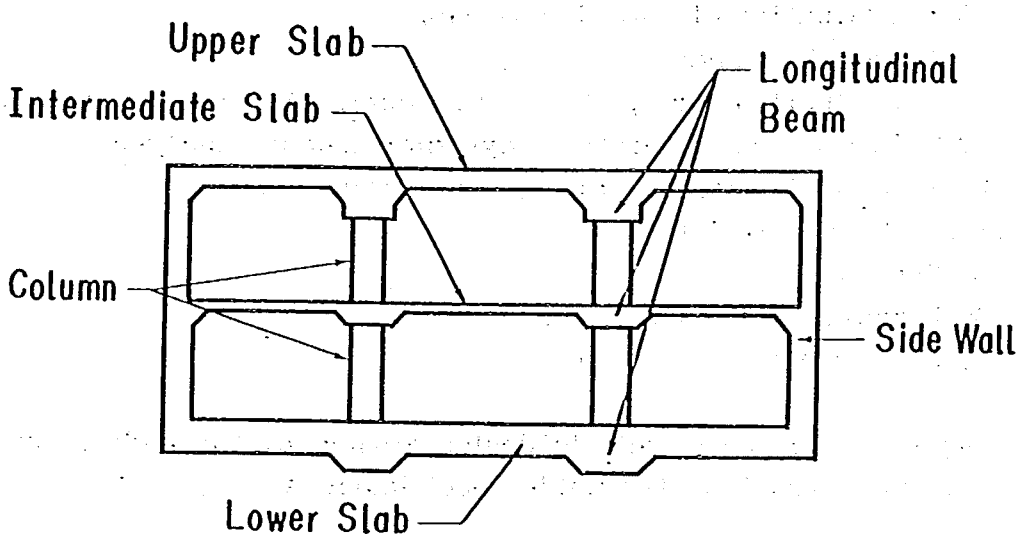
This paper outlines the seismic design method of the underground parking garage structures based on the Guide Specifications.

STRUCTURAL TYPE OF UNDERGROUND PARKING GARAGE

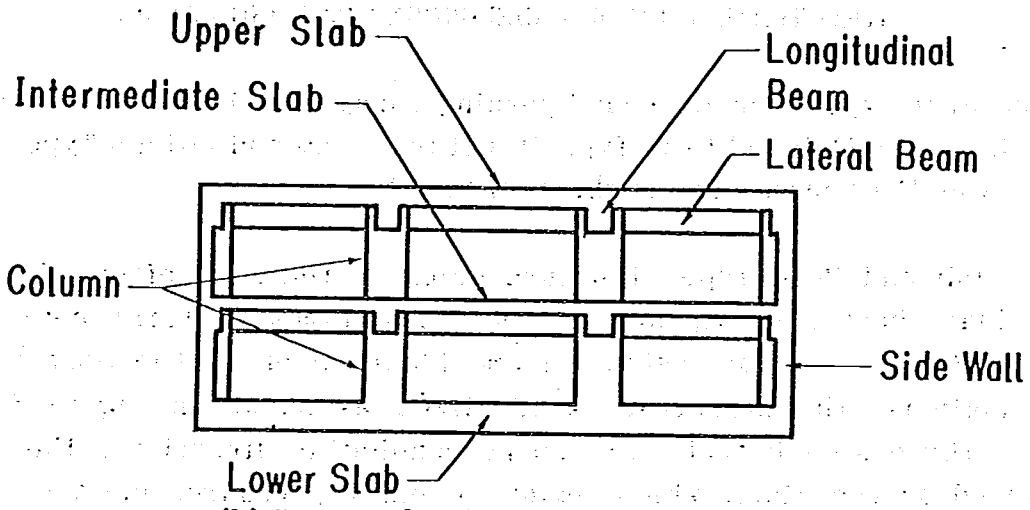
Structural type of underground parking garage may be classified into three groups, i.e., the Slab and Beam Type Structure, Beam and Column Type Structure and Flat Slab Type Structure as shown in Fig. 1.

The Slab and Beam Type Structure which is the most often adopted is of longitudinal beams, slabs, side walls and columns. Lateral beams are not provided. Because two dimensional frame idealization is the most popular in design analysis, the structure is idealized as shown in Fig. 2 for design purpose. The design is made for two perpendicular directions. The side walls are assumed as the plates which resist for earth pressure, and are assumed to be supported by the lateral beams, columns and slabs. Contribution of the slabs is considered in evaluating the equivalent stiffness of longitudinal beams. The upper slab, intermediate slab and lower slab are assumed as beams with the equivalent stiffness. Thus, the structure is idealized as an elastic frame consisting of beams (slabs) and columns as shown in Fig. 2.

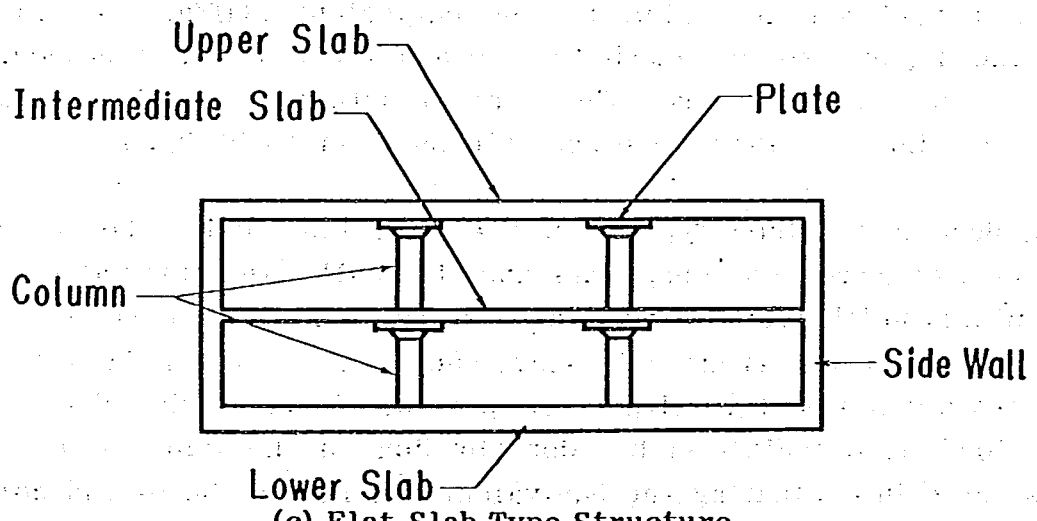
The Beam and Column Type Structure is of longitudinal beams, transverse beams,. lateral beams, columns, slabs and side walls. The side walls are assumed as the plates which resist for earth pressure, and are assumed to be supported by the lateral beams, transverse beams and columns. The slabs are assumed as the plates which resist to either soil pressure (upper slab and lower slab) or vehicle load (intermediate slab). Contribution of the slabs and the side walls is considered in evaluating the equivalent stiffness of beams and columns. The structure is idealized as shown in Fig. 3.



(a) Slab and Beam Type Structure

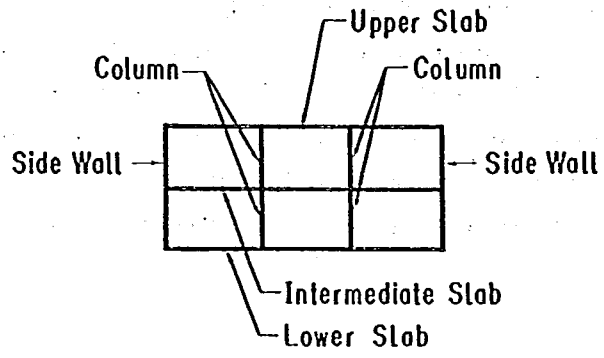


(b) Beam and Column Type Structure

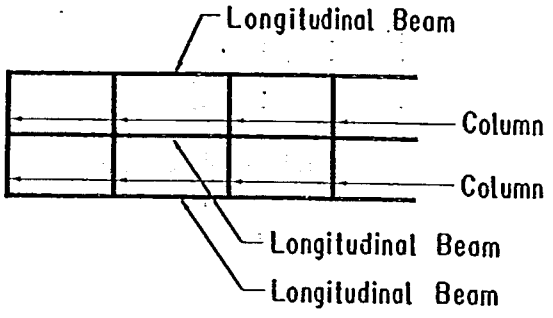


(c) Flat-Slab Type Structure

Fig. 1 Major Structural Type of Underground Parking Garage (2 Story)

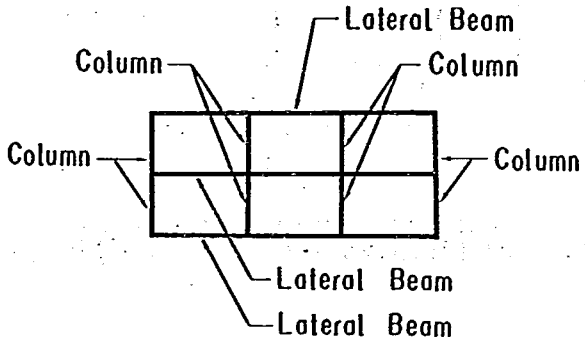


(a) Lateral Direction

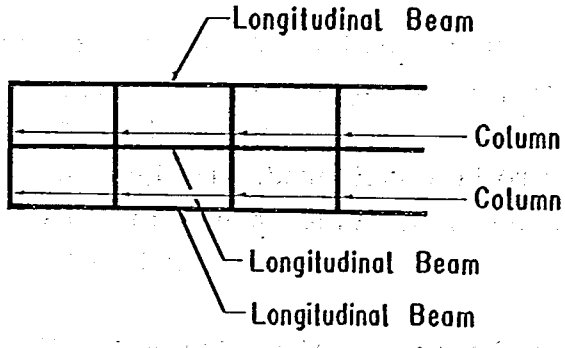


(b) Longitudinal Direction

Fig. 2 Analytical Idealization of Slab and Beam Type Structure



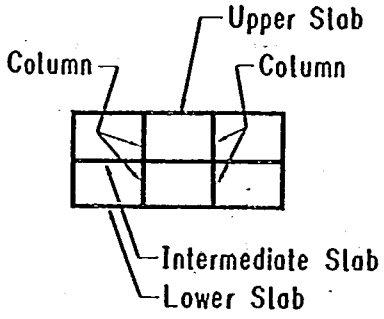
(a) Lateral Direction



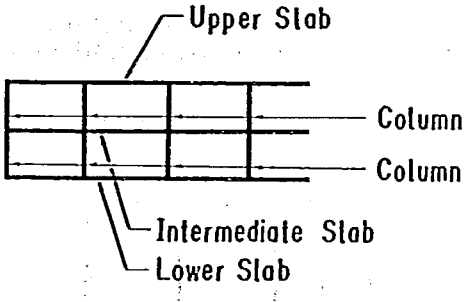
(b) Longitudinal Direction

Fig. 3 Analytical Idealization of Beam and Column Type Structure

The Flat-Slab Type Structure is of slabs, side walls and columns. Because no lateral beams and longitudinal beams are provided, slab-column connections require special attention in their strength. The slabs are assumed as beams with the equivalent stiffness. The side walls are assumed as the plates which resist for earth pressure, and are assumed to be supported by the columns and slabs. The idealization of the Flat Slab Type Structure is shown in Fig. 4.



(a) Lateral Direction



(b) Longitudinal Direction

Fig. 4 Analytical Idealization of Flat Slab Type Structure

DESIGN FORCE AND BASIC PRINCIPLE OF DESIGN

In design of underground parking garage structures, ① dead weight, ② active load (vehicle load), ③ earth pressure, ④ hydraulic pressure, ⑤ uplift force, ⑥ seismic effects, ⑦ load during construction, ⑧ effect of soil settlement and ⑨ other effects have to be considered. All the loads are not always need to be considered in design, and those which are required to be considered have to be selected. Table 1 shows the standard combination of the loads.

The design is made based on the allowable design approach. Design calculations are therefore made assuming the elastic behavior of the

Table 1 Standard Combination of Loads

Loads	Static	Construction Stage	Seismic
Dead Weight	○	○	○
Active Load	○	△	○
Earth Pressure	○	○	○
Hydraulic Pressure	○	○	○
Uplift Force	○		○
Seismic Effects			○
Temporary Load during Construction		○	
Effect of Ground Settlement	△		
Other Loads	△		△

○ has to be considered
△ considered if required

structures. The calculation of forces and stress have to be principally made based on the frame analysis, in which the structure is assumed as a two dimensional frame consisting of beams and columns. Safety has to be examined in the two perpendicular directions.

SEISMIC DESIGN

Basic Principle of Seismic Design

Seismic design is made by the Seismic Deformation Method[2]. In the Seismic Deformation Method, the displacement and deformation developed in the subsurface ground during an earthquake are taken as the major seismic effects to underground structures. The seismic response of underground structures is distinguished by the small mass effect and the large damping ratio from regular structures on ground, i.e.,

a) mass effect is small because unit weight of underground structures is smaller that that of subsurface ground, and

b) damping is very large because radiational damping due to energy dissipation from underground structures to subsoils is very large.

Therefore, it is assumed in the Seismic Deformation Method that underground structures deform following the deformation of subsurface ground during an earthquake. Modelling of underground structures has to be made so that structural response of the underground structures be correctly represented.

Because only the increase of stress and deformation of underground structures due to seismic effects are evaluated by the Seismic Deformation Method, the stress and deformation actually developed during an earthquake have to be computed by adding them with those developed due to the static loads such as the dead weight.

When liquefaction of sandy soil layers is developed around the underground parking garage, the uplift associated with the increase of pore water pressure has to be examined.

Dynamic response analysis is recommended for the underground parking garages with complex structural response.

Loads Considered for Seismic Design

In seismic design, dead weight, earth pressure, water pressure, uplift force, ground settlement and seismic effects are to be considered. The loads have to be combined so that the most critical stress or displacement be developed. As the seismic effects, the following loads have to be considered[3),4)]:

(a) Inertia Force

The lateral force coefficient has to be evaluated as

$$k_h = c_z \cdot c_G \cdot c_U \cdot k_{h0} \qquad (1)$$

where,

k_h : lateral force coefficient

c_z : modification factor for zone (refer to Fig. 5)

c_G : modification factor for ground condition (refer to Table 2)

c_U : modification factor for depth, and is evaluated as

$$c_U = 1.0 - 0.015z \qquad (2)$$

z : depth from ground surface (m)

k_{h0} : standard lateral force coefficient (= 0.2)

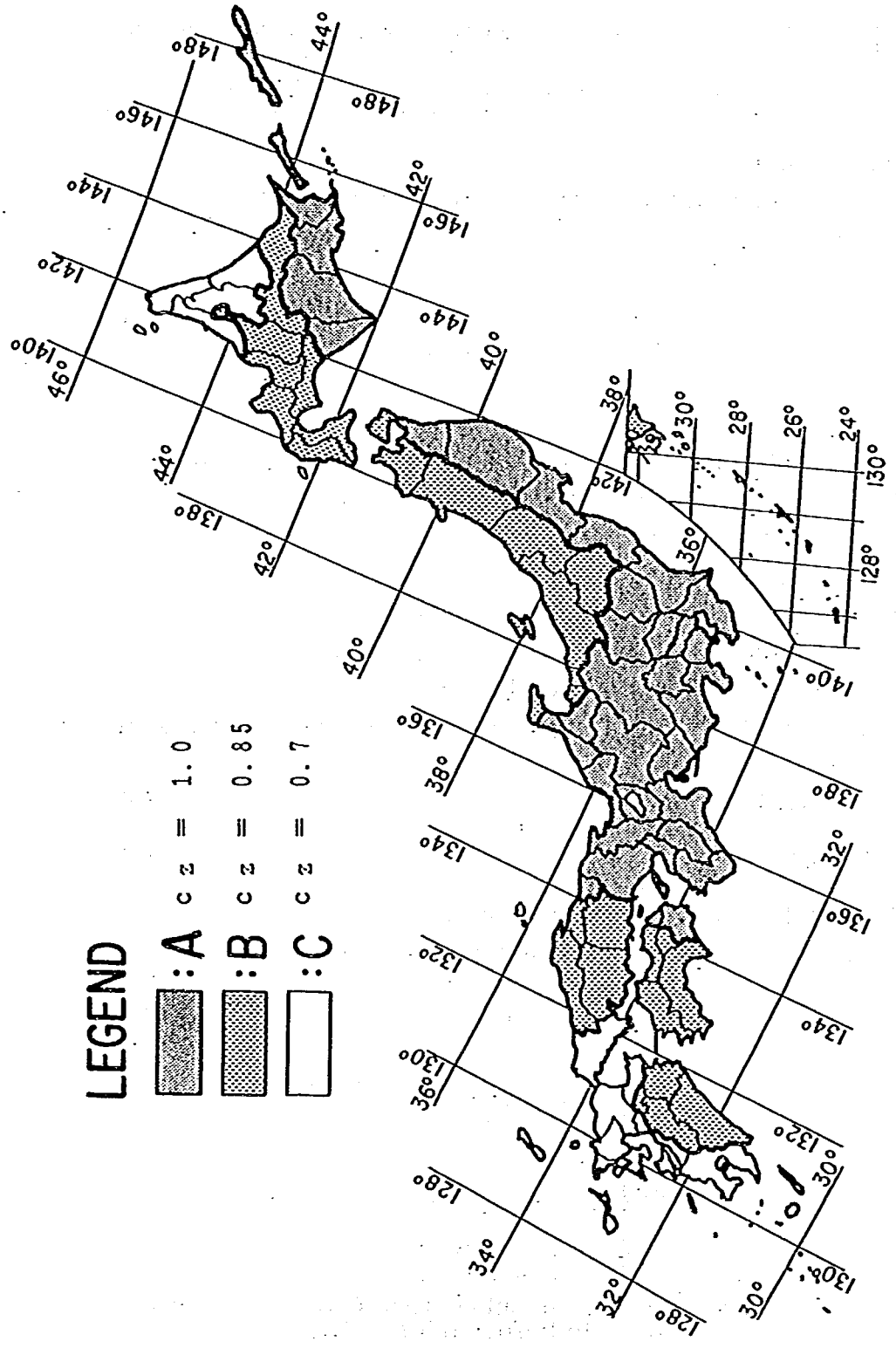


Fig. 5 Modification Factor for Zone

Table 2 Modification Factor for ground Condition

GROUND CONDITION	DEFINITION	APPROXIMATE ESTIMATION
GROUP I	$T_G < 0.2$SEC	TERTIARY OR OLDER
GROUP II	$0.2 \leqq T_G < 0.6$SEC	ALLUVIUM AND DILUVIUM
GROUP III	$0.6\text{SEC} \leqq T_G$	SOFT ALLUVIUM

(b) Design Ground Displacement

The design ground displacement is evaluated depending on the depth as (refer to Fig. 6) :

$$u(z) = \frac{1}{\pi^2} S_V \cdot T_S \cdot \cos\left(\frac{\pi z}{2H}\right) \tag{3}$$

where,

$u(z)$: design ground displacement (m) at depth z (m)

S_V : design velocity response spectrum at design base rock (cm/sec), and is given as

$$S_V = c_Z \cdot S_{VO} \tag{4}$$

c_Z : modification factor for zone (refer to Fig. 5)

S_{VO} : standard velocity response spectrum (cm/sec) at design base rock, and is given by Fig. 7

T_S : natural period of subsurface ground (sec), and is evaluated as

$$T_S = 1.25 \cdot T_G \tag{5}$$

$$T_G = 4\Sigma \frac{H_i}{V_{Si}} \tag{6}$$

H_i : thickness of i-th soil layer (m)

V_{Si} : shear wave velocity of i-th soil layer (m/sec)

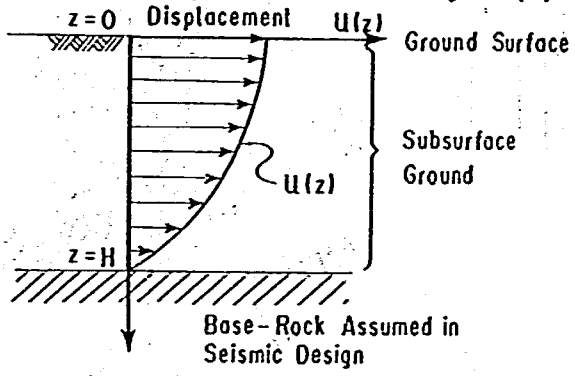


Fig. 6 Deformation of Subsurface Ground Assumed in Seismic Deformation Method

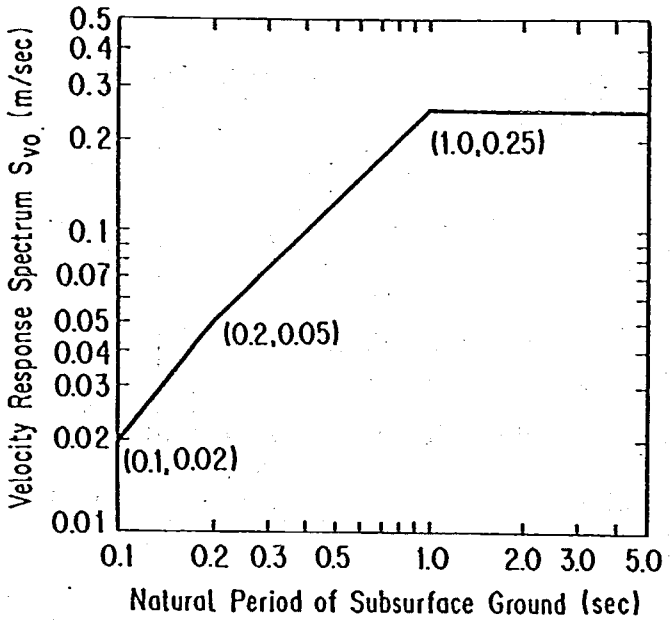


Fig. 7 Standard Velocity Response Spectra

(c) Design Shear Stress around Surface

At the surface of underground parking garage structures contacting with soils, the design shear stress around surface has to be applied to the structure as shown in Fig. 8. The design shear stress around surface is given by Eq. (7). If the design shear stress around surface by Eq. (7) is larger than the strength of soils, the design shear stress around surface shall be the strength of soils.

$$\tau = \frac{G_D}{\pi H} S_V \cdot T_S \cdot \sin\left(\frac{\pi Z}{2H}\right) \qquad (7)$$

where,

τ : design shear stress around surface (tf/m^2)

S_V : design velocity response spectrum at design base rock (cm/sec), and is given by Eq. (4)

G_D : shear modulus of subsurface ground (tf/m^2)

T_S : natural period of subsurface ground (sec), and is computed by Eq.(5)

H : thickness of subsurface ground (m)

(d) Dynamic Earth Pressure

Dynamic earth pressure by Eq. (8) is applied to side walls of underground parking garage structure as shown in Fig. 9.

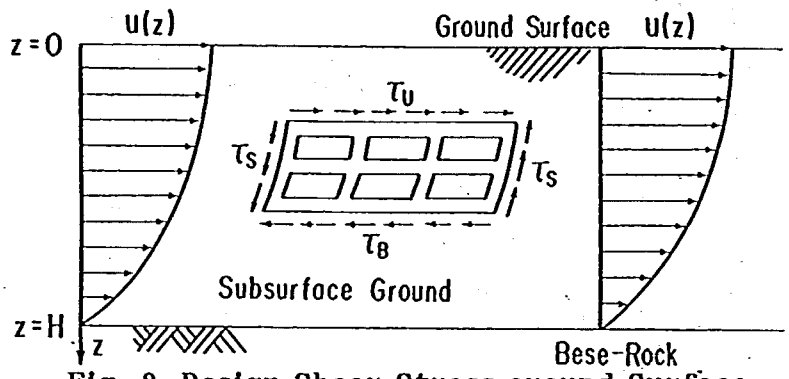


Fig. 8 Design Shear Stress around Surface

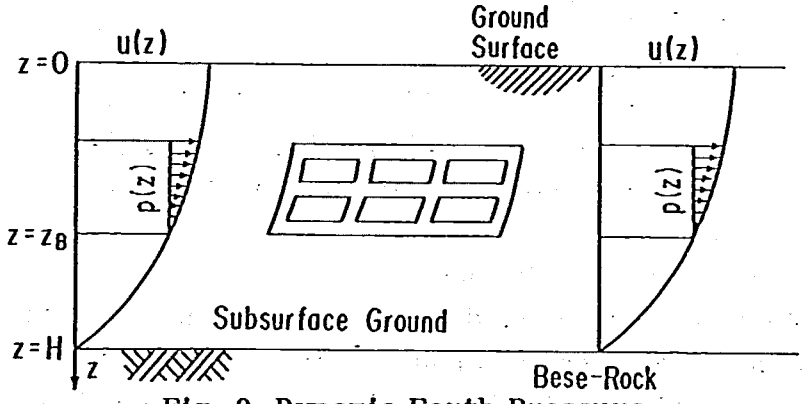


Fig. 9 Dynamic Earth Pressure

$$p(z) = k_H \cdot \{u(z)-u(z_B)\} \qquad (8)$$

where,

p(z) : dynamic earth pressure per unit area (tf/m^2) at depth z (m)

k_H : spring stiffness of soils per unit area (tf/m^2)

u(z) : design ground displacement (m), and is given by Eq. (3)

z_B : depth of base of structure (m)

Effect of Liquefaction

(a) Estimation of Liquefaction

Saturated alluvial sandy layers which have the water table within 10 m from the ground surface and have D_{50}-values on the grain size accumulation curve between 0.02 and 20. mm are vulnerable to liquefaction up to a depth of 20 m below the ground surface.

For those soil layers which were judged to be vulnerable to liquefaction, liquefaction potential shall be checked based on the liquefaction resistance factor F_L[5] defined as

$$F_L = R / L \tag{9}$$

where,

F_L : liquefaction resistance factor

R : resistance of soil elements against dynamic load defined as

$$R = R_1 + R_2 + R_3 \tag{10}$$

$$R_1 = 0.0882\sqrt{\frac{N}{\sigma_v' + 0.7}} \tag{11}$$

$$R_2 = \begin{cases} 0.19 & (0.02\ \text{mm} \leqq D_{50} \leqq 0.05\ \text{mm}) \\ 0.225 \log_{10}(0.35/D_{50}) & (0.05\ \text{mm} < D_{50} \leqq 0.6\ \text{mm}) \\ -0.05 & (0.6\ \text{mm} < D_{50} \leqq 2.0\ \text{mm}) \end{cases} \tag{12}$$

$$R_3 = \begin{cases} 0.0 & (0\ \% \leqq F_C \leqq 40\ \%) \\ 0.004F_C - 0.16 & (40\% < F_C \leqq 100\ \%) \end{cases} \tag{13}$$

N : N-value of standard penetration test

D_{50} : averaged grain size on grain size accumulation curve

F_C : fine sand (grain size less than 74 μm) content

L : dynamic load induced in soil elements during an earthquake defined as

$$L = k_s \frac{\sigma_v}{\sigma_v'} \tag{14}$$

k_s : seismic coefficient for evaluating liquefaction, and shall be determined as

$$k_s = c_z \cdot c_G \cdot c_u \cdot k_{s0} \tag{15}$$

c_z and c_G : modification factors for zone and ground condition (refer to Fig. 5 and Table 2)

c_u : modification factor for depth, and is given by Eq. (2)

k_{s0} : standard design horizontal seismic coefficient for check of liquefaction (= 0.15)

σ_v: total overburden pressure (kgf/cm^2), and

$$\sigma_v = \{\gamma_{t1} h_w + \gamma_{t2} (z - h_w)\} / 10 \tag{16}$$

σ_v': effective overburden pressure (kgf/cm^2), and

$$\sigma v' = \{\gamma_{t1} h_w + \gamma_{t2}' (z - h_w)\} /10 \quad (17)$$

z : depth from ground surface (m)
h_w : depth of water table (m)
γ_{t1} : unit weight of soils (tf/m^3) on water table
γ_{t2} : unit weight of soils (tf/m^3) under water table
γ_{t2}' : effective unit weight of soils (tf/m^3) under water table, and is given as

$$\gamma_{t2}' = \gamma_{t2} - 1.0 \quad (18)$$

Soil layers having the liquefaction resistance factors, F_L, smaller than 1.0 shall be judged to liquefy during an earthquake.

(c) Treatment of Liquefaction

If the soils underneath the bottom of underground parking garage structure is judged to develop liquefaction, countermeasures have to be considered regardless of the degree of uplift. There are basically three measures for the liquefaction as shown in Table 3. The first is to excavate the soils which liquefy during an earthquake for placing the bottom of the structure on deeper stable soil layers. The second method is to strengthen the foundation of the structure. The foundation should be designed strong enough for uplift force. Consideration should be paid to the settlement after an earthquake due to liquefaction. The third is to prevent the liquefaction by either replacing or strengthening the soils. The appropriate countermeasures have to be selected considering effectiveness and cost.

Table 3 Countermeasures for Soil Liquefaction

<table>
<tr><td colspan="3">Place the bottom at deeper stable soil layer</td></tr>
<tr><td colspan="2">Strengthening of Foundation</td><td>Use of Piles</td></tr>
<tr><td rowspan="2">Prevention of Liquefaction</td><td>Increase of Soil Density</td><td>Vibro Floatation, Sand Compaction Rod Compaction</td></tr>
<tr><td>Improvement of Grain Size or Solidification</td><td>Replacement, Injection, Deep Mixing</td></tr>
</table>

When there are soils which have the liquefaction resistance factor $F_L < 1.0$ at side of the underground parking garage as shown in Fig. 10, the uplift of the structure has to be checked even if the soil layers under the bottom of the structure are stable against liquefaction. This is because the pore water pressure at the side of the structure tends to propagate to result in the

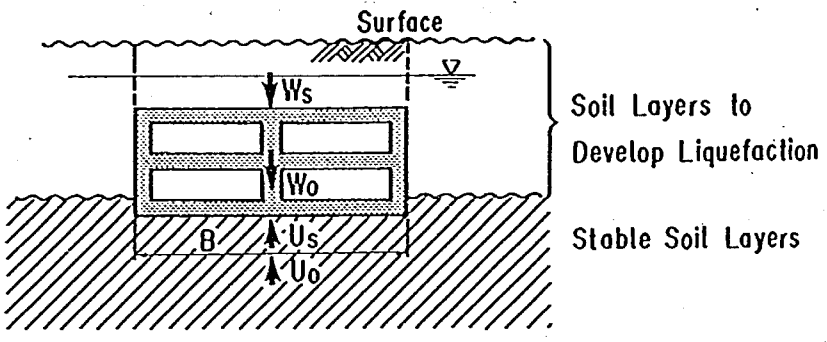


Fig. 10 Check against Uplift due to Soil Liquefaction developed at Side of Structure

propagate to result in the increase of the pore water pressure at the bottom of the structure. It is usual to have water-path due to disturbance during excavation. The safety against uplift shall be examined as

$$F_S = \frac{W_S + W_B}{U_S + U_D} \qquad (19)$$

where,

F_S : safety factor against uplift

W_S : weight of overburden soils (tf)

W_B : weight of underground parking garage (tf)

U_S : uplift force due to static hydraulic pressure (tf)

U_D : uplift force due to increase of pore water pressure associated with liquefaction (tf), and shall be evaluated as

$$U_D = \Delta_u \cdot A = L_u \cdot \sigma_v' \cdot A \qquad (20)$$

Δ_u : pore water pressure (tf/m^2)

A : sectional area of bottom of structure (m^2)

L_u : pore water pressure ratio ($L_u = \Delta_u / \sigma_v'$)

σ_v' : effective overburden pressure (tf/m^2) at surface of stable soil layer

If the safety factor F_S is less than 1.0, measures against the uplift have to be taken.

Dynamic Response Analysis

Dynamic response analysis is recommended for the underground parking garage structure with complex structural response. In the dynamic response

analysis, design acceleration response spectrum at the design base rock is given as

$$S = c_Z \cdot c_D \cdot S_0 \qquad (21)$$

where,

S : design acceleration response spectrum (cm/sec) at design base rock

c_Z : modification factor for zone (refer to Fig. 5)

c_D : modification factor for damping ratio, and is given as

$$c_D = \frac{1.5}{40h_i + 1} + 0.5 \qquad (22)$$

h_i : modal damping ratio of critical for i-th mode

S_0 : standard acceleration response spectrum at design base rock, and is given by Fig. 11

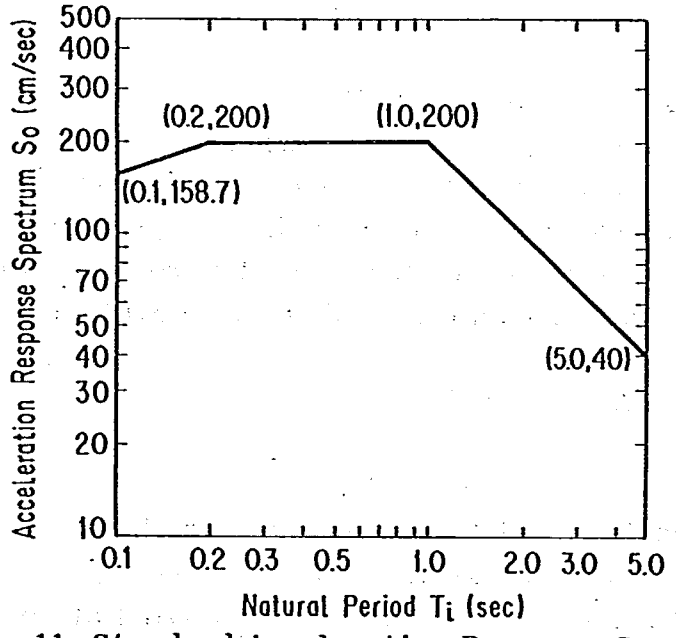


Fig. 11 Standard Acceleration Response Spectrum for Dynamic Response Analysis

Input accelerations for time response analysis shall be either selected from strong motion records which have the close response spectral characteristics with S by Eq. (22) or obtained by adjusting the strong motion records in frequency domain so that the acceleration response spectrum be matched with S by Eq. (22).

STRUCTURAL DETAILS

In addition to design calculation, attention should be paid to structural details. Table 4 summarizes the major structural details. Special attention is placed on the amount of tie and stirrup reinforcement.

Table 4 Major Structural Details

Beam	① $A_s \geqq 0.005bd$ where A_s: reinforcement in tension (cm^2) b : height of beam (cm) d : effective width of beam (cm) ② Interval of stirrup should be less than 1/2d or 25cm. ③ Stirrup ratio ≧ 0.2%
Column	① Diameter of main reinforcement ≧ 13mm ② Number of main reinforcement ≧ 4 ③ Main reinforcement ratio ≧ 0.8% ④ Diameter of tie reinforcement ≧ 13mm ⑤ Interval of tie reinforcement ≦ 1/2d ≦ 15mm ≦ 12 ϕ where d : smaller size (width) of column ϕ : diameter of main reinforcement ⑥ Tie reinforcement ratio ≧ 0.2% ⑦ Minimum width of column ≧ 30cm
Beam-Column Connection	① At column between ±2 times larger width of column from the beam-column connetion a) Interval of tie reinforcement ≦ 10cm b) Tie reinforcement ratio ≧ 0.3% ② At beam between ±2 times height of beam from the beam-column connetion a) Interval of stirrup ≦20cm b) Stirrup ratio ≧0.3%
Slab	① Thickness ≧ 20cm ② Diameter of reinforcement ≧ 13mm ③ Interval of main reinforcement ≧ 125mm ④ Interval of sub reinforcement ≧ 200mm
Structural Wall	① Thickness ≧ 20cm ≧ 1/30×Height ② Double-sided reinforcement ③ Reinforcement ratio ≧ 0.25% ④ Interval of reinforcement ≧ 30cm

CONCLUDING REMARKS

The preceding pages presented the outline of the seismic design method of

reinforced concrete underground structure for parking garage based on the Guide Specifications of Design and Construction of Park Garage issued by the Ministry of Construction in March 1992. Although there are various specifications which describes seismic design method of underground structures of road, most of them are for specific projects. This is the third specifications, following the petroleum pipe line[6] and common utility ducts[7], which comprehensively specifies seismic design method of underground facilities of road. Because seismic safety is one of the most critical issues, it is expected that the specifications contribute for design and construction of underground parking garage with enough seismic safety.

ACKNOWLEDGEMENT

Drafting of the Guide Specifications was made in a Working Group formulated in the Subcommittee of Parking Garage, Japan Road Association.

REFERENCES

1) Japan Road association : Guide Specifications of Design and Construction of Parking Garage, 1992 (in Japanese)
2) Ministry of Construction : New Seismic Design Methods, Technical Note, No. 1185, Public Works Research Institute, March 1977 (in Japanese)
3) Public Works Research Institute : Guidelines for Seismic Design Methods of Underground Structures, Technical Note, March 1992 (in Japanese)
4) Asakura, H., Kawashima, K. and Sugita, H. : Guidelines for Seismic Design Methods of Large Underground Structures, Proc. 24th Joint Meeting, Panel on Wind and Seismic Effects, UJNR, Gaithersburg, Maryland, U.S.A., May 1992
5) Japan Road Association : Part V Seismic Design , Specifications of Design of Highway Bridges, 1990
6) Japan Road Association : Technical Standard for Petroleum Pipeline, June 1971 (in Japanese)
7) Japan Road Association : Design Method of Common Utility Ducts, March 1986 (in Japanese)

Session-7

Bridge

U-7) Caltrans' Foundation Seismic Research Program
(Roblee, C.J.)

J-15) Seismic Strengthening and Retrofitting of Highway Bridges in Japan
(Kawashima, K. and Unjoh, S.)

U-8) Research Based Bridge Seismic Design and Retrofit Program Criteria, Standards and Status
(Roberts, J.E.)

CALTRANS' FOUNDATION SEISMIC RESEARCH PROGRAM

Clifford J. Roblee
DNTMR, Office of Geotechnical Engineering

ABSTRACT: An overview of the Caltrans-sponsored research program focused on the seismic performance of substructures is presented. A current listing of projects sponsored by each of two Divisions is tabulated. Selected projects related to ground-motion prediction and foundation performance are discussed individually.

1. Introduction

In response to the recommendations of the Governor's Board of Inquiry into the Loma Prieta Earthquake of 1989, Caltrans initiated a comprehensive research effort to examine various aspects of the seismic behavior of bridge structures. A large proportion of this work is administered by the Division of Structures (DOS) which has reviewed more than 130 research proposals, and let more than 40 contracts worth in excess of $8 million to both public and private organizations. This research is supported with both special state (SB-36) funds as well as conventional federally-matched highway research (SP&R) allocations. The DOS seismic research program focuses on all aspects of seismic bridge design including subsurface considerations such as regional and local seismicity, ground response characterization, and substructure performance. For information on the broader structural-related seismic research sponsored by DOS, the reader is directed to the following references {1,2,3}.

The Division of New Technology, Materials and Research (DNTMR) within Caltrans provides both internal-staff studies and external-contract research on a wide variety of transportation-related topics while providing numerous specialty services to both DOS and Caltrans Districts. The Offices of Geotechnical Engineering and Engineering Geology within DNTMR routinely provide both site-specific ground response analyses and subsurface characterization information, respectively, to DOS. Seismic research administered by DNTMR is complementary to the larger DOS program, and is funded exclusively through SP&R allocations. The seismic research performed by DNTMR is focused primarily on subsurface considerations including site and material characterization, ground response analysis, and field load testing of foundations.

This paper is intended to provide a current overview of the seismic foundation-related research program sponsored by Caltrans. The overall scope of the program is reflected in Table 1 which provides a listing of the current projects administered by both DOS and DNTMR along with the project identification, Caltrans manager, principal investigators, research organization, current status, and

#	Project	Project Type/ID/ Contract or EA	Manager/ Division	Investigators/ Organization	Status/ Term	Approx. Budget
Performance During Loma Prieta						
1	Evaluation of Dumbarton Bridge Response in the Loma Prieta Earthquake.	Contract w/UCB ID: 59I5D86 RTA 59N206	Sheng @ DOS	Fenves @ UC-Berk	100% Complete 5/90 - 6/91	$50,000
2	Phase I: Inspection and Data Collection on the Substructure of the Bay Bridge. Phase 2: Seismic Condition Assessment of the Bay Bridge.	Contract w/UCB Ph1 ID: F90SD23 Ph1 RTA 59N062 Ph2 ID: 59I5D88 Ph2 RTA 59N580	Sheng @ DOS	Astaneh, Bolt, Lysmer, Powell, Fenves, Monteiro, Stephen @ UC-Berk	90% Complete 1/90 - 12/92 50% Complete 1/90 - 6/93	$50,000 $637,000
Seismic Response Studies						
3	Seismic Evaluation of Northern California Bridge Sites.	Consultant Contract # 59N772	Wilhelms @ DNTMR	Powers @ Geomatrix	75% Complete 11/91 - 3/93	$900,000
4	Seismic Evaluation of Southern California Bridge Sites.	Consultant Contract # 59N771	Mealchin @ DOS	Moriwaki @ Woodward-Clyde in Santa Ana	50% Complete 2/92 - 12/92	$371,000
5	Multiple-Support Response Spectrum Analysis of Bridges.	Contract w/UCB ID: not assigned	Kirkland @ DOS	Der Kiureghian @ UC-Berk	0% Complete 1/93 - 6/94	$94,000
6	Seismic Analysis of the San Francisco-Oakland Bay Bridge	Contract w/UESC ID: 59I5D87 RTA: 59N616		Duggan @ GENSYS/UESC	In Contract Execution	$170,000
Ground-Motion Prediction						
7	Seismic Response of Deep Soil Sites in the San Francisco Bay Area.	Contract w/UCB ID: 59I5D85 RTA 59N224	Mealchin @ DOS	Seed, Lysmer @ UC-Berk.	80% Complete 7/90 - 6/93	$315,000
8	Comparison of Geophysical Methods for In Situ Velocity Measurement - Islais Site.	Internal Minor ID: F92RM01 EA: 638005-32138		Roblee @ DNTMR	60% Complete 2/92 - 12/92	$13,000
9	Examination of the Impact of Updated Soil Models on Caltrans Standard ARS.	Internal Minor ID: F93RM01 EA: 638041-33152		Shantz, Roblee @ DNTMR	25% Complete 8/92 - 1/93	$10,000
10	Response of Soil Sites During Strong Seismic Shaking.	Contract w/UCD ID: F92SD29 RTA 59T342	Moese @ DOS	Idriss, Kutter, Li @ UC-Davis	10% Complete 8/92 - 8/93	$125,000
11	Development of a Prototype Tool for In Situ Determination of High-Strain Dynamic Properties of Soft to Medium-Stiff Clays.	Contract w/UCD ID: F92TL05 RTA: 65T324	Roblee, Jackura @ DNTMR	Li, Idriss, Herrmann @ UC-Davis Chan @ UC-Berk.	5% Complete 8/92 - 6/95	$709,000
12	Review of Soil Amplification Provisions in Current World-Wide Seismic Design Codes.	Internal Minor ID: F93RM01 EA: 638041-33151		Shantz, Roblee @ DNTMR	5% Complete 9/92 - 3/93	$10,000
13	Evaluation of Non-linear Seismic Site Response Models.	Contract/Internal ID: F92TL13	Roblee @ DNTMR		In Proposal	$70,000
14	Strong-Motion Instrumentation of Subsurface Profiles.	Contract ID: F92TL14	Roblee @ DNTMR		In Proposal	$230,000
Soil-Structure Interaction						
15	Improved Mathematical Idealizations to Include Foundation Effects on the Seismic Response of Highway Bridges.	Contract w/UCB ID: F78SD15 RTA 59F453	Gates @ DOS	Penzien @ UC-Berk Imbsen @ Imbsen & Assoc.	100% Complete 7/81 - '90	$398,000
16	Parametric Studies for the Seismic Modeling of Two-Level Elevated Freeways: Work Package 11.	Contract w/Cygna		Ghose @ Cygna Group	100% Complete 11/89 - 6/91	
17	Implementation of Advanced Soil-Structure Interaction Techniques for Analysis of Bridge Structures.	Contract w/C. A. ID: 59I5D13 RTA 59S035	Mitchell @ DOS	Sweet @ Coast Analytics	30% Complete 4/92 - 4/93	$82,000
18	Development and Evaluation of Dynamic Soil-Pile Interaction Models, Phase I.	Internal Minor ID: F93RM01 EA: 638041-33155		Slyh, Jackura @ DNTMR	20% Complete 9/92 - 12/92	$10,000
19	Development & Implementation of Impr. Seismic Design and Retrofit Procedures for Bridge Abutments.	Contract w/USC ID: not assigned		Martin @ USC	In Contract Execution	$122,000
20	Pile Survivability and Soil-Pile Interaction.	Internal Minor ID: F93RM01 EA: 638041-331xx		Slyh, Jackura @ DNTMR	In Proposal 10/92 - 3/93	$10,000
Review of Design Procedures						
21	ATC-32 Review and Revise Standards, Performance Criteria, Specifications and Practices for the Design of New Bridge Structures and Rehab of Existing Structures.	Contract w/ATC ID: 59I5D11 RTA 59N203	Sultan @ DOS	Rojahn, Nutt @ Applied Technology Council	40% Complete 8/91 - 12/93	$555,000
22	Study of Caltrans' Seismic Evaluation Procedures for Short Bridge Overcrossing Structures.	Contract w/D&M ID: 59I5D15 RTA 59Q122	Huang @ DOS	Werner @ Dames & Moore	10% Complete 8/92 - 7/93	$312,000
Structural Aspects of Substructures						
23	Experimental Testing of Epoxy-Injected Steel Shell Retrofitted Sections from the Collapsed Struve Slough Bridge - Phase 1 and 2.	Contract w/UCD ID-Ph1: 59I5D82 ID-Ph2: F92SD28 RTA-Ph1: 59N204 RTA-Ph2: 59S814	Travis @ DOS	Ramey, Ramstad @ UCD	50% Complete 1/90 - 7/93	$100,000
24	Seismic Retrofit of Bridge Column Footings.	Contract w/UCSD ID: F91SD80 RTA 59M494	Mitchell @ DOS	Priestley, Seible @ UC-San Diego	25% Complete 10/91 - 6/93	$375,000
Field Load Tests						
25	Lateral Load Tests on Driven Pile Footings at Cypress Viaduct.	Demolition Contract w/ Christie Const.	Jensen @ DOS	Abearius @ DOS	100% Complete 11/89 - 2/90	~$45,000
26	Full-Scale Medium-Level Vibration Test at Meloland Road Overcrossing.	Contract w/UNR ID: F88SD16 RTA 59G454	Klein @ DOS	Douglas @ UN-Reno	90% Complete 1/88 - 2/93	$375,000
27	Full-Scale Lateral Load Test of Large-Diameter Drilled Shafts Founded in Fractured Rock.	Design-Phase Contract for DOS EA: 04-191794	Seaberg @ DOS	Speer @ DNTMR	75% Complete 10/91 - 12/92	$300,000
28	Experimental Measurement of Bridge Abutment Behavior; Stiffness, and Ultimate Strength Characteristics.	Contract w/UCD ID: 59I5D10 RTA 59Q183	Moese @ DOS	Ramstad, Kutter @ UCD Maroney @ DOS	50% Complete 4/91 - 9/93	$423,000
29	Tension and Compression Testing of 9 Pile Types in Bay Muds Underlain By a Firm Stratum.	Construction-Phase Contract for DOS EA: 04-191794	Mason @ DOS	Speer, Morris @ DNTMR Mason @ DOS	50% Complete 11/91 - 6/93	$750,000

Table 1. Summary of current Caltrans-sponsored seismic foundation research projects.

total budget for each project. Note that both the status and budget figures appearing in Table 1 are approximate. For purposes of providing a framework for discussion, the projects have been grouped into broad categories such as "ground motion prediction". It should be recognized that many projects overlap into several of these categories. Within a particular grouping, the projects are listed in descending order according to the approximate completion status.

The remainder of this paper will provide both a brief review of the general objectives of each project listed in Table 1, as well as a more detailed discussion and some preliminary findings from selected projects for which the author has greater familiarity. In-depth results are beyond the scope of this paper, therefore, the reader is encouraged to contact the appropriate project manager listed in Table 1 for additional information and/or reports pertaining to specific topics of interest. To facilitate project identification in the remainder of the text, numbers appearing in square brackets (e.g. [1]) will denote the project number appearing to the extreme left in Table 1.

2. Performance During Loma Prieta [1, 2]

Shortly after the Loma Prieta earthquake of 1989, research contracts were let by Caltrans DOS to perform preliminary investigations on each of two long multi-span Bay Area bridges. First, the dynamic response of the Dumbarton Bridge was examined because of the extensive data set which was collected during the event by a network of 24 strong-motion accelerometers installed on the structure. Second, documentation of damage sustained by the East Crossing of the Bay Bridge was collected. Detailed presentations on each of these projects can be found elsewhere, therefore, discussion herein will be brief.

The data recorded at the Dumbarton Bridge provides a unique case history of the seismic response of a long structure which is partially founded within deep soft clay. Records from the Loma Prieta event indicate that significant soil amplification effects occurred, and that over 60 seconds of strong bridge response were caused by approximately 30 seconds of free-field input motion. Fenves et al [1] {4, 5, 6} of the University of California at Berkeley (UCB) analyzed the dynamic response of the bridge-foundation-soil system using a linear elastic model having 6500 elements and 12,600 degrees of freedom. Embedded portions of substructure components were modeled with translational and rotational springs according to a method developed by Novak. Free-field ground motion was prescribed at the foundation elements using a combination of recorded and calculated displacement histories which varied along the length of the bridge. Analysis results indicate excellent correlation with recorded mode periods, and reasonable correlation with recorded displacement histories. These investigators conclude that bridge response modeling is very sensitive to both the varying input motion specified along the length of the bridge, and to assumptions regarding modeling of the foundations. An additional investigation into the seismic response of the Dumbarton Bridge has been proposed

by Heuze of LLNL, and will take advantage of supplemental subsurface information which Caltrans is currently acquiring.

The unsatisfactory performance of the East Crossing of the Bay Bridge during the Loma Prieta event focused intense scrutiny on the anticipated structural behavior of this system during future events. Shortly after the earthquake, both Caltrans and NSF provided funds to Astaneh [2, phase 1] of UCB to perform preliminary research which focused on a detailed documentation of the "perishable data" pertaining to damage sustained by the structure. These and other results were compiled into the Governor's Report {7} which concluded that there was no evidence of foundation failure in terms of settlement, displacement, or loss of bearing capacity. However, it also states that soil-structure interaction at the piers may have influenced the dynamic response of the bridge. A comprehensive state-of-the-art seismic assessment of the Bay Bridge is currently underway by a group of UCB researchers under the general direction of Astaneh [2, phase 2] {8, 9}.

3. Seismic Response Studies [3, 4, 5, 6, 7]

Several investigations are underway which focus on various aspects of the seismic response of certain Caltrans structures. The studies identified in this and the following section on "ground motion prediction" are closely related. However, the investigations discussed here are primarily from the perspective of the seismologist, while those presented in the following section are oriented toward the geotechnical engineering perspective.

Two separate investigations are underway to characterize local seismicity in terms of both deterministic and probabilistic analyses for specific major bridge sites in northern and southern California. Although these projects are not part of the official research program of Caltrans, both investigations represent current state-of-the-art assessments, and are viewed as contributing to the overall seismic research goals of Caltrans. Geomatrix [3] was selected to perform seismic evaluations for Northern California bridge sites including: 1) San Joaquin River Antioch Bridge, 2) Dumbarton Bridge, 3) Richmond - San Rafael Bridge, 4) West Crossing of the Bay Bridge, 5) San Mateo - Hayward Bridge, and 6) three Humboldt Bay Crossings. Woodward-Clyde of Santa Anna [4] was selected to perform seismic evaluations for Southern California bridge sites including: 1) San Diego Coronado Bridge, 2) Vincent Thomas Bridge, 3) Gerrald Desmond Bridge, and 4) Schulerheim Bridge. In addition to providing a characterization of local seismicity, these investigations are expected to provide both maximum credible rock spectra and representative rock acceleration histories for each of the sites.

The impact which incoherent seismic ground motions may have on the dynamic response of bridge structures is receiving serious attention by a number of investigators under Caltrans sponsorship. Eidinger and Abrahamson {10} identify the mechanisms of incoherence for long structures in terms of attenuation with distance from a fault, out-of-phase arrivals associated with non-horizontal wave

fronts, scattering boundaries within a profile, and near-source effects associated with the passage of the fault rupture. These investigators are expected to begin a research project with Duggan of GENSYS/UENC [6] to evaluate the impact incoherence has on the dynamic response of the East Crossing of the Bay Bridge. This investigation will also focus on a state-of-the-practice assessment of the Bay Bridge to supplement the state-of-the-art investigation by UCB. As part of a separate UCB effort sponsored by Caltrans [7], Lysmer and Deng [11] have developed a new finite element method to perform 2-D analyses of ground response. This method utilizes "hyperelements" to reduce the requisite number of elements for large dynamic models, and therefore can be efficiently implemented on a microcomputer. This method is capable of modeling response to both inclined body waves and surface waves. Finally, Der Kiureghian [5] will utilize a newly developed response-spectrum method for multiple-support structures [12] for the seismic analysis of a viaduct in San Francisco. This new method recognizes the variability in ground motion associated with differing soil profiles over short distances as well as the incoherence effects previously discussed for longer structures.

4. Ground Motion Prediction

The significance of site amplification effects were fully recognized after the engineering community witnessed the concentration of destruction in localized regions underlain by soft soil deposits during both the 1985 Mexico City and the 1989 Loma Prieta earthquakes. The collapsed portions of the Cypress Freeway were founded almost exclusively within profiles containing soft clay soils. In response to these events, Caltrans began to re-examine its procedures for specification of ground motion, particularly for soft soil sites.

Caltrans utilizes a response spectrum approach for the seismic design of most bridge structures. Standard procedure since the 1970's involves specification of design spectral acceleration values from a family of "standard ARS" curves which appear in the Caltrans manual called Bridge Design Specifications [13]. The appropriate ARS curve is selected on the basis of both a seismicity map and the depth of alluvium at a site. Since the Loma Prieta event, site-specific ground response predictions are being developed for selected structures which are either founded on soft soil profiles or are identified as "important" (usually in terms of providing secondary life safety).

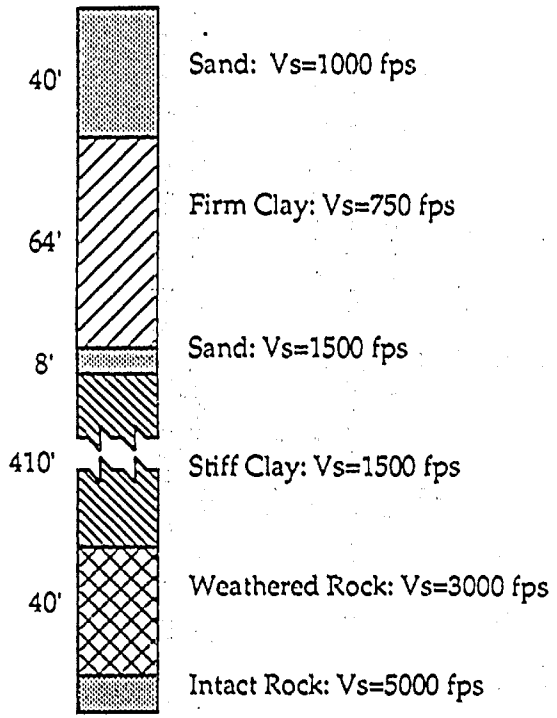
Caltrans is currently sponsoring several research projects related to geotechnical ground-motion prediction. This effort is a combination of both internal staff and contract projects directed toward improvements in site-specific material characterization capabilities, verification of analysis procedures, and development of improved standard ARS. Each of these topics will be discussed in this section after first providing some background on current site-specific procedures.

4.1 Current Caltrans Site-Specific Design Procedures

Site specific ground response predictions are performed within Caltrans by the Office of Geotechnical Engineering at DNTMR. Standard procedure [14] utilizes the program SHAKE [15, 16] along with site-specific characterization of both the input bedrock motions and the soil profile. The input bedrock motions are established using one of several alternative procedures, and typically involve formulation of a site-specific target spectrum based primarily on methodology originally proposed by Sadigh et al [17] and later updated by Geomatrix [18]. The target spectrum is scaled such that the spectral value at "zero" period matches the peak bedrock acceleration established on the basis of both seismic maps and various published attenuation relationships. Once the site-specific target spectrum is established, either a suite of at least three bedrock acceleration histories are established by modifying selected earthquake recordings to match the target spectrum, or a larger suite of recordings is selected and scaled to collectively "fill" various spectral regions of the target spectrum.

Soil profile characterization is accomplished through a combination of routine geotechnical investigation techniques and in situ seismic testing. Site stratigraphy is established using a combination of historical drilling logs, cone penetration data for softer near-surface layers, and conventional drilling and sampling techniques into bedrock. Low-strain modulus for the various stratigraphic units is established using one or more of a variety of in situ seismic techniques. High-strain normalized-modulus-degradation and hysteretic-damping properties of soils are established on the basis of published curves [19, 20]. Both sets of curves provide estimates of dynamic properties to approximately 1% shear strain, and must be extended to 10% shear strain in order to facilitate analysis of many sites of concern. This extension is made by assuming a stress-strain curve which accounts for either the measured or correlated strength of a soil under dynamic loading. (Please note that a previous reference [14] on this topic contains an error. If clarification is needed, feel free to contact DNTMR, Office of Geotechnical Engineering)

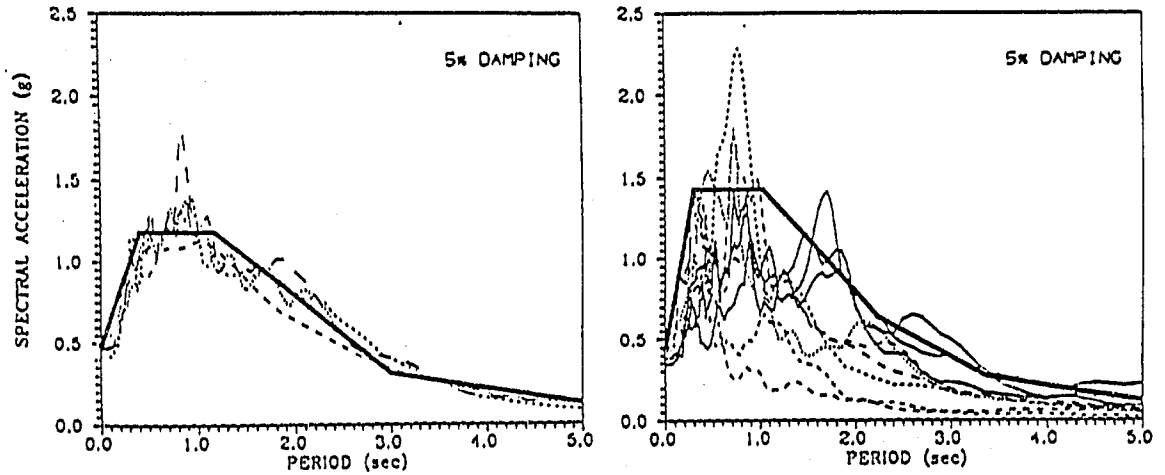
The soil-profile and bedrock-motion information established using the above procedures are input into the SHAKE program to determine free-field ground response. The sensitivity of the results to potential variations in material properties is typically considered. All analysis output is scrutinized for obvious errors as well as potentially excessive values of both shear stress and shear strain. A suite of output response spectra for the various input motions are then plotted, and engineering judgment is utilized to establish a design envelope which encompasses the majority of the spectral content exhibited by the record suite. Figure 1 presents example results from utilization of this methodology. The upper pair of spectral plots shows both individual response from a number of separate input motions along with a design envelope which is drawn to encompass the majority of spectral energy. The left-hand plot utilized acceleration histories which were modified to a target spectrum, while the right-hand figure utilized a larger suite of acceleration



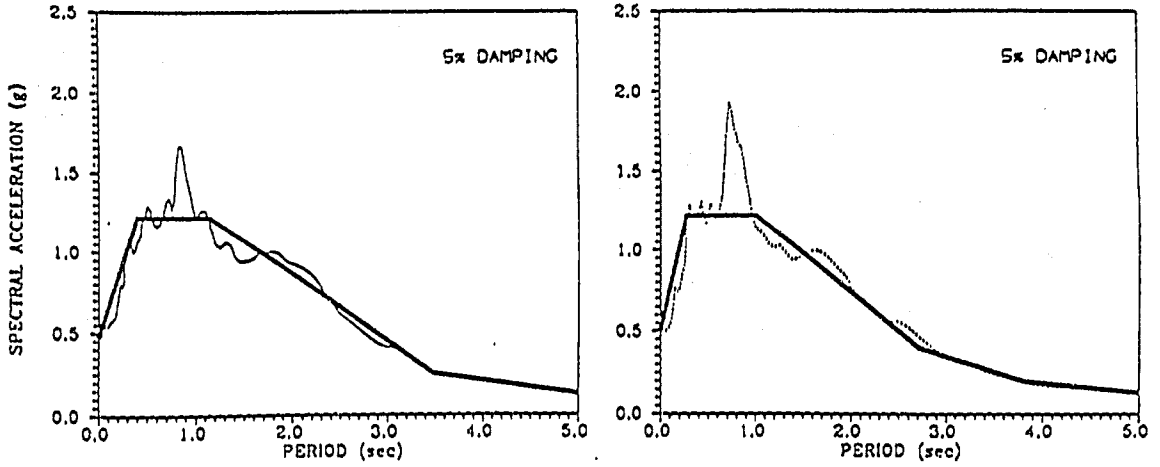
a) Soil Profile

Input Modified to Target Spectrum

Input "Fills" Target Spectrum



b) Suites of Individual Response Spectra with Design Envelope



c) Mean + 1σ of Individual Response Spectra with Design Envelope

Figure 1. Example Results for Site-Specific Ground Response Analysis Using Current Caltrans Methodologies [14].

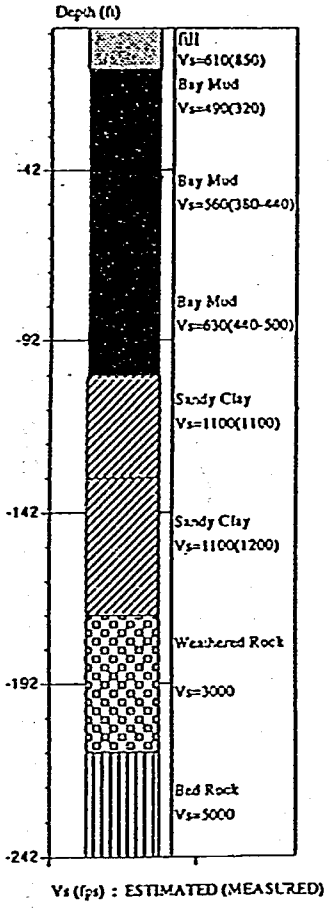
histories which collectively fill the target spectrum The lower pair of spectral plots show the mean plus one standard deviation of the individual response spectra from the upper figures along with an appropriate design envelope.

4.2 Site-Specific Material Characterization [8, 11]

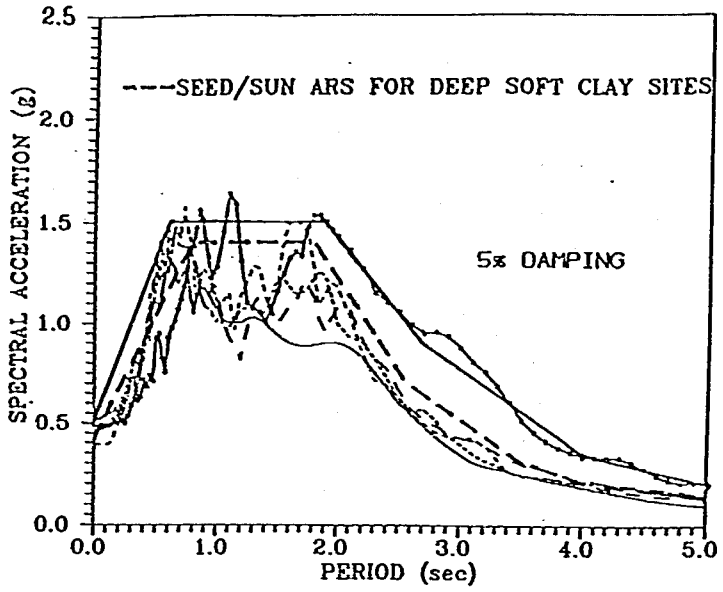
Three types of information are required by all ground response analyses: 1) input "bedrock" acceleration histories, 2) site stratigraphy, and 3) material properties for the various stratigraphic units. Issues related to appropriate characteristics of input motion are typically considered by seismologists, and uncertainties in specification are accommodated in design through modeling of several independent scenarios. Characterization of site stratigraphy is primarily constrained by the level of effort put into the geotechnical investigation rather than the current state of knowledge. Finally, the material properties of soils, typically expressed in terms of modulus and damping, have recently been recognized as having a profound impact on ground response predictions. Due to the highly non-linear behavior of soils with strain level, material properties are typically characterized separately for low-strain ($<10^{-3}$ %) and high-strain (10^{-3} % to ~10%) behavior. This subsection will briefly discuss two on-going research projects directed toward improvements in site-specific characterization of low- and high-strain material properties, particularly for soft soils.

Figure 2 presents results of an actual design case which illustrates the impact which modification of low-strain material properties can have on a site-specific response analysis. The analyses used to determine the spectral design envelopes shown in the upper and lower plots of Fig. 2 differ only in the values of low-strain modulus which were assigned to the upper strata of the profile. This level of analysis sensitivity prompted initiation of an internal minor research investigation [8] into the effectiveness of various seismic techniques used to establish in situ shear-wave velocity (which is directly related to low-strain modulus) of soil strata. This investigation focused on a side-by-side comparison of four methods for velocity determination including: 1) crosshole testing, 2) downhole testing with the seismic cone, 3) downhole testing using conventional borehole receivers, and 4) in-hole testing using the proprietary Oyo P-S Suspension Logger system. All data has been acquired, and results will be contrasted and compared with various established correlations. Additionally, the crosshole investigation at this site was performed along two mutually perpendicular orientations using a five-borehole array. These results will be examined for potential anisotropy in the horizontal plane. Pending results of this investigation, two additional sites are currently being considered for future side-by-side comparisons. Finally, it should be noted that low-strain damping values can also play a critical role in ground response, especially for deep alluvial profiles. At this time, no work is being sponsored by Caltrans on this topic, however, an investigation by EPRI is underway.

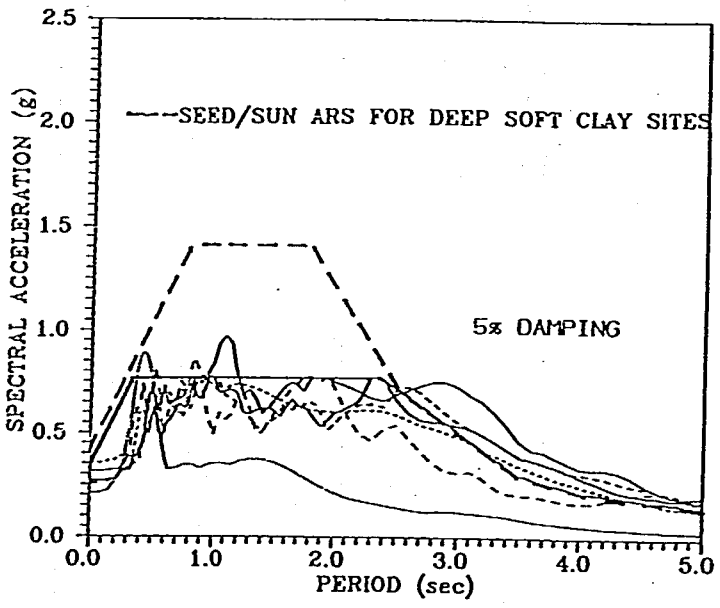
The impact which high-strain properties can have on ground response predictions is illustrated in Figure 3. Each of the three plots along the upper row of



a) Soil Profile

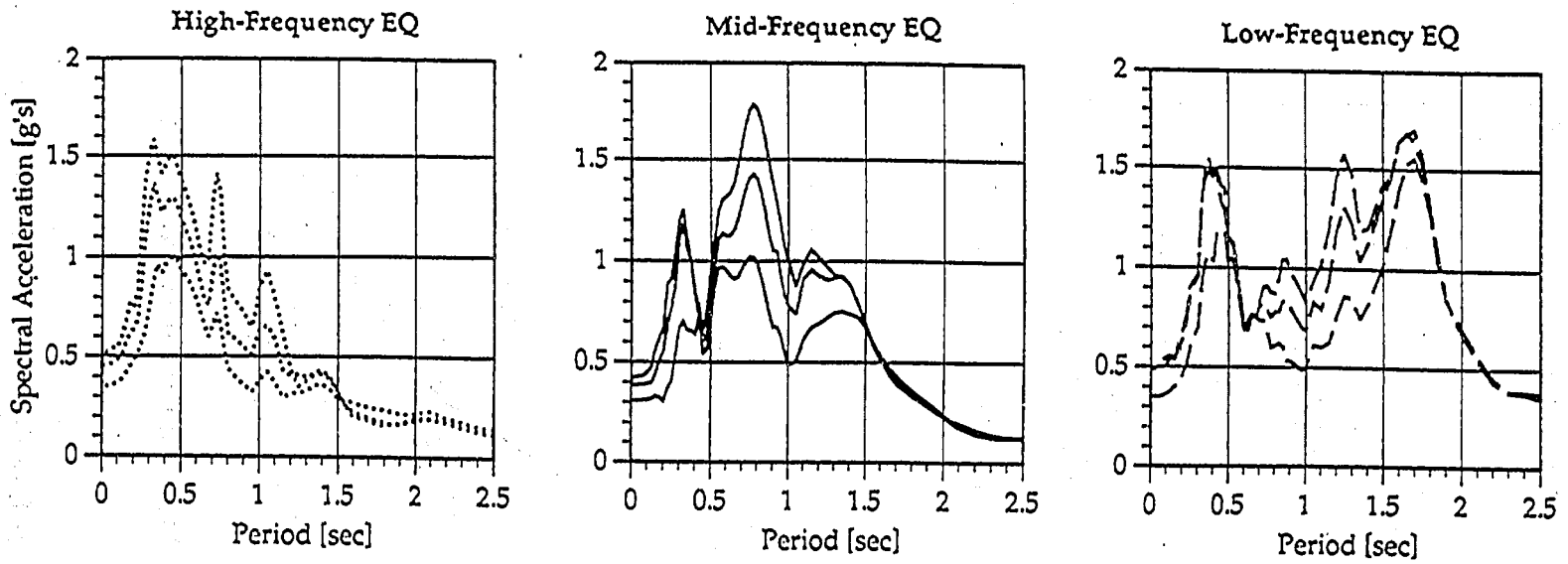


b) ARS Based on Estimates of Shear Wave Velocity

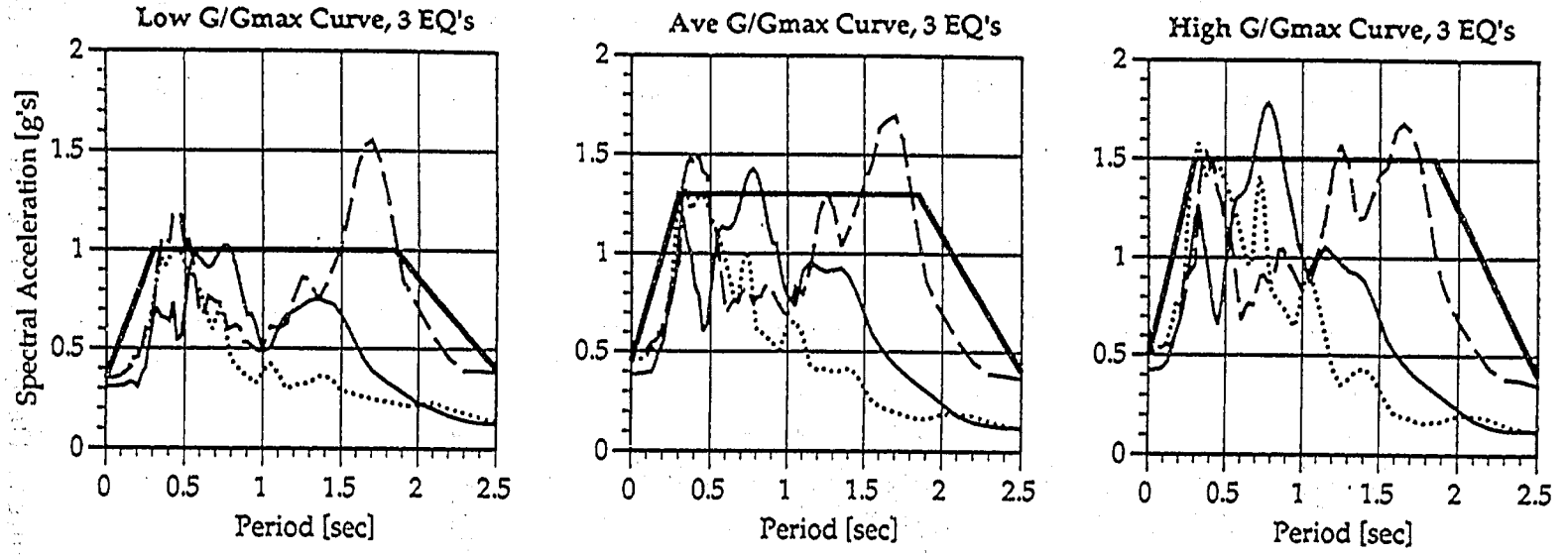


c) ARS Based on Measured Shear Wave Velocity

Figure 2. Design Example Illustrating the Impact of Low-Strain Modulus on Response.



a) Effect of Varying Modulus Reduction Curve for Each of 3 Earthquakes (PBA=0.4g).



b) Impact of Varying Modulus Reduction Curve on Design Envelope.

Figure 3. Synthetic Example Illustrating the Impact of Typical Range in Modulus Reduction Curves on Response.

the figure present results of three separate ground response analyses for a single idealized Bay Area site. Within each plot, high-strain properties were varied according to published ranges [19, 20] of material properties for a moderately-plastic marine clay. Note that the same low-strain modulus and implied strength (at 10% strain) are used for all analyses. Between plots in the upper row, the specified input motion is varied from left to right to include earthquakes rich in a short, medium, and long period energy, respectively. Note that all input motions were scaled to a moderate value (0.4g) of peak bedrock acceleration. The same spectra shown in the upper row of plots are reorganized into the lower row such that a single plot shows spectra for each of the three input motions using a common set of high-strain material properties. These results clearly indicate a significant level of sensitivity of ground response calculations to high-strain properties. Note that while the results presented here were determined using SHAKE, very similar results were determined using a fully non-linear analysis.

Recognition of the impact which high-strain properties have on ground response predictions led to the recent initiation of a major research contract with the University of California at Davis [11]. This project will work toward development of a prototype tool for direct in situ measurement of shear-modulus degradation and damping curves for soft to medium-stiff clays over a wide strain range. The focus of the project on in situ rather than laboratory measurements is intended to both overcome many potentially degrading effects of sample disturbance on material properties, and to provide a tool which could be utilized for site-specific investigations in a timely manner. Currently, the project staff is examining the feasibility of various alternative tool configurations.

4.3 Analysis Verification [10, 13, 14]

Caltrans currently makes extensive use of the program SHAKE for design-level site-specific ground response prediction. This program uses an equivalent linear approximation for the stress-strain behavior of soil. Although recent publications [21, 22, 23] support the adequacy of this procedure for analysis of moderate-level earthquakes such as the Loma Prieta event, questions have been raised about its appropriateness for higher levels of acceleration. This is particularly true for profiles containing materials such as soft clays and loose sands which may undergo large strains during excitation. Alternatively, a number of "fully non-linear" procedures exist which include more realistic models of soil behavior under high strain. These models should be capable of better estimates of spectral response as well as provide reasonable estimates of residual displacements caused by plastic strains. However, these analyses have been notoriously difficult to implement on a design level due to both the large number of parameters required to characterize soil behavior (typically 10 to 20), and the numerical subtleties of running the code. Furthermore, there is a complete lack of supporting high-strain field data for verification of these analyses under relevant conditions. Since the potential benefits of adopting fully non-linear analyses are great, Caltrans has shown interest in

sponsoring verification studies which might lead to more confidence with these procedures.

Three research projects are either currently underway or being considered by Caltrans which will attempt to provide verification of ground response procedures. The first is a contract research program [10] with UCD to perform a series of centrifuge experiments which will record the behavior of six separate soil profiles at several depth intervals for each of four levels of shaking ranging from 0.1g to 0.6g. Results from these experiments can be utilized immediately for calibration of existing models. The remaining two research projects under this category are in the proposal stage, and are closely related. The first project [13] proposes a side-by-side comparison of forward response predictions for a single field site using a number of alternative programs. The site under consideration is the "Islais Site" which has been well characterized as a result of the seismic testing program [8]. The second project [14] proposes to install an array of strong motion sensors at this same site for purposes of verifying analysis predictions. Although the benefits of this type of study are subject to the occurrence of a large magnitude event (estimated to be ~60% probability within the next 30 years [24]), the unique profile at this site provides an excellent long-term verification opportunity which will incorporate macroscopic effects not well modeled in laboratory settings.

4.4 Improvements in Standard ARS [7, 9, 12]

Considering the thousands of Caltrans structures of various sizes throughout the State, comprehensive site-specific evaluations of ground motion for all bridge sites must be considered as infeasible, and use of some form of standardized response spectrum approach must be adopted for routine bridge design. Three research investigations are currently underway to examine potential improvements in Caltrans standard ARS.

The most comprehensive of the investigations has been performed by Seed et al. of UCB as part of the research project focused on the behavior of deep soil sites in San Francisco [7]. This project, which is nearing completion, initially concentrated on the response of soft soil profiles, but has since been expanded to consider stiff soil profiles as well. Early work [21, 25, 26] concentrated on both establishment of a set of typical properties for Bay Mud, and verification of modeling procedures through comparison with Loma Prieta case histories. Subsequent work has focused on a comprehensive series of ground response analyses for a number of different combinations of idealized soil profiles and earthquake magnitude. Analyses were performed using SHAKE for low to medium level inputs, and with a modified version of DESRA-2 [27] for medium to high levels of acceleration. Input motions for each level of acceleration were selected from a database of recorded and synthetic records so that the need for amplitude-scaling was minimized. Soil properties were assigned on the basis of correlations established during the first phase. Results were grouped according to stratigraphic criteria and viewed in terms of normalized spectra combined with a peak-acceleration site-amplification factor similar to ones

previously published {22, 28, 29}. Based on this work, a new set of generic seismic design guidelines are being proposed by Seed and his co-investigators. A preliminary draft of this proposal appears in Table 2 and Fig. 4, and currently proposes use of six separate site classes having ten identifiable site profile combinations. Each site class is associated with both a normalized spectral envelope and a magnitude-dependent amplification factor. Seed {30} indicates that modifications to these guidelines are forthcoming, so the information presented herein should be viewed as tentative. These recommendations (and any future revisions) will be independently reviewed within Caltrans through examination of a database of recent case histories for which site-specific analyses are available.

Two minor research projects regarding standard ARS have recently been initiated by staff at DNTMR. The first project [9] examines the impact which updated material properties for plastic soils have on Caltrans standard ARS. The existing standard ARS curves were developed {31} under the assumption that all alluvium could be conservatively characterized using the high-strain material properties of sands which, at the time, were thought to behave more elastically than clays. Since soft-soil sites are now routinely characterized using a site-specific analysis, the primary focus of this investigation will be on the response of stiff soil profiles for which standard ARS curves are still commonly employed. In particular, the adequacy of the existing curves will be assessed both relative to results of selected site-specific analyses, and with results from a series of analyses using synthetic profiles containing plastic strata of varying thickness. The second minor project [12] will focus on a current review of seismic design provisions which appear in various world-wide building codes. The objective of this project is to assimilate a variety of perspectives regarding design specification of ground motion.

5. Soil-Structure Interaction

The phrase "soil-structure interaction (SSI)" is arguably one of the most vague terms used by the Civil Engineering profession. It encompasses many different categories of both soil and structural problems and solution approaches which are grouped under one label. For purposes of this paper, three SSI problems of interest to Caltrans will be discussed: 1) foundation flexibility, 2) pile survivability, and 3) substructure effects on ARS.

5.1 Foundation Flexibility [15, 16, 17, 19]

In recent years, there has been increasing recognition of the impact which the flexibility of foundation elements such as pile groups and abutments have on the seismic performance of bridges. In the past, Caltrans had assumed that foundation systems provide a "fixed" boundary for purposes of dynamic analyses. Current Caltrans procedures require consideration of foundation-flexibility effects in design. These effects can significantly increase both the structural period and deck displacements, as well as cause a redistribution of load within the structure relative to the fixed-boundary case. Numerical parametric studies completed by the Cygna Group [16]{32} using the general-purpose linear structural analysis program SAP {33}

Site Class	Site Condition	General Description	Site Characteristics[1,2]
(A_0)	A_0	Very Hard Rock	$V_s > 5{,}000$ ft/sec
	A_1	Rock and/or Weathered Rock.	$2{,}500$ ft/ sec $\leq V_s \leq 5{,}000$ ft/sec
A	A_2	Stiff, Shallow Soil.	$H_{soil} \leq 50$ ft, and $V_s \geq 800$ ft/sec (in all but top few feet.[3])
	B_1	Deep, Primarily Cohesionless[4] Soils. ($H_{soil} \leq 250$ ft.)	No "Soft Clay" (see Note 5), $H_{cohesive\ soil} < 0.2\ H_{cohesive\ soil}$, and $H_{cohesive\ soil} < 50$ ft
B	B_2	Medium Depth, Stiff Cohesive Soils and/or Mix of Cohesionless with Stiff Cohesive Soils; No "Soft Clay".	$H_{all\ soil} \leq 150$ ft, and V_s (cohesive soils) > 500 ft/sec. (see Note 5.)
C	C_1	Medium Depth, Stiff Cohesive Soils and/or Mix of Cohesionless with Stiff Cohesive Soils; Thin Layer(s) of Soft Clay	Same as B_2 above except 0 ft $< H_{soft\ clay} \leq 10$ ft (see Note 5.)
	C_2	Deep, Stiff Cohesive Soils and/or Mix of Cohesionless with Stiff Cohesive Soils; No "Soft Clay".	$H_{soil} > 150$ ft, and V_s (cohesive soils) > 500 ft/sec.
D	D_1	Soft, Cohesive Soil.	10 ft $\leq H_{soft\ clay} \leq 90$ ft, and $A_{max,\ rock} \leq 0.3$ g, or [$A_{max,\ rock} \leq 0.45$ g and $M \leq 7.5$]
	E_1	Very Deep, Soft Cohesive Soil.	$H_{soft\ clay} > 90$ ft (see Note 5.)
(E)[6]	E_2	Soft, Cohesive Soil and Very Strong Shaking	$H_{soft\ clay} > 40$ and either: $A_{max,\ rock} > 0.45$ g, or $A_{max,\ rock} > 0.3$ g and $M > 7.5$

1 H = total (vertical) depth of soils of the type or types referred to.

2 V_s = seismic shear wave velocity (ft/sec) at small shear strains (shear strain ~10^{-4}%).

3 If surface soils are cohesionless, V_s may be less than 800 ft/sec in top 10 feet.

4 "Cohesionless soils" = soils with less than 30% "fines" by dry weight;
"Cohesive soils" = soils with more than 30% "fines" by dry weight, and PI (fines) ≥ 15%.

5 "Soft Clay" is defined herein as cohesive soil with: a) Fines content ≥ 30%
b) PI (fines) ≥ 20%, and
c) $V_s \leq 500$ ft/sec.

6 Site-specific geotechnical investigations and dynamic site response analysis are strongly recommended.

Table 2. Proposed Simplified Site Classification System (from Seed {30})

Effective Peak Ground Acceleration

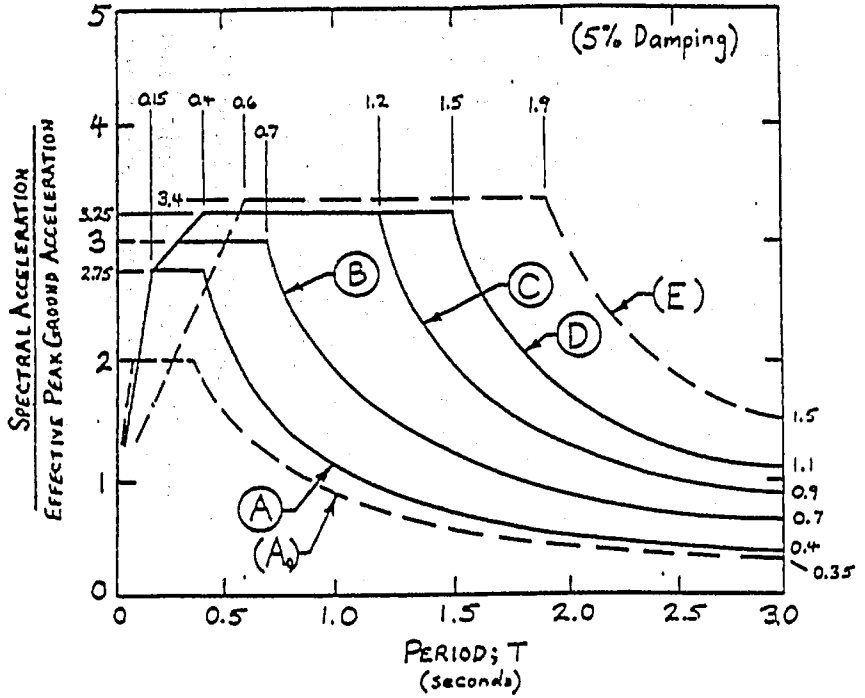
$$PGA_{eff.} = [(A_{max,\,rock})(F_A) + 0.04g$$

$$\text{where } F_A = \frac{A_{max}}{A_{max\ rock}}$$

A_{max} Amplification Factors (F_A)

Site Conditions \ $A_{max,rock}$	0.05 g	0.1 g	0.2 g	0.3 g	0.4 g	0.5 g	0.6 g	0.7 g
A	1.0	1.0	1.0	1.0	1.0	1.0	1.0	1.0
B, C_1	1.5	1.5	1.25	1.13	1.04	0.94	0.90	0.86
C_2, D, E	3.0	2.3	1.5	1.2	1.0	0.86	0.76	0.71

Site-Dependent Design Elastic Response Spectra



PGA vs. $A_{max,\,rock}$ for Defined Site Classes

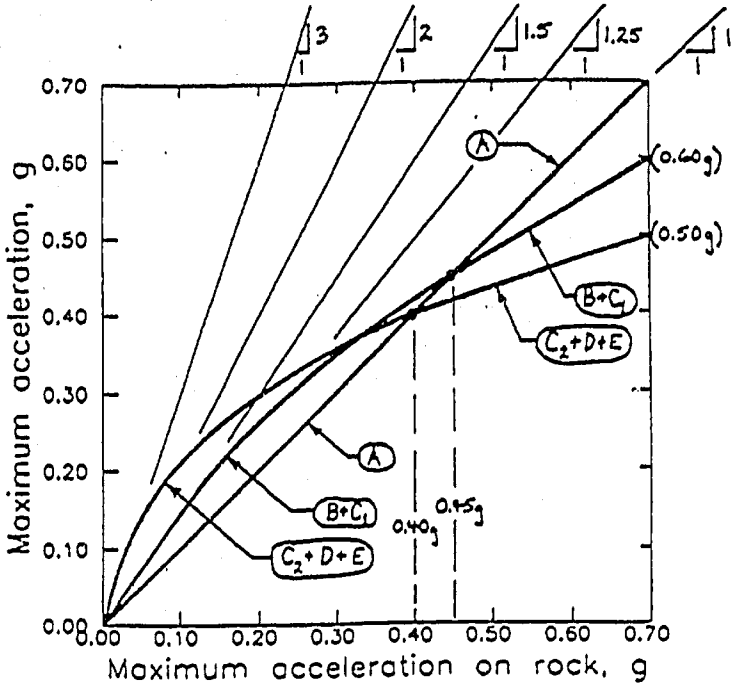


Figure 4. Proposed Method for Standard Specification of Site Response. (from Seed {30})

illustrate the impact which foundation-flexibility effects can have on selected dual-level bridge designs. This and other work indicates that fundamental mode periods of particular bridge designs shift between 40% and 300% relative to the fixed case. This period shift can profoundly affect the value of column base shear determined from a response spectrum.

Incorporation of foundation flexibility effects into structural design can be implemented using solutions exhibiting a wide range of sophistication. Ideally, a structural analysis should consider both the highly non-linear stress-strain behavior of soil as well as the pile-soil-pile interaction ("group effects") problem. Comprehensive consideration of this problem is generally impractical for design-level calculations, therefore, considerable effort is expended in identifying an appropriate level of analysis which adequately predicts response behavior without incurring excessive computational sophistication.

Current Caltrans design methodologies for column footings {34} utilizes perhaps the simplest approach to foundation flexibility where axial, lateral and rotational elastic "soil springs" are specified at each foundation boundary. Spring stiffness values are estimated using either the computer program GROUP1 {35} which utilizes P-Y and T-Z curves for soil-pile interaction, or a combination of methods which estimate foundation performance on the basis of Caltrans minimum axial performance criteria for piles and translational stiffness using modifications to methods presented by Lam et. al. {36} and Broms {37, 38}. Current Caltrans design guidelines for abutments utilize a similar soil-spring concept with empirically-derived values for horizontal stiffness (200 kips/in per lineal foot of wall width) and ultimate dynamic capacity (7.7 ksf).

Caltrans-sponsored research on the topic of foundation flexibility primarily examines either the applicability of current design procedures or assesses alternative design methodologies. Penzien [15] had investigated both the linear substructure method and the non-linear "hybrid model" for developing frequency-independent impedance matrices for substructure components to be used in the non-linear bridge analysis program NEABS {39}. Coast Analytics [17] is developing procedures to examine the SSI effects of a particular bridge structure (to be determined) using the finite element program SATURN {40}. This program can accommodate the fully non-linear behavior of soil including pore-pressure build-up and liquefaction. Martin et al. [19] propose to utilize the finite element program LINOS {41} to examine the soil-structure interaction behavior of various abutment configurations. After performing sensitivity studies pertinent to retrofit evaluations and new design criteria, simplified abutment modeling procedures are to be developed and checked using the program SEISAB {42}.

5.2 Pile Survivability Under Seismic Load [2, 20]

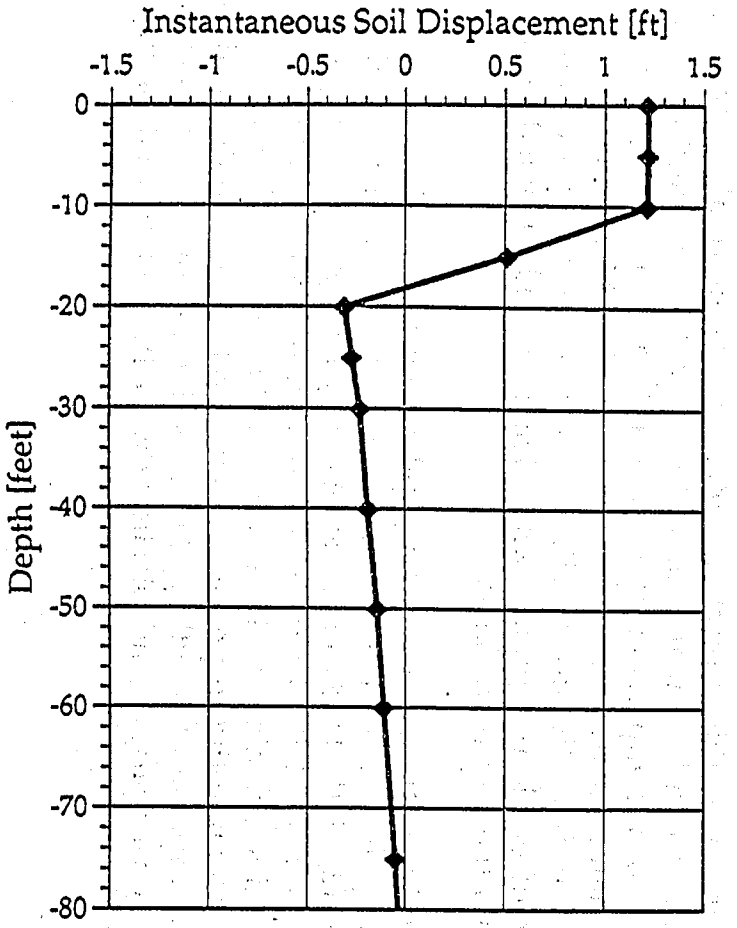
Pile survivability under seismic load is a soil-structure interaction issue which is separate from the effects which foundation flexibility have on structural

response. The objective of a seismic pile-survivability study is to determine transient profiles of shaft deformation, shear, and bending moment for the foundation which are caused by the relative lateral movement between the free-field soil and the pile system during seismic events. This general analysis is also applicable to the problem of displacements caused by liquefaction and lateral spreading. It is important to note that this problem is different from conventional lateral response analyses which account for the superstructure load only.

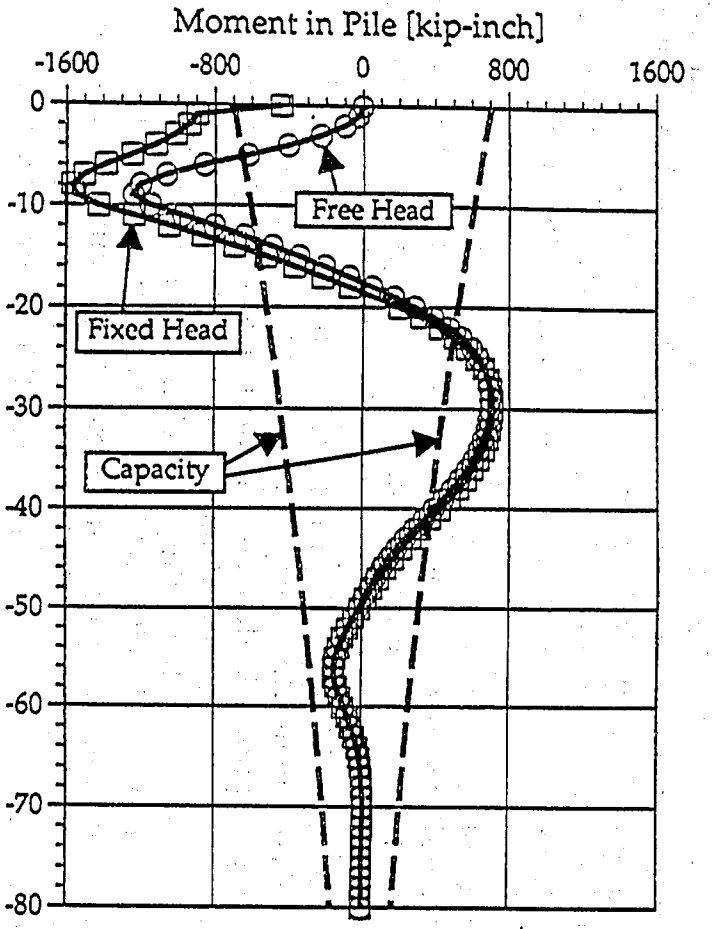
Recent analyses of several Caltrans bridge foundations performed by Slyh and Jackura of DNTMR indicate that certain pile types (typically timber and under-reinforced concrete of various configurations) are susceptible to unacceptable damage during design seismic events, and therefore require retrofit. Figure 5 presents example results of this type of analysis for a timber pile. These results are based on a P-Y analyses using the computer program BMCOL76 [43] where the profile of "soil spring" supports is deflected according to a specified displacement field indicative of worst-case free-field soil motions. At this time, the critical displacement profiles are estimated using two alternative methods which utilize response calculations estimated with SHAKE. The first alternative specifies a displacement profile by integrating peak free-field strain values over depth. The second method considers differential displacement profiles determined at various times from double-integrated acceleration histories. Pile group effects are estimated on the basis of static interaction factors.

An internal minor research project [20] recently proposed by Slyh of DNTMR will document the aforementioned methodology as well as assess alternative approaches. In particular, this project will focus on: 1) alternative procedures for estimating the critical displacement profile, 2) alternative assumptions regarding group effects, and 3) a comparison of both results and useability with existing comprehensive dynamic-analysis programs such as SPASM [44] and FLUSH [45]. Additionally, future investigations will attempt to examine the problem of progressive failure of brittle pile groups where loads are redistributed to inner piles as outer piles within the group are failed.

The pile-survivability of the very large pile groups of the East Crossing of the Bay Bridge is being investigated by Lysmer and Chin [46] as part of the overall seismic assessment [2, Ph2]. Due to the exceptionally large numbers of piles in each group (between 297 and 625), careful consideration of group-effects is critical to overall response and survivability. These investigators are developing a numerical model which will examine the response of a single pile in an infinite field of piles. This model will be capable of handling the redistribution of stress within the pile group caused by non-linearities and plastic flow of the soil as well as slip at the pile/soil interface.



a) Critical Transient Free-Field Displacement Profile.



b) Instantaneous Moment in Pile vs Pile Capacity.

Figure 5. Example of a Pile Survivability Analysis for a Timber Pile Subjected to Large Localized Displacement.

5.3 Substructure Effects on ARS [18]

Caltrans routinely employs the response spectrum approach to the seismic design of bridge structures in the form of either standard or site-specific ARS. Since these response spectra are representative of free-field motion, there is an implicit assumption that the foundation "tracks" free-field motion and that no soil-pile interaction effects occur. This assumption is reasonable for firm soil profiles in which pile systems are likely to comply with dynamic soil strains. However, this is not necessarily the case for sites underlain by soft-soil profiles where substructure stiffness may significantly affect foundation response at ground level.

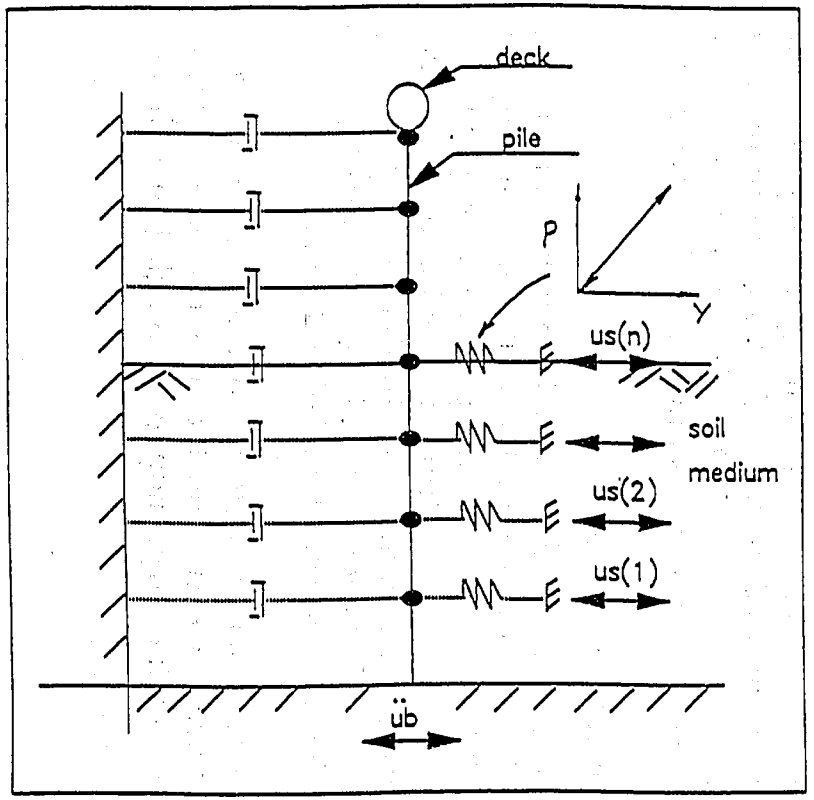
Slyh and Jackura at DNTMR [18] have begun evaluation and modification of numerical procedures to include soil-structure-interaction effects in the determination of site-specific foundation response and ARS. This investigation is an extension of the work initiated by Cafe {47} and utilizes modified versions of the BEAM1DYN program. Refinements to the program include changing the soil elements to accommodate non-linear hysteretic behavior. Preliminary parametric studies indicate that stiff foundation systems within soft-soil profiles experience significantly different acceleration and displacement behavior than that of the surrounding soil in the free field. Fig. 6 presents example results of this behavior for one particular foundation-design/soil-profile combination. Results for this case show significant amplification over free-field motion at periods of less than 1 second, and attenuation of motion for longer periods.

The impact of superstructure inertial "feedback" to the foundation system is also being investigated as part of this project. Preliminary parametric studies which include representative mass and stiffness elements to model the superstructure have shown further significant changes in pile-cap response. These effects appear to be a function of both the added mass and stiffness independently rather than to the stiffness/mass ratio commonly utilized in the single-degree-of-freedom model. To accommodate this behavior, the use of a 3-D surface of peak elastic structural response versus both representative mass and stiffness is under consideration.

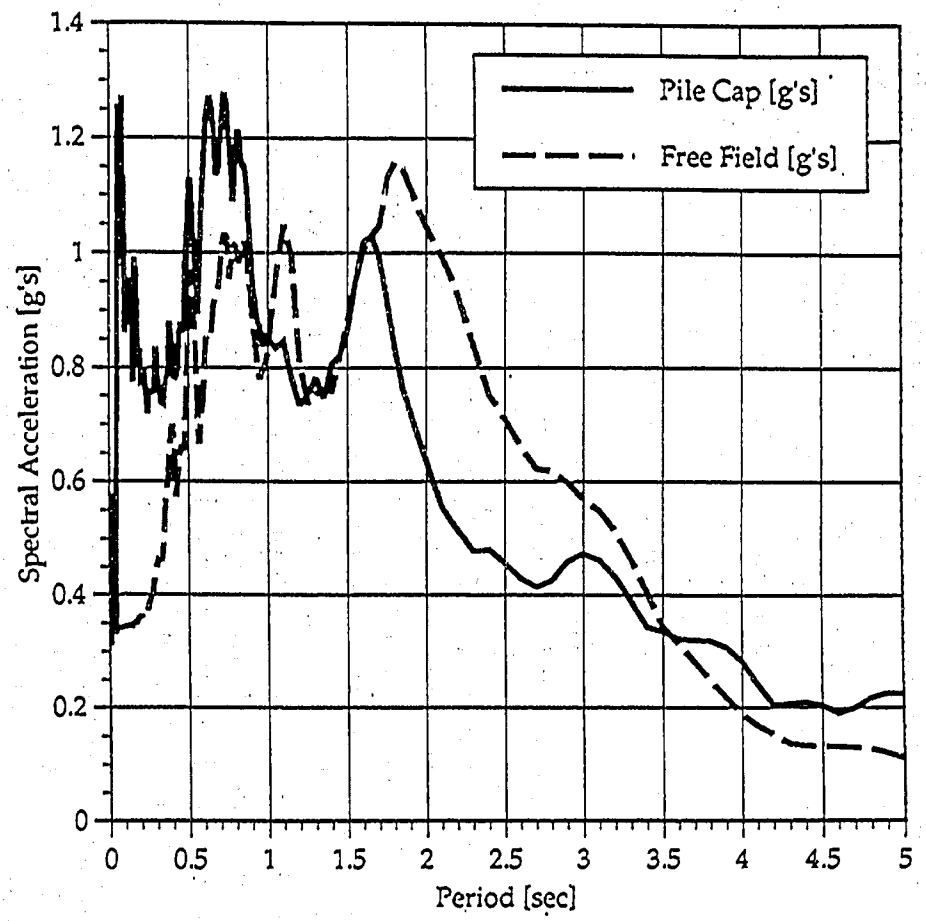
6. Review of Design Procedures [21, 22]

Two separate contract research projects have been initiated by DOS to review various aspects of Caltrans bridge design procedures. The first study by the Applied Technology Council (ATC) [21] is broad based and provides a complete review of the entire bridge design process ranging from rehabilitation prioritization to requirements for design checks. The second study by Dames and Moore (D&M) [22] is more narrowly focused on the behavior of short bridge overcrossings. Portions of both of these studies are relevant to seismic foundation design.

The ATC study involves seven separate subcontractors, one for each of seven areas identified for assessment. Geospectra, Inc. was chosen to review Caltrans seismic loading guidelines. Preliminary findings by Singh {48} indicate concerns



a) Linear P-Y Model Used for Analysis of SSI Effect on ARS. (After Cafe [47])



b) Spectral Response at Ground Level for Free-Field and Cap Motion

Figure 6. Example of the Effect of Pile Stiffness on Response Using a Linear P-Y Approximation.

regarding: 1) the representativeness of Caltrans standard ARS, 2) the use of a "maximum credible" design earthquake, and 3) the use of both target spectra and SHAKE analysis for estimation of site-specific response spectra. This report also discusses the applicability of probabilistic approaches for specification of design earthquakes, key issues related to site effects, and appropriate development of strong-motion records for site-specific response analyses.

Earth Mechanics, Inc. was selected as the ATC consultant for foundation design and rehabilitation. Lam and Martin [49] have reviewed all Caltrans documents pertaining to the standard design practice for substructure elements. Relevant Caltrans guidelines and procedures related to abutments, pile footings, drilled shafts, spread footings, retaining structures, and ground failure hazards are summarized and discussed individually. Key recommendations include the need within Caltrans: 1) for both expansion and improved synthesis of information related to foundations which currently appears in a number of separate documents, 2) to verify abutment stiffness and damping parameters, 3) to examine both the lateral stiffness and lateral capacity of pile groups through a destructive testing program so as to identify the separate contributions provided by the individual piles and the pile cap, 4) for routine determination of site-specific ultimate capacity estimates for piles, especially for uplift loading, and 5) for improved design guidelines for footing-connection details to provide the requisite uplift capacity to resist overturning moment.

The D&M study is focusing on evaluation procedures used by Caltrans to identify retrofit needs for two-span short bridge overcrossing (SBO) structures. Current evaluation results for selected structures have implied a need for retrofit of thousands of older SBO's constructed throughout California. D&M plans to assess the current seismic evaluation procedure for SBO structures, and to develop a new procedure which may lead to a more "realistic basis" for assessing retrofit needs. In addition to purely structural considerations, this study will focus on improvements in the modeling of foundation flexibility at both the abutments and central column, as well as the appropriateness of using 5% modal damping in the specification of ARS design spectra.

7. Structural Aspects of Substructures [23, 24]

Two contract research projects sponsored by DOS are currently underway which focus on structural aspects of two different substructure systems. The first is a project through UCD [23] which is examining the behavior of pile-extension substructures, and the second is a project through UCSD [24] which is examining the structural performance of bridge column footings.

The failure of the Struve Slough Bridge during the Loma Prieta event focused attention on the performance of "pile cap extension" substructures. These substructure elements are simply columns which extend from individual piles at ground line to a bent cap located directly beneath the deck beams. Ramey et al [50] at

UCD are performing experimental investigations to determine the actual bending/shear strength behavior of pile extensions which were "harvested" from the Struve Slough Bridge. Additional experiments on newly-constructed members will be performed to assess both a scheme to rehabilitate cracked column sections using epoxy pressure injection methods, as well as various retrofit schemes involving confinement strategies for increased strength and ductility.

The seismic performance of conventional footing designs is the focus of a combined analytical and experimental research program underway at UCSD. Priestley et al [51] are investigating potential design problems and alternative retrofit strategies for various footing configurations. The potential design problems under investigation include: 1) inadequate anchorage of longitudinal column rebar in the footing, 2) inadequate shear strength of the joint region under the column, 3) inadequate footing flexure and shear strength, and 4) inadequate restraint against overturning. Experimental work will utilize large-scale laboratory models including tests on a rubber substrate to investigate footing performance under rocking motion.

8. Field Load Tests

A key component in Caltrans' seismic research program has been the use of field load tests as a means to verify modeling and design assumptions. The following subsections will briefly discuss five projects related to substructure performance.

8.1 Cypress Footings Lateral Load Tests [25]

The demolition of the Cypress Street Viaduct after the Loma Prieta event provided a unique opportunity to perform full-scale load tests on typical pile-group foundations used for bridge structures. Under tight time constraints, Abcarius [52] supervised lateral load testing of foundation groups at two separate bent locations. Testing at one location involved three pile caps with ~60-ft long piles penetrating into clayey material, while the second location involved two pile caps with ~15-ft long piles set into sandy silt. All piles were 12-inch-diameter closed-ended concrete-filled standard steel pipes, and the individual pile groups consisted of between 10 and 17 piles.

Testing was performed by laterally jacking between pile caps at each bent location with a pair of hydraulic rams while measurements of cap displacement and ram pressure were recorded for one load cycle. The primary objective was to verify the design assumption of 5 kips/pile at 1/4-inch cap deflection. The load tests indicated that average measured lateral pile capacity was between 17 and 26 kips per pile at 1/4-inch cap deflection, while average ultimate lateral capacities exceeded 35 kips per pile. Subsequent axial tension testing of single piles at each of three separate bent locations was performed by staff of DNTMR. Although the implemented lateral-load-test program precluded determination of individual pile capacity, group effects, soil P-Y behavior, or the behavior of the pile group under

repeated load cycles, results from these tests clearly demonstrated that Caltrans' design criteria of 5 kips/pile was conservative.

8.2 Meloland River Overcrossing Dynamic Testing [26]

The Mololand River Overcrossing (MRO) is a monolithic, two-span, reinforced concrete box girder bridge which is located along Interstate Highway 8 adjacent to the Imperial Fault. This bridge became the focus of research interest after strong-motion accelerometers located at this site successfully recorded both free-field and bridge-deck motions during the 1979 Imperial Valley earthquake (M=6.8). Since that time, Caltrans has sponsored research which has investigated the response of this bridge under both low-amplitude ambient vibrations {53} and under medium-level forced vibration tests {54}. This research has led to general recognition within Caltrans of the effects which soil-structure interaction of bridge abutments have on the overall seismic response of bridges.

The primary focus of research on the MRO has been the determination of global response characteristics such as structural mode shapes, natural frequencies, and modal participation factors. However, back-analysis of the performance of this structure at the various levels of excitation has been used to estimate foundation flexibility values (translational and rotational stiffness) for both the central pier and bridge abutments {55, 56, 57, 58}. This and other case histories have provided a baseline for comparison of alternative design methodologies for estimation of foundation flexibility values {59}. Key findings from this work include the documentation of a significant reduction in the fundamental transverse frequency of the bridge (from ~3.4 Hz to between 1.3 and 2.6 Hz) as vibration amplitude increases. This reduction is primarily attributed to large decreases in foundation stiffness values at high strain.

8.3 Terminal Separation Lateral Load Test [27]

The Terminal Separation is a series of interwoven ramps connecting I-80 with downtown San Francisco at the western terminus of the Bay Bridge. This structure was closed after the Loma Prieta event due to concern over design details which were similar to the collapsed Cypress Freeway. Cooper {60} provides an excellent discussion of both the decision to replace the existing structure, as well as the unique features of the replacement design. The new design utilizes a dual-independent framing concept with increased span lengths relative to the existing structure. The alignment crosses several stratigraphic profiles, and requires use of six different site-specific ARS over its 0.7-mile length. The combination of longer spans, tight alignment tolerances, and high seismic design loads necessitated careful analysis of the lateral capacity of both drilled shaft foundations for rock sites and pile-group foundations for soil sites. Preliminary analyses for the drilled shafts (based on limited P-Y behavior data for fractured rock) indicated the need for an embedment length into the Franciscan rock of six diameters or approximately 45 feet. Estimated costs for drilled shaft construction exceeded $3.5 million.

To verify modeling assumptions regarding the behavior of the fractured rock at the Terminal Separation, a full-scale lateral load test of drilled shafts was implemented by Speer of DNTMR at the Rincon Hill site. The test utilized a pair of highly-instrumented 7-ft-diameter drilled shafts embedded directly into fractured bedrock (surface alluvium removed) to a depth of approximately 45 feet. Instrumentation internal to each of the shafts included strain gages fixed to the reinforcing cage at each of six radial positions around the shaft at either 9-inch or 18-inch depth intervals, Carlson gauges located at each of four radial positions around the shaft at 36-inch intervals, and a slope inclinometer casing down the center of each shaft. Figure 7 illustrates the loading scheme where the shafts were pulled together using a pair of hydraulic rams which stressed a pair of multi-strand cables which passed through and were locked-off to each of the shafts. A pair of load cells measured tensile load on each of the two cables, and displacements of each of the two shafts were measured at three locations above ground line on each of two sides of the shafts.

Figure 8 presents preliminary load-displacement results for one shaft during the load sequence which consisted of a series of four load-unload loops of increasing magnitude to a maximum value of approximately 2000 kips. The final load cycle caused a lateral ground-level displacement of approximately 2 inches, and produced a plastic hinge in one shaft at a depth of approximately 5 feet below the top of rock. Figure 9 presents preliminary results of both strain and displacement profiles for one shaft for each of the four peak loads. These data indicate that the peak moment occurred at a depth of approximately five feet, and the entire load was shed at a depth of approximately 20 feet below top of rock. Additionally, forward predictions of shaft load-deformation behavior using pressuremeter-derived P-Y curves and COM624 analysis appear to correlate well with the measured data for all load ranges. A final report incorporating more refined analysis of the over 100,000 data points acquired at this site is being prepared by Speer, and will be published in 1993. Presuming the shaft tip elevations can be raised between 10 and 15 feet, the direct cost savings resulting from this investigation are estimated to be in the range of $1 million.

8.4 Large-Scale Modeling of Bridge Abutment Behavior [28]

The sensitivity of bridge-response calculations to assumed boundary conditions at abutments has highlighted the need for direct physical measurements of abutment behavior under cyclic loading. In response to this need, a joint research effort involving Caltrans and the University of California at Davis (UCD) was initiated to systematically examine the response characteristics of a "near full-scale" model of a typical California-type bridge abutment system (61). In particular, this experimental program will focus on both the evaluation of longitudinal, transverse, and rotational stiffness, as well as ultimate load capacity provided by the abutment. These measured values will be used to assess existing analytical or empirical models including current Caltrans bridge modeling guidelines (stiffness of 200 kips/in/ft of width, and dynamic capacity of 7.7 ksf). These results, in particular the ultimate

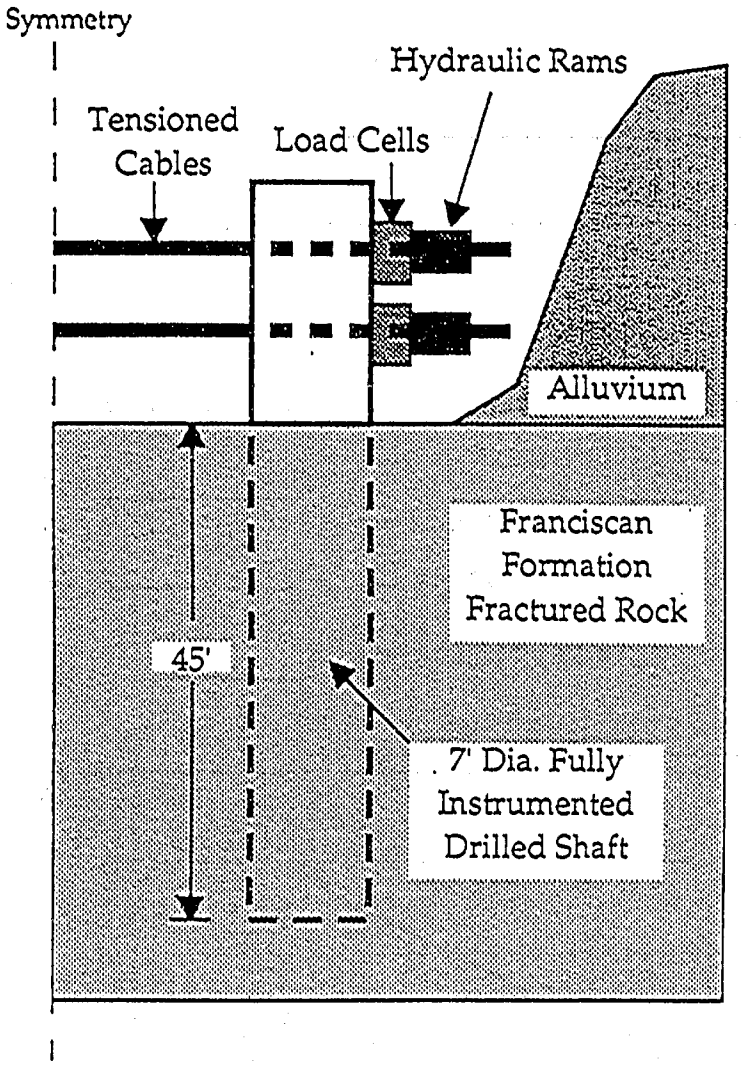


Figure 7. Conceptual Configuration of Terminal Separation Lateral Shaft Load Test

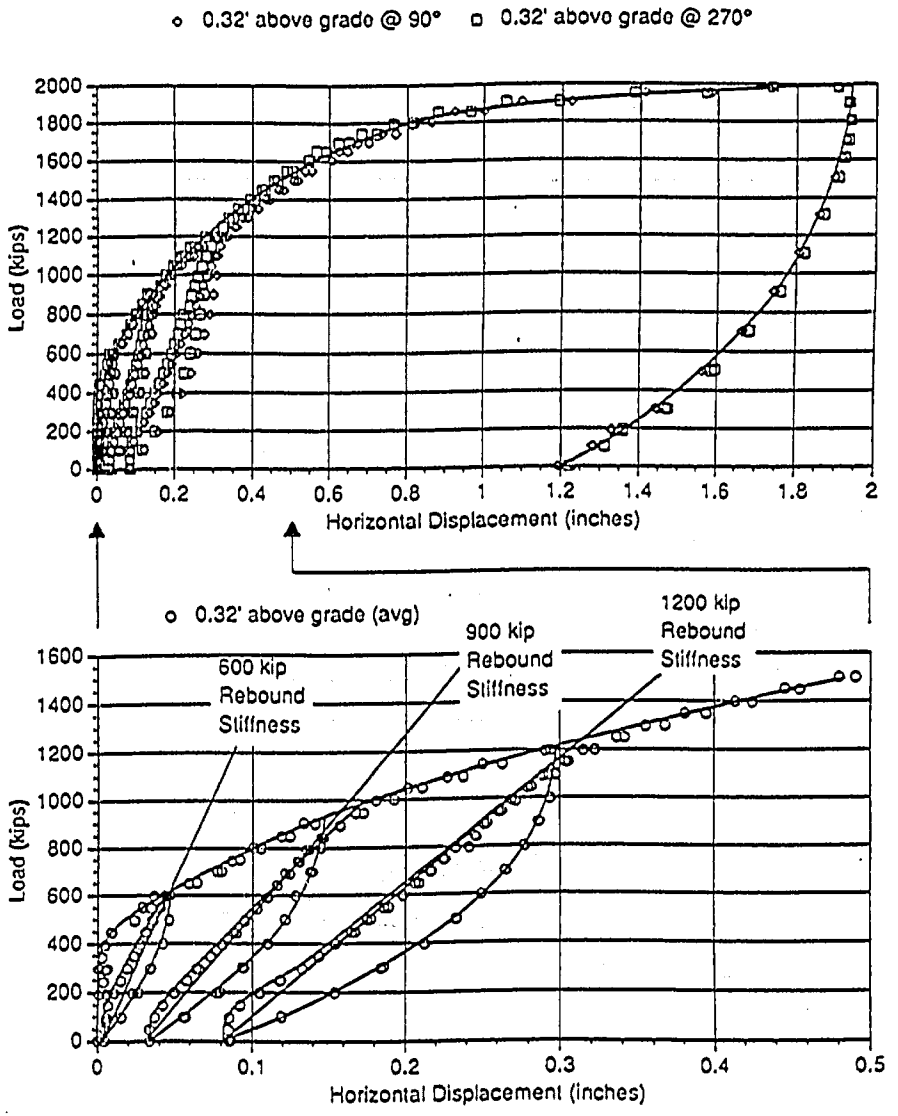
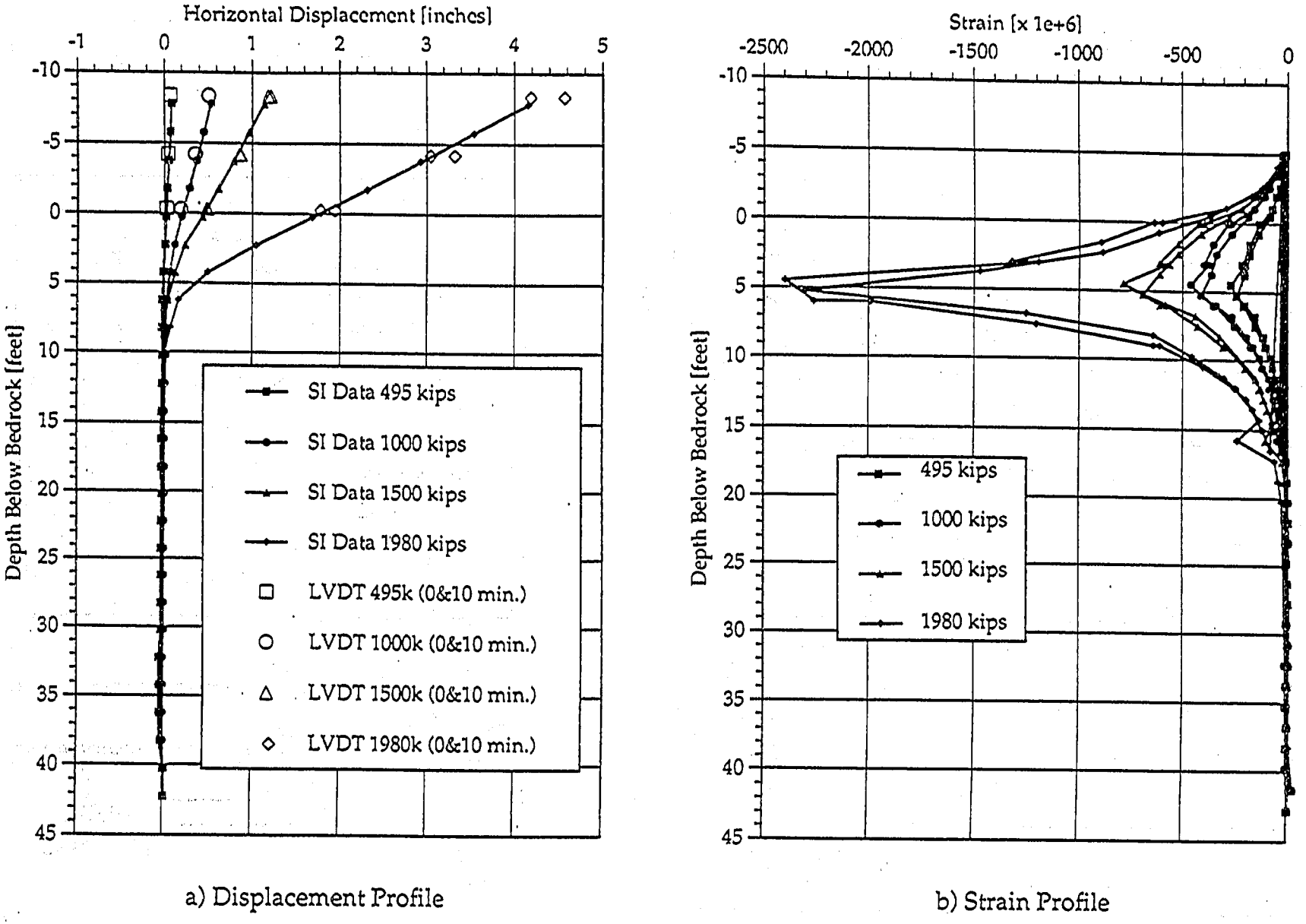


Figure 8. Shaft Head Load vs Horizontal Deflection Near Ground Line for Shaft B



a) Displacement Profile

b) Strain Profile

Figure 9. Terminal Separation Lateral Load Test Results. Displacement and Strain Profiles for 4 Peak Load Levels.

capacity, could have significant impact on the number of California bridges which will require retrofit.

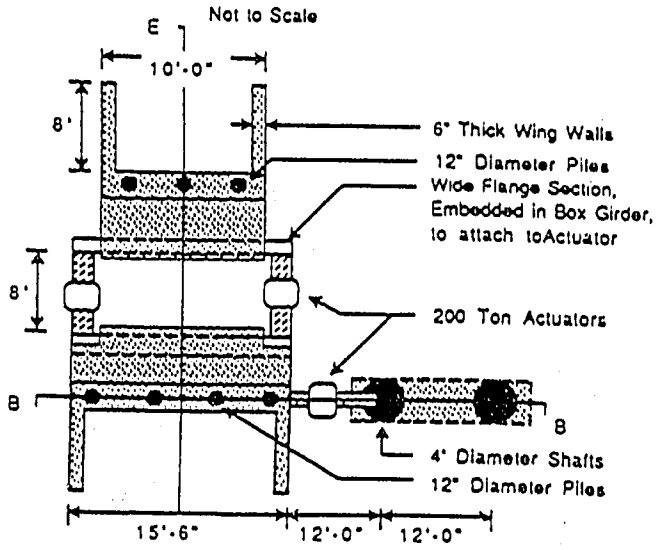
The test facility which is located at UCD has been carefully planned to enable independent examination of several critical factors affecting abutment performance. Figure 10 illustrates the general layout of both the primary abutment facility and the supplemental pile facility. The primary facility consists of two opposing abutments of different sizes and a separate pier-group reaction frame adjacent to the larger abutment. The smaller abutment is backfilled with low-plasticity silt, and the larger abutment is backfilled with a clean sand. The supplemental facility consists of a pair of perpendicularly-oriented two-pile groups. Instrumentation of the abutment facility will include interface-pressure cells for measurement of backfill pressure on structural components, inclinometer casings to determine displacement profiles at various points within the soil and in selected piles, strain gages to record stress histories within the piles, and LVDT's, magnarules, and surveying targets to measure gross displacement of various points on the structure.

The load test program has been planned in three major phases. The first phase involves lateral load testing of the pile groups of the supplemental facility, and has recently been successfully completed. Results from this test phase will be used to isolate the contribution of the piles from the overall lateral behavior of the abutment system. The second phase of the test program will involve jacking horizontally between the two abutments using a pair of 200-ton rams positioned toward the outer edges of the abutments. The rams will be activated both individually and simultaneously to statically drive the abutments both longitudinally and in torsion about the vertical axis. Loading will be displacement controlled, and will provide two full cycles of each load combination. After forcing a pre-determined maximum level of cyclic displacement, an attempt will be made to establish the ultimate longitudinal capacity of the smaller abutment by statically driving it to "failure". The third and final testing phase will involve transverse loading of the larger abutment by jacking against the pier-group reaction frame.

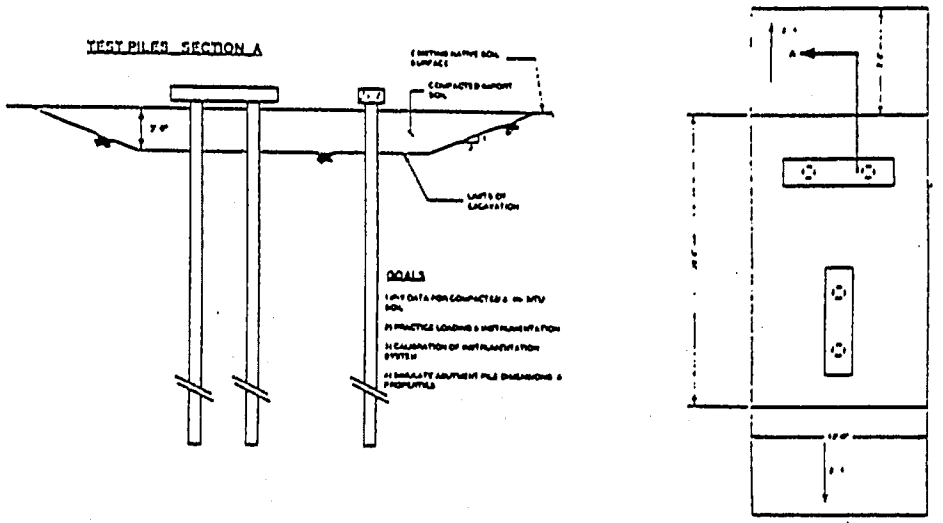
In addition to the field load-test program, 1/12-scale models of both the piles and abutments of the field-test facilities will be built and tested within the large centrifuge at UCD. Provided that test results can be achieved which are reasonably representative of the "near full scale" behavior, additional studies investigating a number of different design alternatives will be evaluated using centrifuge models.

8.5 Highway 280 Axial Load Tests [29]

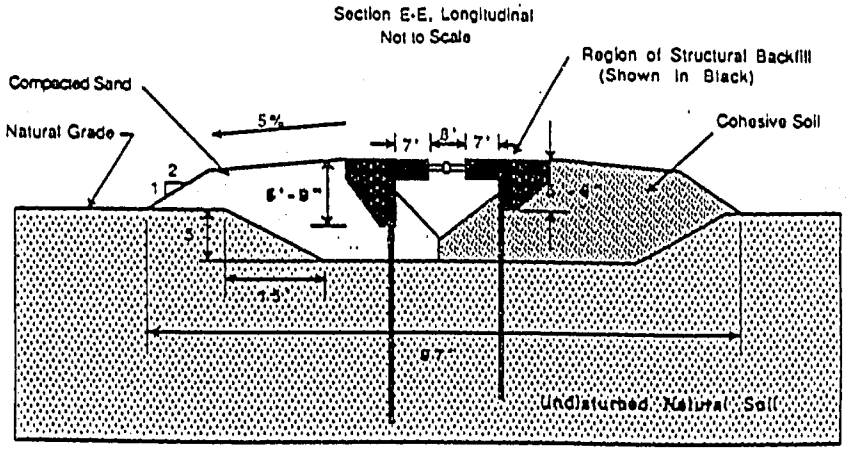
Caltrans has initiated a field load-test program targeted at an improved understanding of the tensile behavior of pile systems in soft clays. This research is motivated by more the stringent design requirements implemented since Loma Prieta for new and retrofitted bridge foundation systems to resist overturning moments. Current Caltrans designs require a tensile capacity of 200 kips at 1/2-inch deflection for each Class 100 pile. Prior to this time, Caltrans designs have conservatively assumed no tensile capacity could be developed within soft clays



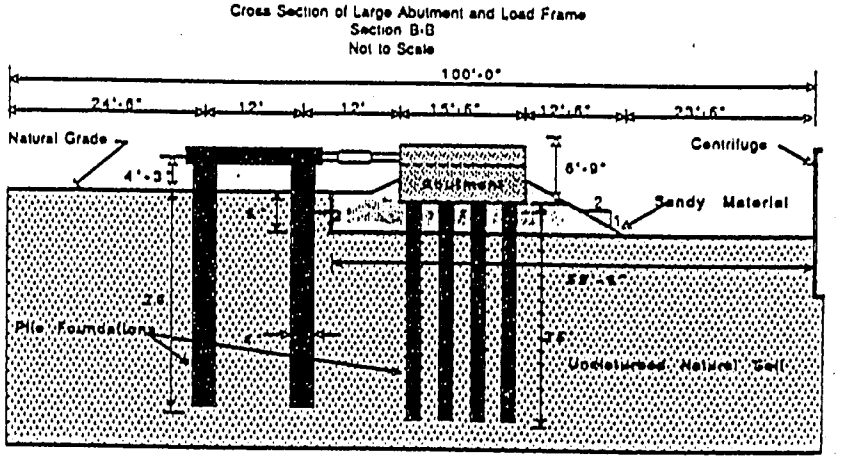
a) Plan of Primary Abutment Facility and Actuators



b) Plan and Section of Supplemental Pile Facility



c) Section thru Longitudinal Axis of Both Abutments



d) Section thru Large Abutment and Reaction Frame

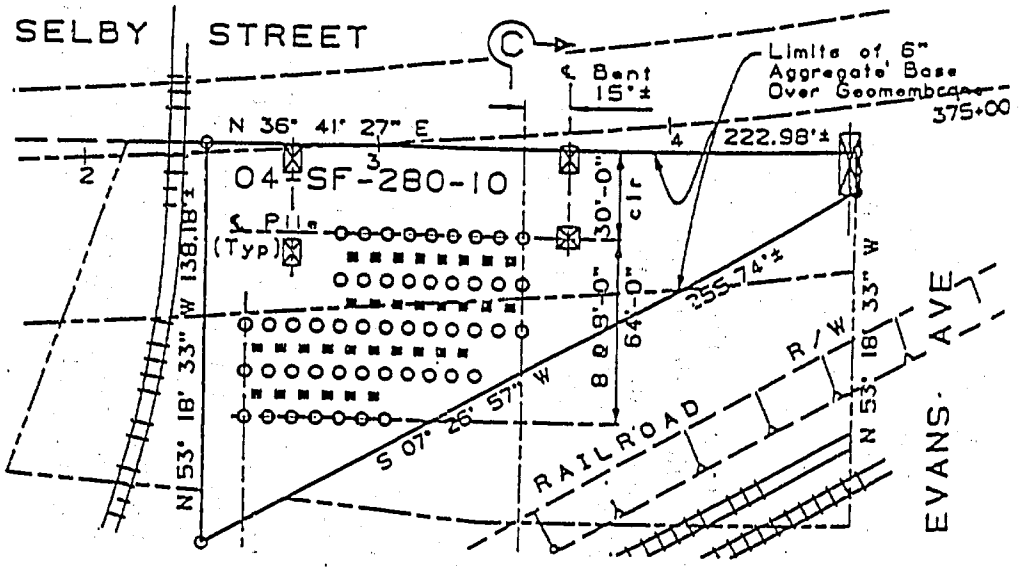
Figure 10. General Layout of UC-Davis Facilities for Large-Scale Testing of Abutment Behavior.

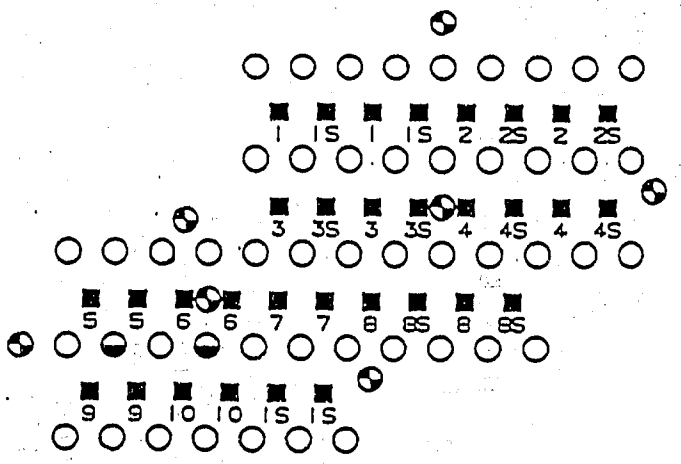
such as the Bay Mud. The field test program will directly measure the tensile, as well as compressive capacity of several pile systems in a side-by-side comparison. At the time of this publication, all test piles have been installed, and testing is planned to begin within 1992.

A total of 28 piles representing 9 separate pile systems have been installed at a site below the Southern Freeway Viaduct (Hwy 280) near Evans Street. This site was chosen because of its unique subsurface profile which includes a 90-ft-thick layer of relatively uniform soft Bay Mud overlying a dense granular formation. These strata are overlain by a 20-ft-thick layer of miscellaneous fill. Two piles of each design were installed such that the tip elevation terminates within the Bay Mud. An additional pair of several of the designs were installed such that the tip is within the dense underlying strata. To avoid uncertainties associated with shaft friction in the miscellaneous surface fill, a casing of sufficient diameter to assure a clear space between the pile and fill was installed through the entire depth of fill at each test-pile location prior to pile installation.

Figure 11 illustrates the general site layout which involves alternating rows of test piles and reaction piles. All reaction piles are HP14x89 steel H-sections, and the test-pile systems include both five standard Caltrans designs and four newer proprietary systems. The standard designs are: 1) a 16-inch I.D. by 0.5-inch thick open-ended steel pipe pile, 2) a pre-loaded steel-pipe pile/tiedown system, 3) a HP14x89 steel H-pile, 4) a 14-inch square prestressed concrete pile, and 5) a timber pile. All standard designs were installed into the ground using conventional driving techniques except for the pile/tiedown system which involved both driving and a subsequent drilling/grouting operation. The proprietary designs are: 1) a tapered and fluted pile provided by Monotube Piling Co. which was driven using conventional methods, 2) a system provided by Fundex (Holland) which uses a pipe pile and a conical auger-flight tip which is first screwed into the ground and then followed by grout injection through the tip, 3) a pile/tiedown system provided by Nicholson Construction Co. which differs from the Caltrans pile/tiedown design primarily by the method of installation, and 4) a reinforced soil-grout column provided by Halliburton/Brown and Root which is installed using a specialized jet-grouting rig.

Load testing will be accomplished with the DNTMR 500-ton-capacity load frame which mounts atop of four reaction piles. All piles will be tested first in tension, then in compression. It is recognized that the compression-test results will be affected by prior tension testing, however, the tension results have been prioritized for this project. Each pile will be cycled through a series of progressively increasing load loops. Applied force will be measured with load cells and pile-head displacements will be measured relative to an independent reference frame using linear optical displacement gauges. Additionally, load-shedding behavior with depth will be documented during load application by recording either strain or displacement measurements (as appropriate to pile type) within the test piles at multiple depths. Pneumatic piezometers have been installed at three depths within





LEGENDS

- Indicates Existing Boundary
- Indicates Reaction Pile
- Indicates 14x14 Class 100 Pile
- Indicates Approximate Location of Piezometer (To Be Installed By CALTRANS)
- Indicates Test Pile

PILE NUMBER:

* 1 - Nicholson(Anchored)
* 1S- Nicholson Pin-Pile(Short)
* 2 -
* 2S-
* 3 - Monotube(Anchored)
* 3S- Monotube(Short)
* 4 - Fundex(Anchored)
* 4S- Fundex(Short)
5S- 16"Ø Steel Pipe Pile(PP16x.500)
6S- 14"x14" Prestressed
7S- Timber
* 8 - Halliburton-Pressure Grouted Soil-Concrete Pile(Anchored)
* 8S- Halliburton(Short)
9S- H-P (HP14x89)
10- Preloaded Steel Pipe Pile/Tiedown

S = Short Adhesion Piles

*To be furnished & Installed by others.

Figure 11. Location and General Layout of Highway 280 Pile Load Test Facility

the clay at each of four separate locations on the site to document regional pore-pressure fluctuations caused by both driving and testing operations. Finally, driving data (acceleration and stress) was recorded for all driven test-pile systems for both the final 30 to 40 feet of initial driving as well as during a subsequent re-strike.

Test results will yield both capacity and stiffness parameters for each of the pile systems being tested. Additionally, measured capacity results will be compared with predictions prepared on the basis of driving data. Finally, an overall evaluation of pile systems will be made which considers both economy and ease of installation in addition to capacity. Additional information on this project will be presented by Mason (62) at the Structures Congress at the UC-Irvine in April of 1993.

9. Conclusions

This paper has provided a current broad overview of the Caltrans-sponsored seismic foundation research program. The intent of this summary has been to provide the reader with both an abstract understanding of each of the individual projects, as well as a means to access more in-depth information on topics of particular interest. In addition to the projects discussed herein, an extensive research program is being conducted on purely structurally-related issues of seismic bridge design. These projects include a number of full-scale physical tests of both various structural components and alternative retrofit concepts as well as analytical studies. Considering the comprehensive scope of the Caltrans-sponsored seismic research program, the ~$5 million annual cost of continuing this aggressive effort is relatively low as it represents only ~10% of the current annual allocations for the retrofit of deficient structures, or ~2% of the current annual expenditures on new bridge construction. The problems associated with understanding the seismic behavior of the wide range of unique Caltrans structures spanning the unprecedented array of subsurface conditions which exist in California is indeed challenging. The continued dedication of research community in providing applications-oriented results will help Caltrans meet that challenge and assure both the efficiency and reliability of the California transportation system.

References

1. Caltrans Division of Structures, 1991, "First Annual Seismic Research Workshop", Proceedings, State of California, December, 244 p.
2. Roberts, J.E., 1991, "Seismic Design of Bridge Foundations", Transportation Research Record, Proceedings of the 3rd TRB Bridge Engineering Conference, March 10-13.
3. Thorkildsen, E., 1992, "Overview of Caltrans' Bridge Seismic Research Program", Structures Notes, No. 27, July, pp. 11-15.
4. Fenves, G.L., F.C. Filippou, and D.T. Sze, 1991, "Evaluation of the Dumbarton Bridge in the Loma Prieta Earthquake", Proceedings, First Annual Seismic

Research Workshop, Caltrans Division of Structures, State of California, December, pp 67-76.

5. Fenves, G.L., 1992, "Earthquake Analysis and Response of Multi-Span Bridges and Viaduct Structures", Proceedings, Seismic Design and Retrofit of Bridges, UC-Berkeley, June, 31 p.

6. Fenves, G.L., F.C. Filippou, and D.T. Sze, 1992, "Response of the Dumbarton Bridge in the Loma Prieta Earthquake", Report No. UCB/EERC-92/02, Earthquake Engineering Research Center, University of California at Berkeley, Berkeley, CA.

7. Housner, G.W. (Chairman), 1990, "Competing Against Time", Report to Governor George Deukmejian from The Governor's Board of Inquiry on the 1989 Loma Prieta Earthquake, C.C. Thiel Jr. (editor), Department of General Services, Publications Section, North Highlands, CA, 264 p.

8. Astaneh, H., B. Bolt, G. Fenves, J. Lysmer, P. Monteiro, and G. Powell, 1991, "Seismic Condition Assessment of the Bay Bridge", Proceedings, First Annual Seismic Research Workshop, Caltrans Division of Structures, State of California, December, pp 87-96.

9. Astaneh, H., 1992, "Seismic Evaluation and Retrofit of the Bay Bridge", Proceedings, Seismic Design and Retrofit of Bridges, UC-Berkeley, June, 31 p.

10. Eidinger, J., and N. Abrahamson, 1991, "Seismic Response of Long Span Bridges to Incoherent Ground Motion", Proceedings, First Annual Seismic Research Workshop, Caltrans Division of Structures, State of California, December, pp 101-110.

11. Lysmer, J. and N. Deng, 1991, "Two-Dimensional Site Response Analysis", Proceedings, First Annual Seismic Research Workshop, Caltrans Division of Structures, State of California, December, pp 97-100.

12. Der Kiureghian, A., and A. Neuenhofer, 1992, "Response Spectrum Method for Incoherent Support Motions", Proceedings, Seismic Design and Retrofit of Bridges, UC-Berkeley, June, 6 p.

13. Caltrans, June 1990, Bridge Design Specifications, Office of Structural Design, pp. 3-15 to 3-18.

14. DNTMR, Office of Geotechnical Engineering, 1992, "Caltrans Procedures for Development of Site-Specific Acceleration Response Spectra", Proceedings, Seismic Design and Retrofit of Bridges, UC-Berkeley, June, 16 p.

15. Idriss, I.M., and J.I. Sun, 1992, "SHAKE91 - A Computer Program for Conducting Equivalent Linear Response Analysis of Horizontally Layered Soil Deposits", Users Manual, University of California at Davis, Davis, CA.

16. Schnabel, P. B., J. Lysmer, and H.B. Seed, 1972, "SHAKE, A Computer Program for Earthquake Response Analysis of Horizontally Layered Sites", Report No. EERC 72-12, University of California, Berkeley.

17. Sadigh, K., J. Egan, and R. Youngs, 1986, "Specification of Ground Motion for Seismic Design of Long Period Structures", Earthquake Notes, Vol 57, No. 13.

18. Geomatrix Consultants, Inc., San Francisco, CA, "Seismic Response Study for Proposed Benicia-Martinez Bridge, Contra Costa and Solano Counties", Draft Report to California, Department of Transportation, in-press.

19. Sun, J.I., R. Golesorkhi, and H.B. Seed, 1988, "Dynamic Moduli and Damping Ratios for Cohesive Soils", Report No. UBC/EERC-88/15, Earthquake Engineering Research Center, 42 p.

20. Vucetic, M., and R. Dobry, 1991, "Effect of Soil Plasticity on Cyclic Response", ASCE, Journal of Geotechnical Engineering, Vol 117, No. 1, pp. 89-107.

21. Dickenson, S.E., R.B. Seed, J. Lysmer, and C.M. Mok, 1991, "Response of Soft Soils During the 1989 Loma Prieta Earthquake and Implications for Seismic Design Criteria", Proceedings of the Pacific Conference on Earthquake Engineering, Aukland, New Zealand, Nov. 20-23, 13 p.

22. Idriss, I.M., 1990, "Response of Soft Soil Sites During Earthquakes", Proceedings of the Memorial Symposium to Honor Professor Harry Bolton Seed, Berkeley, CA, May 10-11, 16 p.

23. Hryciw, Roman D., K.M. Rollins, M. Homolka, S.E. Shewbridge, and M. McHood, 1991, "Soil Amplification at Treasure Island During the Loma Prieta Earthquake", Proceedings: Second International Conference on Recent Advances in Geotechnical Earthquake Engineering and Soil Dynamics, Paper Number LP20, St. Louis, MO., March 11-15, pp. 1679-1685.

24. Working Group on California Earthquake Probabilities, 1990, "Probabilities of Large Earthquakes, San Francisco Bay Region, California", Circular Report No. 1053, United State Geological Survey.

25. Dickenson, S.E., and R.B. Seed, 1991, "Correlations of Shear Wave Velocity and Engineering Properties for Soft Soil Deposits in the San Francisco Bay Region", Report No. UCB/EERC-91/xx, Earthquake Engineering Research Center University of California, Berkeley, in press.

26. Seed, R.B., S.E. Dickenson, and C.M. Mok, 1992, "Recent Lessons Regarding Seismic Response Analyses of Soft and Deep Clay Sites", Proceedings, Seismic Design and Retrofit of Bridges, UC-Berkeley, June, 15 p.

27. Lee, M.K.W., and W.D.L. Finn, 1978, "DESRA-2, Dynamic Effective Stress Response Analysis of Soil Deposits with Energy-Transmitting Boundary Including Assessment of Liquefaction Potential", Users Guide, University of British Columbia, Vancouver.

28. Idriss, I.M., 1991, "Earthquake Ground Motions at Soft Soil Sites", Proceedings, 2nd International Conference on Recent Advances in Geotechnical Earthquake Engineering and Soil Dynamics, St. Louis, MO, March.

29. Seed, R.B., S.E. Dickenson, and C.M. Mok, 1992, "Recent Lessons Regarding Seismic Response Analyses of Soft and Deep Clay Sites", Proceedings, 4th

Japan-US Workshop on Earthquake Resistant Design of Lifeline Facilities and Countermeasures Against Soil Liquefaction, Honolulu, HA, May 27-29, 15 p.

30. Seed, R.B., Personal Communication 9/30/92.

31. Gates, James H., 1975, "California Seismic Design Criteria for Bridges", ASCE National Convention, Meeting Preprint 2607, 30p.

32. Luo, J.S., P.R. Kich, A. Ghose, R.M. Polivka, 1991, "Parametric Studies for the Seismic Modeling of Two-Level Elevated Freeways, Work Package No. 11, Effects of Foundation Flexibility", Report to Caltrans Division of Structures, Cygna Group, Walnut Creek, CA, Revision 0 Dated June 14, 22 p.

33. Bathe, K.J., E.L. Wilson, and F.E. Peterson, 1974, "SAP IV - Structural Analysis Program for Static and Dynamic Response of Linear Systems", User Guide, Report No. 73-11, Earthquake Engineering Research Center, University of California, Berkeley, CA.

34. Seible, F., I.M. Idriss, J. Nicoletti, 1992, "I-880 Reconstruction Project Seismic Design Critical Reiview - Assessment by the Independent Seismic Safety Review Panel, Appendix B", Report to Caltrans Division of Structures, June 30.

35. Reese, L., Awashika, Lam, and Wang, 1987, "Documentation of Computer Program GROUP1: Analysis of a Group of Piles Subjected to Axial and Lateral Loading", User Guide, Ensoft, Inc, Austin, TX.

36. Lam, I.P., G. Martin, and R. Imbsen, 1991, "Modeling Bridge Foundations for Seismic Design and Retrofitting", Transportation Research Record 1290, Proceedings of the 3rd TRB Bridge Engineering Conference, March 10-13, pp. 113-126.

37. Broms, B.B., 1964, "Lateral Resistance of Piles in Cohesive Soils", ASCE, Journal of Soil Mechanics and Foundation Division, SM2, March, pp. 27-63.

38. Broms, B.B., 1964, "Lateral Resistance of Piles in Cohesionless Soils", ASCE, Journal of Soil Mechanics and Foundation Division, SM3, May, pp. 123-156.

39. Penzien, J., R. Imbsen, and W.D. Liu, 1981, "NEABS - Non-Linear Earthquake Analysis of Bridge Systems", User Guide, Earthquake Engineering Research Center, University of California, Berkeley, CA.

40. Sweet, J., 1979, "SATURN - A Multi-Dimensional Two-Phase Computer Program Which Treats the Nonlinear Behavior of Continua Using the Finite Element Approach", Report No. JSA-79-016, Joel Seet and Associates , September.

41. Bardet, J.P., "LINOS - A Non-Linear Finite Element Program for Geomechanics and Geotechnical Engineering", User Guide, Research Center for Computational Geomechanics, University of Southern California, Los Angeles, CA.

42. Imbsen & Associates, 1984, "SEISAB-1 User Manual and Example Problems", User Guide, Engineering Computer Corporation, Sacramento, CA.

43. Matlock, H.S., D. Bogard, I. Lam, 1981, "BMCOL76: A Computer Program for the Analysis of Beams-Columns Under Static Axial and Lateral Loading", User Guide, Ertec, Inc., Long Beach, CA.

44. Matlock, H.S., H.C. Foo, C-F. Tsai, and I. Lam, 1979, "SPASM8 - A Dynamic Beam-Column Program for Seismic Pile Analysis With Support Motion, User Guide, Fugro, Inc. Long Beach, CA.

45. Lysmer, J., T. Udaka, C.F. Tsai, and H.B. Seed, 1975, "FLUSH - A Computer Program for Approximate 3-D Analysis of Soil-Structure Interaction Problems", User Guide, Report No. UCB/EERC-75/30, Earthquake Engineering Research Center, University of California, Berkeley, CA.

46. Lysmer, J., and C.C. Chin, 1991, "Seismic Response of Piled Bridge Piers", Proceedings, First Annual Seismic Research Workshop, Caltrans Division of Structures, State of California, December, pp. 21-24.

47. Cafe, P.F.M, 1991, "Dynamic Response of a Pile-Supported Bridge on Soft Soil", Masters Thesis, Department of Civil Engineering, Univerity of California at Davis, 152 p.

48. Singh, J.P., 1992, "ATC-32, Design Earthquakes and Seismic Loading Guidelines", Report to ATC Dated 6/3/92, Geospectra, Inc., 17 p.

49. Lam, I.P., and G. Martin, 1992, "Review of Caltrans Bridge Design Specifications and Practice for Abutments and Foundations", Report to ATC, Earth Mechanics, Inc., 17 p.

50. Ramey, M.R., K.M. Romstad, R. Dougherty, and J.P.M. Mwangi, 1991, "Experimental Testing of Epoxy Injected and Steel Shell Retrofitted Sections from the Collapsed Struve Slough Bridge", Proceedings, First Annual Seismic Research Workshop, Caltrans Division of Structures, State of California, December, pp. 157-165.

51. Priestley, M.J.N., F. Seible, and N. Hamada, 1991, "Retrofit and Assessment of Foundations", Proceedings, First Annual Seismic Research Workshop, Caltrans Division of Structures, State of California, December, pp. 21-24.

52. Abcarius, J., 1991, "Lateral Load Tests on Driven Pile Footings", Proceedings, Third Bridge Engineering Conference, Denver, CO, March, 8 p.

53. Gates, J.H., and M.J. Smith, 1982, "Verification of Dynamic Modeling Methods by Prototype Excitation", Report No. FHWA/CA/SD-82/07, California Department of Transportation, Office of Structures Design, Sacramento, CA, November.

54. Douglas, B.M., C.B. Crouse, S.D. Werner, and E.A. Maragakis, 1992, "Quick-Release Dynamic Tests of the Meloland Road Overcrossing", Report in Preparation, University of Nevada at Reno, Center for Civil Engineering Earthquake Research.

55. Crouse, C.B., 1992, "Estimation of Foundation Stiffnesses of Meloland Road Overcrossing During Quick-Release Tests", Report, University of Nevada at Reno, Center for Civil Engineering Earthquake Research.

56. Douglas, B.M., E.A. Maragakis, and S. Vrontinos, 1991, "Parameter Identification Studies of the Meloland Road Overcrossing", Proceedings, Pacific Conference on Earthquake Engineering, Vol 1, pp. 105-116.

57. Norris, G.M., 1986, Nonstable Rotational Stiffness of a Pile Group", Proceedings, Third U.S. National Conference on Earthquake Engineering, pp. 635-646.

58. Wilson, J.C., and B.S. Tan, 1990, "Bridge Abutments: Assessing Their Influence of Earthquake Response of Meloland Road Overpass", ASCE, Journal of Engineering Mechanics, Vol 116, No. 8, pp. 1838-1856.

59 Crouse, C.B., T. Price, and R. Mitchell, 1992, "Evaluation of Methods to Estimate Pile Foundation Stiffnesses for Bridges".

60. Cooper, T.R., 1992, "Terminal Separation Design Criteria: A Case Study of Current Bridge Seismic Design and Application of Recent Seismic Design Research", Proceedings, Seismic Design and Retrofit of Bridges, UC-Berkeley, June, 17 p.

61. Romstad, K., B. Kutter, B. Maroney, M. Griggs, E. Kasper, X.S. Li, and E. Vanderbilt, 1991, "Experimental Measurements of Bridge Abutment Behavior", Proceedings, First Annual Seismic Research Workshop, Caltrans Division of Structures, State of California, December, pp. 31-40.

62. Mason, J.A., 1993, "Tension Pile Test", Proceedings, ASCE Structures Congress, UC-Irvine, April.

SEISMIC STRENGTHENING AND RETROFITTING OF HIGHWAY BRIDGES IN JAPAN

Kazuhiko KAWASHIMA and Shigeki UNJOH

Earthquake Engineering Division, Public Works Research Institute

SUMMARY

Presented are current technical developments for seismic strengthening and retrofitting of highway bridges in Japan. Seismic inspections, history of provision of seismic design codes, and seismic strengthening methods for highway bridges and the applications are described with emphasis on practical applications of strengthening and retrofitting.

INTRODUCTION

Japan is one of the most seismically disastrous countries in the world and has often suffered significant damages from large earthquakes. More than 3,000 highway bridges have suffered damages in the past earthquakes since the Kanto Earthquake of 1926. It should be noted here that although there were many bridges which suffered damages due to earthquakes, number of bridges which fell down was only 15 except number of bridges which fell down by fires. Since the damage to highway bridges loses functions as an emergency evacuation route and a transportation route for emergency relief goods and it takes a long time to be repaired, it significantly affects social and economical activities in the area. Therefore, it is important to provide appropriate seismic resistance for highway bridges.

This paper presents the factors which affect seismic vulnerability of highway bridges and the seismic strengthening and retrofitting for the substructures with emphasis on the practical applications.

DETAILS OF THE PAST SEISMIC INSPECTIONS OF HIGHWAY BRIDGES IN JAPAN

The Ministry of Construction has made several seismic inspections of highway bridges throughout the country since 1971 as a part of comprehensive earthquake disaster prevention measures for highway facilities. Seismic strengthening work for vulnerable highway bridges has been successively made according to these seismic inspections. Table 1 shows the history of past seismic inspections of highway bridges in Japan.[1)-9)]

Table 1 Details of the Past Seismic Inspections of Highway Bridges in Japan

Year	Highways Inspected	Inspection Items	Number of Bridges		
			Inspected	Require Strengthening	Strengthened
1971	All Sections of National Expressways and National Highways, and Sections of the Others (Bridge Length ≧ 5m)	① Deterioration ② Bearing Seat Length S for Bridges supported by Bent Piles	18,000	3,200	1,500
1976	All Sections of National Expressways and National Highways, and Sections of the Others (Bridge Length ≧ 15m or Overpass Bridges)	① Deterioration of Substructures, Bearing Supports and Girders/Slabs ② Bearing Seat Length S and Devices for Preventing Falling-off of Superstructure	25,000	7,000	2,500
1979	All Sections of National Expressways, National Highways and Principal Local Highways, and Sections of the Others (Bridge Length ≧ 15m or Overpass Bridges)	① Deterioration of Substructures and Bearing Supports ② Devices for Preventing Falling-off of Superstructure ③ Effect of Soil Liquefaction ④ Bearing Capacity of Soils and Piles ⑤ Strength of RC Piers ⑥ Vulnerable Foundations (Bent Pile and RC Frame on Two Independent Caisson Foundation)	35,000	16,000	13,000
1986	All Sections of National Expressways, National Highways and Principal Local Highways, and Sections of the Others (Bridge Length ≧ 15m or Overpass Bridges)	① Deterioration of Substructures, Bearing Supports and Concrete Girders ② Devices for Preventing Falling-off of Superstructure ③ Effect of Soil Liquefaction ④ Strength of RC Piers (Bottom of Piers and Termination Zone of Main Reinforcement) ⑤ Bearing Capacity of Piles ⑥ Vulnerable Foundations (Bent Piles and RC Frame on Two Independent Caisson Foundation)	40,000	11,800	6,000 (As of the End of 1989 Fiscal Year)

Note) Number of bridges inspected, number of bridges that required strengthening and number of bridges strengthened are approximate numbers.

The first seismic inspection was made in 1971 in order to strengthen and promote earthquake disaster prevention measures in Japan. The damage experiences of highway bridges caused by the San Fernando Earthquake (Magnitude = 6.6) close to Los Angeles, USA, in February, 1971 was a turning point of the initiation of the inspection. Highway bridges with span length greater than or equal to 5m on all sections of national expressways and national highways, and sections of the others were inspected in which attention was paid to detect deterioration such as cracks of reinforced concrete structures, tilting, sliding, settlement and scouring of foundations, etc. Approximately 18,000 highway bridges in total were inspected and approximately 3,200 bridges were found to require retrofitting.

Following the first seismic inspection, it has been subsequently made in 1976, 1979 and 1986, with gradually expanding highways inspected and inspection items. The latest inspection of 1986 was made with the increase of social needs to insure seismic safety of highway traffic after the damage experiences caused by the Urakawa-oki Earthquake of 1982 and the Nihon-kai-chubu Earthquake in 1983. The highway bridges with span length greater than or equal to 15m on all sections of national expressways, national highways and principal local highways, and sections of the other, and overpass bridges were inspected. The inspection items included deterioration, devices for preventing falling-off of superstructure, strength of substructures and stability of foundations.

A series of these seismic strengthening works, approximately 23,000 highway bridges were successively strengthened by the end of 1989 fiscal year.

SEISMIC DAMAGE TO HIGHWAY BRIDGES AND PROVISIONS OF SEISMIC DESIGN CODES

It was in 1927, which was the next year of the Kanto Earthquake in 1926, to initiate introducing the seismic effect in the design of highway bridges. The Civil Engineering Bureau of the Ministry of Internal Affairs in those days notified "the method of seismic design of abutments and piers". The seismic design method has been developed and improved with progress of comprehensive technology on earthquake engineering and a number of damage experiences. In particular, the seismic design technology was integrated and summarized by the establishment of "Specifications for Seismic Design of Highway Bridges" in 1971, which independently provided seismic design issues. Furthermore, it was revised in 1980 and integrated in "Design Specifications of Highway Bridges" as "Part V : Seismic Design." And the "Part V : Seismic Design" was revised in 1990 and is currently in practice. In the latest specification for seismic design, design seismic loads, bearing capacity of reinforced concrete pier for lateral force, soil liquefaction, design details in seismic design and so on are prescribed and it may be an unique specification for seismic design in the world. It should be noted here that the remarkable attentions were paid to the seismic design of highway bridges after 1971.

Table 2 shows the provisions of design issues for the seismic design method of highway bridges. In this table, the design issues for seismic design of substructures are shown.

Table 2 History of Seismic Design Methods for Highway Bridges in Japan

		1926 Details of Road Structure (draft), Road Law, MIA	1939 Design Specifications of Steel Highway Bridges (draft), MIA	1956 Design Specifications of Steel Highway Bridges, MOC	1964 Design Specifications of Substructures (Pile Foundations), MOC	1964 Design Specifications of Steel Highway Bridges, MOC	1966 Design Specifications of Substructures (Survey and Design), MOC	1968 Design Specifications of Substructures (Piers and Direct Foundations), MOC	1970 Design Specifications of Substructures (Caisson Foundations), MOC	1971 Specifications for Seismic Design of Highway Bridges, MOC	1972 Design Specifications of Substructures (Cast-in-Piles), MOC	1975 Design Specifications of Substructures (Pile Foundations), MOC	1980 Design Specifications of Highway Bridges, MOC	1990 Design Specifications of Highway Bridges, MOC
Seismic Loads	Seismic Coefficient	Largest Seismic Loads k_h =0.2 varied dependent on the site	k_h =0.1 ~ 0.35 varied dependent on the site und ground Condition							k_h =0.1 ~ 0.3 Standardization of Seismic Coefficient Provision of Modified Seismic Coefficient Method			Revision of Application range of Modified Seismic Coefficient Method	k_h =0.1 ~ 0.3 Integration of Seismic Coefficient Method and Modified one.
	Dynamic Earth Pressure	Epuations proposed by Mononobe and Okabe were supposed to be used.						Provision of Dynamic Earth Pressure						
	Dynamic Hydraulic Pressure	Less Effect on Piers except High Piers in Deep Water.						Provision of Hydraulic Pressure		Provision of Dynamic Hydraulic Pressure.				
Reinfored Concrete Column	Bending at Bottom	Supposed to be designed in a similar way provided in current Desigin Specifications						Provisions of Definite Design Method						
	Shear	Less Effect on RC Piers except those with Smaller section area such as RC Frame and Hollow Section						Check of Shear Strength					Provision of Definite Design Method, Decreasing of Allowable Shear Stress	
	Termination of Main Reiforement at Mid-Hieght											Elongation of Anchorage Length of Terminuted Reinforcement at Mid-Height		
	Bearing Capacity for Lateral Fore							Less Effect on RC Piers with Larger Section Area				Ductility Check	Check of Bearing Capacity for Lateral Force	
Footing							Provisions of Definite Design Method (Designed as a Cantilever Plate)					Provisions of Effective width and Check of Shear Strength		
Pile Foundation		Bearing Capacity in vertical direction was supposed to be checked.			Provisions of Definite Design Method (Bearing Capacity in vertical and horizontal directions)						Special Condition (Foundation on Slope, Consolidation Settlement, Lateral Movement)	Provisions of Design Details for Pile Head		
Direct Foundation		Stability (Overturning and Slip) was supposed to be checked.						Provisions of Definite Design Method (Bearing Capacity, Stability Analysis)						
Caisson Foundation					Supposed to be designed in a similar way provided in Design Specification of Caisson Foundation of 1969				Provisions of Definite Design Method					
Soil Liquefaction									Provisions of Soil Layers of which Bearing Capacity shall be Ignored in seismic design			Provisions of Evaluation Method of Soil Liquefaction and the treatment in seismic design		Consideration of effect of fine sand content
Bearing Support	Bearing Support		Provisions of Design Methods for Steel Bearing Supports (Bearing, Roller, Anchor Bolt)							Provision of Transmitting Method of Seismic Load at Bearing				
	Devices Preventing Falling-off of Superstructure							Provision of Bearing Seat Length S	Provisions of Stopper at Movable Bearings, Devices for Preventing Superstructure from Falling (Seat Length S, Connection of Adjacent Decks)			Provisions of Stopper at Movavle Bearings, Devices for Preventing Superstructure from Falling (Seat Length S_E, Devices)		

FACTORS WHICH AFFECT SEISMIC VULNERABILITY OF HIGHWAY BRIDGES AND FEASIBILITY OF SEISMIC STRENGTHENING

Table 3 summarizes the factors which affect seismic vulnerability of highway bridges and feasibility of seismic strengthening which was obtained through the statistical analyses of the damaged bridges in the past earthquakes in Japan.[10),11)] According to the results, 16 factors in total are significantly associated with the damages of highway bridges, in which 8 factors of ①design specifications, ⑥ devices for preventing falling-off of superstructure, ⑨ ground condition, ⑫effect of scouring, ⑬materials of substructures, ⑭type of foundations, ⑮ intensity of ground motion, and ⑯effect of termination of main reinforcement at mid-height significantly affect seismic performance of highway bridges.

From the viewpoint of seismic strengthening, these 8 factors can be categorized as follows :

1) ⑥devices for preventing falling-off of superstructure
   → Installation of devices
2) ⑦ type of substructure, ⑩ effect of soil liquefaction, and ⑫ type of foundation
   → Improvement of seismic strength of foundations
3) ⑬type of substructure, ⑭materials of substructure, and ⑯effect of termination of main reinforcement at mid-height
   → Improvement of seismic strength of substructures
4) ⑮intensity of ground motion
   → Distribution and decrease of seismic loads

Fig.1 shows the typical and effective seismic strengthening measures for the above categories.

SEISMIC STRENGTHENING METHODS OF FOUNDATIONS AND THE APPLICATIONS

Seismic strengthening of foundations are required in cases of 1)weak bearing capacity of soils induced by soil liquefaction, 2)weak bearing capacity of soils by scouring, and 3)vulnerable foundations which were built of bricks and masonry without sufficient consideration for seismic design.

In the above items, seismic strengthening measures to soil liquefaction is becoming the most important a seismic strengthening one. There are two measures to mitigate the effect of soil liquefaction, which include measures to prevent or mitigate occurrence of soil liquefaction itself, and measures to resist the effect of soil liquefaction by strength of foundations. The former measures include increase of strength of soils against soil liquefaction and replacement of liquefiable soils by non-liquefiable ones. On the other hand, in order to resist the effect of soil liquefaction by the latter measures, foundations have to be supported by non-liquefiable layer so as to prevent the settlement and tilting.

Table 3 Factors which Affect Seismic Vulnerability of Highway Bridges and Feasibility of the Seismic Strengthening

Items	Seismic Vulnerability	Feasibility of Seismic Strengthening	Principles of Countermeasures
① Design Specifications	Those designed in accordance with 1926 or 1939 Specifications have higher vulnerability	○	Strengthening of inadequate members from the viewpoint of current Design Level
② Type of Superstructure	·Gerber or simply supported girders with 2 or more spans have higher vulnerability ·Arch, frame, continuous girders, cable-stayed bridges or suspension bridges have lower vulnerability	×	———
③ Shape of Superstructure	Skewed or curved bridges do not necessarily have higher vulnerability than straight bridges	×	———
④ Materials of Superstructure	Reinforced concrete bridges or prestressed concrete bridges have lower vulnerability than steel bridges although the difference is small	×	———
⑤ Slope in Bridge Axis	Bridges with slope in bridge axis have higher vulnerability	×	———
⑥ Device for Preventing Falling-off of Superstructure	Bridges with devices for preventing falling-off of superstructure have lower vulnerability	○	Installation of Devices
⑦ Type of Substructure	Bridges supported by single-line bent piles or by reinforced concrete frame placed on two separte caisson foundations have higher vulnerability	○	Strengthening of Substructures
⑧ Height of Piers	Bridges supported by higher piers have higher vulnerability	×	———
⑨ Ground Condition	Bridges constructed on soft soil have higher vulnerability	×	———
⑩ Effect of Soil Liquefaction	Bridges constructed on sandy soil layers susceptible to liquefaction have higher vulnerability	○	Strengthening of Foundations or Strengthening of Surrounding Soils
⑪ Irregularity of Supporting Soil Condition	Bridges constructed on soils with irregularity of supporting conditions have higer vulnerability	×	———
⑫ Effect of Scouring	Bridges where the surface soils are scoured have higher vulnerability	○	Treatment for Prevention of Scouring or Strengthening of Foundations
⑬ Materials of Substructures	Bridges supported by plane-concrete substructures designed in accordance with 1926 or 1939 specifications have higher vulnerability	○	Strengthening Substructures, Renewal of Substructures
⑭ Type of Foundation	Bridges supported by timber, brick, masonry or other old unknown type substructures have higher vulnerability	○	Strengthening of Foundations
⑮ Intensity of Ground Motion	Bridges subjected to higer intensity of ground acceleration have higher vulnerability. In particular, vulnerability becomes quite high when the bridges are subjected to peak ground acceleration larger than 400 gal (0.4g)	○	Application of Base-Isolation
⑯ Effect of Termination of Main Reinforcement at Mid-height	Bridges wich RC Piers which do not have enough anchorage length for terminated reinforement have higher vulnerability	○	Strengthening of Substructures

Note ○ Items for which seismic strengthening is feasible
× Items for which seismic strengthening is not feasible

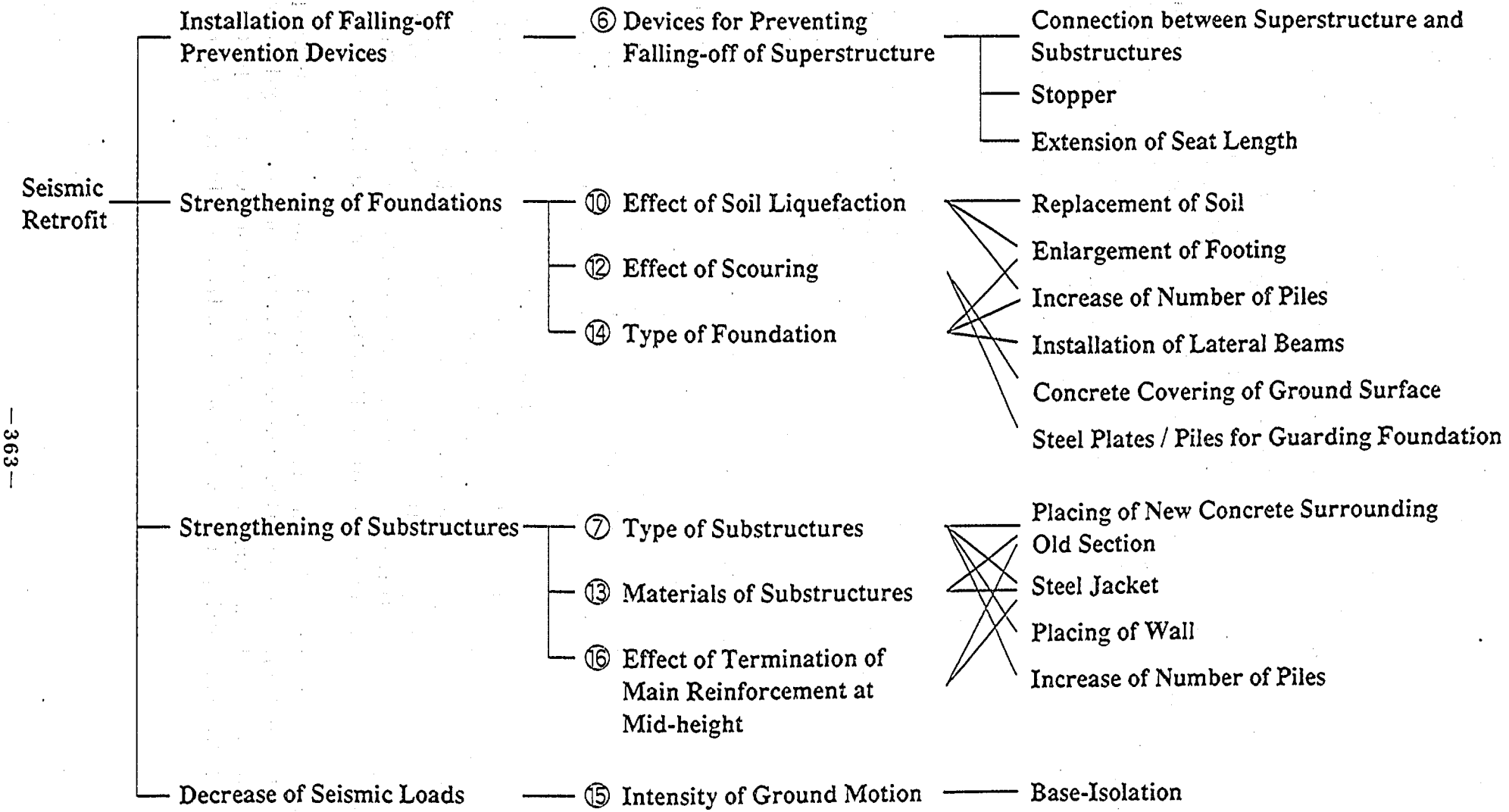


Fig.1 Selection of Seismic Strengthening Measures for Highway Bridges

Although the selection of the above two measures depends on the ground conditions and structural conditions of each site, the strengthening measures by increasing strength of foundations may generally be reliable and economical.

Table 4 and Table 5 show the seismic strengthening methods for abutment foundations and pier foundations, respectively.[12]

Two strengthening practices to soil liquefaction are shown as follows:[13]

A SEISMIC STRENGTHENING PRACTICE BY INCREASING NUMBER OF PILES

The strength of piers and piles as shown in Fig.2 were found to be sufficient, but the bearing capacity of soils became vulnerable when the soil liquefaction occurred. Three strengthening methods by ①ground improvement by soil cement, ②increase of number of piles in the transverse direction by using steel pipe piles, and ③covering of the existing foundations by steel sheet piles were investigated and compared as a strengthening measure. Since Method ① was relatively expensive, Method ② was finally adopted as a result of comparison of Methods ② and ③ with consideration of construction method, economy and reliability.

In the strengthening design, it was assumed that the existing piles resisted seismic load up to the designed level and that the force beyond the design force was supported by newly constructed piles. Since the pier to be strengthened was on the high water channel, the temporary road to the pier was provided and steel pipe pile was placed by using a vibro hammer. The new footing was constructed by shutting-up by steel sheet piles from water around the pier. Integration between existing and new footings were made by anchoring reinforcing bars and injecting resin mortar.

A SEISMIC STRENGTHENING PRACTICE BY CONNECTING BEAMS

Fig.3 shows a strengthening practice of 11-span simply-supported pretension concrete slab bridge. Reinforced concrete bent plies were used for piers and abutments. It was found that the liquefaction resistance factor, F_L, of the layer with thickness of 3.2m under the river bed was less than 1.0 and pile length which was supported by the stable soil layer was 1/3 of total pile length of 12m.

Three strengthening measures by ①strengthening of all 12 substructures, ②strengthening of one substructure per two spans, and ③strengthening of both abutments and connecting all pier crests by continuous beams were investigated as a strengthening method. Alternative methods by ④replacement of liquefiable soil layer by non-liquefiable soils and ⑤chemical grouting were also investigated. As a result of the investigation of these measures, Method ③ was selected with consideration of reliability, construction method and economy.

In the strengthening design, it was assumed that existing bent piles supported the vertical load and that seismic loads was supported by integrated structure of new and existing ones. Since pier crests of bent piles were strengthened by connecting beams, it was required to insure appropriate

Table 4 Seismic Strengthening Methods for Abutment Foundations

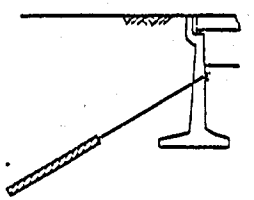
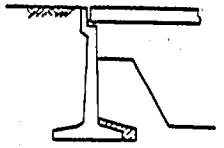
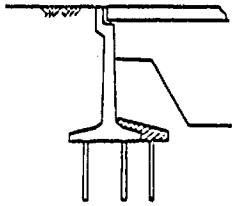
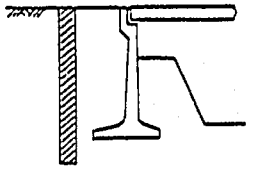
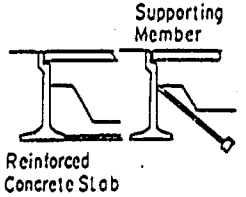
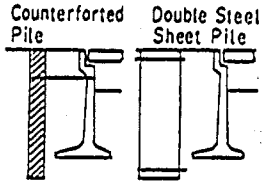
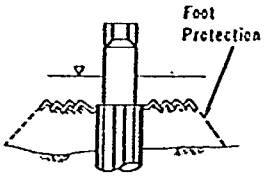
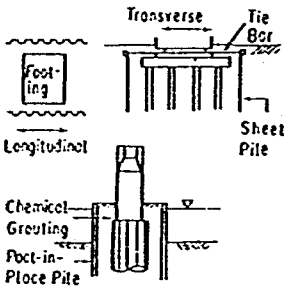
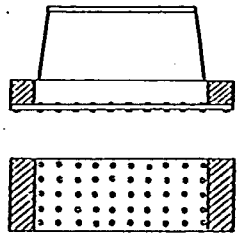
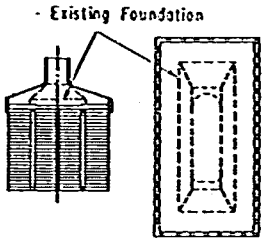
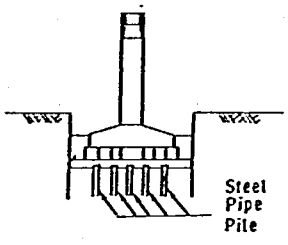
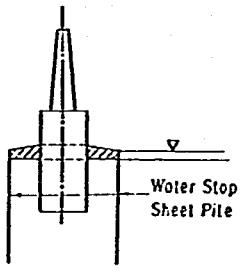
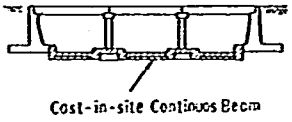
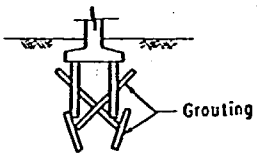
Method		① Earth Anchor	② Enlargement of Footing	③ Increase of Number of Piles	④ Piles for decreasing earth pressure	⑤ Others (Measures in the front of Foundation)	⑥ Others (Measures in the back of Foundation)
Illustration							
Outline		Increasing resistance to sliding and overturning by earth anchor constructed from the abutment wall to the ground.	Excavating ground in the front of footing and enlarging the footing	Excavating ground in the front of footing, constructing piles and enlarging the footing	Constructing piles in the back-filling ground and decreasing earth pressure to the foundation	Increasing resistance to sliding and overturning by reinforced concrete slab or supporting member	Decreasing earth pressure by counterforted pile, double steel sheet pile, improvement of ground, etc.
Strengthening Item		· Bearing Capacity of Soils · Displacement of Foundation	· Bearing Capacity of Soils	· Bearing Capacity of Soils · Bearing Capacity of Piles	· Displacement of Foundation	· Bearing Capacity of Soils	· Displacement of foundation
Points to be considered in the Design		Share of loads between earth anchor and existing footing	Connection of new and existing footing	Share of loads betwen new and existing piles. Connection of new and existing footing	· Share of earth pressure between piles and abutment	· Connection of new and existing structures	· Share of earth pressure between new and existing structures.
Points to be considered in the Construction	Traffic Regulation, Construction Space	Construction can be made by relatively small-scale construction machines. Clear headway under the girder at reast up to 3m is necessary.	Construction space can be small.	Constuction method for placing piles is restricted because of limitted construction space. Cast-in-place pile (reverse circulation drill methed) and steel pipe pile with joints can be applicable.	Traffic regulation is necessary during construction	Construction space can be small.	Traffic regulation is necessary during construction.
	Cofferdam	Construction of cofferdam is necessary but may be small-scale.	Construction of cofferdam by sheet pile is necessary. Special construction method under the girder using short sheet piles with joints is necessary.	same as ②	not necessary	same as ②	not necessary
	Effect on Existing Structure	Attention should be paid to cut of reinforcing bars of abutment wall. Strength of fixing section of earch anchor should be checked.	Stability of foundation should be checked during construction.	Stability of foundation during construction should be checked. Placing point of piles is limitted if buttered pile is used in the existing piles.	Decrease of bearing capacity of soils by soil relaxation should be checked in case of constructing cast-in-place piles	same as ① and ②	same as ④
	Effect on Surrounding Structures	Attention should be paid to underground structures in the back of abutment.	———	———	same as ①	———	same as ①
Commentary		· Earth anchor method has been applied in many practices since the construction cost is cheaper. · Careful consideration to effectiveness of strengthening should be given because the back ground may move during earthquake. · Anchorage portion should be leveled under the bottom of footing.	· Reliable construction for connecting new and existing footings is necessary. · By installation of projection in the bottom of footing increase of bearing capacity to lateral loading is possible.	· Reliable construction for connecting new and existing footings is necessary.	———	· Although increase of resistance to lateral force is reliable, this method can be applicable only for short span bridges.	———

Table 5 Seismic Strengthening Methods for Pier Foundations

Method	① Foot Protection	② Cofferdam	③ Inueese of Number of Piles	④ Cast-in-Site Diaphragms Wall
Illustration				
Outline	Protecting foundation from scouring by blocks, cover concrete and matress shaped gabion	Constructing cofferdom by sheat pile or pact-in-place pile around foundation and filling soils inside. Chemical grouting and prepacked concrete can be used for soil filling.	Increasing number of piles and enlarging the footing	Constructing cast-in-site diaphragms wall and integrating new structure with existing foundation
Strengthening Item	· Scouring	· Scouring · Bearing Capacity of Piles	· Bearing Capacity of Soils · Bearing Capacity of Piles	· Bearing Capacity of Soils · Scouring
Points to be considered in the Design	· Strengthening Area · Can not be a parmanent strengthening method	· Blocking of drainage area of river	· Reliable effectiveness of strengthening · Share of loads between new and existing structures · Connection between new and existing structures	· Reliable effectiveness of strengthening · Blocking of drainage area of river · Effect of water flow pressure
Points to be considered in the Construction	· Relatively easy construction	· Construction machine for sheet piles may be restricted by limitted construction space.	· Relatively easy for constructing piles in transverse direction · Construction machine is restricted for constructing piles under the girder · Cofferdam and dry-up construction is necessary for connection of new and existing footings.	· Apporopriate construction method for ground condition should be selected.

Method	⑤ Strengthening by Stell Pipe Pile	⑥ Enlargement of Footing	⑦ Cast-in-site Beam, Reinforced Concrete Plate	⑧ Foundation Improvement
Illustration				
Outline	Strengthening by constructing steel pipe piles under existing footing	Constructing footing at the design ground surface and resisting to moment and lateral loads	Increasing stability of foundations by connecting adjacent foundations by cast-in-site beam or reinfored concrete plate. Applicable for short span bridges.	Increasing bearing capacity of soft soils by placing quicklime pile, sand compaction pile, gravel drain, chemical grouting, soil coment, etc.
Strengthening Item	· Bearing Capacity of Foundation · Bearing Capacity of Soils	· Bearing Capacity of Soils · Scouring	· Bearing Capacity of Soils · Displacement of Foundation.	· Bearing Capacity of Soils · Effect of Soil Liquefaction
Points to be considered in the Design	———	· Share of loads between new and existing structures. · Connection of new and existing structures	———	· Evaluation of effectiveness of foundation improvement · Improvement area
Points to be considered in the Construction	· Construction of cofferdam and placement of pile under foundation is generally difficult. · Construction cost is relatively expensive.	· Construction of cofferdam is necessary	· Construction of cofferdam under the girder is necessary. · In case of river crossing bridge, transference of river course is necessary.	———

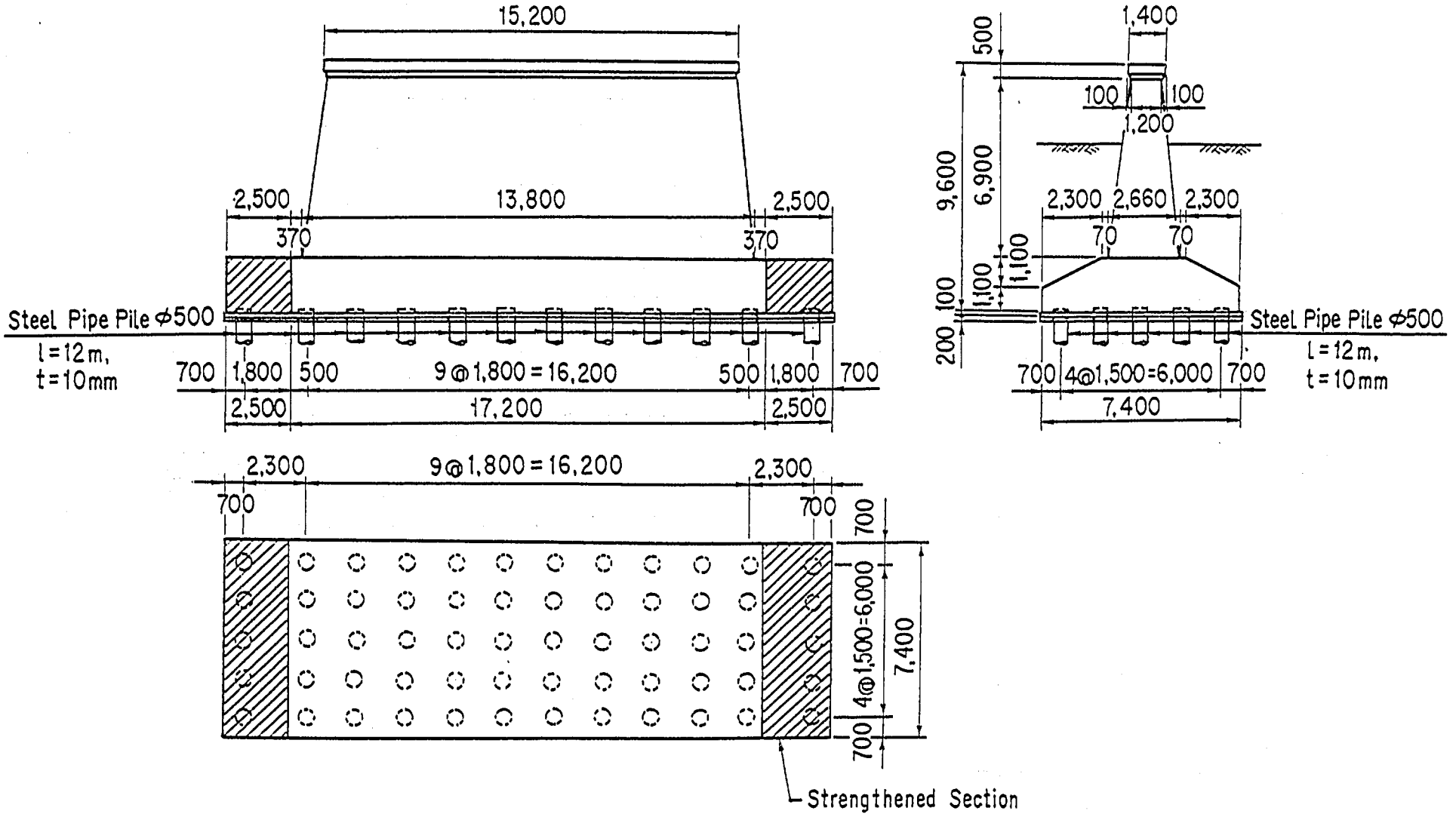


Fig.2 Seismic Strengthening of A Foundation on Liquefiable Soils by Increasing Number of Piles

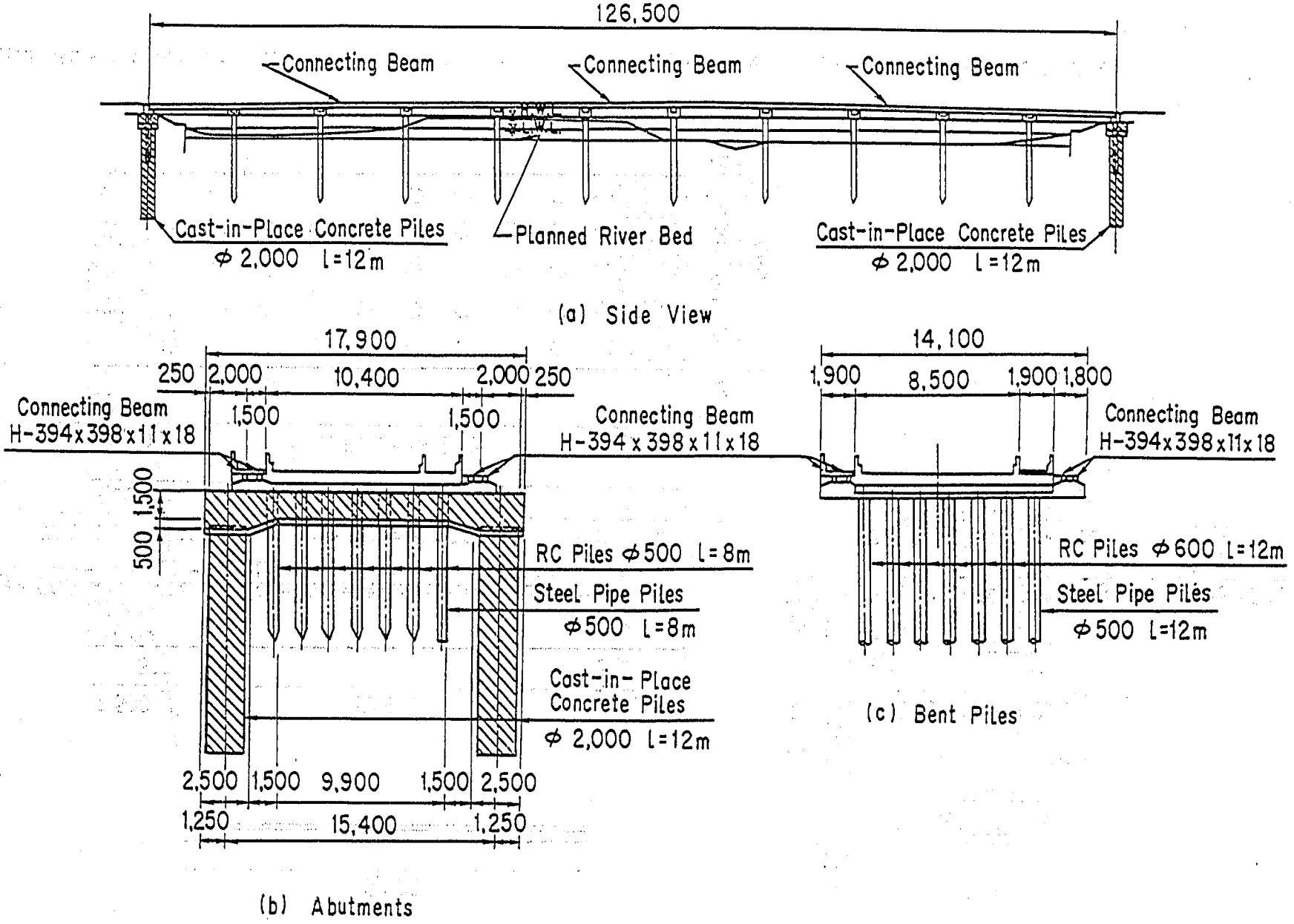


Fig.3 Seismic Strengthening of A Bent Pile on Liquefiable Soils by Connecting Beams

strength for the connecting beams. Therefore, the connecting beams were designed as a device for preventing falling-off of superstructure. The connecting beams and fix bearing on the lateral beams were designed using two times horizontal seismic coefficient. It should be noted here that the connecting beams were also used as girders of pedestrian decks.

SEISMIC STRENGTHENING METHODS OF PIERS AND THE APPLICATIONS

There are two cases that required strengthening of substructures, which include vulnerable type and materials of substructures, and weak strength of reinforced concrete piers at the bottom and termination zone of main reinforcement at mid-height.

Type of foundations vulnerable to seismic damage includes single-line bent piles and reinforced concrete frame on two independent caisson foundation. Substructures made of plain concrete, brick and masonry which were constructed in the old ages are also vulnerable to brittle failure.

On the other hand, substructures which have weak strength at the bottom include the cases in which the design seismic force is smaller than current design level or arrangement of tie reinforcement is not adequate. The strength at the termination zone of main reinforcement at mid-height had not generally checked before 1980. When the anchorage length of terminated reinforcement is not enough long, brittle failure at the zone is anticipated similarly to the damage of the piers of the Shizunai Bridge during the Urakawa-oki Earthquake of 1982.

There are two strengthening methods for such weak reinforced concrete piers, which include placement of new reinforced concrete or steel jackets. In both cases, it is important to integrate new and existing structures. Recently, jacketing method by using new materials such as carbon fiber and fiber reinforced plastic are also being studied.

Table 6 and Table 7 show the seismic strengthening methods for vulnerable bent piles and reinforced concrete piers.[12]

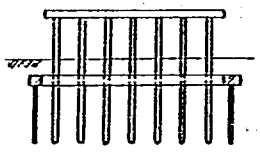
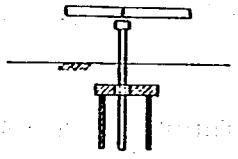
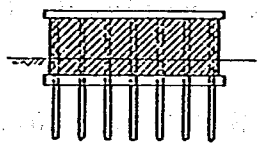
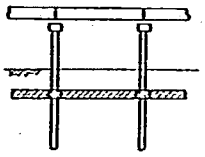
The seismic strengthening practices of substructures are shown as follows.[13]

A SEISMIC STRENGTHENING PRACTICE BY PLACING NEW REINFORCED CONCRETE (CASE 1)

Fig.4 shows a seismic strengthening practice for increasing ductility of a reinforced concrete pier by placing new reinforced concrete. The cover concrete of the existing pier was chipped-out up to the surface of longitudinal reinforcing bars, anchoring reinforcing bars were newly installed and new reinforced concrete with thickness of 17cm was placed.

The longitudinal reinforcing bars were anchored with necessary anchorage length and anchorage portion was inclined toward the pier center in order to anchor them to the existing footing.

Table 6 Seismic Strengthening Methods for Bent Piles

Method		① Increase of Number of Piles in Transverse Direction	② Increase of Number of Piles in Longitudinal Direction	③ New Reinforced Concrete Section	④ Connection of Adjacent Piers by Cast-in-site Beam
Illustration					
Outline		Constructing piles outside of deck	Constructing piles in longitudinal direction under the girder and connecting new and existing piles by new footing	Placing new reinforced concrete and integrating new and existing structures	Connecting adjacent piers and/or abutment by cast-in-site beam
Strengthening Item		Type of Substructure (Bent Pile) (Bearing Capacity of Pile)	Type of Substructure (Bent Pile)(Bearing Capacity of Pile)	Type of Substructure (Bent Pile)(Strength of Pile, Stiffness of Pile)	Type of Substructure (Bent Pile)(Bearing Capacity of Pile)
Points to be considered in the Design		Connection of new and existing section	same as ①	Check of pile stress caused by increase of weight	Connection of beam and existing piles
Points to be considered in the Construction	Traffic Regulation, Construction Space	not necessary in general. When construction of piles is mede from the deck, partial traffic regulation is necessary.	Construction method is restricted for placing piles under the girder.	Construction space is relatively small.	same as ①
	Cofferdam	Cofferdam is necessary for constructing footing. Special construction method is required for constructing sheet pile conder the girder.	same as ①	Construction of cofferdam under the gider is necessary. same as ①	Construction of cofferdam under the girder is necessary. In case of river crossing bridge, transference of river course is necessary.

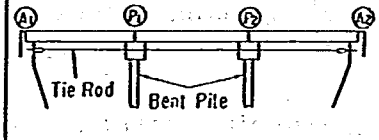
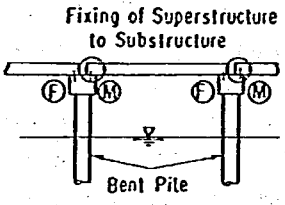
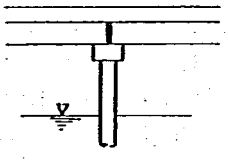
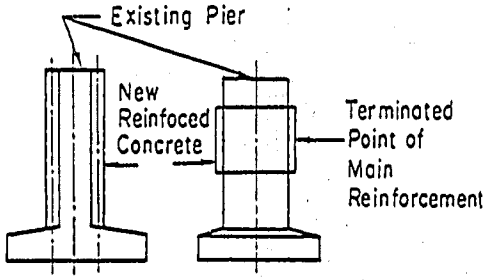
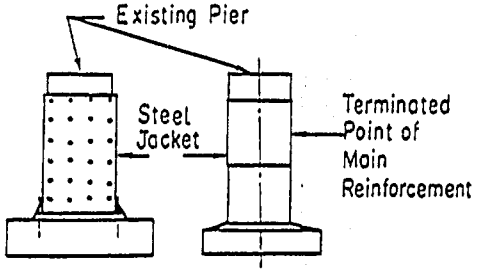
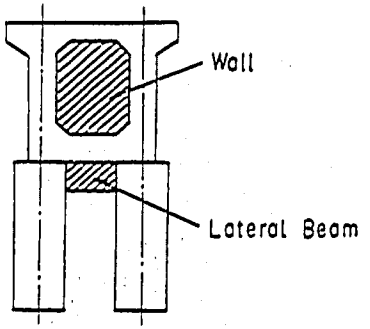
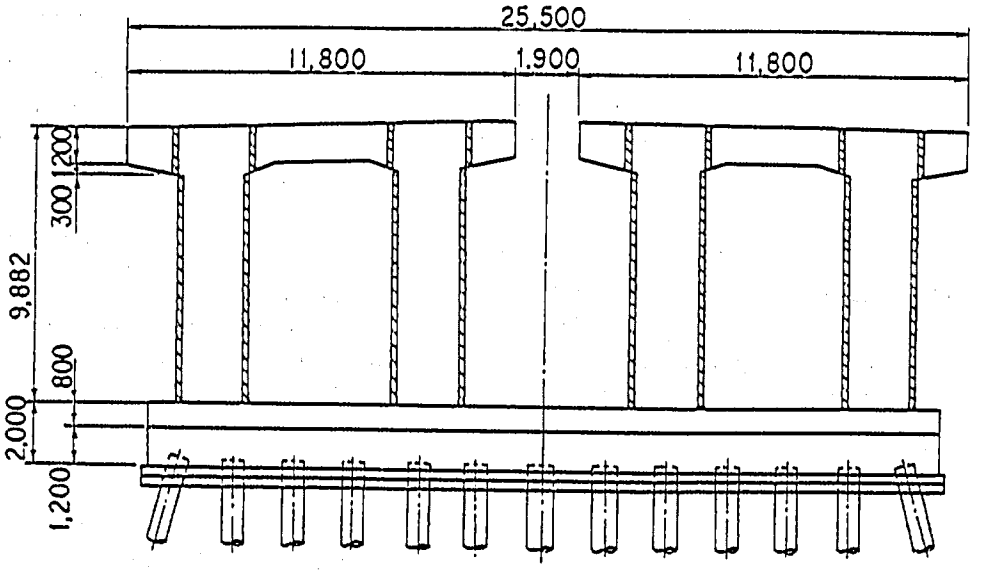
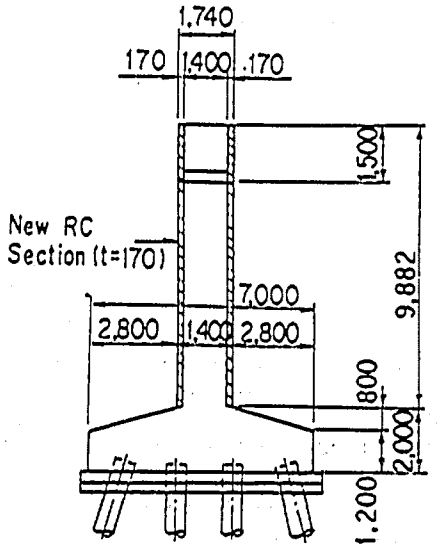
Method		⑤ Connection of Piers and Abutments by Tie-Rod	⑥ Replacement of Movable Bearing by Fixed Bearing	⑦ Connection of Deck Slab
Illustration				
Outline		Connecting piers and abutments by tie-rod and increasing stiffness in the longitudinal direction.	Fixing superstructure to substructure, and increasing stiffness in the longitudinal direction.	Connecting adjacent deck slabs and increasing drivability.
Strengthening Item		Type of Formdation (Bent Pile) (Bearing Capacity of Pile Stiffness of Pile)	Type of Foundation (Bent Pile) (Bearing Capacity of Stiffness of Pile)	Type of Foundation (Bent Pile) (Stiffness of Pile)
Points to be considered in the Design		· Design method for devices for preventing falling-off of superstructure is applicable. · Anchorage of tie-rod and anti-corrosive coating of tie-rod	· Connection between superstructure and substructure · Strengthening of fixing portion of pier crest and girder	Strengthening of connection portion of slab is necessary.
Points to be considered in the Construction	Traffic Regulation, Construction Space	not necessary	Partial traffic regulation is necessary.	Traffic regulation is necessary for removing expansion joint and replacing a part of deck slab.
	Cofferdam	not necessary	not necessary	not necessary

Table 7 Seismic Strengthening Methods for Piers

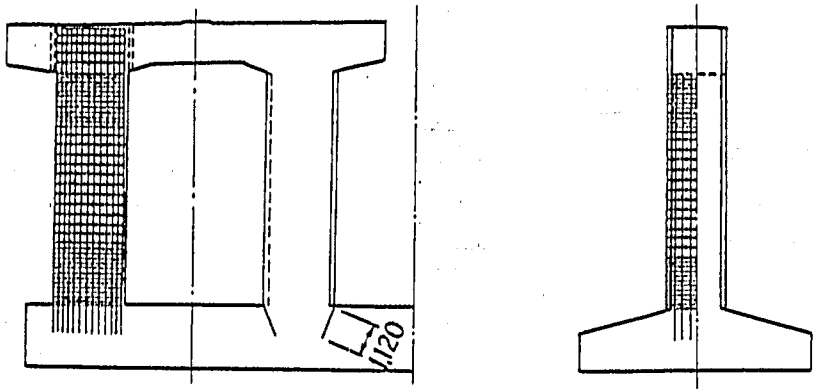
Method	① New Reinfored Concrete Section	② Steel Jacket	③ Wall and Lateral Beam
Illustration			
Outline	· Placing new reinforced concrete on existing piers · A number of practices for repairing damaged pier	· Placing steel jacket on existing piers	· Construction of wall to increase lateral strength of reinforced concrete frame. · Connecting two independent caisson foundation by lateral beam for reducing the relative displacement
Strengthening Item	· Strength of Pier	· Strength of Pier	· Strength of Reinforced Concrete Frame · Two Independent Caisson Foundation
Points to be considered in the Design	· Anchorage of reinforcing bars to footing, chipping at cover concerte of existing pier and anchoring reinforcing bars for integration of new and existing structures · Thickness and width of new reinforced concrete · Blocking of drainage area of river	· Anchoring method of steel jacket to existing pier and footing · Thickness, width and anchor bolt density · Future maintenance (painting, etc)	· Connection between new and existing structures
Points to be considered in the Construction	· In case of a river crossing bridge, construction of cofferdam is necessary.	same as ①	same as ①



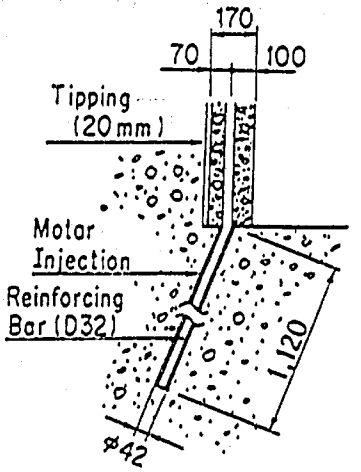
(a) Elevation



(b) Side View



(c) Arrangement of Reinforcement



(d) Anchorage of Reinforcing Bars

Fig.4 Seismic Strengthening of A Reinforced Concrete Frame by Placing New Reinforced Concrete

A SEISMIC STRENGTHENING PRACTICE BY PLACING NEW REINFORCED CONCRETE (CASE 2)

Fig.5 shows a seismic strengthening practice of a multi-column reinforced concrete frame pier. Three strengthening methods by ①replacement of pier, ② placement of new lateral beam, and ③placement of new reinforced concrete so as to change a structure-type from multi-column to oval section type were investigated. Method ③ was finally selected as a result of investigation with consideration of the viewpoint of river administration.

In the strengthening design, it was assumed that the seismic force was supported by the integrated structure of new and existing ones. All of cover concrete of the existing structure was chipped-out in order to insure integration between exiting and new structures. Although the weight of substructure increased, strengthening of foundation was not required because the foundation was on the stiff ground with N-value of more than 50.

A SEISMIC STRENGTHENING PRACTICE OF REINFORCED CONCRETE FRAME BY PLACING REINFORCED CONCRETE WALL

Fig.6 shows a strengthening practice of a reinforced concrete frame to increase lateral strength in the transverse direction by placing new reinforced concrete wall. Thickness of the wall was designed as 40 cm, and it was assumed that seismic loads was supported by the integrated structure of new and existing ones. Cover concrete of the connection portion of the existing structure was chipped-out and anchoring reinforcing bars were installed for reliable integration between new and existing structures.

A SEISMIC STRENGTHENING PRACTICE OF BENT PILE BY INCREASING NUMBER OF PILES

Fig.7 shows a seismic strengthening practice of a bent pile by increasing number of piles. Since the existing steel pipe piles were corroded and heavily damaged, the bent piles were strengthened by placing new reinforced concrete and the structure-type was changed to wall-type. Since the deck width was enlarged for increasing the number of traffic lanes, enlargement of pier width and construction of new piles were required.

In the strengthening design, it was assume that seismic loads was supported by the integrated structure of new and existing ones. In order to insure reliable integration between new and existing structures cover concrete of existing structure was chipped-out and anchoring reinforcing bars were installed. Since necessary pile length was 42m long, a steel pipe pile with larger diameter of 1.2m was selected. In the strengthening construction, a steel shell frame, which was a part of mold for concrete was used. The construction of piles and setting of the steel shell frame was made from the ship.

A SEISMIC STRENGTHENING PRACTICE OF REINFORCED CONCRETE PIER BY STEEL JACKETS

Fig.8 shows a seismic strengthening practice of a reinforced concrete pier at the termination zone of main reinforcement at mid-height. Instead of placing new reinforced concrete, steel jackets were used for covering the existing reinforced concrete pier. This was to mitigate the environmental effects such

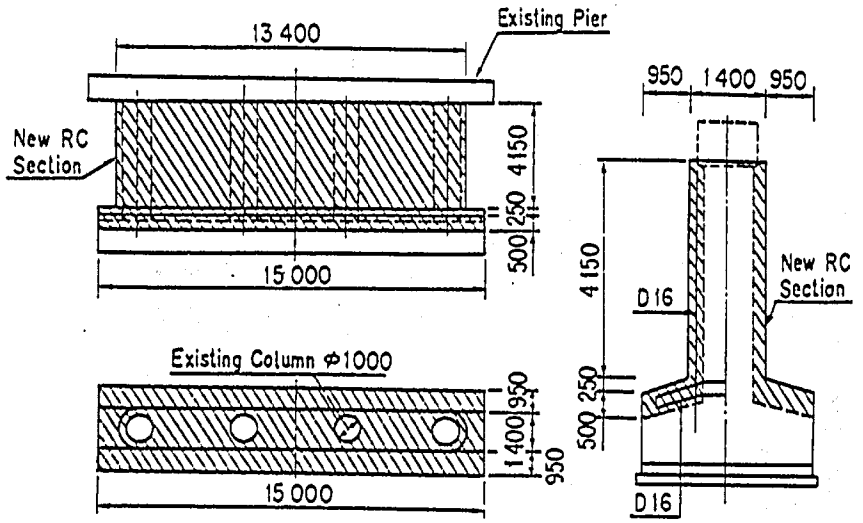


Fig.5 Seismic Strengthening of A Reinforced Concrete Columns by Placing New Reinforced Concrete

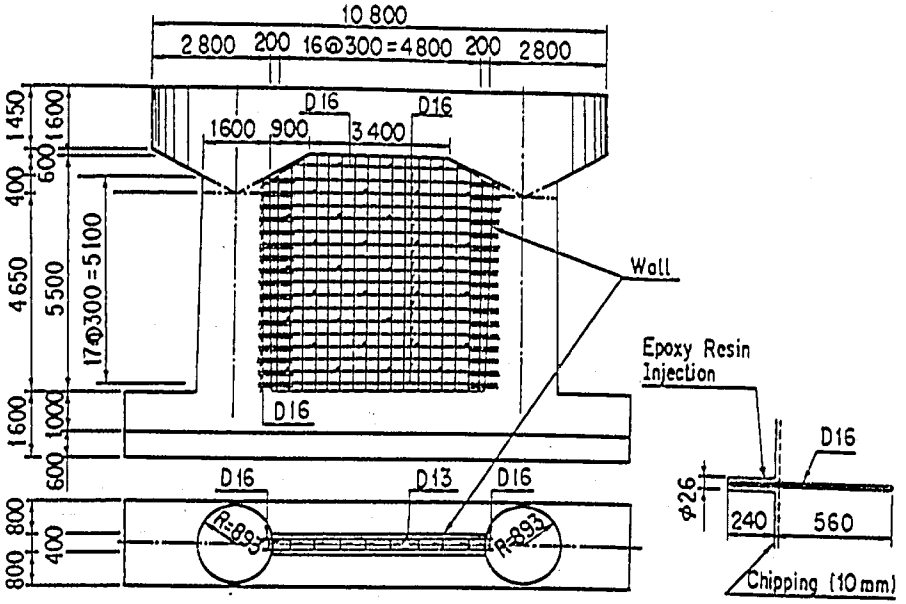


Fig.6 Seismic Strengthening of A Reinforced Concrete Frame by Placing New Reinforced Concrete Wall

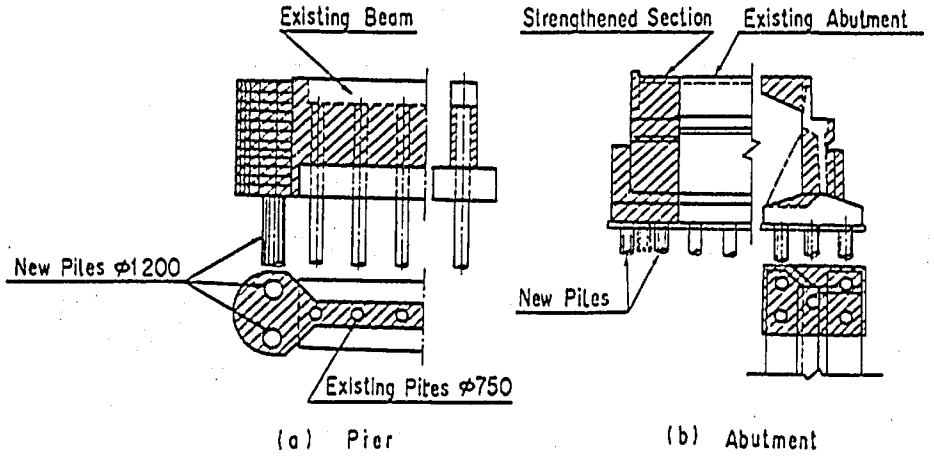


Fig.7 Seismic Strengthening of A Bent Pile by Increasing Number of Piles

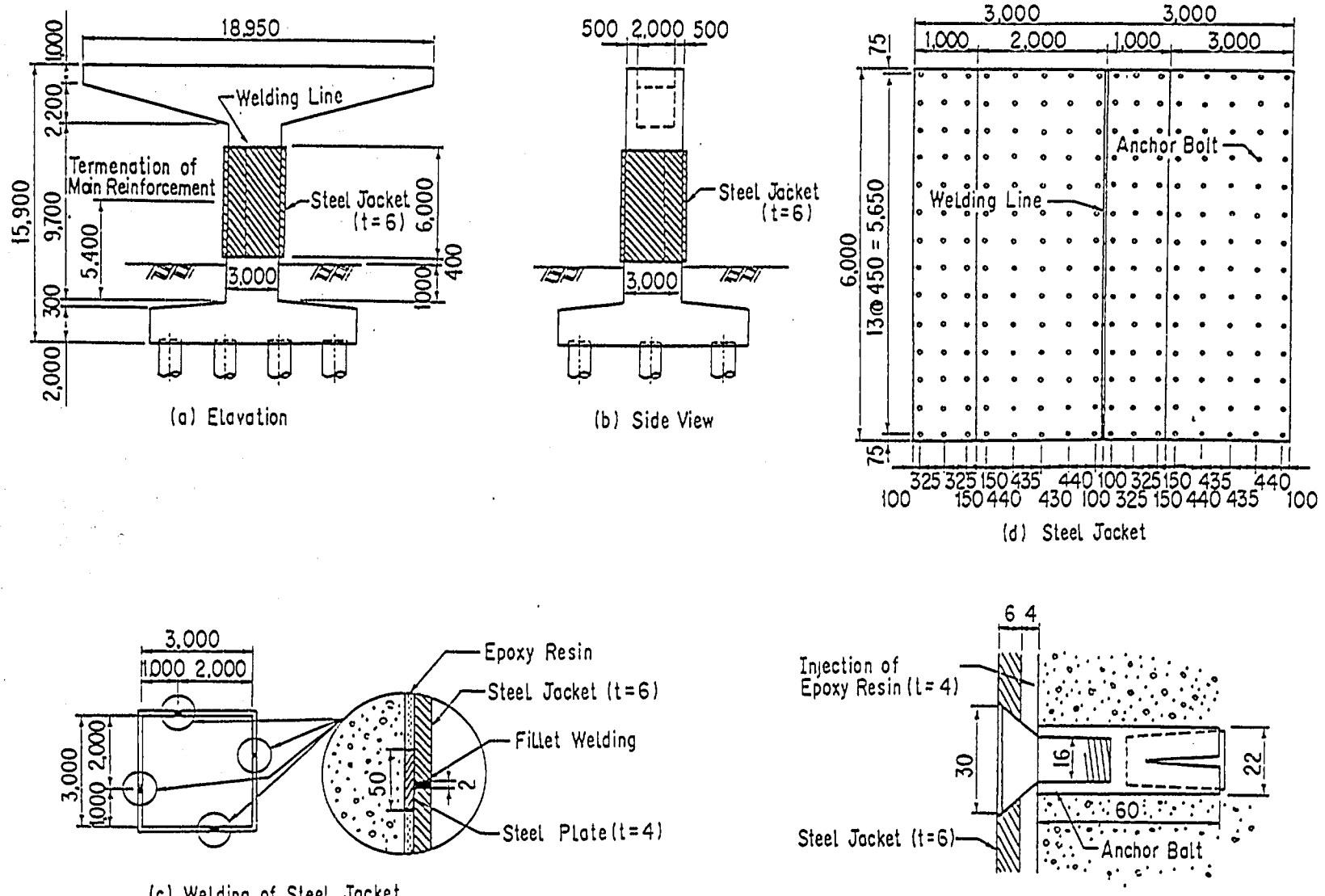


Fig.8 Seismic Strengthening of A Reinforced Concrete Pier at Termination Zone of Main Reinforcement by A Steel Jacket

as noise and air pollution caused by chipping-out of cover concrete of existing piers during construction, and to prevent increase of weight of pier because residual bearing capacity of the foundation was not enough. The minimum width of a steel jacket was determined to be more than two times section width through the dynamic loading tests conducted at the Public Works Research Institute. In the strengthening construction, the pier was covered by steel jackets from the bottom to crest of the pier for better outside appearance.

CONCLUDING REMARKS

This paper presents seismic strengthening methods for highway bridges with emphasis on practical applications. In the past seismic strengthening work in Japan, installation of devices for preventing falling-off of superstructure has successively been made. However strengthening of substructures has had difficulties such as cost problem and lack of reliable strengthening methods, so promotion of the strengthening work for substructures is now being required. Therefore, it is significantly important to develop rational and effective seismic strengthening methods with application of new materials and construction methods. It should be noted here that strengthening methods by connecting girders of a multi-span simply-supported bridge and base-isolation design are also being developed and applied.

REFERENCES

1) Edited by Planning Division, Road Bureau, Ministry of Construction : Notifications on Technical Standard for Road Facilities, Gyosei Publishing Co., March, 1978
2) Edited by Planning Division, Road Bureau, Ministry of Construction : Notifications on Technical Standard for Road Facilities, 3rd edition, Gyosei Publishing Co., April, 1978
3) Headquarters Office for Earthquake Disaster prevention Countermeasures, Ministry of Construction, Countermeasures against Large-scale Earthquakes, Monthly Journal of Construction, Vol.25, No.1, January, 1972
4) Fujii, T. : Road Disaster Prevention Measures, Road Journal, September, 1978
5) Fujii, T. : Road Service and Road Disaster Prevention Measures, Road Journal, June, 1980
6) Yamauchi, Y. : Present Status of Road Disaster Prevention Measures, Road Journal, December, 1980
7) Yoshikoshi, H. : Present Status and Subjects of Road Disaster Prevention Measures, Road Journal, September, 1982
8) Miyaji, A. : Road Disaster Prevention Measures, Road Journal, September, 1990
9) Edited by Road Bureau, Ministry of Construction : Road Traffic and Economy Survey, 1992 Version, December, 1990
10) Kawashima, K. and Unjoh, S. : An Inspection Method of Seismic Vulnerability

of Existing Highway Bridges, Proceedings of Japan Society of Civil Engineers, Vol.7, No.1, April, 1990
11) Japan Road Association : Manual for Earthquake Disaster Prevention of Road Facilities (Pre-earthquake Countermeasures), February, 1988
12) Road Bureau and Public Works Research Institute, Ministry of Construction : Investigation on Assessment of Durability and Improvement Technology for Existing Highway Bridges, Proceedings of the 42nd Meeting on Construction Technology, Ministry of Construction, November, 1989
13) Earthquake Engineering Division, Public Works Research Institute : Case Survey of Seismic Strengthening Practices of Existing Highway Bridges Based on Seismic Inspection of 1979, Technical Memorandum of Public Works Research Institute, No.2674, October, 1989
14) Kawashima, K. : Seismic Design and Earthquake Disaster Countermeasures for Highway Bridges, Road Journal, September, 1990

RESEARCH BASED BRIDGE SEISMIC DESIGN AND RETROFIT PROGRAM CRITERIA, STANDARDS AND STATUS

James E. Roberts, Chief
Division of Structures
California Department of Transportation

ABSTRACT

Post earthquake evaluation of bridge damage revealed that the major causes of bridge structural failure during the October, 1989 Loma Prieta event were the inadequate beam-column joint reinforcing details; the lack of adequate reinforcement for combined bending, axial loads and torsion in long outrigger type bent caps and columns; and the lack of accurate predictions of response spectra for deep, soft bay muds.

The California Department of Transportation (Caltrans) immediately accelerated its Bridge Seismic Research Program with the funding of 23 major research projects for a total cost of over $8 million. This research was "problem focused" on those areas that proved to be vulnerable during the recent earthquakes. Most of the research involved half-size model testing of bridge components and joint details.

Seismic retrofit details to strengthen existing bridges were developed and proven with this research program and their good performance in three recent earthquakes in California prove the validity of the ductile design and retrofit approach adopted by Caltrans.

Additional large scale and full size model research is continuing to develop improved solutions for bridge foundations in liquifiable soils; a family of Deep, Soft Soil Acceleration Response Spectra for the more typical and shorter Freeway bridges; bond development length criteria for large diameter reinforcing steel bars; and column-cap joint confinement details for combined torsion, bending and shear.

BACKGROUND AND HISTORY

The California Department of Transportation (Caltrans) owns and maintains over 12,000 bridges (spans over 20 feet). There are an equal number on the City and County system. We maintain the condition data for all these and some 6,000 other highway structures such as culverts and tunnels. Structural details and the condition data are maintained in the Bridge Maintenance files as a part of the National Bridge Inventory System (NBIS) required by Congress and administered by the Federal Highway Administration (FHWA).

Immediately after the February 9, 1971 San Fernando earthquake Caltrans began a comprehensive upgrading of the Bridge Seismic Design Specifications and Construction Details. Caltrans' bridge design specifications were modified to correct the identified deficiencies on newly designed bridges. This work was completed with contributions by the Applied Technology Council (ATC) and project ATC-6 became the basis for Caltrans' Bridge Seismic Design Code. A similar bridge seismic design code was later adopted by the American Association of State Highway and Transportation Officials (AASHTO) as the national standard. Existing structures, however, proved to be a substantially more challenging problem. Research was undertaken in the United States and overseas (New Zealand and Japan) to improve analytical techniques, and to provide basic data on the strengths and deformation characteristics of lateral load resisting systems for bridges. Caltrans identified the vulnerable elements of existing bridges and began a statewide bridge seismic retrofit program to systematically reinforce the older non-ductile bridges.

The initial phase of the Caltrans' Bridge Seismic Retrofit Program involved installation of hinge and joint restrainers to prevent deck joints from separating. This was the major cause of bridge collapse during the San Fernando earthquake and was judged by Caltrans engineers to be the highest risk to the traveling public. Included in this phase was the installation of devices to fasten the super- structure elements to the substructure in order to resist vertical accelerations and also to prevent superstructure elements from falling off their supports. This phase was essentially completed in 1989 after approximately 1,260 bridges on the State Highway System had been retrofitted at a cost of over $55 million. Funding for this program competed with other highway safety programs, which were arguably more critical in terms of statistical support, and we were allocated an average of only $4 million annually for bridge seismic retrofitting. These joint restrainer systems have performed well in subsequent earthquakes, including the Whittier (1987) Loma Prieta (1989), Cape Mendocino (1992) and the three most recent Southern California events of 1992.

While the hinge and joint restrainers performed well, shear failure of columns on the I-605/I-5 separation bridge in Los Angeles during the moderate Whittier Earthquake of October 1, 1987 reemphasized the inadequacies of pre-1971 column designs. Even though there was no collapse, the extensive damage resulted in plans for basic research into practical methods of retrofitting bridge columns on the existing pre-1971 bridges. That research program was initiated in early 1987 and is currently being conducted at the University of California at San Diego, the University of California at Berkeley, and other University and private research facilities. Funding levels for implementation were increased four fold after the Whittier earthquake to an annual program of $16 million. Even at that level it would require some 50 years to complete the retrofitting program. After the Loma Prieta earthquake caused 44 fatalities on the State Highway System, capital funding for seismic retrofitting was increased to $300 million per year. At the same time bridge seismic research funding was increased from $0.5 million annually to $5.0 million annually with an initial $8.0 million allocation from the special State Emergency Earthquake Recovery legislation of November, 1989, Senate Bill 36X (SB 36X).

The Loma Prieta earthquake of October 17, 1989 again proved the reliability of hinge and joint restrainers but the tragic loss of life at the Cypress Street Viaduct on I-880 in Oakland emphasized the necessity to immediately accelerate the column retrofit phase of the bridge seismic retrofit program with a higher funding level for both research and implementation. Other structures in the earthquake affected counties performed well, suffering the expected column damage without collapse. With the exception of a single outrigger column-cap joint confinement detail, those bridges using the post 1971 design specifications and confinement details performed well. Damage to long, multiple level bridges showed the need to more carefully consider longitudinal resisting systems because earthquake forces cannot be carried into abutments and approach embankments as they can on shorter bridges. Using the special research funding provided in SB 36X the department engaged additional research facilities to assist in this massive program.

CALTRANS' POST LOMA PRIETA SEISMIC RETROFIT PROGRAM

After the Loma Prieta earthquake the State Legislature passed Senate Bill 36X and Assembly Bill 38X which directed the Department of Transportation to take the "Lead Agency" role in preparing projects for the replacement or upgrading of all "publicly owned" bridges in the state to meet current Seismic Safety Criteria. Funds were provided to initiate the program and

match available federal funds. In addition to the City, County and State bridges there are "publicly owned" bridges under the jurisdiction of more than 50 other agencies over which Caltrans has no legal authority (Local Transit Agencies, State Department of Water Resources, Federal Highway Administration, US Forest Service and other state and local agencies). Most of the agencies have been cooperative in identifying and prioritizing their bridges. For example, working cooperatively with the US Forest Service in screening their bridges and conducting a vulnerability analysis, Caltrans' staff has identified only five bridges on the USFS system that require seismic retrofitting.

The first substructure retrofit projects were approved by the California Transportation Commission (CTC) in December, 1989 and contracts were awarded in early 1990. These projects were for single column supported structures that had been identified for retrofit prior to Loma Prieta and plans were "on the shelf" awaiting funding.

By July, 1990 the Caltrans Division of Structures (DOS) staff had completed an initial "Vulnerability Analysis" of the 24,000 state, county and city bridges and produced a prioritized list from which to complete the program implementation. The logical strategy was to retrofit or replace the most vulnerable bridges on the list first, when this approach is possible. That initial list contained nearly 7000 state and 4500 city and county bridges which required further analysis and evaluation. The list of potentially vulnerable state owned bridges was submitted to the Governor on August 31, 1990 in response to his Executive Order of June 2, 1990.

A schedule for seismic retrofit project completion and cost estimates was submitted to the Governor on January 1, 1991 in response to Senate Bill 2104. For the first time an attempt to segregate the 7000 bridges into priority groups was included in the report. This was for the purpose of identifying those most critical bridges that needed immediate repair versus those which would only be repaired for purposes of reducing future damage. A form of triage if you think of it that way. We believe, based on our past experience, that the number of state bridges actually needing any element of retrofit work will be pared down to approximately 4000. For the local systems that number is closer to 1500. Not all of these bridges will need immediate retrofit to meet the Seismic Safety Criteria and, therefore, State owned Bridges were grouped into three categories:

1. Category 1-<u>Seismic Safety Category</u>-Those bridges which must be replaced or retrofitted to meet the current "Seismic Safety Criteria". The seismic safety criteria adopted is, NO COLLAPSE; NO MAJOR DAMAGE; NO SECONDARY DAMAGE OR INJURIES

BECAUSE DAMAGED STRUCTURES PRECLUDE MOVEMENT OR ACCESS BY RESCUE AND RECOVERY PERSONNEL. There are approximately 800 state bridges in this category with a retrofit cost estimate of $750 million. For the local system the numbers are 170 bridges and a cost estimate of $110 million.

2. Category 2-Seismic Protection Category-Those bridges which will be needed for recovery from the disaster. These are bridges which meet the seismic safety criteria of "no collapse" but could sustain damage in a major earthquake. The damaged bridges must be reopened for service within hours or days of the disaster. After the Loma Prieta event several bridges, which would fall into this category, were supported on shoring or falsework and repaired while traffic flowed over and under them.

3. Category 3-Seismic Protection Category-Those remaining bridges which are needed to maintain the transportation system in its normal manner. These bridges need to be repaired and reopened for service within a reasonable time but are not needed for the disaster recovery.

The cost to repair the 3200 bridges in categories 2 and 3 could be another $3 billion. The budget issue is "how much do we spend for insurance versus the cost of repairing the future damage when and if it occurs?" Given the probabilistic nature of earthquakes and the intense competition for scarce transportation funds it is rational to evaluate these needs in competition with other highway safety projects.

The toll bridges over the major waterways were not included in the above estimates because of the complex and time consuming dynamic analyses required to make a reasonable cost estimate. There are 11 toll bridges but at least 2 are not in highly vulnerable locations and the newest, the Dumbarton, over the southern end of San Francisco Bay, was designed for the current seismic criteria. Studies are underway to produce hazard analyses and retrofitting requirements for these toll bridges. Based on the initial studies of the San Francisco-Oakland Bay Bridge and the Golden Gate Bridge, estimated costs for seismic upgrading of the eight remaining toll bridges is expected to exceed $500 million.

Similar priority lists have been published for the City and County bridges. Because the ratio of deck surface area between the 12,000 state bridges and the 12,000 local bridges is 4 to 1 and most local bridges are less complex, the program numbers are 1500 estimated to need any work and only 170 in the seismic safety category. It was and still is Caltrans philosophy to first retrofit those structures which pose the greatest risk to the public and are the most vital to the transportation system.

Recent changes in the Federal Interstate Surface Transportation Efficiency Act (ISTEA) provide sufficient funding to match available State funds and complete the local program.

Working with the new Seismic Advisory Board, the Department has recently adopted a Bridge Seismic Performance Criteria for design of all new bridges. This criteria is also applied to seismic retrofitting design for older bridges where it is practical. In some cases it is more prudent to replace rather than retrofit a structure, because of age or high retrofit costs. **Attachment 1** is the newly adopted Seismic Performance Criteria for the State Highway System.

The Senate Bill 2104 requirement to complete retrofitting the **Seismic Safety Category** for State bridges is to have all projects advertised for contract by December 31,1993. This goal is attainable for all but the toll bridges because we are utilizing a large number of consultants to augment the engineering staff. Some of the toll bridge retrofitting will be started by the end of 1993 but we will need to ask the legislature for an extension of the deadline for completing all of these bridges. Most of them are complex and old. These conditions require more comprehensive analysis and more field work to bring them up to current seismic performance criteria. It is the Caltrans' bridge staff belief that the toll bridge retrofit contracts can be underway by the end of December, 1994 (a one year extension of the legislative mandate).

BRIDGE SEISMIC RESEARCH

The Department has engaged several research facilities in a major Bridge Seismic Research effort and that will continue for several years to solve the problems we have encountered in the areas of non-uniform and out-of-phase foundation response, dynamic response of deep soft soils, soil liquifaction, joint confinement, torsional performance in large beam and column members, and other structural problems. We have already derived much useful information from the ongoing seismic research in the areas of ground response spectra for deep, soft soil sites and for the seismically resistant reinforcement details.

A manual has been developed to provide guidance for seismic retrofitting of bridges, and site specific Design Criteria have been developed for the replacement structures on the new alignment of I-880 in Oakland (replacing the Cypress Street Viaduct) and for the I-480 Terminal Separation structures in San Francisco. These design documents represent the latest technical information on bridge seismic design. Research is continuing in the areas of large reinforcing steel bond developoment, joint performance,

multi-level and complex framing system performance and detailing procedures, performance and design of outrigger and "C" bents and other structural members subject to torsion, identification of and design for liquifiable foundation sites, and ground response spectra for deep, soft soils.

One of the Research Projects which was funded is the Applied Technology Council (ATC) ATC-32 Project to review and revise the entire Caltrans Bridge Seismic Design Specifications. That project is in its first year and the specific areas that need revision have been identified and work plans have been approved for the various sub-contractors to complete the project. Several Structural Engineers Association of California (SEAOC) members and prominent Professors are members of the Project Engineering Panel (PEP) which meets semi-annually to provide guidance to the project consultant and sub-contractors.

Many of the details utilized in Phase I of the seismic retrofit program had been tested using full size elements but this was not practical from a logistics and cost standpoint for large substructure members. Since little research had been previously accomplished in the area of seismic upgrading for older non-ductile bridges, it was important to accelerate the program and implement results as soon as research was completed

The University of California at San Diego (UCSD) was chosen for the initial testing in 1987 because they had a new structural engineering laboratory with a five story strong wall and other necessary equipment to conduct the tests. More important, the Principal Investigator, Doctor M.J. Nigel Priestley, had recently moved from Canterbury University in Christchurch, New Zealand where he had been testing smaller scale models of bridge columns using a steel jacket concept to provide exterior confinement for older, non-ductile columns. With that combination of research background and the testing facility Caltrans awarded contracts to UCSD early in 1987 and had completed several tests by the time the Whittier earthquake of October, 1987 again showed the weakness of pre 1972 non-ductile column designs. The test series was accelerated after the Whittier earthquake and by the time of the October, 1989 Loma Prieta disaster Caltrans had enough test results from Dr. Priestley's work that plans were on the shelf ready to be advertised for the first column retrofit projects. Those first projects were advertised within two months of the Loma Prieta event and work was started in early January, 1990 and completed by the end of that year. Subsequently, more than 60 construction contracts have been awarded for seismic upgrading of bridge columns by retrofitting with steel jackets and other improvements to footings and connections to provide ductile performance on older bridges. Over 100 bridges have been retrofitted in projects that have been completed and 200 more are

under construction. Of the 281 identified single column supported bridges which need retrofitting, only 25 have yet to be designed and advertised for construction. Work is now underway to design the retrofitting projects for multiple column supported bridges and over 35 are under construction. The remaining 450 bridges have been assigned to designers and consultants for analysis and plan preparation.

These seismic research projects are exclusively applied research rather than theoretical research. They are specific problem-focused research directed at bridge details which were determined to be weak after investigation and analysis of earthquake damage, especially from the Loma Prieta event. Eight different univertsity research facilities are conducting this research and testing work and interim, implementable results are an annual contract requirement. Most of the work involves full size or half size model testing of prototype details and proposed designs for both new construction and seismic retrofitting of older structures. The UC San Diego researchers have completed more than 30 different sets of tests on column retrofit details, using various materials and techniques. Work was started in late 1991 to test Column-Cap joints on outrigger bents, pullout tests on number 18 column reinforcing steel, and the torsion resistance of outriggers. The UC Berkeley (UCB) Earthquake Research Institute (ERI) laboratory at the Richmond Field Station is testing half size models of complex, multi-level bents and column-cap details for seismic resistance. The UC Irvine laboratory is testing column-footing hinge pin details and long, slender pier walls.

MAJOR ACCOMPLISHMENTS IN SEISMOLOGY SINCE LOMA PRIETA

Research and analysis subsequent to the Loma Prieta event have shown conclusively that a lightly reinforced column pedestal detail unique to the Cypress structure was the main cause of the total collapse. Immediately following the Loma Prieta earthquake the Structural Engineering Department at the University of California at Berkeley requested that we salvage a section of the damaged Cypress Street Viaduct which had not collapsed for the purpose of conducting a series of seismic performance experiments. **Figure 1** shows the overall location and test setup for the three span, four bent section that was utilized for these tests. UCB has published reports of the experiments which were to determine the fundamental period of the complex structure under low intensity seismic loading. Additional tests were performed to measure the actual lateral resistance of the framing system up to yield. Experiments on several proposed column retrofit details were also conducted on this structure.

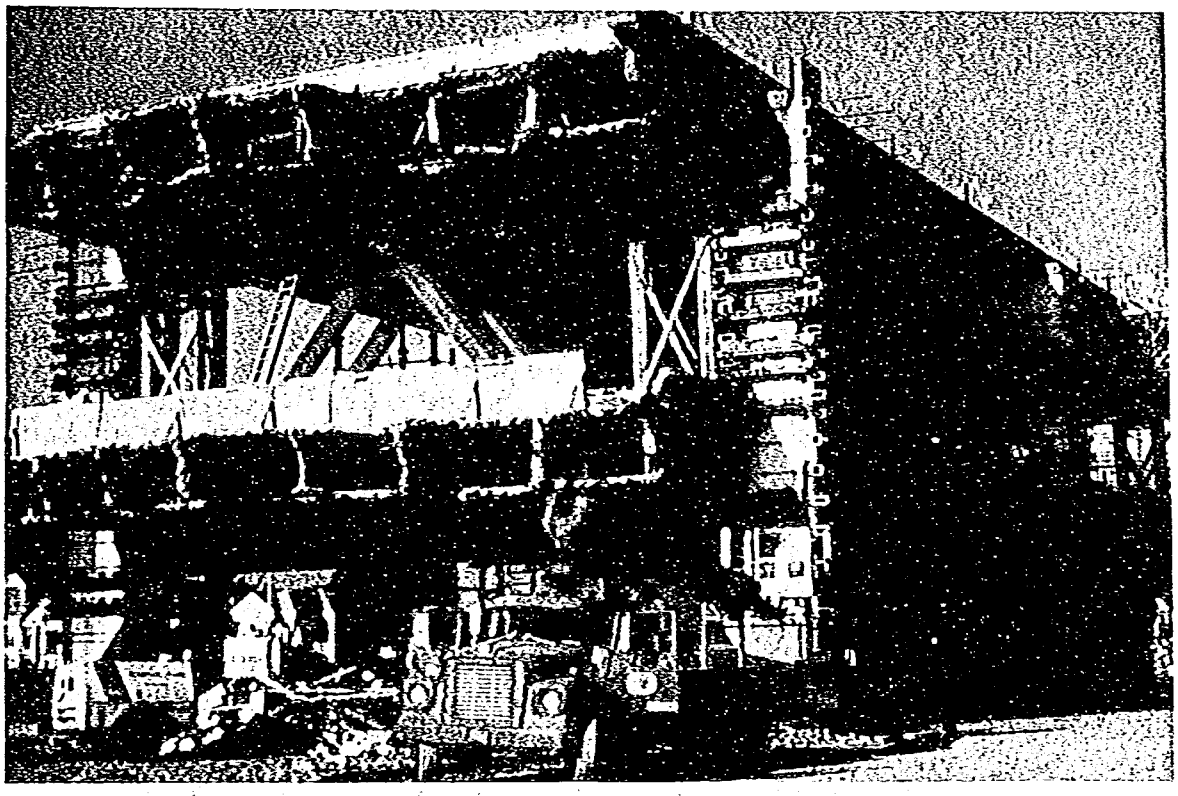


Figure 1-Full Size Tests At Cypress Street Viaduct

The effect of the dynamic response of deep soft soils in the structure foundations also proved to be a contributing factor to the collapse of the Cypress Viaduct and must be analyzed and included in future design procedures, especially for long, tall structures with relatively high periods of vibration.

Soft Soil Dynamic Response-On some of the major retrofitting projects, new site specific acceleration response spectra have been developed on an individual basis for these deep soft soil foundations. Professors John Lysmer and Raymond Seed at U C Berkeley are assisting in development of a series of deep, soft soil Acceleration Response Spectra (ARS curves) for statewide use on typical freeway bridges but we will continue to develop individual site specific spectra for large structures. These ARS curves are similar to those developed by Professor Harry Seed for harder soils and alluvium after the 1971 San Fernando earthquake.

Deep, Soft Soil Sites-The Caltrans staff Seismologist, Engineering Geologist and Geotechnical Engineers have identified and mapped the deep, soft sites throughout the state and this information has been entered into the Geographic Information System (GIS) and Bridge Data Base. Site specific ground response spectra have been prepared for the replacement structures at the

Terminal Separation interchange in San Francisco and I-880 replacement in Oakland, and for the retrofit upgrading of multi level structures on both I-280 and US 101 in San Francisco.

Liquifaction Potential Sites-The Engineering Geologist and Geotechnical Engineers have also completed identification and mapping of the potential liquifiable soil sites throughout the state. These sites are also recorded in the Bridge Data Base.

Column and Joint Design-Bridge columns designed before the 1971 San Fernando earthquake typically contain very little transverse reinforcement. A common detail for both circular and rectangular columns consisted of #4 (1/2 inch diam.) transverse peripheral hoops at 12 inch to 18 inch centers, regardless of column size and area of main reinforcement. Also, it was common practice to extend short lengths of dowel or tails from the footing reinforcing steel out of the footing and lap splice them with the main column reinforcing steel cage at that point. As a consequence of these details, the ultimate curvature capable of being developed within the potential plastic region is limited by the strain at which the cover concrete starts to spall. The result is flexural failure resulting from inadequate ductility capacity, or shear failure due to lack of adequate shear reinforcement. Tests conducted at UC San Diego confirm this theory. Several bridges suffered column shear failures due to the elastic design philosophy under which they were designed prior to 1971.

Columns designed since 1971 contain a slight increase in the main column reinforcing steel and a major increase in confinement steel over the pre-1971 designs. All new columns, regardless of geometric shape, are reinforced with one or a series of spiral wound circular cages. The typical transverse reinforcement detail now consists of #6 (3/4 inch diam.) hoops or continuous spiral at three inch pitch. This provides approximately eight times the confinement reinforcing steel in columns than what was used in the pre 1972 non-ductile designs. All main column reinforcing is continuous into the footings and superstructure. Splices are mostly welded or mechanical, both in the main and transverse reinforcing. Transverse reinforcing steel is designed to produce a ductile column by confining the plastic hinge areas at the top and bottom of columns. The use of grade 60, A 706 reinforcing steel in bridges has recently been specified on a few projects on a trial basis.

The largest number of large scale tests have been conducted to confirm the calculated ductile performance of older, non-ductile bridge columns that have been strengthened by application of structural steel plate, pre-stressed strand and fiberglass-composite jackets to provide the confinement necessary to insure ductile performance. Since the Spring of 1987 the

researchers at UC San Diego have completed 30 sets of tests on bridge column models. Figures 2 through 4 show various column tests at UCSD.



Figures 2 and 3-Half Scale Model Tests-Column Retrofit

Both UCB and UCSD will be conducting tests on the column-footing joint details as other work is completed. Results of previous column retrofit tests indicate that pre-1972 footing details need substantial improvement. These improvements have already been made in the retrofit contract plans but the research is necessary to confirm theoretical calculations of performance and to continually improve details.

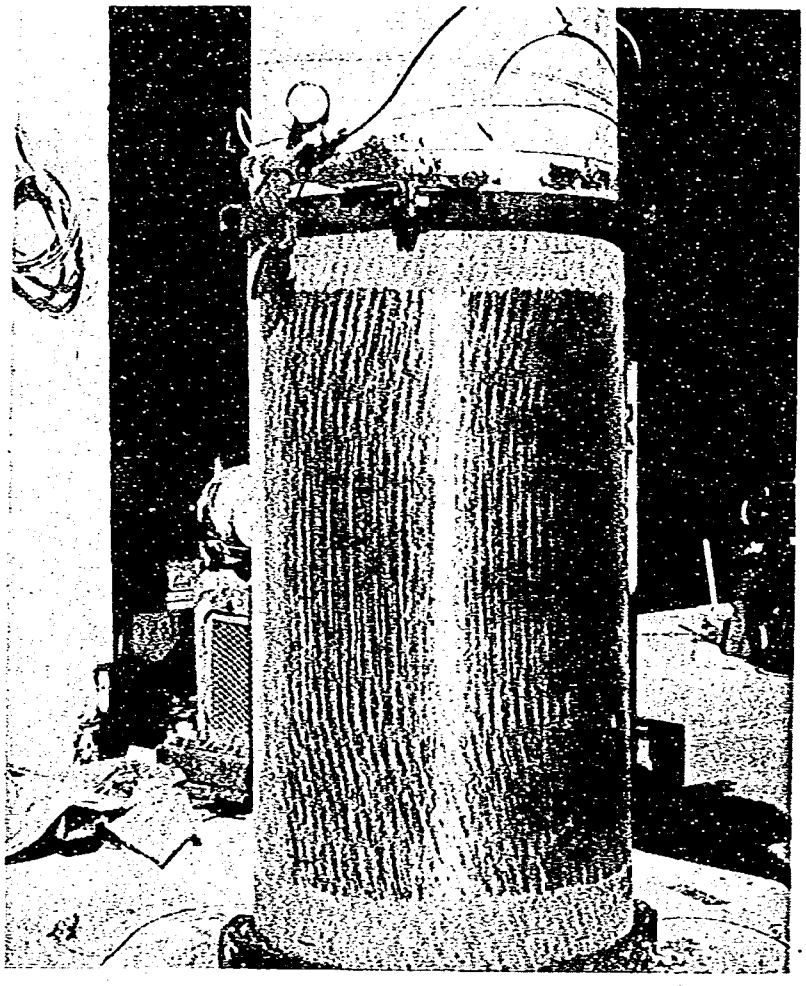


Figure 4-Fiberglass Column Retrofit

Outrigger bent cap-column joint details. The Earthquake Research Institute (ERI) of the University of California at Berkeley (UCB) began a series of tests on the performance of outrigger joints in 1991. They tested a model of the outrigger joint of the I-980 structure which was damaged in the Loma Prieta earthquake using the identical prototype details. **Figures 5 and** 6 show the results of those tests. They replicated very closely the actual field damage, then tested the retrofitted joint as Caltrans had redesigned it and confirmed the validity of the redesigned joint details. **Figure 7** shows results of the tests on

the retrofitted joint detail. Based on these tests Column-cap joint details have been improved; column transverse reinforcement is typically continued up through the joint regions and the joints are further confined for shear and torsion resistance. The details for these joints usually require 1% to 3% confinement reinforcing steel.

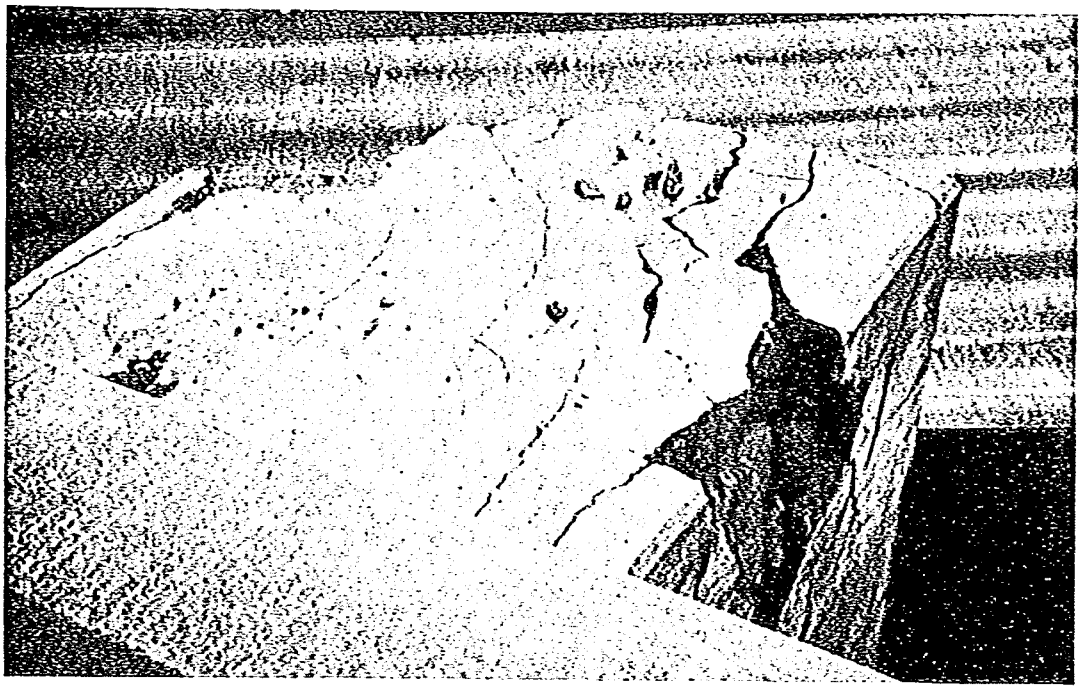


Figure 5-Damaged Outrigger Column-Cap Joint



Figure 6-Half Scale Model Test of Prototype Joint

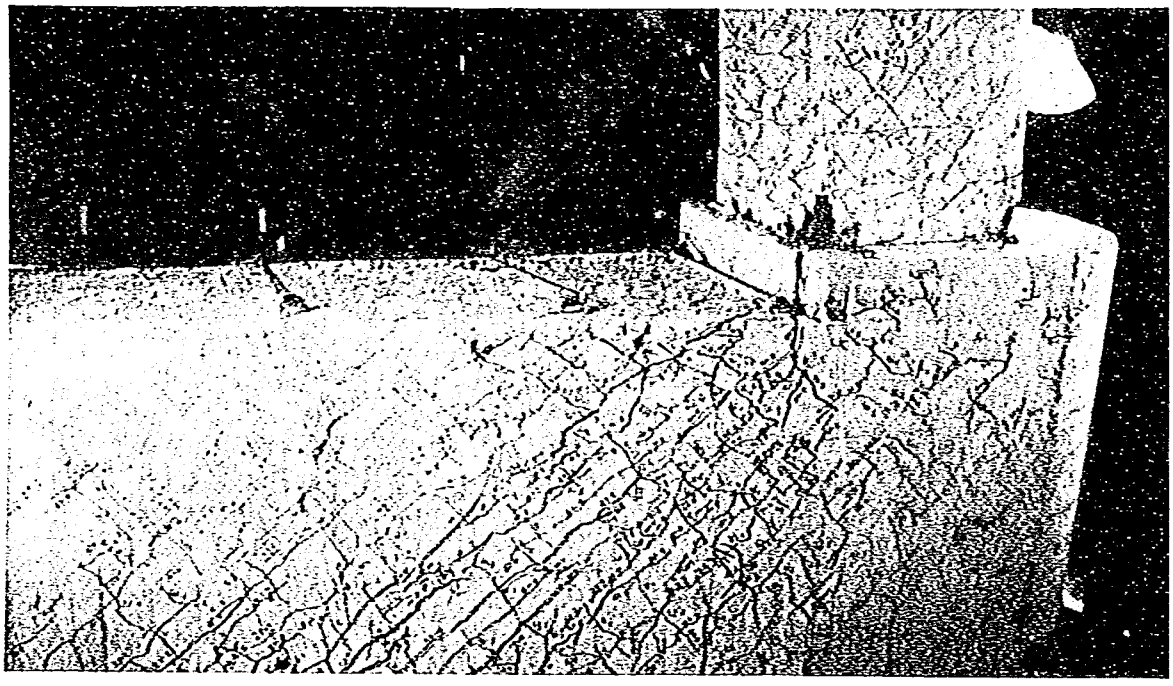
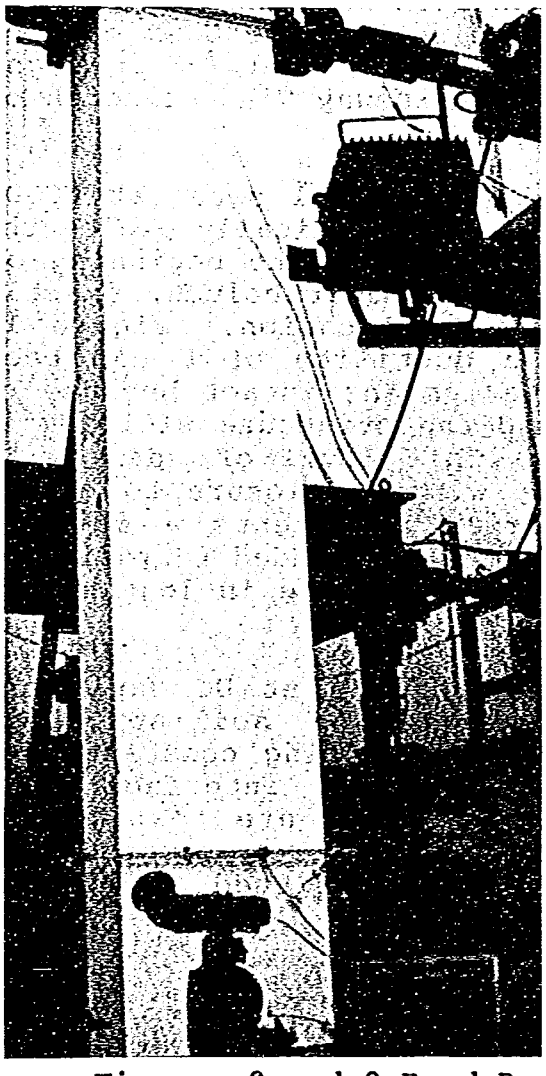


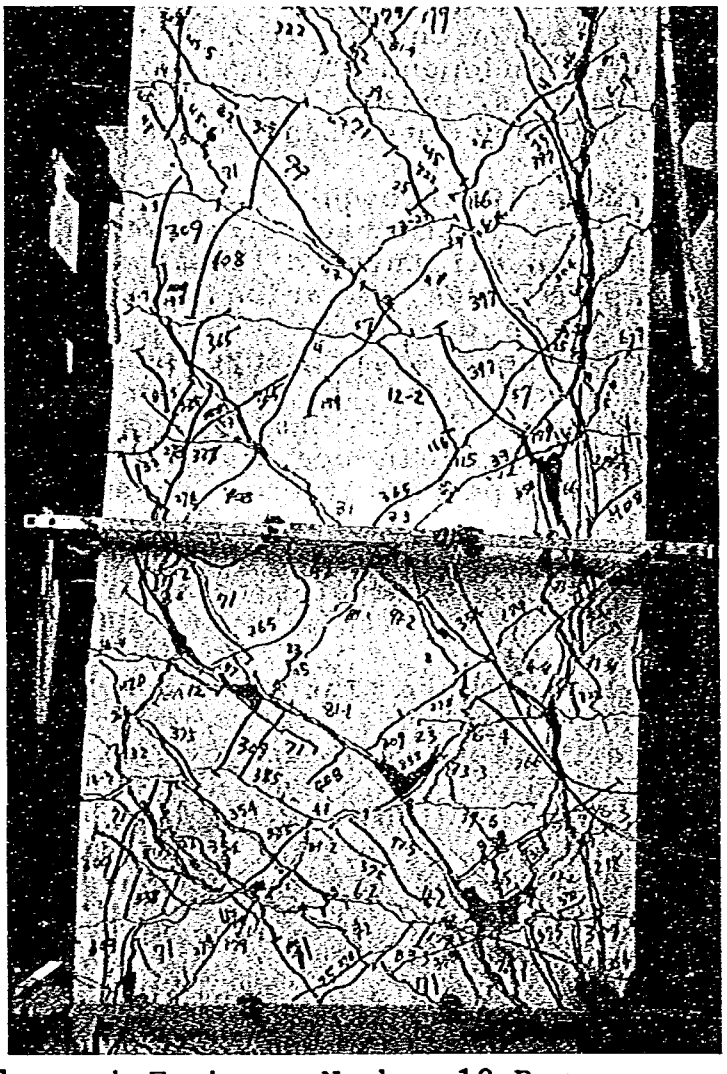
Figure 7-Half Scale Model Test of Retrofitted Joint

Peer Review Panel concerns about the adequacy of the AASHTO design code provisions for bond development length for number 14 and number 18 reinforcing steel bars, which are typically used in large bridge columns in California, prompted additional research testing. Full size elements of the column-cap connection are being built and tested at UC San Diego. The Earthquake Research Institute (ERI) of the University of California at Berkeley (UCB) also conducted tests of the bond development length as a function of concrete cover. Full size tests of these details have been conducted because of concerns regarding scaling of such large bars. These tests will confirm the adequacy of current provisions or recommend changes to be made to the current code requirements at the AASHTO Bridge Engineer's meeting in May, 1993. Results of the UCB tests are shown in Figures 8 and 9.

Multi-Level Member Joint Design-Major advances have been made in this area based on the results of research at both UC Berkeley and UC San Diego. The performance and design criteria and structural details developed for the Terminal Separation and I-880 replacement structures reflect the results of this research. Research is continuing at both Institutions to further refine the design details to ensure ductile performance of these joints. Large one-half size models of the most critical longitudinal edge beam, transverse bent cap, colmun joint detail were built and tested at both UC San Diego and UC Berkeley as a major element of the joint and column testing program. Additional large scale

model testing programs are planned for the more complex multi-level beam column details commonly used in major highway interchange structures.Pier Walls, Column Pins and Miscellaneous Details-UC Irvine has a series of research projects and large scale model tests to investigate the performance of long bridge pier walls under dynamic loading. They are also investigating the performance and shear strength of column hinge pin details. The University of Nevada at Reno research facility is testing the performance of Bridge Hinge and Joint, Cable Restrainers under dynamic loading. They also have an ongoing research program to measure the dynamic response characteristics of a full-sized bridge on the California State Highway system near the San Andreas fault at El Centro, California.





Figures 8 and 9-Bond Development Tests on Number 18 Bars

Edge Beam-Column-Bent Cap joint detail. The most elaborate and expensive tests conducted to date have been the half scale and third scale models of the proposed retrofit details for the double deck viaduct structures in San Francisco. Models, using two different seismic retrofit techniques, were tested at both UCSD(Half scale) and UCB(Third Scale) in order to obtain the performance characteristics of the two different details so we could make the final design and construction decisions and get the construction contracts started in 1992. Both models were nearly 50 feet long by 20 feet wide and 20 feet high. They included one-half of each span adjacent to the joint and half the column above and below the joint. Half width of the superstructure was also modeled to recreate the actual contributing dead load and stiffness of the elements that frame into these columns. The difference in the concepts is in the connection to edge of deck of the original structure. The UCB concept uses an integral edge beam detail which is necessary on curved alignments, such as the Central Viaduct (US 101) in Downtown San Francisco and the Alemany Interchange on US 101 in South San Francisco. The UCSD concept is an independent edge beam which will be used on straight alignments, primarily the IS 280 Southern Freeway Viaduct north of the Alemany Interchange with US 101.

Figures 10 through 12 show the details and model setup at UCSD. Thirteen dynamic actuators were required to dynamically excite the model in all three directions. **Figure 13** shows the beginning of plastic hinge formation at the top of the lower column, exactly where the design is intended to force its location. **Figure 14** shows the plastic hinge zone after a ductility of 8 had been achieved. Note that the core concrete remains intact because of the heavy confinement reinforcement and the structure will remain standing and in operational service. This level of damage is easily repaired after a seismic event without closure to public traffic. Each of these test series represents a cost of $500,000 but they are used to proof test the intended retrofitting scheme for structures totalling more than one mile in length with a replacement cost of over $200 million.

Soil-Structure Interraction-Research projects at UC Davis and other facilities are intended to test the soil-structure interraction and help develop reliable soil-spring constants for advanced analysis and design of this important interface under dynamic loading. Other projects at UC Davis are testing the performance of bridge foundation piles which were removed from the Collapsed Struve Slough Bridge and retrofitted to current criteria.

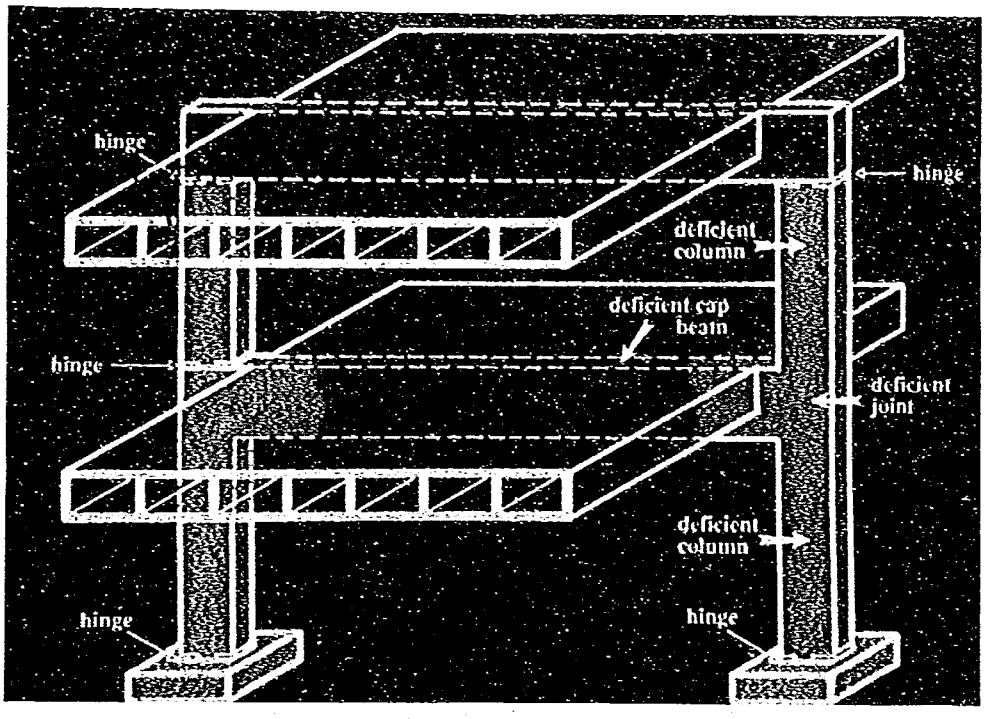


Figure 10-Schematic of Prototype Structure

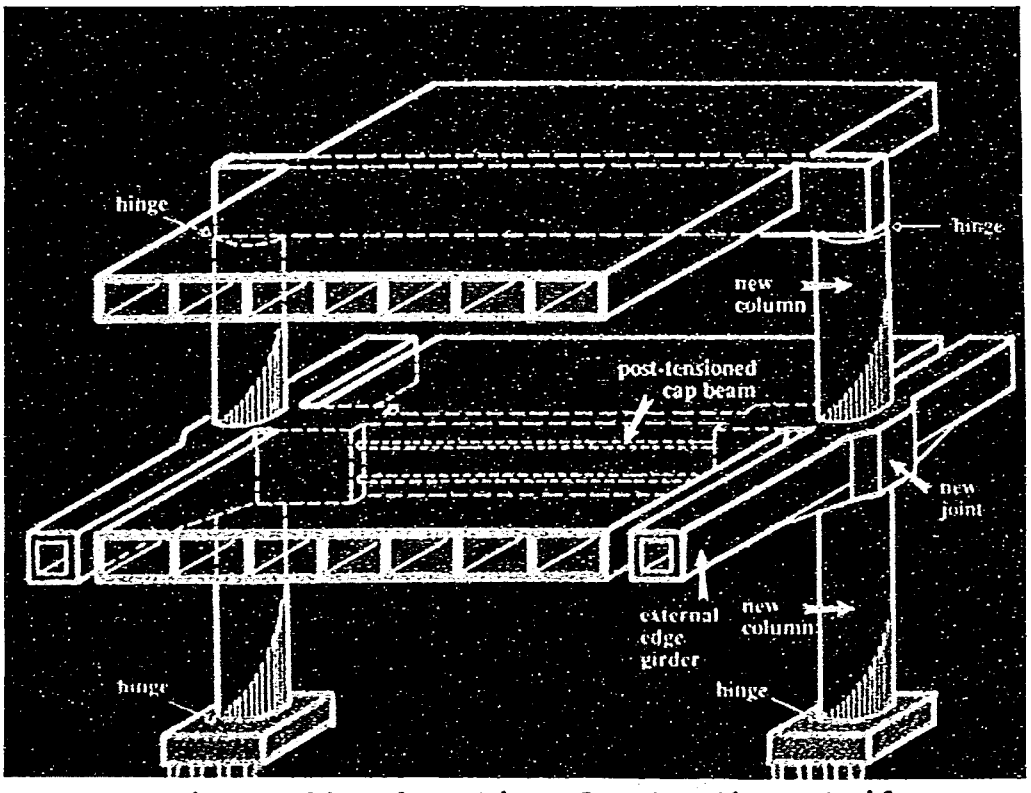


Figure 11-Schematic of Retrofit Details

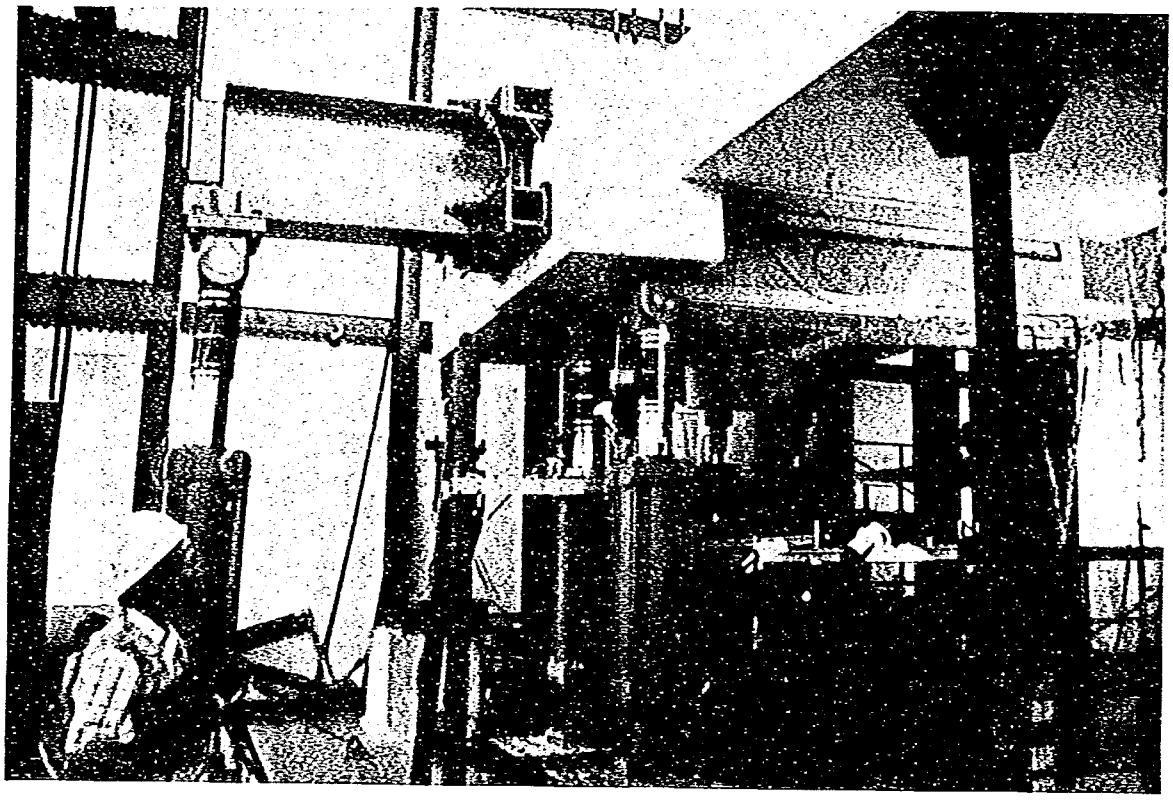


Figure 12-Model Test Setup, Showing Dynamic Actuators

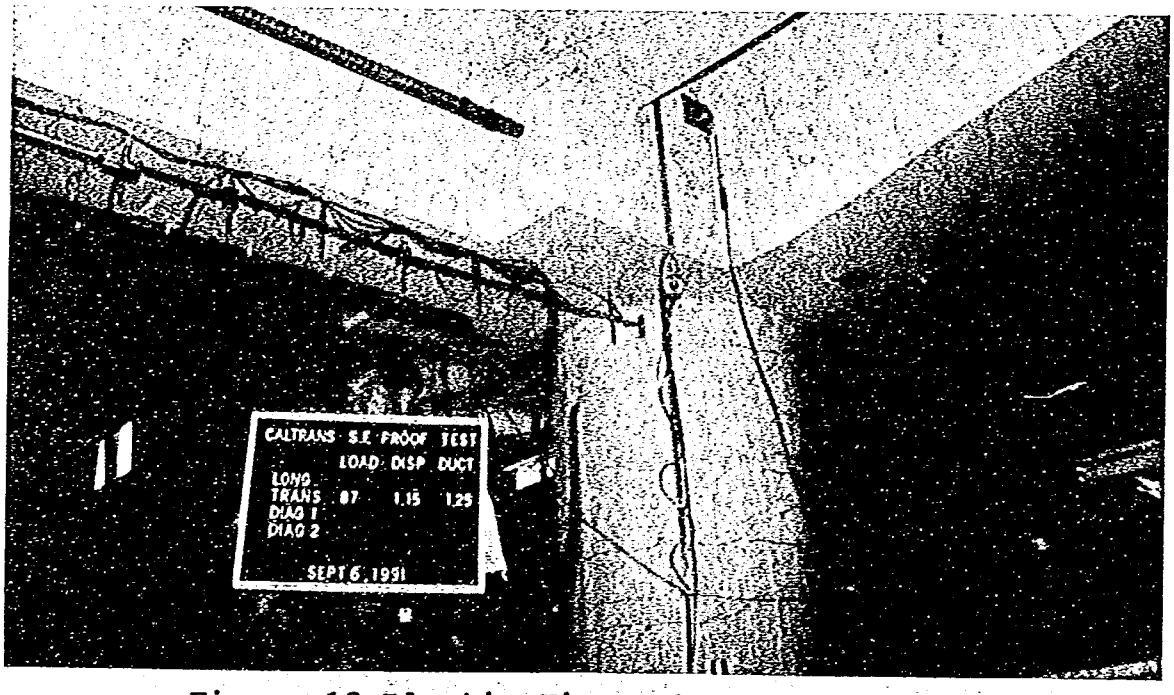


Figure 13-Plastic Hinge at Top of Column

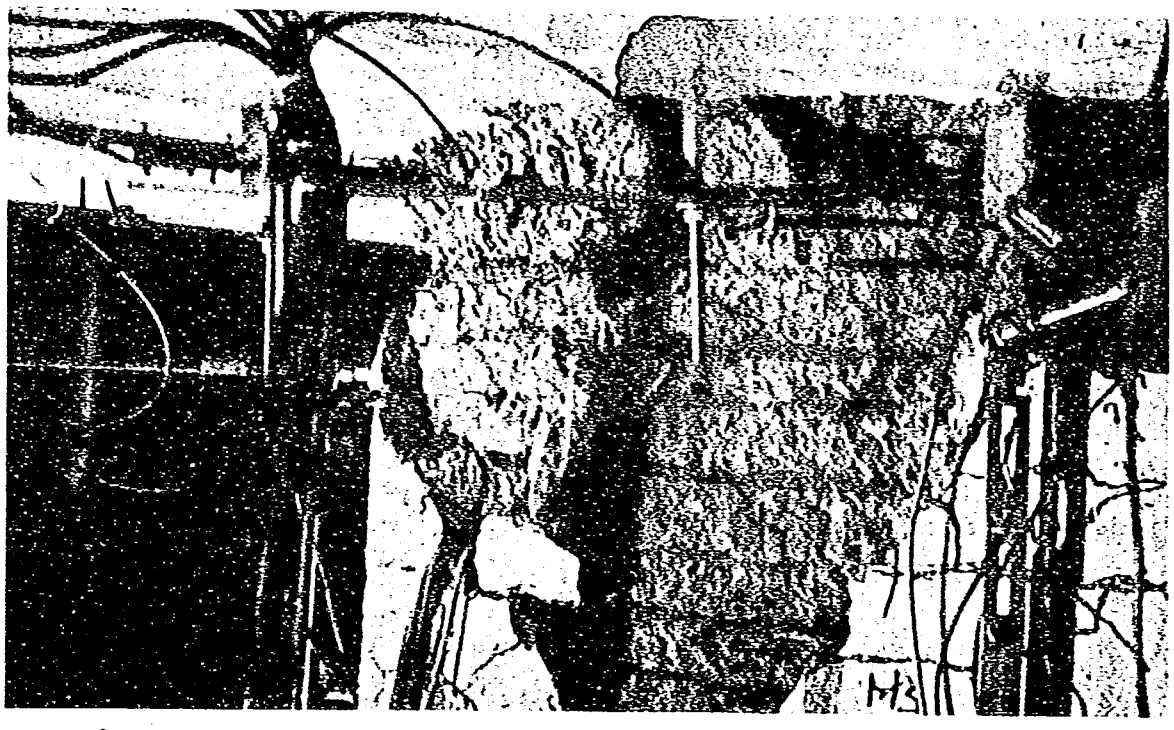


Figure 14-Plastic Hinge Zone at Ductility Factor 8

RETROFIT PHILOSOPHY

There are some 24,000 highway structures for which the State of California is responsible in some capacity. It is economically unrealistic to suggest that every structure be immediately retrofitted to withstand maximum magnitude earthquakes without some damage. The retrofit philosophy adopted at the start of the superstructure joint restrainer retrofit phase of the program offers reasonable direction to the remaining phases of the retrofit program and, for that reason, we have continued implementation of all phases of the retrofit program using that philosophy.

It was and still is Caltrans philosophy to first retrofit those structures which pose the greatest risk to the public and are the most vital to the transportation system. The ultimate goal is to see that all of the bridges in the state will be capable of surviving maximum credible earthquakes without collapse. Some damage is inevitable but, with proper retrofitting, it is believed that collapse is preventable and, further, it is believed that damage can be held to a minimum, to the extent that the critical elements of the transportation system can remain open and functioning during a civil disaster and during repair. As we get

into the actual analysis and design it is becoming apparent that retrofitting many older structures to this standard may not be cost effective. It is highly probable that we may have to accept some period of closure on many structures to effect repairs. It is also apparent that some structures will be replaced rather than retrofitted simply as an economic decision. Time and further analysis will bring this problem to the decision makers.

As a direct result of the one month loss of the San Francisco-Oakland Bay Bridge during the Loma Prieta earthquake, it has been recommended that major transportation structures be designed for higher elastic seismic force levels and longer shaking periods to reduce the damage to non structural type. To accomplish this goal a new "importance factor" was introduced into the design and retrofit performance criteria. This represents a major change in the seismic design criteria for bridges and also represents introduction of a subjective factor which will be based on judgement more than engineering principles.

SUMMARY

The Bridge Seismic Retrofit Program which was initiated after the 1971 San Fernando earthquake and accelerated after the 1989 Loma Prieta earthquake is progressing on schedule. The program is designed and funded to replace or retrofit all publicly owned bridges that need upgrading to meet current seismic safety criteria. Design criteria and details have been developed in conjunction with a major "problem-focused" research program which relies heavily on large scale model testing to prove the theoretical designs. Analysis of the performance of seismic retrofit details during recent California earthquakes have proved the validity of the ductile performance philosophy utilized in the retrofit designs. The California Department of Transportation has over 800 bridges which need seismic upgrading and the current plans are to have them all retrofitted by the end of 1995.

SEISMIC PERFORMANCE CRITERIA FOR THE DESIGN AND EVALUATION OF BRIDGES

Ground Motion at Site	Minimum Performance Level	Important Bridge Performance Level
Functional Evaluation	Service Level-Immediate 'Repairable' Damage	Service Level-Immediate 'Minimal' Damage
Safety Evaluation	Service Level-Limited 'Significant' Damage	Service Level-Immediate 'Repairable' Damage

DEFINITIONS

Service Level-Immediate: Full access to normal traffic available almost immediately.
Service Level-limited: Limited access possible within days, (reduced lanes, light emergency traffic). Full service restorable within months.

'Minimal' Damage: Essentially elastic performance.
'Repairable' Damage: No collapse, but damage that can be repaired without closure.
'Significant' Damage: No collapse, but damage that may require closure to repair.

Important Bridge (one or more of the following):

- Bridge required to provide secondary life safety. (example: access to emergency facility)
- Loss of bridge creates major economic impact.
- Bridge formally identified by a local emergency plan as critical.

Safety Evaluation Ground Motion (Up to two methods of defining ground motions may be used):

- *Deterministically assessed ground motions from the maximum earthquake as defined by the Division of Mines and Geology Open File Report 92-1 (1990).*
- *Probabilistically assessed ground motions with a long return period (approx. 1000 years).*

For Important bridges both methods shall be given consideration, however the probabilistic evaluation shall be reviewed by a CALTRANS approved consensus group. For all other bridges the motions shall be based only on the deterministic evaluation. In the future, the role of the two methods for other bridges shall be reviewed by a CALTRANS approved consensus group.

Functional Evaluation Ground Motion:

Probabilistically assessed ground motions which have a reasonable (approx. 30 to 40%) probability of occurring during the useful life of the bridge. The determination of this event shall be reviewed by a CALTRANS approved consensus group. A separate Functional Evaluation is required only for Important Bridges. All other bridges are only required to meet specified design requirements to assure Minimum Functional Performance Level compliance.

Session-8

Hazard Mitigation

U-9) Pipeline Damage Mitigation Using TCLEE Pipeline Failure Database
(Lund, L.V.)

J-16) Study on Socio-Economic Effects of Lifeline Earthquake Disaster in Urbane Transportation Networks
(Kuribayashi, E., Chartchai, L., Suzuki, G. and Kawabe, H.)

U-10) Lifeline Interaction and Post-Earthquake Functionality: Case Study for Fire Following Earthquake
(Scawthorn, C.)

U-11) Proposed Plan for Developing and Adopting Seismic Guidelines and Standards for Lifelines
(Chung, R.M.)

PIPELINE DAMAGE MITIGATION USING TCLEE PIPELINE FAILURE DATABASE

Le Val Lund, P.E., M. ASCE

Civil Engineer, Los Angeles, CA,

ABSTRACT

The Technical Council on Lifeline Earthquake Engineering, American Society of Civil Engineers, has developed a methodology for a computer-based database for documenting pipeline failures in earthquakes. The purpose of the "TCLEE Pipeline Failure Database" is to preserve information on the location, pipe size, pipe material, type of pipeline damage and other useful characteristics of the damage for the engineering, geological, seismological, and seismic risk communities; for lifeline researchers. The ultimate goal is to develop pipeline mitigation measures to prevent earthquake disasters of lifeline network systems. Data collected from the Loma Prieta, California, USA, earthquake on October 17, 1989 was initially entered into the database. The methodology is of a general nature so that data can be entered from future earthquakes. The resulting database and methodology is available in a public depository, in diskette format for use on personal computers, to the engineering and scientific community.

INTRODUCTION

Lifelines and Pipelines

Lifelines are those services are vital to the health and safety of the community and to the functioning of an urban and industrialized society. Lifelines are critical for emergency response and recovery of a community after a disaster such as an earthquake. Lifelines include power, communication, transportation, water, sewage, gas and liquid fuel network systems.

Functional seismic performance of pipelines is necessary to facilitate emergency response and recovery of a community after an earthquake. Uninterrupted water supply is necessary for public health and safety, including fire fighting, drinking, cooking and sanitary use. Functional sewer pipelines are necessary to carry wastewater away and to prevent pollution and the spread of illness or disease. Gas supplies are critical for heating and cooking in essential facilities such as hospitals. Also, gas and liquid fuels are essential for operation of emergency vehicles and equipment. Electric power generation is critical to support emergency services. In addition to public health and safety issues, lifeline operability can be critical to the economy of the effected region. In some cases, lifeline damage can reach far beyond the local economy, producing serious economic effects at the state and even national level.

OBJECTIVES

The objectives of the "TCLEE Pipeline Failure Database" project is to develop a computer-based database and initially enter data collected from the Loma Prieta, California, Earthquake. Information to be preserved on the location, pipe size, pipe material, type of damage, and other pipeline damage characteristics for use by the engineering, geological, seismological, and seismic risk communities, and lifeline researchers. Also it is to encourage and facilitate the use of these data and methodology in future earthquakes, and ultimately to help improve the seismic pipeline performance of lifeline network systems for the public welfare. It should be noted, this is the first known attempt to document

pipeline damage on a region wide basis, and to establish a common methodology for collecting, storing, and disseminating pipeline damage data in an electronic format.

LOMA PRIETA EARTHQUAKE

Initially data from the Loma Prieta earthquake was entered into the TCLEE Pipeline Failure Database. On October 17, 1989 at 5:04 p.m. (PDT), a magnitude Ms 7.1 earthquake occurred along the San Andreas Fault in the Santa Cruz Mountains of California. The epicenter was located 100 km (60 miles) south of San Francisco, California. This event killed 63 people, injured 3,757 people, destroyed 366 businesses, damaged 3,530 businesses and left more than 12,000 temporarily displaced. The strong shaking lasted less than 15 seconds, but is estimated to have caused more than $7 billion in damage, not including economic losses.

The Loma Prieta Earthquake affected the performance of almost every type of lifeline system in the San Francisco and Monterey Bay areas. The most significant were in transportation, especially the loss of the Cypress Street viaduct on US Interstate 880, and the collapse of a linking span on the San Francisco-Oakland Bay Bridge. Significant damage to pipelines occurred in the Marina and South of Market Street areas of San Francisco, areas along the San Francisco Bay in Oakland and Alameda, in the Los Gatos area and areas along the San Lorenzo River in Santa Cruz. Underground pipelines were affected in unstable ground areas, especially those subjected to liquefaction. In a few cases the inability of the these pipelines to function affected emergency response and recovery activities.

AMERICAN SOCIETY OF CIVIL ENGINEERS NATIONAL SCIENCE FOUNDATION

The Earthquake Investigation Committee, Technical Council on Lifeline Earthquake Engineering (TCLEE), American Society of Civil Engineers (ASCE) conducted a preliminary investigation of lifeline damage from the Loma Prieta Earthquake of October 17, 1989. This investigation evaluated the performance of transportation, power, gas, communications and water and sewage facilities, and

subsequently prepared a report on lifeline performance. The report was published in the Earthquake Engineering Research Institute's professional journal, Earthquake Spectra (EERI, 1990).

ASCE-TCLEE, responding to a request for proposal (RFP), was awarded a grant (BCS-9011325) by the National Science Foundation (NSF) to develop the TCLEE Pipeline Failure Database and initially input data from the Loma Prieta earthquake. The methodology will permit data to be added from future earthquakes. The resulting electronic database was made available in a number of public depositories for use by the engineering and scientific community for the cost of duplication. The database is stored in files on a single 5-1/4 in., 1.2 Mb diskette formatted for IBM-type personal computers.

TCLEE PIPELINE FAILURE DATABASE METHODOLOGY DESCRIPTION

Scope

1. An advisory group was established to review objectives of the project to develop the TCLEE Pipeline Failure Database and to determine the type of data to be preserved and to how it might be used.
2. Lifeline agencies are identified who operate pipelines that might have been affected by an earthquake.
3. Data is collected on pipeline damage from agencies using a standard form.
4. Location of pipeline damage is determined by longitude and latitude.
5. For each location, added data fields describing the pipe characteristics and damage.
6. Compiled pipe break and leak data into electronic format, thereby creating computer database adaptable to existing commercially available software for use on the personal computer.
7. Placed methodology and computer data diskette in public depositories, available for use by researchers and practitioners.

8. Publish and make oral presentations on the general methodology for collecting pipeline break and leak data to collect data from future earthquakes to develop a similar database.
9. Future researchers and practitioners to develop pipeline damage prevention measures for pipeline network systems from future earthquakes.

Data Collection

The advisory group recommended collecting the following basic information on pipeline damage locations (Appendix A):

Lifeline conveyed: Water, sewage, storm water, natural gas or liquid fuels

Size: Pipe diameter and thickness

Material: Steel, cast iron, ductile iron, plastic, copper, concrete (reinforced or unreinforced), concrete cylinder, etc.

Pipe or fitting: Pipe, valve, elbow, tee, reducer, etc.)

Joint type: Bell and spigot, welded (gas or electric arc), rubber

Age: Year of installation.

Type of damage: Tension, compression, bending, corrosion, etc.

Leak or Break: Leak: lifeline continued to function with minimum loss of service.
Break: lifeline damaged with complete loss of function.

The advisory group also recommended collecting several other items, although with the knowledge these data may not be as readily available as those listed above as follows:

Method of Repair: Repair clamp, welding, coupling, replace pipe or fitting, etc.

Water Table: Elevation or depth to water from the ground surface.

Foundation Material: Description of bedding or trench material.

Coating and Lining: Cement mortar lining or coating, coal tar enamel lining or coating, multiwrap coating, etc.

Cathodically Protected: Yes or no.

A letter was sent to pipeline lifeline agencies in the Loma Prieta earthquake requesting this information using the Pipeline Damage Check Sheet (Appendix A), to more than 65 water, sewer, drainage, and gas agencies. . Telephone calls and personal visits were made to approximately 25 agencies in an effort to collect pipeline damage data.

In the process of contacting these lifeline agencies, it has become evident that many, but not all of them have documented the location of damage to underground pipelines. Some identified the size, pipe material, type of damage and other features of the damage. In contrast, about one-half of agencies concentrated on restoring the lifeline service, and on documenting the cost of repair for use in preparing Agency's Damage Survey Reports, which are documents used for soliciting federal damage reimbursement from the Federal Emergency Management Agency (FEMA). Damage Survey Report forms were available from public utilities, as only public agencies are eligible for reimbursement from FEMA. In summary, the availability and detail of pipeline damage data varied between agencies. Though most agencies did respond to our requests for damage data, some did not, even though their systems experienced damage. The database provided with this report contains 862 pipeline failure records from the Loma Prieta Earthquake. Indeed, since records were made only of reported repairs, much damage may have occurred has not yet been discovered, let alone documented.

Some agencies were fortunate and had no damage. The project does not include data on service connections, meters and private lines. There were no reported breaks or leaks to pipelines transporting

petroleum. Although substantial damage is known to have occurred to gas pipelines, the only damage data contained in the database is from Palo Alto.

Coordinate Determination

Contributing utilities generally provided street addresses or street intersections of pipe repairs. These were converted to global latitude/longitude coordinates using EQEHAZARD, a proprietary program of EQE International; however, this may be done by other methods such as scaling locations on maps showing latitude and longitude. Global coordinates were chosen to provide the most-commonly accessible location context, although it is recognized that some areas have more sophisticated coordinate systems. The address database used by EQEHAZARD is drawn from the United States Census Bureau's most recent address files.

Pipe Damage Electronic Database

The database is composed of records, one record for each pipe failure. Each record consists of 51 data fields, which describe the earthquake and the pipe damage. The fields are defined in the database format (Appendix B). Field names are shown on the left; explanatory text is provided opposite the field names. For example the first field in each database record is EARTHQUAKE, that is, the causative earthquake. Every record in this database refers to damage that occurred in the Loma Prieta earthquake, and therefore every record has the text "17 OCT 1989 Loma Prieta" entered in the first field. Future earthquakes will be similarly identified. Field names are based on the entries in the pipeline damage check sheet (Appendix A) which contributing utilities filled out to supply pipe repair data. It should be noted that terminology used to describe pipeline material, construction, and repair varies between agencies. This fact is reflected in the data the agencies provided, and therefore is also reflected in the database. A glossary of relevant terms was developed.

The diskette prepared contained the following files:

TCLEE_DD.DBF: Pipeline damage database, compatible with dBase III database software.

TCLEE_DD.PRN: Pipeline damage database in comma-and-quote delimited format, which is readable by virtually any database or spreadsheet program. These programs, such as dBase, FoxPro, and Lotus 1-2-3, have functions that enable the user to analyze, search, or print the data.

Methodology Dissemination

The computer diskette and report were distributed for permanent storage in a number of public depositories, including: the National Information Service for Earthquake Engineering and Bechtel Engineering Library at University of California, Berkeley; National Center for Earthquake Engineering Research at State University of New York; Terman Engineering Library at Stanford University; Southern California Earthquake Center, at University of Southern California; Library of Congress; California Institute of Technology; University of California, Davis; University of California, Los Angeles; University of California, Irvine; San Jose State University; Public Works Research Institute, Tsukuba and available to any researcher for nominal cost. Also oral presentations were made and publication in professional journals.

Problems

Immediately after the Loma Prieta earthquake, a flyer with a check sheet (similar to that shown in Appendix A) was distributed by the TCLEE Earthquake Investigation Committee (EIC) to a number of lifeline agencies, requesting they collect the information described In Appendix A. The agencies were informed a TCLEE EIC representative would contact them in about 30 days to collect damage information for inclusion in a report on the performance of lifelines in the earthquake. When TCLEE EIC personnel telephoned or visited the agencies, it was found that only a very few respondents

followed these suggestions. The information they provided was the basis for the 1990 EERI Spectra Loma Prieta Preliminary Reconnaissance report on water and sewage facilities.

There are significant differences in the amount of damage information available from different agencies. Not all agencies kept detailed records of the type of damage and method of repair. Most public agencies kept records on the cost of repair for possible reimbursement by FEMA. This reimbursement was not available to private agencies, although they may be eligible for low interest loans if the earthquake impact area is declared a "disaster area" by a state and federal governments.

Some agencies lack extensive information on the systems they operate. In some cases a utility acquired an old system for which detailed records were never kept. Some utilities were created through the merger of a group of smaller agencies, and therefore lack common records. Some small agencies lack technical staff. The quality and detail of data provided by these agencies may therefore be lower than that provided by larger utilities.

The methodology used in this project is the first known attempt to collect and digitize pipeline damage on a region wide basis. Like all first attempts, it is subject to improvement in future events. In future earthquakes in the United States, the flyer and check sheet, with a format similar to that shown in Appendix A, should be distributed. The format should be modified if appropriate; however, the value of the database may be degraded by inconsistencies between events. It should be recognized that there may be varying degrees of compliance.

DISASTER PREVENTION APPLICATIONS

Statistics - Inventory

The TCLEE Pipeline Failure Database provides the opportunity to collect information on pipeline failures from may earthquakes under different soil, seismic and geological conditions. It is necessary to have a total inventory (size, material, age, joints, geology, etc.) of the pipe in the system, so that a true comparison can be made of damage and good seismic performance can be identified. Agency pipe inventory was not made from the Loma Prieta earthquake.

Figure 1a: Pipeline Damage, Loma Prieta Earthquake, by material and diameter and Figure 1b: Pipeline Damage, Loma Prieta Earthquake, by material and UBC Soil Types are samples of data collected from the 862 damage locations in the Loma Prieta earthquake.

Pipeline Damage

The pipeline damage can be plotted on maps of the earthquake impact area to identify concentrations of damage. TCLEE Pipeline Failure Database can plot damage in the general area of impact as shown on Figure 2: Pipeline Damage, Loma Prieta Earthquake. The program has the capability of focusing (zooming into) the damage in a small area to analyze the detail of the pipe damage location as shown on Figure 3: Pipeline Damage, Loma Prieta Earthquake, in the San Francisco Marina District. This also may allow a better determination of breaks per 1,000-feet (per 1,000-kilometres) to be used in the a seismic risk analysis.

Faulting

Fault location maps are available in most seismic areas. This information can be overlaid on to the pipeline damage map to identify any damage due to faulting. Figure 4: Pipeline Damage, Loma Prieta Earthquake,and Major Faults shows the major faults as related to the actual damage in the Loma Prieta earthquake. This program allows for focusing into a small area for detail.

Soil Types

A valuable illustration of the utility of the TCLEE Pipeline Failure Database is the application of soils data to pipeline damage record. Two soil classifications, United States Geological Survey (USGS) and Uniform Building Code have been provided for each pipe repair location. The former system, by Evernden and others of the USGS (1981), describes soil type in terms of ground condition units A through J, as defined in Appendix C. The latter system (also in Appendix C) classifies a soil profile (types) as S1 through S4, for the purpose of characterizing seismic frequency response content at the ground surface.has been extracted from the Uniform Building Code (ICBO, 1991).

Soil data presented in the sample application from the Loma Prieta earthquake is shown on Figure 5 is based primarily on high resolution geological maps digitized by EQE. These electronic maps cover the urbanized San Francisco Bay area, and are based on 1:24,000 and 1:62,500-scale geological maps published by such

agencies as USGS and the California Division of Mines and Geology (CDMG). Slightly over one-half of the San Francisco Bay area was digitized using the higher-resolution maps. In addition, Santa Cruz has been digitized using a 1:24,000 scale geological map. The small scale provides for an accuracy of between 25 and 100 metres (75 and 300 feet) in the location of soil type boundaries.

Except for Santa Cruz, soil data for regions outside the urbanized San Francisco Bay area are based on 1/2-minute geological maps provided by Evernden and Thompson of the United States Geological Survey. The USGS 1/2-minute maps present average soil types in rectangles whose dimensions are approximately 730 metres (east-west) by 900 metres (north-south)(2,400 feet (east-west) by 3,000 feet (north-south)); accuracy of soil data drawn from this source is therefore limited.

Water Table - Liquifaction

It is known that pipe damage in earthquakes is frequently concentrated in zones of liquefaction. Liquefaction typically occurs where loosely-consolidated saturated alluvium is subjected to strong ground motion. Therefore, the tendency for pipe breakage to occur in saturated alluvial soils may be evaluated by overlaying the data from the TCLEE Pipeline Failure Database with peak ground acceleration or other appropriate measure of seismic intensity.

Seismicity

Seismicity maps are available for seismic areas and the data from the TCLEE Pipeline Failure Database can be overlaid on to the pipeline damage map to identify if seismicity affects pipe materials in a different manner. The program has the capability to zoom into small areas for details.

Seismic Risk Analysis

Seismic risk analysis have been preformed on existing pipeline network systems. Data collected from the TCLEE Pipeline Failure Database will be valuable in the analysis, including a better determination of the breaks per 1,000-feet (per 1,000 kilometres).

The purpose of the TCLEE Pipeline Failure Database is to supply researchers and practitioners with a single, consistent database of pipe damage in a format usable to all database and spreadsheet programs. The future investigations using this data for earthquake

disaster prevention of lifeline systems is, up to the researchers and practitioners themselves.

CONCLUSIONS

The data provided with this report may be used by geotechnical researchers to determine damage as related to different geological conditions or seismicity. Seismic risk researchers may employ the information to analyze lifeline systems, to understand better the performance of lifeline systems in earthquakes, and to identify regions where soil, seismicity or geological conditions would affect seismic risk or damage. The ultimate goal for these data is to improve the performance of lifeline systems.

RECOMMENDATIONS

1. The methodology presented herein should be used in future earthquakes for the collection of pipeline damage data. As future earthquakes occur, new data should be collected in the same manner and compiled into the same database, so that accumulated data can be placed in a TCLEE Pipeline Failure Database data bank representing different seismicity, geological and topographical conditions.

2. There is a need to obtain an inventory of pipe by length, size and material for each agency reporting damage to enhance the value of the data in the statistical reports..

3. There is a need to obtain a description of the operational pipeline network system, including pumps, tanks, pressure regulators, etc. from each agency at the time of the earthquake to enhance system seismic vulnerability analysis

4. The collection of pipeline data is different than other post-earthquake investigation activities in that it is often several months before most of the damage information is available or is finally discovered and repaired. Thus, the data collection of pipeline damage cannot meet the needs for most early reconnaissance activities, which are typically to be completed within 2 months

after the earthquake. Thus, there is a need for a mechanism to financially support the detailed effort needed to document pipeline damage at a later time period.

5. There is a need for better coordination between investigators in the collection of pipeline damage data. After significant earthquakes, many teams go into the field to collect data, including pipeline damage data. As a result, water and other lifeline agencies get several requests for the same damage information.

ACKNOWLEDGMENTS

The author wish to express his appreciation to the National Science Foundation for supporting this project.and to also thank the representatives of the many lifeline agencies who took the time to provide damage data. Marie McGuinness of ASCE, the members of the advisory group, and Anshel Schiff provided invaluable assistance. EQE's, San Francisco, staff who compiled the database into an electronic format, digitized pipeline damage, fault and soils data, their participation was appreciated.

REFERENCES

1. Earthquake Engineering Research Institute, Loma Prieta Earthquake Reconnaissance Report, Earthquake Spectra, Supplement to Volume 6, May 1990, El Cerrito, CA. pp. 239 - 338.

2. Evernden, J.F., Kohler, W.M., and Clow, C.D., 1981. Seismic Intensities of Earthquakes of Conterminous United States -- Their Prediction and Interpretation. Geological Survey Professional Paper 1223. 55 pp.

3. International Conference of Building Officials (ICBO), 1991. Uniform Building Code. p. 184.

4. Personal communications with lifeline agency representatives by Le Val Lund.

LL 10-13-92

MATERIAL	BREAKS/ LEAKS	DIAMETER, in. Unknown	>=72	(36-72)	(24-36)	(12-24)	(8-12)	(4-8)	(2-4)	<2
WELDED STEEL	33	1	0	0	2	7	4	19	0	0
OTHER STEEL	145	7	0	3	0	5	2	53	59	16
CLAY	31	1	0	0	0	3	7	20	0	0
SHEET IRON	2	0	0	0	0	0	1	1	0	0
PVC	25	0	0	0	0	0	1	11	8	5
OTHER PLASTIC	3	0	0	0	0	0	0	1	2	0
DUCTILE IRON	9	0	0	0	1	0	2	6	0	0
COPPER	2	0	0	0	0	0	0	0	1	1
CONCRETE	8	1	2	4	0	1	0	0	0	0
CAST IRON	148	24	0	0	0	10	18	80	13	3
ASBESTOS CEMENT	46	4	0	0	0	6	6	30	0	0
TOTAL	452	38	2	7	3	32	41	221	83	25

Figure 1a: Pipeline Damage, Loma Prieta Earthquake, by material and diameter (1-inch = 25.3 milimetres)

MATERIAL	BREAKS/ LEAKS	UBC SOIL PROFILE (ESTIMATED) Unknown	S1	S2	S3	S4
WELDED STEEL	33	3	4	24	2	0
OTHER STEEL	145	9	62	41	33	0
CLAY	31	0	1	1	26	3
SHEET IRON	2	0	1	1	0	0
PVC	25	1	20	1	3	0
OTHER PLASTIC	3	0	0	3	0	0
DUCTILE IRON	9	0	0	5	3	1
COPPER	2	0	0	1	1	0
CONCRETE	8	1	0	3	3	1
CAST IRON	148	2	55	25	53	13
ASBESTOS CEMENT	46	5	9	8	22	2
TOTAL	452	21	152	113	146	20

Figure 1b: Pipeline Damage, Loma Prieta Earthquake, by material and UBC Soil Types

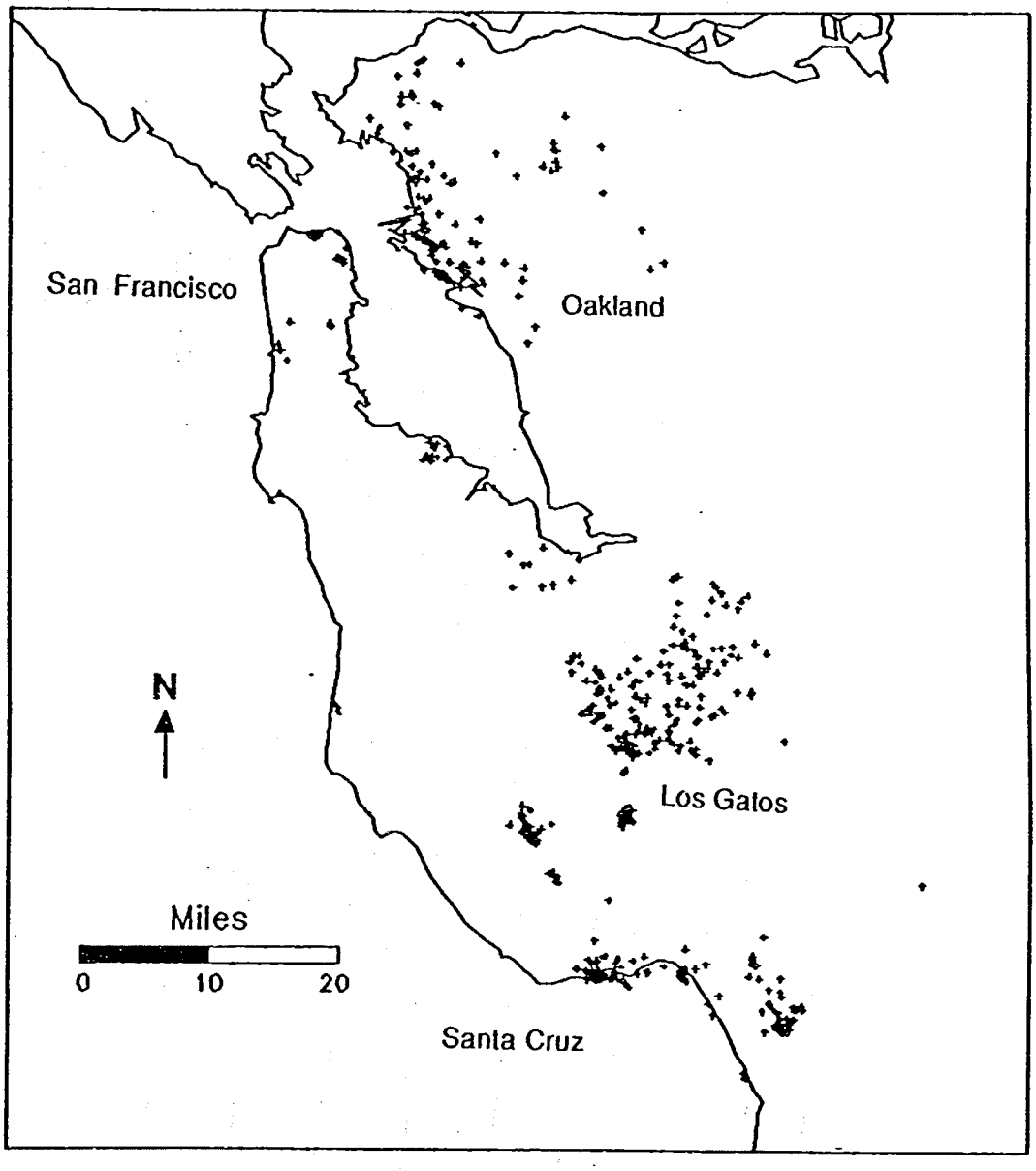


Figure 2: Pipeline Damage, Loma Prieta Earthquake

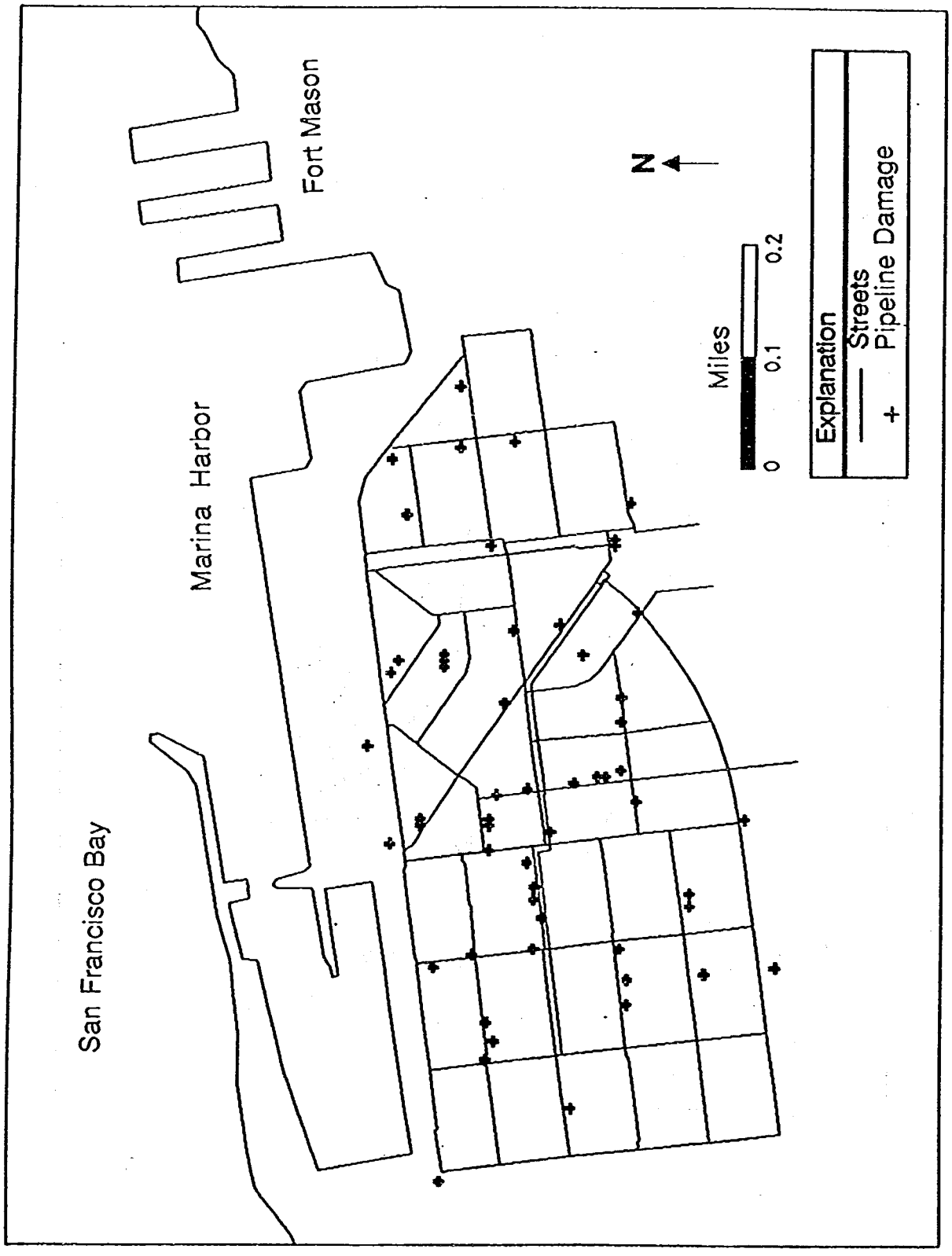


Figure 3: Pipeline Damage, Loma Prieta Earthquake, in the San Francisco Marina District

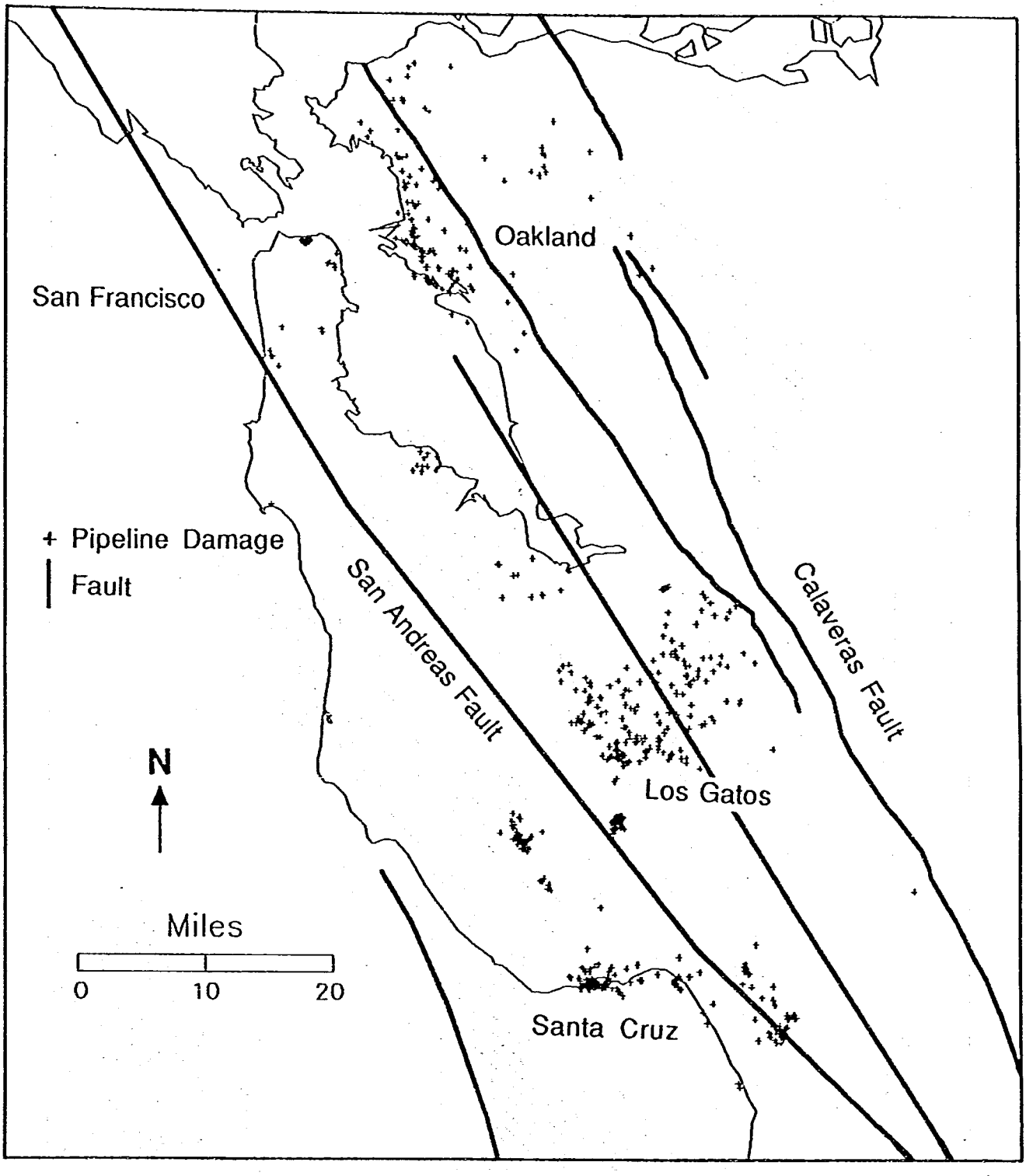


Figure 4: Pipeline Damage, Loma Prieta Earthquake, and Major Faults

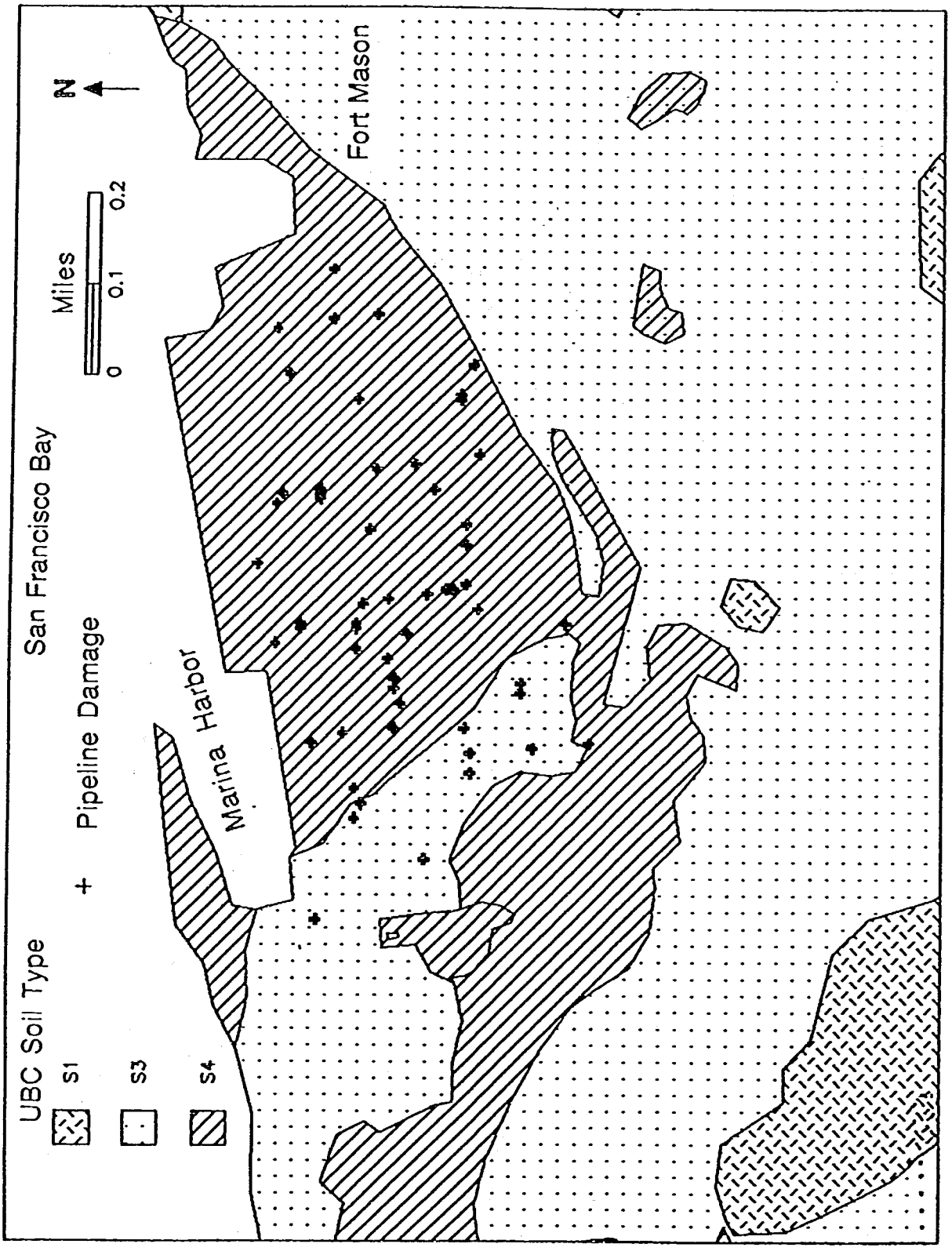


Figure 5: Pipeline Damage, Loma Prieta Earthquake, San Francisco Marina District, and UBC Soil Types

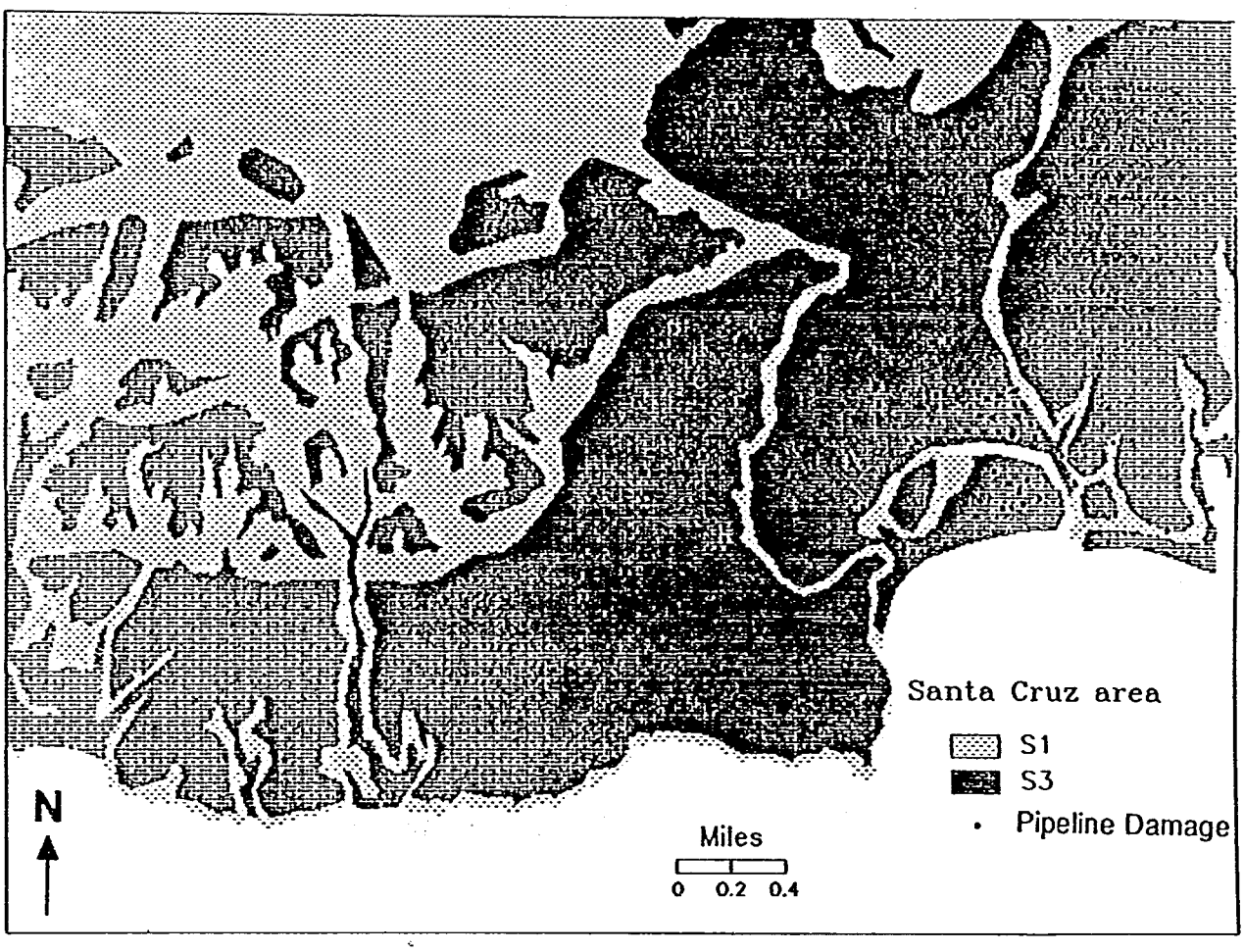


Figure 5: Pipeline Damage, Loma Prieta Earthquake, Santa Cruz Area, and UBC Soil Types

American Society of Civil Engineers
Technical Council on Lifeline Earthquake Engineering

Pipeline Damage Check Sheet

Location of Damage _____.

Pipe Description

Size ____, Thickness ____, Material _____, Lining ____,
Coating ____, Date of Installation _____

Type of Joints _____, Burial Depth ____,
Bedding Material _____,Type of Backfill _____

Ground Water Present ____, Depth to Water Surface ____

Damage

Impact on Flow: Break (flow disrupted) ____
or Leak (flow continued) _____

Pipe Failure: Circumferential (round crack) ____,
Change in Pressure (blowout) ____, Longitudinal (split) ____,
Corrosion ____, Other (describe)____

Joint Failure: Cracked ___ Pulled ___, Compression ___, Gasket ___,
Other (describe) _____

Fitting Failure: Elbow ___,Tee ___, Cross ___,Offset ___,Flange ___, Flange ___,
Hydrant ___, Other (describe) _____

Repair Method: Repair Clamp ___, Butt Strap ___, Welded ___, Replaced pipe or fitting ___, Other (describe) _____

Supervisor _____ Date _____

Comments _____
_____
_____

LL 8-8-90

Pipeline Damage Check Sheet - APPENDIX A
406

Field no.	Field name	Explanation
1	EARTHQUAKE	Name and date of causative earthquake
2	AGENCY	Name of responding agency
3	MEDIUM	Medium carried by pipeline (e.g., water)
4	CONTACT	Name of person providing data
5	PHONE	Telephone number of person providing data
6	LOCATION	Approximate address of pipeline damage
7	CITY	City of same address
8	ZIP	5-digit zip code of same address
9	LAT	Location of damage, degrees latitude (+N, -S)
10	LONG	Location of damage, degrees longitude (+E, -W)
11	SOIL_USGS	Soil type: USGS ground condition unit
12	SOIL_UBC	Soil type: UBC soil profile classification
13	SIZE	Pipe nominal diameter, inches
14	THICKNESS	Pipe wall thickness, inches
15	MATERIAL	Pipe material
16	LINING	Pipe lining, applied to inside of pipe
17	COATING	Pipe coating, applied to outside of pipe
18	YEAR_INST	Year of installation
19	JOINT_TYPE	Type of joint
20	BUR_DEPTH	Depth of pipe invert below ground surface, feet
21	BEDDING	Material on which pipe rests
22	BACKFILL	Material in which pipe is buried
23	GW_PRESENT	Groundwater present when excavating pipe
24	GW_DEPTH	Depth to groundwater below ground surface, feet
25	BREAK	Flow disrupted, loss of function
26	LEAK	Damage caused leak, but pipeline function continued
27	ROUND	Circumferential pipe crack
28	BLOWOUT	Blowout-type damage
29	SPLIT	Longitudinal pipe crack
30	CORROSION	Corrosion evident at damage
31	PIPE_OTHER	Pipe damage caused by other phenomenon (described)
32	CRACK	Joint failure caused by crack
33	PULL	Joint pulled apart
34	COMPRESSION	Joint failure caused by compression
35	GASKET	Joint gasket failure
36	JT_OTHER	Other type of joint failure (described)
37	ELBOW	Failure at elbow fitting
38	TEE	Failure at tee fitting
39	CROSS	Failure at cross fitting
40	OFFSET	Failure at offset fitting
41	FLANGE	Failure at flange fitting
42	HYDRANT	Failure at fire hydrant
43	FITG_OTHER	Failure at other type of fitting (described)
44	CLAMP	Damage repaired with repair clamp
45	STRAP	Damage repaired with butt strap
46	WELD	Damage repaired with weld
47	REPLACE	Damage repaired by replacing pipe or fitting
48	REP_OTHER	Damage repaired with other method (described)
49	COMMENTS1	Comments, 1st line
50	COMMENTS2	Comments, 2nd line
51	COMMENTS3	Comments, 3rd line

Database Format - APPENDIX B

Geologic map units	Ground-condition unit
Granitic and metamorphic rocks (Kjfv, gr, bi, ub, JT_{RV}, m, mV, PpV, PmV, Cv, Dv, pS, pSv, pCc, pCgr, pC, epC, Tl)	A
Paleozoic sedimentary rocks (Ms, PP, Pm, C, CP, CM, D, S, pSs, O, E)	B
Early Mesozoic sedimentary rocks (Jk, Ju, JmE, Tr, Kjf)	C
Cretaceous through Eocene sedimentary rocks (Ec, E, Epc, Ep, K, Ku, KE)	D
Undivided Tertiary sedimentary rocks (QTc, Tc, TE, Tm)	E
Oligocene through middle Pliocene sedimentary rocks (PmEc, PmE, Mc, Muc, Mu, Mmc, Mm, ME, Φe, Φ)	F
"Plio-Pleistocene" sedimentary rocks (Qc, OP, Pc, Puc, Pu)	G
Tertiary volcanic rocks (Pv, Mv, Olv, Ev, QTv, Tv)	H
Quaternary volcanic rocks (Qrv, Qpv)	I
Quaternary sedimentary deposits (Qs, QaE, Qsc, Qf, Qb, Qst, QE, Qq, Qt, Qm)	J

Explanation of USGS ground condition units
From Evernden et al., 1981

TYPE	DESCRIPTION
S_1	A soil profile with either: (a) A rock-like material characterized by a shear-wave velocity greater than 2,500 feet per second or by other suitable means of classification, or (b) Stiff or dense soil condition where the soil depth is less than 200 feet.
S_2	A soil profile with dense or stiff soil conditions, where the soil depth exceeds 200 feet.
S_3	A soil profile 70 feet or more in depth and containing more than 20 feet of soft to medium stiff clay but not more than 40 feet of soft clay.
S_4	A soil profile containing more than 40 feet of soft clay characterized by a shear wave velocity less than 500 feet per second.

Explanation of UBC site soil profile classifications
From 1991 Uniform Building Code

Soil Classifications - APPENDIX C

ASCE - Technical Council on Lifeline Earthquake Engineering

Lifelines Performance in the Landers - Big Bear (CA) Earthquakes of June 28, 1992.

Two earthquakes occurred in the San Bernardino County high desert and mountain regions of southern California on Sunday, June 28, 1992. The first event was a magnitude 7.5, at 4:58 am PDT, on the Johnson Valley fault near the community of Landers in Yucca Valley and the second was a magnitude 6.6, at 8:04 am, east of the community of Big Bear Lake on an unnamed fault in the San Bernardino Mountains. The two events were followed by many aftershocks with some of magnitude 5.0 and greater. The epicenters of both earthquakes was approximately 100 miles (160 kilometres) easterly of Los Angeles, California. The estimated damage to public and private facilities is $92 million.

The most significant geotechnical feature of the earthquake is the surface expression of the faulting along a 44 mile (71 kilometres) length with a maximum reported right lateral horizontal slip of approximately 21 feet (6.5 metres).

While most of the faulting occurred in a isolated region of the desert, the surface expression of the faulting in the vicinity of the communities of Yucca Valley and Landers had significant effect on the highway and water supply lifelines. In this area the horizontal displacement ranged from 5 to 9.5 feet (1.5 to 3.0 metres) in a disrupted zone, which at places is several hundred feet (100 metres) wide. State Highway No. 247 (Old Woman Springs Road) was disrupted in 10 locations. Eight days later traffic was fully restored by the California Department of Transportation. Other county roads in the area were similarly disrupted, mostly gravel roads, and were restored by San Bernardino County Road Department. There was no reported damage to state highway bridges. State Highway No. 38 to Big Bear Lake remained closed for two weeks because of rock slides. Operations at three small civilian and one military airport in the Yucca Valley area were not affected by the earthquakes, other than minor cracking of runways and taxiways and loss of power.

Water supply is from wells from the several groundwater basins in the area. Water customers were without water from several hours to two weeks because of the damage to water lines from wave propagation, ground subsidence and crossing the fault zone. Most of the pipeline damage occurred in the fault zone,.where the pipes were not able to take such a large displacement. It was preliminarily reported there was approximately 700 water pipe breaks, even some as far away as Los Angeles and Phoenix, AZ.

At least six water tanks were damaged, ranging in size from 42,000 gallons (160,000 litres) to 417,000 gallons (1.6 megalitres), four of which were removed from service. Damage consisted of a bulge at the base of the tank (elephants foot), shell and roof damage, shell splitting at access hatches and severed piping attached to the tank. There was no reported damage to water wells or booster pumping plants other than the loss power supply and ground displacement adjacent to wells..

Approximately one dozen water agencies along with private contractors, responded with mutual aid equipment and personnel to help the local agencies restore the water distribution systems in the Yucca Valley area. Some agencies advised their customers to boil the water to protect the people from possible contamination. California Office of Drinking Water personnel supervised the disinfection of restored water mains and lifted the boil water notice on July 13th. Beverage companies, U. S. Marine Corps and California National Guard provided emergency water for those people in need of water.

Wastewater disposal in the Yucca Valley area is handled by private individual sewage disposal facilities. In the Big Bear Lake area a regional waste water agency collects sewage from the several communities, treats the water and discharges the treated water to Lucerne Valley for agricultural irrigation. Damage occurred within the secondary treatment plant 1.5 million gallons per day (5.7 megalitres per day); however, with adequate storage, the biological treatment process was maintained and there was no loss in operation of the system. There was no operational damage to the collection and discharge lines.

The major electric power agency in the area experienced lost of service to 550,000 customers due to localized damage within the distribution system. Most of the service was restored to the customers by late the same night of the earthquakes. There was no operational damage to their high voltage system. The Big Bear Lake area is served by another electric agency which purchases energy from the major utility. 5,000 customers in this area lost service,

also due to localized failures, 95% of the customer's service was restored within two hours. In the Los Angeles area power service was lost to 51,000 customers, again due to distribution system failures. Nearly all had their service restored within 24 hours.

An interesting situation.occurred when the northwesterly extension of the fault rupture zone passed beneath a steel tower supporting a 220 kilovolt transmission line. There was no loss of service, even though the tower was badly damaged and displaced approximately 9-feet(2.75-metres). Two temporary wood frame "H" structures were installed each side of the fault zone. Ultimately these two wood structures will be replaced by two steel towers.

A portion of the Yucca Valley area is served with natural gas and there was no reported leaks in the gas distribution system. Most people in the area rely on bottled gas (propane). The Big Bear Lake area is serve by another gas agency and also reported no gas leaks. There was no damage to two high pressure gas transmission lines passing through the area, one 6 inch (152 millimetres) south of the primary rupture zone and the other 30 inch (760 millimetres) north of the primary rupture zone. There was some nonstructural damage to a compressor station on the 30 inch (760 millimetres) line.

Telephone service was affected by the usual congestion due to the high volume of calls and an overhead cable was down along State Highway No. 247. There were very limited service outages due to a few tension failures on buried telephone cable from the earthquake. Line load control was implemented.

San Bernardino County activated there Emergency Operations Center in the City of San Bernardino and at a field location in the county services center in Yucca Valley. Some of the local lifelines also activated their emergency operations plan. Four structure fires were reported in Yucca Valley due to overturned water heaters and propane tank. One FM radio station in Yucca Valley, which had a emergency backup power supply continued to operate after the earthquakes providing valuable local emergency public information. The local radio station in big Bear also remained in service.

Prepared by Le Val Lund
Information collected by ASCE-TCLEE Earthquake Investigation Committee.

STUDY ON SOCIO-ECONOMIC EFFECTS OF LIFELINE EARTHQUAKE DISASTER IN URBANE TRANSPORTATION NETWORKS

by

Eiichi Kuribayashi[1], Leelawat Chartchai[2], Go Suzuki[3], and Hiroaki Kawabe[4]

ABSTRACT

One of the major lifelines, transportation system has a great responsibility on evacuation, rescue, and rehabilitation after earthquakes. Also, it gives large effects on socio-economic situation if damage is severe, and the recovery delayed in modern urbane areas.

It is important to prepare for the future disasters for decreasing the socio-economic loss. This paper presents some of the recommendations on principle for preparation, and degree of damage on the system so that future loss to be estimated. There also case study was carried out based on the Loma Prieta Earthquake of 1989.

---

1) Professor, Dept. of Civil Engineering/Regional Planning, Toyohashi University of Technology, Toyohashi 441 Japan
2) Research Associate, ditto
3) Graduate student, ditto
4) Graduate student, ditto

INTRODUCTION

Referring to the Bible, "When God saw what they did and how they returned from their evil ways, he had compassion and did not bring upon them the destruction he had threatened." Jonah Chapter 3 Verse 10. "Believe in the Lord, Jesus, and you will be saved." Acts Chapter 16 Verse 31.

When the natural hazards occur, sometimes it may strongly affect to the human life by the damages on the lifeline systems. In this report earthquake disasters are discussed, with emphasys on the transportation systems.[1] Systems usually include road, railway, navigation channel, and airway, but since only the small region was dealt in this paper, airway is not discussed. Further more it is an important factor, of course for our daily life, and for the recovery on any other facilities damaged by the earthquake.

In common sense, when the system is damaged, it must be recovered as soon as possible. Even in any authorities, there are many things to be considered like how to make the recovery quick: in how much function the system could resume.

GENERAL CONSIDERATIONS ON TRANSPORTATION SYSTEM

System Networks

As we consider the function of the road facility, it is more natural to treat them as a network rather than just as lines. In urbanizedareas, there are some substitute ways to get to one point from another. All of the route is not perfectly sevicable. One of the important thing after the disaster is to not make the people isolated from their needs. There may be casualties must be carried to the hospital in different area. They might lack food and water supply. If at least one branch of the network is connected to the point, these indirect loss or secondary disaster may decreased.

Any how, the needs would increase as the days pass by. It can be estimated that the maximum demand could be greater than that of the before-quake, for there will be increased traffics for the recovery of the area. The final volume of the transportation is expected as before the earthquake, so that strongly recommended is to have data of traffic amount on each route, such as result of "origin and destination survey," for the use of recovery and future planning to disaster mitigation.

However, this survey takes a lot of time and expenditures, either actual cost for the equipment or for the labor costs. And also, it is impossible to

survey all the traffic on every route, especially on before the earthquake and right after the quake. So in general, in finding out the image of traffic flow, the only data which can be used without special effort is the population. Using the population related traffic amount, calculation can be made.

Utilization of Transportation Lifeline System

There are three different measures according to the damage on the traffic system.[2] They are categorized as 1)ALTERNATIVE measures, 2)EMERGENCY repairs, and 3)SUSPENSIVE measures, provided on Fig. 1.

When damage is light and other transportation method can take place of the traffic of damaged line, total traffic will not change, and will be called alternative measures. Following are the example equations.

$$P1+P2+P3 = P1+P2+P3 \quad (1)$$

Here P1, P2, and P3 are the traffic amount(number of person) of each transportation method. On this study, three method of automobile, railroad, and ship has been taken. P1, P2, and P3 are the amount of after the quake. This equation shows that total amount of traffic on before and after the earthquake is equal.

$$P1+P2+P3 > P1+P2+P3 \quad (2)$$

Equation 2 shows the function of emergency repairs. This measure signifies that total amount of traffic before the quake is greater than that of before quake. This means some trips are restricted, so that one must give up the trip or delay the schedule.

$$P1+P2+P3 = 0 \quad (3)$$

Equation 3 is a function of suspensive. All of the transportation method are closed, and must give up any trip relating to that area.

OVER HEAD LOSS ESTIMATION OF THE TRANSPORTATION NETWORK

Concepts on the Traffic Flow Simulation

Estimating the over head loss for the transportation system, computer simulation was used. Fig. 2 shows the concept of the simulation method.

On the figure, small circles inside the large one, are the district or region inside the city. Within the small circle, there are groups of person which want to trip to some region of the other city. In this study, each person within this small group is postulated to trip together. This group choose the route of minimum cost, distance, or time for the trip between origin and destination. Trip will be an addition of three. They are:

(1) the trip from the origin to the key point of trans-city, either road, train, or ship;
(2) the trip of trans-city;
(3) the trip from the key point of other city to the final destination.

Case study - Loma Prieta Earthquake[3]

The Loma Prieta Earthquake of October 17, 1989 caused many damages on the highway structures in San Francisco Bay area.[4][5] Closing the San Francisco - Oakland Bay Bridge, and collapsing of viaducts, there are many disturbances and inconveniences both on business and household. Fortunately there are some substitute traffic route, which are other bridges, train, and ship, between San Francisco and Oakland. There is a counting on the number of the trip around the bay area, before and after the earthquake,[6] but the increased/decreased cost of trip are not shown, for the survey is only done by the crossings.

On the case study, expecting the average amount of one day traffic on the closed route, to be assigned to other route. The traffic amount is distributed according to the rate of the population of each district. [7]

The simulation was to find out a minimum trip cost on each travel, and also for estimating the indirect loss of transportation system on the area. Fig. 3 and 4 shows the simulation model of the San Francisco Bay area. As in the modeling, first, done by each zone, second, by connecting all zones to form whole area. Each model was expressed by nodes and branches. Nodes are either dense inhabited district (D.I.D.), major railway stations, or freeway interchanges. Branches signify transportation facilities. Since necessity time between nodes are not considered in this study, the weight of the branch due to the trip cost. Closed route, like Bay Bridge, are also included in the figure with dotted line.

Result

The result of the simulation is listed on Table 1. The amount of the loss

was rather small, comparing to the regional G.N.P. ($125 billion) or total loss from this earthquake ($7 billion). Some of the reason for this are:

1) 24 hours of Energency schedule on BART;
2) Low price of gasoline;
3) Flexibility and redundancy of the system in this area.

On the other hand, simulating the situation if the BART did not change its schedule, 30,000 of automobiles were overflowed. If this happened, there may be a great loss in the economy of this area. As a result, massive transportation method like railway is an important factor of raising a redundancy of the transportation lifeline network system. Further study may be required on its earthquake resistance, both on structurally and systematically.

EARTHQUAKE PREPAREDNESS

Preparedness on Transportation Facilities

Since it is well known for every one of the technical field that the earthquake resistance on the structures are important, save details of this field for other researches. One proposition on this field is to have "easy-to-recover" design. Optimizing the investment for earthquake resistance, this conception could accepted. In the case of the Loma Prieta Earthquake, one of the major issue, as a good example, San Fransisco Bay bridge caused great effects, but the damage itself was small. On the other hand, some of the viaducts like I-880 Cypress Viaduct collapsed and made a large number of casualties. Avoiding the loss of human life from the collapse of the structure is necessary. Considering this and designing structures with the manner of "easy-to-recover" may be the future style of designing.

As for an example, say "make the foundation vulnerable only by the human hands," that is for the complete replacement in case the structure damaged heavily.

Preparedness on People

The earthquake happens when we can not expect. For it is difficult to be at the safe place during the movements, but the preparation can save lives from the disaster of aftershock. As for a transportation, either driver, customer, or even the pedestrian should better to have knnowledge on the

characteristic of the earthquake. Public education for the earthquake is one of the most affective preparedness. This could be done by the community meeting, teaching at school, send round a circular, governmental notice, and so on. Using a modern information, like computer networks could be a future. Mass media should have role on broad understanding on hazard so that the loss could be minimized.

CONCLUSIONS

Treating transportation lifeline system as a network, it is clear that there is a redundancy itself unless one region is connected with single line. In urbane area, this case is rare so that the redundancy depends on the earthquake resistance and the traffic capacity of the system. Results from the case study of the San Francisco Bay Area, socio economic loss from damages on the transportation system is rather small, within the sphere of "ALTERNATIVE measures." Exceeding this and being "EMERGENCY repairs," a great loss might happen. Reconsideration on today's system in many of urbane areas and future research must be strongly recommended.

FUTURE DIRECTIONS

In this paper, the effect of earthquake to the transportation system has studied, but only dealt with subject related to before the quake. Total guide line for the transportation lifeline system must be made.

The case study here dose not include required time for each trip. Time - cost relationship should analyzed and more detailed simulation would give another face of socio economic losses.

REFERENCES

(1) Eiichi Kuribayashi, Present Status and Problems on Countermesures to Earthquake Disasters with Emphasis on Disaster-Resistivities of Cities and their Lifelines, Technical Memorandum of PRWI No. 1342

(2) Eiichi Kuribayashi, Study on Emergency and Alterrnative Function of Damaged Lifelines, Toyohashi Univ. of Tech. May 1986 (in Japanese)

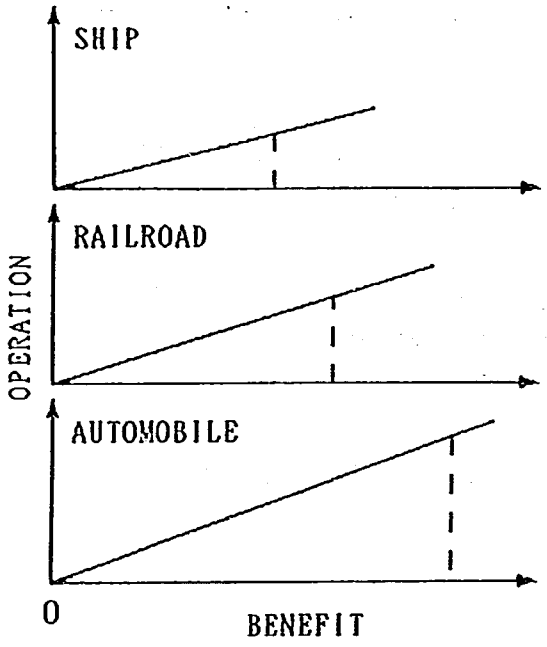
(3) Hiroaki Kawabe, Socio-Economic appraisal of damaged Lifelines on Urbane space, Conference of the Japan Society of Civil Engineers, March, 1992 (in Japanese)

(4) Loma Prieta Earthquake Reconnaissance Report, Earthquake Spectra, Supplement to Volume 6, May 1990

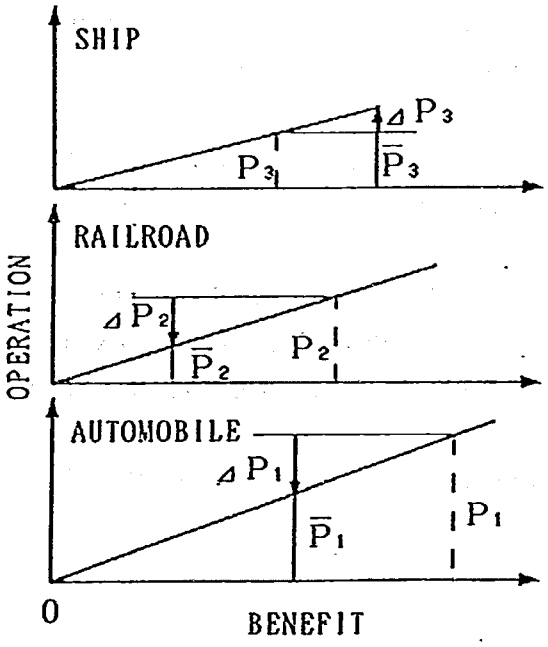
(5) Lessons Learned from the 1989 Loma Prieta Earthquake, International Symposium on Safety of Urbane Life and Facilities, Nov. 1990

(6) George W. Housener, Competing against time, Report to Governor George Deukmejian, The Geovernor's Board of Inquiry on the 1989 Loma Prieta Earthquake, May 1990

(7) National Resarch Council(U.S.):Highway Capacity Manual, 1985

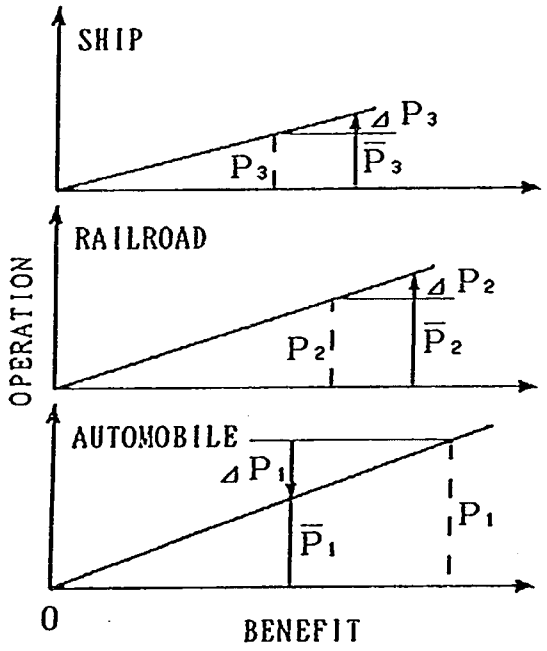


Coefficient of Utilization of Lifeline System



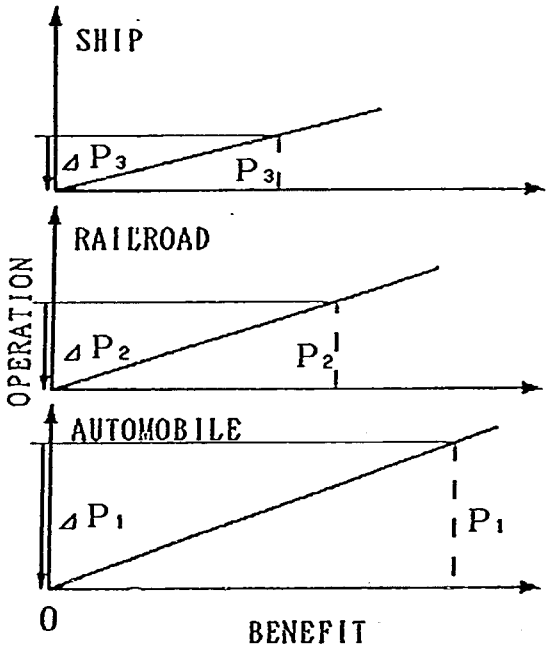
EMERGENCY repairs

$$P_1 + P_2 + P_3 > \bar{P}_1 + \bar{P}_2 + \bar{P}_3$$
$$\Delta P_1 + \Delta P_2 + \Delta P_3 < 0$$



ALTERNATIVE measures

$$P_1 + P_2 + P_3 \equiv \bar{P}_1 + \bar{P}_2 + \bar{P}_3$$
$$\Delta P_1 + \Delta P_2 + \Delta P_3 = 0$$



SUSPENSIVE functions

$$\bar{P}_1 + \bar{P}_2 + \bar{P}_3 = 0$$
$$\Delta P_1 + \Delta P_2 + \Delta P_3 = -\{P_1 + P_2 + P_3\}$$

Fig. 1 Coefficient of Utilization of Lifeline System

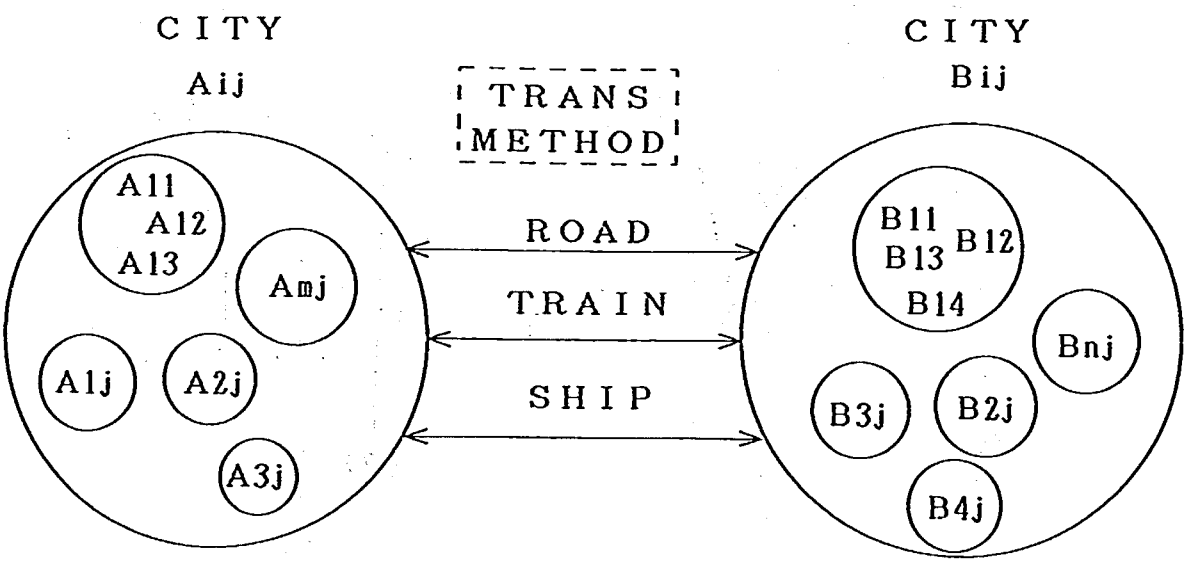


Fig. 2 Concept of the Simulation Method

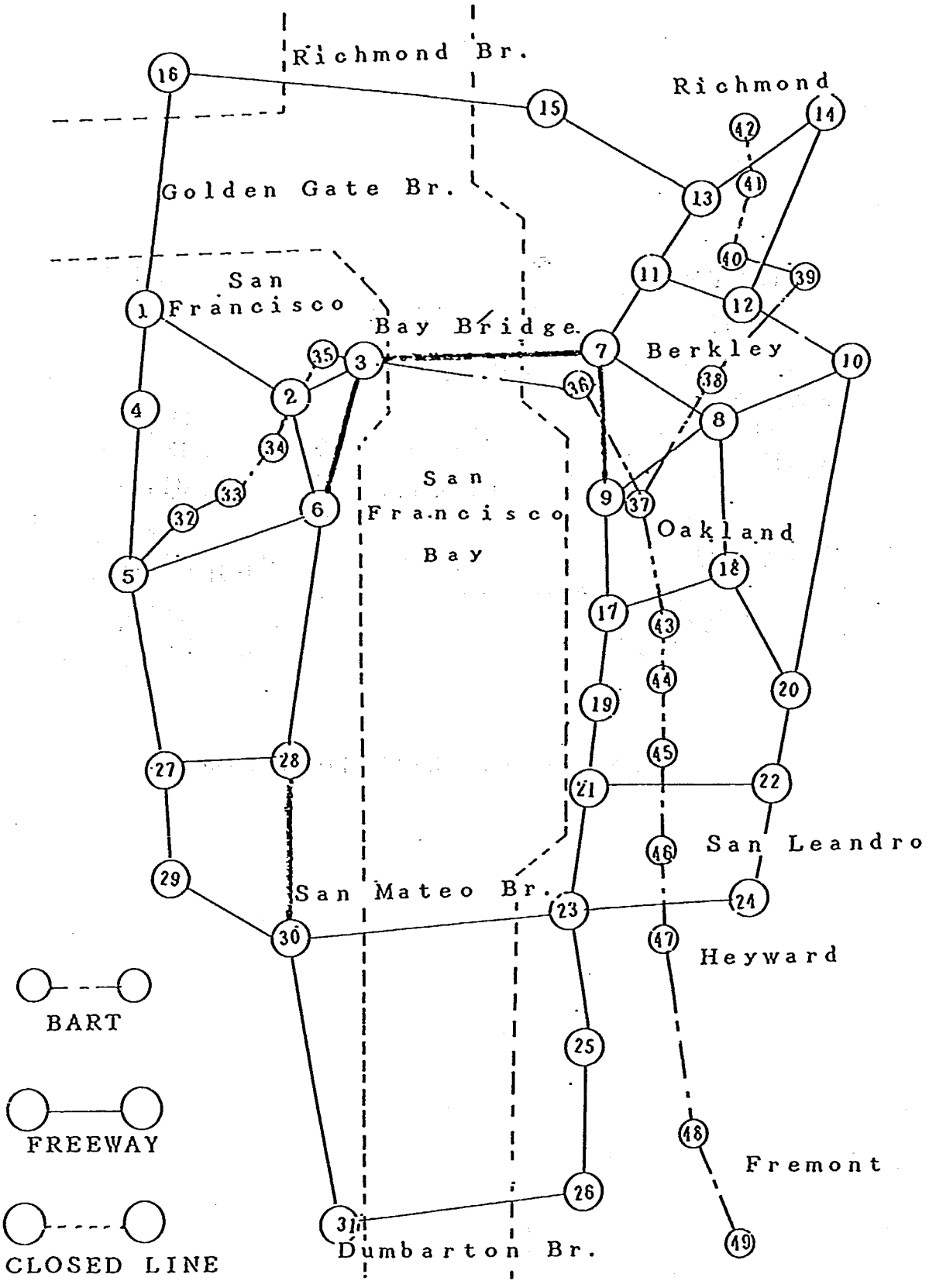


Fig. 3 Model of the San Francisco Bay Area

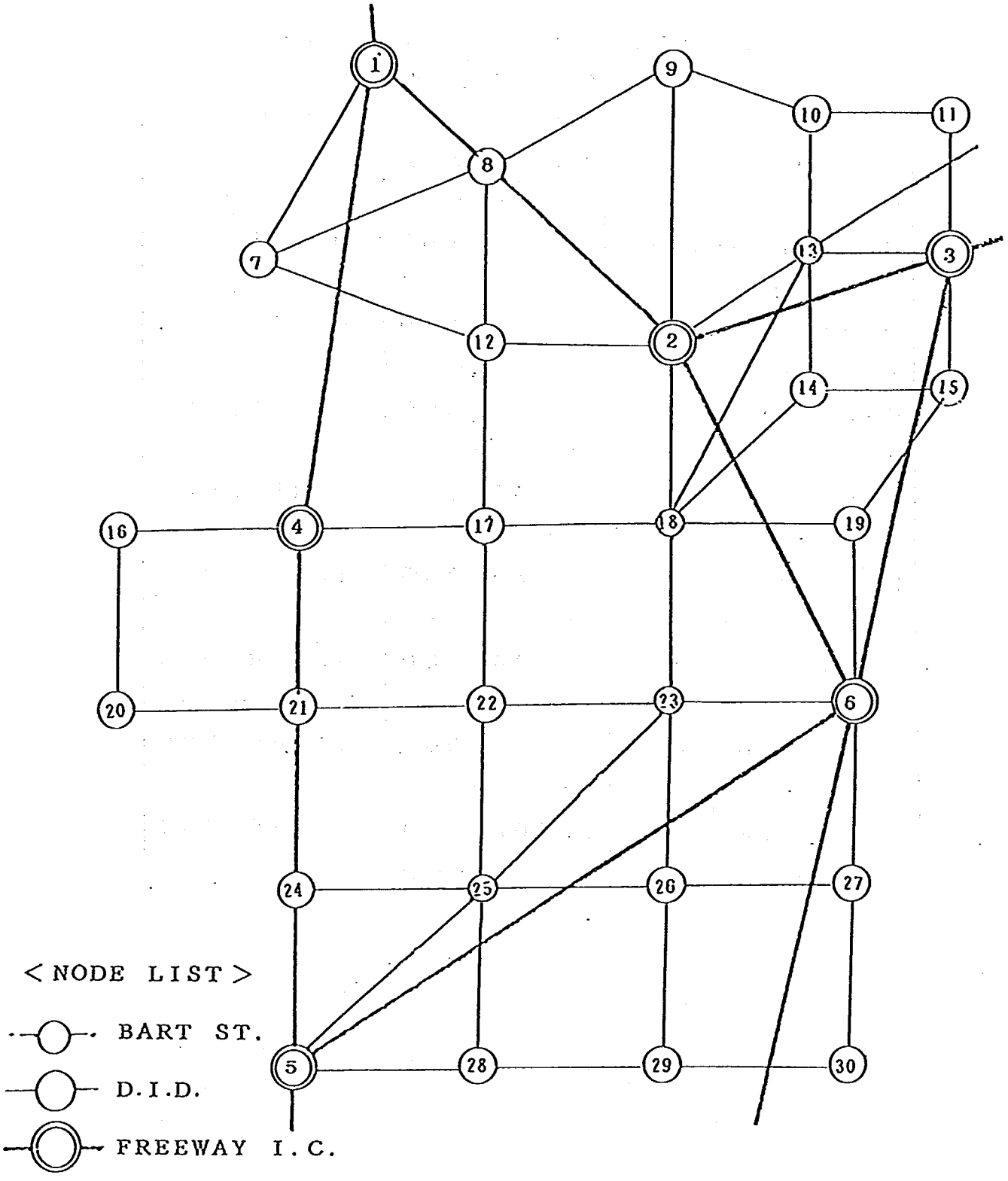


Fig. 4 Model of an exanple zone

Table 1 Estimated user loss related to the damage on transportation system

City	Loss ($/day)	Loss ($/mon.)
San Francisco	654,600	19,638,000
Oakland	350,600	10,518,000
Berkley	112,000	3,360,000
Heyward	46,800	1,404,000
Fremont	56,200	1,686,000
Richmond	144,600	4,338,000
San Leandro	38,000	1,140,000
total	1,402,800	42,084,000

LIFELINE INTERACTION AND POST-EARTHQUAKE FUNCTIONALITY

Case Study for Fire Following Earthquake

Charles Scawthorn, S.E.

Vice President
EQE International
San Francisco, CA 94104

ABSTRACT

Seismic vulnerability studies have generally examined the post-earthquake functionality of lifeline systems in isolation-that is, without consideration of interaction, where the degraded performance of a lifeline impacts the performance of a second lifeline (e.g., loss of electric power degrades water supply due to lack of pumping). Recent lifeline experiences, including the 1989 Cajon Pass, 1989 Loma Prieta earthquake, 1991 Shasta spill, 1991 East Bay Hills fire, and 1992 Hurricanes Andrew and Iniki events all indicate that interaction effects can be very significant. Based on a review of these events, three types of interaction are identified: cross-impact, collocation, and cascade. A simple model of initial and final functional states linked by a lifeline interaction matrix is presented, together with results from an example application for water supply impacts on the post-earthquake fire problem in San Francisco, which indicates differing impacts of water supply dysfunction, depending on post-earthquake conflagration potential.

INTRODUCTION

Reliable performance of lifelines such as water supply, transportation, and communications is essential following a major earthquake. While the seismic vulnerability of these systems has been studied in a number of urban areas, these studies have generally examined the post-earthquake functionality of these systems in isolation-that is, without consideration of interaction, where the degraded performance of a lifeline impacts the performance of a second lifeline (e.g., loss of electric power degrades water supply due to lack of pumping). A further consideration in this regard is collocation where, due to physical constraints, a number of lifelines are located in proximity, such that a single relatively small event can simultaneously disrupt most or all of the lifelines. In recognition of these aspects, several investigators have recently begun to identify potential interactions[1,2] and have examined the collocation problem within a limited context.

This paper first reviews recent lifeline experience, drawing on the 1989 Cajon Pass, 1989 Loma Prieta Earthquake, 1991 Shasta spill, 1991 East Bay Hills fire, and 1992 Hurricanes Andrew and Iniki events. This paper discusses these events in the context of interaction and collocation effects, and draws on the lessons of these events to construct a model and analytical methodology for lifeline interaction. The model examines the impacts of lifeline interaction on potential losses due to fire following earthquake.

REVIEW OF RECENT LIFELINE EXPERIENCE

This section reviews recent lifeline experience, drawing on the Cajon Pass, 1989 Loma Prieta Earthquake, 1991 Shasta spill, 1991 East Bay Hills fire, and 1992 Hurricanes Andrew and Iniki events.

1989 Cajon Pass

In May 1989 a train derailment in San Bernardino, California, occurred, resulting in severe property damage and loss of life. The Office of the Fire Marshall responded to determine if the derailment had impacted a petroleum products pipeline that was buried along the railroad right-of-way. It was decided that the pipeline was not damaged, and the fire and safety personnel turned over the site to the railroad to allow site cleanup. About a week later, the pipeline ruptured and the resulting fire caused considerable property damage and loss of life. The subsequent investigation[3] concluded that the pipeline may have been damaged during the derailment, but the most probable cause of its damage was the derailment cleanup operations. *[Foregoing paraphrased from a secondary source[4].]*

1989 Loma Prieta Earthquake

Impacts of the 17 October 1989 Loma Prieta earthquake on lifeline performance have been reviewed by a number of authors. While some failures occurred in virtually all lifelines[5], relatively few significant lifeline interactions occurred. Transportation cross-impacts were noted[6], but most interaction was not particularly significant relative to primary damage to structures and lifelines[7]. Nojima and Kameda have compiled instances of interactions, several of which are worth noting:

a. One interaction was loss of wastewater treatment capability, due to loss of electric power at treatment plants (electric power is required to continuously mix sludge digesters, otherwise changes in temperature and oxygen conditions result in die-off of the microbial flora, requiring new startup, with loss of several days in treatment).

b. A significant interaction was that between power, transportation, and telecommunications. Several central business district telephone facilities were not immediately affected by the earthquake, but they lost commercial power supply, requiring them to shift to backup on-site power generation. This was adequate for several hours, until fuel ran low. Transport of fuel to the facilities was severely hampered by highway problems. In a large event, it is likely that these telephone switches would have lost all service. Central business district telephone facilities are particularly vulnerable and significant in this regard, due to the large number of critical customers they serve, as well as the difficulties likely to be encountered in supplying them with fuel after a major earthquake.

Figure 1, from Nojima and Kameda, summarizes lifeline interactions in the Loma Prieta Earthquake.

1991 Shasta Spill

In 1991, a railroad train traversing a sharp-curved railroad bridge at Dunsmuir, California, derailed. The derailment occurred directly over a river feeding Shasta reservoir, the largest potable water reservoir in California. One of the cars contained a toxic pesticide, which spilled into the river and reached Shasta reservoir within 48 hours. Fortunately, the pesticide was short-lived, and rapid response permitted swift degradation of the pesticide to harmless constituents. This event is significant due to the interaction of the railroad and water supply lifelines, illustrating the potential for major disruption of potable water. Highway, railroads, and pipeline lifelines traversing pathways capable of draining into reservoirs are sources of potential lifeline interactions, and major consequences. This aspect is currently under study in the central United States[8].

1991 East Bay Hills Fire

On October 20, 1991, one of the largest fires in U.S. history occurred in Oakland and Berkeley, California, destroying approximately 2,700 homes and 440 apartment units, and resulting in at least 25 fatalities. A total of approximately 1,800 acres (2.8 square miles) were devastated, although the fire was only unchecked for about 8 hours (see Figure 2).

The Oakland fire is significant in its effects on lifelines. Due to the hilly terrain, water supply is from ridge-top tanks of limited volume, resupplied almost daily from lower pump stations. These tanks were drained early in the fire, due to both firefighting demands and more importantly, breakage of service connections in structures collapsing in the fire. Another important aspect was the interaction of electric power and water supply-early in the fire, overhead electric supply lines were destroyed by the fire, so pump stations lost all power and could not resupply the tanks. Analyses for the water utility indicates that loss of power was not a critical issue, since pump capacity would have been insufficient in any case[9].

Other lifeline interaction problems that exacerbated the situation included transportation and communications. Because the fire imperilled the Chabot Canyon/Caldecott Tunnel area from all sides, Highways 24 and 13 had to be closed early in the incident. This resulted in traffic jams and impeded access for arriving strike teams. Compounding this situation was the necessary curtailment of service by the Bay Area Rapid Transit (BART), the major commuter system for the area, which utilizes the median of Highway 24. The fire area was also the site of a major substation and several high-voltage transmission lines, which were shut down due to contamination of the power lines by smoke and soot from the fire. Saturation of the telephone lines and emergency radio frequencies was also a major

problem, impeding both emergency operations as well as attempts by the public to contact friends and relatives[10].

1992 Hurricanes Andrew and Iniki

In August and September 1992, the United States sustained two of the largest hurricanes in its history- first Andrew, which caused the highest property losses in history in the south Miami, Florida, area, followed by Iniki, which devastated the island of Kauai, Hawaii. In both cases, property loss was dominated by residential damage, but significant lifeline impacts occurred. These included:

a. Widespread loss of electric power, due to downing of overhead electric distribution lines and failure of the supporting pole structures. Five weeks later (as of this writing), most residents remain without power[11]

b. similar but less widespread loss of telephone service, since telephone lines were often carried on the same pole structures. Five weeks later, half of Kauai's telephones were still out of service (*ibid*).

c. In Florida (and to some extent in Kauai), widespread loss of water service, due primarily to loss of electric power for pumps (the flat terrain in Florida results in widespread use of elevated tanks for water supply, while Kauai's water is generally from wells).

d. Major road passability difficulties for the first several days, due again to downed power poles.

In summary, significant lifeline interactions occurred in both storms, due primarily to widespread downing of power poles, which caused widespread loss of water service, widespread and extended loss of telephone service, and short-term roadway problems.

ANALYSIS AND APPLICATION

The foregoing summary provides a number of occurrences of lifeline interaction, both in earthquakes and in other disasters which provide analogous data for potential earthquakes. These occurrences can be categorized into three types:

TYPE ONE, CROSS-IMPACT: defined as the impact on one lifeline's function due to impairment of service to that lifeline by a second lifeline. Cross-impacts can occur at great distances. An example is reduction in water service due to loss of power.

TYPE TWO, COLLOCATION: defined as direct damage or impact on one lifeline's function due to failure of another lifeline in a very proximate location. An example is failure of a pipeline crossing a bridge, when the bridge collapses due to an earthquake. Strictly speaking, collocation simply means located at the same spot or having a similar alignment, but can be employed to identify this type of interaction.

TYPE THREE, CASCADE: defined as increasing impacts on a lifeline due to initial inadequacies. An example is increasing degradation of water service in a conflagration due to service connections breaking as structures collapse as the conflagration grows.

That is, as the conflagration increases in size, more and more structures burn and collapse, resulting in more and more broken services, resulting in greater and greater pressure loss in the water service, further impairing water supply and leading to further growth in the conflagration. The cycle then repeats itself. A similar phenomenon can be hypothesized for road transport in a conflagration.

A *qualitative* tabulation of Type One lifeline cross-impacts has been compiled by Nojima and Kameda, Figure 3, which captures many of the occurrences discussed above. Similar to Figure 3, a *quantitative* tabulation of lifeline interactions can be constructed, such that:

$$D_f = [L]\, D_i \qquad (1)$$

where D_f is a vector of *final* functional states, given lifeline interactions,

Di is a vector of initial lifeline functional states, without consideration of lifeline interactions, and

[L] is a matrix quantifying lifeline interactions

The [L] matrix is actually a supply matrix, quantifying in each cell per row the fraction of that row's corresponding lifeline, which is furnished by the lifeline corresponding to the column.

Considering only water and power, we have seen water functionality significantly impacted due to loss of power, in the incidents described in the preceding section. This can be modeled as,

$$Df = [L]\, Di = \begin{bmatrix} 0.83 \\ 0.2 \end{bmatrix} = \begin{bmatrix} 0.9 & 0.1 \\ 0.0 & 1.0 \end{bmatrix} \begin{bmatrix} 0.9 \\ 0.2 \end{bmatrix} \begin{matrix} \text{Water} \\ \text{Electric} \end{matrix}$$

which simply captures the Type One Cross-Impact phenomenon, showing that although water had low initial impacts, major loss of electric power resulted in significantly larger final impacts than initial considerations would have indicated. In this, the [L] matrix indicates that 90% of water supply is due to the function of the water system (i.e., gravity flow) and 10% is related to electric power (e.g., power for pumps).

A simple example illustrates the significance of quantifying these factors. A model has been previously developed for post-earthquake conflagration in San Francisco, which accounts for degraded water supply[12]. Using considerations as outlined above, with realistically hypothesized interaction factors, the model was used to examine the additional degradation to water supply, that might result from lifeline interactions, and the resulting final water supply state and impacts on the final burnt area. Figure 4 shows that the impacts vary, with major impacts in the high conflagration prone areas, and moderate to nil impacts in the lower density portions of the city. The implication is that greater reliability of water supply is required in the higher value districts-a lesson San Francisco drew from the 1906 earthquake and fire, following which the city constructed a redundant water supply system. Other cities, however, have not followed this example.

ACKNOWLEDGEMENTS

This work is supported by a grant from the National Center for Earthquake Engineering Research, SUNY-Buffalo, which is gratefully acknowledged.

REFERENCES

1. Nojima, N., and Kameda H. (1991) Cross-Impact Analysis for Lifeline Interaction, Proc. 3rd U.S. Conf. Lifeline Earthquake Engg., TCLEE/ASCE, Los Angeles.

2. Kameda, H., and Shinozuka, M. (1990) Urban Lifeline Systems - Its Vulnerability and Reconstruction Following Earthquakes, UEHR Report No. 4, Urban Earthquake Hazard Research Center, Disaster Prevention Research Institute, Kyoto University, Kyoto 911, Japan.

3. National Transportation Safety Board Railroad Accident Report NTBS/RAR-90/02 (PB90-916302), June 19, 1990.

4. FEMA (1992) Collocation Impacts on the Vulnerability of Lifelines During Earthquakes with Applications to the Cajon Pass, California, FEMA 226.

5. Khater, M. et al (1990) Lifeline Performance During the October 17, 1989 Loma Prieta Earthquake, Proc. 1990 UJNR Panel on Natural Hazards, Natl. Inst. Standards and Technology, Gaithersburg MD.

6. Kameda, H. et al (1990) Effects of the 1989 Loma Prieta Earthquake on the Bay Area Transportation Systems, 8th Japan Earthquake Engg. Symposium, Tokyo.

7. Isenberg, J., Phipps, M.T., and Scawthorn, C. (1990) Watsonville Regional Study: Interaction among Damaged Lifelines, Proc. of *Putting the Pieces Together*, presented by BAREPP and FEMA, Hyatt Regency San Francisco Airport, pp. 119-128.

8. Eguchi, R.T. et al (1992) An Assessment of Environmental Costs Associated with Crude Oil Pipeline Damage Caused by Earthquakes, Proc. Lifeline Earthquake Engg. in the Central and Eastern U.S., D. Ballantyne, ed., ASCE, New York.

9. EBMUD (1992) East Bay Hills Firestorm Response Assessment, Phase I Final Report, prepared for the East Bay Municipal Utility District by VSP Associates et al., Sacramento, CA 95825.

10. Scawthorn, C., Blackburn, F., and Friedman, L.R. (1991) "Fire in the East Bay Hills," article in *EQE Review*, Fall Issue, EQE International, San Francisco, CA 94104.

11. San Francisco Examiner, October 18, 1992, p. A-4.

12. Scawthorn, C. (1987) Fire Following Earthquake, All-Industry Research Advisory Council, Oak Brook, IL.

	electric power supply	gas supply	water supply	sewage disposal	transportation		telephone
					road traffic	urban railway	
electric power supply	*	Santa Cruz: gas explosion due to electricity comback (spark ignition) recovery work arrangement with electric power supply system	Santa Cruz: pump stopped for 18hrs (gravitative flow area survived: no water in pump-based supply area) S.F.: power failure due to gas leak inspection, no water in pump-based supply area and Marina district no power for repair work EBMUD: short-term loss of power at Lafayette filtration plant, Oakland Control Center power loss, no service	S.F. and Santa Cruz: power failure at pump station	S.F. and Santa Cruz: traffic jam due to malfunction of traffic signal	S.F.: BART omitted stops at some stations to save electricity	capacity diminished due to use of storage cell PBX with no battery, malfunction Pacific Bell: Bush/Pine Office(S.F.) coolant trouble no service for 3 hrs Hollister Office generator failure no service for 3 hrs GTE: Menlo Bello Office (Los Gatos) failure of fuel tank of generator malfunction(6-7hrs)
gas supply	S.F. & Santa cruz: gas leak inspection before recovering electricity	*	Santa Cruz: no home treatment recovery work arrangement with gas supply system		S.F.: road closed due to propane fire (Rte. 80 VB Central Ave.)		
water supply		Santa Cruz: recovery work arrangement with water supply system	*	Santa Cruz: damage detection by analogy	S.F.: road failure due to water leakage (Marina District)		
sewage displsal			Santa Cruz: suspection of underground water contamination due to outflow of crude sewage from pipeline	*			
road traffic			Santa Cruz: no transporting machinery due to damage to bridge	Santa Cruz: damage detection by analogy	*	BART riders increased due to Bay Br. closure (Oct.23 : +40%)	
urban railway						*	
telephone			S.F. and Santa Cruz: overload				*

Figure 1: Lifeline Interactions in the Loma Prieta earthquake (after Nojima and Kameda 1991).

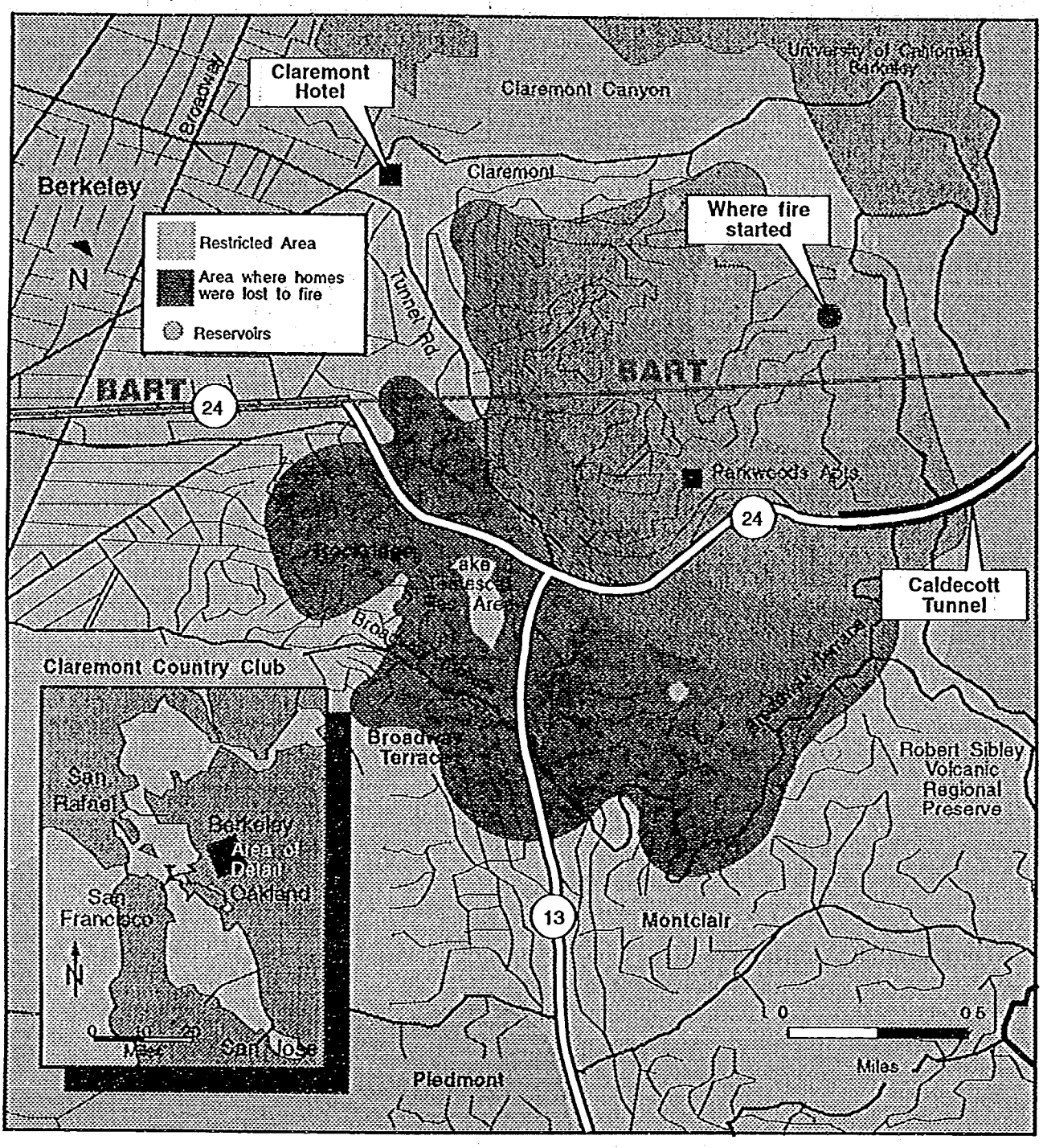


Figure 2: Area affected by East Bay Hills Fire.

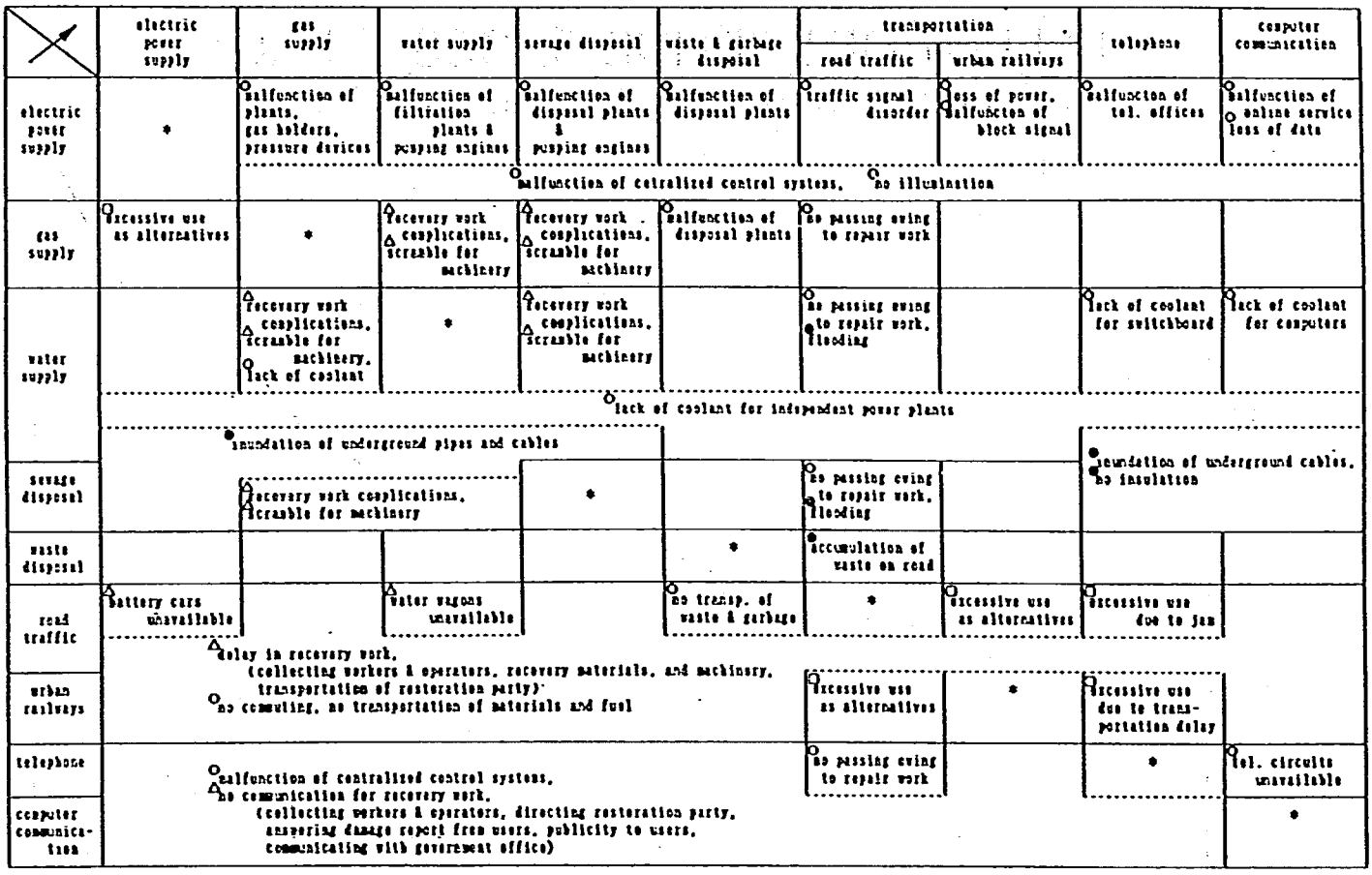


Figure 3: Lifeline Interaction, Qualitative Aspects (after Nojima and Kameda 1991).

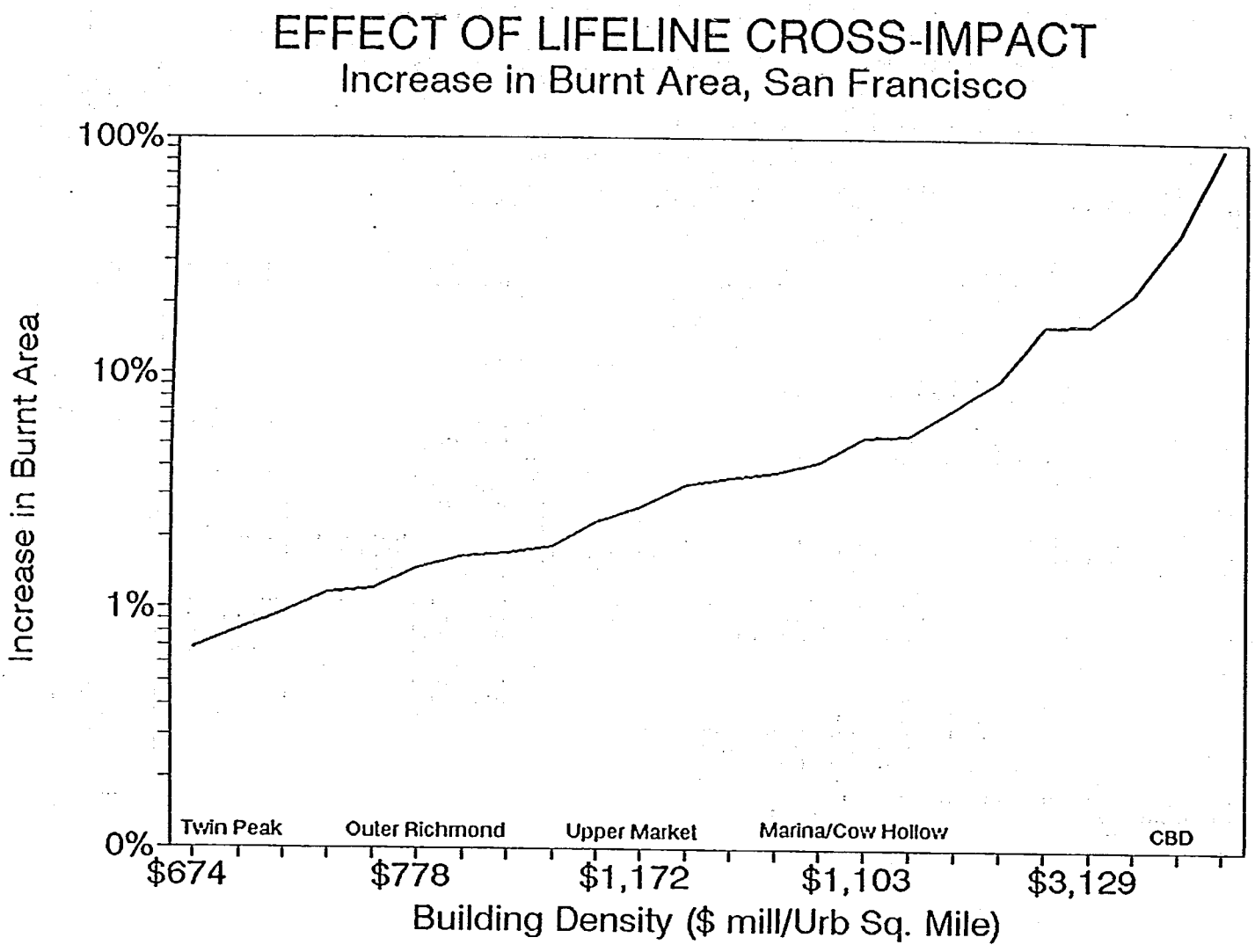


Figure 4: Impacts of Cross-Impacted Water Supply on Final Burnt Area, City of San Francisco.

PROPOSED PLAN FOR DEVELOPING AND ADOPTING SEISMIC GUIDELINES AND STANDARDS FOR LIFELINES

by

Riley M. Chung, Leader
Earthquake Engineering Group
Structures Division
BFRL/NIST

CONGRESSIONAL MANDATE

The plan is prepared in response to Public Law 101-614, The National Earthquake Hazards Reduction Program Reauthorization Act, 1990.

LIFELINE SYSTEMS TO BE CONSIDERED

- Electric Power
- Gas and Liquid Fuels
- Telecommunications
- Transportation
- Water Supply and Sewers

OBJECTIVES

- Establish performance criteria that must be achieved in construction, maintenance, and operation of existing and proposed lifeline systems

- Provide a basis for technical specifications for use by buyers and sellers of lifeline products and services to reduce the vulnerability of lifeline systems to earthquakes

- Provide a reliable basis for regulations to protect the public health, safety, and welfare

BASIS FOR THE PLAN'S DEVELOPMENT

- Workshop on Developing and Adopting Seismic Design and Construction Standards for Lifelines, September 25-27, 1991, Denver, Colorado

- Review Comments by NEHRP's Advisory Committee

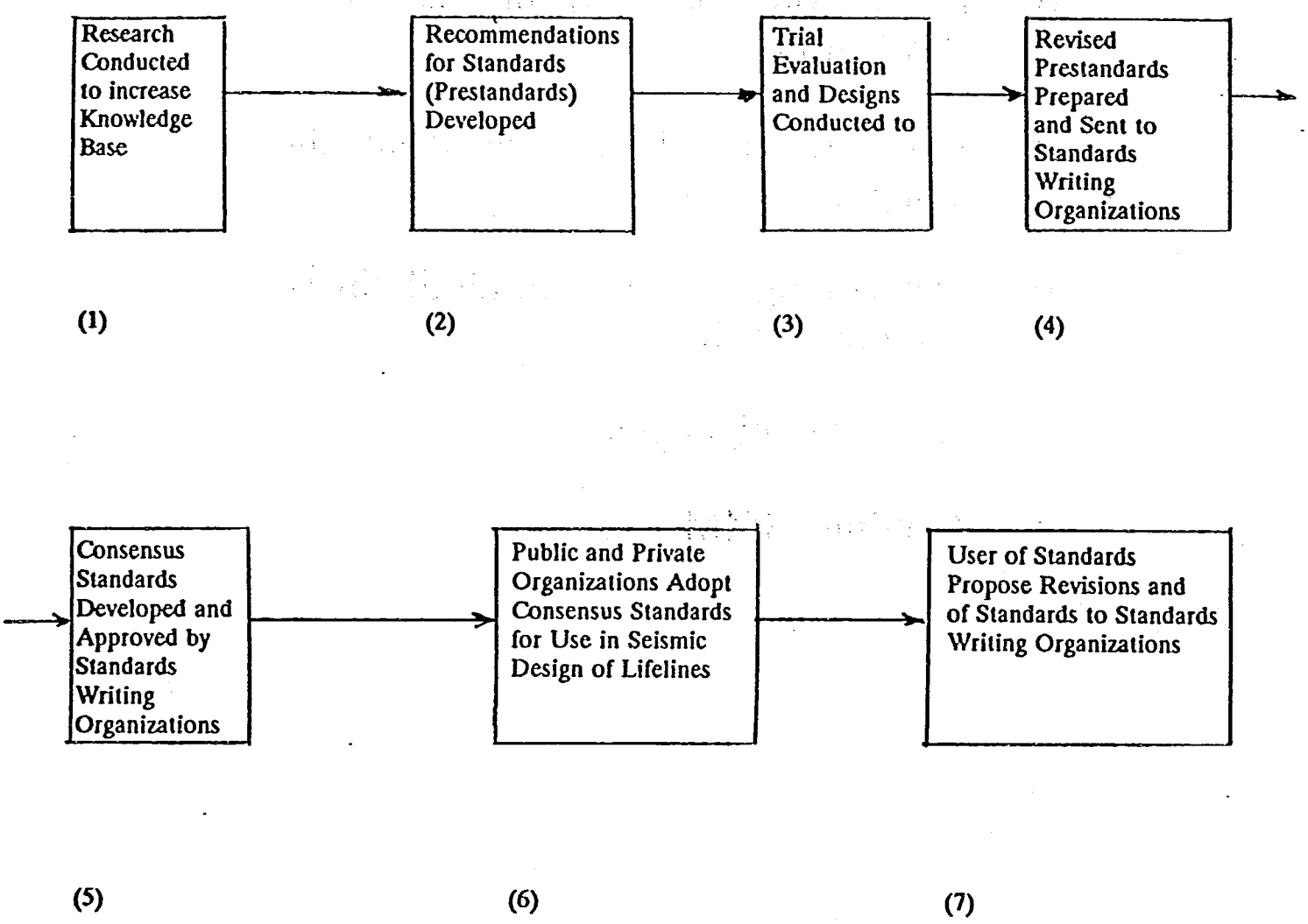
ALTERNATIVES FOR GUIDELINES AND STANDARDS DEVELOPMENT

- A Detailed Approach
- A Pragmatic Approach

A DETAILED APPROACH

- Based on input from the 1991 Workshop
- Full support of funding from the Congress
- Developing standards in all lifelines simultaneously
- Duration: eight years
- Funding: $54M

Figure 4.1 Detailed Approach: Activities in the Development and Implementation of Lifeline Seismic Standards



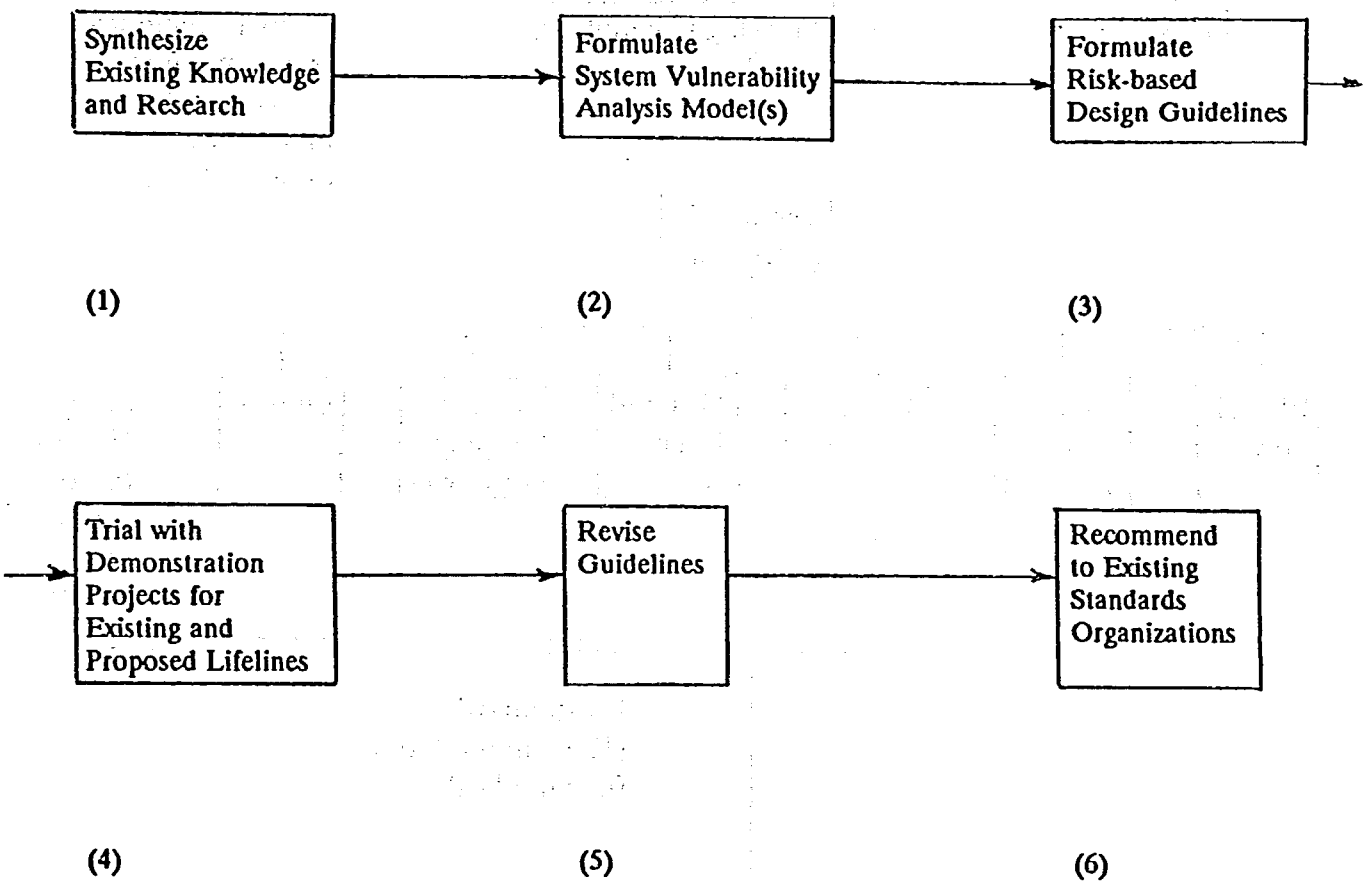
A PRAGMATIC APPROACH

- o Recognizing current fiscal constraints
- o Focusing initially on the highest priority types of lifeline systems
- o Focusing on earlier realization of benefits to the public
- o Duration: eight to ten years
- o Funding:
  - vary depending on the stage of the project
  - beginning with $3M per year and reviewed annually

ELEMENTS IN THE PRAGMATIC APPROACH

- Policy statement/Strategy
- Strong leadership through FEMA, NIST, LSPS, and CCLSS
- DEMONSTRATION PROJECTS
- Implementation

Figure 4.3 Pragmatic Approach: Activities in the Development and Implementation of Lifeline Seismic Guidelines and Standards for Each Lifeline Type



Prestandardization

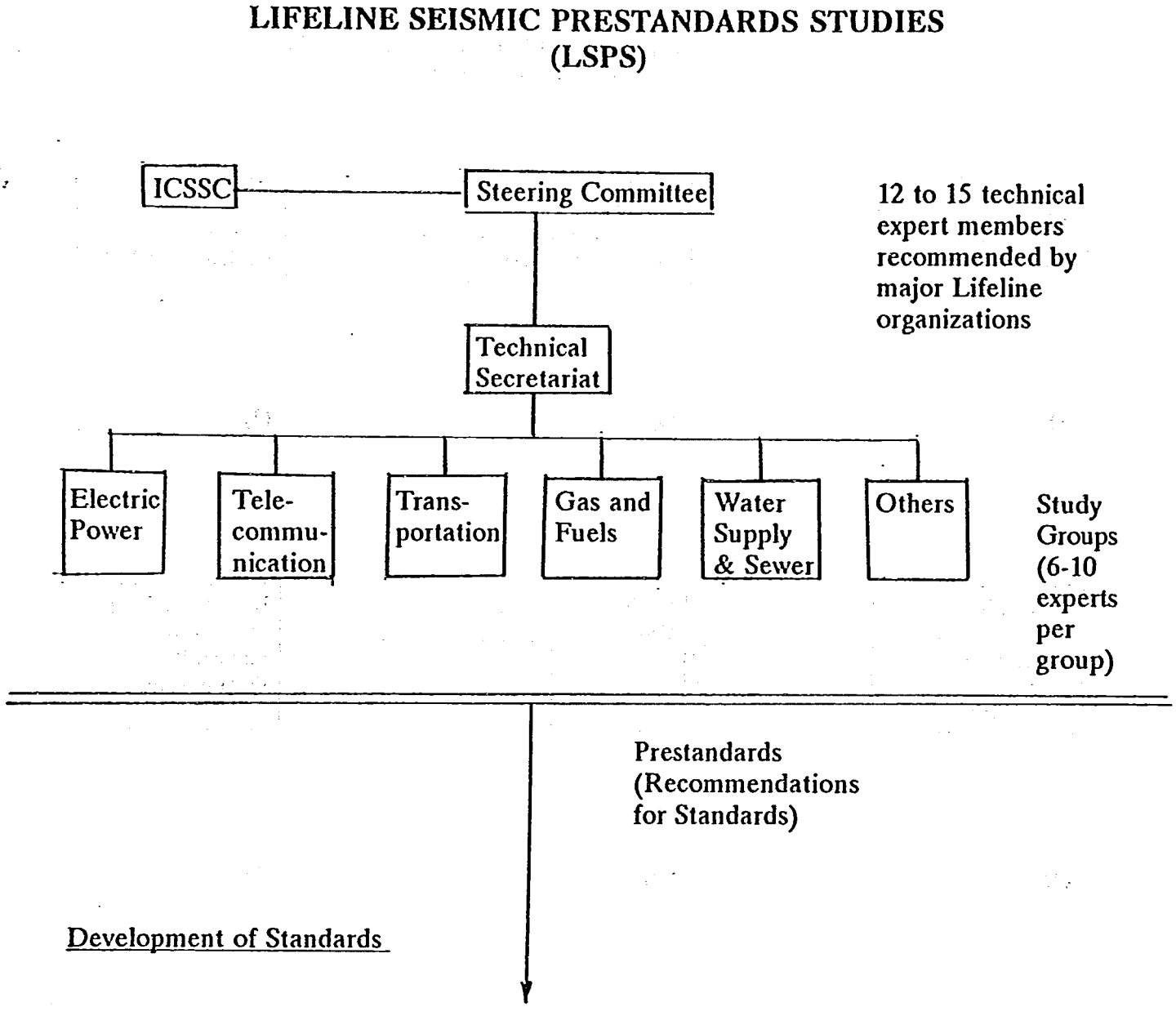


Figure 5.1 Organization Chart for Developing and Adopting Seismic Guidelines and Standards for Lifelines

MAJOR FUNCTIONS OF LSPS

- Address needs and issues of all lifeline systems
- Develop a prioritized overall program plan
- Select demonstration projects
- guide the operation of the Technical Secretariat and the technical studies by the Study Groups

MAJOR FUNCTIONS OF CCLSS

- Support the development and adoption of national voluntary consensus standards for lifelines

- Serve as an independent and authoritative focal point and primary resources for establishing broad representation for voluntary coordination of private standards developments

- Encourage lifeline industries and associated manufacturers, associations, and professionals to consider earthquakes and their impact in planning, design, construction, and operation of lifeline systems

- Develop recommendations, including priorities, for lifeline safety design and construction standards development, research, and implementation activities.

Session-9

Observation and Seismic Monitoring

J-17) Seismic Behavior of Beried Pipelines Through Field Observation
(Kawashima, K., Sugita, H. and Nakajima, T.)

J-18) Seismic Monitering and System Control for Lifelines
(Takada, S., Fuke, T. and Ueno, J.)

U-12) Monitoring, Instrumentation and Innovative Devices for Lifeline Systems
(Ballantyne, D.)

U-13) Vulnerability of Fiber Optics Cables to Fault Rupture, A Proposed Field Experiment
(Wong, F.S. and Isenberg, J.)

SEISMIC BEHAVIOR OF BERIED PIPELINES THROUGH FIELD OBSERVATION

By Kazuhiko KAWASHIMA[1], Hideki SUGITA[2] and Tomoru NAKAJIMA[2]

ABSTRACT

This paper presents seismic response characteristics of embedded pipes based on field measurements. Strains induced in steel pipe and ductile pipes with expansion joints are studied. Special attention is placed for effect of bends on pipe response. Soil springs which are important in seismic design by means of the seismic deformation method is also studied based on the measured data.

INTRODUCTION

Seismic design of embedded pipes is generally made by the seismic deformation method[4)] in which embedded pipes are assumed to respond in accordance with strain induced in ground during earthquakes. Pipes are considered to be beams elastically supported by soils when the stiffness of the soil is modelled by springs. Although the seismic deformation method has been adopted for seismic design of embedded lifeline facilities, measured data available for evaluation pipe response during earthquakes is very limited. Strong motion observation was initiated for measuring pipe response, because precise evaluating of pipe response in ground is essential for improving seismic design method. Special attention was paid to obtain response data for pipe with bends and expansion joints.

This paper presents an analysis of the measured data of pipe response, and soil spring stiffness to be used in the seismic deformation method is also presented.

---

1 Head, Earthquake Engineering Division, Public Works Research Institute, Ministry of Construction, Tsukuba Science City, Japan

2 Research Engineer, ditto

OBSERVATION SYSTEMS

Fig.1 and Photo 1,2 shows the observation systems placed at Sodegaura city, about 50 km east of Tokyo, for measuring seismic behavior of embedded pipes. Continuous steel pipe with a diameter of 15 cm and ductile pipes with diameters of 15 cm and 30 cm are embedded 1 m below the ground surface as shown in Photo 3-7. The length of the continuous steel pipe is 120 m and there is a bend at 20 m from the right end. The length of one element of the ductile pipe is 5 m in the 15 cm diameter pipe and 6 m in the 30 cm diameter pipe. They were jointed together by expansion joints which are capable of absorbing a relative deformation of ± 10 % of pipe length in the axial direction and a rotation of ± 6 degrees. Stoppers for preventing excessive pulling-out are provided at the expansion joints.

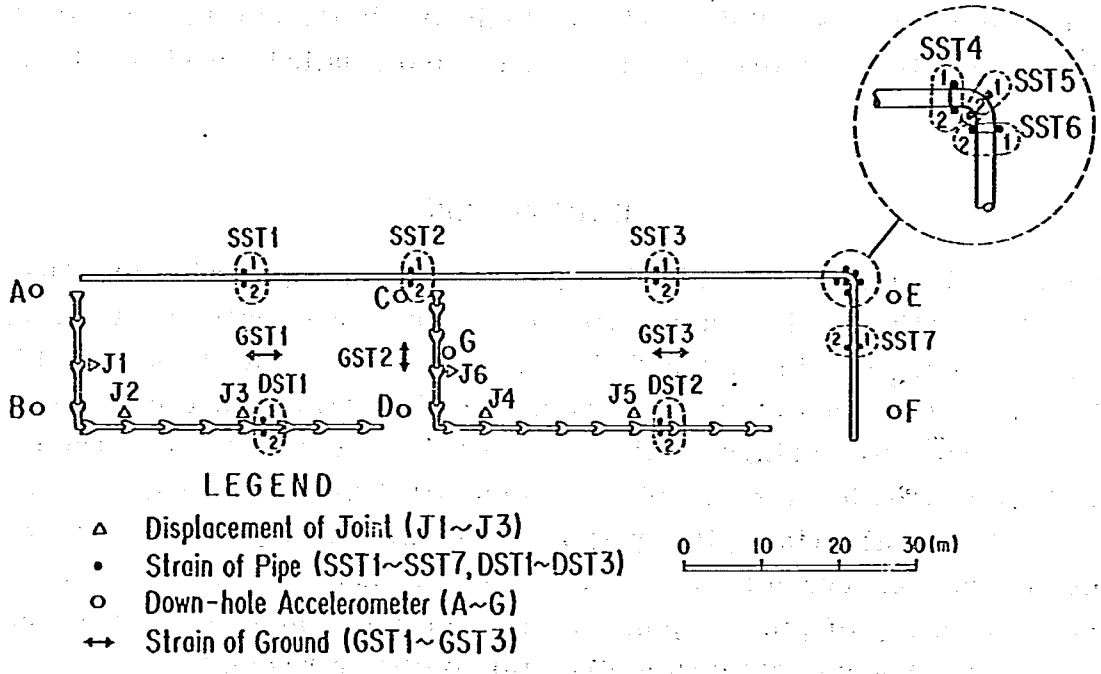


Figure 1. Observation Systems

Dense instrumentation is made to measure the pipe response. The strain induced in the steel and ductile pipes as well as relative displacements developed between two adjacent ductile pipe sections were measured. Strain gauges with coating against water are placed on the both sides of the pipes so that the flexural strain as well as the axial strain could be detected.

The ground acceleration and ground strain were measured. Three-components down-hole accelerometers were installed at six points to measure ground acceleration. The measured data was used to compute the averaged ground

strain induced at the site. Special devices were installed 1 m below the ground surface to directly measure ground strain. The devices consist of two 80 cm diameter circular plates and a 6 cm diameter double tubed steel rod. The circular plates were connected to the double tubed steel rod.

Movement of the circular steel plates in accordance with soils vibration during earthquakes would develop small relative displacements between the two circular plates. Ground strain may be evaluated by dividing the relative displacement by the length of the double tubed steel rod. This device has been successfully used for measuring ground strain at several observation sites1)3).

All the measured signals are digitized with an interval of 1/100 second and recorded with a digital acquisition systems. Pre-event memory of about 10 seconds are provided to get full records from their start.

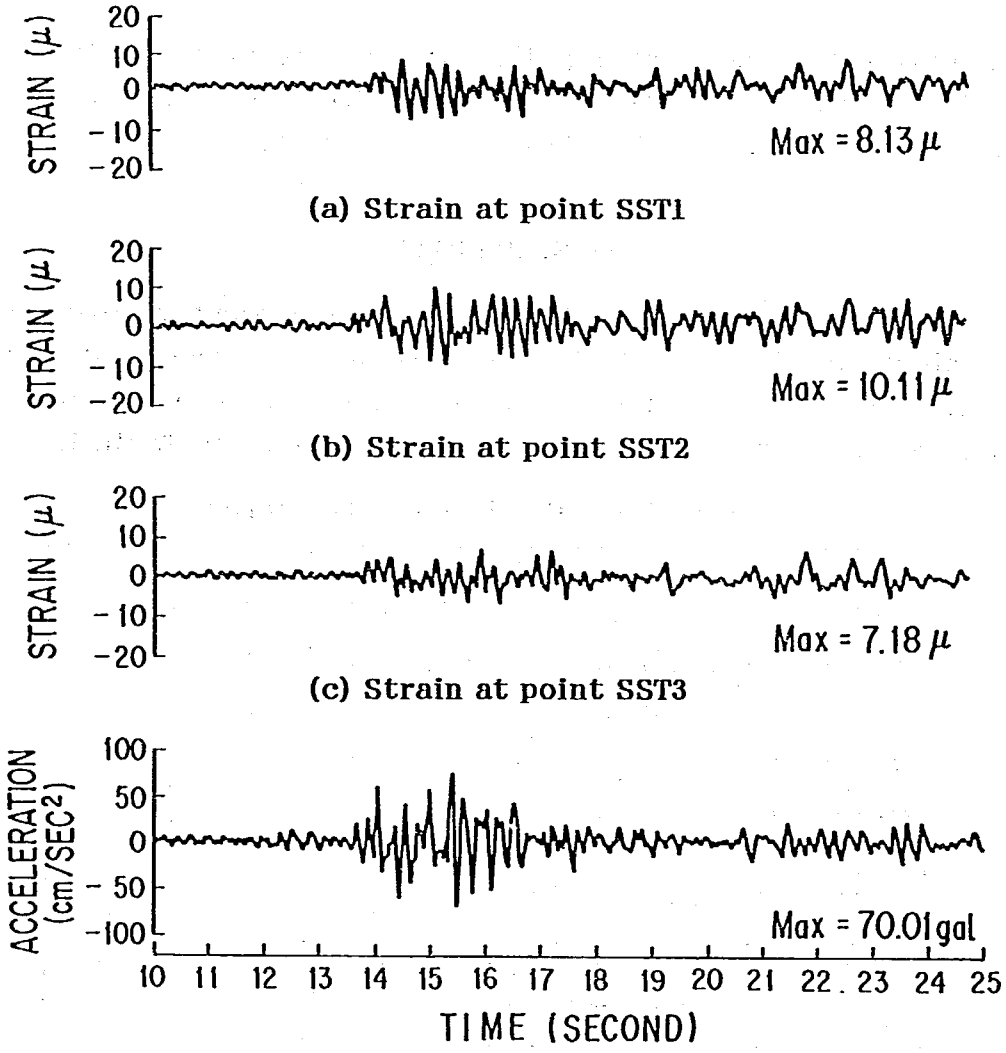
MEASURED DATA

Observation was initiated in January 1989 and many records have been already obtained. In this report the pipe response was analyzed based on the measured data obtained after October 1989. Record which are large enough for analysis were measured by thirteen earthquakes as shown in Table 1.

Table 1. Major Earthquakes Triggered

NO. OF EQ.	DATE	EPICENTER			MAGNITUDE (M)	FOCAL DEPTH (km)
		EPICENTRAL REGION	LONGITUDE	LATITUDE		
EQ-1	1989. 10. 14	NEAR IZU-OHSHIMA	135° 03'	34° 54'	5.7	25
EQ-2	1990. 6. 1	EAST OF CHIBA-KEN	140° 40'	35° 38'	6.0	70
EQ-3	1990. 6. 5	MIDDLE OF KANAGAWA-KEN	139° 20'	35° 50'	5.3	120
EQ-4	1990. 6. 27	SAGAMI-BAY	139° 07'	35° 00'	5.4	148
EQ-5	1990. 8. 23	MIDDLE OF CHIBA-KEN	140° 24'	35° 21'	5.4	50
EQ-6	1990. 8. 23	MIDDLE OF CHIBA-KEN	140° 24'	35° 21'	5.2	49
EQ-7	1990. 12. 11	MIDDLE OF CHIBA-KEN	140° 19'	35° 19'	4.0	35
EQ-8	1990. 12. 16	MIDDLE OF CHIBA-KEN	140° 13'	35° 37'	4.6	77
EQ-9	1991. 6. 28	TOKYO-BAY	139° 52'	35° 29'	4.6	68
EQ-10	1991. 7. 14	EAST OF NAGANO-KEN	138° 31'	36° 25'	5.4	187
EQ-11	1991. 9. 29	NORTH OF CHIBA-KEN	140° 06'	35° 45'	4.9	80
EQ-12	1991. 11. 19	TOKYO-BAY	140° 02'	35° 36'	4.9	81
EQ-13	1992. 2. 2	TOKYO-BAY	139° 08'	35° 20'	5.7	90

Fig. 2 shows the measured axial strain induced in the steel pipe and ground accelerations developed by an earthquake with epicentral distance of 75 km and an earthquake magnitude of 5.7. This earthquake is designated hereinafter as EQ 3 earthquake. The peak ground acceleration was about 65 to 70 cm/sec^2 and the peak pipe strain was about 7.2 to 10.1 μ. It is interesting to note in Fig. 2 that although there are many similarities of the pipe strains between the three locations, the pipe strain are considerably different each other. This clearly shows that the pipe response in axial direction depends considerably on the response of nearby soil.



(a) Strain at point SST1

(b) Strain at point SST2

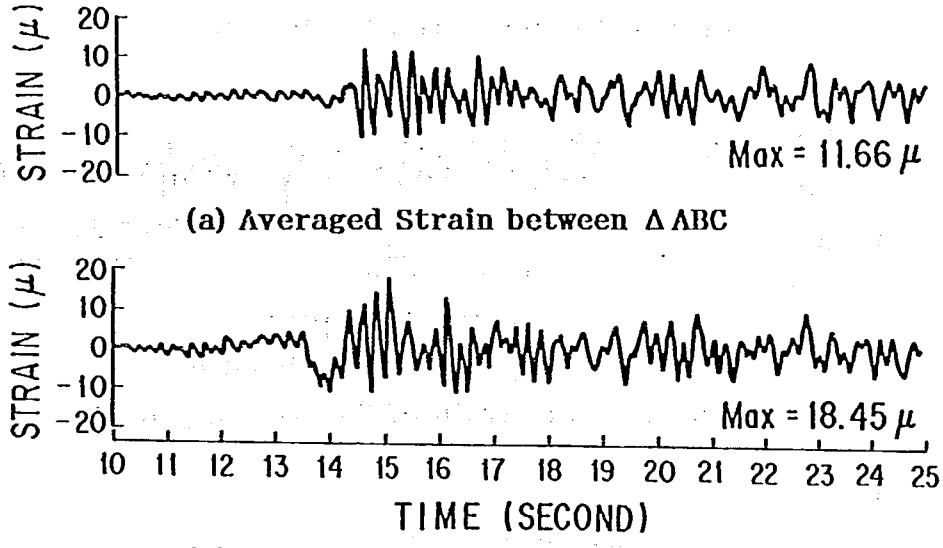
(c) Strain at point SST3

(d) Acceleration at point C

Figure 2. Measured Axial Strain of Steel Pipe and Ground Acceleration C Point during EQ 13

Because the ground motion was small, the devices for measuring ground strain did not directly detect ground strain. Fig. 3 shows ground strains

computed for the EQ 13 earthquake from measured ground accelerations. The measured ground accelerations were double integrated to obtain the ground displacements[7]. Assuming triangular elements such as Δ ABC and Δ BCD, the ground strain along pipe axis was computed with use of the standard finite element method[5]. Linear interpolation function for displacements was assumed in each finite element. If the ground strain computed for Δ ABC, which is the averaged ground strain between points A and C, is compared with the axial pipe strain at point SST1, in Fig. 2, it is found that the strains obtained are quite similar.



(a) Averaged Strain between Δ ABC

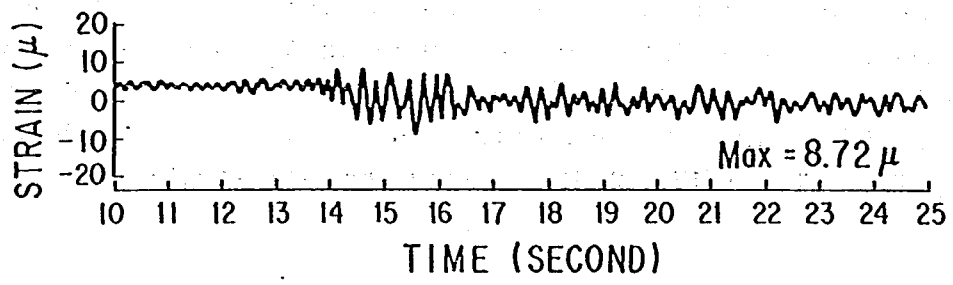
(b) Averaged Strain between Δ BCD

Figure 3. Ground Strain Computed for EQ 13 from Measured Ground Acceleration

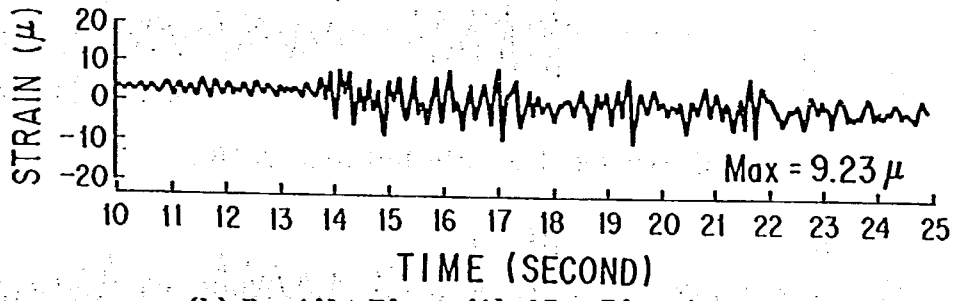
Fig. 4 shows axial strain induced during the EQ 13 earthquake in the ductile pipes. Almost no relative displacement was developed at the joints. It is interesting to note that the strain of the ductile pipe at the point DST-1 is quite similar with the strain of the steel pipe at the point SST-1. The strain of the ductile pipe is not necessarily smaller than the strain of the steel pipe. This implies that reduction of axial force induced in the ductile pipe due to the expansion joints was quite small during the EQ 13. The forces developed at the expansion joints during the EQ 13 were so small that friction at the expansion joints prevented slippage to occur between the adjacent pipe sections.

Fig. 5 shows a distribution of peak strain along the steel pipe for the EQ 13 earthquake. Both axial and flexural strains are presented. It should be noted that although axial strain is predominant in the straight section, flexural

strain becomes larger than the axial strain at the bends. Flexural strain has to be therefore taken into account in seismic design of pipes at bend sections.

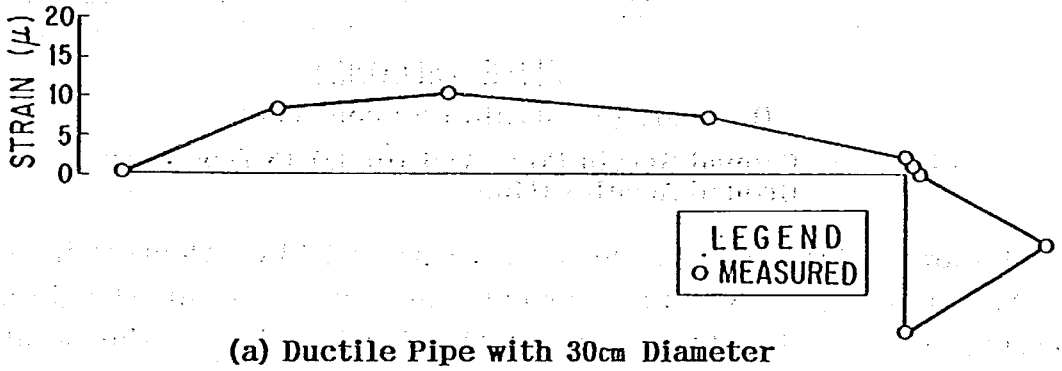


(a) Ductile Pipe with 30cm Diameter

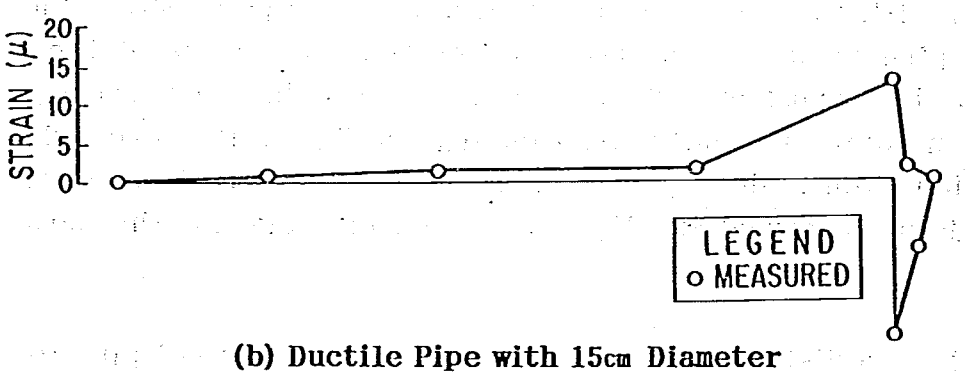


(b) Ductile Pipe with 15cm Diameter

Figure 4. Measured Axial Strain of Ductile Pipe during EQ13



(a) Ductile Pipe with 30cm Diameter



(b) Ductile Pipe with 15cm Diameter

Figure 5. Peak Strain of Steel Pipe during EQ 13

Fig. 6 shows the axial strain of steel pipe vs. peak ground acceleration relation for the data obtained by the eight earthquakes presented in Table 1. Although number of the data obtained is still small, clear correlation between the pipe strain and the peak ground acceleration is observed. By increasing the number of data, this is expected to provide a practical estimation for the pipe strain induced during earthquakes.

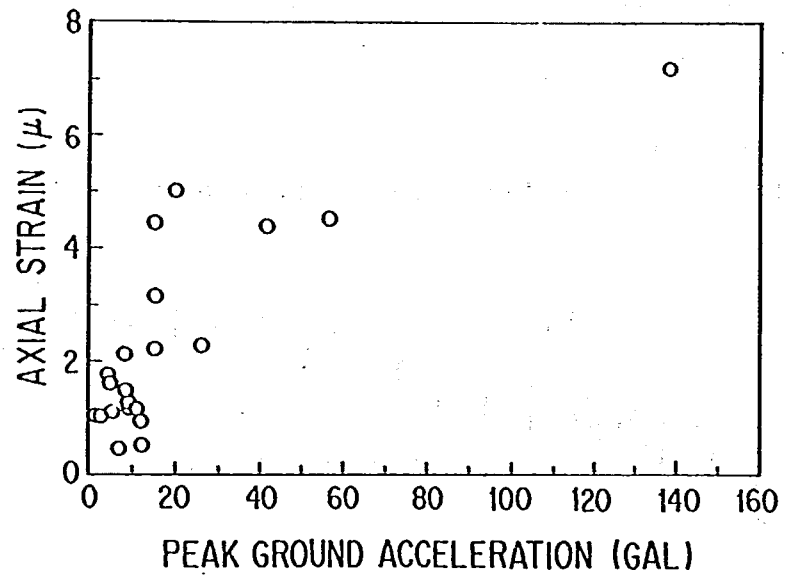


Figure 6. Axial Strain of Steel Pipe vs. Peak Ground Acceleration Relation

EVALUATION OF SOIL SPRING STIFFNESS

An analytical model presented in Fig. 7 is often adopted to estimate dynamic response analysis of embedded pipes[6]. The pipe is idealized by a beam elastically supported by springs which represent pipe -soil interaction. Soil response is computed by prescribing the input ground motion at the base rock.

In the analytical model presented in Fig. 7, it is essential to determine the stiffness of the soil springs which elastically support correctly the pipe. Various methods have been proposed from analytical and experimental studies to estimate the soil springs. However due to limitation of measured data available for estimating soil springs based on measured seismic response data of pipes, few studies have been made for soil springs. Therefore, with use of the analytical model presented in Fig. 7, the soil springs stiffness were studied.

The response displacements of soils which were estimated from the measured accelerations were used for computing the pipe responses. The steel pipe was

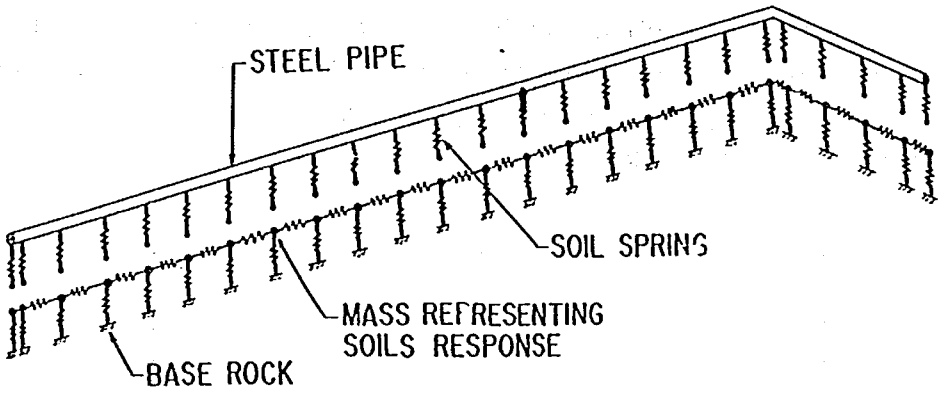


Figure 7. Analytical Model for Dynamic Response Analysis of Embedded Pipes

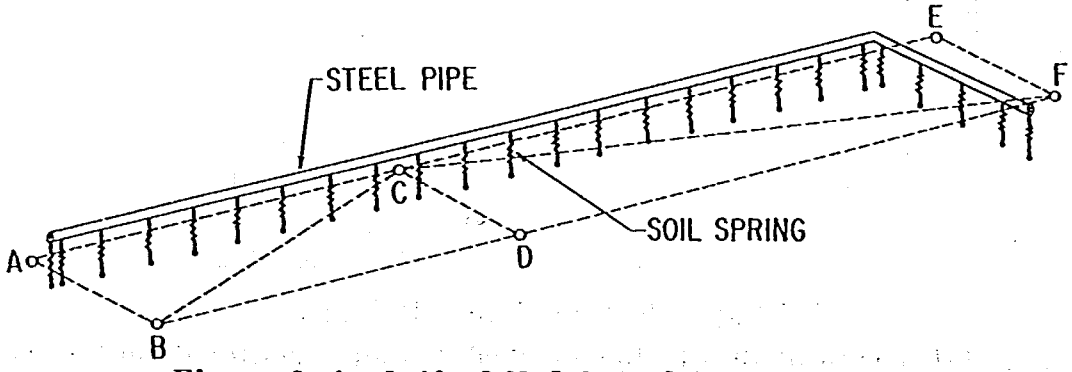


Figure 8. Analytical Model Used for Pipe Response

idealized by a discrete analytical model with 24 beam elements as shown in Fig. 8. Because the displacements which were computed from the measured accelerations were available at only six points, the displacements at each nodal point of the analytical model were computed from either linear interpolation or extrapolation of the displacements from the six points.

In the Design Specifications of Petroleum Pipelines[2], the soil spring stiffness is stipulated to be estimated as

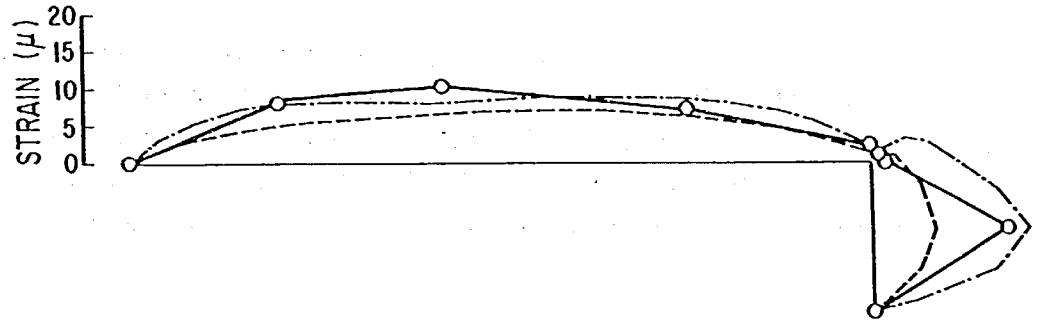
$$K = c \times G_s \tag{1}$$

where K : stiffness of soil spring per unit length, c : a coefficient, and Gs : shear moduli of soils. The shear moduli of soils are estimated as

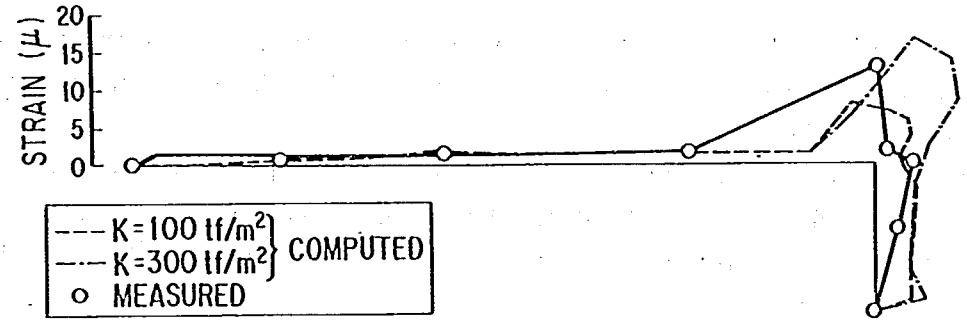
$$G_s = \gamma_t \times V_s^2 / g \tag{2}$$

where γ_t : unit weight of soils, V_s : shear wave velocity of soils, and g : acceleration of gravity. In the specifications the coefficient c is stipulated to be determined by appropriate tests, and a value of 3.0 is recommended when such test data is not available.

The soil spring which gives realistic estimation for the measured pipe strain was therefore studied. Fig. 9 shows the approximation of the computed pipe strain assuming a soil spring stiffness of 100 tf/m^2 and 300 tf/m^2. The computed axial and flexural strain approximates quite well the measured pipe strain. Because shear wave velocity which was measured at three points in the observation site was about 150 m/sec at the depth between the ground surface and 15 meters below the ground surface, the soil spring stiffness of 100tf/m^2 and 300tf/m^2 are predicted by assuming a coefficient "c" of about 0.05 and 0.16 respectively in Eq.(1). From such evidence it may be said that the recommended value of 3.0 for the coefficient "c" in Eq.(1) is excessively conservative. It is important to precisely study the coefficient "c" which gives a realistic soil spring stiffness.



(a) Axial Strain



(b) Flexural Strain

Figure 9. Best Correlation of Pipe Strain for EQ 13 CONCLUSIONS

For accumulating actual seismic behavior of embedded pipes during earthquakes, seismic observation of two types of pipes was initiated. Based on the analyses of the measured data on the strain of embedded pipes, the following conclusions may be deduced:

1) Although axial strain was predominant in the straight section, flexural

strain is more predominant than axial strain at the bend section of the pipe. Flexural strain should be considered in seismic design at bend sections.

2) Considerably good correlation was observed between the measured axial strain of the pipe and the peak ground acceleration. Accumulation of measured data is expected to provide a realistic estimation method for the pipe strain based on the peak ground acceleration.

3) The computed pipe strain assuming Eqs.(1) and (2) was excessively larger than the measured pipe strain. It is thought that the spring stiffness predicted by Eq.(1) assuming the coefficient "c" of 3.0 is too conservative. Coefficient "c" has to be precisely studied by analyzing more measured data.

FUTURE DIRECTIONS

Accumulation of measured data is required for providing a realistic estimation method for the pipe strain based on the peak ground acceleration, and for studying the coefficient "c" which gives a realistic soil spring stiffness. Because the observation site is located at one of the highest seismicity area in Japan, it is anticipated to have a number of mesuared data in a short time.

REFERENCES

1) Iawamoto, T.et.al.: Observation of Dynamic Behavior of Buried Pipelines during Earthquakes, Eighth World Conference on Earthquake Engineering, San Francisco, U.S.A., 1984
2) Japan Road Association : Design Specifications of Petroleum Pipelines, 1974
3) Katayama, T. and Sato, N. : Ground Strain Measurement by a Very Densely Located Seismometer Array, Proc. 6th Japan Earthquake Engineering Symposium, Tokyo, 1982
4) Ministry of Construction : New Seismic Design Methods, Technical Note of PWRI, No. 1185, Public Works Research Institute, 1977
5) Okubo, T., Arakawa, T. and Kawashima, K. : Dense Instrument Array Program of the Public Works Research Institute and Preliminary Analysis of the Records, Eighth World Conference on Earthquake Engineering, San Francisco, U.S.A., 1984
6) Tamura, C., Okamoto, S. and Hamada, M. : Dynamic Behavior of a Submerged Tunnel during Earthquakes, Report of the Institute of Industrial Science, University of Tokyo, Vol.24, No.5, 1975
7) Tamura, K., Kawashima, K., Aizawa, K. and Takahashi, K. : Recording Accuracy

of Digital Strong Motion Accelerographs with Independent Triggering and Recording Systems for Analysis of Finite Ground Strains Induced during Earthquakes, Proc. Japan Society of Civil Engineering, Vol. 392/I-9, 1988

8) Kawashima, K., Hasegawa, K. and Nagashima, H.: Seismic Behavior of Buried Pipelines through Field Observation, Proc. of 3rd U.S. National Conference on Lifeline Earthquake Engineering, Los Angeles, CA, August 1991

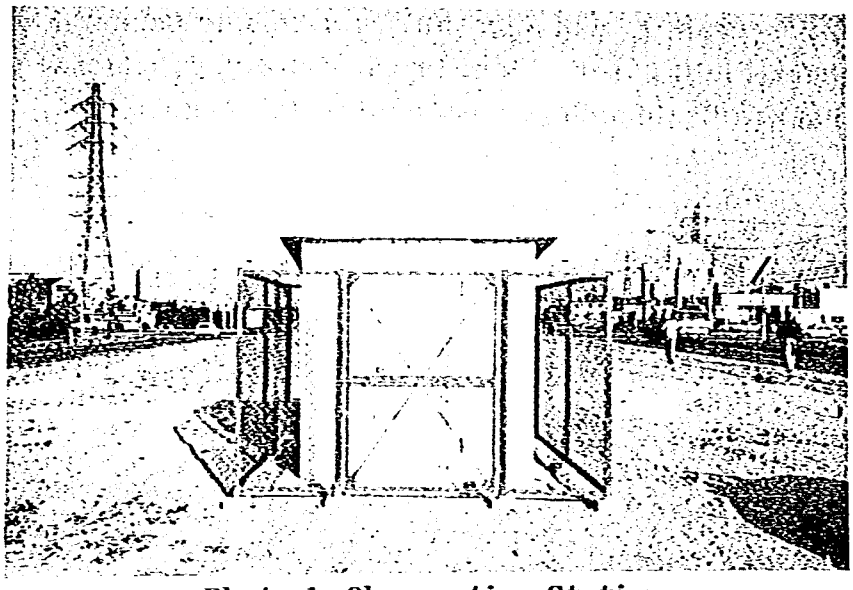


Photo 1. Observation Station

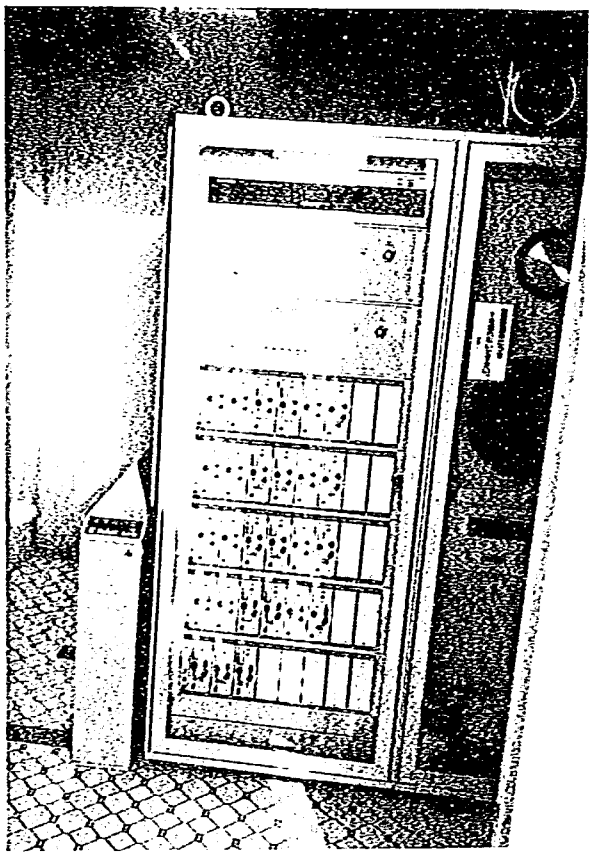


Photo 2. Data Acquisition System

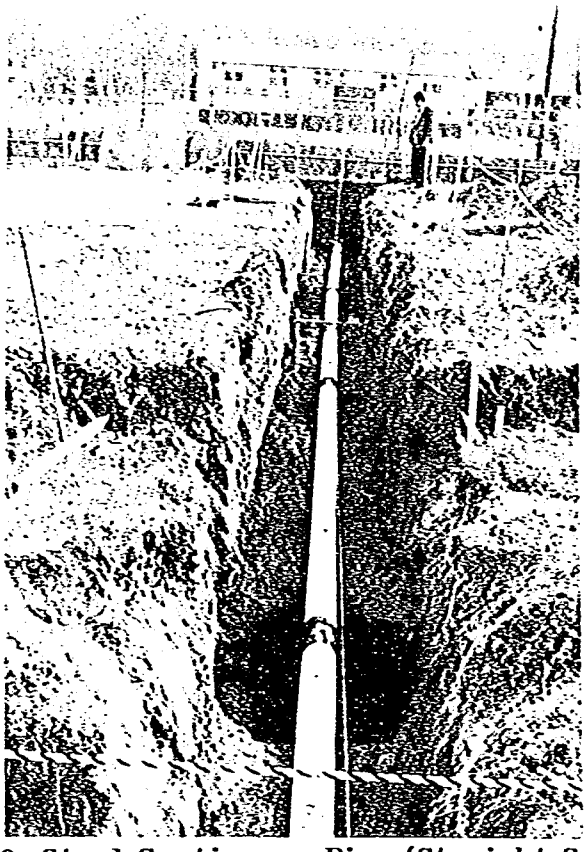


Photo 3. Steel Continuous Pipe (Straight Section)

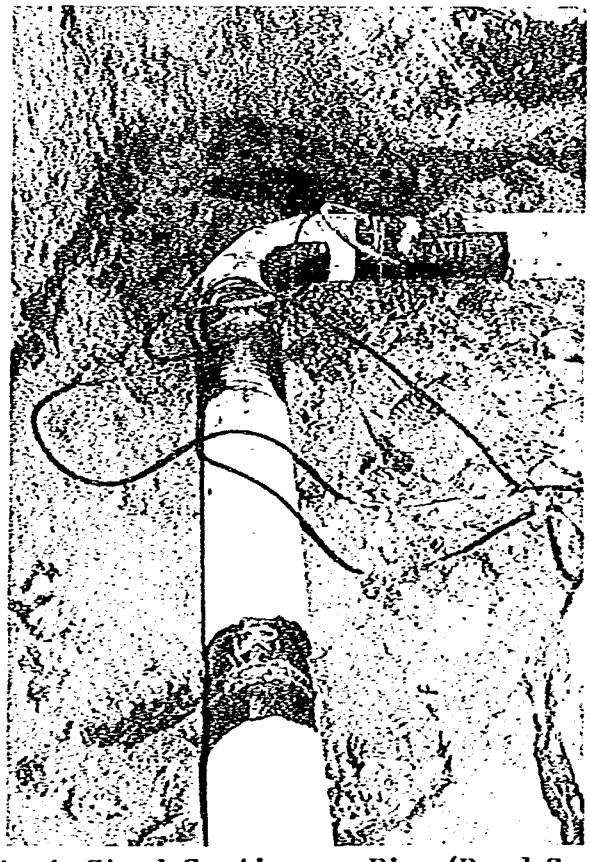


Photo 4. Steel Continuous Pipe (Bend Section)



Photo 5. Ductile Pipe with Expansion Joints



Photo 6. Expansion Joint

SEISMIC MONITERING AND SYSTEM CONTROL FOR LIFELINES

by

S.Takada[1] T.Fuke[2] and J.Ueno[3]

1 Professor, Department of Architecture and Civil Engineering, Kobe Univ.
2 Senior Engineer, Osaka Gas Co.,Ltd.
3 Senior Engineer, Konoike Construction Co.,Ltd.

ABSTRACT

It is important to obtain various information of seismic damages to lifeline systems as quickly and accurately as possible in order to make quick functional recovery for damaged lifeline facilities. A problem for making an effective arrangement of seismometers is discussed from the viewpoints of both spacing and installing locations. An optimum spacing of seismometers is developed by minimizing the total costs of both equivalent costs to earthquake damages and installing costs of seismometers. An optimum installing location of seismometers for a given spacing is evaluated by using a neural network system with a pattern recognition of earthquake damages to lifeline systems during recent earthquakes. In addition to these, a method to estimate seismic ground motions at arbitrary locations by using remote monitoring seismometer data observed at limited locations. The shape interpolating function is applied to the estimation method of seismic ground motions. Based on these basic discussions, a design scenario of seismic monitoring network has been proposed for an existing gas supply system,providing locations of telemeter and seismometer. An application of the seismic monitoring network is shown as a real time damage estimate for emergency responses immediately after an earthquake.

INTRODUCTION

Urban functions in highly developed modern cities are greatly dependent on lifeline systems such as electric power, gas, water and communication network, and the earthquake damages to those facilities cause urban functional disorder by which various activities in modern cities are seriously affected. The functional restoration

of damaged lifeline facilities must be recovered as quickly as possible. It is indispensable, in the view of decision making of restoration strategies to damaged lifeline facilities, to obtain information of earthquake damages to lifeline systems as quickly and accurately as possible. Generally several seismometers are installed in the vicinity of important facilities of lifeline systems in order to obtain records for seismic ground motions which are closely related to the earthquake damages to lifeline systems.

Fig.1 shows a time flow for intra- and post-earthquake operations of lifeline systems under earthquake emergency response. If the information of earthquake damages to lifeline systems can be obtained within one hour after the occurrence of an earthquake by an earthquake early detection system, and some emergency management of restoration works for lifeline systems can be accurately operated, the restoration works and functional recovery for lifeline systems may be smoothly and quickly performed. An effective arrangement of remote monitoring seismometers is necessary for the accurate estimation of seismic ground motions over an entire supply-region of lifeline systems, and for an accurate detection of earthquake damages to lifeline systems as quickly as possible. This paper proposes a method to design a seismic monitoring network and its application for emergency response after earthquakes. First of all, a problem for making an effective arrangement of remote monitoring seismographs is discussed taking consideration of both spacing and installing locations of seismometers. An optimum spacing of seismographs can be evaluated for minimizing not only the disadvantage costs due to both seismic damages and secondary disasters but also the cost of installing of seismometers. An optimum installing locations of seismographs under a given optimum spacing can be numerically evaluated by means of a neural network system whose learning data have various information as to seismic damages of lifeline systems during recent earthquakes. Moreover, an estimation method of seismic ground motions at arbitrary locations over an entire supply-region is proposed by using some remote monitoring seismometer data observed at limited locations in order to make quick and accurate activities for damage inspection after an earthquake as shown in Fig.1.

OPTIMUM SEPARATION DISTANCE OF SEISMOMETERS BY COST-BENEFIT ANALYSIS

An optimum separation distance between each seismometer in a monitoring network, which is associated with an optimum number of seismometers of the network for an objective area, is decided by a cost-benefit analysis. In the following chapter, an

optimum location will be decided considering other factors like as seismological history, active faults and so on.

Definition of an objective function for optimum separation distance of seismometers

An optimum separation distance of seismometer R can be so determined that make an efficiency function Z take the maximum value (Ref. Fig.2).
The efficiency function Z is defined as follows.

$$Z=\frac{B}{C} \qquad (1)$$

where, B is amount of money saved by quick and accurate countermeasures based on informations of seismometer network. C is installation cost for the seismometer network.

In Fig.2, following notations are employed. C_0 is total cost paid by lifeline industry. C_1 is cost irrelevant to monitoring networks such as survey and repair costs. L is total amount of money loss for the society including customers. L_0 is loss irrelevant to the monitoring network. L_{01} is loss due to outbreak of direct disaster. L_{02} is loss due to the minimum (inevitable) outbreak of the second disaster. These second disasters are considered to occur by the time an emergency response is executed. L_{03} is loss due to disadvantages to customers in the minimum supply-stop. This is loss when lifeline service in the area ought to be stopped is stopped correctly and quickly. L_1 is loss due to outbreak of the second disaster when necessary supply-stop was not taken. L_2 is loss due to disadvantages to customers in unnecessary supply-stop.

The L_1 occurs when severely damaged areas are left without supply-stop whereas the L_2 occurs when non-damaged areas are forced to stop their service by incorrect judgement. Therefore L_1 and L_2 can be reduced according to informations by the seismometer network information.
Again, it should be made sure that this project of the monitoring network can't minimize the number of damages but minimize the risk of the second disaster and unnecessary supply-stop.

Assume that when the accuracy of damage estimation is improved by the information of seismometer network under an optimum separation distance R', the L_1 and L_2 have been reduced to L_1' and L_2' respectively.

$$B=(L_1-L_1')+(L_2-L_2') \tag{2}$$

In the first term of Eq.(2),

$$L_1= E_{1,P=0} \sum_{i=1}^{m} (F_i \cdot a \cdot k \cdot l_i) \tag{3}$$

$$L_1'= E_1 \sum_{i=1}^{m} (F_i \cdot a \cdot k \cdot l_i) \tag{4}$$

$$E_1= G_1 \cdot e^{-\beta_1 \cdot P} \tag{5}$$

$$L_1-L_1'= G_1 \cdot (1-e^{-\beta_1 \cdot P}) \cdot \sum_{i=1}^{m} (F_i \cdot a \cdot k \cdot l_i) \tag{6}$$

where,E_1 is the probability of outbreak of the second disaster due to error judgement for supply-stop. E_1 is defined as follows.

$$E_1=\frac{\text{(Area which should be stopped but taken no measures)}}{\text{(Total area for supply service)}} \tag{7}$$

Assume E_1 is the function of the separation distance R and expressed by a variable P and Coefficient β_1. Here, P is a detecting rate of damages defined by follows.

$$P=\frac{\left(\begin{array}{c}\text{Detected number of damaged location based on survey}\\ \text{following informations by the monitoring network}\end{array}\right)}{\text{(Total number of damaged locations)}} \tag{8}$$

These relation is shown in Figs.3 and 4.

A coefficient a is the rate of the second disaster defined as follow.

$$a=\frac{\text{(Number of location of second disaster)}}{\text{(Total number of location of direct disaster)}} \tag{9}$$

F_i is disadvantage cost (Yen/Number) by the second disaster on i-th area.
F_i is assumed to be depending on following 3 factors. A Factor : Character of area classified into industry, commercial, residential and agricultural areas, B Factor :

Population density such as heavy, intermediate and low, C Factor : Existence of important facilities such as hospital, fire station and etc.

A coefficient k(Number/km) is damage ratio per unit length of pipeline depending on materials of pipes or seismic intensity. A coefficient l_i is the construction length of pipeline in i-th area. A coefficient m is entire area on supply service.

In the second term of Eq.(2),

$$L_2 = E_{2,P=0} \sum_{i=1}^{m} (M_i \cdot T_{ave}) \tag{10}$$

$$L_2' = E_2 \sum_{i=1}^{m} (M_i \cdot T_{ave}) \tag{11}$$

$$E_2 = G_2 \cdot e^{-\beta_2 \cdot P} \quad) \tag{12}$$

$$L_2 - L_2' = G_2 \cdot (1 - e^{-\beta_2 \cdot P}) \cdot \sum_{i=1}^{m} (M_i \cdot T_{ave}) \tag{13}$$

Where, E_2 is the probability of doing unnecessary supply-stop due to error judgement.
E_2 is defined as follows.

$$E_2 = \frac{\text{(Area which should not be stopped but taken measures)}}{\text{(Total area for supply service)}} \tag{14}$$

Assume E_2 is the function of R and expressed by the variable P and coefficient β_2. These relations are shown in Figs.4 and 5.

In Eq(10), T_{ave} is an average supply-stop hour. The relationship between T_{ave} and seismic intensity has to be estimated by empirical data during past earthquakes. M_i is an average disadvantage cost (Yen/hour) due to troubles caused by damages of pipeline on i-th area. M_i is assumed to be depending on the following 2 factors. A Factor : Character of area classified into industry, commercial, residential and agricultural areas, B Factor : Population density such as heavy, intermediate and low. The m is entire area on lifeline service.

Numerical example

As a numerical example, following assumptions are used here.

Dimension of lifeline service area : 12km x 24km
Dimension of mesh : 400m x 400m
Relationship between R and P : Fig.4
In Fig.3, G_1=0.5, β_1=1.6. In Fig.5,G_2=0.5, β_2=1.6.
The lifeline service area is here assumed to be a residential one.
a=0.01, F_i=10,000,000(Yen/one second disaster), k=1.5, l=0.12(km/mesh),
M_i=1500(Yen/day), T_{ave}=1.5(day), n=10,000,000(Yen/seismometer)

We can give upper and lower limit values of the separation distance such as 12km and 0.4km respectively, taking consideration of entire lifeline service area and mesh size. Under above conditions, the relationship between R(km) and Z in Eq.(2) is evaluated as shown in Fig.6. This figure shows that the optimum distance is turned out to be about 8.5km.

PRIORITY FOR LOCATING SEISMOMETERS

A neural network system is introduced to obtain optimum installing locations of seismographs in this paper. The learning procedure of the neural network is called 'back-propagation' for networks of neurone-like units.[1] This learning procedure repeatedly adjusts the weights of the connections in the network so as to minimizing the measure of the difference between an actual output vector of the network and a desired output vector.

In this paper the information of earthquake damages to gas and water pipelines in four recent urban earthquakes is used as learning data of the neural network system. The learning data generally consists of input and output data. The input data in each damaged area including seismic intensity, ground classification, active faults, important pipeline facilities, pipeline density and strength of pipeline joint are used for the neural network system, while the information of earthquake damage states such as severe, medium, slight and no damage is used as output data of the neural network.

The learning of neural network is to find a set of weights which ensure that for each input vector an actual output vector produced by the network is sufficiently close to the desired output vector. Total error can be evaluated by comparing the actual and desired output vectors for every learning case. In this paper the total error E is defined as follows.

$$E=\frac{1}{N}\sum_i \sum_j (y_{ij}-d_{ij})^2 \qquad (15)$$

where i is an index over input-output pairs, j is an index over output units, y_{ij} is the actual state of the output unit, d_{ij} is its desired state, and N is number of learning data. In back propagation method it is, in general, necessary to numerically evaluate the partial derivative of total error E with respect to each weight in the network system in order to minimize E by gradient descent. The neural network system consists of three layers and input layer has 20 units, hidden one is 40 units, and output one is 4 units. The number of learning data is 590 and that of repetitions is 150,000. This neural network system whose learning has already finished for input-output pairs of past earthquake damages to pipelines are applied to a problem of installing locations of seismographs. It is necessary to investigate this neural network system for 14 standard pattern recognition data of earthquake damages to lifeline systems in Table 1 before using this system.

The characteristics of damages of each earthquake for a learning data can be represented by multiplying an appropriate weight to the output vector of this system whose 4 neuron-like units have four damage grades such as severe, medium, slight and no damage. Fig.7 shows output results of this neural network system for learning data by multiplying the following weight to each damage grade of the output vector.

$$\text{Output value}=(\text{severe damage})+(\text{medium damage})*0.7 +(\text{slight damage})*0.3 \qquad (16)$$

This figure indicates that the factors such as high potential of liquefaction, existing of faults, weak pipe material and high seismic intensity are closely related with pipe damages.

Next, the results of the neural network system described above are applied to existing practical problems. We divide gas supply-regions in Osaka area into small meshes as 382m × 308m which have a weight including various information of each input datum in learning data of the neural network described above. In doing so, the seismic intensity grade for each mesh is analytically evaluated for a presumed earthquake with given location and magnitude. The neural network system can estimate the grade of earthquake damages to lifeline systems.

Fig.8 shows a weight distribution for each mesh and locations of telemeter stations which are illustrated in dot marks in Osaka area. The locations of telemeter stations are chosen as a subject to the installing locations of seismographs. The priority for installing locations of seismographs can be in order by the weight summation of meshes within the region bounded by a circle whose center and radius are the location of telemeter station and a given spacing of seismometer, respectively.

Fig.9 illustrates resultant order for installing locations of seismographs for the case of optimum spacing R=7km. It is evident from this numerical example that the effective installing locations and order of seismographs can be numerically evaluated by the neural network system whose learning data have various information of damaged lifeline systems.

INTERPOLATION METHOD OF SEISMIC GROUND MOTIONS AND ITS ACCURACY

Outline of interpolation method

A shape interpolating function used in FEM and/or BEM can be applicable for deterministic estimation of seismic ground motions at arbitrary locations from data observed at limited sites over an entire region of lifeline systems. Under given values of ground motion at four points shown in Fig.10, a value at arbitrary location can be calculated by following formulae with the aid of the shape interpolating function.[2)]

$$A_{max}=\sum_{i=1}^{4} N_i(\xi,\eta)A_i \qquad (-1\leq\xi\leq1,\ -1\leq\eta\leq1) \tag{17}$$

where, $N_1(\xi,\eta)=+0.25\xi\eta(1-\xi)(1-\eta)$,
$N_2(\xi,\eta)=-0.25\xi\eta(1+\xi)(1-\eta)$,
$N_3(\xi,\eta)=+0.25\xi\eta(1+\xi)(1+\eta)$,
$N_4(\xi,\eta)=-0.25\xi\eta(1-\xi)(1+\eta)$,

and Ai(i=1-4) is a value observed at i-th location. The observation points rarely locate at corners of square shape as shown in Fig.11 and then some modification for Eq.(17) is required for an arbitrary quadrangle shape. Fig. 11 indicates the mapping between the arbitrary quadrangle shape in global coordinate(x,y) and the square shape in local coordinate(ξ,η) The relation between both coordinates can be represented by following equations.

$$x=\sum_{i=1}^{4} N_i(\xi,\eta)x_i\ ,\quad y=\sum_{i=1}^{4} N_i(\xi,\eta)y_i \tag{18}$$

where, xi and yi are x and y coordinates of the i-th observation location, respectively. Ground motions are strongly dependent on surrounding topography and surface soil layers beneath the location. An amplification factor for the surface

soil layers is introduced here to estimate ground motion at an arbitrary location , neglecting three dimensional effects of the topography. Then ground motions can be estimated by the next Equation.

$$A_{max}=\sum_{i=1}^{4} N_i(\xi,\eta)A_i\times\frac{A_m}{A_{m_i}} \qquad (19)$$

where, A_{m_i} and A_m are amplification factors at the i-th observation point and the estimated point respectively.

Proposed method for estimating ground motions based on seismic monitored data is a deterministic way taking consideration of linear variation of ground motion among the monitored data. In fact, the ground motion should be taken account for random variables depending on soil and topographical conditions. The present paper takes advantage of saving computational time for rapid estimate of ground motions over entire regions of lifeline system immediately after earthquakes. A broad-gauged value of ground motions associated with MMI or JMAI would be sufficient for emergency response after earthquakes from practical view points of engineering. The accuracy of the value estimated by proposed method would be governed by factors such as area of network, location of epicenter, topography, sudden change of ground amplification and ground instability like liquefaction phenomena.

Figs.12 and 13 show the comparison of observed maximum acceleration values during recent earthquakes with estimated ones by the proposed method. A monitoring network of seismometers shown in these figures are existing ones for emergency response after earthquakes. Fig.12 indicates the effects of epicentral location of earthquakes providing observed data for a near field earthquake and for a far field earthquake. Estimated acceleration values for the far field earthquake give a satisfactory results than those for the near filed earthquake. For near field earthquake, the maximum accelerations monitored by seismometers are variated in wide ranges especially in observed points between sites in the vicinity of epicenter and ones far from there whereas the maximum accelerations are almost uniformly distributed for the far field earthquake. The size of network of seismometer should be reduced under these conditions. Fig.13 is the effects of a size of network of seismometers on estimated acceleration values. The smaller size of the network gives better results.

DESIGN FOR MONITORING NETWORK OF SEISMOMETERS FOR EXISTING GAS SUPPLY SYSTEMS

Based on discussions in previous Chapters, a seismic monitoring network for existing gas supply systems has been designed in order to hold damage states immediately after earthquakes. Design scenarios for the monitoring network are as follows.

(1) Range of separation distance between locations of seismometers is specified based on previous analytical results. A range of 5 to 15 km is being proposed depending on easily damaged areas, density of population and buried pipelines , and urban or rural areas .

(2) There exists more than thirty sites where seismometer and telemeter are already working. These sites has been fixed with first priority as points constituting of the monitoring network.

(3) Possible sites for locating seismometer and telemeter system are selected from among sites of gas regulator station, gas tank, office building for gas supply, and existing telemeter station for other purposes.

(4) The priority for selecting sites is followed by the proposed method of neural algorithm.

(5) An whole monitoring network is divided into dozens of sub-network which constitutes of a four to twelve polygon.

(6) The monitoring sub-network is considered to locate in a uniform ground and topographical conditions as much as possible and also the shape of a polygon is close upon a circle.

(7) A future planning for increasing gas supply in the areas is taken consideration to set the whole monitoring network.

Fig.14 is a designed whole monitoring network which covers areas of 4,000 km^2 and 600 million customers of gas consuming. Total numbers of monitoring stations are 37 and 10 sub-network composing the whole network. Fig.15 is a seismic intensity mapping in terms of ground acceleration which has estimated by a proposed interpolating method based on given acceleration values at monitoring stations. Fig.15 can be calculated and drawn in computer screen in less than one minute by a personal computer(PC-H98).

REAL TIME DAMAGE ESTIMATE AND SYSTEM CONTROL WITH THE AID OF MONITORING NETWORK

Real time damage estimate

A damage prediction of buried pipelines under scenario earthquakes is the first step for urban disaster mitigation planning though it involves so many uncertain factors such as seismic ground intensity , ground instability and liquefaction. A real time damage estimate , in which monitored seismic ground motions as acceleration and velocity are able to be employed, could specify severe damaged areas with much higher precision than the damage prediction before earthquakes, allowing easy emergency response. Fig.16 indicates flow chart of real time damage estimate of buried pipelines with the aid of monitoring network. The procedure of the real time damage estimate is as follows.

(1) Seismic intensities in term of ground acceleration and velocity in each regional mech(300mx400m) are identified from monitored data and following estimated values by the interpolating method.

(2) Ground conditions I,II and III are assigned in each mesh based on the criteria in Seismic Design Code for Road Bridge, and also micro-topographical conditions A,B, and C are assigned such as A: river basin,B:plain and C:terrace and mountain side. The conditions in the largest areas are employed when a mesh includes different ground and topographical conditions.

(3) Each mesh is classified into five levels as shown in Table 2 depending on ground acceleration and velocity. Ground shaking,crack and subsidence are considered as seismic causes of damage in non-liquefied mesh.

(4) PL-value for evaluating possible liquefaction is calculated in each mesh by using next empirical formula.

$$PL=a \times Amax + b \tag{20}$$

where, a and b are coefficients specified in each mesh, which can be given by analyzing bore hole data and micro-topography in the mesh.

(5) A mesh is considered as non-liquefied area when it satisfies following all conditions. (a) Intensity level for acceleration is 1, (b) Micro-topographical condition is C, (c) Ground condition is I, and (d) PL-value is less than 5.

(6) Rating of possible liquefaction area in a mesh is calculated by next empirical formula.

$$S=2.9 \times PL \times A + 1.9 \times PL \times B \tag{21}$$

Here, S: Rating of possible liquefaction area in a mesh, A and B: Area ratios(%) for micro-topographical condition A and B in a mesh.

(7) Damage rate (Number/km) is empirically obtained for cast iron pipeline with screw joint under non-liquefied and liquefied conditions with the aids of damage data during past earthquakes.

(8) Theoretical damage probabilities for gas pipelines such as welded steel, ductile iron with mechanical joint, cast iron with screw joint and polyethylene are obtained by response analyses for different seismic inputs as ground shaking, crack,subsidence, buoyancy and lateral flow due to liquefaction.

(9) Relative damage ratios of i-type pipeline to cast iron pipeline with screw joint are calculated based on the theoretical damage probabilities.

(10) Fragility curves for any types of buried pipelines can be provided by multiplying the relative damage ratio with damage rate of cast iron with screw joint for different ground intensity and for different diameter of pipelines.

(11) Number of damage in a mesh for various types of buried pipelines are calculated under non-liquefied or liquefied conditions by using following formulae.

$$N_n=\sum_{i=1}^{M} \beta_{ni} \cdot \alpha_n \cdot L_i \quad : \text{for Non-liquefied mesh} \qquad (22)$$

$$N_L=(1-\frac{S}{100})\sum_{i=1}^{\overline{M}} \beta_{ni} \cdot \alpha_n \cdot L_i+\frac{S}{100}\sum_{i=1}^{\overline{M}} \beta_{Li} \cdot \alpha_L \cdot L_i \quad : \text{for Liquefied mesh} \qquad (23)$$

where, N_n and N_L: Numbers of damage of buried pipelines in non-liquefied and liquefied meshes, β_{ni} and β_{Li}: Relative damage ratios of i-type buried pipeline to damage rates of cast iron pipeline with screw joint in non-liquefied and liquefied meshes, α_n and α_L : Damage rates of cast iron pipeline with screw joint in non-liquefied and liquefied meshes, and Li: Length of i-type buried pipeline in a mesh.

Fig.17 (a) and (b) shows an example of computer-screen output for the real time damage estimate in center areas of the monitoring network. It takes five minutes in computer calculations for entire regions of the monitoring network. Present damage estimate based on seismic monitoring data can be done 5-6 minutes later after the occurrence of earthquake including process time of the telemeter system.

SYSTEM CONTROL WITH THE AID OF SEISMIC MONITORING

Fig.18 indicates the scenario of emergency responses for gas supply system. The first stage is to specify severely damaged areas based on results by real time damage estimate, damage facts acquired by offices controlling lower levels of hierarchy gas supply networks and on news by mass medias. Route and region could be indicated for surveying damage states by helicopters or examiners. These emergency response should be done within half an hour after an earthquake. The second stage is the system control including shut down of gas supply in severely damaged areas, making zonal blocking to continue to supply gas in slightly or non-damaged areas. The zonal blocking will be performed based on informations by the damage survey above mentioned. The real time damage estimate by seismic monitoring will help the decision making for gas shut down and zonal blocking. In fact, the decision making for gas shut down is extremely delicate judgement because rehabilitation works for shut lines take so many times due to the nature of gas substance. Judgement of shutting gas supply and zonal blocking should be done within 1-2 hours after an earthquake. The third stage of emergency response is an additional zonal blocking for gas shut down based on informations from job sites of rehabilitation works and variation of required gas consuming after an earthquake.

Data on seismic ground motions monitored by network of seismometers will play an important roll for the system control of lifelines as mentioned above.

CONCLUSIONS

Present research introduces a methodology to design a monitoring network for early detection of severely damages areas immediately after earthquakes. Research results so far can be summarized as follows even though the monitoring network for existing gas supply systems is still under developing based on the proposed methodology.

(1) The importance of monitoring network for lifelines has been discussed from the view points of real time damage estimate and system control of lifelines.
(2) Optimum separation distance for seismometers is analyzed based on cost benefit conception. An optimum separation distance is turned out to be around 10 km for the areas interested.
(3) Priority for locating seismometers can be given by a neural network algorithm by which damage data of buried gas pipelines during past earthquakes are analyzed taking consideration of affecting factors such as ground and topographical

conditions, density of pipeline, active faults, strength of pipeline and seismic ground intensity.

(4) An estimating method of seismic ground motions in an entire supply region has been proposed by using remote monitored at limited locations. An accuracy of the method is discussed by applying it to an existing monitoring network.

(5) Scenario for designing a monitoring network is proposed taking for an example of existing gas supply systems based on analyzing and discussion results in previous Chapters.

(6) Procedure for a real time damage estimate of buried pipelines has been shown with advantage of the seismic monitoring network and system control as an emergency response for lifelines was discussed including the application of the monitoring network.

REFERENCES

1) Rumelhart, D.E., McClelland, J.L. & PDP Research Group 1986. Parallel Distributed Processing. Vol 1&2, MIT Press, Cambridge.

2) Washizu, H., Miyamoto H., Yamada Y., & Kawai T. 1981. Handbook of Finite Element Method I, Baifukan (in Japanese).

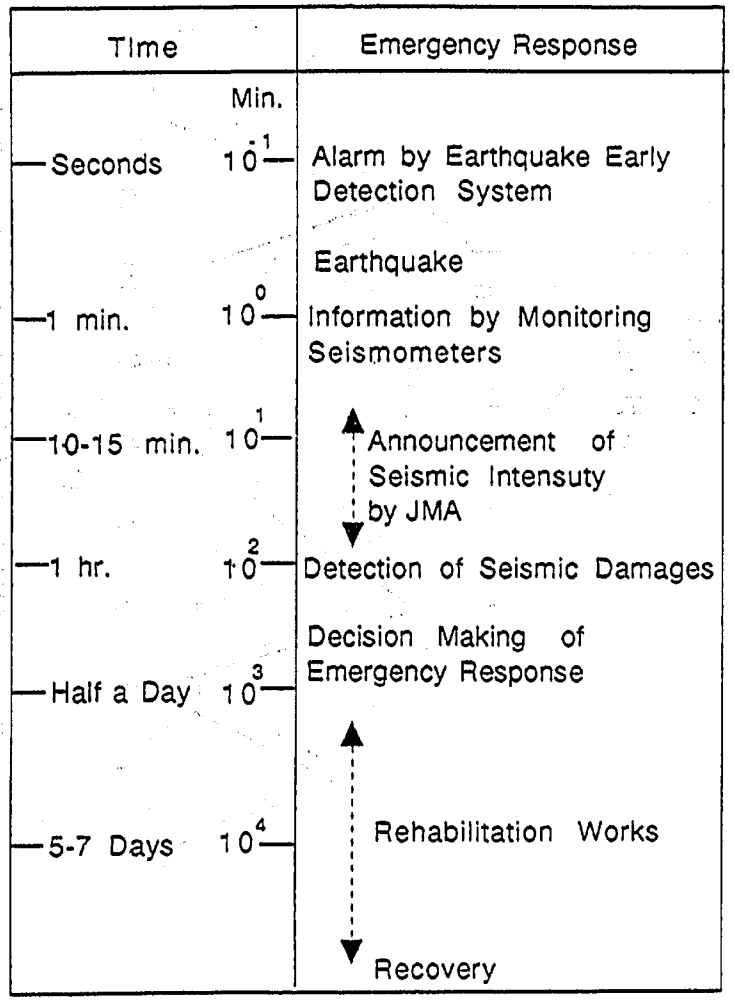


Fig.1 Time Flow of Intra- and Post Earthquake Emergency Response for Lifelines

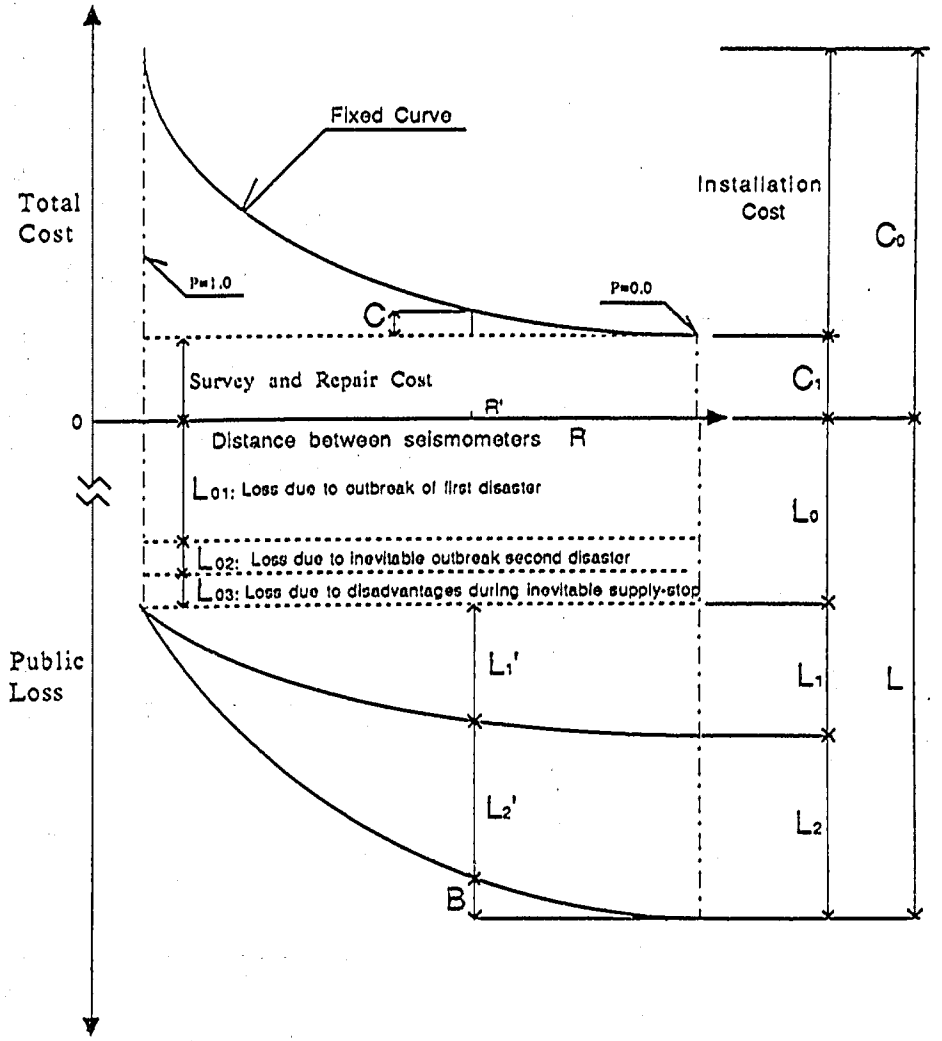


Fig.2 Objective Function for Cost Benefit Analysis

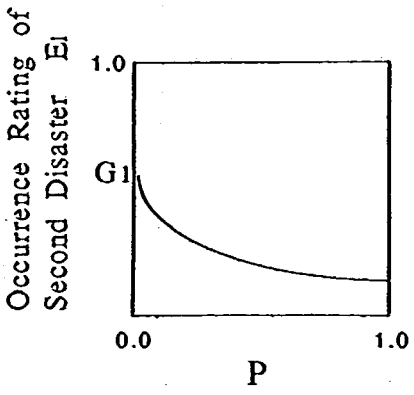


Fig.3 Relation between E_1 and P

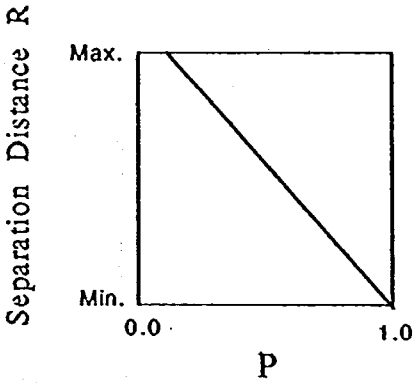


Fig.4 Relation between P and R

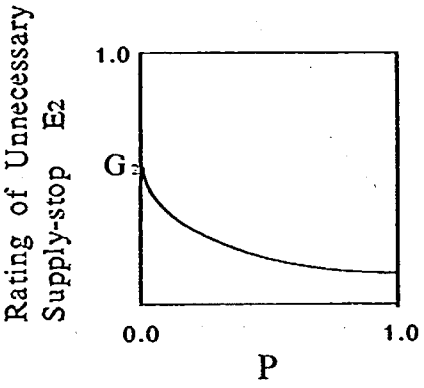


Fig.5 Relation between E_2 and P

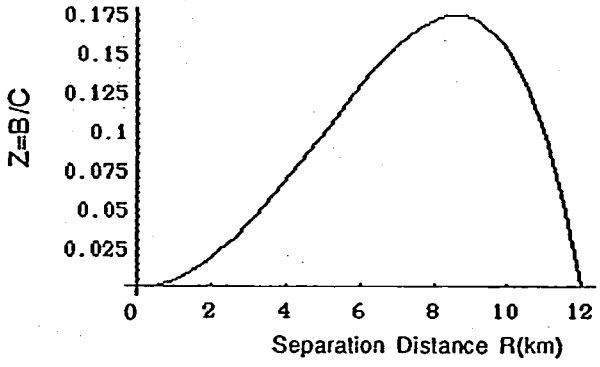


Fig.6 Optimum Separation Distance

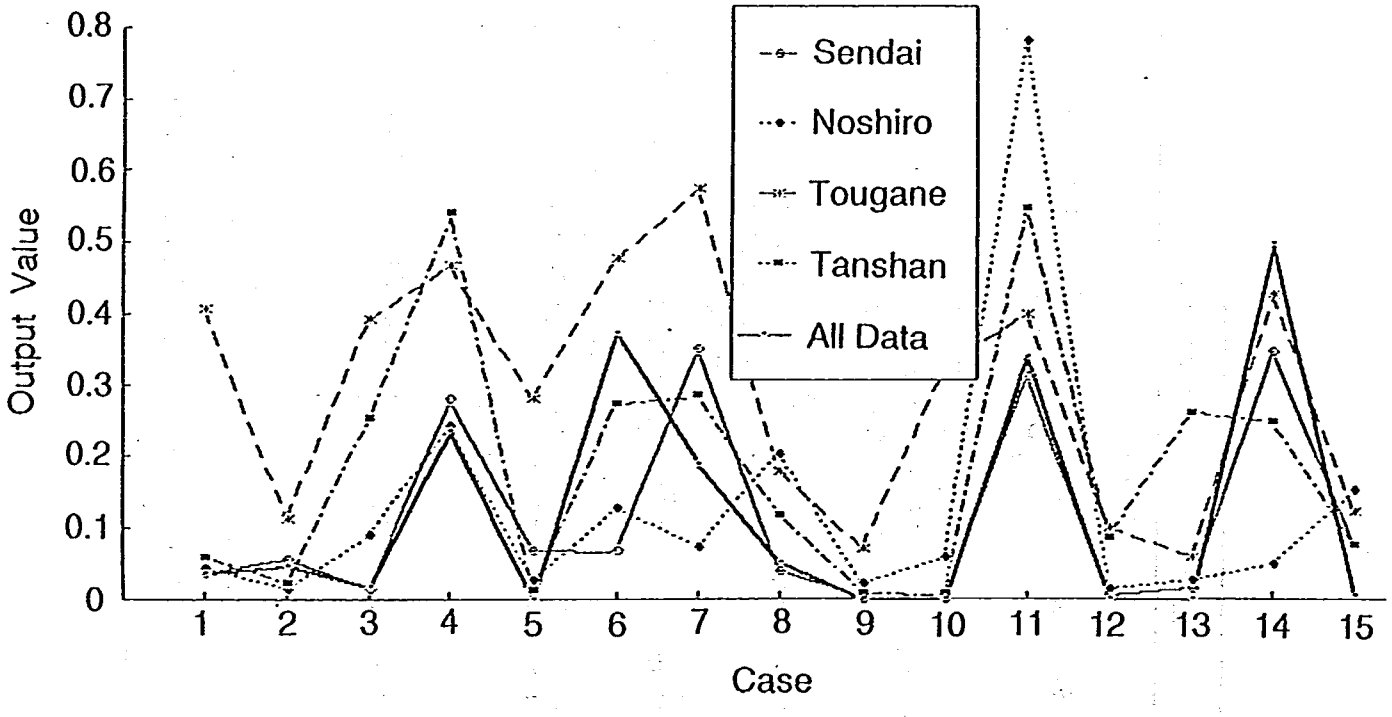


Fig. 7 Effects of Weight of Each Factor to Learning Results of Neural Network

Table 1 Recognition Data for Learning Result of Neural Network

Input factors / CASE 1~14	Ground Classification			Geographical Features			Region where geological state changes suddenly		Active Faults		Density of Pipeline Network			Strength of Pipeline Joint			Seismic Intensity			
	I	II	III	A	B	C	Exist	No	Exist	No	High	Medium	Low	Strong	Medium	Weak	IV	V⁻	V⁺	VI
1. Standard		O			O			O		O		O			O				O	
Ground Classification																				
2. I (Hard)	O				O			O		O		O			O				O	
3. III (Soft)			O		O			O		O		O			O				O	
Potential of Liquefaction																				
4. High		O		O				O		O		O			O				O	
5. Low		O				O		O		O		O			O				O	
6. Region where geological state changes suddenly		O			O		O			O		O			O				O	
7. Active Faults		O			O			O	O			O			O				O	
Density of Pipeline Network																				
8. High		O			O			O		O	O				O				O	
9. Low		O			O			O		O			O		O				O	
Strength of Pipeline Joint																				
10. Strong		O			O			O		O		O		O					O	
11. Weak		O			O			O		O			O			O			O	
Seismic Intensity																				
12. IV (~ 80gal)		O			O			O		O		O			O		O			
13. V⁻ (80~150gal)		O			O			O		O		O			O			O		
14. VI (250~400gal)		O			O			O		O		O			O					O

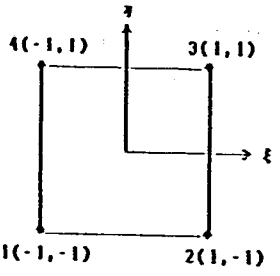
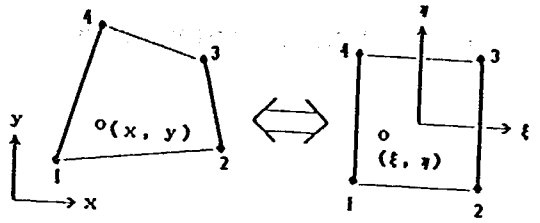


Fig.10 Observation Points by Seismometers



Global Coordinate Local Coordinate

Fig.11 Mapping between Global Coordinate and Local Coordinate

Table 2 Levels of Seismic Intensity

Level	1	2	3	4	5
Acceleration(gal)	Less 80	80-150	150-250	250-400	Over 400
Velocity(kine)	Less 5	5-15	15-25	25-40	Over 40
Strain(μ) x1000	0-1	1-2	2-3	3-4	4-5
Ground Subsidence(cm)	0-5	5-15	15-30	30-50	50-80
Ground Crack(cm)	0-1	1-5	5-10	10-20	20-30



Fig.8 Weight Distribution and Locations of Telemeter Station

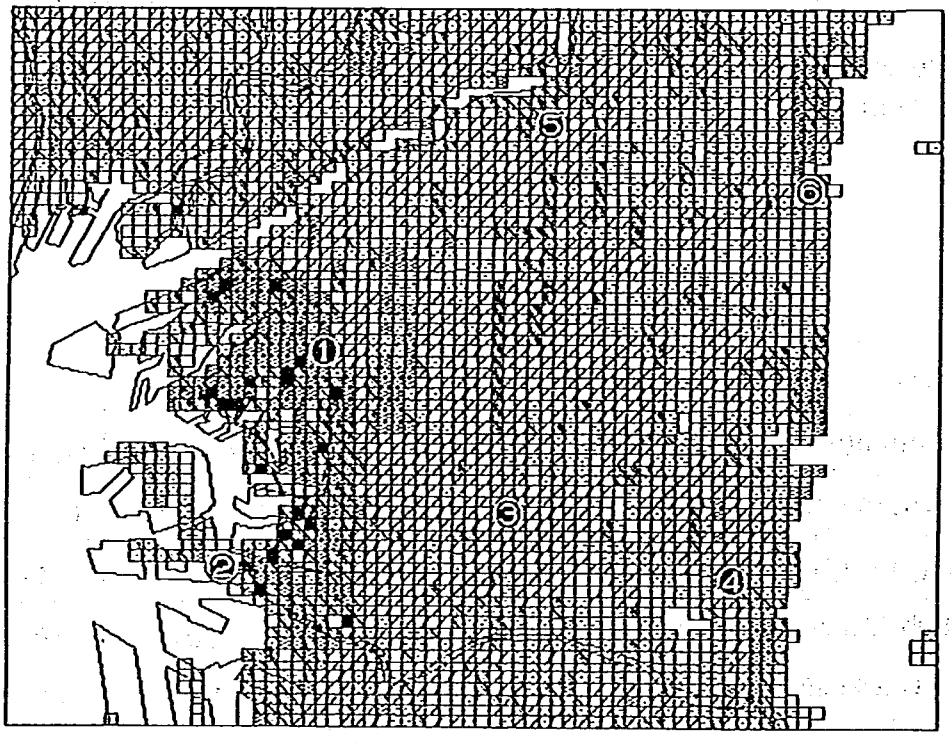
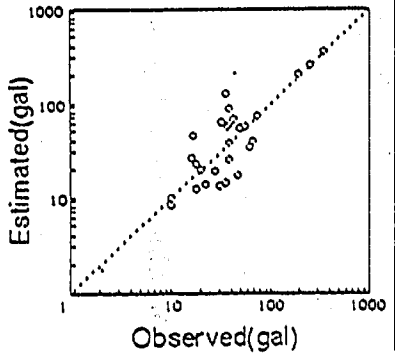
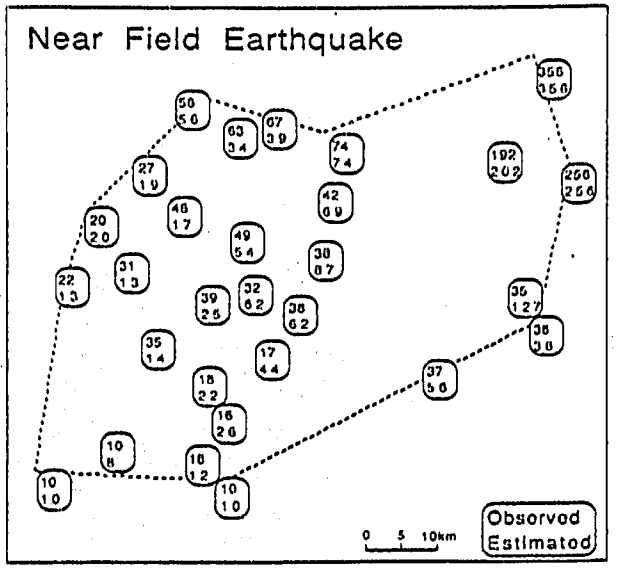


Fig.9 Resultant Order for Installing Locations of Seismometer
(Optimum Distance R=7 km)

Conformability=1.136

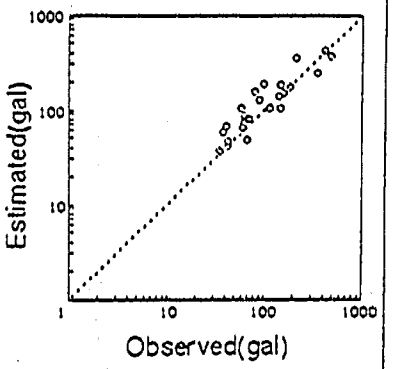
Standard Deviation=0.620

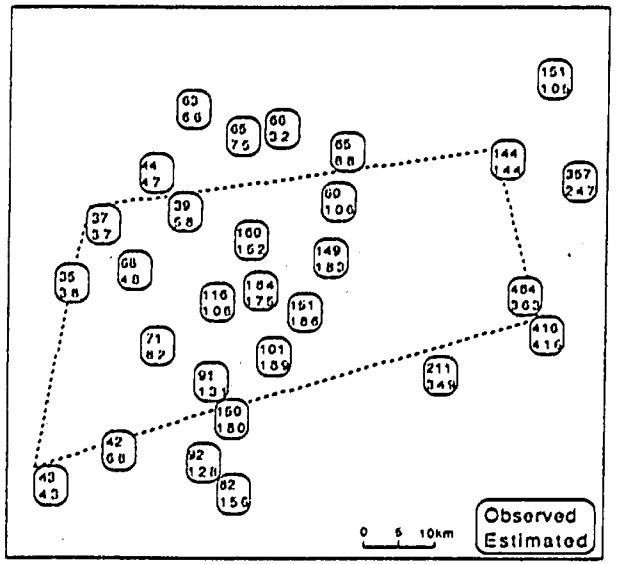




Conformability=0.903

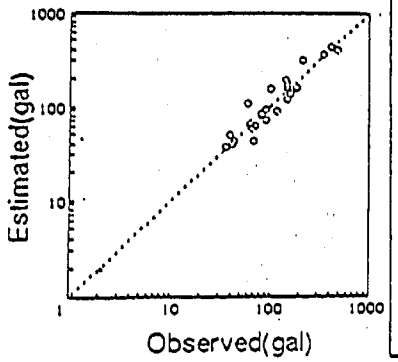
Standard Deviation=0.273





Conformability=1.026

Standard Deviation=0.214



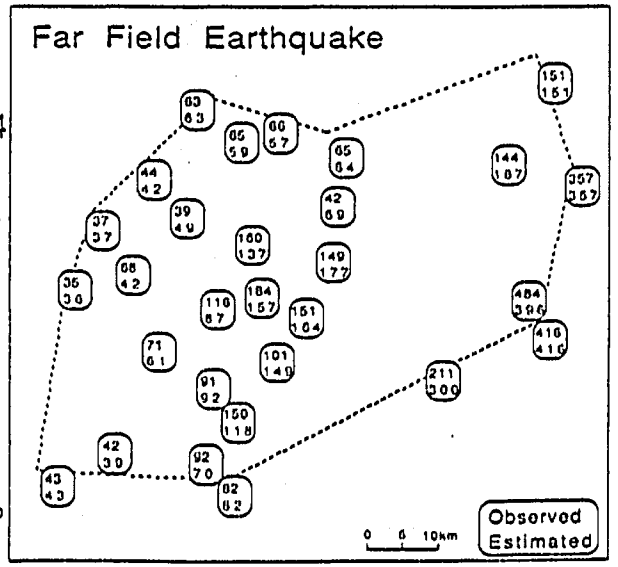
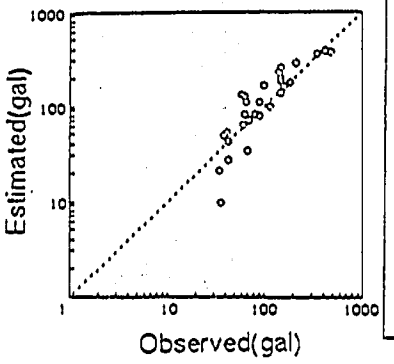


Fig.12 Accuracy of Interpolating Method
(Effects of Epicentral Location)

Conformability=1.069

Standard Deviation=0.631



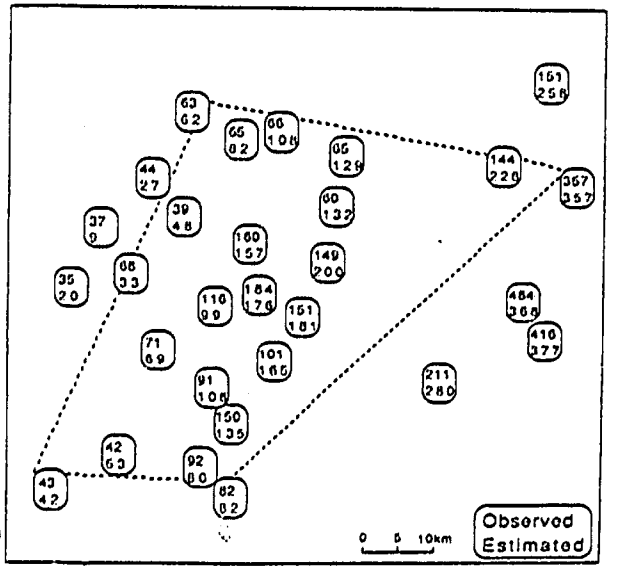


Fig.13 Accuracy of Interpolating Method
(Effects of of Configuration of Monitoring Network)

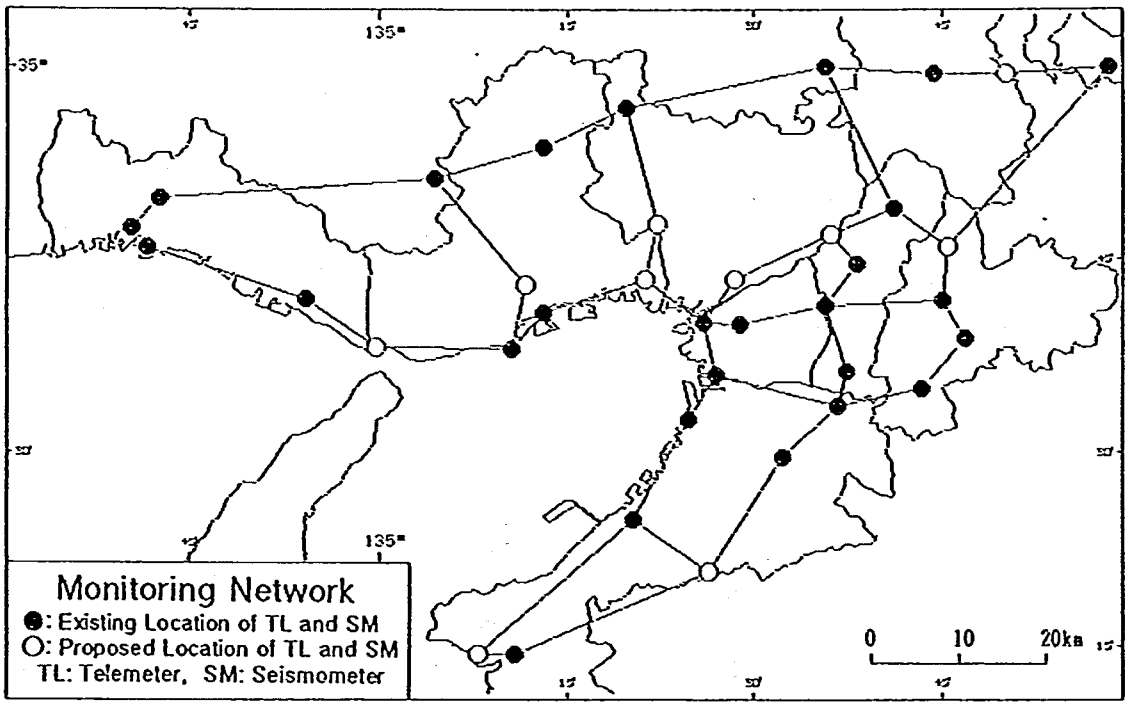


Fig.14 Monitoring Network for Gas Supply System

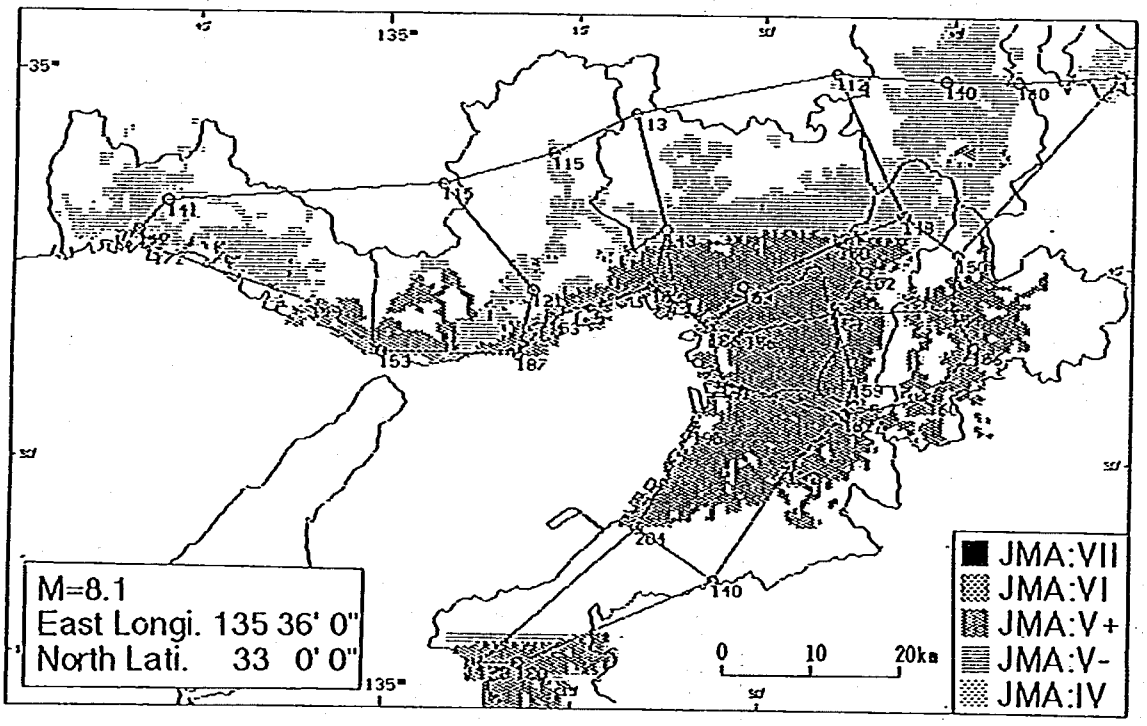


Fig.15 Estimated Ground Intensity Based on Monitoring Network

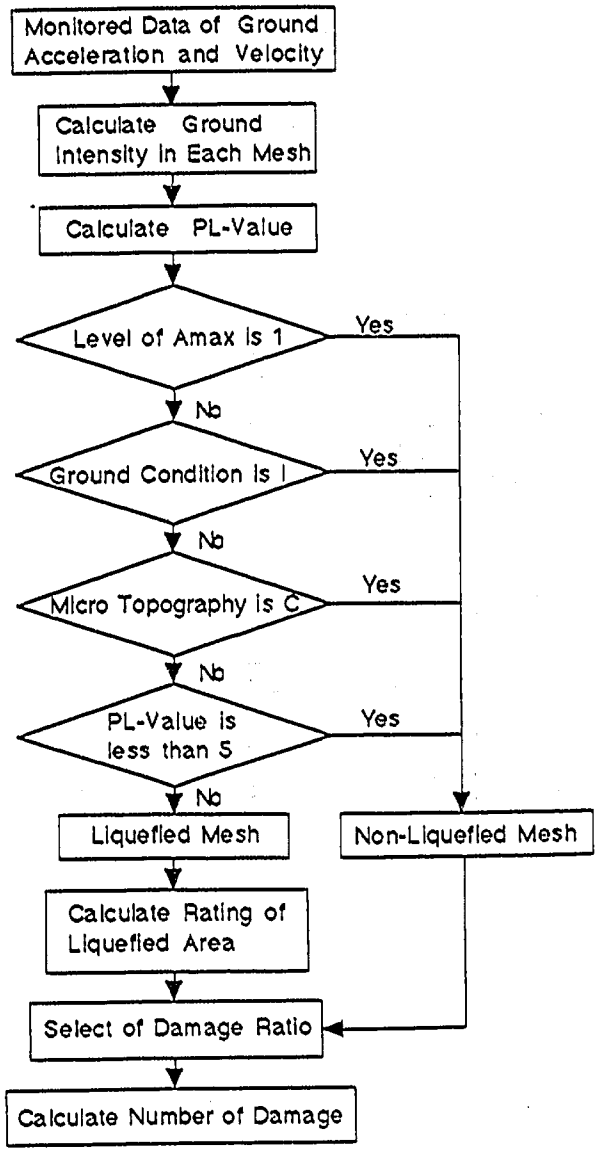


Fig.16 Flow of Real Time Damage Estimate

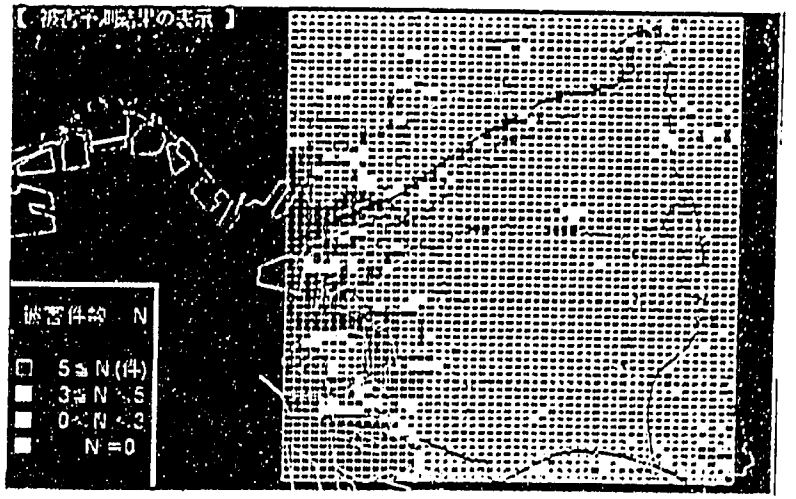


Fig.17(a) Real Time Damage Estimate
(Far Field Earthquake)

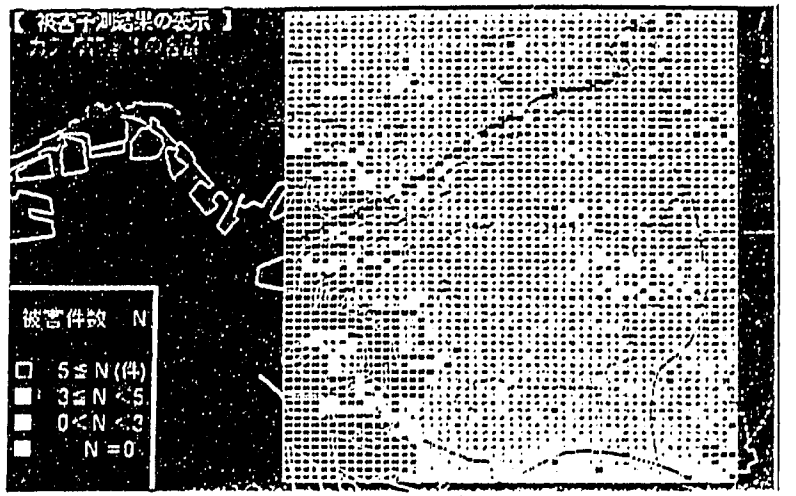


Fig.17(b) Real Time Damage Estimate
(Near Field Earthquake)

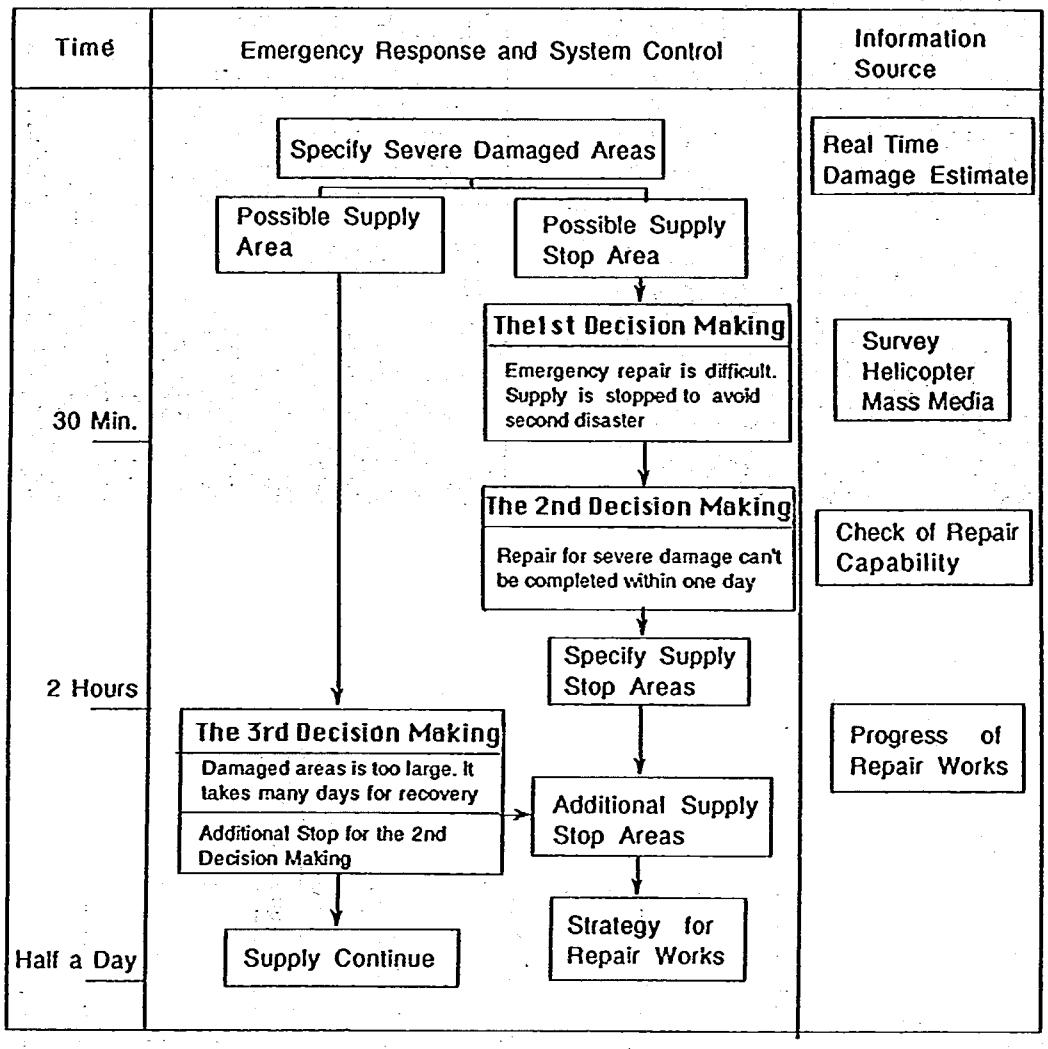


Fig.18 Flow of Emergency Response for Lifelines

MONITORING, INSTRUMENTATION AND INNOVATIVE DEVICES FOR LIFELINE SYSTEMS

Donald Ballantyne, P.E.

Senior Sanitary Engineer
Kennedy/Jenks Consultants

ABSTRACT

Post-earthquake lifeline system function can be maximized by monitoring system operating parameters and using the information to make system control decisions. The background and findings of this ongoing study are discussed in this paper. Failure of lifeline system pipelines has resulted in loss of system function and secondary damage. Loss of fire fighting capability is loss of function; fire damage from leaking natural gas is secondary damage. Wholesale replacement of the pipe with earthquake-resistant materials may be too expensive for system owners. Isolating the damaged portion of the system may be an effective earthquake damage mitigation alternative.

The focus of this phase of the project is on water systems. Monitoring can include system pressure and flow as well as use of seismic switches for input to system control. System isolation valves can be controlled manually or automatically either by self-contained local controllers or central operations centers. Isolation valves can be located on storage tanks, at faults, or around areas vulnerable to ground failure. System reliability, including telemetry and power, is critical.

Concerns arise from this control strategy: 1) liability associated with automatic shutdown of a water system serving a building sprinkler system or other critical services such as hospitals, 2) contamination of the shut-down potable supply system, 3) quick system reactivation, 4) reliability of such systems, and 5) implementation costs. These concerns can be mitigated by improving control system reliability and using dual water sources/reservoirs. Costs can be minimized by piggy-backing the system on an existing system.

This paper also presents preliminary conclusions drawn from interviews with lifeline system owners as to the possible application of post-earthquake system control in their systems. This project is being funded by the National Center for Earthquake engineering Research.

INTRODUCTION

Objective and Approach

The status of this ongoing study is reported herein. The objective of this study is to identify, develop, and evaluate devices to assess system post-earthquake status and to respond by appropriately controlling the system to minimize earthquake effects. The focus of this phase of the study is water systems. One significant element of this study is conducting interviews with water system owners who either have earthquake monitoring and control systems in place or could potentially use such systems.

Post-earthquake System Monitoring and Control Strategy

The proposed strategy to overcome water loss from pipeline failure following an earthquake is to monitor earthquake ground motion and/or water system pressure or flow. Based on that information, damaged segments of the water system can be isolated to save water. Either reservoirs can be isolated from damaged piping in the distribution system or damaged areas of the transmission/distribution system can be isolated from the system segments that remain intact.

This paper discusses water system disfunction in recent earthquakes and the cost of mitigation by pipeline replacement. Monitoring and control strategies, as well as system hardware alternatives are discussed. Isolation control configurations for water systems of varying designs are described. Five concerns that should be addressed before a monitoring and control system is installed are discussed. Four existing monitoring and control systems are described. Conclusions about such systems are drawn. Preliminary recommendations including improved control reliability and use of dual supplies/reservoirs are presented. Ten conclusions are drawn.

Water System Disfunction in Recent Earthquakes

Pipeline failure during earthquakes, and resulting reservoir drainage, is common. Water that is lost immediately following an earthquake often cannot be replaced for days as a result of power outage making pumps inoperable or transmission system pipeline damage.

In the 1987 Whittier Narrows earthquake, one reservoir in the City of Whittier, California water system drained down approximately four feet through damaged system piping before crews could isolate the tank. The earthquake occurred during normal working hours. Had it occurred at night or during a weekend, the tank would likely have drained completely (phone interview with Mr. Jim Johns, City of Whittier).

In the Loma Prieta earthquake, the San Francisco Auxiliary Water Supply System (AWSS) did not provide water needed for fire protection in the Marina District because pipeline system damage caused the Jones Street Tank to drain (Khater, 1991). In that same earthquake, the reservoir serving a key pressure zone in the Santa Cruz water system that served two hospitals, drained (Lund, 1990). That loss of water can be attributed to approximately 85 pipe leaks and breaks. The system could not be refilled after damage was isolated because of a power outage.

In Rio Dell, following the 1992 Cape Mendocino earthquakes, a reservoir drained because of a pipe failure at a bridge crossing (Schiff, under preparation). The city was without water for four days.

Cost of Pipeline Replacement

Replacement of water system pipeline materials vulnerable to earthquake would be prohibitively expensive as an earthquake mitigation measure. The Seattle water system has approximately 2,400 km of pipelines less than or equal to 30.5 cm in diameter and approximately 550 km of pipelines larger than 30.5 cm in diameter (Ballantyne, 1988). Approximately 6 percent is in areas highly vulnerable to liquefaction. The large majority of the system is constructed of cast iron pipe. The estimated cost to replace the entire system with ductile iron or welded steel pipe would be over $1.5 billion. Replacing just the pipelines in particularly areas would cost an estimated $100 million. These costs exceed the Seattle Water Department's financial capability to replace vulnerable pipelines.

A monitoring and control system alternative will mitigate the effects of some pipeline damage at a cost less than replacing vulnerable pipelines.

MONITORING AND CONTROL APPROACHES

Peak ground acceleration, pipeline flow, and system pressure can be monitored to provide input for post-earthquake system control. Control decisions can be made locally or in a central location. Two types of valves are typically used for isolation. Monitoring parameters, control location, and control valves are discussed in this section.

System Monitoring Parameters

Earthquake control of a water system can be initiated by seismic switches triggered by a threshold peak ground acceleration, excess flow through a pipeline, or reduction in system pressure. A combination of the three alternatives can also be employed.

Seismic switches shut the system down before any flooding or secondary losses such as erosion occur. Unfortunately, they would activate regardless of the actual system performance. It may be that pipeline damage was only moderate, and that the water supply could keep up with the system demand/system leakage. If that was the case, keeping the system in operation would be preferable to shutting it down. The peak ground acceleration triggering device threshold should be set to the point where significant pipeline damage is expected.

The advantage of triggering the isolation valve using excess flow is that it is representative of the actual system condition, that is, the valve will only close if the flow rate is high. It may also be useful to monitor for non-earthquake related pipeline failures. Care must be used in selecting the excess flow threshold where the isolation valve would close. It must allow for peak demands in addition to fire-flow. It would be unsatisfactory to shut down a system that is delivering water for fire suppression but is not damaged.

The advantage of triggering the isolation valve based on system pressure is that it may better account for overall system function rather than localized flows; the disadvantage is that it may not adequately define local system function.

These three alternatives require additional study, and should be evaluated for each new application.

Local Versus Central Monitoring and Control

System monitoring and control decisions can be performed locally using an automated system. Local control decisions would be based on predefined threshold levels, as previously discussed. The major advantage of local monitoring and control is good reliability. The disadvantage is that the predefined threshold values may not be appropriate for all situations.

For smaller systems, it may be possible to incorporate manual valve closure for system segment isolation as part of the emergency response plan (Ballantyne, under preparation).

System status information can be transmitted to a central location using a Supervisory Control and Data Acquisition (SCADA) system, where control decisions can be made either manually or using a computer. System operators can be trained to manually isolate transmission or distribution system segments from their central location using the SCADA system. They would make their decisions based on the system status information received. System operators generally have an excellent understanding of how their systems operate and could be trained to further consider earthquake operating conditions.

The information could be fed directly to a computer where control decisions could be made, and transmitted back to the remote location using SCADA. Eguchi (1991) explored this approach. An intermediate alternative would be for the operator use the computer as a tool to assist him in making operating decisions.

The major disadvantage of central decision making is poor reliability of the SCADA system.

Control Valves

A range of control hardware is available, including a variety of valves and valve actuators. The primary consideration in selection of the system is reliability. The two most likely types of valves to be used for isolation would be globe valves and butterfly valves. Gate valves have been used, but are difficult to operate with stored energy sources.

Globe valves, configured as pressure-reducing or altitude valves, make use of system water pressure to actuate. They will not operate if the system has been drained. They are commonly used as altitude valves to limit the maximum water level in a reservoir or as pressure-reducing valves to feed water from a higher to a lower operating pressure zone. Their advantage is the use of system pressure for activation and the likelihood that they are already in place being used for other purposes. Their disadvantage is that they will not operate if there is no water in the system. There is some speculation that they may not operate if they have not been operated for several years, allowing scale to build up and restrict their movement.

Butterfly valves are used because they are actuated by rotating one-quarter turn, rather than multiple turns as required by a gate valve. This can be achieved by pneumatic or hydraulic cylinder actuators. Energy can be readily stored in the form of compressed air or nitrogen to power the actuators. Kanair (1987) offers such as system. Butterfly valve operator design must take into account the torque required to close the valve when there are high flows going through the valve.

Alternatively, electric actuators are available. The system should not be dependent on continued electric power for operation. Valves that require electric actuators require emergency generators. Their capital and maintenance cost, and reliability are disadvantages.

Batteries, continually recharged by trickle chargers, are useful for operation of SCADA systems, seismic switches, and solenoids for valve piloting.

Isolation valve selection is system-dependent but should take into account the considerations addressed above.

ISOLATION CONFIGURATIONS

Three monitoring and isolation control system configurations are described in this section.

Reservoir Isolation

Reservoirs can be isolated from damaged piping in the distribution system, as shown in Figure 1. An isolation valve would be installed on or near the reservoir to isolate it from the system when triggered by earthquake ground motion, excess flow, or reduced system pressure. Water would be saved in the reservoir, but the distribution system would be put out of service. Operations staff would respond by assessing the transmission and distribution systems, and isolating damaged areas. After those areas were isolated, the reservoir isolation valve would be reopened, restoring function to the undamaged portion of the system. This activity would hopefully take place quickly and in close coordination with the fire department. Potentially, water would be directed to areas where fires erupted by operations staff opening and closing appropriate valves. Saved water could also be available for tank trucks for fire fighting or drinking.

There are several advantages to this approach. It would save water regardless of pipeline damage, assuming that the reservoir remained intact. It would be less expensive than area isolation, requiring only a single valve for each reservoir. The valve may already be in place as an altitude valve and only require additional piloting hardware.

There are several disadvantages to this approach. There would be no water pressure available to help operations staff locate leaks. The entire system would be shut down during the leak location process. This could result in liability associated with critical water service water system contamination, or quick system reactivation concerns.

Isolation of Fault or River Crossings

An isolation valve could be installed on either side of a pipeline section that was highly vulnerable, such as a fault or river crossing. This configuration is shown in Figure 2. The same concerns for reservoir isolation are applicable for isolation of fault crossings or river crossings.

Isolation of Vulnerable Areas

Predefined areas of vulnerable transmission/distribution system piping can be isolated from the areas of the system that will likely remain intact, such as shown in Figure 3. Areas that are particularly vulnerable to pipeline damage, such as those that are susceptible to liquefaction, would be isolated from the remainder of the system. The isolation valves would be triggered by earthquake ground motion, excess flow, or reduced system pressure.

The major advantage to this approach is that significant areas of the system would remain on-line following the earthquake. This could mitigate liability associated with critical water service, water system contamination, or quick system reactivation concerns.

This type of system may require installation and maintenance of new valves specifically for this purpose. It also relies on knowing where the pipelines will fail. If there was significant pipeline damage in the area not isolated, the reservoir could still drain.

WATER SYSTEM CONFIGURATIONS AND ISOLATION CONSIDERATIONS

Water system configurations vary considerably. Whether or not a water system may lend itself to monitoring and control is dependent on the water system configuration. This section describes configurations of existing systems.

Systems such as the Seattle, Washington water system have large reservoirs feeding a few major distribution pipelines. This may lend itself to isolation of those reservoirs. Also, the Seattle system has one particular area that is much more vulnerable to liquefaction than other areas. This area could potentially be isolated.

The City of Bellevue, Washington system is fed by a single major transmission pipeline traversing its system from north to south. The hydraulic grade line of this pipeline is high enough to feed the majority of the system by gravity. The system is divided into 23 pressure zones that are fed through pressure reducing valves which cascade water down through the system. The Bellevue system may lend itself to a monitoring and control system by monitoring and isolating entire pressure zones. Control systems could be added to existing pressure-reducing valves. No new isolation valves would be required, reducing installation costs significantly.

The Memphis, Tennessee water system is supplied by a large number of small well supplies and associated at-grade reservoirs. The system is extensively intertied by a pipeline network. It would be easy to isolate a storage reservoir by shutting down a booster pump that pumps the water into the system. Unfortunately, the system is so intertied that isolating a single reservoir would not be very effective. Trying to isolate a vulnerable section of distribution system would be difficult, requiring a large number of control valves. Also, the geotechnical situation in the Memphis area is such that there are no significant areas that have a vulnerability much higher than other areas. The Memphis system may lend itself to isolation of particularly vulnerable pipeline sections such as river crossings.

CONCERNS

Isolation of reservoirs or damaged segments of a water system following an earthquake to allow operation of undamaged areas of the systems is a viable mitigation alternative. There are concerns that system segments will inadvertently be isolated either when no earthquake has occurred, or when an earthquake has occurred but has not done much damage to the water system. This section addresses those concerns.

Liability Associated With Critical Service

Continued water supply is critical for service categories such as kidney dialysis patients, hospitals, large computer/communications installations, and fire sprinkler systems. Fire sprinkler systems may be even more critical following and earthquake. The isolation control systems discussed herein propose automatically shutting segments of a water system. There is a concern that there may be liability associated with such systems, particularly if the shut-down occurs as a result of control system malfunction. For example, a building with fire sprinklers could burn; hospital operations could be impaired.

Contamination of Potable Supply

When a water system is shut down and drained by continued water use, there is an increased probability that the system will be contaminated by back-siphoning through cross-connections or infiltration of contaminated groundwater. The probability is increased following an earthquake if water and sewer mains are broken, which may allow passage of sewage into the water main. For this reason, water purveyors have procedures in place to keep systems in operation. If systems are intentionally shut down, operations personnel go to great lengths to minimize the chance that lines are contaminated. This is a time-consuming process.

Quick System Reactivation

Filling pipelines can be a time-consuming process. Normally, when a pipeline is emptied and being refilled, or being filled for the first time, it is done very slowly to allow air to escape and minimize water hammer, which may result in pipe damage. Following the Loma Prieta earthquake, a portion of the San Francisco AWSS drained. The fire department decided against refilling it quickly because of concerns over water hammer and further system damage. If a segment of a water system is inadvertently shut down and drained, air release and water hammer should be taken into account when refilling to minimize any damage.

Reliability

There are significant concerns regarding monitoring and control system reliability. Systems that are designed only to control post-earthquake system operation may be used only once every 25 years or longer. Operations staff are skeptical about maintenance of equipment used regularly, let alone equipment that would be used once in a lifetime. Piggy-backing an earthquake control system on a system that is used and maintained regularly may mitigate this concern.

The local monitoring and control system may be preferable to a centralized system. The SCADA system is not only dependent on transmitting and receiving hardware at both ends, but on the transmission corridor connecting the two. Buried cables are subject to damage in earthquakes caused by lateral spreading and fault movement. Microwave towers for radio-based SCADA systems are subject to misalignment in earthquakes. Failure of a SCADA system in the Seattle water system resulted in an incorrect activation signal under non-earthquake conditions. Also in Seattle, disruption of a single buried cable resulted in water system disfunction.

Specific hardware concerns about valve sticking and energy supply reliability were previously addressed. The reliability of each monitoring and isolation control system should be evaluated when it is configured.

Cost

Installation of SCADA systems and isolation valves specifically for post-earthquake system control is expensive. It is better to use existing valves and modify their control strategy to accomplish the desired post-earthquake system control. One example is the Bellevue water system, where the system is served through a series of pressure-reducing valves. Seismic switches could be added to the pilot systems of selected pressure-reducing valves for minimal cost.

EXISTING SYSTEMS

Four monitoring and control systems in place in the United States and Japan are described below.

Alameda County Water District

The Alameda County Water District, Hayward, California, has had a monitoring and control system in place for over 30 years. Their service area is divided by the Hayward fault similar to the configuration shown in Figure 2. Most of their storage is east of the fault in reservoirs located in the hills. Most of their customers are to the west of the fault, in the coastal lowlands adjacent to San Francisco Bay. Their oldest monitoring and control system is a specially designed hardware system located on a reservoir outlet line, and is triggered on excess flow. If flow increases beyond a predefined point, the increasing vacuum in a venturi tube closes an isolation valve. In their newest system, both excess flow and/or seismic switch will trigger valve closure. They use three different stored energy sources to close isolation valves in three different systems: 1) hydraulic pressure from the water supply, 2) high-pressure air stored in a receiver (continually replenished with a compressor when power is on), and 3) compressed nitrogen. Alameda uses both globe and butterfly valves for isolation.

One significant factor allowing their use of an isolation system is having a dual water source. They are isolating their storage reservoirs on the east side of the fault, which is supplied by a surface water supply. They also have a well field source on the west side of the fault. Their standard earthquake response procedure is to close the reservoir isolation valves (done automatically) and turn on the wells (which are fitted with emergency generators). This will keep the water system on-line unless damage is severe. If damage is severe, heavily leaking segments of the water system can be isolated by manual valve closure before the east side reservoir isolation valves are opened.

San Francisco Auxiliary Water Supply System

The San Francisco AWSS is designed to provide a highly reliable water supply for fire protection, particularly following an earthquake. The AWSS supplies a set of fire hydrants that are independent of the Municipal Water Supply System (MWSS). The MWSS supplies all other services and connections to buildings, including fire sprinklers. The AWSS was designed to allow isolation of segments of the system that were particularly vulnerable to earthquake damage, similar to the configuration shown in Figure 3.

The isolation system did not function properly following the Loma Prieta earthquake, for a number of reasons. The San Francisco Fire Department is modifying the system to mitigate the problems encountered in Loma Prieta. Control system flexibility is being added to allow either remote or local valve actuation using electric operators, as well as local mechanical actuation, using truck mounted operators. Both radio and hard-wired telemetry is provided between critical valves and the central control facility.

One deficiency was dependence on electrical power. The AWSS isolation system valve actuators required electrical power. Power was out in San Francisco following Loma Prieta, making the actuators unusable. A battery operated system is being installed at each valve site.

A major advantage of having a water system delegated solely for fire protection separate from the potable water and fire sprinkler water system is elimination of concern over liability associated with critical water services and water system contamination. Intra-department communications required for system operation during fires may be better than inter-department communication required in other system between the fire department and water department in other cities.

City of Whittier and other Cla-Val/Flo-Loc Systems

The City of Whittier, California installed several excess flow-triggered reservoir isolation control valve systems following the 1987 Whittier Narrows earthquake. The configuration shown in Figure 1 is similar to these systems. They use globe valves (manufactured by Cla-Val) with a

pilot system triggered by excess flow/pressure drop across the valve. The normal system hydraulic pressure is used to close the valve. Since those systems were installed, Cla-Val has configured a system where the pilot system is triggered with a Flo-Loc seismically actuated switch. That system, marketed commercially in the United States, addresses the hardware considerations described herein.

City of Yokosuka, Japan City Waterworks Bureau

The City of Yokosuka, Japan, has a earthquake control valve system said to be one of the most sophisticated in Japan. The City of Yokosuka serves about 450,000 people and is located south of Tokyo on Tokyo Bay. They were heavily impacted by the 1923 Kanto earthquake. Their system employs a combination of seismic switches and flow monitoring to shut down key pipeline links with electrically operated butterfly valves. The telemetry is intertied, using a microwave system. Additional information on the detailed control strategy for this system is being sought.

PRELIMINARY RECOMMENDATIONS

Liability, contamination, quick system reactivation, and reliability all relate, at least in part, to inadvertent system shutdown. Inadvertent system shutdown can be mitigated by providing improved control reliability and/or use of dual supplies/reservoirs.

Improved Control Reliability

Control reliability can be achieved either by hardening the control system or providing redundancy/flexibility. System hardening can include selection of seismic-resistant systems and seismic-resistant design of each system component, such as:

- Radio telemetry systems rather than hard-wired systems because of the vulnerability of buried conduits to permanent ground movement
- Seismic-resistant structures housing system components
- Component equipment anchorage
- Backup power supplies for electric power-dependent systems.

Control system redundancy/flexibility can include:

- Both radio and hard-wired telemetry systems

- Combined seismic and excess-flow activated valves, requiring both to exceed their design threshold before activation
- Local valve control open/close decisions with central operations center control override
- Electric/pneumatic actuated operators with provision for manual override (truck-mounted valve operators)
- Control system with redundant components
- Trained emergency response personnel with clear system operations understanding and communications capability.

Use of Dual Supplies/Reservoirs

Provision of dual or redundant supplies/reservoirs for each system or system segment, such as shown in Figure 4, will minimize inadvertent shutdown concerns. The control strategy would be to isolate one of the supplies/reservoirs and allow the other to continue on-line. Two scenarios are described below: 1) an earthquake causing significant water system damage, and 2) inadvertent isolation system activation.

If an earthquake causes significant water system damage, the isolated supply/reservoir's water would be saved until the damaged segments were isolated. The supply/reservoir left on-line would be lost. Maintenance personnel would locate and isolate leaks, and open the reservoir isolation valve.

If the isolation system activation is inadvertent, the entire water system would remain in operation served by the on-line reservoir. The isolated reservoir would be brought back on-line when the isolation was identified by operations personnel.

There may be an instance where one supply/reservoir is inadequate to provide normal demands, but two supplies/reservoirs are. This needs to be considered in design of isolation systems.

CONCLUSIONS

Ten conclusions can be drawn from the study to date:

- Post-earthquake water system function is poor
- Earthquake damage mitigation by pipeline replacement is too expensive

- Post-earthquake monitoring and control system are a mitigation alternative
- Earthquake ground motion, flow, or pressure can be monitored to provide information for post-earthquake system control; control decisions can be made locally or at a central location
- Monitoring and control hardware are readily available; systems are in place in California
- Systems can be isolated at reservoirs or on the periphery of vulnerable pipeline areas
- Monitoring and control system designs should be system-dependent
- Liability associated with critical service, contamination of the potable water supply, quick system reactivation, and reliability are concerns associated with inadvertent isolation system activation
- Monitoring and control system costs can be minimized by piggy-backing them on other water system control system hardware
- Improved control reliability and use of dual supplies/reservoirs will help mitigate inadvertent shutdown concerns

ACKNOWLEDGEMENTS

This project is being funded by the National Center for Earthquake Engineering Research. Their support is greatfully acknowledged.

The author has conducted interviews with each of the following water purveyor organizations, specifically asking questions about the issues presented in this paper. Their time and insight are greatfully recognized. Representatives from each organization typically included operations and engineering staff. The contact person is shown for each organization.

California

Alameda County Water District, Hayward - Mr. William Blair
City of Los Angeles Department of Water and Power - Mr. Fred Barker
City of San Francisco Fire Department - Chief Scales
City of Whittier Water Department - Mr. Jim Johns (phone interview)

Oregon

City of Portland, Water Bureau - Mr. William Elliott

Tennessee

City of Memphis Light, Gas and Water Division - Mr. Kevin Poe

Washington

City of Bellevue Department of Public Works and Utilities - Mr. Wes Jorgenson
Sammamish Plateau Water and Sewer District, Issaquah - Mr. Ron Little
City of Seattle Water Department - Ms. Laurel Harrington

Japan

Yokosuka City Waterworks Bureau - Professor H. Sato, National Defense Academy

Equipment Suppliers

Two equipment manufacturers are actively promoting use of earthquake control system for post-earthquake water system control: Cla-val Co., Mr. Ray Williams; and Flo-Loc Control Systems, Inc., represented by GC Systems, Mr. Jack Boyd. There input is acknowledged.

REFERENCES

Ballantyne, D.; *Earthquake Loss Estimation Modeling of the Seattle Water System; Year End Status Report*, Kennedy/Jenks Consultants No. 886005; supported by USGS Project Number 14-08-0001-G1526, 1988.

Ballantyne, D.; K. Parker; *Emergency Response Plan*; Sammamish Plateau Water and Sewer District, Issaquah, Washington; under preparation by Kennedy/Jenks Consultants.

CH2M Hill, *Bellevue Water Comprehensive Plan*, City of Bellevue Washington, May 1985.

Eguchi, R.T.; J.D. Chrostowski; C.W. Tillman; A. G. Ayala; *A Rapid Post-Earthquake Damage Detection Method for Underground Lifelines*; Lifeline Earthquake Engineering; ASCE, Technical Council on Lifeline Earthquake Engineering; Monograph No. 4; Michael Cassaro, Editor; August 1991.

Flo-Loc Control Systems Inc., Product Information Literature, San Clemente, California, 1992

Kanair Controls, *Instruction Manual for Nitrogen Powered Hydraulic Actuator System*, Alameda County Water District; Hayward, California, October 1987.

Khater, M.; C. Scawthorne; T.D. O'Rourke; F. Blackburn; *Performance of AWSS of San Francisco During and After Loma Prieta Earthquake*; Presentation at the 4th U.S. - Japan Workshop on Earthquake Disaster Prevention for Lifeline Systems, August 19-21, 1991, Los Angeles, California.

Lund, L.; G. Laverty; D.B. Ballantyne; et al; *Water and Sewage Systems*, Lifeline Chapter in the Loma Prieta Earthquake Reconnaissance Report, Earthquake Spectra of the Earthquake Engineering Research Institute, Supplement to Volume 6, May 1990.

Memphis Light, Gas and Water Division; *Master Plan for Future Development of Water System, 1991 Planning Edition*; Memphis, Tennessee.

Schiff, A.; L. Lund; *Reconnaissance Report on Lifeline Performance in the Cape Mendocino Earthquakes*; ASCE Technical Council on Lifeline Earthquake Engineering; under preparation.

Also, see interviews listed under acknowledgements.

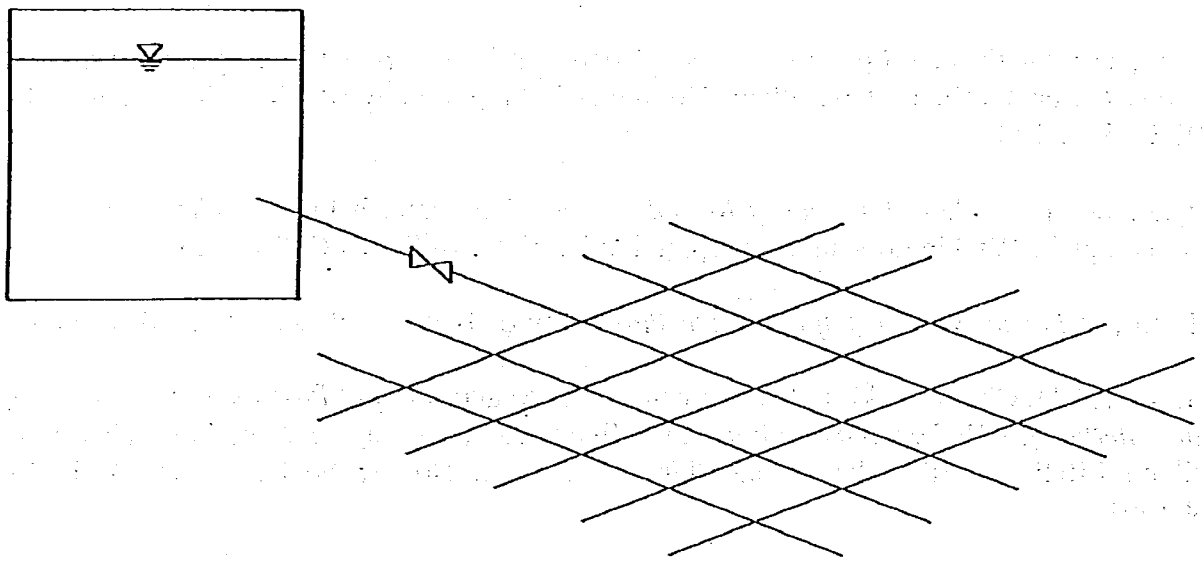


Figure 1 - Reservoir Isolation
(Whittier, California)

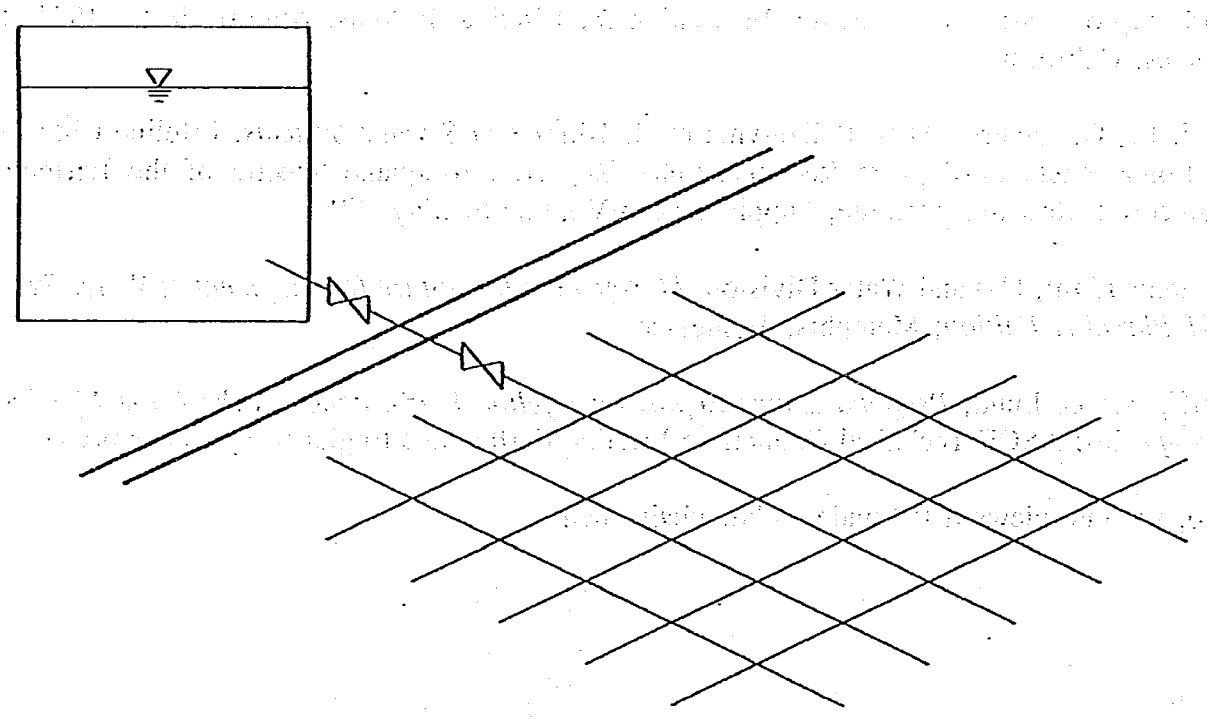


Figure 2 - Isolation of Fault or River Crossings
(Alameda County Water District, Hayward, California)

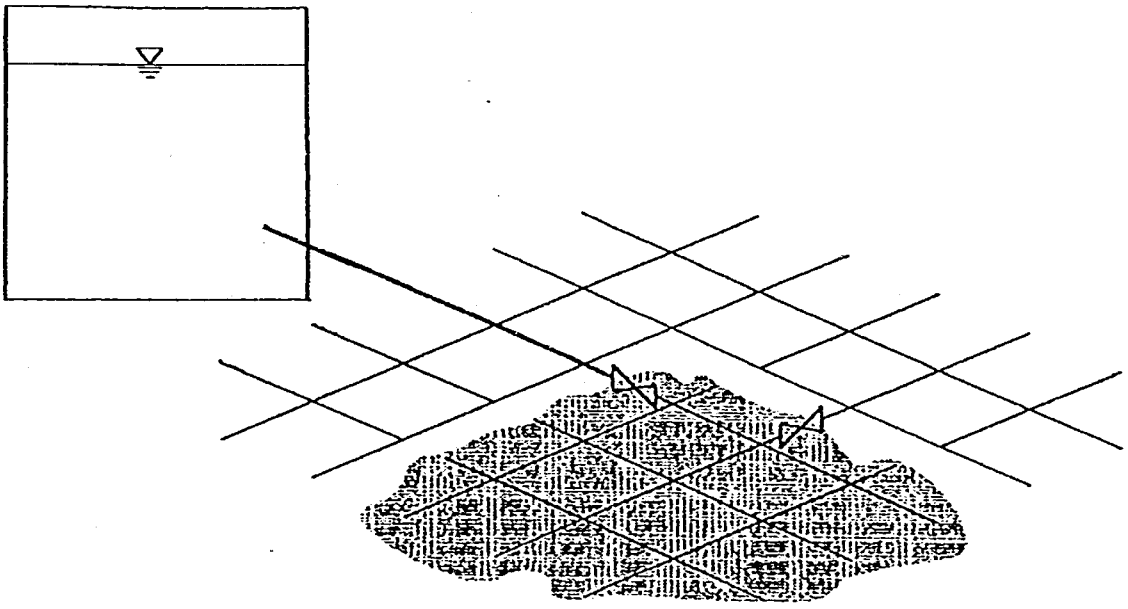


Figure 3 - Isolation of Vulnerable Areas
(San Francisco, California AWSS)

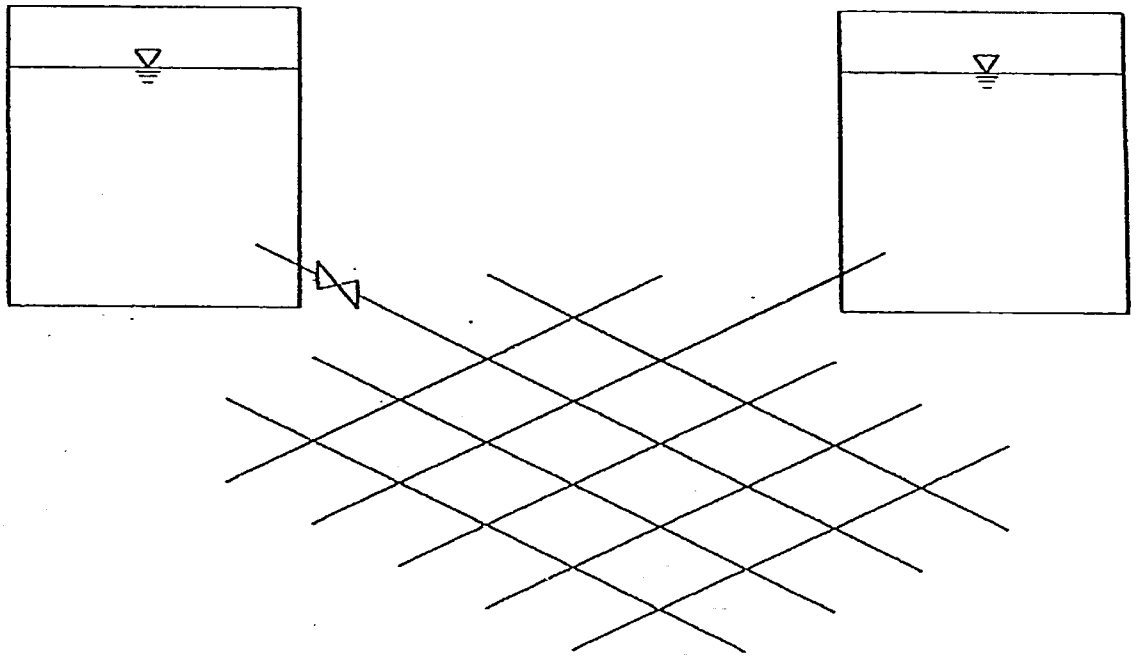


Figure 4 - Dual Supply/Reservoir

VULNERABILITY OF FIBER OPTICS CABLES TO FAULT RUPTURE, A PROPOSED FIELD EXPERIMENT

Felix S. Wong and Jeremy Isenberg
Weidlinger Associates, Los Altos, California, USA

INTRODUCTION

Weidlinger Associates, which has been engaged since 1975 in lifeline earthquake engineering applied to buried pipelines and telecommunications facilities, has suggested an experiment to study buried fiber optical cables subjected to surface rupture accompanying fault movement. The site of the proposed work is the field station at Parkfield, California where an experiment is currently in place that will provide data on the performance of buried pipelines subjected to lateral offsets and to ground strains from seismic wave propagation. The experiment, which is sponsored jointly by American (NSF and NCEER) and Japanese (University of Kyoto, Osaka Gas and Tokyo Gas Companies) institutions, is designed to capitalize on a recurrance of the 1966 Parkfield-Cholame earthquake sequence on the San Andreas Fault. This event has not yet occurred, making it possible to develop further experiments of the type described below. Successful operation of the recording system was confirmed during low intensity shaking from the Loma Prieta earthquake (October 17, 1989)[1].

We propose to bury fiber optics cables, an essential component of a modern communications system, across a strand of the San Andreas Fault where fault creep is currently taking place and where 4 inches of lateral offset occurred in the earthquake sequence of 1966. Unlike transmission and switching equipment, computers, etc. which constitute the inside plant of a communications network, cables are spread over large urban and surburban areas where they are exposed to such hazards as ground strains from travelling waves; to ground failure from landslides, liquefaction and fault rupture; and to collateral hazards. Their distributed nature makes damage mitigation measures (such as armour, sheathing, conduit) cost-prohibitive. In some circumstances such as the crossing of a fault or at narrow bridges, the hazard is unavoidable.

Data on the vulnerability of fiber optics cables exposed to ground rupture are scarce, although anecdotal evidence from the Loma Prieta Earthquake indicates they can be robust. Adding selected cable articles to the field experiment prior to the main Parkfield event can yield much valuable data A preliminary study of requirements for an add on experiment is described below.

PARKFIELD TEST SITE

The test site is located at Owen's Pasture near the hamlet of Parkfield in Central California, at the intersection of locked and creeping segments of the San Andreas Fault (see Fig.1). The layout of the test site is shown in Fig.2 which shows a number of pipe segments already in place. The basic objective is to study how travelling waves and surface offset

[1] The U. S. Geological Survey is a participant of the project, and Osaka Gas, Tokyo Gas and Kyoto University donated transducers and electronics equipment to monitor the pipeline response.

transmit strains to welded steel and ductile iron pipe segments crossing the fault zone and to estimate ground strains in the regions surrounding the fault. Figure 3 illustrates the mechanics of idealized slip and its effect on a buried lifeline.

To investigate the behavior of pipelines intersected by surface ruptures, the welded steel pipes are instrumented with strain gages, and the jointed ductile iron pipes are instrumented with displacement transducers. A line of monuments is placed cross the predicted location of the surface rupture by the USGS to measure the lateral offset during pre-earthquake creep and earthquake-induced surface rupture phases. A USGS creepmeter XPK1 measures the coseismic creep. One of the most important issues which the experiment is designed to address is the anchor length, i.e., the distance from the center of the fault rupture zone to the anchor point.

Ground strains are derived from records of three seismographs contributed by the Urban Hazards Research Institute of Kyoto University. Strain components are computed from the horizontal components of ground displacements imposed the vertices of a triangular finite element corresponding the the region of ground delineated by the three seismograph stations. By comparing the ground strain with pipe strain obtained from strain gages, one can deduce the relationship between ground strain and pipe strain and the relative importance of wave propagation and surface offset.

FIBER OPTICS CABLES AND THEIR SEISMIC VULNERABILITY

An optical fiber communication system consists of a light source, the fiber itself, and a light detector at the distant end, as shown in Fig.4. Input electrical signals are converted to optical signals which are then transmitted over an optical fiber waveguide to a receiver. At the receiver, the optical signal is converted back into electrical format by an optical-to-electrical converter. Optical-fiber transmission links accept electrical input in digital or analog form. The transmitter sends the optical signal by modulating the output of a light source by varying the source drive current[2].

The transmission distance is set by the available power margin between the transmitter and receiver (i.e., the difference in decibels between the transmitter optical output and required reciever input). Each optical data transmission system element has its associated losses expressed in decibels. The power margin has to match the accumulated losses of the associated hardware to ensure that the optical signal reaching the receiver falls withn its sensitivity. If necessary and depending on the degree of smearing, noise, and losses in the fiber, the light pulses are detected and regenerated along the length of the system at regular intervals by repeaters.

Light is the carrier wave for signals multiplexed together and transmitted over optical fiber. Whereas it is difficult to modulate the frequency or amplitude of the light in a highly linear fashion, it is very simple to turn the light on and off. Optical fibers thus are particularly well suited for carrying digital signals that have been time-division multiplexed together; light has an extremely high frequency and can be turned on and off at an extremely fast rate, and hence a very large amount of information can be carried over a single optical

[2] When the speed of the system is less than 100 Mbps, simple light-emitting-diodes are usually used as the light source, as they are economical and reliable. For speed higher than 100 Mbps, a laser must be used. The light output of a laser is a collimated beam of single-frequency coherent light which makes it easy to couple the beam to single-mode fiber. A light-sensitive semiconductor diode, such as the PIN (positive-doped, intrinsic and negative-dope sandwich) or avalanche diode, is usually used as the light detector.

fiber[3]. This large capacity combined with their freedom from noise and interference, low cost, low loss and small size are some of the reasons why optical fibers have truly revolutionized transmission technology.

Optical fiber offers many advantages over other transmission media. The fiber itself is flexible, inexpensive and light-weight. Because light is carried by the fiber, optical fiber is not prone to electrical and electromagnetic interference. Because no light escapes from the fiber nor can enter it from outside, there is no leakage or crosstalk between adjacent fibers. The bandwidth and capacity are extremely high, and losses are quite small. On the other hand, the extremely small size of the fiber - one-tenth the diameter of a human hair for single-mode fiber - makes it delicate in other ways. For instance, splicing becomes very tricky. A lateral or angular misalignment will result in signal degradation. For example, as Fig.5a shows, a lateral misalignment of one-fifth of the fiber core diameter results in a 1 dB loss, and the degradation increases exponentially so that it is infinite at 1/2 core diameter. Loss due to angular misalignment varies with the fiber type (single or multi-mode) but are significant even for misalignments of a few degrees as fiber loss specifications are in the 1-1.5 dB range (Fig.5b).

Other factors cause signal degradation in a fiber-optic system but are not relevant to our project. They are absorption loss caused by the presence of impurities in the fiber material, scattering losses resulting from fundamental fluctuations in glass density and composition, and the degradation of light by differential delay (pulse broadening or spreading). Finally, microbends in the fiber can cause radiation losses. The microbends are sometimes incurred during cable fabrication, and radiation losses can be minimized by minimizing all contact between the fibers and other bodies. Radiation losses can also results from abrasions or dirt on the outer surface of the fiber.

Structurally, fibers are extremely strong. High quality fibers have a tensile strength of 100,000 psi when first manufactured, but the strength decreases with time and micro-fracture growth. To overcome problems such as fragility, microscopic fractures, and weakened fiber strength due to bending, flexing, or stretching, fibers are made into cables. Cables are built in various configurations, but all have, in addition to the fibers, one or more strength members, some kind of buffing, and an overall sheath. Figure 6 uses single-fiber cable for illustration. The optical fiber is located in the center an surrounded by the buffering material. This material has good chemical resistance and buffers against abrasion. A strength member forms the next layer, providing protection against impact, crushing, and longitudinal stretching. The outer jacket is a tubular sheath that minimizes microbending, shields from the environment, and establishes a limit of cable bending.

Most commercial cables have a rated maximum load of 600-1,000 lbs as stated in most installation manuals, but the actual strength is much higher[4]. Consequently, structural failure of fiber cables by ground straining is seldom observed. Most failures are due to concentrated shear displacement such as from an accidental backhoe blow (Fig.7), or as the proposed experiment is designed to ascertain, fault rupture. Hence, the size of the rupture

---

[3] The theoretical maximum capacity of a single light channel in single-mode fiber is about 200 Gbps, or the equivalent of 30,000 paperback books per second, 3 million digital voice circuits, or 4,000 television signals. If the entire light spectrum operable for fiber was used through color multiplexing, the theoretical capacity increases to 50,000 Gbps.

[4] The exact consequence of over-stretching a fiber optics cable is not clear. It is believed that repeated overloads will cause the crystal structure to change with time, leading to significant degradation in performance.

zone, in addition to the amount of slip, is an important parameter to be investigated in the experiment. However, as signal transmission quality can degrade significanly with minute changes to the fibers, fiber optics cables do not need to sustain significant physical damage to fail. Stretching or shearing may induce pinching, lateral and angular shifts such that even if the fibers are still structurally intact, the function of the cable is lost[5]. For this reason, the field testing of cables should not focus only on the structural aspect of the test specimen. A measure of vulnerability must include transmission loss, and the experiment must include testing of the signal transmission characteristics of the fibers before and after the event.

PROPOSED ADD-ON EXPERIMENT

We propose to add several segments of fiber optics cable to the experiment, installed (buried and inside conduits) according to industry procedure across the fault. The cables will be installed on the Northwest side of the site, between the TR FLEX jointed pipe and the compression segment of welded steel pipe. Each cable segment is approximately 200' long and there is a clear strip of 40' width in the field for trenching.

Parameters to be investigated are:

- Fiber Type: For example, 96 strand, bi-directional, 8 micronfiber; 24 strand
- Burial Configuration: For example, bare in sand, in vitrified or PVC conduits
- Slack Condition: For example, manhole, snaking or straight.

There are many variations of cable type, burial configuration and slack condition. As it is impossible to address them all with limited space and resources, only the most common type/configuration (i.e., cables that are prevalent in Northern California) will be considered.

Success of the experiment requires participation of the telecommunications industry (telcos, cable vendors, construction firms, and equipment manufacturers). We should jointly identify the configuration(s) for testing, the fiber type, burial configuration, etc. Second, we need to acquire the cables, and install the cables/conduits at the site according to standard procedure. Third, we need (portable) equipment and personnel to measure the signal transmission characteristics of the cables before and after the event, and probably several times in-between.

We would ask the industry to donate the cables, handle the special requirments in installation, and perform the measurements. A similar cooperation effort with the piping industry has worked to every one's benefit. Telecommunications also requires specialized equipment and specially trained personnel, which make industry cooperation even more imperative.

In particular, from recent discussions with industry sources, we have identified the following procurement requirements:

1. Cables - While 200 ft segments of cables are not expensive (about $500-1000 each), most vendors do not sell them in such quantities.

---

[5] For example, a general rule of thumb for inside plant cable placement is that the minimum curvature should be 10D, where D is the diameter of the cable (usually 4 inch) when the cable is unloaded, and 20D if it is stretched.

2. Installation - Installation has two phases. The ends of the fibers must be prepared so that are ready for hook-up and test. This means a pigtail and splice per fiber, which connects the fiber to a connector in an end-box. The cost is about $50 per fiber, and trained telecommunications technicians are needed to perform the work. For a 96-fiber cable, the cost of this preparation is about $5,000. Fortunately, only one end of the cable needs to be prepared this way. The other end can be unconnected. As long as the fibers at the free end are cut cleanly, they will behave as a mirror and reflector for the test signals.

The prepared cables will then be laid in the ground and in conduit as needed. Outside contractors can be used for this purpose as was done for the laying of the water/gas pipes. One needs to make sure that the cables/conduits are placed at the right depth, properly sand backfilled, and tamped.

3. Testing - To measure the transmission degradation inflicted by seismic hazards, a light source and power meter (about $1,500) and a high precision OTDR[6] (Optical Time Domain Reflector, about $23,000) are needed. The OTDR works much like a radar; a blurp in the reflected signal at a particular part of the waveform indicates where the anomaly is.

SUMMARY

As seismic protection of telecommunications equipment continues to improve to the point where direct failure of the critical equipment is unlikely, vulnerability of a telecommunications lifeline network may be governed by the vulnerability of the outside plants (cables, CEV, towers, etc.). In particular, transmission fiber optics cables, because they are spatially distributed, are exposed to seismic hazards such as fault rupture, land failure and collateral damage from failure of supporting structures. Recent trends in the industry towards more concentration and less dispersion (fewer but higher capacity trunks) heighten the importance of these assets to the robustness of the overall system.

We have described a proposed field experiment to study the seismic performance of buried fiber optics cables. Testing of cables differ from testing of pipes in two aspects. First, structural failure or damage need not take place for the fibers to lose their transmission function. This is analogous to leakage in water pipes except that transmission effectiveness is extremely sensitive to slight physical impairment to the fibers. Second, preparation, placement and testing of fiber optics cables require expensive and specialized equipment and personnel. Cooperation of the industry is essential to the success of the project.

---

[6] High precision is required because of the short length of the cable.

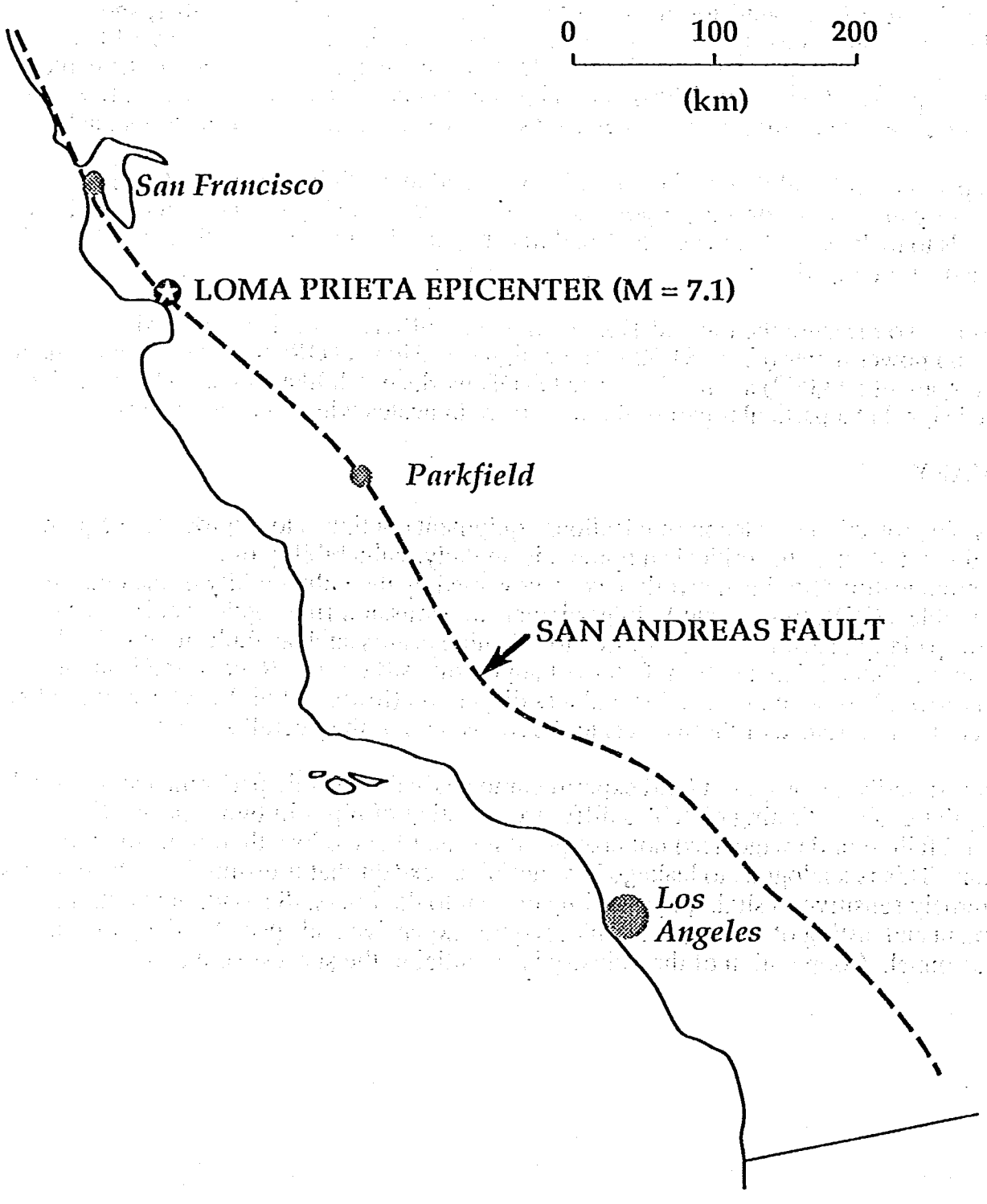


Figure 1. Location of Parkfield Test Site

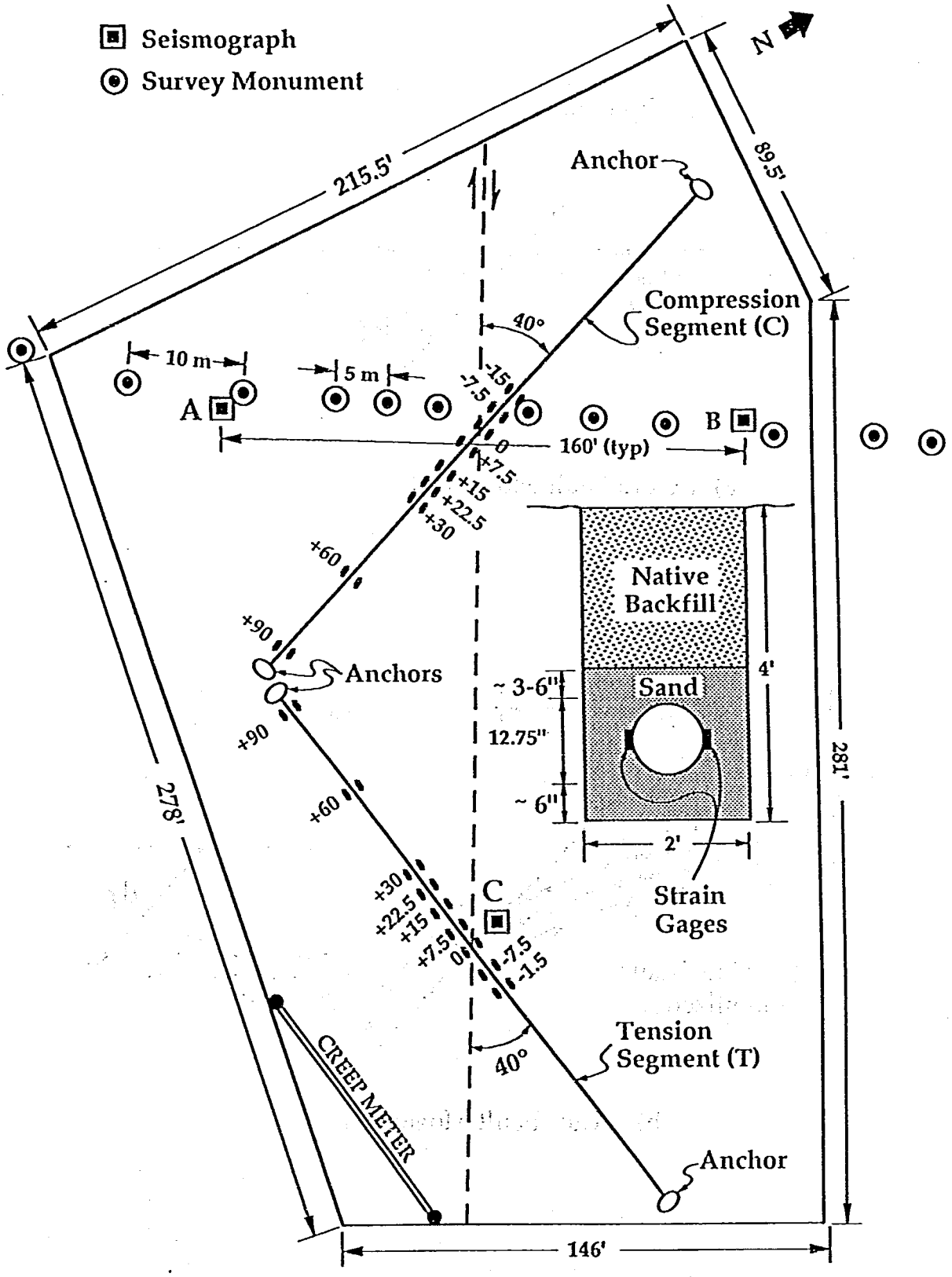
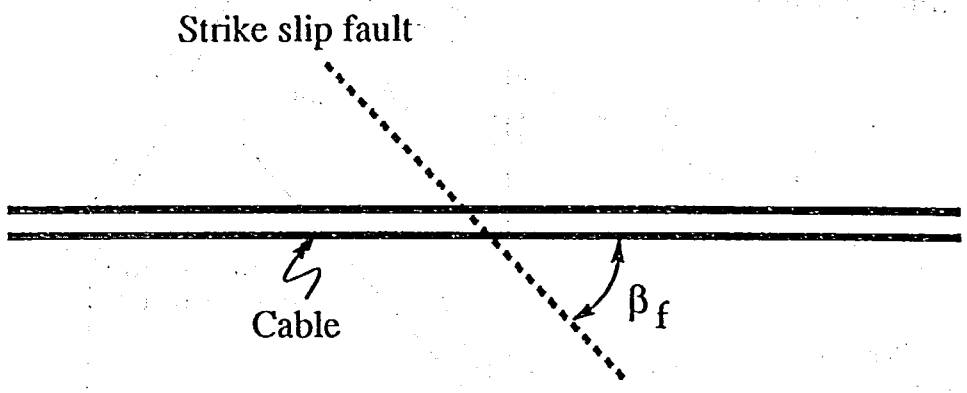
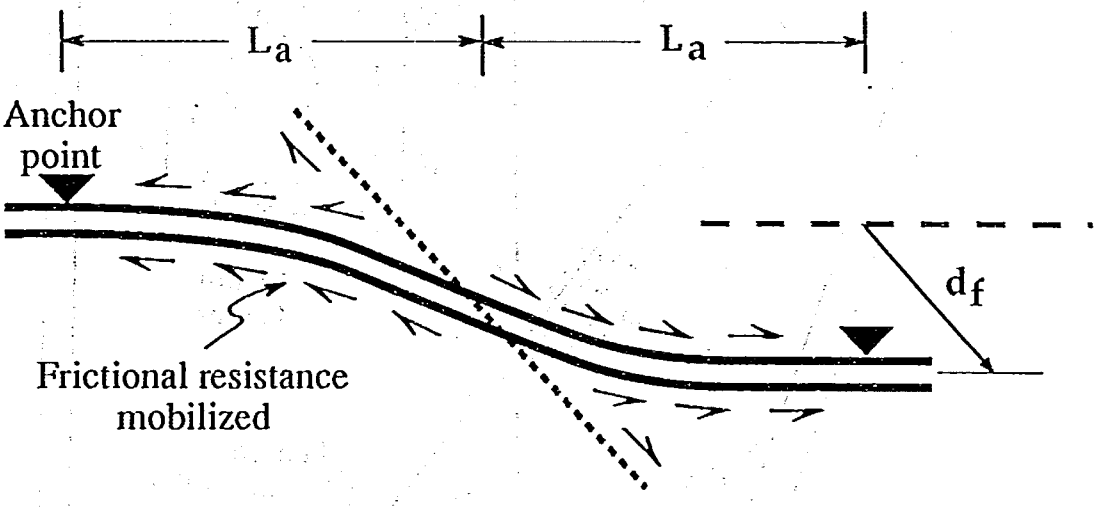


Figure 2. Parkfield Test Site, Plan View



a) Before Fault Movement



b) After Fault Movement

Figure 3. Stretching and Offset of Cable Due to Fault Movement

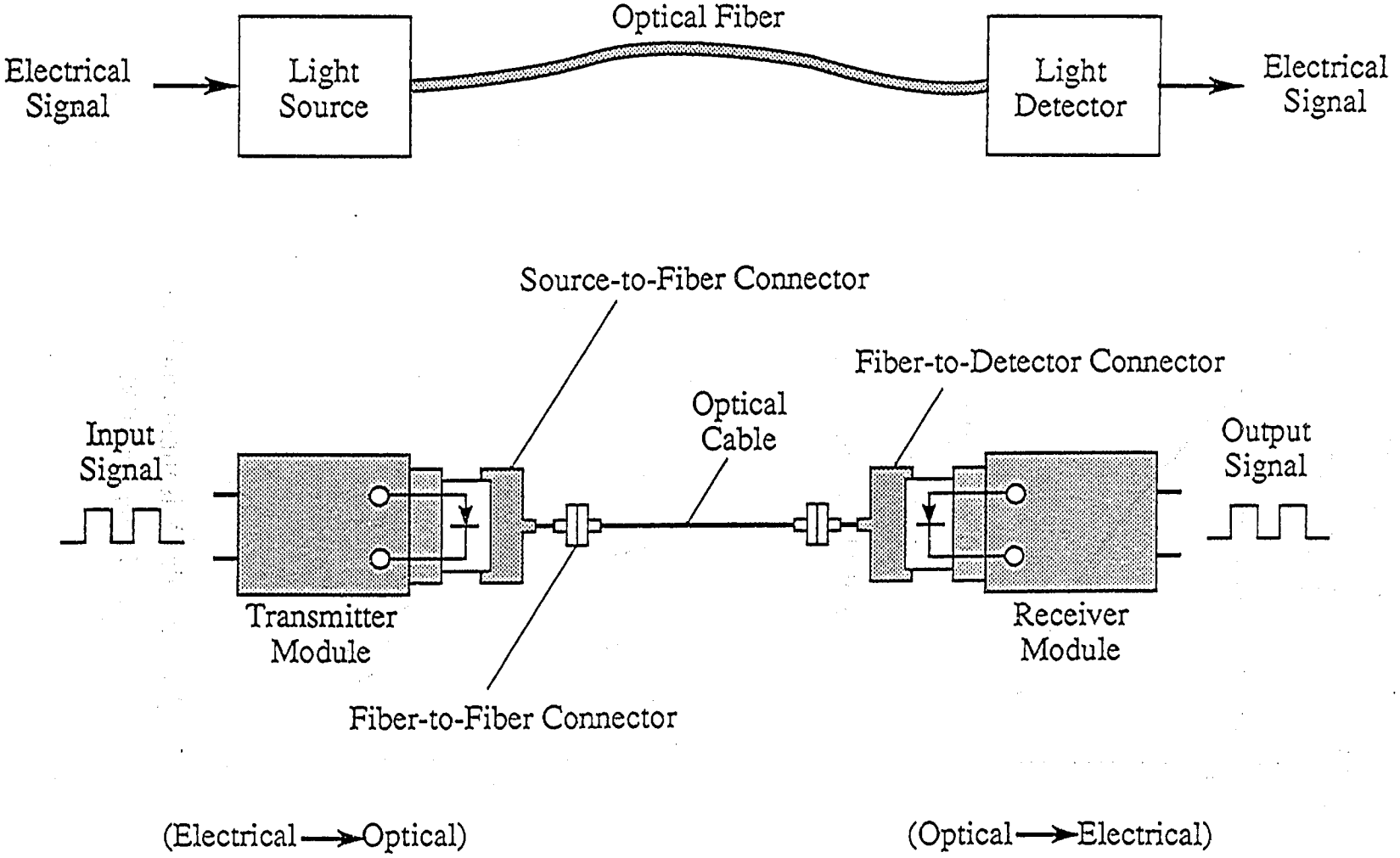
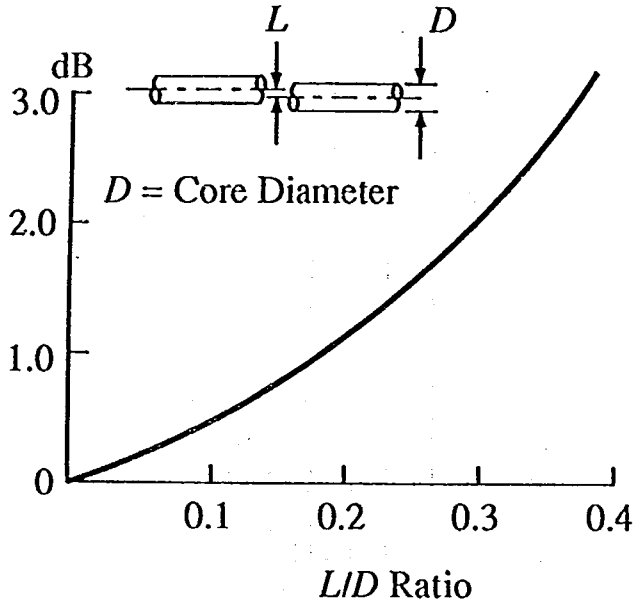
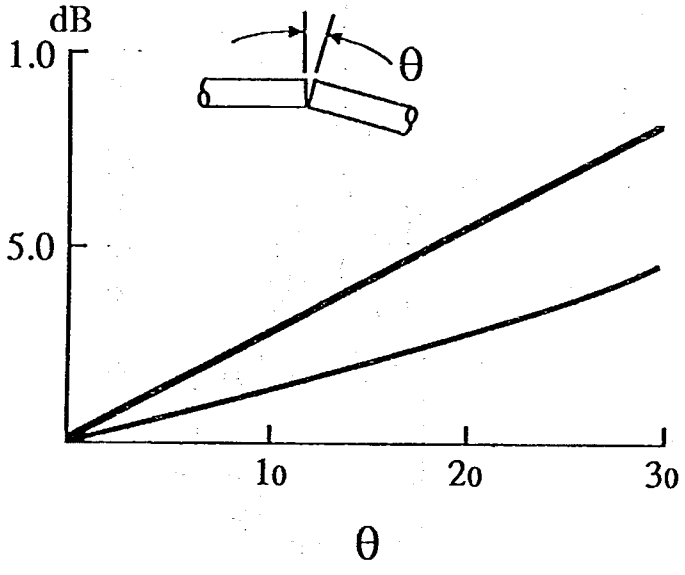


Figure 4. Typical Optical-Fiber Data Transmission Link

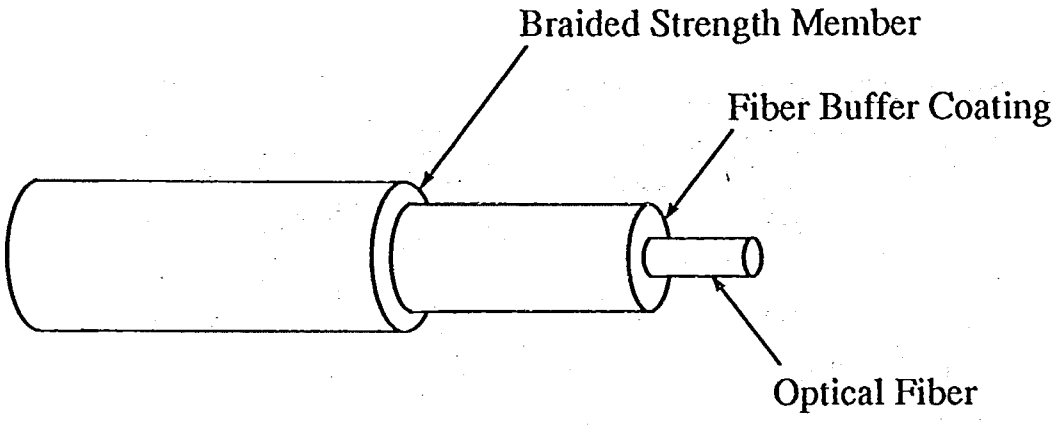


(a) Lateral Misalignment Loss



(b) Angular Misalignment Loss
(from Pooch et al, 1991)

Figure 5. Signal Degradation in Optical Fibers



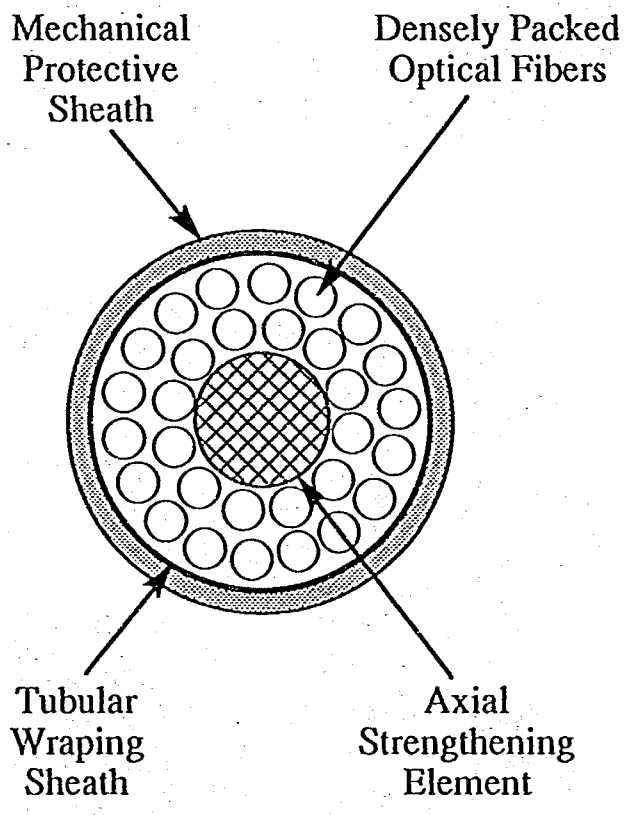


Figure 6. Example of Single-Fiber Cable with Axial Strengthening

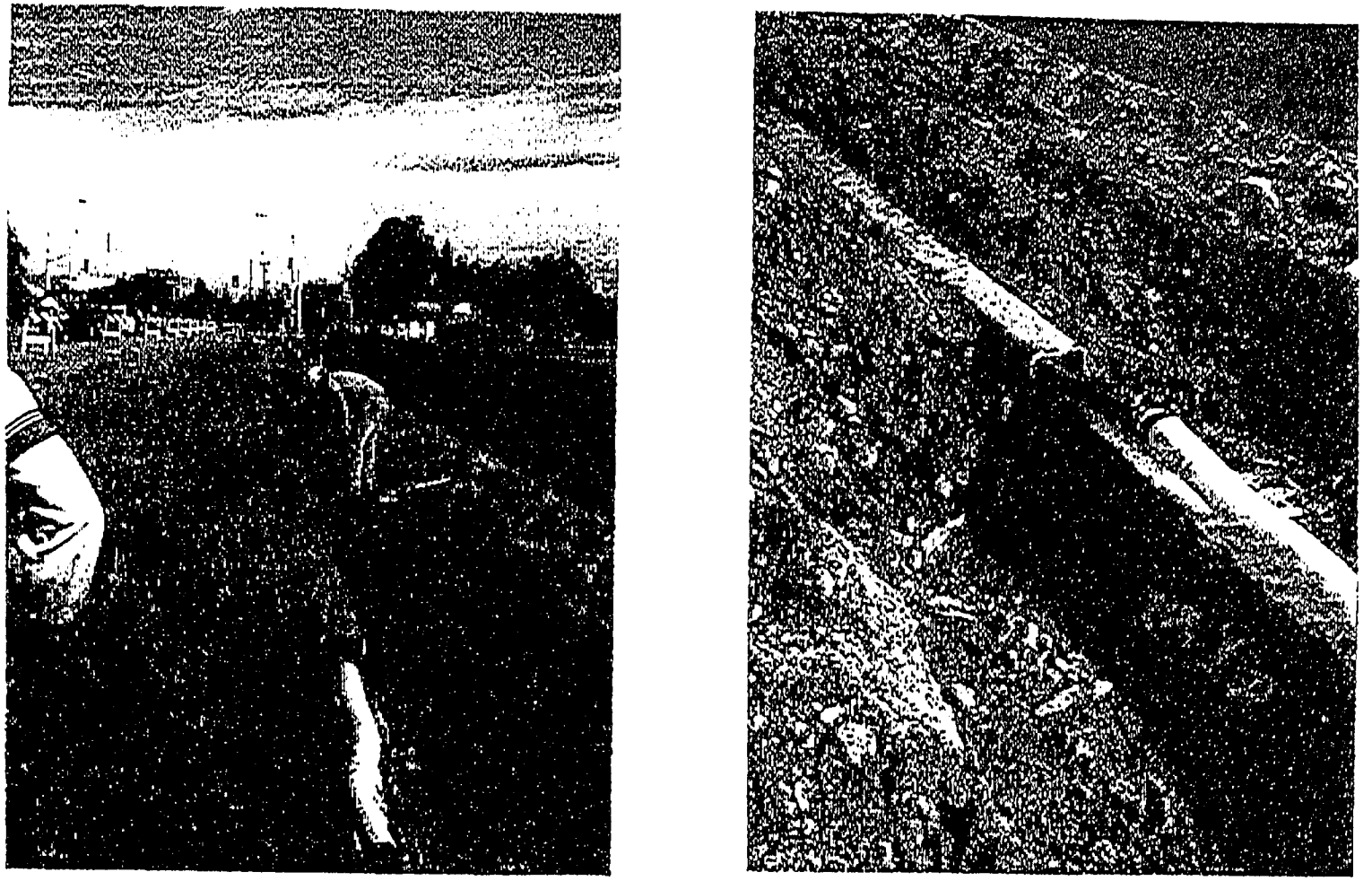


Figure 7. Examples Of Damaged Cables.

Session-10

Impact of Seismic Effects

J-19) Effective Measures for Reducing People's Anxiety in Underground Spaces During Earthquakes
(Saito, E., Ikemi, H., Nakano, H. and Kobayashi, N.)

U-14) Indirect Losses Caused by Lifeline Damage or Disruption
(Eguchi, R.T., Seligson, H.A. and Wiggins, J.H.)

U-15) Earthquake-Induced Congestion Impacts on Local Telephone Networks
(Forys, L.J.)

EFFECTIVE MEASURES FOR REDUCING PEOPLE'S ANXIETY IN UNDERGROUND SPACES DURING EARTHQUAKES

By E.Saito,H.Ikemi,H.Nakano and N.Kobayashi

Dept. of Civil Engineering,Technical Research Institute, FUJITA CORPORATION

ABSTRACT

This study concerns methods for reducing lurking anxiety people could have about earthquakes when they are in underground urban spaces.
A survey using a questionnaire was conducted to study factors belonging to the bottom layer of the hierarchical model the authors already proposed as a structural model of anxiety about earthquakes in underground urban spaces. The factors in the bottom layer are fundamental causes of lurking anxiety felt by people. This survey was conducted in two underground malls: one old mall which started in the 1950s and a new mall which started in after 1985. People were asked about the degree of anxiety about each factor listed in the questionnaire and the reason for the anxiety or suggestions of remedies.
The results of the survey have revealed that there are a number of bottom-layer factors which causes people in the new mall to feel the same degree of anxiety as in the old mall. According to the results of inference based on the structural model, factors specific to underground environment are characterized by a smaller difference in the degree of anxiety between new and old malls than any other major factors of lurking anxiety.
This paper proposes a number of methods to reduce such anxiety according to the results of the above analysis and the answers to the questionnaire stating the reason for anxiety and suggestions of remedies. It also numerically demonstrates the effects of these methods using an inference model. One of these method is a method which could be achieved through earthquake engineering efforts; it is to clearly show people how the underground structures resist earthquakes (what degree of earthquake resistance is assured in the event of an earthquake with a particular intensity).

INTRODUCTION

In Tokyo and other large urban areas, the construction of large underground structures is expected because of serious restriction on use of land on the ground. It is generally said that underground facilities are more resistant to earthquakes than ground facilities. However, since Japan is a country distinguished from most of other countries in the world by frequent earthquakes, seismic design is a primary importance in constructing large-scale underground structures.

For underground malls, underground parking lots, underground road tunnels, and underground urban complexes combining the above in which people act in different ways, it is necessary not only to provide the underground facilities with earthquake resistant properties, but also to reduce anxiety felt by people about earthquakes. According to a survey using a questionnaire to 720 passengers in an underground malls[1], for example, anxiety about earthquake disaster ranked second to anxiety about fire. Another survey using a questionnaire to 1713 people consisting of underground mall managers and employees[2] indicates that over one half of the people feel anxiety about

earthquake disaster. Such lurking anxiety might cause unexpected confusion in the event of an earthquake. This study aims at proposing methods for reducing such anxiety.

The paper discusses the following subjects:
1) A survey using a questionnaire was conducted in new and old underground malls to study the difference in the degree of anxiety about each factor given in the questionnaire between the old and new malls. These factors belong to the bottom layer of the hierarchical model[3] already proposed as a structural model of anxiety about earthquakes in relation to the underground malls. The bottom-layer factors are fundamental causes of lurking anxiety.
2) The examinees were also asked about the reason for anxiety about each factor or any suggestion for remedies. The replies to these questions and the results of the study in Item 1) above were analyzed to propose a number of measures for reducing anxiety.
3) On the assumption that the proposed measures are implemented to give intended effects, how the anxiety will be reduced by these measures was numerically estimated according to inference from the hierarchical model.

QUESTIONNAIRE

Subjects of survey

The survey was conducted by visiting users of a particular old underground mall (which opened in the 1950s) and a new underground mall (which opened in after 1985). The examinees were general people who used either mall at least twice a month. The answers assume that a great earthquake might happen and affect the underground mall. The number of examinees and their age ranges are given in Table 1.

The survey items are as follows:

a. Degree of anxiety about factors (input factors) belonging to the bottom layer of the hierarchical model

Questions were created from the input factors (Table 2) of the hierarchical model. The examinee was asked to choose a point on the line divided into 17 segments, each corresponding to a degree of anxiety (Figure 1).

b. Question about reason or remedy to examinees who reply that they feel anxiety

Examinees who replied "absolutely yes" or "yes" when asked if they feel anxiety were also asked to give descriptive answers about reasons for anxiety or suggestions of remedy. However, no descriptive answer was requested for factors which would require special knowledge or for which only one reason or remedy would be expected (Table 3).

c. Degree of anxiety about staying in an underground mall during earthquake

The examinees were asked about the anxiety about staying in the underground mall during an earthquake in order to estimate the degree of overall anxiety inferred using the hierarchical model according to the results of the survey explained in Item a above. A segmented line similar to that in Figure 1 was used for answers about degrees of anxiety.

Degree of anxiety about each factor listed in the questionnaire

Figure 2 shows the averages of the answered degrees of anxiety about each factor in the questionnaire. The comparison in the degree of anxiety between the new and old malls is as follows:

The degree of anxiety is lower in the new mall than in the old mall regarding "fire inclosed space" (Q5), "fire extinguishing facilities" (Q11), "fire prevention facilities" (Q12), "facilities and equipment for refuge" (Q26), and "capacity of refuge routes" (Q28).

There was almost no difference in the degree of anxiety between the new and old malls regarding "echo of sound due to closed space" (Q1), "lack of the sense of time due to closed space" (Q2), "lack of the sense of directions due to closed and unfamiliar space" (Q3 and Q4), "refuge in artificial space" (Q8), "earthquake resistance of facilities" (Q9), "falling of equipment and other things" (Q10), "fire handling" (Q13), "water blocking" (Q14), "means for transmitting damage information" (Q18), "training of people working in underground spaces" (Q19), "recognition of the direction of refuge" (Q25), and "knowledge about the place of refuge" (Q27).
The new underground mall is better than the old underground mall in terms of anxiety about earthquakes, but only to a slight extent.

The above tendency suggests the following:
The new underground mall is considerably improved in terms of reduction of anxiety about fire which is secondary disaster subsequent to earthquakes, disaster prevention facilities and equipment against such secondary disasters, and the capacity of passages as refuge routes. The new mall selected for the survey is bright, has wide passages, looks equipped with high-tech facilities, and gives passengers such an impression that the mall is well furnished with disaster prevention facilities. Such appearance of the mall seems to help reduce the anxiety.

On the other hand, consider primary damage caused by earthquakes, such as collapse of structures and falling of equipment. Even if the underground facilities are sufficiently resistant to earthquakes, passengers cannot understand such advantage when they are simply walking around the mall. To reduce this kind of anxiety, it is necessary to well inform people what degree of earthquake resistance is assured against earthquakes with a particular intensity, how underground facilities resist earthquakes when compared with ground facilities.

Although anxiety about the capacity of passages as refuge routes is reduced in the new mall, there is no significant difference between the new and old malls in the degree of anxiety about the recognition of the correct direction for refuge. In general, new underground malls are larger than old underground malls and have a greater number of exits. Many examinees answered that they were often lost even in ordinary condition (as will be discussed later). This seems to be one of the reasons for such anxiety.

The refuge destinations from the new and old underground malls are on the ground. People can reach them by taking routes through emergency exits. However, passengers are not well informed of the routes at present. Many examinees made descriptive answers stating that they felt anxiety because the ground would be crowded with automobiles and people when they were to go to the ground (as will be discussed later). Since underground facilities are expected to be built at increasingly deep levels, it seems necessary for users to be well informed of the refuge destinations and the capacity of refuge routes.

Users of underground malls have almost no opportunity to participate in disaster prevention training or similar events. Therefore, they know little about training given to people working in the underground mall or how information will be transmitted in the event of a disaster. This seems to be a reason why good appearance of new underground malls does not lead to reduction of anxiety about disasters.

Reason for anxiety and suggestion of remedy as stated by examinees who reply that they feel anxiety

Reasons for anxiety and suggestions of remedies as stated by examinees are summarized below.

a. Lack of the sense of time due to closed space (Q2)

The percentage of examinees who feel that they lose the sense of time when staying in the underground mall is 37.3% in the new mall and 56.0% in the old mall. As attempts to recover the sense of time, some examinees who are users of the new underground mall suggest that chimes or music should be made to tell the time directly, that nature should be simulated using natural light, flowers, and plants, and that a TV board or similar means should be used to give an image of the condition on the ground. On the other hand, in addition to similar suggestions to the above, examinees who are users of the old underground mall suggest as high-priority remedies that the underground mall should be bright and clean and have wider passages and exits as have already been adopted in new underground malls to some extent.

b. Lack of the sense of direction due to closed and unfamiliar space (Q3 and Q4)

The percentage of examinees who feel that they lose the sense of direction when staying in the underground mall, so are anxious about refuge is 20.0% in the new mall and 46.7% in the old mall. Examinees who are users of the new mall suggest that users should compose themselves and check the refuge route and exits by their own eyes. On the other hand, examinees who are users of the old mall suggest as high-priority remedies that the underground mall should have wider exits and passages and should be arranged more simply and neatly as have already been adopted in new underground malls to some extent. A certain examinee suggests that the refuge destination should be indicated. Now that underground facilities are located considerably deep, clear indication of where refuge destinations are located is a noteworthy means for reducing anxiety about refuge.

c. Rescue activities from outside (Q7)

The percentage of examinees who feel anxiety about rescue activities from outside is 18.0% in the new mall and 51.3% in the old mall. Some examinees suggest that a rescue brigade should reside underground and that places of refuge should be provided underground. Another examinee suggests that since earthquake damage will be more serious on the ground than underground, the exits to the ground should always be clear. Many users of the old mall suggest that passages and exits should be improved and that exits dedicated to rescue activities should be provided. Most of such remedies have already been implemented in new underground malls.

d. Central supervisory system (Q17)

This question was not asked to users of the old mall because the old mall has no disaster prevention center. In the new mall, 2.6% of all examinees feel anxiety about the disaster prevention center. A few examinees who feel such anxiety suggest that the staff members

of the center should have a strong sense of responsibility and should be well acquainted with their duties and that the emergency power supply should be safe.

e. Means for transmitting damage information (Q18)
The percentage of examinees who feel anxiety about means for transmitting damage information is 9.3% in the new mall and 30.0% in the old mall. Many users of the new mall suggest that staff members of the mall and tenant employees should be trained to stay calm in the event of a disaster. Many users of the old mall suggest that the mall should have visual means for transmitting much damage information, including a system allowing damage conditions to be displayed on TV screens and blinking illuminations indicating refuge routes.

f. Training of personnel dealing with business in the mall (Q19)
The percentage of examinees who feel anxiety about refuge directions despite training ordinarily given is 10.0% in the new mall and 36.6% in the old mall. Both users of the old mall and users of the new mall consider the reason in the same way: Training is different from actual situations. In the event of a disaster, mall staff members and tenant employees might be afraid of their own danger and be confused. This could be likely if the damage is considerable and the environment is much crowded. Some examinees point out that an increasing number of part-timers are adopted in tenant stores and that they do not seem to be trained adequately. Users of the old mall state that there are problems as to relief for aged or other people who are particularly vulnerable to disasters and that many tenant employees are aged and look rather inactive and trustless.

g. Users' trust in damage information (Q20)
The percentage of examinees who feel anxiety about users' not following refuge directions is 7.3% in the new mall and 20.0% in the old mall. Both users of the new mall and users of the old mall consider that it is important for mall staff members and tenant employees to give passengers refuge directions briskly, but calmly so that a panic will not happen.

h. Information collection by refuge guides (Q21 and Q22)
The percentage of examinees who feel anxiety about information exchange between refuge guides is 5.3% in the new mall and 20.0% in the old mall. Both users of the new mall and users of the old mall suggest that specially trained guides should always be alert, be adequately taught about what to do and how to act, and be trained to prevent a panic from happening. In addition, some users of the old mall suggest that it is important to have close communication with people on the ground and furnish tenant stores with radio communication equipment.

i. Directions by refuge guides (Q23 and Q24)
The percentage of examinees who feel anxiety about refuge guides' directions is 9.3% in the new mall and 29.3% in the old mall. Both users of the new mall and users of the old mall suggest that dedicated disaster prevention staff members should always be alert and that guides should keep calm and give refuge directions so that no panic will happen. Other examinees suggest that the mall should have a refuge system which allows people to take refuge without directions from guides, such as a TV board which displays vivid images of the condition and such design of the floor and ceiling that will give signs of refuge directions in an emergency. Some users of the old mall suggest that people working in the mall, particularly tenant employees, should look active to build up passengers' trust in them.

j. Recognition of the direction of refuge (Q25)
The percentage of examinees who feel anxiety about the correct direction of refuge is 10.7% in the new mall and 36.7% in the old mall. Regarding the reason for this, users of the new mall state that they are often lost even in ordinary condition, that the mall is always crowded, that direction signs are unreadable, and that they suppose themselves to get confused in an emergency. Users of the old mall point out unclear direction signs, narrow passages and exits, and the presence of blind alleys.

k. Equipment for refuge guidance (Q26)
The percentage of examinees who feel anxiety about refuge guidance equipment is 3.3% in the new mall and 40.0%, that is nearly one half, in the old mall. To explain the reason, users of the old mall point out that installed equipment is inconspicuous, old, and contaminated so that there is fear about correct operation.

INFERENCE OF OVERALL ANXIETY

Inference of degrees of overall anxiety

Degrees of overall anxiety felt by questionnaire examinees were inferred using a hierarchical model through the analytical hierarchy process (AHP) method[4]. The inferred degrees of anxiety are considered as major factors of the model: underground-specific anxiety factors(A), damage factors(B), refuge information factors(C), refuge guidance factors(D), refuge facilities and equipment factors(E), and action-at-earthquake factors(F), and overall anxiety degrees summarizing the above(G). The degrees of overall anxiety about the conbination of all major factors numerically represent the lurking anxiety felt by people in underground urban spaces during earthquakes.

As explained earlier, the individual questions in the questionnaire are designed to correspond to the input factors of the hierarchical (inference) model. This means that examinees' answers about their anxiety are input to the inference model as they are. Figure 3 shows the averages of the inferred values of overall anxiety degrees for individual major factors and their combination.

In the new underground mall, the degrees of overall anxiety are characterized by the underground-specific factors slightly within the "anxious" side; the damage factors, refuge information factors, refuge guidance factors, and refuge facilities and equipment factors are slightly within the "easy" side. In the old underground mall, the major factors except action-at-earthquake factors are within the range between "uncertain" and "rather yes."

The difference between the new and old malls in the degrees of overall anxiety about the major factors is large with regard to refuge information factors and refuge facilities and equipment factors, which are less anxious in the new mall. The difference is small with regard to underground-specific factors. Then, anxiety about this major factor does not seem to be reduced so much in the new mall.

The degree of overall anxiety about the combination of all factors is in the "uncertain" range in the new mall. It is slightly lower than in the old mall. Because underground

facilities are expected to be build deeper, measures for further reduction of anxiety are desirable.

Evaluation of degree of overall anxiety about the combination of all factors

The inferred degrees of overall anxiety about the combination of all factors was evaluated by comparing with the answers to added questions as to anxiety about large earthquakes in the underground mall the examinees use.

Figure 4 shows the numerical representation of degrees of anxiety on the segmented line contained in the questionnaire. Considering that the answers to the questionnaire are concentrated on the 1/9, 1/5, 1, 5, and 9 points and, in most cases, do not fall on intermediate points, the results of inference well agree with the results of the survey using the questionnaire. Therefore, the average of the answers to the questionnaire suggests that the proposed inference model is nearly reasonable.

REMEDIES

A number of methods for reducing anxiety are proposed according to the results of the survey using the questionnaire, and their effects are numerically evaluated through inference. Descriptive answers (called remedies I) stating remedies or their reasons are ranked by feasibility. If a descriptive answer states a reason for anxiety, remedies for the anxiety are devised and ranked by feasibility. Remedies I of rank A are already implemented in some way in many underground malls in Japan. Remedies I of rank B are, in most cases, not implemented, but are technically feasible. Remedies I of rank C are characterized by individual options or emphasis on mental aspects. The method of their actual implementation is not so clear. Specific means for remedies belonging to each rank are listed below.

Remedies I of rank A

- Widening passages and exits, raising ceilings, and providing a center square to make the entire mall simple.
- Ringing a chime or providing music at constant intervals so that people will not lose the sense of time. Keeping bright and clean. In particular, keeping the disaster prevention facilities and equipment clean so that people can trust their operation.
- Improving disaster prevention facilities and equipment.
- Providing a dedicated space for access from the ground if rescue activities are mainly from the ground.

Remedies I of rank B

- Introducing natural light and arranging plants to simulate environment on the ground.
- Installing TV boards with a large screen at many places to always display the environment on the ground so that people can keep the sense of directions by identifying their position in relation to the scenery on the ground. In an emergency, the TV boards will display damage conditions and indicate how to take refuge, thus providing a visual means for information transmission to users.
- Making tenant employees cheerful and active so that they look trustworthy to users. In particular, give good consideration for training occasional employees in disaster prevention and rescue.

- Improving the environment around the exits if the refuge is on the ground. Providing adequate information about the position and capacity of the refuge if it is underground.

Remedies I of rank C

- Users should usually check the refuge routes and exits. In an emergency, they should be calm when acting and should follow guides' directions.
- If the damage is serious and the environment is crowded, a panic could happen. In this event, the environment could differ from the situation assumed during training. Guides should keep calmness, have good communication with others, remember instructions given during training, and take appropriate action.

Table 4 shows average overall anxiety data obtained by modifying the answers on the assumption the remedies are implemented effectively, subjecting the modified answers to recalculation and inference, determining the degrees of overall anxiety about the combination of all major factors, and calculating averages.
In this table, rank AB denotes the case where remedies of rank A and rank B are implemented effectively; rank ABC denotes the case where remedies of rank A, rank B, and rank C are implemented effectively.
Modification was made only to the descriptive answers (Figure 5a) so that answers to the question "Do you feel anxiety?" became "rather no" (1/3) or "no" (1/5).
Table 4 indicates that, at each rank, the degree of overall anxiety about the combination of all factors is somewhat reduced in both the new and old malls. If remedies of rank A are implemented in the old mall, the degree of overall anxiety about the combination of all factors should become nearly equal to the unmodified degree in the new mall; however, the two differ in fact.
The modification was made only to descriptive answers. If an answer pointed to a degree of anxiety within the range from 1/3 (or 1/5) to 5, it was not modified. Therefore, the average of modified overall anxiety seems to be deviated towards the "anxious" side.

Remedies I in Table 4 are such that if a descriptive answer is modified to 1/3, the previous answer indicated a higher degree of anxiety (Figure 5b), and this is also true of modification into 1/5. However, since non-descriptive answers cannot be ranked, the response to them is assumed to be the implementation of remedies of rank ABC.

There is another type of remedies (remedies II). Remedies II were devised through analysis of non-descriptive answers to the questionnaire. These answers were modified on the assumption that remedies II were implemented. The modification method is similar to the method used in the case of remedies I. Principal remedies II are as follows:

- Adequately informing general people of the present earthquake resistance of the underground facility (what degree of earthquake resistance is assured against earthquakes with a particular intensity).
- Allowing users of the underground facilities to receive disaster prevention training about once a year.

The implementation of these remedies leads to a reduction in anxiety to nearly the same extent as when remedies I are implemented.

The answers corresponding to remedies I of ranks A, B, and C and to remedies II were modified at the same time, and the averages were obtained through inference. The results are given in Table 5. Considering that answers corresponding to remedies I of rank AB are on the "anxious" side as discussed earlier, effective implementation of remedies I of rank

AB and remedies II leads to the effect that the degree of anxiety in the new mall is reduced to "rather unanxious" (Table 6). If remedies I and II are implemented effectively, the degree of anxiety can be reduced to the range from "rather unanxious" to "unanxious".

CONCLUSIONS

Conclusions of the study are as follows:
1)The underground mall which opened in after 1985 give people a considerably reduced degree of anxiety about disaster prevention equipment against fire and other secondary damage subsequent to earthquakes. However, the degree of anxiety about primary damage is nearly equal to that in the underground mall which opened in the 1950s. Therefore, it is specially important to implement remedies against such anxiety.
2) Major factors of lurking anxiety concerning earthquakes in underground urban spaces include underground-specific factors, damage factors, refuge information factors, refuge facilities and equipment factors, and action-at-earthquake factors. Among these factors, anxiety caused by refuge information factors and refuge facilities and equipment factors is reduced in the new mall, but anxiety caused by underground-specific factors is still nearly equal to that in the old underground mall.
3) Some of the proposed remedies require handling in earthquake engineering. They include a method for adequately informing general people of present earthquake resistance of underground facilities (what degree of earthquake resistance is assured against earthquakes with a particular intensity).

FUTURE DIRECTIONS

This paper has proposed a number remedies for reducing lurking anxiety felt by people about earthquakes when they are in underground urban spaces. The authors plan to conduct surveys using questionnaires and experiments in order to study how to implement each of these remedies specifically and what effects will be produced by them.

ACKNOWLEDGMENTS

This study was conducted as a part of study on "A Cooperative Research in Development of Seismic Design of Underground Structures" in "Technology Research and Development Regarding Use of Underground Space" of "A Comprehensive Research Project". The writers thank cooperative researchers.

REFERENCES

1) Osamu Hiroi: Great Earthquakes and Underground malls, Monthly Fire Services Journal, 1990.
2) Tokyo Fire Defense Agency and Fire Prevention Council: Report on Research on Actual
3) E.Saito,H.Ikemi,H.Nakano and M.Nakamura : Estimation of Degree of Anxiety Felt by People in Underground Urban Space during Earthquakes, Proceedings of the 4th U.S.-Japan Workshop on Earthquake Disaster Prevention for Lifeline Systems, Los Angeles, California, 1991.8. Conditions of Underground Malls, March 1979.
4) Saaty, T.L.: The analytic hierarchy process, McGrow-Hill, Book Co.,1980.

Table 1 Number of examinees of the questionnaire

	Total Number of examinees (Persons)	Teens		Twenties		Thirties		Forties		Fifties	
		M	W	M	W	M	W	M	W	M	W
Old Underground Mall	150	15	15	15	15	15	15	15	15	15	15
New Underground Mall	150	15	15	15	15	15	15	15	15	15	15

Note W : Woman M : Man

Table 2 Questions in the questionnaire

A. Underground-specific factors
- Q1: Echo of sound due to closed space
- Q2: Lack of the sense of time due to closed space
- Q3 and Q4: Lack of the sense of directions due to closed and unfamiliar space
- Q5: Fire in closed space
- Q6: Power failure in artificial space
- Q7: Rescue activities from outside
- Q8: Refuge in artificial space

B. Damage factors
- Q9: Earthquake resistance of facilities
- Q10: Falling of equipment and other things
- Q11: Firefighting equipment
- Q12: Fire prevention facilities and equipment (such as fire wall and shutters)
- Q13: Fire handling
- Q14: Water blocking
- Q15: Power supply for emergency

C. Refuge information factors
- Q16: Means for collecting damage information
- Q17: Central supervisory system
- Q18: Means for transmitting damage information
- Q19: Training of people working in underground spaces
- Q20: Users' trust in damage information

D. Refuge guidance factors
- Q21 and Q22: Information collection by refuge guides
- Q23 and Q24: Refuge guides' directions

E. Refuge facilities and equipment factors
- Q25: Recognition of the direction of refuge
- Q26: Facilities and equipment for refuge guidance
- Q27: Knowledge about the place of refuge
- Q28: Capacity of passages (refuge routes)
- Q29: Disaster prevention equipment along refuge routes

F. Action-at-earthquake factors
- Q30: Disaster prevention training for users
- Q31: Experience in earthquake underground

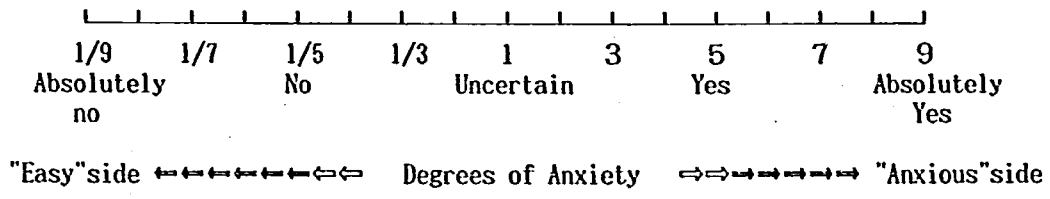


Figure 1 Segmented line for answering degrees of anxiety

Table 3 Input factors requiring descriptive answers

Descriptive Answers	Input factors
Remedies	Q2, Q3. Q4, Q7, Q17, Q18, Q20, Q21. Q22, Q23. Q24
Reasons	Q19, Q25, Q26

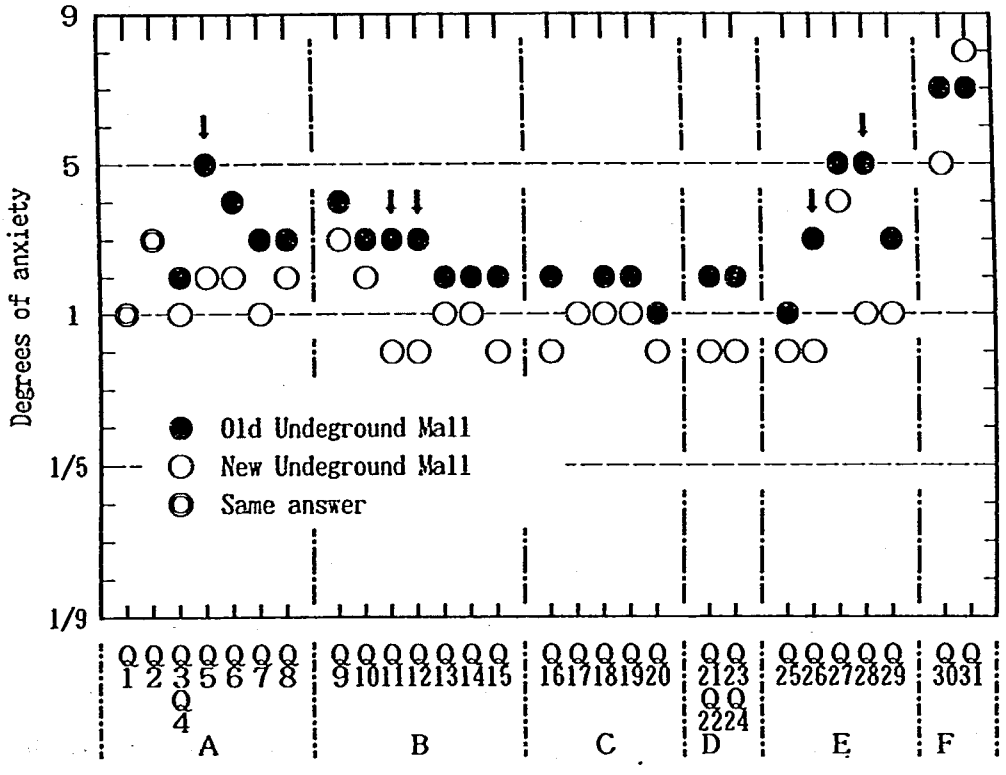


Figure 2 Averages of answers regarding anxiety in new and old malls

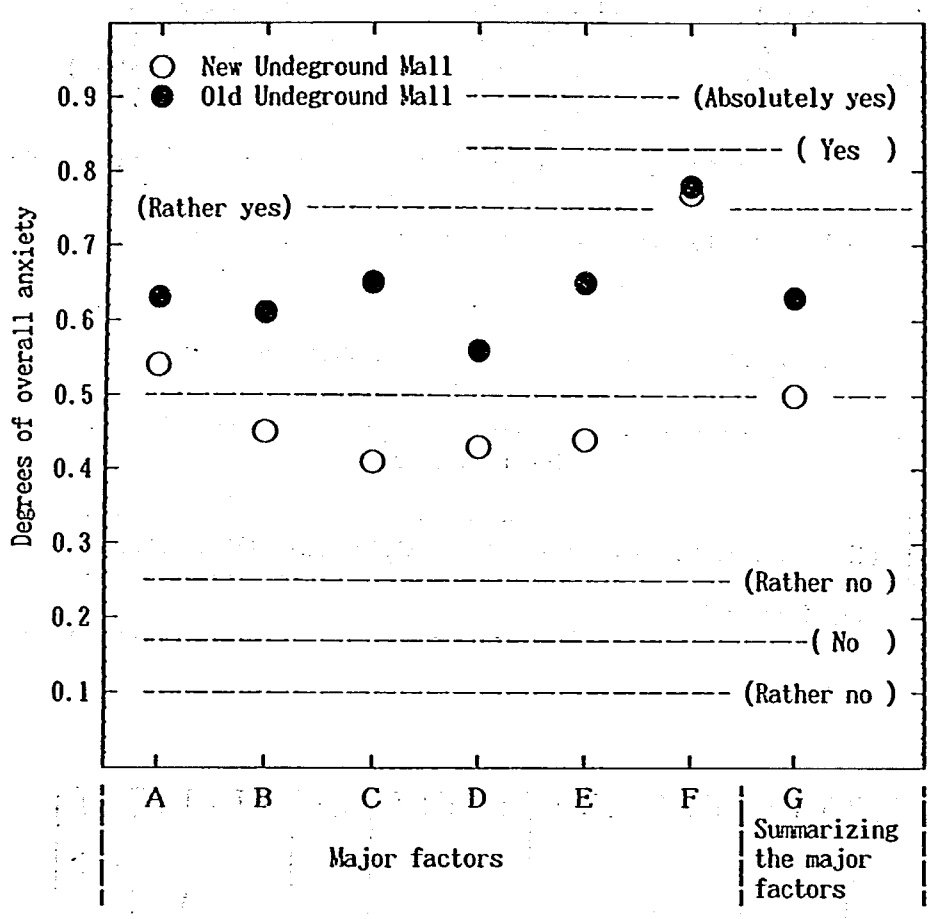


Figure 3 Averages of degrees of anxiety felt during earthquake in new and old malls

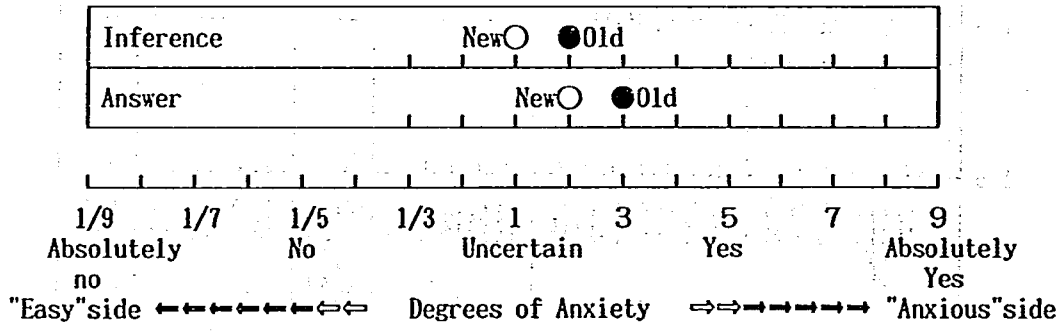
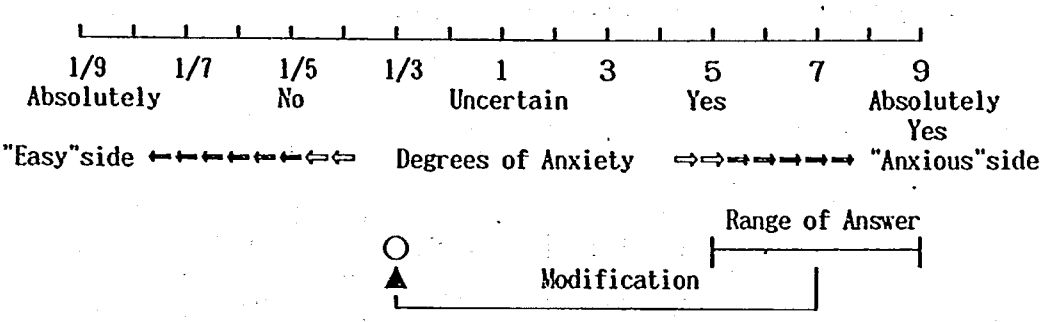
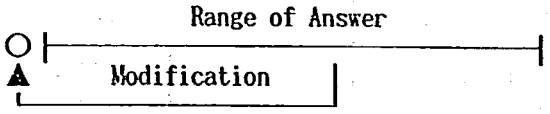


Figure 4 Matching and division of degrees of anxiety



a. Remedies I −rankA, Remedies I −rankA B, Remedies I −rankA B C



b. Remedies I and Remedies II

Figure 5 Modification to answers (in the case of 1/3)

Table 4 Averages of modified degrees of overall anxiety about the combination of all factors (assuming the implementation of remedies I or II)

Revel of remedies	Modified to 1/3		Modified to 1/5	
	New Underground Mall	Old Underground Mall	New Underground Mall	Old Underground Mall
Original	0.50(5)	0.64(5)	0.50(5)	0.64(5)
remedies I −rankA	0.50(5)	0.60(5)	0.50(5)	0.59(5)
remedies I −rankAB	0.48(4)	0.58(5)	0.48(4)	0.58(5)
remedies I −rankABC	0.47(4)	0.56(5)	0.47(4)	0.55(5)
remedies I	0.40(4)	0.46(4)	0.37(4)	0.43(4)
remedies II	0.37(4)	0.45(4)	0.34(4)	0.41(4)

Note ( ) : Classes of degrees of overall anxiety in Table 6

Table 5 Averages of modified degrees of overall anxiety about the combination of all factors (assuming the implementation of both remedies I and II)

Revel of remedies	Modified to 1/3		Modified to 1/5	
	New Under-ground Mall	Old Under-ground Mall	New Under-ground Mall	Old Under-ground Mall
Original	0.50(5)	0.64(5)	0.50(5)	0.64(5)
remedies I -rankA +remedies II	0.37(4)	0.41(4)	0.33(4)	0.37(4)
remedies I -rankAB +remedies II	0.35(4)	0.39(4)	0.32(4)	0.35(4)
remedies I -rankABC+remedies II	0.34(4)	0.37(4)	0.31(4)	0.33(4)
remedies I +remedies II	0.26(4)	0.27(4)	0.20(3)	0.20(4)

Note ( ) : Classes of degrees of overall anxiety in Table 6

Table 6 Classes of degree of overall anxiety

Classes	Degrees of overall anxiety (DOA)	Definition
1	0.10≦DOA <0.12	Absolutely no ～ Rather no
2	0.12≦DOA <0.17	Rather no ～ No
3	0.17≦DOA <0.25	No ～ Almost no
4	0.25≦DOA <0.50	Almost no ～ Uncertain
5	0.50≦DOA <0.75	Uncertain ～ Almost yes
6	0.75≦DOA <0.83	Almost yes ～ Yes
7	0.83≦DOA <0.88	Yes ～ Rather yes
8	0.88≦DOA ≦0.90	Rather yes ～ Absolutely yes

INDIRECT LOSSES CAUSED BY LIFELINE DAMAGE OR DISRUPTION

By

Ronald T. Eguchi[1]
Hope A. Seligson[2]
Jack H. Wiggins[3]

ABSTRACT

The failure of lifeline systems in natural disasters can be devastating, hampering both response and recovery. Recent events, such as the 1989 Loma Prieta earthquake, have demonstrated that indirect impacts associated with the failure of lifeline systems may far outweigh the direct costs associated with system repair. As a result, the problem of quantifying possible indirect losses is currently receiving increased attention. This paper addresses previous, current and future efforts in the field of indirect loss assessment. A general methodology for indirect loss assessment is presented, along with a review of previous loss assessment studies and summaries of several state-of-the-art studies currently underway. In addition, possible future directions, with respect to models and methodologies, are explored.

INTRODUCTION

The failure of critical lifeline systems during earthquakes can be devastating and costly. The failure of the water supply system in the city of San Francisco during the 1906 San Francisco earthquake resulted in over 8 square miles of the business district being burned and completely destroyed. More recently, the failure of the Cypress viaduct structure during the 1989 Loma Prieta earthquake resulted in 46 fatalities. In each of these examples, the secondary or indirect impacts associated with the failure of the lifeline far exceeded the actual cost to repair the damaged system. However, even with these examples as motivation, the state-of-the-art in indirect loss assessment has not progressed significantly.

Part of the reason for this slow development has been the lack of empirical data with which to validate analytical or theoretical predictions of secondary or indirect loss. Recent disasters, such as Hurricanes Hugo in 1989 and Andrew in 1992, and the 1989 Loma Prieta earthquake have underscored the need to collect information on indirect loss impacts.

---

1 Vice President, EQE Engineering and Design, Irvine, California
2 Project Research Engineer, EQE Engineering and Design, Irvine, California
3 Project Engineer, EQE Engineering and Design, Irvine, California

Another reason for this slow development has been that indirect loss assessment requires a multi-disciplinary effort. Engineers and social scientists must work together to develop models to assess economic and social impacts. Until recently, engineers have not completely understood the measures or dimensions used by social scientists to quantify socioeconomic impact. By the same token, social scientists have not completely communicated to the engineers the importance of quantifying effects, other than direct damage, to buildings or lifelines.

Recently, there has been a concerted effort to have engineers work with social scientists to address these multi-dimensional issues. A program initiated by the National Science Foundation (NSF) through the National Center for Earthquake Engineering Research (NCEER) focuses specifically on measuring the socioeconomic impact of lifeline failures and disruption. Because research tasks have been defined within a larger project scope, it has been possible to bring together researchers from the engineering and social science disciplines to resolve these complex issues. Examples of some of these projects will be discussed later in this paper.

The purpose of this paper is four-fold. First, a review of previous lifeline earthquake loss studies is presented in order to gain an understanding of the current state-of-the art. Included in this review are studies that address direct loss assessment, as well as indirect loss estimation. Second, this paper outlines the major elements and methodology required to estimate the indirect impact of lifeline failures or disruption. Third, in order to demonstrate the application of these methods to the lifeline problem, two case histories are presented. In these examples, environmental and higher order economic loss issues are addressed. The final topic addressed is future needs and directions with regard to improvement of methods and models used in indirect loss assessment.

PREVIOUS EARTHQUAKE VULNERABILITY STUDIES

Compared to other areas of earthquake engineering (e.g., analysis of buildings), the analysis of lifeline seismic vulnerability is a relatively new field. Prior to the 1971 San Fernando earthquake, even the most seismically-active regions of California were not seriously concerned with the regional impact of large earthquakes on lifeline systems. With the exception of the 1906 San Francisco earthquake, no earthquake has been more devastating to lifeline systems in the U.S. than the 1971 San Fernando earthquake. This particular event caused significant damage to virtually every type of lifeline system and has been the major catalyst for modern seismic design measures for lifelines.

Even with the San Fernando earthquake acting as a catalyst for the development of new seismic design procedures, the amount of research money spent on lifelines relative to other areas of earthquake engineering has been limited. For example, between the years of 1980 and 1990, the National Science Foundation funded approximately $160 million in earthquake hazard mitigation research, of which roughly $18 million was designated for the specific study of lifelines (Seligson et al., 1991).

Despite this limited funding, much progress has been made in developing procedures to estimate potential earthquake damage to lifelines. Much of this progress has been summarized in technical journals and conference proceedings (ASCE 1977, 1980, 1981, 1983, 1984, 1991).

To date, seven areas of the U.S. have benefitted from some type of lifeline vulnerability study. These areas include:

1. Southern California
2. Northern California
3. The New Madrid Seismic Zone
4. The Wasatch Front Area in Utah
5. The Pacific Northwest, including Seattle, Washington and Portland, Oregon
6. The Charleston, South Carolina Area
7. The Northeast, including Boston, Massachusetts

These areas have been ranked roughly in order of comprehensiveness, i.e., geographic areas having more in-depth lifeline studies have been ranked higher. The federal agencies responsible for funding research in lifeline earthquake engineering include the Federal Emergency Management Agency (FEMA), the U.S. Geological Survey (USGS), the National Science Foundation (NSF), the National Institute of Standards and Technology (NIST) and the National Center for Earthquake Engineering Research (NCEER).

Since the early seventies, there have been at least 20 published reports that have focused on earthquake loss or reliability assessment of lifelines. In addition, there are probably an equal number of studies that have been performed for private sector entities, such as utility companies, that have not reached the general research community. Only a handful of these studies, however, provide quantitative estimates of loss or vulnerability. Fewer consider the secondary or indirect effects caused by lifeline failures or disruption.

Many of these studies have focused on the performance of lifelines in California (approximately one-third). This is understandable considering the frequency of significant earthquakes and the recent history of damaging events (1971 San Fernando, 1983 Coalinga, 1987 Whittier Narrows, 1989 Loma Prieta and 1992 Landers earthquakes). However, in recent years, a considerable amount of attention has been given to earthquake risks outside of California. Regions receiving increased attention include the Wasatch Front area in Utah, the Pacific Northwest and the New Madrid Seismic Zone.

Table 1 provides a list of some of the earthquake loss studies published to date. In this table, communication lifelines such as radio, television, and telephone have been grouped together, as have transportation lifelines, such as highways, bridges, railroads, and airports. Several major loss studies of buildings have also been included and losses from all types of building structures have been totaled. The lifelines which have been reported individually are natural gas, electric power, petroleum, water supply, and waste water. Where available, indirect losses resulting from lifeline failures have been included.

The losses estimated are primarily associated with direct damage. They may be measured as; damage as a percent of the replacement cost of the damaged facility; percent of functionality which is lost; number or rate of breaks in a pipeline; or dollar cost of repairs. Many studies have been produced for the sole purpose of providing a damage scenario for emergency response planning. In these studies, earthquake damage has not been quantified or

Table 1:

SUMMARY OF PREDICTED EARTHQUAKE LOSSES

Location	Magnitude	Nat'l Gas	Elec.	Oil	Water	Waste W.	Comm.	Trans.	Indir. L.L.	Bldgs.	Reference
Central	Ms = 8	$56 M	$4860 M	$75 M	$880 M			$3620 M	$14.6 B		ATC (1991)
Central	Ms = 7	$19 M	$1730 M	$28 M	$280 M			$640 M	$4.9 B		
Central, East	Various	Qual	Qual	Qual							AAES (1990)
Central	Ms = 8.6								$.3 B (ENV)		Pelmulder & Eguchi 1992
Kentucky	Ms = 8+							Qual			Allen et al, (1988)
Memphis, TN	Mw = 7.5				- 30% Fn Loss						Shinozuka et al, (1992)
Six cities in	Ms = 7.6	$646.4 M	$3323 M		$456.4 M	$495.6 M		$588.0 M		$32.7 B	FEMA/CUSEPP (1985)
Central	Ms = 8.6	$997.6 M	$4902 M		$693.0 M	$733.4 M		$841.5 M		$43.6 B	
St. Louis, MO	Ms = 7.6	$68.1 M	$262 M		$148.1 M			$212 M		$2.2 B	FEMA/CUSEPP (1990)
	Ms = 8.6	123.0 M	$333 M		$187.7 M			$418 M		$5.2 B	
Southeast	Ms = 7.5	$0	$2000 M	$0	$310 M			$1270 M	$10.2 B		ATC (1991)
Charleston,	MMI = VII	Few Brk	Qual		Qual	Few Brk	Qual	Qual		$1.89 B	Harlan and Lindbergh
S.C.	MMI = IX	3000 Brk	Qual		Qual	700 + Brk	Qual	Qual		$4.89 B	(1988)
Northeast	Ms = 7	$0	$2200 M	$0	$300 M			$980 M	$9.1 B		ATC (1991)
Boston, MA	Ms = 6.25	$3.9 M	$57.7 M	$2.3 M	$2.3 M	$3.8 M	$14.5 M	$70.8 M		$3.51 B	Ebel et al. (1990)
No. California	Ms = 7.5	$6 M	$2210 M	$0	$200 M			$460 M	$11.1 B		ATC (1991)
S.F. Bay Area	Ms = 8.3	Qual	Qual	Qual	Qual	Qual	Qual	Qual			CDMG (1982b)
S.F. Bay Area	Ms = 7.5	Qual	Qual	Qual	Qual	Qual	Qual	Qual			CDMG (1987)
So. California	Ms = 8	$11 M	$1800 M	$28 M	$230 M			$700 M	$11.7 B		ATC (1991)
San Diego, CA	Ms = 6.8	Qual	Qual	Qual	Qual	Qual	Qual	Qual		Qual	CDMG (1990)
Southern CA	Ms = 8.3	Qual	Qual	Qual	Qual	Qual	Qual	Qual			CDMG (1982a)
Southern CA	Ms = 7	Qual	Qual	Qual	Qual	Qual	Qual	Qual		Qual	CDMG (1988)
LA & Orange	Ms = 8.3	1510 Brk,	0-10% Fn	Qual	1180 Brk,	4570 Brk	Qual	Qual		Qual	NOAA (1973)
Counties	(SA)	67.5 K Sv			2 K SvLk						
	Ms = 7.5	4410 Brk,	0-25% Fn	Qual	3620 Brk,	13429 Brk	Qual	Qual		Qual	
	(NI)	197 K Sv			6 K SvLk						
Los Angeles City	Ms = 8+ (SA)									$1.1 B	Spangle (1987)
	Ms = 6+ (LA)									$3.9 B	
	Ms = 6+ (LA)									$2.9 B	
San Bernardino,	Ms = 8.3 (SA)									$12.8 M	SCEPP (1983)
CA	Ms = 6.8 (LA)									$20.2 M	
	Ms = 6.8 (LA)									$19.6 M	

B = Billion
Brk = Pipeline Break
Comm. = Communications
ENV = Environmental
Elec. = Electric Power
Fn = Functionality
K = Thousand
L.L. = Lifeline
M = Million
MI = Body Wave Magnitude
MMI = Modified Mercalli Intensity
Ms = Surface Wave Magnitude
Mw = Moment Magnitude
O( ) = On the Order of ( )
Oil = Crude or Refined
W, = Water
Qual = Qualitative Assessment
Sv = Services
SvLk = Service Leak
Trans. = Transportation

Table 1: (Continued)

SUMMARY OF PREDICTED EARTHQUAKE LOSSES

Location	Magnitude	Nat'l Gas	Elec.	Oil	Water	Waste W.	Comm.	Trans.	Indir. L.L.	Bldgs.	Reference
Northwest	Ms = 7.5	$6 M	$2410 M	$0	$90 M			$780 M	$6.1 B		ATC (1991)
Everett, WA	Ms = 6.5	$65 K	$710 K		$5.4 M	$6.2 M	$24.4 M	$265 M	$135.9 M		Kennedy/Jenks/
	Ms = 7.0	$25 K	$175 K		$2.3 M	$3.3 M	$11.2 M	$92 M	$32.2 M		Chilton (1991)
	Ms = 8.25	$175 K	$277 K		$4.8 M	$8.9 M	$31.7 M	$171 M	$136.4 M		
Seattle, WA	Ms = 6.5				$1.1 M				$54 M		Kennedy/Jenks/
	Ms = 7.5				$3.5 M				$243 M		Chilton (1990)
	Ms = 8.5				$7.6 M				$567 M		
Portland, OR	Ms = 6.5				$129 K	$255 K					Wang et al (1990)
	Ms = 8.4				$1.5 M	$2.6 M					
Wasatch Front	Ms = 7.5	$6 M	$1280 M	$0	$130 M			$580 M	$3.9 B		ATC (1991)
Weber, Davis	Ms = 7.5	360 Brk/	2960 Tr,	Qual	360 Brk	1130 Brk	30-65%	Qual		10-60% Fn	USGS (1976)
Salt Lake		17 K Sv	7670 Cr,		510 SvLk		Fn loss			either E'Q	
& Utah	Ms = 7.5	310 Brk/	19 Sub	Qual	300 Brk	840 Brk	to	Qual			
Counties		13860 Sv	either E'Q		410 SvLk		Phones				
Weber, Davis	Ms = 7.5									$5.2 B	Algermissen et al.
Salt Lake	Ms = 7.5									$5.5 B	(1988)
& Utah	Ms = 7.5									$5.0 B	
Counties	Ms = 7.5									$4.5 B	
	Ms = 6.5									$3.1 B	
	Ms = 6.5									$4.0 B	
	Ms = 6.5									$2.3 B	
	Ml = 5.5									$1.3 B	
	Ml = 5.5									$1.9 B	
	Ml = 5.5									$0.8 B	
Utah	Ms = 6.1-7.5	Qual		Qual							Taylor & Ward (1981d)
Utah	Ms = 6.1		Transm.								Taylor & Ward (1981a)
			100% Fn								
			w/in 4 hr								
Utah	Ms = 6.1-7.5						Qual				Taylor & Ward (1981b)
Utah	Ms = 6.1-7.5							Qual			Taylor & Ward (1981c)
S. Salt Lake					Qual						Taylor & Bigler (1982)
Salt Lake and	Various	Brk Rates			Break					$260 M	Taylor et al. (1986)
Weber Counties					Rates					UT owned	
Weber & Utah	Various	Brk Rates			Break						Taylor et al. (1988)
Counties					Rates						

B = Billion
Brk = Pipeline Break
Comm. = Communications
ENV = Environmental
Elec. = Electric Power
Fn = Functionality
K = Thousand
L.L. = Lifeline
M = Million
Ml = Body Wave Magnitude
MMI = Modified Mercalli Intensity
Ms = Surface Wave Magnitude
Mw = Moment Magnitude
O( ) = On the Order of ( )
Oil = Crude or Refined
W. = Water
Qual = Qualitative Assessment
Sv = Services
SvLk = Service Leak
Trans. = Transportation

2HD 208nb/TABLE-1B

tallied in a form which can be summarized in a table. This type of damage analysis is described in Table 1 as qualitative, even though a specific damage state may have been postulated for planning purposes.

In almost all cases where quantitative losses have been estimated, the largest direct losses are attributed to either transportation or electric power systems. Direct damage to other energy systems (i.e., natural gas and oil) tends to be significantly lower (as much as an order of magnitude) than losses associated with electric power and transportation facilities.

To a great extent, the data collected from the 1971 San Fernando and 1989 Loma Prieta earthquakes substantiate these relative vulnerabilities. In the 1971 San Fernando earthquake, direct damage to electric power and transportation systems were among the most costly. For electric power systems, direct losses exceeded $33 million (1971 dollars). In comparison, direct losses to natural gas systems in this event were approximately $2 million. In the 1989 Loma Prieta earthquake, the most significant direct losses to lifeline systems were associated with transportation and electric power system failures.

Perhaps the most comprehensive study performed to date on indirect losses resulting from lifeline failures is the Applied Technology Council (ATC) study on "Seismic Vulnerability and Impact of Disruption of Lifelines in the Conterminous United States." This report, published in 1991 by FEMA, estimates direct and indirect losses to lifelines in seven separate earthquake scenarios around the U.S. The report shows that indirect losses can exceed direct losses by up to a factor of 3.

DEFINITION OF LOSS MEASURES AND PERFORMANCE STANDARDS

In order to assess the performance of a lifeline system during and after an earthquake, performance or loss measures must be identified. In this paper, direct loss is defined by those costs associated with the repair of a damaged system.

Secondary losses include a variety of post-earthquake costs:

- Business interruption losses
- Environmental damage
- Collateral damage, e.g., fire following

In addition, secondary impacts can also be measured by the level of social disruption caused by the failure of a lifeline system. For example, evacuation of areas or buildings because of damage to utilities can displace individuals, causing some to be without shelter. Furthermore, some lifeline failures can result in death and injury. Tierney (1992) provides a list of socio-economic impacts related to oil pipeline spills.

Secondary impacts are difficult to quantify because their assessment requires detailed databases and models. In order to compile the data needed for these assessments, detailed information on exposed facilities must be collected. In the case of business interruption loss, all businesses potentially affected by a interruption in lifeline service would have to be

identified and categorized. In a large city, identifying these businesses could be an enormous task. One method of quantifying regional economic impacts is through the use of Input-Output models which assess the ripple effects of economic disruption.

Another aspect of performance evaluation is the definition of performance criteria or standards. Normally, performance standards are specified for individual components. Rarely are standards specified for complete systems. However, in order to measure the effectiveness of a particular lifeline after an earthquake, it is critical that the overall functionality of the system be considered.

Table 2 shows a summary of suggested performance measures and criteria for various lifelines. This summary was developed in 1979 by Campbell, et al. In this table, performance is generally measured by the percent of serviced population without service, the maximum duration of an outage, and the time to full restoration of the system. The more critical the lifeline, the more stringent the criteria. In order to assess whether these performance criteria can be met or not, system vulnerability studies would have to be performed.

TABLE 2

POSSIBLE PERFORMANCE LEVELS FOR LIFELINE SYSTEMS

Performance Level (1)	Maximum Percent of Serviced Population Without Service (2)	Maximum Duration of Outage in Days (3)	Time to Full Restoration in Days (4)
AA	Fully Functional		
A	0.1	¼	1
B	0.5	1	7
C	1	3	14
D	2	7	30
E	10	14	90
F	50	14	180

Source: Campbell, et al., 1979.

The following section provides further discussion of these measures and how they can be used to gauge the effectiveness of a lifeline system during an earthquake. It must be understood that the measures discussed above and in the remaining part of this paper are but a small subset of the measures that can be used to assess post-earthquake lifeline performance.

GENERAL METHODOLOGY FOR INDIRECT LOSS ASSESSMENT

The procedure for estimating secondary or indirect impacts begins with an assessment of damaged lifelines and of the extent to which they have been rendered inoperable. Methods for estimating these direct impacts are fairly well established and can be found in many conference proceedings and journals. One excellent reference is a document prepared by the ASCE Technical Council on Lifeline Earthquake Engineering (ASCE/TCLEE, 1983).

Figure 1 illustrates the steps required to determine some of the indirect impacts resulting from lifeline failures. The initial step is the lifeline damage or vulnerability assessment, wherein lifeline damage states and outage are determined. This step includes the compilation of seismic hazard data, the characterization of the lifelines under study, and the application of damage and outage algorithms. In general, the output from these direct loss assessments includes the locations of damaged lifeline elements, expected repair costs, and an identification of potential outage areas. Usually, to estimate potential outage areas, additional operational data (e.g., the results of hydraulic studies for water supply systems) are needed.

The second step is to define the indirect loss measures of interest, such as environmental, social, and economic costs. Such costs might include the cost of environmental remediation of oil spills or expected decline in economic productivity or reduced industrial production.

This step is followed by the compilation of exposure data. Data may be readily available, as in population data from the U.S. Census, or may need to be compiled from various agencies, through research or the administration of questionnaires. Data may be collected explicitly, as in the development of a detailed regional business inventory or the collection of topographic and geophysical maps along a pipeline route, or it may be collected to allow for the reduction of a complex physical problem to a few generalized models, as in the development of a handful of environmental models to represent possible exposure along the same pipeline route.

The fourth step is to determine the extent of secondary impact, or to translate the direct lifeline losses into secondary losses. For instance, the direct loss may be pipeline damage modelled by the number of leaks. The secondary impact of interest may be environmental contamination, modelled through drainage and soil migration models. Another example might be damage to a large dam, while the secondary impact would be the number of people facing inundation from flooding caused by a dam break.

The fifth and final step is to determine the cost associated with the given secondary impact. This usually entails a quantification of dollar costs in an area that the risk analyst is unfamiliar, necessitating the input of outside experts. Cost estimates, such as the cost to clean-up contaminated groundwater, or losses associated with refinery shutdown and start-up, can only be developed with the aid of experts in the field. Generalized cost estimates may be used to develop cost models for this type of analysis.

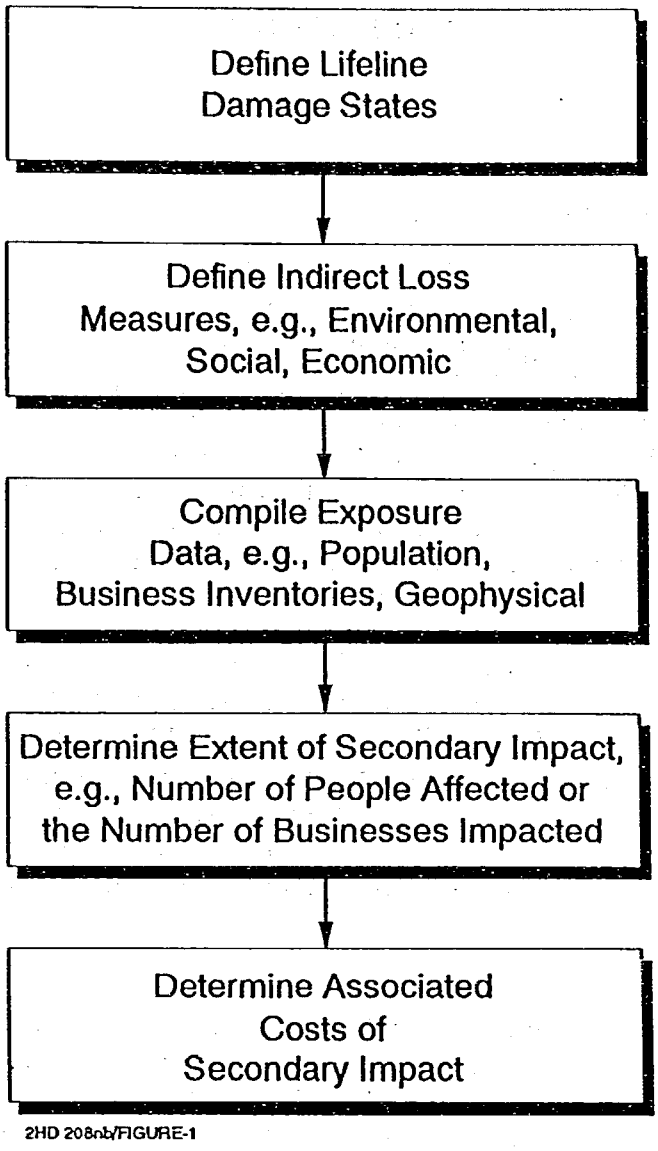


Figure 1: Steps in Estimating Indirect Impacts of Lifeline Failures Due to Earthquakes

CASE STUDIES

ENVIRONMENTAL LOSS

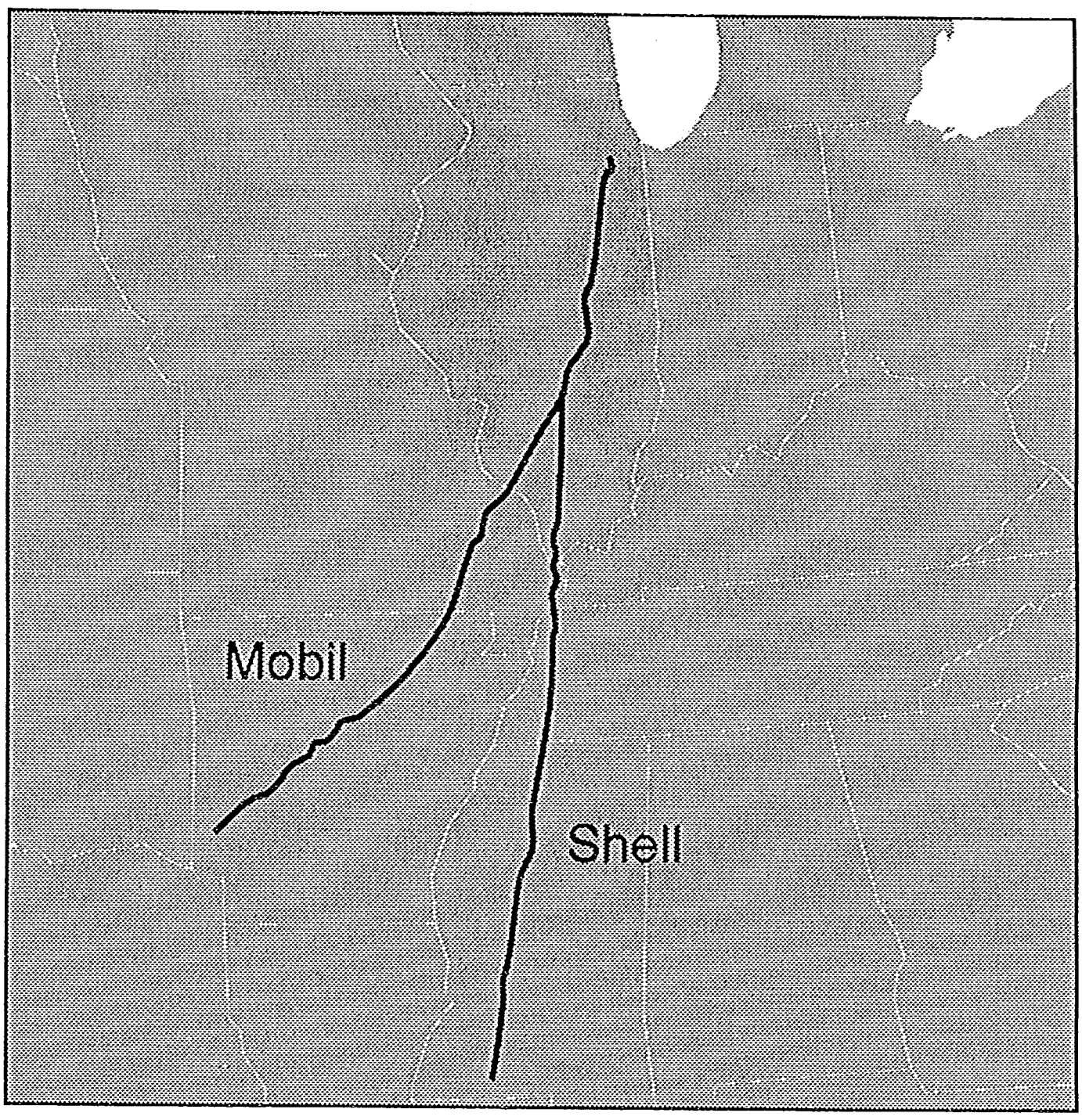
The secondary cost of lifeline failures may include the cost of environmental remediation when the lifeline failure is such that damage to the environment results. The earthquake-induced failure of oil pipelines may cause such contamination. A methodology for assessing the risk of environmental contamination and associated cost of remediation from oil pipeline failures in earthquakes has been developed under contract to NCEER. The methodology combines Monte Carlo techniques for earthquake simulation, a deterministic model to estimate oil volumes released, and a library of cost models to estimate contamination and remediation costs. The methodology was developed for use on a regional scale, and therefore relies on a limited amount of input data.

While oil pipeline systems have generally performed well in moderate to large earthquakes, examples of serious damage have been observed. In the 1987 Ecuador earthquake (M 6.9), 6.5 miles of transmission pipeline were destroyed by landslides, 10 miles were damaged by mud flows, five miles were deformed with distortion of above ground pipeline supports, and 2 miles of pipeline were pulled off supports when a pipeline bridge was destroyed by flooding. Lost revenue and the cost of reconstruction totalled $1 - 1.5 billion dollars (Crespo, 1987). The extent of other costs, including environmental clean-up, were not quantified.

The mid-western oil transportation network is both linearly extensive and critical from an economic standpoint. Over 650 million barrels are transported annually from the south, to refineries in the midwest through large underground pipelines. The disruption of this supply due to damage in a large earthquake in the New Madrid Seismic Zone (NMSZ) would have a major impact on the regional economy. Losses due to direct damage to all major lifeline systems may reach $11.8 billion, while business interruption losses could exceed $14.6 billion (ATC-25, 1991). Other losses could add significantly to this figure, including the remediation cost associated with the clean-up of spilled oil. To begin quantifying such costs, this methodology was applied to two oil pipelines that traverse the New Madrid Seismic Zone (NMSZ) shown on Figure 2; the Shell Capline, a 40 inch welded steel pipe with arc-welded joints installed in 1968 and the Mobil Line Number 68, 18 to 20 inches grade B steel with welded joints, installed around 1948 (Ariman et al., 1990).

The overall methodology is outlined in Figure 3. The approach uses Monte Carlo techniques to simulate earthquake events, but operational risks may be assessed in this manner as well. For this application, each simulation trial represents a possible outcome of the earthquake simulated. The combined results from all simulation trials allows development of a distribution of possible losses from the simulated event. To develop a loss distribution for many possible earthquakes in a region, a series of events would be simulated, and results combined, weighted by each earthquake's probability of occurrence.

Seismic hazard data utilized for this study was developed by the U.S. Geological Survey. Modified Mercalli Intensity maps for the M 8.6 NMSZ event (Figure 4) were developed by



SOURCE: Obermeier, 1985

2HD 208nb/PIPE-LNE

Figure 2: Pipelines Studied in New Madrid Seismic Zone Scenario

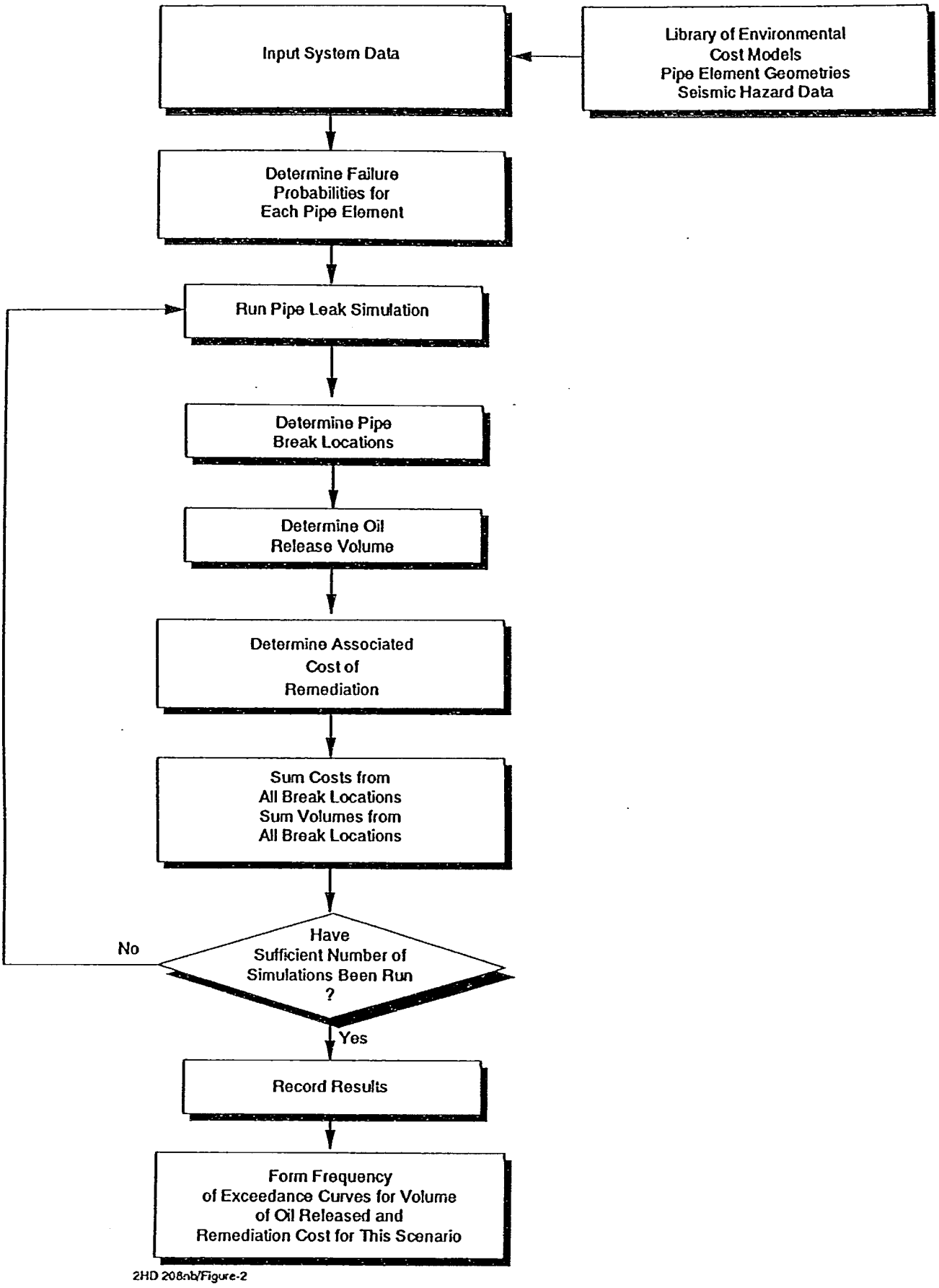
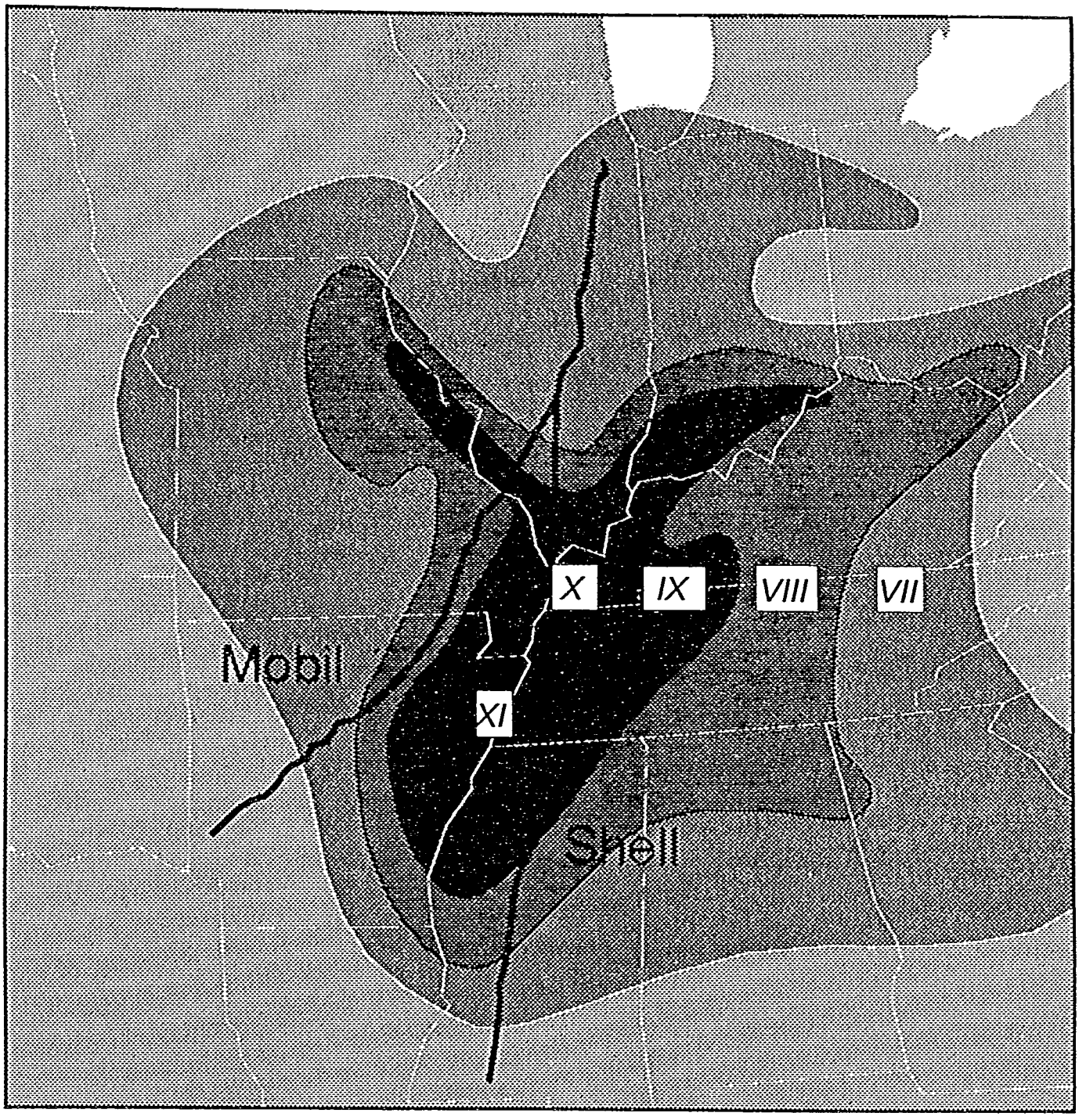


Figure 3: Procedure for Estimating Frequency of Exceedance Curves for Volume of Oil Released and Remediation Cost.



SOURCE: Algermissen and Hopper, 1984

2HD 208nb/MM-M88

Figure 4: Modified Mercalli Intensity for a Magnitude 8.6 Event Anywhere Along the New Madrid Seismic Zone. (After Algermissen and Hopper, 1984).

Algermissen and Hopper (1984), and areas of moderate to high liquefaction potential in areas identified by Algermissen and Hopper as MMI IX and above (Figure 5), were developed by Obermeier (1985). This event has an estimated 0.3 - 1.0 percent probability of occurrence by the year 2000 (Johnston and Nava, 1984). For this case study, a value of 0.5 percent probability of occurrence was assumed. Earthquake vulnerability models for underground pipelines (Eguchi, 1983, 1991) were used to determine failure probabilities for each pipeline segment. Within each simulation trial, a random number is generated for each segment. If the random number exceeds the failure probability, the pipeline element is assumed to have broken for that trial.

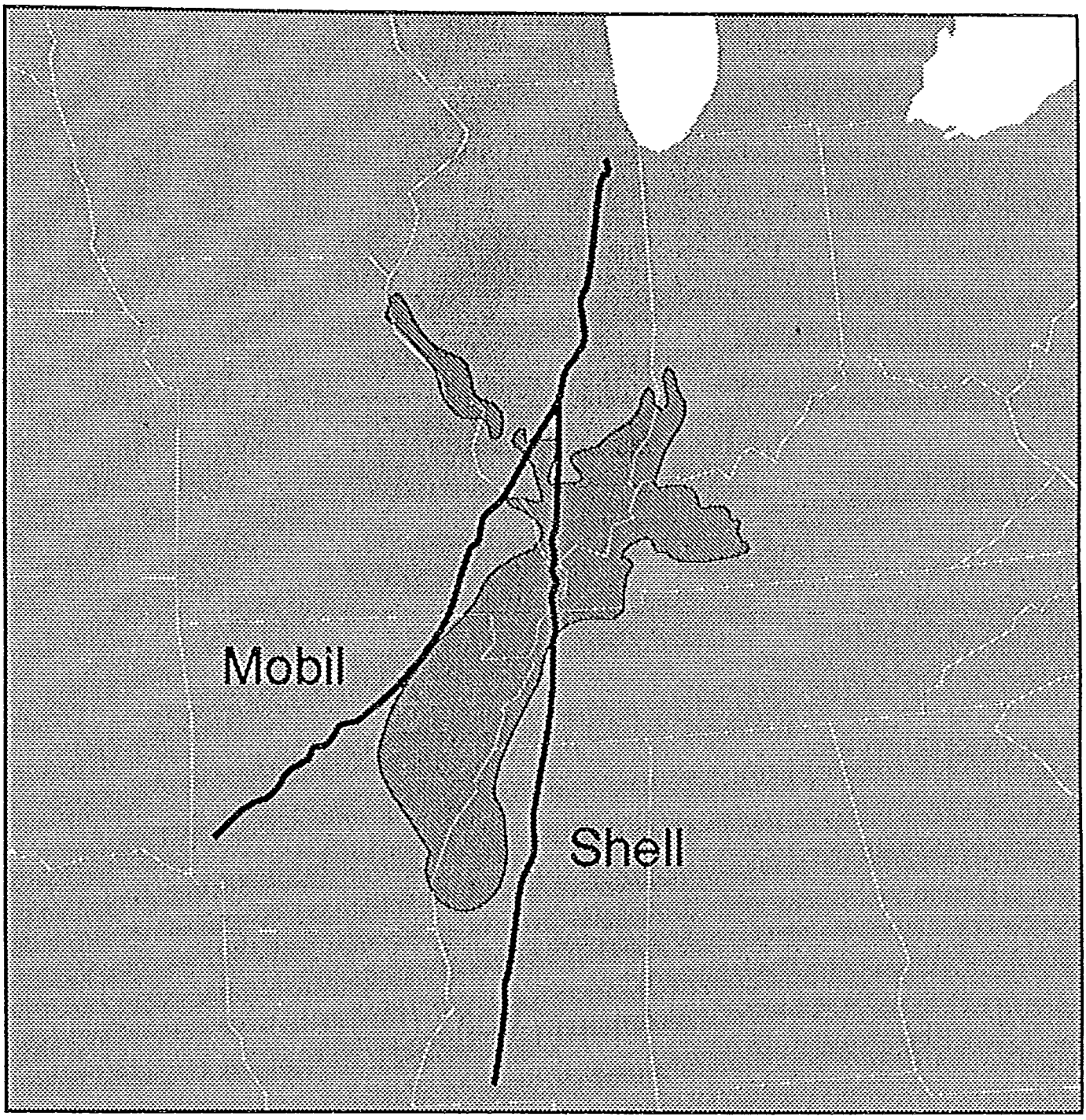
Once the locations of all breaks for a particular trial are known, a deterministic "drain down" model is employed to estimate the volume of oil released at each location. This drain down model employs several simplifying assumptions, such that the only data required to estimate the volume of oil lost is the elevation at the pipeline segment endpoints and the pipe diameter. Combining spill volume data with the selection of the proper environmental model (i.e., river crossing, flood plain, etc.) allows application of one of the library of cost models.

The cost models developed estimate both the extent of environmental contamination and the cost of remediation. Five generalized models were developed to characterize various types of contamination, based on the general topography of the area, depth to groundwater, and proximity to surface water. The contamination models estimate the vertical extent and rate of oil migration in soil, to estimate the extent of ground and surface water contamination. To develop remediation cost models, estimates of remediation costs for soil, ground and surface water contamination were obtained from experts in the field. Average remediation costs for a given contamination model were estimated using fault trees to allow consideration of numerous variables (e.g., depth to water table, soil permeability, oil type, response time and cost schedule). For each model, the average or expected cost of remediation was developed for the range of oil volumes specified.

Both volume and dollar losses are aggregated for all pipe failures resulting from the simulation trial to determine total losses from the simulated event. The simulation process continues until a stable distribution of loss are obtained. After all trials are completed, curves depicting annual frequency of exceedance are developed by normalizing the frequency curves by the number of trials performed and by the annual earthquake probability.

Preliminary results from the pipeline analysis are shown in Figures 6 (frequency of exceedance of total spill volume) and 7 (frequency of exceedance of dollar loss). The range of volumes leaked during this earthquake scenario is 150,000 to 2,350,000 barrels, with an average spill volume of 400,000 barrels. (This volume is the sum of spill volumes from all leaks occurring in this event). The average spill volume expected at a single site is 4700 barrels. Because this is a extreme earthquake scenario, at least one leak occurred in every simulation of the event, and the maximum frequency (the frequency with which at least one leak occurs) is equal to the probability of the event.

Possible dollar losses range from 30 million to 2.4 billion dollars. The large range of costs may be attributed, in part, to the difference between remediation cost models for surface water and soil. When a large number of leaks occur in a simulation, many are on flood plains or rivers, with high clean up costs. However, many more moderate cases are possible, and the average loss is expected to be 310 million dollars. The expected loss at a single leak is 3.6 million dollars.



SOURCE: Obermeier, 1985

2HD 208nb/PIPE-LNE

Figure 5: Areas of Moderate to High Liquefaction Potential in the New Madrid Seismic Zone During a Major Earthquake. (After Obermeier, 1985).

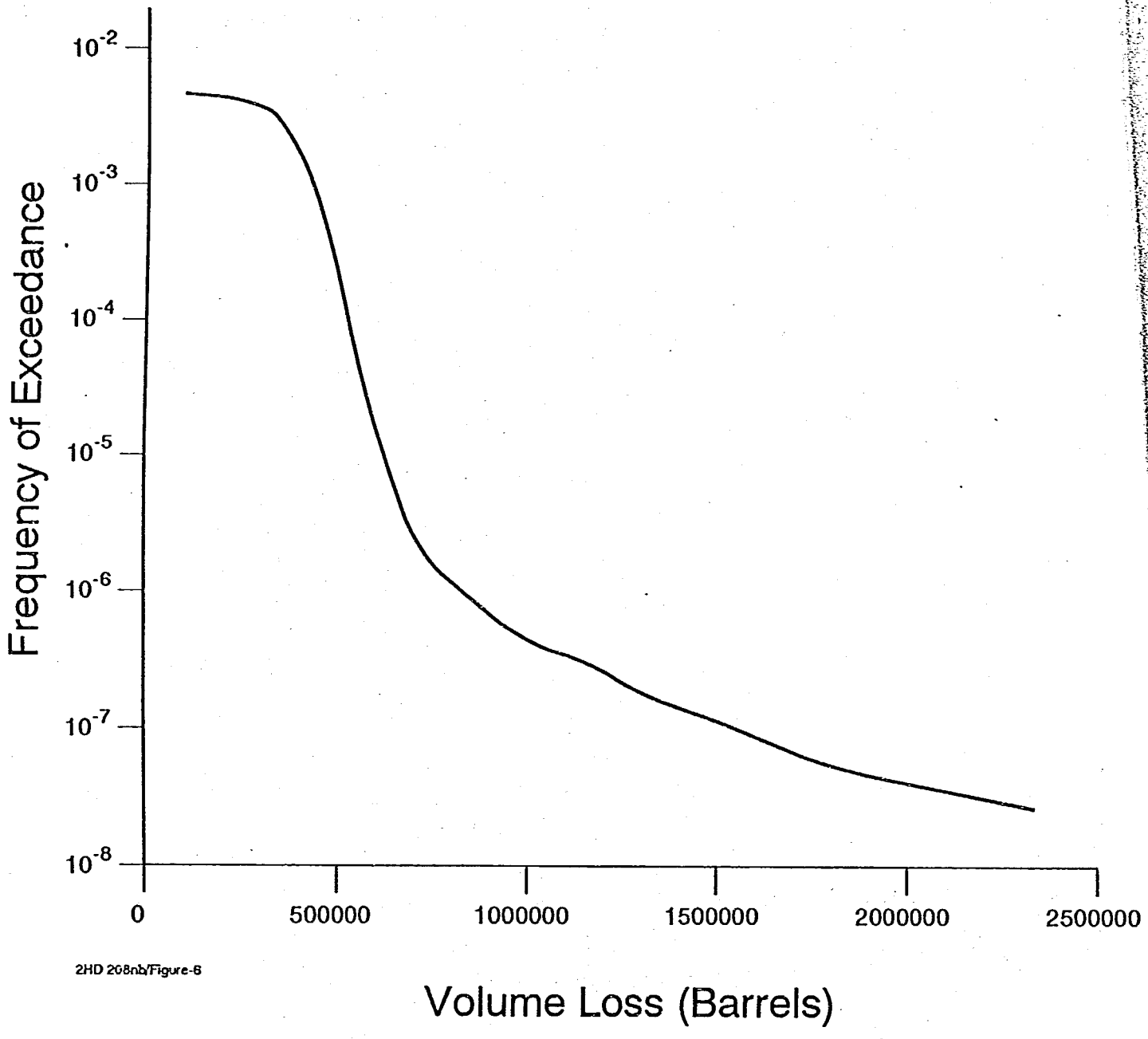


Figure 6: Frequency of Exceedance Curve for Total Spill Volume in a Major Earthquake in the New Madrid Seismic Zone.

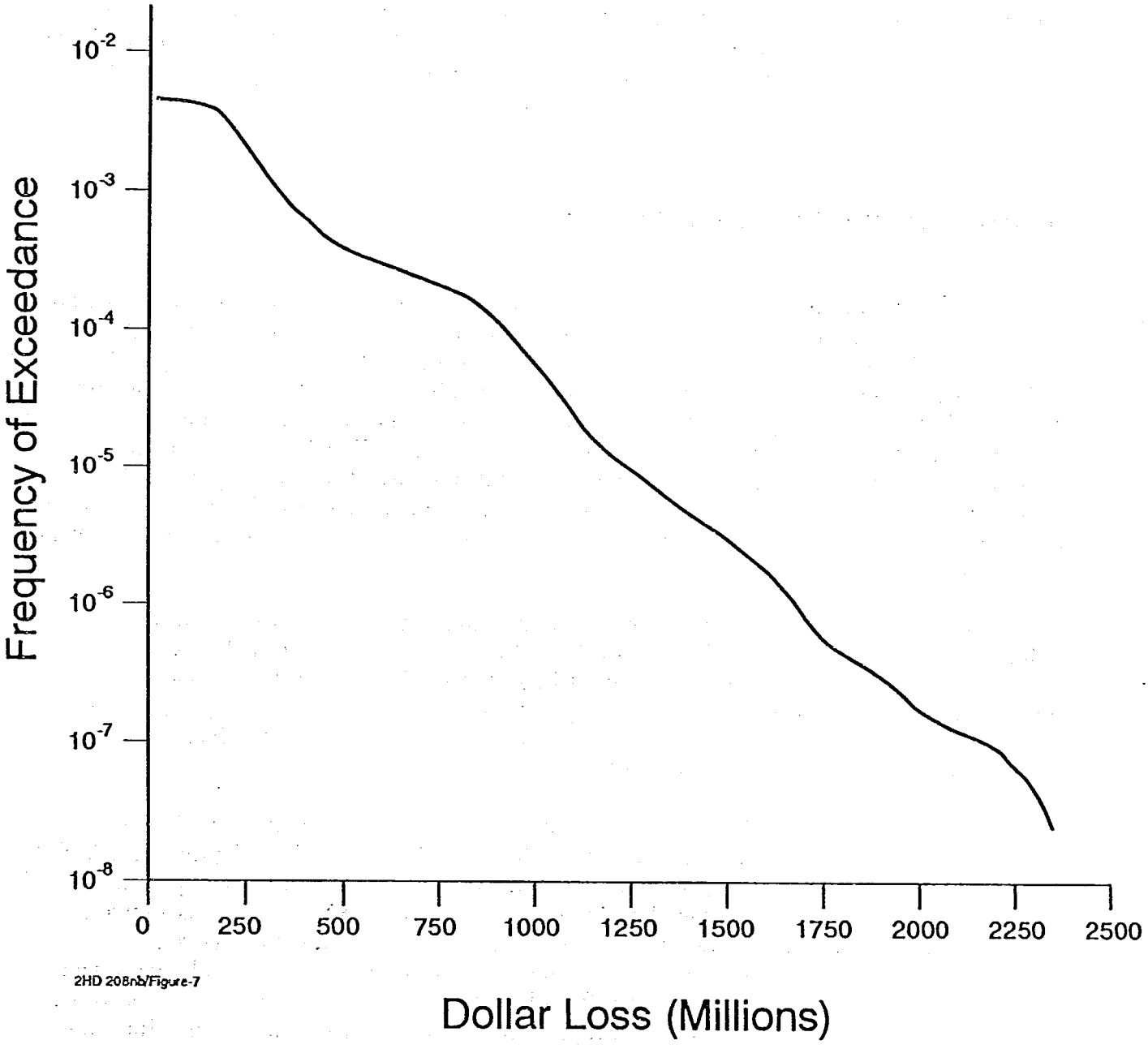


Figure 7: Frequency of Exceedance Curve for Dollar Loss in a Major Earthquake in the New Madrid Seismic Zone.

This example demonstrates the advantage of a probabilistic or risk-based approach. Had a worst-case approach been taken, high-end losses may have been predicted without an estimate of the associated likelihood. The frequency curves developed show that the high-end losses have frequencies three to four orders of magnitude lower than the average expected values.

HIGHER ORDER ECONOMIC LOSSES

In addition to the losses resulting from environmental clean-up and spill remediation, oil pipeline failures due to earthquakes may result in indirect economic losses to local economies dependent upon the impacted petroleum refineries. A recent study prepared for NCEER has examined this issue of higher order economic losses for the two oil transmission pipelines discussed in the previous section, plus a third pipeline located within the same general area for the Magnitude 8.6 scenario earthquake in the NMSZ. The methodology combines previously developed hazard and vulnerability information with expert opinion restoration estimates to develop estimates of direct economic losses to refineries. These direct losses are entered into a regional Input-Output (I-O) model to estimate economic losses for the regional economy.

The general methodology has three major components; the pipeline exposure and vulnerability assessment, the estimation of direct losses to the petroleum industry, and the estimation of indirect losses for the region of impact through the Input-Output model. All three components of the general methodology use previously accepted techniques, however, their combined use to assess indirect economic losses is unique. The study includes losses due to the economic ripple effects of lifeline failures during earthquakes.

The pipeline vulnerability assessment utilized facility and seismic hazard data as referenced in the previous section. The three subject pipelines; the Shell Capline #22, Mobil Pipeline #68, and the additional Mid-Valley Pipeline #66 (22 inch welded steel pipe installed in 1949), were overlain onto the ground shaking and liquefaction potential maps as shown in Figures 4 and 5. These maps were used to estimate the length of pipe through areas of potential liquefaction and strong ground shaking. Similar to the environmental consequence analysis, pipeline failure rates were taken from Eguchi (1991). Liquefaction failures were found to govern, and the total number of liquefaction-induced breaks on each pipeline was estimated. A total of 105 pipeline repairs were estimated for the three pipelines during a large earthquake on the NMSZ.

To estimate economic loss suffered by the refineries as a result of the pipeline damage, an estimate of restoration time was developed. Repair-time estimates were generated from an expert opinion modification to the methodology developed for California in ATC-13, "Earthquake Damage Evaluation Data for California" (1985). Pipeline restoration may be accomplished through a combination of two activities; pipeline repair and pipeline replacement. Based on historic performance in the 1971 San Fernando, 1987 Ecuador, and 1983 Coalinga earthquakes, it was concluded that replacement was more likely to be performed in areas of ground failure or large earth movements. That is, concentrated damage in areas of ground failure necessitated the replacement of some length of pipe, rather than the repair of individual leaks or breaks. Pipeline replacement was divided into 3 sub-tasks; mobilization, physical replacement, and reconnection. Estimated replacement time will depend upon the area's development density:

- Urban - 16 - 21 days per mile of pipe replaced
- Suburban - 13 - 18 days per mile of pipe replaced
- Rural - 10 - 15 days per mile of pipe replaced

Individual repairs of isolated damage or damage in areas of little ground failure are anticipated to take 5 days each, assuming that several crews will be available and that an average leak size is approximately 4,700 barrels, as estimated in the previous environmental assessment.

To distinguish between areas requiring replacement from those requiring repair, the severity of ground deformation was evaluated on the basis of the Liquefaction Severity Index (LSI), as reported by a previous NCEER investigator (Ariman et. al, 1990). When the LSI along the pipeline route exceeded 100 inches, that stretch of pipeline was assigned a replacement probability of 60%.

Total restoration of the three pipelines was estimated to require approximately 63 pipeline segment replacements, and 41 pipeline repairs. Assuming an average replacement length of one mile, and development density probabilities for the pipeline routes of 10%, 15%, and 75% for urban, suburban, and rural development, respectively, restoration estimates for the three pipelines were made, as follows:

- Pipeline 22 - 21 days
- Pipeline 66 - 88 days
- Pipeline 68 - 76 days.

These restoration estimates became the basis for estimating second order losses, or the impact of pipeline outage on the destination refineries. By multiplying the outage estimates by the average daily volume of crude oil per pipeline, it is possible to estimate the amount of crude oil not delivered to the refineries, assuming no deliveries are made until the pipeline is fully restored. To estimate the reduction in output caused by the loss of supply, an estimate of the dollar value per barrel of refined product was made by dividing the total value of shipments of U.S. refiners by the yearly volume of crude oil refined in the U.S. Multiplying the dollar value per barrel by the outage volume resulted in an estimate of refiner direct losses. This loss was calculated to be approximately $1.1 billion.

To estimate higher order losses, this study utilized an Input-Output modeling technique to represent the interdependency of various economic sectors. The selected I-O model divides the economy into 39 economic sectors. For a given industry, the model contains a coefficient representing the fractional amount of input required from every other industry to produce a unit value of output. This can, in turn, be interpreted in terms of loss. That is, if the petroleum industry suffers a drop in final output, all contributing industries will be forced to reduce their corresponding input. Losses to the regional economy are calculated by multiplying the refinery direct loss by the coefficients for each contributing economic sector.

Coefficients within an I-O model vary with the size and location of the study region. To develop the Mid-West regional I-O model, coefficients from existing United States and San Francisco Bay Area I-O models (Brady and Yang, 1991) were interpolated, based on the relative populations of the three areas. The final coefficients for the petroleum industry in the Mid-west are presented in Table 3.

Higher order losses were then calculated by multiplying each economic sector's petroleum coefficients by the reduction in output for the petroleum industry as a result of the NMSZ earthquake. These losses were further modified to take into account permanent vs. time-dependent losses. Losses by sector are also presented in Table 3. The total higher order losses were estimated to be $3.3 billion. When added to the refiner's losses, the total estimated losses for the petroleum refiners and affected economic sectors total $4.5 billion.

These results may be combined with the loss estimates developed for the environmental loss assessment. Although the environmental study includes only two pipelines, the expected losses for spill clean-up range from $30 million to $2.4 billion. Added together, damage to oil transmission pipelines in a large NMSZ earthquake, excluding direct losses to repair the pipelines, may result in second and higher order economic losses as large as $6.9 billion.

The results may also be compared to those of the ATC-25 study, which estimates business interruption, or secondary losses for various earthquakes, including a M8.0 event in the NMSZ. For the ATC-25 study, coarse estimates of direct damage were made, and importance weights were used to capture each economic sectors' lifeline dependence. The study predicts $0.4 billion in losses due to damage to national crude oil delivery lifelines. While this estimate is an order of magnitude less than the $3.3 billion estimated for the current study, the ATC-25 estimate is based on a cursory damage assessment, and does not include any economic ripple effects.

FUTURE DIRECTIONS

In order to improve our ability to assess the indirect impacts of lifeline failures and disruptions, many new issues will have to be addressed. These issues will be complex, necessitating the involvement of a multi-disciplinary team of investigators. Some of the issues which will require immediate response are:

1. Determination of impacts resulting from lifeline failures. Tierney (1992) has identified a list of 12 impacts associated with the spillage of oil during an earthquake. These effects range from environmental pollution, to threats to wildlife and vegetation, to threats to economic activity. Similar definitions need to be identified for all lifeline systems and their failure modes.

2. Quantification of lifeline dependencies for urban businesses. In order to assess the impact of lifeline disruption on business continuity, a more refined model of lifeline usage needs to be developed for small, medium and large cities. Seasonal and regional factors are important and must be considered.

3. Development of regional and local economic models to characterize business interruption loss exposure. Coarse information is currently available on a state by state basis. We know, however, that shaking intensities from an earthquake will vary significantly within a particular state. Depending upon the intensities experienced, some businesses

Table 3

INPUT-OUTPUT COEFFICIENTS FOR THE PETROLEUM INDUSTRY IN THE MIDWEST & HIGHER ORDER LOSSES (IN $ MILLION)

	ECONOMIC SECTOR	I-O COEFFICIENT	TOTAL
1.	Agriculture, Forestry, and Fisheries	0.07	$47.7
2.	Mining	0.50	223.5
3.	Construction, Residential	0.07	30.0
4.	Construction, Non-residential	0.07	30.0
5.	Construction, Highways and Public Utilities	0.07	30.0
6.	Maintenance and Repair	0.01	6.0
7.	Food and Beverage Processing	0.09	83.3
8.	Textile and Apparel Products	0.03	26.6
9.	Lumber, Wood, Paper Products, and Furniture	0.02	12.5
10.	Printing and Publishing	0.01	10.5
11.	Chemicals and Allied Products	0.04	38.5
12.	Petroleum Refining and Related Industries	1.39	1,246.2
13.	Rubber and Leather Products	0.01	9.0
14.	Stone, Clay, Glass, and Concrete Products	0.01	3.7
15.	Primary Metal Industries	0.00	2.1
16.	Fabricated Metal Products	0.01	4.1
17.	Non-electrical Machinery, except Computers	0.00	2.0
18.	Computers and Office Equipment	0.07	46.0
19.	Electric Transmission and Industrial Apparatus	0.07	60.1
20.	Household and Lighting Appliances, Radio, TV	0.02	7.2
21.	Communication Equipment	0.07	30.3
22.	Electronic Components and Equipment	0.01	4.2
23.	Transportation Equipment	0.02	13.7
24.	Professional, Scientific, Misc. Manufacturing	0.01	8.6
25.	Transportation Services	0.07	60.1
26.	Motor Freight Transport and Warehousing	0.02	10.2
27.	Communications	0.02	20.0
28.	Utilities	0.09	84.9
29.	Wholesale Trade	0.07	78.9
30.	Retail Trade	0.11	74.4
31.	F.I.R.E.	0.20	88.7
32.	Hotels and Lodging Places	0.02	21.2
33.	Personal and Repair Services	0.08	53.4
34.	Business, Professional, Engineering Services	0.05	24.4
35.	Amusement and Recreation Services	0.01	12.1
36.	Health Services	0.10	44.7
37.	Education, Non-commercial R&D, Non-profit Services	0.07	31.2
38.	Government not elsewhere Classified	0.01	5.6
39.	Households	1.17	788.9
	TOTAL	4.73	$3,344.7

may be affected while others may not. It is important to develop economic models at the same level of refinement as the patterns of earthquake intensities experienced in a region.

4. Refinement of lifeline restoration estimates. Initial estimates have been provided by ATC reports. These estimates reflect the results of surveys of expert opinion. While these estimates are useful, quantitative information must be collected to validate or modify these results. Case studies of response and restoration of lifelines from recent (last 15 to 20 years) earthquakes would provide a valuable resource for researchers.

5. Collection of post-earthquake data on indirect impacts. The 1983 Coalinga (Tierney, 1985), 1987 Whittier Narrows (FEMA/California OES/SCEPP, 1987), and 1989 Loma Prieta (EERI, 1990) earthquakes all provided information on socioeconomic impacts. These data must be collected in formats that would allow the quantification of secondary impacts. In order to facilitate this development, information collection guidelines must be developed that can be implemented after each major earthquake. These guidelines should be assembled by a team of engineers and social scientists.

REFERENCES

AAES (1990), Vulnerability of Energy Distribution Systems to an Earthquake in the Eastern United States: An Overview, American Association of Engineering Societies.

Algermissen, S.T. and M.G. Hopper (1984), "Estimated Maximum Regional Seismic Intensities Associated with an Ensemble of Great Earthquakes that Might Occur along the New Madrid Seismic Zone, East-Central United States," U. S. Geological Survey Miscellaneous Field Studies Map MF-1712.

Algermissen, S.T., E.P. Arnold, K.V. Steinbrugger, M.G. Hopper and P.S. Powers (1988), Earthquake Losses in Central Utah, United States Geological Survey Open File Report 88-680.

Allen, David L. et al., (1988) Earthquake Hazard Mitigation of Transportation Facilities, Kentucky Transportation Research Program, University of Kentucky.

Ariman, T. et al., (1990) Pilot Study on Seismic Vulnerability of Crude Oil Transmission Systems, National Center for Earthquake Engineering Research, NCEER Technical Report NCEER-90-008.

ASCE (1977), The Current State of Knowledge of Lifeline Earthquake Engineering, American Society of Civil Engineers, New York.

ASCE (1980), Social and Economic Impact of Earthquake on Utility Lifelines, American Society of Civil Engineers, New York.

ASCE (1981), Lifeline Earthquake Engineering: The Current State of Knowledge, American Society of Civil Engineers, New York.

ASCE (1983), Advisory Notes on Lifeline Earthquake Engineering, Technical Council on Lifeline Earthquake Engineering, American Society of Civil Engineers, New York.

ASCE (1984), Guidelines for Seismic Design of Oil and Gas Pipelines, Technical Council on Lifeline Earthquake Engineering (Gas and Liquid Fuels Committee), New York.

ASCE (1991), Lifeline Earthquake Engineering, Technical Council on Lifeline Earthquake Engineering, American Society of Civil Engineers, New York.

Applied Technology Council (1985), Earthquake Damage Evaluation Data for California, Report ATC-13, Redwood City, California.

Applied Technology Council, (1991), Seismic Vulnerability and Impact of Disruption of Lifelines in the Conterminous United States, Applied Technology Council Report ATC-25.

Campbell, K.W., R.T. Eguchi and C.M. Duke (1979), "Reliability in Lifeline Earthquake Engineering," Journal of the Technical Councils, ASCE, Vol. 105, No. TC2, December, 1979, pp. 259-270.

REFERENCES (CONTINUED)

Cassaro, M.A., M.J. Cassaro, R.K. Ragade, and S. Alexander, (1992), "Risk Based Decision Support Model for Water Delivery Systems Subject to Natural Hazards", Lifeline Earthquake Engineering in the Central and Eastern U.S., TCLEE Monograph No. 5, D. Ballantyne, Editor.

CDMG (1982a), Earthquake Planning Scenario for a Magnitude 8.3 Earthquake on the San Andreas Fault in Southern California, California Division of Mines and Geology, Special Publication 60.

CDMG (1982b), Earthquake Planning Scenario for a Magnitude 8.3 Earthquake on the San Andreas Fault in the San Francisco Bay Area, California Division of Mines and Geology, Special Publication 61.

CDMG (1987), Earthquake Planning Scenario for a Magnitude 7.5 Earthquake on the Hayward Fault in the San Francisco Bay Area, California Division of Mines and Geology, Special Publication 78.

CDMG (1988), Planning Scenario for a Major Earthquake on the Newport-Inglewood Fault Zone, California Division of Mines and Geology, Special Publication 99 (Preprint).

CDMG (1990), Planning Scenario for a Major Earthquake, San Diego - Tijuana Metropolitan Area, California Division of Mines and Geology, Special Publication 100.

Crespo, E., et al. (1987), "1987 Ecuador Earthquake of March 5, 1987: EERI Special Earthquake Report," EERI Newsletter, Vol. 21, No. 7, July.

Development Technologies, Inc. (1992), Indirect Economic Consequences of a Catastrophic Earthquake, Prepared for FEMA.

Ebel, John et al., (1990), Metropolitan Boston Area Earthquake Loss Study, Loss Analysis Committee Report and Recommendations, Massachusetts Civil Defense Agency.

Earthquake Engineering Research Institute (1990), Loma Prieta Earthquake Reconnaissance Report, Earthquake Spectra, Supplement in Volume 6, May.

Eguchi, R.T., (1983), "Seismic Vulnerability Models for Underground Pipes," Earthquake Behavior and Safety of Oil and Gas Storage Facilities, Buried Pipelines and Equipment, PVP - Vol. 77, ASME, New York.

Eguchi, R.T., (1991), "Seismic Hazard Input for Lifeline Systems," Structural Safety, 10, Elservier Science Publishers B.V., pp. 193-198.

Eguchi, R.T. and S.D. Pelmulder (1992), "Indirect Economic Impacts of Energy Network Failure," Indirect Economic Consequences of a Catastrophic Earthquake, Development Technologies, Inc. Report Prepared for FEMA.

FEMA (1987), "The Los Angeles - Whittier Narrows Earthquake of October 1, 1987: Federal/State hazard Mitigation Survey Team Report," Prepared by the Federal

REFERENCES (CONTINUED)

Emergency Management Agency, Region IX; California Governor's Office of Emergency Services, Southern California Earthquake Preparedness Project and Planning Division.

FEMA/CUSEPP (1985), An Assessment of Damage and Casualties for Six Cities in the Central United States Resulting from Earthquakes in the New Madrid Seismic Zone, Prepared by the Central United States Earthquake Preparedness Project (CUSEPP) for the Federal Emergency Management Agency (FEMA, 1990).

FEMA/CUSEPP (1990), Estimated Future Earthquake Losses for St. Louis City and County, Missouri, Prepared by the Central United States Earthquake Preparedness Project (CUSEPP) for the Federal Emergency Management Agency (FEMA).

Harlan, M.R. and C. Lindbergh (1988), An Earthquake Vulnerability Analysis of the Charleston, South Carolina Area, Department of Civil Engineering, The Citadel, Charleston, South Carolina.

Johnson, A. and S.J. Nava (1984) "Recurrence Rates and Probability Estimates for the New Madrid Seismic Zone," Proceedings of the Symposium on "The New Madrid Seismic Zone, P.L. Gori and W.W. Hays, eds., USGS Open File Report 84-770.

Kennedy/Jenks/Chilton (1990), Earthquake Loss Estimation of the Seattle Water System, Prepared for U.S. Geological Survey.

Kennedy/Jenks/Chilton (1991), Earthquake Loss Estimation for the City of Everett, Washington's Lifelines, Prepared for U.S. Geological Survey.

NOAA (1973), A Study of Earthquake Losses in the Los Angeles, California Area, National Oceanic and Atmospheric Administration for the Federal Disaster Assistance Administration, Department of Housing and Urban Development.

Obermeier, S.F. (1985), Plates 1-7, in Estimation of Earthquake Effects Associated with Large Earthquakes in the New Madrid Seismic Zone, M.G. Hopper, ed., U.S. Geological Survey, Open File Report 85-457.

Pelmulder, S.D. and Eguchi, R.T. (1992), "Regional Risk Assessment of Environmental Contamination from Oil Pipelines," Proceedings of the 4th U.S. - Japan Workshop on Earthquake Disaster Prevention for Lifeline Systems."

SCEPP (1983), Pilot Project for Earthquake Hazard Assessment, Southern California Earthquake Preparedness Project.

Seligson, H.A., R.T. Eguchi, L. Lund and C.E. Taylor (1991), Survey of 15 Utility Agencies Serving the Areas Affected by the 1971 San Fernando and the 1987 Whittier Narrows Earthquakes, Prepared for the National Science Foundation, Dames & Moore Research Report 91-01.

Shinozuka, M., M. Murata and T. Iwata (1992), "Strategies for Repair and Restoration of Seismically Damaged Gas Pipeline Systems," Proceedings of the 4th U.S. - Japan Workshop on Earthquake Disaster Prevention for Lifeline Systems.

REFERENCES (CONTINUED)

Spangle, W.E. (1987), Pre-Earthquake Planning for Post-Earthquake Rebuilding, Prepared for the National Science Foundation.

Taylor C.E., M. Salmon, R. Eguchi, R. Campbell, C. Tillman and J. Haber (1988), Continuing Investigations of Earthquake Risk to Utah Water and Gas Systems, Prepared by NTS Engineering, Long Beach, CA, for the U.S. Geological Survey.

Taylor, C.E. and D.B. Ward (1981a), Seismic Risk Assessment of Electric Power Systems in Utah and Recommendations for Risk Reduction, Utah Seismic Safety Advisory Council, USSAC-15.

Taylor, C.E. and D.B. Ward (1981b), Seismic Risk Assessment of Principal Communications Systems in Utah and Recommendations for Risk Reduction, Utah Seismic Safety Advisory Council, USSAC-20.

Taylor, C.E. and D.B. Ward (1981c), Seismic Risk Assessment of Utah Transportation Systems and Recommendations for Risk Reduction, Utah Seismic Safety Council, USSAC-18.

Taylor, C.E. and D.B. Ward (1981d), Seismic Risk Assessment of Oil and Natural Gas Systems in Utah and Recommendations for Risk Reduction, Utah Seismic Safety Advisory Council, USSAC-16.

Taylor, C.E., and C.E. Bigler (1982), Preliminary Investigation of Possible Earthquake Effects on Salt Lake County Water Supply Systems, Utah Division of Comprehensive Emergency Management.

Taylor, C.E., J.H. Wiggins, J.M. Haber and D.B. Ward (1986), A Systems Approach to Wasatch Front Seismic Risk Problems, Prepared by NTS Engineering, Redondo Beach, CA, and Structural Facilities Inc., Salt Lake City, UT for the U.S. Geological Survey.

Taylor, Craig E., ed. (1991), Seismic Loss Estimates for a Hypothetical Water System: A Demonstration Project, American Society of Civil Engineers Technical Council for Lifeline Earthquake Engineering (ASCE/TCLEE) Monograph No. 2.

Tierney, K.J. (1985), Report on the Coalinga Earthquake of May 2, 1983, Prepared for State of California, Seismic Safety Commission.

Tierney, Kathleen J. (1992), Literature Review on Socioeconomic Impacts, NCEER Pipeline Study (DRAFT), Prepared by the Disaster Research Center, University of Delaware for the National Center for Earthquake Engineering Research.

USGS (1976), A Study of Earthquake Losses in the Salt Lake City, Utah Area, United States Geological Survey, Open-File Report 76-89.

Wang, L.R.L. et al., (1990), Development of Inventory and Seismic Loss Estimation Model for Portland, Oregon Water and Sewer Systems, Prepared by the Department of Civil Engineering, Old Dominion University, Norfolk, Virginia for the U. S. Geological Survey.

EARTHQUAKE-INDUCED CONGESTION IMPACTS ON LOCAL TELEPHONE NETWORKS

L. J. Forys

Director, System Performance Modeling Group

Bell Communications Research, USA

ABSTRACT

Earthquakes have two major impacts on traffic congestion in local networks. There is a large increase in demand, and the connectivity of the network decreases. Both of these can cause long delays in obtaining dial tone, and in completing calls. We discuss preliminary work indicating the potential severity of dial tone delays, and also quantify the potential benefits of providing priority dial tone for selected customers. In addition, a number of proposed enhanced priority call completion strategies are discussed. Finally, we outline what work needs to be done to predict the impact of earthquakes on congestion in realistic local telephone networks, and to determine the benefits of priority enhancements.

INTRODUCTION

Earthquakes can impact the local telecommunications network in obvious ways by destroying local exchanges, or subscriber loop access to a local exchange. In this paper we concentrate on analyzing less severe impacts which do not involve local exchange or local loop failures. If the local exchange and local loop are intact, subscribers still experience service degradation through two mechanisms. The first involves service degradation due to unusually high demands placed on local switching equipment. In analyzing data from several stressful scenarios (tornados, snowstorms, hurricanes), it is common for a local exchange to experience a 100% increase in offered attempts. In these scenarios, no extensive damage was done to connecting facilities, the additional attempts were due to the criticality of the situation. As we indicate later, if a local exchange is not loaded to its maximum capacity, the impact of the additional load may not be severe. However, it is becoming common to consolidate several analog switches and replace them with a single, large digital switch, often increasing processor loading.

The second mechanism that impacts performance involves service degradation due to loss of connectivity in the local (or long distance) network. This loss of connectivity will not only cause network blockages, but in addition can additionally increase the attempt load on local exchanges due to customer reattempts. We will first deal with the issues involved in switch overloads. We provide an approximate analysis to quantify the severity of dial tone delays (switch access delays). We then outline several mechanisms which are expected to enhance call completion probabilities for critical users. Finally we propose a work plan that is required in order to provide a benchmark for existing local networks, and which may also be used to assess the efficacy of enhanced call completion mechanisms.

DESCRIPTION OF CURRENT SWITCH OVERLOAD CONTROLS

In order to understand the impact of heavy loads on local exchanges, it is important to understand the overload logic used by the processors in these exchanges. The overload strategies result in giving priority treatment to calls in progress, by controlling the processing of new call attempts. This results in the occurrence of dial tone delays when switches are overloaded. In fact, the primary cause of dial tone delays in modern switches is processor overload. Most modern switch processors incorporate some version of the "LIFO" (Last-In-First-Out) overload strategy required by the LATA Switching System Generic Requirements (LSSGR) produced by Bellcore. This strategy was originally incorporated in 1ESS over a decade ago and has been documented in detail in references 1 and 2. We will only summarize it here. Basically, the LIFO strategy was introduced in order to mitigate the abnormally high ineffective attempts caused by customers dialing before dial tone during overloads thus resulting in partial dials. High numbers of ineffective attempts cost system resources and reduce the number of completed calls that can be processed. Previous overload controls basically handled bids for dial tone in a

First-In-First-Out (FIFO) manner, serving the oldest waiting bid first. During overloads, dial tone delays would increase for all customers. A large fraction (40% and more) of customers do not wait for dial tone, but begin dialing as though tone were present. Since dial tone is sent only when the resources (e.g. digit receivers) necessary to process digits are allocated, customer calls that receive dial tone while dialing result in partial dials, and are ineffective. They waste system resources and often customers reattempt their bids for service, further exacerbating the overload.

Field data and analytic studies indicate that with FIFO, the percentage of successfully handled calls (calls to ringing, busy or successfully outpulsed) declines to 70% and less of what is achievable if there were no increase in ineffective attempts. The LIFO strategy overcomes this problem by insuring that a significant fraction of customer attempts do not experience any delay in receiving dial tone. This is accomplished by processing the freshest bid for service before other bids for service. Unfortunately, although this will insure high levels of call completions (high throughput), it does not reward the "patient" customer. This is resolved by having the processor artificially reoriginate attempts for patient customers, who have waited for a prescribed timing interval. Thus, patient customers become "fresh" customers. Any customer actions, such as flashing, or disconnect and reorigination are ignored while a customer is enqueued for dial tone. The algorithm results in dial tone delays which are either very short, or long enough (e.g. 15-20 seconds) so that early dialers abandon and so are not seen by the system, and only patient customers are handled.

A decade of field experience with the LIFO control indicates that ineffective attempts are minimized, resulting in significantly higher levels of completed calls. For example, reference 2 presents field data that demonstrates that call completions are maintained at high levels (95% of capacity) even during a 50% overload. Also, customer complaints are substantially lessened. Many customers do not experience dial tone delays during modest overloads. If they do experience dial tone delays and abandon their attempts, subsequent attempts by the customer may result in no delay for dial tone.

DIAL TONE DELAY PERFORMANCE DURING SEVERE OVERLOADS

Under exceptional (e.g. 100%) overloads, however, it is likely that a significant number of customers will experience long dial tone delays. Table 1 summarizes the results of approximately analyzing the dial tone delay distribution for a sample case of a modern digital switch having a 20 second timing interval.

A key assumption used in this analysis is that the calls incoming from other offices are always completed and that their calling rate is fixed. Thus, only an originating overload is modeled. Should the incoming calling rate increase in the same manner as originations, the delays would be substantially greater, particularly in switches where incoming trunk requests receive higher priorities for processor resources than line originations. The details of our analysis, including further discussion of the assumptions, are documented in Appendix A.

In Table 1, the percentage of calls experiencing dial tone delays greater than a given length of time are tabulated for various overload levels. Here, the percent overload is the percentage of attempts which are greater than the maximum capacity of the switch processor (peripheral processor or central processor, as appropriate). The "Total Attempts" includes both the customers' first attempts to receive dial tone together with reattempts resulting from ineffective call attempts. It is assumed that there are sufficient hardware resources available, and that the only cause for dial tone delay is processor overload.

As the table indicates, when the overload is sufficiently great, some customers could be experiencing significantly large delays. As an example, if the overload were 100% more than the processor capability, 9% of customers, who waited patiently, would not receive dial tone within 80 seconds. It is unlikely that customers would be willing to wait this long for dial tone. Our analysis of several overload scenarios indicates that overloads in excess of 100% are possible for natural disasters. The basic reason for this is that, if a call does not complete, it is highly likely that the call will be reattempted within a short period of time. Various studies indicate that approximately 70% of ineffective attempts will result in at least one reattempt.

If we now consider the % overload as being the % of *first offered* attempts in excess of capacity, we can derive results similar to Table 1. These results are depicted in Table 2. As this table indicates, a 30% *first offered* overload corresponds to a 100% *total attempt* overload as indicated in Table 1.

PRIORITY DIAL TONE STRATEGIES

There are a number of current trends, in both the government sector as well as the public sector to provide priority service to critical users. One such example is priority restoral and initiation of service for critical users as outlined in Part 64 of the FCC Rules and Regulations. There are two other mechanisms which address the problem of giving priority access to dial tone. These are called "Line Load Control" (LLC) and "Essential Service Protection" (ESP). Line Load Control has existed for a number of years. A manual means of controlling traffic by denying access to groups of non-critical users was available in No. 5 Crossbar Switches, and it may have been available even earlier. The basic idea was that in extreme conditions, the load on the switch could be reduced by this means, thus giving critical users more ready access to the switch. In No. 5 Crossbar, groups of lines would have their service manually inhibited and they would have to be manually restored. In 1ESS, the Line Load Control feature was enhanced so that the removal and restoral of lines for non-critical users could be done automatically, and only when required. Essential Service Protection was introduced shortly after the introduction of the LIFO strategy, and builds on this strategy. It differs from LLC in that no lines are ever deliberately denied access to the switch.

In the next two sections, we briefly discuss the performance of LLC both before LIFO and after the introduction of LIFO. We also analyze the performance of ESP and show

how it provides superior service to essential customers, while only minimally impacting non- essential customers.

Characterization of LLC performance

In this section we will focus on LLC as implemented in the 1/1A ESS, since most of the field experience with LLC in the U.S. has been with this implementation. Line Load Control has the characteristic that during periods of long dial tone delays, certain groups of lines will be denied service in order to relieve processor congestion. "Essential" or "priority" lines are never denied service. As dial tone delays subside, a fraction of denied lines will be brought back into service. Initiation of LLC is done by manual means. However, once initiated, dial tone delays are periodically monitored on artificial bids for service and the fraction of lines which are scanned is determined from this measurement. Besides consciously denying service to groups of lines for potentially long periods of time, there are other major problems with this mechanism: the dial tone delays experienced by essential lines can still be long and the throughput of the system can be degraded. Simulation studies of the 1ESS implementation of LLC without LIFO indicate that even during modest overloads (10%), the fraction of *priority* calls experiencing dial tone delays in excess of three seconds was very high, .90. The overall call throughput dropped to 80% for these same load levels. When LIFO was implemented, LLC did not activate until 100% overloads occurred. This was due to the fact that LIFO allows a subset of calls to receive nearly instantaneous dial tone. Test calls, would only randomly experience dial tone delays, and hence the mechanism not activate. Because of these performance attributes, LLC is not a recommended form of overload control and call prioritization in the LSSGR, and is almost never used in the U.S..

Characterization of Essential Service Protection performance

Essential Service Protection was originally designed to work synergistically with the LIFO overload strategy. Instead of reducing the offered attempt load by selectively denying service to groups of customers, ESP gives preferential treatment to a subset of lines. ESP makes no attempt to reduce the load through the deliberate denial of service to specific lines. In this section we will analyze how ESP impacts the dial tone behavior of non-ESP calls and the expected performance of ESP calls during severe overloads. The performance of ESP depends on switch architecture. In the sections below we will focus on a specific, but common architecture to illustrate the characteristics of ESP.
In digital offices, there is a great degree of flexibility in assigning customers the Essential Service Protection feature. Rather than designating entire line groups for ESP, as in a 1/1A ESS, individual lines are designated for this service. As a result, the percentage of ESP lines in a digital office is typically only a few percent. However, as we indicate

below, a penetration of 15% still has minimal impact on the dial tone availability for non-ESP customers.

ESP performance for peripheral processors

In almost all modern digital switches, peripheral processors provide dial tone. In Appendix B, a generic mathematical model is developed to approximately analyze the dial tone behavior of both ESP and non-ESP calls for peripheral processors. The way that ESP is typically implemented is to have the microprocessor that does line scanning distinguish an ESP origination from a non-ESP origination, and to enqueue the ESP originations into a higher priority queue than non-ESP originations. It does this when the ESP feature is activated, which typically requires a manual input. Call-in-progress work, such as digit analysis, network connections and disconnects is done at an even higher priority level. Often, trunk originations are also processed at a high priority level, especially if they are originated on SS7 trunks. In our model, we assume that the mode of operation is to first process all non-origination related work, if time is available to then process ESP bids for dial tone, (in a first-in-first-out FIFO manner), and finally to process non-ESP bids for dial tone (using the LIFO algorithm). In actual practice, this strict priority is not exactly followed. For example, several bids for dial tone are often processed together even if call-in-progress work is detected while they are being processed. Thus, our model is somewhat conservative in assessing the dial tone delay performance for ESP calls. The analysis of dial tone delay behavior for non-ESP calls is an expansion of the model developed in Appendix A, and tends to be somewhat optimistic, although its accuracy improves for large overloads.

Figure 1 illustrates the impact of ESP calls on the dial tone delay performance of non-ESP calls. The term α in the figure represents the fraction of initial attempts which are ESP. Thus, the four curves in Figure 1 represent values of $\alpha = 0, .05, 10,$ and $.15$. The value $\alpha = 0$ is depicted to indicate the expected performance when ESP is not activated. Thus, it serves as a benchmark with which to compare the impact of ESP.

Two points of the delay distribution were chosen for comparison. The top set of curves represent the probability that the dial tone delay for non-ESP calls exceeds 20 seconds, while the lower set of curves is that for 40 seconds. For the heavy overload case of 30% first offered overload (or 100% total offered overload), the probability of dial tone delay exceeding 40 seconds increases from .3 at $\alpha = 0$ to .36 at $\alpha = .15$. The impact of providing ESP is thus estimated to be minimal for non-ESP customers even with 15% penetration of ESP service.

The predicted dial tone delay for ESP calls is indicated in Figure 2. As can be seen in the figure, the average dial tone delay is almost independent of overload for the region of interest. It also increases only slightly as the penetration of ESP increases. For ESP calls, not only is the mean dial tone delay modest, but the probability of long delays is small. For example, we estimate that the percentage of ESP calls experiencing a dial tone delay in excess of 20 seconds is negligibly small (less than a .3% chance) in the region of

interest. Only if the offered load is extremely high does the likelihood of excessive dial tone delay become apparent. In the extreme case of $\alpha = .15$, the first offered load would have to approach 600% overload before excessive dial tone delays would become apparent.
In certain switch architectures, the central processor is also involved in providing dial tone. In these processors, ESP is also implemented in the central processor. The results are similar to that presented for peripheral processors, except that the delays are about a factor of 40 less for ESP calls, 100 milliseconds. The impact of ESP calls on non-ESP calls is similar to that depicted in Figure 2.

PROPOSALS FOR ENHANCED CALL COMPLETION FOR PRIORITY CALLS

Even though ESP does provide effective prioritization in obtaining dial tone, ESP attempts could still experience severe difficulties in completing their calls. This factor, together with the costs of administering ESP, is a key of the reasons why several BCCs have chosen not to offer ESP. In this section we explore several proposals which extend the aim of ESP. These proposals concentrate on the providing of priority service not only for dial tone, but also for other switch resources and even network resources. Their objective is to provide adequate end to end completion of calls to priority callers during emergency situations such as earthquake disasters.

Queueing for selected trunk groups

During severe overloads, trunk groups can often become congested, causing ESP calls to be sent to reorder, if no alternative path exists. A possible extension of ESP is to allow ESP calls to queue for an outgoing trunk on selected trunk groups. In typical BCC networks, the sizes of the trunk groups, particularly to tandems (via exchanges),is large. Often several hundred trunks are in such groups. If a trunk group is of size 100, and the average holding time of calls is 180 seconds, then a trunk within a congested group will become idle, on average, in under two seconds. By allowing ESP calls to queue for certain trunk groups, some post-dial delays would occur for these calls, but for a wide range of scenarios, these would be short. For example, assuming that ESP calls comprise 5% of the total outgoing calls offered to a trunk group of size 100 and assuming a 100% overload on the trunk group, we estimate that the expected time that a queued call will have to wait for a trunk to become free is just over 2 seconds. The size of the queue could be set in order that the post-dial delays would be reasonable. This setting would depend on the trunk group size. If the queue were full, the ESP call would then be sent to reorder as before. The impact on non-ESP calls by permitting queueing is expected to be small if the ESP penetration is small.
However, there is a real time penalty for queueing calls for a trunk group. With ESP calls

restricted to less than 15% of the first first offered calls in the switch, the effects should be minimal, but this needs to be further explored. Also, it may be preferable to only queue for final routes, since this will allow for the full availability of routes. The potential for significant call completion improvement for ESP customers is high and the impact on non ESP customers is minimal.

Queueing for other switch resources

In all current switch implementations, when all network paths within the switch which are required for call completion are unavailable, the call is sent to reorder. An exception to this is the case of "blocked dial tone", when all paths to an appropriate digit receiver are unavailable. In the blocked dial tone case, the attempts are enqueued until an appropriate path becomes available.
In observed field data, as many as 5% of attempts may be sent to reorder due to internal network congestion during periods of severe (100%) overload. Although this may not be as pressing a problem as trunk blocking, a similar queueing strategy to that of blocked dial tone could be used to enhance call completions for ESP calls. The feasibility of this needs further investigation. What needs to be assessed is the expected queueing delay that would be experienced by ESP calls, the amount of real time expenditure required to implement the feature, and the impact of the feature on non-ESP customers. In addition, switch vendors are providing switching fabrics which cause less blocking than those currently available. The impact of these new switching fabrics on overload performance has not yet been established.

Exemption from Network Management controls

Certain types of network management controls e.g. call gapping controls would cause ESP calls to be sent to reorder even though facilities exist to handle the call, especially if trunk queueing is allowed. In emergency situations, it may be especially important for ESP calls to reach congested destinations. Thus, the issue of exempting ESP calls from certain NM controls should be examined.

Exemption from CCS congestion controls

The (CCITT SS7) Common Channel Signalling (CCS) network is being widely deployed in the U.S.. It is designed to be totally redundant, should links or other network elements fail. Each network element is engineered to handle a 100% overload. However, should the network become severely damaged, through, e.g. a severe earthquake, congestion can

develop. The CCS network has a number of congestion controls which are intended to alleviate congestion should portions of the network overload. Several of these controls are necessary so that CCS messages will not attempt routes which do not exist, e.g. Transfer Prohibit (TFP), and Transfer Restrict (TFR). Clearly, it does no good to have messages associated with ESP calls exempted from these types of controls. However, other controls are sent when certain links (or link sets) are available, but congested. This mechanism makes use of Transfer Control (TFC) messages, which indicate to the originating point that messages of a given priority are temporarily not allowed into the network to a given destination. There are currently 4 priority levels assigned to CCS messages, the highest of which is reserved for network management messages e.g. TFPs, TFRs.
Call set-up messages, Initial Address Messages (IAMs) currently have the second lowest priority of non-NM messages, but recent changes to Bellcore requirements indicate that they should have the lowest priority. However, the U.S. version of the protocol does allow a fraction of IAMs to have higher priorities. This could be used to enable ESP calls to have higher priority in the CCS network.
The way that TFCs are implemented within Service Switching Points (SSPs) needs to be modified in order to take advantage of the possibility of higher priorities for IAMs. Currently, all SSPs that are used by the BCCs implement the blocking of IAMs in the following manner. Upon reception of a TFC indicating that IAMs are to be blocked, the trunk group which services the destination is artificially made busy. Thus, even though an IAM of an ESP call may have a higher priority than IAMs of non-essential calls, the call will be route advanced, or sent to reorder. SSPs would need to be modified to allow essential calls to be exempted from this situation. An analysis of the estimated benefit of providing IAMs priority within the CCS network is required in order to justify the associated development costs. In addition, an analysis of alternative CCS network architectures through the use of "E-links" needs to be performed.

ESP for trunks

In certain applications, especially access tandems, it may be desirable to extend the concept of ESP to certain trunks, or trunk groups. Currently, all trunks are handled at the same priority level and are subjected to the same internal overload controls. If certain trunks or trunk groups were designated as handling ESP calls, priority treatment for these calls within the switch could be introduced. This could include exemption from internal overload controls, queueing for switch fabric and other resources, and possible exemption from CCS congestion controls for calls leaving the switch.

AUTOVON priority software

Specialized software was developed for several switches to handle high priority,

government, traffic. It has the generic name, AUTOVON. Several of its features may help implement the specific proposals indicated above. The feasibility of using AUTOVON software needs to be assessed for civilian applications.

Dynamic routing strategies

Current local networks use static routing strategies to determine the choice of a route between two destinations. Thus, should severe damage occur because of earthquakes, it may not be possible to find an undamaged path to certain destinations without significant manual intervention and changes to the network topology. However, there are several proposed dynamic strategies which enable the determination of routes to be done on the basis of network conditions in real time without involving manual intervention. These strategies hold the promise of being able to optimally reconfigure a damaged network. One of the difficulties of implementing such strategies is that they tend to be specific to a switch vendor. Thus, it is necessary to assess the benefit of incorporating only a partially deployed dynamic strategy.

WORK REQUIRED

In order to assess the benefits of the call completion enhancement proposals indicated in the previous section, a study network and performance analysis tools are required. The impact of earthquakes on local networks is critically dependent on the state of loading of network elements as well as damage scenarios. We currently have a variety of performance tools to study individual network components. In the course of analyzing vendor switches, Bellcore has developed performance models of such switches. Trunk network models have been used to investigate dynamic routing strategies. Simulations of CCS networks exist to characterize CCS network performance. However, we do not currently have a tool (simulation or analytic models) which combines all of these network elements. Yet, in order to investigate the types of scenarios that earthquake damage presents, it will be necessary to have an integrated tool.
Such a tool would require, as inputs, several factors:

- Undamaged network topology including types of switches, trunk connectivity, CCS network topology.
- Estimates of damage to CCS network elements, trunking network, and switches.
- Degree of loading of the network elements at time of earthquake, and estimates of load increases due to the quake. This would require inputs from interexchange carriers as well.

- Candidate enhancements and how they might be implemented in realistic network elements.

The size of local networks is large. LATAs may often have 100-200 (and more) local exchanges, and hundreds of trunk groups connecting them. It does not appear to be feasible to model each local exchange exactly. Rather, a more realistic approach would be to concentrate on accurate modeling of a relatively small number(10-20) of "critical" exchanges, and to have "representative" models of the other exchanges. This in itself is a study issue, and is the most crucial item to be initially researched.

CONCLUSIONS

We have indicated, through the use of approximate mathematical models that dial tone access can be severely impacted during earthquakes, even for critical users unless priority access is provided. With Essential Service Protection, priority users can gain quick access to a local exchange without severely impacting non-priority users. We propose a number of call completion enhancements for critical users and detail the work that must be done to assess their efficacy during earthquake scenarios.

References

[1] L. J. Forys, "Performance Analysis of a New Overload Strategy", 10th International Teletraffic Congress, 1983, Montreal, Canada
[2] J. Borchering, L. J. Forys, A. A. Fredericks, G. J. Hejny, "Coping With Overloads", Bell Laboratories Record, pp. 183-185, July/August 1981.
[3] L. Kleinrock, *Queueing Systems, Volume II; Computer Applications*, John Wiley & Sons, 1976.

APPENDIX A: APPROXIMATE ANALYSIS OF DIAL TONE DELAY DISTRIBUTIONS

In this section, we develop an approximate model to analyze the dial tone delay distribution when the LIFO overload strategy is implemented. The strategy handles both new bids for service and patient customers who are made to appear as new bids in the same manner. A critical parameter to analyze is the fraction of bids that are not served immediately, i.e. are not the "freshest" bids for service. If a bid is not served immediately, it is enqueued in an "origination queue". We will assume that the bid must wait for a timing interval before it can be considered again. This is a very reasonable assumption for the case where the offered load exceeds the capability of the processor, i.e. when there are more demands offered than the processor can handle.

In a 1AESS, this timing interval is uniformly distributed between 20 and 30 seconds. This is achieved by examining the origination queue every 10 seconds, and timing-out a call which is seen three times. In other switch implementations, the timing interval is typically constant, and often somewhat shorter. We will concentrate on implementations where the timing interval is constant, which we will assume to be 20 seconds. Several switches have constant timing intervals.

While a customer is enqueued, waiting for dial tone, line state changes are ignored (e.g. flashing or disconnects are not detected). Thus, if a customer is patient, and is not served immediately, it will experience *at least* a 20" delay before obtaining dial tone. At the end of the timing interval, the bid is erased from the queue and line scanning is resumed on the line, with its line status (artificially) set to "on-hook". If the customer is still off-hook, the next scan will interpret that line as generating a new origination, which will be loaded into the origination queue. Thus, in effect, the processor automatically reattempts the call of a patient customer. If this bid is not served immediately, it is again enqueued for the length of the timing interval. We will denote the probability that a bid is not served immediately (in actuality, after a small delay), i.e. is delayed and timed-out, by p_d. We denote the total originating offered attempt load, (which includes the bids automatically reattempted by the processor) by λ_T and the processed originating attempt load (or carried load) by λ_c.

We will approximate the effects of LIFO by the following equation, which is most accurate for heavy overloads.

$$\lambda_T = \lambda_c + p_d \lambda_T \tag{1}$$

Or,

$$\lambda_T = \frac{\lambda_c}{1 - p_d} \tag{2}$$

The first equation, (1), reflects the fact that the total offered attempts are either served immediately (and carried) or they are delayed.

While attempts are enqueued, a fraction of the attempts will abandon before they are automatically reattempted by the processor. We will assume that the time a customer waits until abandonment is exponentially distributed. Using a timing interval of 20 seconds, from the data presented in section 5.3 of the LSSGR, only 20% of customers will not have abandoned or attempted dialing. Presumably, a fraction of "early dialers" will still be off hook, or, they will have abandoned their requests and have reinitiated their call before the timing interval expires. The exponential assumption is key to the analysis. Because of the assumption, no matter how many times an attempt is automatically enqueued, the abandonment behavior will be the same. Field data reported on in reference 1 for a 1AESS indicates that as many as 30% of λ_T will still be present and automatically reattempted. This discrepancy may be due to the longer timing interval in a 1AESS which allows more customers to abandon, and then reattempt their call before the timing interval expires. Using a value of 20% will make our calculation of p_d optimistic,

which further motivates the need for ESP.
With these assumptions we can write:

$$\lambda_T = \lambda_{off} + .2\lambda_T p_d \tag{3}$$

Here, λ_{off} is the call attempt load offered to the processor by the customers. It is the similar to λ_T except it does not include the automatic reattempts.
Rearranging equation (3) we get:

$$\lambda_T = \frac{\lambda_{off}}{1 - .2p_d} \tag{4}$$

From equations (2) and (4) we get an expression for p_d in terms of λ_c and λ_{off}:

$$p_d = 1 - \frac{\lambda_c(1 - .2p_d)}{\lambda_{off}} \tag{5}$$

Solving for p_d,

$$p_d = (1 - \frac{\lambda_c}{\lambda_{off}})/(1 - .2\frac{\lambda_c}{\lambda_{off}}) \tag{6}$$

In equation (6), the key parameter is the ratio λ_c/λ_{off}. If the incoming traffic is assumed to be constant, say, e.g., 35% of the capacity of the processor capacity, then λ_c can be assumed to be constant. Thus, λ_c/λ_{off} can be thought of as the degree of originating overload. Note that our assumptions of abandonment behavior appears solely through the coefficient .2 in equation (6). If customers were more prone to abandon, this coefficient would decrease, and the resulting delays would be somewhat less, for the same % overload. Correspondingly, if the coefficient were larger, the resulting delays would be larger.
Although equation (6) represents the delay probability when the total offered load is measured, it often does not reflect the actual overload condition. This is because customers who do not complete often reattempt. Let p represent the probability of reattempting after an ineffective attempt (e.g. an abandonment). Let λ_o represent the first attempted stream of calls. Then,

$$\lambda_{off} = \lambda_o + p(\lambda_{off} - \lambda_c) \tag{7}$$

or,

$$\lambda_{off} = \frac{\lambda_o - p\lambda_c}{1 - p} \tag{8}$$

We can rewrite equation (6) in terms of the first offered overload, $\frac{\lambda_o}{\lambda_c}$, by first using

equation (8) to get that

$$\frac{\lambda_c}{\lambda_{off}} = \frac{(1-p)}{\frac{\lambda_o}{\lambda_c} - p} \tag{9}$$

Using (9) in (6), we then get:

$$p_d = \frac{1 - \frac{\lambda_o}{\lambda_c}}{.8p + .2 - \frac{\lambda_o}{\lambda_c}} \tag{10}$$

Since p_d represents the fact that customers who are delayed are also delayed for a period of time greater than the timing interval, p_d is equal to the probability of dial tone delay greater than 3 seconds. Since all switches implementing LIFO have timing intervals greater than 3 seconds, this conclusion holds for all switches.
The difference between switches is more apparent when other parts of the delay distribution are calculated. For example, because the 1AESS has a timeout interval randomly distributed between 20-30 seconds, a call experiencing a delay greater than 3 seconds will also be delayed greater than 20 seconds. For switches with shorter timing intervals intervals, say e.g. 15 seconds, a delay greater than 3 seconds would also be a delay greater than 15 seconds. Because we have assumed a 20 second timing interval, the probability of being delayed at least k times 20 seconds is p_d^k.

APPENDIX B: APPROXIMATE ANALYSIS OF ESP DELAYS

In all implementations of ESP that we consider, a separate, high priority queue, is used to provide priority service to ESP customers. Bids for dial tone are immediately placed into the high priority queue after detection of the bid. Dial tone requests are served after call-in-progress work, if any, has been processed. Incoming calls often have priority over originations. For simplicity, we will assume that they get processed at the same priority as call-in-progress work. We thus model the processors as having three tasks to be processed: call-in-progress work (and incoming seizures), ESP bids for dial tone, and non-ESP bids for dial tone. ESP bids are handled FIFO, and non-ESP bids are handled by the LIFO algorithm. Maintenance and other overhead functions which are not call dependent are handled by inflating the work for calls by the appropriate amounts. We will use priority queueing models to approximately analyze the delays. There are several references for this theory, see e.g. Chapter 3 of reference 3. The priority queueing results assume that the when the processor is available to do a task, it will select one from the highest priority queue. It will not interrupt the work on a task even if a higher priority

arrival occurs (non-preemptive head of the line priority). Arrivals are assumed to be independent Poisson processes, and processing times can be different for each queue, and can have any distribution.

This priority queue model is expected to produce higher delays than actual systems, since, strict priority is rarely achieved in these systems.

We will let $\overline{W_i}$ denote the average delay in the ith priority queue. The average arrival rate into the ith priority queue will be denoted by λ_i, and the average processing times by $\frac{1}{\mu_i}$.

Denoting $\rho_i = \lambda_i/\mu_i$, we get the following expressions for $\overline{W_i}$:

$$\overline{W}_1 = \frac{\overline{R}}{1 - \rho_1} \tag{11}$$

$$\overline{W}_2 = \frac{\overline{R}}{(1 - \rho_1)(1 - \rho_1 - \rho_2)} \tag{12}$$

$$\overline{W}_3 = \frac{\overline{R}}{(1 - \rho_1 - \rho_2)(1 - \rho_1 - \rho_2 - \rho_3)} \tag{13}$$

The term $\overline{R}$ in the equations represents the mean residual processing time and is equal to $\sum_{k=1}^{3} \lambda_k b_k/2$, and b_k is the second moment of the service time for the kth queue.

To perform our analysis, we will focus on a "typical" peripheral module in a digital switch. We will assume that the overhead in the peripheral processor is embedded into the amount of time it takes to process a call. We will assume a nominal capacity of 4,500 (full) calls/hour (or 1.25 calls/second), which corresponds to a peripheral processor capacity. In addition, we will assume that the time to process abandonments in queue is negligible, which is a good assumption. Thus, each full call will take 3600/4500 = .80 seconds. By making appropriate assumptions on the various call processing segments, we obtain $\overline{R}$ =

$$\left(\frac{1.25}{2}\right)[10.35(.0057) + .65(.0225)]$$

$$= .046$$

The model will predict infinite delays for for the lowest priority queue when $\lambda_2 + \lambda_3 \geq .8125$. Nevertheless, in this region, the delays for ESP calls will still be finite for $\lambda_2 < .8125$. In reality, the delays for the lowest priority queue will also be finite when $\lambda_2 + \lambda_3 > .8125$ because, customers will abandon their attempts. In fact, an analysis similar to that of Appendix A can be used to predict the delay distribution.

The definition of λc in equation (1) and (6) needs to be modified to reflect the fact that ESP calls will decrease the amount of processor time which can be used by non-ESP calls. The term λ_c, which reflects the maximum possible carried load should be reduced by the ESP carried load. We will use superscripts, N and E to indicate quantities related to non-

ESP calls and ESP calls respectively. Thus, in (10), we will replace $\frac{\lambda_o}{\lambda_c}$ by:

$$\frac{\lambda_o{}^N}{\lambda_c{}^N} = \frac{\lambda_o - \lambda_o{}^E}{\lambda_c - \lambda_c{}^E}$$

$$= \frac{\lambda_o - \lambda_o{}^E}{\lambda_c - \lambda_o{}^E}$$

$$= \frac{1 - \alpha}{\frac{\lambda_c}{\lambda_o} - \alpha} \tag{14}$$

Here, $\alpha = \frac{\lambda_o{}^E}{\lambda_o}$, which is the fraction of first attempts which are ESP. We have also made use of the fact, that, for the regions of interest, $\lambda_c{}^E = \lambda_o{}^E$, i.e. the entire load offered by ESP calls is carried.
We now use (14) in (10) to yield:

$$p_d = \frac{1 - \frac{\lambda_o}{\lambda_c}}{.2 + .8p - (1 - .8\alpha + .8\alpha p)\frac{\lambda_o}{\lambda_c}} \tag{15}$$

This expression makes sense provided $\frac{\lambda_o}{\lambda_c} < \frac{1}{\alpha}$. We note that with our definitions, in equation (12) we will make use of the fact that $\lambda_2 = \alpha\lambda o$.
To approximately obtain the delay distribution of ESP calls, we make use of (12) to first calculate the mean delay, $\bar{W}_2$. We next assume that the probability of delay greater than 0 is 1, (which produces higher delays, and is hence conservative) and further assume that the delay distribution is exponential.
As a result, we get:

$$P(ESP\ delay > T) = \exp - T/\bar{W}_2 \tag{16}$$

Table 1: Estimated DTD Distribution
(Total Attempts)

	Percentage Delay				
Percent Overload	>3"	>20"	>40"	>60"	>80"
10%	10	10	1	.1	.01
20%	20	20	4	.8	.2
30%	27	27	7	2	.5
50%	38	38	14	6	3
80%	50	50	25	12.5	6
100%	55	55	30	17	9

Table 2: Estimated DTD Distribution
(First Offered Attempts)

	Percentage Delay				
Percent Overload	>3"	>20"	>40"	>60"	>80"
10%	29	29	8.4	2.4	.7
20%	46	46	21	9	4
30%	55	55	30	17	9
50%	67	67	45	30	20

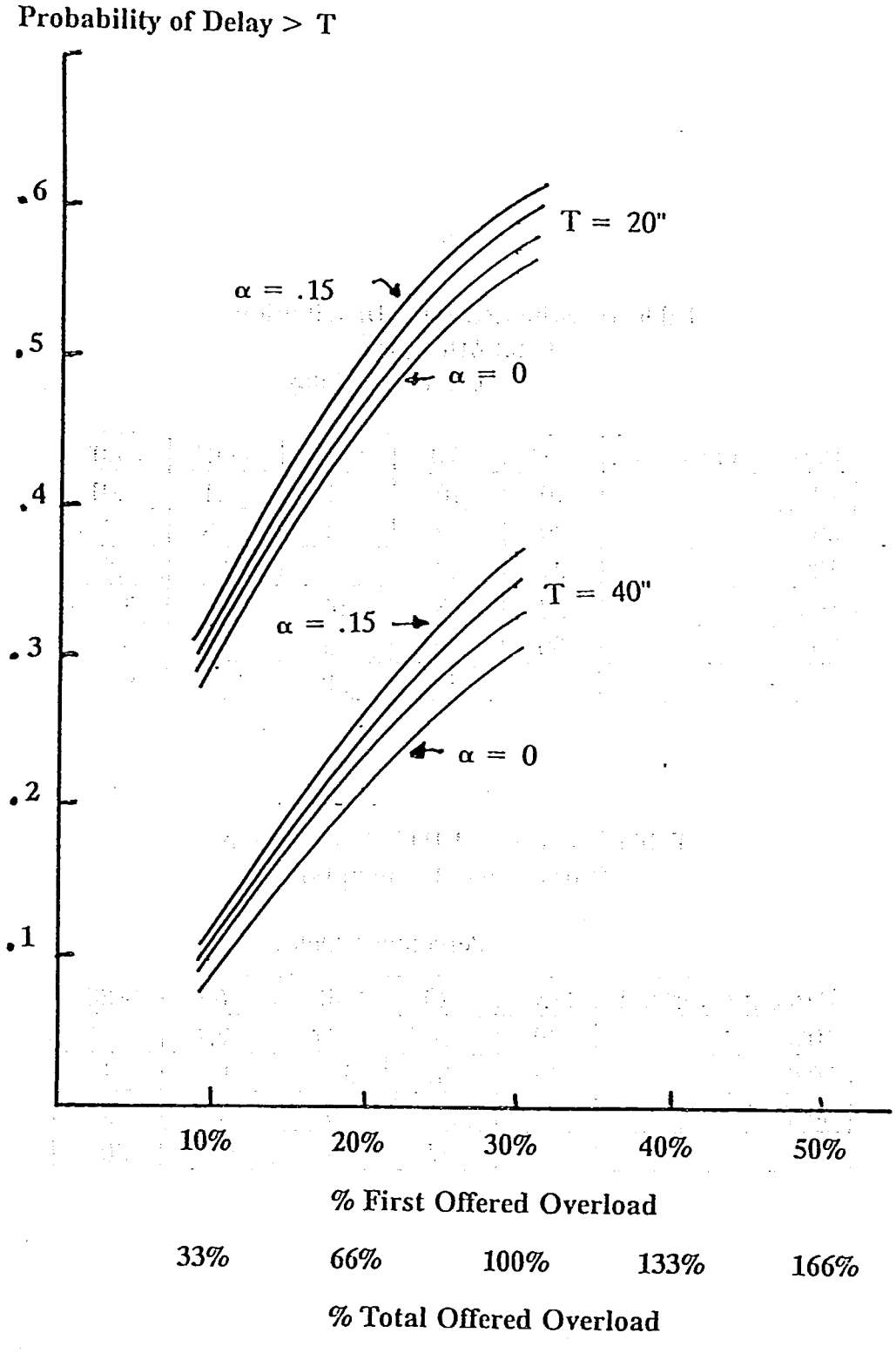


Figure 1: Impact of ESP Calls on non-ESP Dial Tone Delays

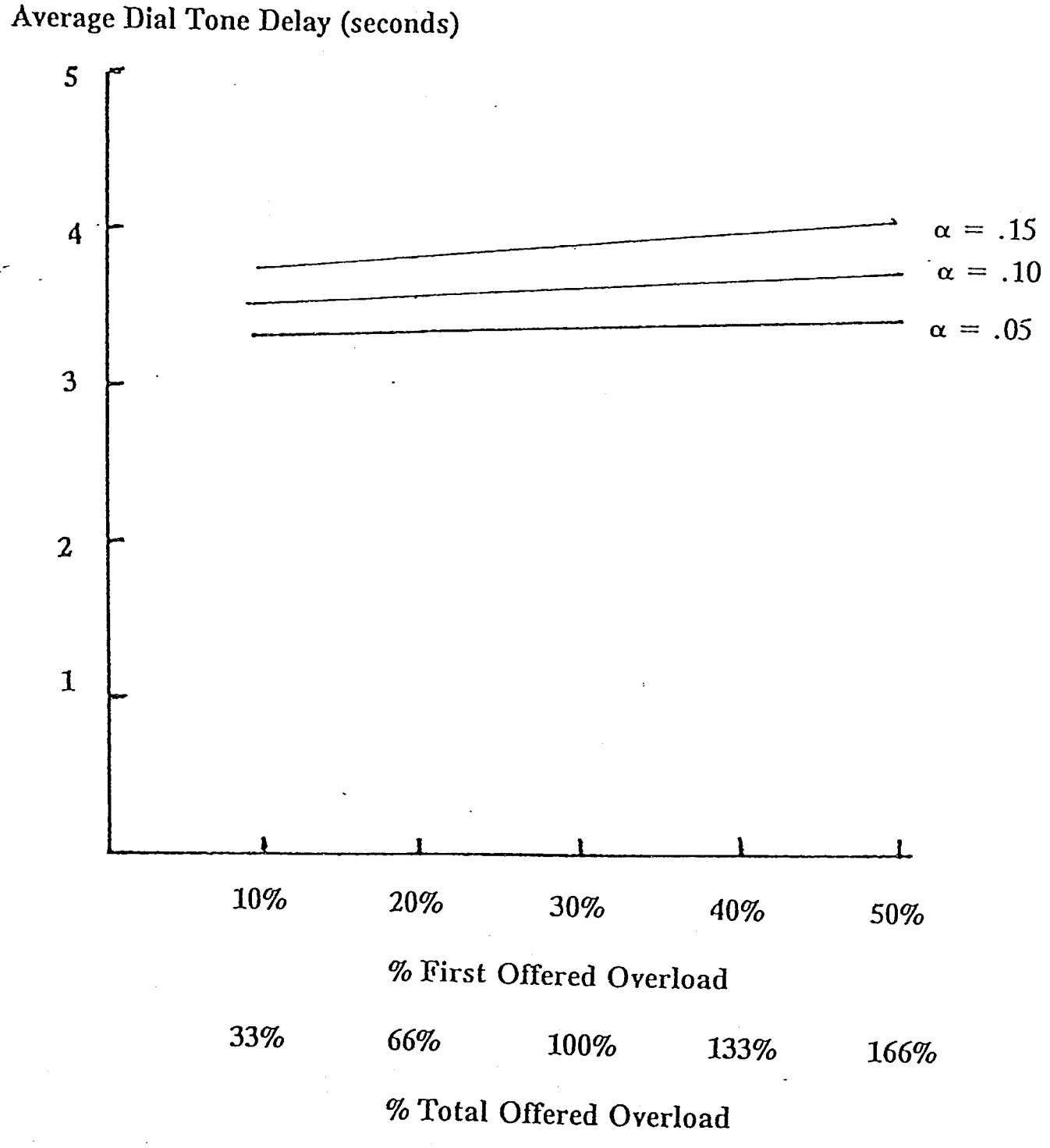


Figure 2: Average Dial Tone Delay for ESP Calls (non-1AESS)

Resolutions

RESOLUTIONS OF THE FIFTH U.S.-JAPAN WORKSHOP ON EARTHQUAKE DISASTER PREVENTION FOR LIFELINE SYSTEMS

Public Works Research Institute, Tsukuba
October 26-30,1992

The Fifth U.S.-Japan Workshop on Earthquake Disaster Prevention for Lifeline Systems was held under the sponsorship of the Public Works Research Institute of Japan and the U.S. National Science Foundation under the auspices of Task Committee F, "Disaster Prevention Methods for Lifeline Systems,"UJNR Panel on Wind and Seismic Effects at the Public Works Research Institute, Tsukuba, October 26-30,1992.

The workshop provided a valuable forum to exchange information and ideas on technical and socioeconomic issues important to the lifeline earthquake engineering communities of both countries. The following topics were addressed:

a. Effect of liquefaction and large ground displacement
b. Network and system performance assessment
c. Observations and seismic monitoring
d. Seismic design and performance of lifeline systems, including telecommunication, electric power, water and natural gas systems
e. Seismic design and performance of highway bridges and tunnels
f. Socioeconomic impact of lifeline failures and disruptions.

The following resolutions were adopted by the Workshop participants:

1. The workshop identified, without priority order, the following topics relevant to lifeline systems for further cooperative research programs:

a. Effect of liquefaction on the performance of Lifeline Systems;
b. Field investigations of seismic damage;
c. Seismic design procedures and engineered safety protection measures;
d. Procedures and instrumentation to detect the behavior of lifeline systems during an earthquake and inspect the damage to lifeline structures following an earthquake;
e. Repair and retrofit procedures and post-event service restoration strategies;
f. Estimation of reliability of lifelines;
g. Vulnerability models for lifeline components, systems, and networks, and models for damage and loss estimates;
h. Systems analysis and network management strategies for lifeline damage

mitigation;

i. Public education and information transfer programs for demonstrating the importance of seismic reliability of lifeline systems for earthquakes;
j. Earthquake hazard reduction programs with US. and Japan Government Agencies;
k. Investigation into requirements for large-scale testing of lifeline systems and laboratory studies using multiple shaking tables and dynamic actuators;
l. Exchange of information on the seismic design and performance of telecommunication facilities;
m. Method to minimize the impact caused by disruption of interdependent lifelines;
n. Earthquake mitigation as a part of overall infrastructure rehabilitation program.

2. The Workshop acknowledges current efforts in both countries to establish seismic design guidelines and standards for lifeline systems. Encouragement in the actual development of such standards should be placed on the U.S. effort. Existing UJNR channels should be fully utilized to facilitate the exchange of relevant technical information concerning standards development. Possible collaboration of joint development of lifeline system standards and guidelines should be pursued.

3. The importance of continued support of "the International Decade for Natural Disaster Reduction"(IDNDR) was acknowledged with respect to lifeline earthquake engineering and disaster mitigation research under the UJNR program. The participants of the Workshop believe that the Fifth U.S.-Japan Workshop on Earthquake Disaster Prevention for Lifeline Systems is a significant contribution to the achievement of the goals of the IDNDR program.

4. The workshop recognizes the importance of continued exchange of research personnel, technical information, research data and use of available research facilities in both countries. The workshop further recognizes the benefit of identifying specific activities to compare the results of different design, analysis and experimental methods, and disaster strategies of both countries.

5. In view of the recent hurricanes and typhoons that caused significant damage to Lifeline Systems in the United States and Japan, the workshop encourages the interaction of this Task Committee with other UJNR Task Committees to quantify the vulnerability of Lifeline Systems to earthquake and wind effects.

6. In view of the importance of cooperative research programs on seismic effects and earthquake disaster prevention methods on lifeline systems, it is recommended to hold the 6th Workshop in May 1994 in U.S.A. The location and time of the workshop will be determined through correspondence between the Co-Chairs of

Task Committee "F" of the UJNR Panel on Wind and Seismic Effects.

Appendices

FIFTH U.S.-JAPAN WORKSHOP ON EARTHQUAKE DISASTER PREVENTION FOR LIFELINE SYSTEMS

OCTOBER 26 AND 27,1992

PUBLIC WORKS RESEARCH INSTITUTE, TSUKUBA, JAPAN

WORKSHOP PROGRAM

October 26 (MON)

9:00 Session-1 Opening Session

(Chairman: Kawashima, K. and Singh, M.P.)

Opening Remarks by Mr. Sumiyoshi, Y., Director-General, PWRI

Address by Dr. Riley Chung, National Institute of Standard and Technology

Address by Mr. Iida, Y., Director, Earthquake Disaster Prevention Department, PWRI

Address by Mr. Eguchi, R.T., EQE International

9:30 Session-2 Telecommunication

(Chairman: Hamada, M. and Lund, L.)

U-1) Earthquake and Lifeline Hazards Reduction Programs at National Science Foundation
(M.P. Singh)

J-1) A Seismatic Countermeasures for Optical Fiber Cable in Liquefied Ground
(Shinji MATAKI)

U-2) Post-Earthquake Performance of Telecommunications Network
(Kenneth Boheim)

U-3) Seismic Considerations of Raised Floor Application for Telecommunication Network Facilities
(Alex Tang)

10:50 Break

11:10 Session-3 Electricity, Water & Gas

(Chairman: Suzuki, H. and Ballantyne, D.)

J-2) Earthquake Engineering Researches for Electric Power Lifeline Systems
(Junichi TOHMA)

J-3) A Method of Evaluating Earthquake Resistance of Buried Pipelines---Recommended Practice of JGA and A Proposal for Its Improvement
(Nobuaki NISHIO)

U-4) Earthquake Hazard Reduction Program for a Water Utility Lifeline Agency
(Ergun Bakall)

J-4) Seismic Design for Pipeline of Waterworks in Tokyo
(Ichiro YOKOTA)

12:30 Lunch (Conference Room at 1st Floor)

13:30 Session-4 Effect of Liquefaction

(Chairman: Tokida, K. and Scawthorn, C.)

J-5) Stress Analysis Method for Steel Pipelines Buried in a Liquefied Ground Layer
(Takashi IWATA)

J-6) A State of the Art of Methodology in Japan for Damage Estimation of Lifeline Facilities in Liquefied Area
(Masanori HAMADA)

J-7) Safety Estimation of Buried Pipes for Permanent Ground Deformation by Liquefaction
(Hideyo SUZUKI)

J-8) Experimental Study on Liquefaction Potential and The Uplift Deformation of Underground Structures
(Yoshio NINOMIYA)

U-5) Lateral Spread Effects on Reinforced Concrete Pile Foundations
(Thomas O'Rourke)

15:10 Break

15:30 Session-5 Network Assessment

(Chairman: Saito, T. and O'Rourke, T.D.)

J-9) Seismic Reliability Analysis of Large Scale Lifeline Networks Using Fuzzy Set Theory
(Tadanobu SATO)

J-10) Network Performance of Highway Systems Under Earthquake Effects: A Case Study of the 1989 Loma Prieta Earthquake
(Hiroshi WAKABAYASHI and Hiroyuki KAMEDA)

U-6) GIS-Based Assessment of the Seismic Performance of a Water Delivery System
(Masanobu Shinozuka)

16:30 Break

16:50 Session-6 Seismic Design

(Chairman: Kameda, H. and Roberts, J.E.)

J-11) Earthquake Response Analysis Method for Shield Tunnels
(Yukio SHIBA)

J-12) A Seismic Design of A Large Shield Tunnel of Trans-Tokyo Bay Highway
(Kenji KURAISHI)

J-13) Design of Tama River and Kawasaki Fairway Tunnels in Expressway Bay-shore Route
(Shinichi EGAWA)

J-14) Seismic Design of Underground Parking Garage
(Kazuhiko KAWASHIMA)

18:10 Adjourn

18:20 Leave PWRI

18:40 Arrive Hotel Grand Shinonome

19:30 Reception Hosted by Director-General, Public Works Research Institute
(Hotel Grand Shinonome)

October 27 (TUE)

9:00 Session-7 Bridge
(Chairman: Katayama, T. and Bakall, E.)
U-7) Effects of Soil Response on Bridge Seismic Performance
(James Roberts)
J-15) Seismic Strengthening and Retrofitting of Highway Bridges in Japan
(Shigeki UNJOH)
U-8) Research Based Bridge Seismic Design and Retrofit Program Criteria, Standard and Status
(James Roberts)

10:00 Break

10:20 Session-8 Hazard Mitigation
(Chairman: Nishio, N. and Shinozuka, M.)
U-9) Pipeline Damage Mitigation Using TCLEE Pipeline Failure Database
(LeVal Lund)
J-16) A Study of Socio-Economic Effects of Lifelines Earthquake Disaster in Urban Transportation Networks
(Chartchai Leelawat)
U-10) Lifeline Collocation, Interaction and Post-Earthquake Functionality: Case Study for Fire Following Earthquake
(Charles Scawthorn)
U-11) Earthquake Hazard Reduction Program for Lifelines at the National Institute of Standards and Technology
(Riley Chung)

11:40 Memorial Group Photo (in front of Main Building)
12:00 Lunch (Conference Room at 1st Floor)

13:00 Session-9 Observation and Seismic Monitoring
(Chairman: Iida, Y. and Tang, A.)
J-17) Seismic Behavior of Buried Pipelines Through Field Observation
(Hideki SUGITA)
J-18) Seismic Monitoring System for Lifelines
(Shiro TAKADA)
U-12) Monitoring, Instrumentation, and Innovative Devices for Lifeline Systems
(Donald Ballantyne)
U-13) Vulnerability of Fiber Optics Cables to Fault Rupture, A Proposed Field Experiment
(Felix Wong)

14:20 Break

14:40	<u>Session-10 Impact of Seismic Effects</u> (Chairman: Kuribayashi, E. and Kelley, C.M.) J-19) Effective Measures for Reducing People's Anxiety in Underground Spaces during Earthquakes (Etsuro SAITO) U-14) Lifeline Damage and Resulting Impacts (R.T.Eguchi) U-15) Earthquake-Induced Congestion Impacts on Local Telephone Networks (Leonard Forys)
15:40	Visit to Laboratories Earthquake Engineering Laboratory Ground Vibration Laboratory
16:40	<u>Session-11 Closing Session</u> (Chairman: Kawashima, K. and Eguchi, R.T.)
17:40	Closure
17:50	Leave PWRI
18:10	Arrive Hotel Grand Shinonome
19:00	Reception Hosted by U.S. Members (Sea Food Restaurant "Isami")

TECHNICAL STUDY-TOUR

October 28 (WED)

9:00 Leave Hotel Grand Shinonome (Tsukuba, Bus)
10:30 Water Purification Plant (Misato, Tokyo Metropolitan Government)
13:00 Construction Site of Water Supply Tunnel
(Tokyo Metropolitan Government, Minato-ku, Tokyo)
15:00 Control Center, Tokyo Electric Company (Shinbashi, Tokyo)
17:00 Shinbashi-Dai-Ichi Hotel (Tokyo)

October 29 (THR)

8:20 Leave Shinbashi-Dai-Ichi Hotel
9:00 Submerged Tunnel Construction Site
(Metropolitan Expressway Public Corporation)
11:00 Trans Tokyo Bay Crossing Highway Construction Site (Boat)
Cruise from Kawasaki to Kisarazu
Tour for Road Tunnel and Bridge Piers
14:30 Leave Kisarazu to PWRI Pipe Response Observation Site
15:40 Tour to Tokyo Electric Tunnel Construction Site
17:58 Leave Kimitu Station to Shinbashi Station (JR Train)
19:30 Shinbashi-Dai-Ichi Hotel (Tokyo)

October 30 (FRI)

9:00 Leave Shinbashi-Dai-Ichi Hotel
9:30 Group A: NTT Network Control Center (Minato-ku, Tokyo)
Group B: Construction Site of A Suspension Bridge on Soft Rock
(Metropolitan Expressway Public Corporation, Minato-ku, Tokyo)
12:30 Construction Site of A Cable Stayed Bridge
(Tsurumi Bridge, Metropolitan Expressway Public Corporation)
15:00 Research Center, Tokyo Gas Company (Tsurumi)
17:30 Shinbashi-Dai-Ichi Hotel(Tokyo)

PARTICIPANTS IN THE WORKSHOP

PARTICIPANTS FROM THE U.S. SIDE

Mr. Ergun Bakall
Chief Engineer
San Diego County Water Authority
3211 Fifth Avenue San Diego,
CA 92103-5718

Mr. Donald Ballantyne
Senior Sanitary Engineer
Kennedy/Jenk Consultants
530 S. 336th Street
Federal Way, WA 98003

Mr. Kenneth Boheim
Assistant Manager
Plans and Program
National Communications System
Office of Plans and Programs
Arlington, VA 22204

Dr. Riley Chung
National Institute of Standards and Technology
Building and Fire Research Laboratory
Building 226
Gaithersburg, Maryland 20899

Mr. Ron Eguchi
Vice President
EQE Engineering and Design
18101 Von Karman Ave. Ste. 400
Irvine, CA 92715

Dr. Leonard Forys
Director of System Performance Modeling Group
Bell Communication Research
331 Newman Springs Rd. Room 2x-157
Red Bank, NJ 07701

Mr. Chris Kelly
Senior Associate
Booz·Allen&Hamilton Inc.
8283 Grensboro Dr.
McLean, VA 22102

Mr. LeVal Lund
Civil Engineer
Engineering Consultant
3245 Lowry Rd.
Los Angeles, CA 90027

Prof.Thomas O'Rouke
Professor
Civil and Environmental Engineering
Cornell University
265 Hollister Hall
Ithaca, NY 14853

Mr. James Roberts
Division of Structures
California Department of Transportation
1801 30th St., Room 211
Sacramento, CA 95816

Dr. Charles Scawthorn
EQE International
44 Montgomery # 3200
San Francisco, CA 94104

Prof. Masanobu Shinozuka
Professor
Department of Civil Engineering and Operations Research
Princeton University
Princeton, NJ 08544

Dr. M. P. Singh
Program Director
Earthquake Hazard Mitigation Program
Directorate for Engineering
National Science Foundation
1800 G Street N.W.
Washington D.C. 20550

Mr. Alex Tang
Manager of Mechanical Engineering
and Regulatory Compliance
Northern Telecom Public Network
Division
8200 Dixie Rd. Department S617
Brampton, Ontario L6V @M6
Canada

Dr. Felix Wong
Weidlinger Associates
4410 El Camino Real
Ste 110
Los Altos, Ca 94022

PARTICIPANTS FROM THE JAPAN SIDE

Mr.Masanobu Arano
Senior Research Engineer
Seismic Engineering Department
Tsukuba Research Institute
Okumura Corp.
Tsukuba, 300-33, Japan

Mr.Shinichi Egawa
Deputy Manager
Bay-shore Route Construction Bureau
Metropolitan Expressway Public Corp.
Minato-ku, Tokyo, 105, Japan

Prof.Masanori Hamada
Professor
School of Marine Science and
Technology
Tokai University
Shimizu, 424, Japan

Mr.Junichi Hoshikuma
Research Engineer
Earthquake Engineering Division
Public Works Research Institute
Ministry of Construction
Tsukuba, 305, Japan

Mr.Yutaka Iida
Director, Earthquake Disaster
Prevention Department
Public Works Research Institute
Ministry of Construction
Tsukuba, 305, Japan

Dr.Takashi Iijima
Assistant Director General
Public Works Research Institute
Ministry of Construction
Tsukuba, 305, Japan

Mr.Takaaki Ikeda
Research Engineer
Research & Development Department
Technology Development Division
Tobishima Corp.
Chiba, 270-02, Japan

Mr.Takashi Iwata
Senior Manager
Transmission Section
Pipeline and Facilities Engineering
Department Tokyo Gas Co.,Ltd.
Minato-ku, Tokyo, 105, Japan

Prof.Hiroyuki Kameda
Professor
Urban Earthquake Hazard research
Center
Disaster Prevention Research
Institute
Kyoto University
Kyoto, 611, Japan

Prof.Tsuneo Katayama
Professor
Institute of Industrial Science
University of Tokyo
Minato-ku, Tokyo, 106, Japan

Dr.Kazuhiko Kawashima
Head, Earthquake Engineering
Division
Public Works Research Institute
Ministry of Construction
Tsukuba, 305, Japan

Dr.Takeji Kokusyo
Director, Siting Technology
Department
Central Research Institute of
Electric Power Industry
Abiko, 270-11, Japan

Mr.Hiroshi Kohno
Deputy Director General
Public Works Research Institute
Ministry of Construction
Tsukuba, 305, Japan

Mr.Nobuo Kubota
Manager
Bay-shore Route Construction Bureau
Metropolitan Expressway Public Corp.
Minato-ku, Tokyo, 105, Japan

Mr.Kenji Kuraishi
Design and Engineering Department
Trans-Tokyo Bay Highway Corp.
Chiyoda-ku, Tokyo, 102, Japan

Prof.Eiichi Kuribayashi
Professor
Department of Civil Engineering
Toyohashi University of Science and Technology
Toyohashi, 440, Japan

Mr.Chartchai Leelawat
Research Associate
Department of Civil Engineering
Toyohashi University of Science and Technology
Toyohashi, 440, Japan

Mr.Tamio Masuda
Manager
Civil Engineering Administration Division
Hydro-Generation and Transmission Engineering Department
Tokyo Electric Power Co. Inc.
Chiyoda-ku, 100, Tokyo, Japan

Mr.Shinji Mataki
Civil Engineering Systems Development Project Group
NTT,Telecommunication Field Systems R&D CenterTsukuba, 305, Japan

Mr.Katsumi Matsubara
Assistant Manager
Technical Research Institute
Hazama Corp.
Tsukuba, 305, Japan

Mr.Hidetoshi Mukai
Assistant Research Engineer
Earthquake Engineering Division
Public Works Research Institute
Ministry of Construction
Tsukuba, 305, Japan

Mr.Kazuhiro Nagaya
Assistant Research Engineer
Earthquake Engineering Division
Public Works Research Institute
Ministry of Construction
Tsukuba, 305, Japan

Mr.Tomoru Nakajima
Research Engineer
Earthquake Engineering Division
Public Works Research Institute
Ministry of Construction
Tsukuba, 305, Japan

Mr.Yutaka Nakajima
Deputy Manager
Design and Engineering Department
Trans-Tokyo Bay Highway Corp.
Chiyoda-ku, Tokyo, 102, Japan

Mr.Yoshio Ninomiya
Senior Research Engineer
Ground Vibration Division
Public Works Research Institute
Ministry of Construction
Tsukuba, 305, Japan

Dr.Nobuaki Nishio
Councilor, Senior Researcher
Fundamental Technology Research Laboratory
Tokyo Gas Co.,Ltd.
Minato-ku, Tokyo, 105, Japan

Dr.Naoto Ohbo
Senior Research Engineer
Earthquake Engineering Section
Civil Engineering Department I
Kajima Technical Research Institute
Kajima Corp.
Chofu, 182, Japan

Mr.Yasuaki Ohtani
Senior Engineer
Super Computing Technology, Division 3
Fuji Research Institute Corp.
Minato-ku, Tokyo, 105, Japan

Dr.Etsuro Saito
Senior Research Engineer
Civil Engineering Research Department
Technical Research Institute
Fujita Corp.
Yokohama, 223, Japan

Mr.Masayuki Satoh
Section Chief
Seismic Engineering Department
Tokyo Electric Power Services Co.,Ltd.
Chiyoda-ku, 100, Tokyo, Japan

Prof.Tadanobu Satoh
Associate Professor
Disaster Prevention Research Institute
Kyoto University
Kyoto, 611, Japan

Dr.Yukio Shiba
Research Engineer
Earthquake Engineering Team
Earthquake & Wind Engineering Research Group, Technology Research Center
Taisei Corp.
Yokohama, 245, Japan

Dr.Yukitake Shioi
General Manager
Design and Engineering Department
Trans-Tokyo Bay Highway Corp.
Chiyoda-ku, Tokyo, 102, Japan

Mr.Hideki Sugita
Research Engineer
Earthquake Engineering Division
Public Works Research Institute
Ministry of Construction
Tsukuba, 305, Japan

Mr.Yukihiko Sumiyoshi
Director General
Public Works Research Institute
Ministry of Construction
Tsukuba, 305, Japan

Dr.Hideyo Suzuki
Chief Researcher
Architecture Department
Engineering Research Center
Tokyo Electric Power Co. Inc.
Chofu, 182, Japan

Prof.Shirok Takada
Professor
Department of Civil Engineering
Kobe University
Kobe, 657, Japan

Mr.Naonobu Takewaki
Senior Research Engineer
Ohsaki Research Institute, Shimizu Corp.
Chiyoda-ku, Tokyo, 100, Japan

Dr.Keiichi Tamura
Senior Research Engineer
Ground Vibration Division
Public Works Research Institute
Ministry of Construction
Tsukuba, 305, Japan

Mr.Masahide Tamura
Director, Planning and Research Administration Department
Public Works Research Institute
Ministry of Construction
Tsukuba, 305, Japan

Mr.Junichi Tohma
Senior Researcher
Earthquake Engineering Section
Central Research Institute of Electric Power Industry
Abiko, 270-11, Japan

Mr.Kenichi Tokida
Head, Ground Vibration Division
Public Works Research Institute
Ministry of Construction
Tsukuba, 305, Japan

Mr.Junichi Ueno
Chief
Civil Engineering Department
Konoike Construction Co., Ltd.
Chuo-ku, Osaka, 541, Japan

Mr.Shigeki Unjo
Senior Research Engineer
Earthquake Engineering Division
Public Works Research Institute
Ministry of Construction
Tsukuba, 305, Japan

Prof.Hiroshi Wakabayashi
Associate Professor
Department of Civil Engineering
Osaka Prefectural College of
Technology
572, Neyagawa, Japan

Mr.Koji Yagi
Senior Manager
Advanced Tunneling Technologies
Development Project Group
NTT,Telecommunication Field Systems
R&D Center
Tsukuba, 305, Japan

Mr.Ichiro Yokota
Head, Second Design Section
Construction Division, Bureau of
Water Works
Tokyo Metropolitan Government
Shinjuku-ku, 163-01, Japan

PROCEEDING OF FIFTH U.S.–JAPAN WORKSHOP ON EARTHQUAKE DISASTER PREVENTION FOR LIFELINE SYSTEMS

ISSN 0386–5878
Technical Memorandum of PWRI No.3198

Kazuhiko KAWASHIMA,
Hideki SUGITA and
Tomoru NAKAJIMA

This proceedings document the results of the U.S.–Japan Workshop on Earthquake Disaster Prevention for Lifeline Systems which was held at the Public Works Research Institute, Tsukuba Science City, Japan, on October 26 and 27, 1992 under the auspices of the Panel on Wind and Seismic Effects, UJNR. The Workshop was organized by the Task Committee F "Disaster Prevention Methods for Lifeline Systems"(U.S. side chairman: R.D.Dikkers, NIST, Japan side chairman: Y.Iida, PWRI) of the Panel.

○

郵 便 はが き

Postage stamp

3 0 5 -□□

建設省土木研究所地震防災部耐震研究室
〒305 茨城県つくば市大字旭１番地

Earthquake Engineering Division,
Public Works Research Institute
Tsukuba Science City
Japan 305

No. 133

No. 133

配布先住所 ○

配布先氏名

Receipt of

Technical Memorandum of PWRI No.3198

Name _____

Address _____

_____

_____